frontiers | Research Topics

Seafloor heterogeneity: Artificial structures and marine ecosystem dynamics - recent advances

Edited by
Toyonobu Fujii, Victoria Louise Georgia Todd, Daniel Joseph Pondella
and Andrew James Guerin

Published in
Frontiers in Marine Science

ISSN 1664-8714
ISBN 978-2-83252-179-3
DOI 10.3389/978-2-83252-179-3

About Frontiers

Frontiers is more than just an open access publisher of scholarly articles: it is a pioneering approach to the world of academia, radically improving the way scholarly research is managed. The grand vision of Frontiers is a world where all people have an equal opportunity to seek, share and generate knowledge. Frontiers provides immediate and permanent online open access to all its publications, but this alone is not enough to realize our grand goals.

Frontiers journal series

The Frontiers journal series is a multi-tier and interdisciplinary set of open-access, online journals, promising a paradigm shift from the current review, selection and dissemination processes in academic publishing. All Frontiers journals are driven by researchers for researchers; therefore, they constitute a service to the scholarly community. At the same time, the *Frontiers journal series* operates on a revolutionary invention, the tiered publishing system, initially addressing specific communities of scholars, and gradually climbing up to broader public understanding, thus serving the interests of the lay society, too.

Dedication to quality

Each Frontiers article is a landmark of the highest quality, thanks to genuinely collaborative interactions between authors and review editors, who include some of the world's best academicians. Research must be certified by peers before entering a stream of knowledge that may eventually reach the public - and shape society; therefore, Frontiers only applies the most rigorous and unbiased reviews. Frontiers revolutionizes research publishing by freely delivering the most outstanding research, evaluated with no bias from both the academic and social point of view. By applying the most advanced information technologies, Frontiers is catapulting scholarly publishing into a new generation.

What are Frontiers Research Topics?

Frontiers Research Topics are very popular trademarks of the *Frontiers journals series*: they are collections of at least ten articles, all centered on a particular subject. With their unique mix of varied contributions from Original Research to Review Articles, Frontiers Research Topics unify the most influential researchers, the latest key findings and historical advances in a hot research area.

Find out more on how to host your own Frontiers Research Topic or contribute to one as an author by contacting the Frontiers editorial office: frontiersin.org/about/contact

Seafloor heterogeneity: Artificial structures and marine ecosystem dynamics - recent advances

Topic editors
Toyonobu Fujii — Tohoku University, Japan
Victoria Louise Georgia Todd — Ocean Science Consulting Ltd., United Kingdom
Daniel Joseph Pondella — Occidental College, United States
Andrew James Guerin — McMaster University, Canada

Citation
Fujii, T., Todd, V. L. G., Pondella, D. J., Guerin, A. J., eds. (2023). *Seafloor heterogeneity: Artificial structures and marine ecosystem dynamics - recent advances*. Lausanne: Frontiers Media SA. doi: 10.3389/978-2-83252-179-3

Table of contents

frontiers | Frontiers in Marine Science

TYPE Editorial
PUBLISHED 31 March 2023
DOI 10.3389/fmars.2023.1181568

OPEN ACCESS

EDITED AND REVIEWED BY
Heliana Teixeira,
University of Aveiro, Portugal

*CORRESPONDENCE
Toyonobu Fujii
toyonobu.fujii.a8@tohoku.ac.jp

SPECIALTY SECTION
This article was submitted to
Marine Ecosystem Ecology,
a section of the journal
Frontiers in Marine Science

RECEIVED 07 March 2023
ACCEPTED 21 March 2023
PUBLISHED 31 March 2023

CITATION
Fujii T, Pondella DJ II, Todd VLG
and Guerin AJ (2023) Editorial:
Seafloor heterogeneity: Artificial
structures and marine ecosystem
dynamics - recent advances.
Front. Mar. Sci. 10:1181568.
doi: 10.3389/fmars.2023.1181568

Editorial: Seafloor heterogeneity: Artificial structures and marine ecosystem dynamics - recent advances

Toyonobu Fujii[1]*, Daniel J. Pondella II[2], Victoria L. G. Todd[3] and Andrew J. Guerin[4]

[1]Graduate School of Agricultural Science, Tohoku University, Sendai, Japan, [2]Department of Biology, Vantuna Research Group, Occidental College, Los Angeles, CA, United States, [3]Ocean Science Consulting Ltd., Dunbar, United Kingdom, [4]Department of Biology, McMaster University, Hamilton, ON, Canada

KEYWORDS

artificial reefs, offshore oil and gas installations, marine renewable energy, aquaculture, anthropogenic stressors, ecological restoration, ecosystem-based management, decommissioning

Editorial on the Research Topic
Seafloor heterogeneity: Artificial structures and marine ecosystem dynamics - recent advances

During the past several centuries, marine coastal ecosystems have been altered at alarming rates as a result of ever increasing anthropogenic influences (McCauley et al., 2015; Halpern et al., 2019; Duarte et al., 2020). While impacts of anthropogenic climate change have already been manifested in the form of, for example, decreased ocean productivity, altered food web dynamics, and reduced abundance of habitat-forming species, e.g. corals, seagrass, mangroves, kelp forests (Waycott et al., 2009; Hoegh-Guldberg and Bruno, 2010; Filbee-Dexter and Wernberg, 2018; FAO, 2020; Souter et al., 2021; FAO, 2022), effects of increasing installations of various artificial structures on marine ecosystems are poorly understood. Drawing on the success of the first edition (Fujii et al.), this volume aims to further advance research in the field of human impact on marine life *via* placement of "sub-sea artificial structures". This Research Topic assembles 15 articles investigating relationships between various types of anthropogenic structure and marine ecosystem dynamics. Here we present an overview of these contributions and highlight emerging views and future directions in this field.

Artificial reefs for ecological restoration

To assess the role of artificial reef construction in coastal management, Wang et al. developed trophic models for established and newly deployed artificial oyster reef ecosystems in comparison with non-reef bare substratum located in Bohai Sea, China. Reefs showed more complicated trophic relationships, greater potential to withstand perturbations, and higher carrying capacities of commercial organisms compared to bare seafloor, demonstrating benefits of constructing artificial oyster reefs for marine ranching. Williams et al. compared growth rates of a shallow-water damselfish in artificial versus natural habitats throughout the Southern California Bight. Adult garibaldi fish (*Hypsypops rubicundus*) are territorial, with limited vagility, linking their growth rates to habitat quality. Garibaldi grew significantly larger on artificial reefs than on natural reefs, a finding consistent with other fishes in the region, providing insights into future reef design and assessments. Williams et al. report on the first restoration rocky reef built on the open coast in California. The Palos Verdes Reef is a series of variable relief rock modules (1-4 m) placed proximate to existing reefs. Due to its novel design, there were rapid recruitment and successional responses. Reef performance quickly exceeded design expectations, including the persistence of giant kelp, fish biomass, and fish density.

Human activities relating to aquaculture and reconstruction of coastal infrastructure

Hashimoto and Sato-Okoshi investigated population dynamics of a capitellid polychaete in Gamo Lagoon (northeast Japan) during restoration works operating in response to the 2011 Tohoku earthquake and tsunami. Daily maximum water level in the inner part of the lagoon, where the capitellid polychaete was most abundant, dropped markedly during the reconstruction of a flow-conducting levee. The maximum water level had a significant effect on maintenance of the polychaete population; sufficiently high water levels enabled dispersion of planktonic larvae, aiding rapid population recovery. Okumura et al. surveyed the coastal environment in Matsushima Bay, northeast Japan, for four years following the 2011 Tohoku tsunami. The lack of differences in nutrient concentrations or eukaryote assemblages between areas with and without aquaculture installations was considered to be a result of efficient seawater exchange, despite the presence of many small islets separating Matsushima Bay from the open ocean. It was concluded that the current aquaculture installations had no major negative impact on the environment in Matsushima Bay.

Continuing importance of archival underwater imagery for ecological assessment of offshore oil and gas installations

Using a remotely operated vehicle (ROV), Biede et al. investigated the response of deep-water benthic megafauna to the installation of a pipeline on the Angolan Margin. While density of megafauna, particularly in mid-slope regions, increased significantly three months after pipeline installation, diversity did not increase consistently. The pipeline appeared to trap organic material and anthropogenic litter, and may have enhanced available food resources locally as well as providing hard substratum. McLean et al. used ROV imagery to assess diversity and abundance of fishery target species on subsea wells and pipelines in relation to structure properties and environmental variables in tropical and temperate Australia. They also used techniques proposed by Smith et al. (2016) to estimate fish production for three species. Many species were associated with these structures, and production estimates were similar to those from other studies of artificial reefs. These data will help inform decommissioning decisions for subsea infrastructure. Sih et al. analyzed industry ROV imagery (2008-2018) at different oil and gas (O&G) structures/pipelines in the Bass Strait, Australia, and compared with fisheries-catch data from the same period. Fish/invertebrate richness, abundance, and diversity were high around O&G platforms, with a different species subset inhabiting pipelines. There was only 10% overlap between species targeted by fishers compared to O&G structures; however, grouped fisheries species data are an under-representation of true diversity. Ierodiaconou et al. reviewed ten years' worth of O&G industry ROV imagery data for wells and flowlines in the Bass Strait, Australia. Sixty-nine taxa were recorded in total, with a higher diversity on flowlines (28 taxa) than wells (19 taxa). High-spatial variability was identified across all sites. Notable protected species were recorded, including Australian fur seal (*Arctocephalus pusillus*).

Variety of techniques for monitoring subsea artificial structures

Boyle et al. used passive acoustic monitoring (PAM) to describe fish sounds in a variety of marine habitats across the Alabama Artificial Reef Zone in the Gulf of Mexico. They showed distinct spatiotemporal sound variation potentially associated with varied species composition and abundance as well as diel and seasonal influences, suggesting soundscape variability may be a consideration for management, as it can provide an acoustic cue for reef location by some fish species. Galaiduk et al. assessed regional patterns in demersal fish assemblages among subsea pipelines and natural habitats across north-west Australia using baited remote underwater video systems (BRUVs). At the regional scale, subsea pipelines showed lower diversity than natural environments, but possessed a higher abundance of piscivorous and herbivorous fish taxa, highlighting a negligible regional influence of subsea pipelines on fish communities, although these structures may be important for some fish species at the local scale. Fernandez-Betelu et al. deployed self-contained, autonomous-underwater-echolocation-click detectors (C-PODs) to investigate presence/foraging of harbor porpoise (*Phocoena phocoena*) around four unmanned oil, gas, and renewable energy installations in the Moray firth, Scotland. Porpoises were encountered on average 17 hrs/day and changed to night-time foraging behavior when the installation was present; foraging activity decreased with distance from structures, highlighting the importance of offshore installations for porpoises.

Theoretical and data-driven approaches for marine habitat assessment and ecosystem-based management

To support ecosystem-based management efforts in the Southeastern US, Steward et al. used multiple data-driven approaches to quantify the amount of seafloor covered by artificial and natural reefs. Artificial reef coverage was several orders of magnitude less than natural reef coverage. While expansive seafloor mapping and characterization efforts are still needed, these results filled critical information gaps and demonstrated an approach applicable to other regions. Pondella et al. synthesized the mechanisms of increasing fish production by maximizing ecological processes. Utilizing structural and ecological theory of artificial reef design based upon physical attributes (i.e., complexity, vertical relief, habitat heterogeneity, and spatial scale), they summarized the mechanisms used to increase secondary fish production and proposed a general theory for optimization of these variables. This theory is applicable to reef assessment and design. Nicolette et al. adapted a Net Environmental Benefit Analysis (NEBA) framework to bolster the comparative assessment (CA) process for decommissioning options of offshore O&G facilities. The NEBA-CA framework is based on integrating ecosystem-service values, site data, and extant scientific information at sites in the North Sea, Australia, Gulf of Thailand, California, Gulf of Mexico, and the Caribbean. A NEBA-CA case study performed on a North Sea offshore installation determined that full removal was the least preferable decommissioning option.

Emerging opinions and future directions

This Research Topic provided further insights into: (1) the importance of considering multiple environmental factors; (2) the scale-dependency of ecological patterns observed on and around sub-sea artificial structures; and (3) the diversity of approaches being developed to investigate impacts of human activities on the marine environment. While many studies reported that sub-sea artificial structures generally have beneficial effects on a range of marine life by providing shelter and/or enhanced food supply (Biede et al.; Fernandez-Betelu et al.; Ierodiaconou et al.; Williams et al.), observed variability in some key ecological properties may also be controlled by other environmental factors such as prevailing hydrodynamics (Hashimoto and Sato-Okoshi; Okumura et al.; Wang et al.), seafloor topography, depth, and sea surface temperature (Galaiduk et al.; Pondella et al.; Williams et al.). Several studies also highlighted that the ecological significance of artificial habitats observed at one spatial scale may become less significant when viewed at another, indicating the importance of scale-dependency when interpreting ecological patterns observed at varying spatiotemporal scales (Galaiduk et al.; Pondella et al.; Steward et al.). An increasing number of studies have also attempted to fill gaps regarding the influence of marine artificial habitats in support of implementing sustainable coastal management, including the ecosystem-based approach (Boyle et al.; Sih et al.; Steward et al.; Wang et al.). With regard to issues surrounding decommissioning, this volume proposes a wealth of approaches in an attempt to facilitate decision-making (Fernandez-Betelu et al.; Ierodiaconou et al.; McLean et al.; Nicolette et al.; Sih et al.). Overall, this Research Topic provided a renewed opportunity to better integrate emerging knowledge and thereby advance our ability to understand, predict, and manage our marine environments and resources.

Author contributions

All authors listed have made a substantial, direct, and intellectual contribution to the work, and approved it for publication.

Funding

TF was supported by Japan Science and Technology Agency (JST) Grant Number JPMJPF2110. DP was supported by California State Coastal Conservancy Grant Agreement # 19-019; COAST State Science Information Needs Program Award # COAST-SSINP-2022-02; NOAA Restoration Center Community-based Restoration Program Project Awards #2008-0073-010 and #2008-0073-046; National Fish and Wildlife Foundation Grant IDs #8006.13.040016 and # 3002.15.049578 under the Damage Assessment, Remediation, and Restoration Program (DARRP) Settlement Restoration Program Cooperative Agreement funded by National Oceanic and Atmospheric Administration Fund # NA12NMF4630196; the US Department of the Interior, Bureau of Ocean Energy Management (BOEM), Environmental Studies Program, Washington, DC, under Agreement Number M21AC00021. The views and conclusions contained in this document are those of the authors and should not be interpreted as representing the opinions or policies of the US Government, nor does mention of trade names or commercial products constitute endorsement or recommendation for use. VLGT was supported by a research fund provided by Ocean Science Consulting Ltd. VLGT declares that this study received funding from the company Ocean Science Consulting Ltd. The funder was not involved in the study design, collection, analysis, interpretation of data, the writing of this article or the decision to submit it for publication. The remaining authors declare that the research was conducted in the absence of any commercial or financial relationships that could be construed as a potential conflict of interest.

Acknowledgments

We thank all authors, reviewers, and the editorial staff of Frontiers in Marine Science for their support in producing this Special Issue.

Conflict of interest

VLGT was employed by the company Ocean Science Consulting Ltd.

The remaining authors declare that the research was conducted in the absence of any commercial or financial relationships that could be construed as a potential conflict of interest.

Publisher's note

References

Duarte, C. M., Agusti, S., Barbier, E., Britten, G. L., Castilla, J. C., Gattuso, J.-P., et al. (2020). Rebuilding marine life. *Nature* 580, 39–51. doi: 10.1038/s41586-020-2146-7

FAO (2020) *Global forest resources assessment 2020: Main report. Rome*. Available at: https://doi.org/10.4060/ca9825en.

FAO (2022). *The state of world fisheries and aquaculture 2022. towards blue transformation.* (Rome: FAO). Available at: https://doi.org/10.4060/cc0461en.

Filbee-Dexter, K., and Wernberg, T. (2018). Rise of turfs: A new battlefront for globally declining kelp forests. *Bioscience* 68, 64–76. doi: 10.1093/biosci/bix147

Halpern, B. S., Frazier, M., Afflerbach, J., Lowndes, J. S., Micheli, F., O'Hara, C., et al. (2019). Recent pace of change in human impact on the world's ocean. *Sci. Rep.* 9 (1), 11609. doi: 10.1038/s41598-019-47201-9

Hoegh-Guldberg, O., and Bruno, J. F. (2010). The impact of climate change on the world's marine ecosystems. *Science* 328, 1523–1528. doi: 10.1126/science.1189930

McCauley, D. J., Pinsky, M. L., Palumbi, S. R., Estes, J. A., Joyce, F. H., and Warner, R. R. (2015). Marine defaunation: Animal loss in the global ocean. *Science* 347, 1255641. doi: 10.1126/science.1255641

Smith, J. A., Lowr, M. B., Champion, C., and Suthers, I. M. (2016). A designed artificial reef is among the most productive marine fish habitats: New metrics to address 'production versus attraction. *Mar. Biol.* 163, 1–8. doi: 10.1007/s00227-016-2967-y

Souter, D., Planes, S., Wicquart, J., Logan, M., Obura, D., Staub, F., et al. (2021). Status of coral reefs of the world: 2020 report. Global Coral Reef Monitoring Network (GCRMN)/ International Coral Reef Initiative (ICRI). Available at: https://gcrmn.net/2020-report/.

Waycott, M., Duarte, C. M., Carruthers, T. J., Orth, R. J., Dennison, W. C., Olyarnik, S., et al. (2009). Accelerating loss of seagrasses across the globe threatens coastal ecosystems. *PNAS* 106 (30), 12377–12381. doi: 10.1073/pnas.0905620106

frontiers in Marine Science

ORIGINAL RESEARCH
published: 16 March 2022
doi: 10.3389/fmars.2022.829557

Structural and Functional Improvements of Coastal Ecosystem Based on Artificial Oyster Reef Construction in the Bohai Sea, China

Xu Wang[1,2,3,4], *Jie Feng*[2,3,4], *Chenggang Lin*[2,3,4]*, *Hui Liu*[5], *Muyan Chen*[1] and *Yunling Zhang*[6]

[1] College of Fisheries, Ocean University of China, Qingdao, China, [2] CAS Key Laboratory of Marine Ecology and Environmental Sciences, Institute of Oceanology, Chinese Academy of Sciences, Qingdao, China, [3] CAS Engineering Laboratory for Marine Ranching, Institute of Oceanology, Chinese Academy of Sciences, Qingdao, China, [4] Laboratory for Marine Ecology and Environmental Science, Qingdao National Laboratory for Marine Science and Technology, Qingdao, China, [5] Key Laboratory of Coastal Zone Environmental Processes and Ecological Remediation, Yantai Institute of Coastal Zone Research, Chinese Academy of Sciences, Yantai, China, [6] Hebei Provincial Technology Innovation Center for Coastal Ecology Rehabilitation, Tangshan Marine Ranching Co., Ltd., Tangshan, China

OPEN ACCESS

Edited by:
Victoria Louise Georgia Todd,
Ocean Science Consulting Ltd.,
United Kingdom

Reviewed by:
Ashley M. Fowler,
New South Wales Department of Primary Industries Fisheries,
Australia
Rodrigo Riera,
University of Las Palmas de Gran Canaria, Spain

***Correspondence:**
Chenggang Lin
Linchenggang@qdio.ac.cn

Specialty section:
This article was submitted to Marine Ecosystem Ecology, a section of the journal Frontiers in Marine Science

Received: 06 December 2021
Accepted: 07 February 2022
Published: 16 March 2022

Citation:
Wang X, Feng J, Lin C, Liu H, Chen M and Zhang Y (2022) Structural and Functional Improvements of Coastal Ecosystem Based on Artificial Oyster Reef Construction in the Bohai Sea, China. Front. Mar. Sci. 9:829557. doi: 10.3389/fmars.2022.829557

Oyster reefs are gaining more and more attention in marine ranching and coastal ecosystem restoration, but tremendous knowledge gaps still exist. In this study, we developed trophic models for the established artificial oyster reef (EAOR), newly deployed artificial oyster reef (NAOR), and non-reef bare substratum (NBS) ecosystems located in the Bay of Xiangyun, Bohai Sea, China, to assess the benefits of artificial oyster reef construction and to characterize the unique role of these reefs in coastal management. The analysis showed that the EAOR and NAOR ecosystems were similar to each other, but both were greatly different than the NBS ecosystem. Reefs showed greater "ecological size" and stronger top-down effects compared to the bare area. The ecosystems were not yet mature, but the EAOR and NAOR ecosystems had more complicated trophic relationships, greater potential to withstand perturbations, and higher biological carrying capacities of commercial organisms compared to the NBS ecosystem. These results demonstrated that artificial oyster reef construction resulted in great advantages to the ecosystem. For example, oysters became the structuring functional group and played a critical role in the trophic structure of the reef areas. The phytoplankton/detritus-oysters-carnivorous macrobenthos pathway developed and became dominant in these areas, thereby contributing to highly efficient secondary production. The ratios of total primary production/total respiration were < 1, indicating that the reef ecosystems responded effectively to nutrient inputs from adjacent ecosystems. We speculate that water exchange might be a critical factor influencing the maintenance of the system. Long-term monitoring of the EAOR and NAOR should be implemented for oyster protection and to assess the need to manipulate carnivorous macrobenthos to keep the systems in balance. Results of this study could benefit the restoration, exploitation, and management of oyster reefs. Further studies should take the adjacent ecosystems and anthropogenic activities into account.

Keywords: artificial oyster reefs, Ecopath model, ecological network analysis, comparative analysis, coastal ecological restoration, Bohai Sea

INTRODUCTION

Oyster reefs, which are formed by clustering oysters, are widely distributed in temperate and subtropical estuaries and coastal areas. Oyster reefs provide the basic structure for the whole ecosystem and support various crucial ecological functions, thus serving as the "ecological engineer" in shallow waters (Gutiérrez et al., 2003; Chowdhury et al., 2021). Filter-feeding oysters ingest suspended detritus and phytoplankton, which can improve water quality and transparency and inhibit eutrophication (Hoellein et al., 2015). The water column and sediment are coupled through the feeding and excreting processes of oysters, further enhancing the ecosystem's denitrification and carbon sequestration functions (Miller et al., 2009; Hoellein et al., 2015). The complex three-dimensional structure of oyster reefs provides habitats for a variety of marine organisms, thus contributing to high biodiversity and complex food webs and increasing fishery resources (Zu Ermgassen et al., 2015; Gain et al., 2016). Furthermore, oyster reefs can act as natural surf shields to buffer wave erosion and protect the coastline (Piazza et al., 2005; Borsje et al., 2011). However, due to destructive fishing and habitat degeneration, more than 85% of natural oyster reefs worldwide have declined in the last 100 years, and $< 10\%$ of historical abundance remains in most bays (Beck et al., 2011). The loss of oyster reefs has caused serious desertification of the seabed, and it is crucial to advance the restoration of oyster reefs (Coen et al., 2007).

Over the last four decades, artificial structures have been developed and deployed in subtidal zones around the world as efficient alternatives to declining natural habitats (Baine, 2001; Layman and Allgeier, 2020). Studies on artificial reefs showed that well-designed artificial reefs could effectively enhance the biomass and biodiversity of ecosystems and provide suitable habitats for organisms in coastal areas, indicating that such restoration approaches are advisable (Lee et al., 2018; Cresson et al., 2019; Wu et al., 2019). When deployed in substrate-limited places, artificial structures would become adherence sites for oyster larvae and thereby benefit oyster reef restoration (Theuerkauf et al., 2014; Walles et al., 2016). Along the coastlines of North America, Australia, and Europe, specially designed artificial structures have been used to promote the preservation and restoration of oyster reefs (La Peyre et al., 2014; Rodriguez-Perez et al., 2019; Gillies et al., 2020). Successful artificial reefs include the Half Moon Reef in Texas' Matagorda Bay, Oyster Castle in Long Island, New York, and the concrete modular reef in the Rappahannock River, Virginia (La Peyre et al., 2014). Some restoration work has also been conducted from northern to southern China in recent years, including Dashentang (Tianjin), Xiangyun Bay (Hebei), Laizhou Bay (Shandong), Xiaomiaohong (Jiangsu), Yangtze River Estuary (Shanghai), and Houhai Bay (Hongkong) (Quan et al., 2017; Liu et al., 2018; Xu et al., 2019; Yang, 2019). Studies have mainly focused on the oyster population status, trophic interactions and enhancement of biodiversity and fishery resources (Powers et al., 2009; Blomberg et al., 2017; Yang, 2019). To date, analyses of the whole ecosystem based on trophic models are rare (Xu et al., 2019; Samonte et al., 2020).

The Bohai Sea is the only semi-closed inland sea in China. It covers an area of 77,000 km^2, with an average depth of < 20 m. Because of its fertile water and abundant prey, the Bohai Sea once was an important habitat for spawning, feeding, and migrating of various organisms, and historically it has supported abundant fishery resources (Jin and Deng, 2000). Massive Holocene oyster reefs and shell ridges once existed along the northwest coast of the Bohai Sea (Yue et al., 2012), but now only patches of oyster reefs distribute in estuaries and shoals. As urbanization progressed, the population in the Bohai Sea coastal region increased dramatically, leading to increases in destructive fishing practices and anthropogenic disturbances (Jin and Deng, 2000). The whole ecosystem of the Bohai Sea changed greatly, and desertification of most coastal seabeds has been occurring since the late 1980s (Jin et al., 2013; Rahman et al., 2019).

To mitigate the current ecosystem decline, restoration and construction of artificial oyster reefs began in Xiangyun Bay in 2011. This bay is located at the confluence of Luan River and Bohai Bay. By the end of 2018, 930,000 m^3 of various kinds of artificial reefs had been deployed, and two artificial oyster reef areas of 200 ha and 57 ha had been successively been constructed. Persistent investigation and monitoring of these artificial oyster reefs showed that significant positive ecological effects were achieved, including a more complex community and higher productivity (Yang, 2018). Combined with bottom seeding of the sea cucumber Apostichopus japonicas and recreational fishing, considerable economic benefits were generated (unpublished commercial data). Previous studies focused on the effects of the artificial oyster reefs on the environment and fishery resources and seasonal differences of the ecosystem (Yang, 2019; Xu et al., 2020). However, a holistic comparison analysis of ecosystem properties has not yet been conducted, and the role of artificial oyster reefs in coastal ecological restoration has not been specified.

Ecological trophic models provide a means to conduct studies at the ecosystem level and thereby deepen our understanding of the ecosystem. The Ecopath with Ecosim (EwE) model is one of the most well-accepted models among those currently available. The Ecopath module is a mass-balanced model based on ecosystem approaches, and it is usually applied to quantitative analysis of aquatic ecosystems (Christensen and Walters, 2004). Its first application was for a coral reef ecosystem at French Frigate Shoals by Polovina (1984). Since then, it has been used for estuaries, lagoons, continent shelfs, lakes, and artificial reefs (Darwall et al., 2010; Blomberg and Montagna, 2014; Heymans and Tomczak, 2016; Wu et al., 2016; Xu et al., 2019). In application, species are grouped in terms of their ecological niches, and all functional groups should basically cover the whole process of energy flow in the ecosystem. The output indicators can be used to describe the energy flow, ecological interactions, stability, and maturity of the ecosystem, and the biological carrying capacities of each group can be calculated. Thus, the results can greatly benefit ecosystem-based management (Heymans et al., 2016).

In this study, we developed three Ecopath models for the established artificial oyster reef (EAOR), newly deployed artificial oyster reef (NAOR), and non-reef bare substratum (NBS) ecosystems based on surveys conducted during 2019–2020 in Xiangyun Bay. Our aims were to: (1) Identify the structural distinctions between the reef and non-reef ecosystems to clarify the benefits of artificial oyster reef construction; (2) summarize the main properties of the artificial oyster reefs and demonstrate their unique role in coastal management; and (3) propose practical strategies for optimizing and managing oyster reef restoration and construction.

MATERIALS AND METHODS

Study Area

The study area is located in Xiangyun Bay, Bohai Sea, China (39°10′N, 119°00′E) (**Figure 1**). The transmeridional semi-diurnal tides flow back and forth from Luan River Estuary to the coast of the Caofeidian district, with an average flow velocity of 0.28~0.37 $m \cdot s^{-1}$ (Sun and Zhang, 2018).

The EAOR ecosystem was constructed between 2011 and 2017 and forms an area of about 200 ha. It is located nearshore, with an average depth of 6.50 m and temperature of 13.34°C during the study year. Tremendous quantities of oysters and macroalgae coexist on the hard substrates, forming a stable kelp-shellfish-reef ecosystem (**Figure 2**). However, it lies next to the channel of Jingtang Port and is susceptible to dredging disturbances [Video data provided by Tangshan Marine Ranching Co., Ltd. (Hebei, China)].

The NAOR ecosystem was constructed between December, 2017 and June, 2018 and covers an area of 57 ha. It is located to the southwest of the EAOR, with a deeper depth of 8.22 m and average temperature of 13.22°C during the study year. The NAOR is more open and is characterized by entire submerged reefs with no macroalgae (**Figure 2**). Its further location from the coast makes it difficult to regulate, and it is more disturbed by navigation issues and illegal fishing.

The NBS ecosystem is located further south and lacks reefs. It had an average depth of 10.44 m and temperature of 12.94°C during the study year. Although the site is deeper than the other sites, the characteristics of the NBS ecosystem are similar to those of the EAOR and NAOR areas before the ecosystems were constructed, and it is located far away from the influence of the NAOR ecosystem. It is subject to intense fishery activities and its species composition has been unchangeable in recent 10 years (Sun and Zhang, 2018). Therefore, we viewed the NBS ecosystem as the background ecosystem before the addition of artificial oyster reefs, and it also represented the current natural marine ecosystem in Xiangyun Bay (Sun and Zhang, 2018; **Figure 2**).

Trophic Model

The Ecopath model is commonly used to quantitatively estimate the mass transfer and energy flow in an ecosystem (Christensen and Walters, 2004; Christensen et al., 2005). According to thermodynamic theories, the energy input and output of a certain biological functional group should be in balance, meaning that

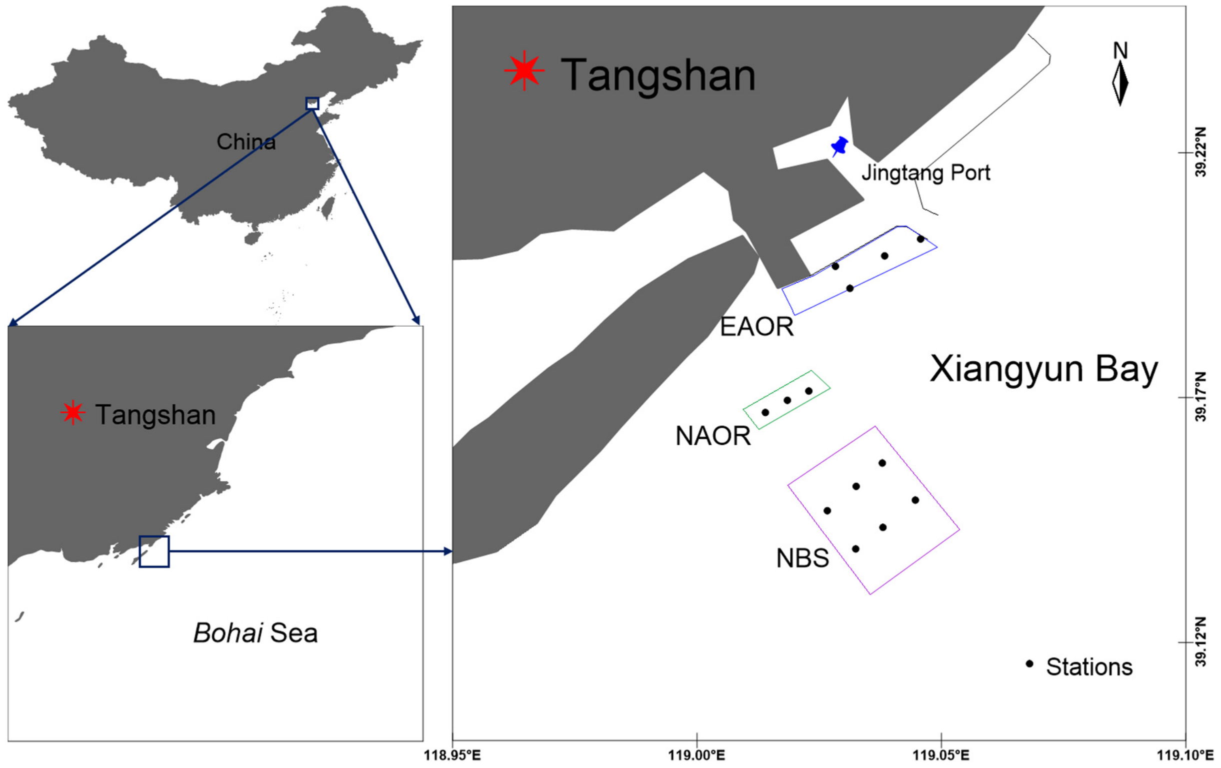

FIGURE 1 | Geographic location and sampling sites of EAOR, NAOR and NBS ecosystems in the Bay of Xiangyun, Bohai Sea, China.

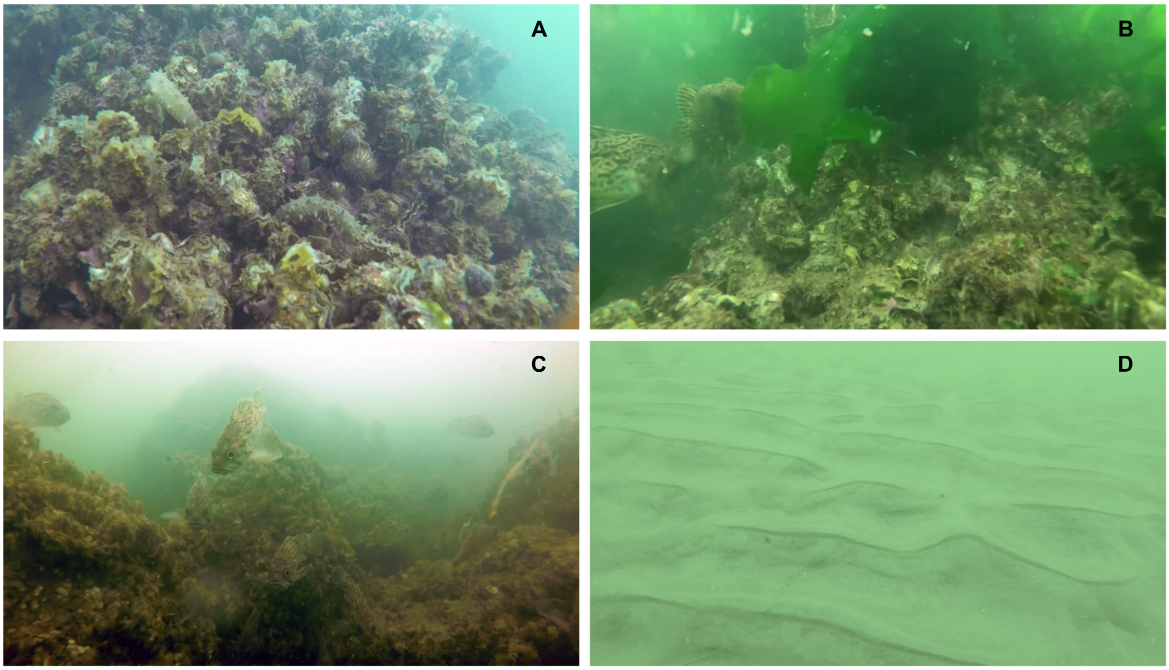

FIGURE 2 | Benthic environment of EAOR **(A,B)**, NAOR **(C)** and NBS **(D)** ecosystems.

productivity equals the sum of mortalities. We used another equation to determine the inner mass balance of the group; the consumption (Q) of each group was equal to the sum of the production (P), respiration (R_i), and unassimilated food (U_i) of the group. The equations are written as follows:

$$B_i \cdot \left(\frac{P}{B}\right)_i \cdot EE_i - \sum_j \left(B_j \times \left(\frac{Q}{B}\right)_j \times DC_{ij}\right) - Y_i - BA_i - E_i = 0 \quad (1)$$

$$B_i \times \left(\frac{Q}{B}\right)_i = B_i \times \left(\frac{P}{B}\right)_i + R_i + U_i \quad (2)$$

where B_i is the biomass of functional group i, $(P/B)_i$ is the production ratio, $(Q/B)_i$ is the consumption ratio, EE_i is the ecotrophic efficiency (the proportion of the production utilized in the system), DC_{ij} is the proportion of prey i in the diet of predator j, Y_i is the fishery mortality, BA_i is the biomass accumulation rate, and E_i is the net migration rate. In the process of parameter input, B_i, $(P/B)_i$, $(Q/B)_i$, and DC_{ij} were required. If one of the first three was missing, the corresponding EE value could be designated. Besides, E_i and catches were also required.

Data Sources

Biological wet weight unit ($t \cdot km^{-2}$) was used in this study to represent the system energy flow. The biomass (B) of each functional group was obtained from the results of ecological surveys conducted during from 2019 to 2020 (Summer: June 2019, Autumn: September 2019, Winter: December 2019, Spring: March 2020). Sampling methods for nekton included trap nets, gill nets, and small trawl nets around reef areas. The biomass of fishes and cephalopods was estimated predominantly from trap nets and gill nets, while trawl nets and underwater videos were used for correction. Fish were collected using the trap nets (section × length × width × height: 5 × 8 m × 30 cm × 20 cm; mesh size: 2 cm) for 72 h each time. Fish biomass was calculated using the following equation (modified from Li et al., 2020, 2021):

$$B = (C \times d)/(v \times t \times a \times q \times h) \quad (3)$$

where B is the fish biomass ($g \cdot m^{-2}$), C is the total catch weight per net (g), v is velocity (here, 0.30 $m \cdot s^{-1}$; Sun and Zhang, 2018), *t* is the effective working time (6 h/d × 3 d), a is the efficient area of the cage (here, 4.0 m^2), and q is the capture efficiency (0.5; Li et al., 2020), h is the height of the nets (0.20 m here), d is the mean water depth (6.50, 8.22 and 10.44 m for EAOR, NAOR and NBS, respectively). When nekton was only caught by trap nets or gill nets, the d-value was divided by 2 (detailed calculation can be seen in **Supplementary Material**).

The biomass and abundance of macrobenthos (the whelks, sea cucumbers, and sea stars) were estimated by SCUBA grasping and videos combined with net operations. Bivalves, epizoites, and macroalgae were scraped from reefs using 0.5 × 0.5 m quadrats by SCUBA diving, with three to six replicates evenly distributed each season. Meiobenthos were sampled using a box sampler (0.05 m^2) at each station. Zooplankton samples were obtained by vertical towing using plankton nets with mesh size of 169 μm. Phytoplankton biomass was calculated in terms of chlorophyll a measured according to standard procedures (Parsons et al., 1984). Detritus was obtained as the organic matter in the water column by filtering 1 L of subsurface and bottom seawater through a mesh size of 77 μm. Physical factors were measured *in situ* using a YSI meter (EXO2, Yellow Springs, OH, United States). The survey design was referred to Xu et al. (2020).

The P/B and Q/B ratios of fishes were calculated using empirical formulas (Christensen and Walters, 2004; Christensen et al., 2005), and the parameters used were from previous reports (Tang et al., 2007; Ouyang and Guo, 2010). The P/B ratios of invertebrates were estimated based on formulas in Tumbiolo and Downing (1994) and Q/B ratios were mainly estimated from previously reported laboratory culture experiments (Xu and Ma, 2009; Zhu et al., 2016; Lv et al., 2018) or expert consultation (**Supplementary Tables 3–5**). The food composition matrix of the functional groups was derived in part from stomach content analysis of sampled fishes and also from literature reports from nearby areas (Wei and Jiang, 1992; Deng et al., 1997; Yang, 2001a,b; Zhang, 2018) and www.fishbase.de. The catch data of EAOR came from the statistics of the fishery company Tangshan Marine Ranching Co., Ltd. (Hebei, China).

Model Balancing and Uncertainty

Ecopath models were balanced followed Heymans et al. (2016). First, the EE of each functional group was set to ≤ 1, meaning that the proportion of the production that was utilized in the ecosystem could not exceed 1. Second, the gross food conversion efficiency (GE = P/Q, acquired through P/B divided by Q/B) values of most functional groups were set to fall between 0.1 and 0.3. For some fast-growing species, they have higher P/Q values. The Production/Respiration (P/R) ratio, which expresses the fate of assimilated food, could not exceed 1, and the group with higher turnover has a greater Respiration/Biomass (R/B) value, which indicates the "metabolic activity level" of a group (Darwall et al., 2010).

The pre-balanced diagnosis (Link, 2010) was used to identify issues in the model structure and in data quality before balancing the network model. The uncertainty of Ecopath model input parameters was analyzed using the pedigree index (Christensen et al., 2005). For B, P/B, Q/B, and diet composition (DC) values, the uncertainty indices were assigned in terms of data resources. Summarizing the uncertainties of all functional groups, pedigree index could evaluate the overall quality of the Ecopath model for a particular ecosystem.

Ecological Indices

Ecological network analysis was performed directly within the EwE software using the network analysis plugin (Christensen and Walters, 2004). A set of ecological indices was employed to describe the structure and function of the ecosystem. The total system throughput (TST), total consumption (TQ), total exports (TEx), total respiration (TR), and flows into detritus (FD), as well as the total primary production (TPP) and total biomass (TB), characterize the overall activity and the size of the ecosystem (Latham, 2006; Ortiz et al., 2015). The TPP/TR and TPP/TB ratios are the most important indicators of the stability and maturity of the ecosystem (Odum, 1969; Christensen, 1995). Finn's cycling index (FCI), the connectance index (CI), and the system omnivory index (SOI) together with the Finn's mean path length (FMPL) represent stress and structural complexity of the ecosystem (Finn, 1976; Christensen and Walters, 2004; Libralato, 2013). Ascendency (A) indicates the degree of development and maturity of an ecosystem, while overhead (O) represents the capacity of an ecosystem to withstand perturbations (Ulanowicz, 1986; Christensen, 1995).

The non-integral trophic level (TL) of each functional group was calculated from the food web matrix. The mean TL (mTL) reflects the structure of the functional groups, and it can be calculated by the weighted average TL for functional groups with TL ≥ 2 (Pauly et al., 1998). The total mean transfer efficiency (mTE) was calculated as the geometric mean of TEs of flow transferred from each discrete TL to the next one starting from TL II (Christensen et al., 2005).

Mixed trophic impact (MTI) analysis provides quantification of direct (predation) and indirect (competition) feeding interactions between compartments in an ecosystem (Ulanowicz and Puccia, 1990). The negative and positive elements of MTI enable estimation of top-down and bottom-up effects, respectively (Libralato et al., 2006). The overall impact (ε_i) of each compartment characterizes its functional role in the system and is useful for identifying key functional groups (Libralato et al., 2006). Key functional groups are distinguished as keystone and structuring groups according to their biomass (Power et al., 1996). Keystone groups have high overall effect but low biomass proportion, while structuring groups have both high overall trophic effect and high biomass proportion (Heymans et al., 2011). The keystoneness index (KS_i) and dominance index (KD_i) were quantified to identify the keystone functional groups (i.e., with KS ≥ 0) and structuring functional groups (i.e., with KD ≥ –0.7) in the three ecosystems following Libralato et al. (2006) and Heymans et al. (2011):

$$KS_i = \log[\varepsilon_i \cdot (1 - p_i)] \tag{4}$$

$$KD_i = \log[\varepsilon_i \cdot p_i] \tag{5}$$

where ε_i represents the overall impact of group i on the other groups (excluding itself), and p_i represents the biomass proportion of group i.

We also estimated the biological carrying capacity (BCC) of the ecologically or economically important functional groups, which is defined as the maximum biomass that could be sustained indefinitely without significantly changing the major energy fluxes or structure of the ecosystem (Jiang and Gibbs, 2005).

RESULTS

In terms of species composition and their ecological traits, we identified 23, 23, and 18 functional groups for the EAOR, NAOR, and NBS ecosystems, respectively (**Table 1** and **Supplementary Tables 6–8**). Commercially or ecologically important species (e.g., black rockfish, whelks, sea cucumbers, et.) were treated as separate functional groups in the models. For commercially important species, they either hold massive biomass or might act as joints in the trophic cascade effect exerted by fishery. Pedigree index values for the EAOR (0.596), NAOR (0.581), and NBS (0.515) ecosystems were within a reasonable range,

TABLE 1 | Biomass (B, t·km^{-2}·yr^{-1}), Ecotrophic Efficiency (EE) and Trophic level (TL) of each group in the three models (EAOR, NAOR, and NBS ecosystems).

EAOR				NAOR				NBS			
Group name	**TL**	**B**	**EE**	**Group name**	**TL**	**B**	**EE**	**Group name**	**TL**	**B**	**EE**
Pelagic fishes	2.896	0.155	0.944	Pelagic fishes	2.838	0.540	0.647	Pelagic fishes	2.903	0.204	0.148
Black rockfish	3.865	1.671	0.556	Sea bass	3.955	0.063	0.000	Benthic fishes	3.889	0.130	0.703
Greenling	3.574	0.395	0.531	Black rockfish	3.950	2.939	0.484	Gobiidae	3.696	0.365	0.653
Sea bass	3.929	0.051	0.000	Greenling	3.710	0.274	0.239	Flatfishes	3.545	0.105	0.780
Gobiidae	3.548	0.709	0.989	*Platycephalus indicus*	3.869	0.127	0.108	Cephalopods	3.985	0.142	0.785
Filefish	3.274	0.869	0.954	Gobiidae	3.608	0.718	0.865	Large crabs	3.600	0.488	0.000
Other benthic fishes	3.426	0.830	0.941	Other benthic fishes	3.635	0.597	0.988	Mantis shrimp	3.462	0.350	0.118
Flatfishes	3.371	0.286	0.674	Flatfishes	3.533	0.246	0.910	Whelk	3.147	0.611	0.000
Cephalopods	3.848	0.814	0.962	Cephalopods	3.945	0.369	0.822	Sea star	3.140	1.060	0.000
Mantis shrimp	3.307	0.341	0.956	Large crabs	3.243	1.631	0.451	*Glossaulax didyma*	3.083	0.332	0.695
Large crabs	3.234	3.849	0.499	Whelk	3.076	27.980	0.007	Luidia	2.971	0.212	0.000
Whelk	3.053	45.360	0.087	Sea star	3.052	22.345	0.005	Bivalves	2.076	4.570	0.936
Sea star	2.999	4.010	0.000	Mantis shrimp	3.372	0.150	0.925	Other macrobenthos	2.123	2.240	0.766
Sea cucumber	2.016	75.311	0.000	Oyster	2.073	171.707	0.572	Small crustaceans	3.089	2.134	0.950
Oyster	2.050	198.950	0.571	Mussel	2.060	30.785	0.655	Meiobenthos	2.064	19.844	0.507
Small crustaceans	2.843	6.149	0.950	Epizoite	2.166	27.211	0.784	Zooplankton	2.053	5.200	0.244
Epizoite	2.111	26.925	0.849	Small crustaceans	2.962	3.946	0.950	Phytoplankton	1.000	16.486	0.335
Other macrobenthos	2.055	1.960	0.709	Other macrobenthos	2.120	0.892	0.986	Detritus	1.000	171.578	0.399
Meiobenthos	2.092	12.047	0.985	Meiobenthos	2.094	15.306	0.873				
Zooplankton	2.087	5.670	0.821	Sea cucumber	2.045	51.962	0.000				
Macroalgae	1.000	75.420	0.252	Zooplankton	2.053	6.150	0.732				
Phytoplankton	1.000	9.720	0.964	Phytoplankton	1.000	13.979	0.956				
Detritus	1.000	86.263	0.898	Detritus	1.000	110.154	0.906				

indicating that input data for the three models were of good quality (Morissette, 2007).

Biomass and Energy Flow

Total biomass (TB) values (except for detritus) of the EAOR, NAOR, and NBS ecosystems were 471.492, 379.915, and 54.474 t·km^{-2}·year^{-1}, respectively (**Table 2**). For all three ecosystems, biomass was mainly concentrated in TL II (**Figure 3**). Oysters, epizoites, and sea cucumbers constituted the major component of the biomass of TL II in the EAOR and NAOR ecosystems. While in the NBS ecosystem, because of the lower biomass in TL II (57.96%), the biomass ratio of TL I was relatively higher (30.27%). The mean EE values of the EAOR, NAOR, and NBS ecosystems were 0.497, 0.572, and 0.417 apart. The EEs of different functional groups varied greatly (**Table 2**). In the EAOR and NAOR areas, the high EE value groups were mainly prey groups in medium and low TLs, whereas the EE values for top predators and macroinvertebrate groups were rather low. But most functional groups in the NBS ecosystem were quite underutilized.

For all three models, the system energy flow was mainly concentrated in TLs I and II, which accounted for over 90% of TST (**Figure 3**). Particularly, in the NBS area, the energy flow in TL I reached more than 70% of the system. The fraction of total energy flew from detritus to TL II was greater than that from primary producers in all three models and increased in sequence as EAOR > NAOR > NBS (**Table 2**). The holistic mTE showed that the EAOR system was more efficient than the NBS and NAOR ecosystems. The mTE originating from detritus (mTEd) exceeded that from primary production (mTEpp) in all three systems (**Table 2**).

In the EAOR ecosystem, we identified four distinctive trophic pathways based on the ecological niches and trophic interactions (**Figure 4**): (1) From macroalgae to herbivorous epizoites and macrobenthos, which were further mainly consumed by euryphagous fishes; (2) from phytoplankton and detritus to zooplankton or meiobenthos; the materials were used by small shrimps/fishes and finally flowed to top nekton predators; (3) phytoplankton and detritus, which were mostly filtered by the massive numbers of bivalves, which then were consumed by carnivorous macrobenthos such as whelks, sea stars, and large crabs; and (4) from detritus to sea cucumbers, which mainly ended to fishery. We identified the latter three pathways in the NAOR ecosystem; it was missing the macroalgae chain. The NBS system lacked sea cucumbers, and only pathways two and three were detected. However, the bivalve pathway was quite weak compared with the two reef ecosystems because of the small number of bivalves present.

Ecological Network Analysis

Table 2 provides aggregated summary statistics and indicators of network analysis for each system. The TSTs estimated for the EAOR, NAOR, and NBS ecosystems were 12,282.800, 11,086.120, and 4848.713 t·km^{-2}·year^{-1}, respectively. Differences in TST and its four distributions illustrated larger size and better energy

TABLE 2 | Ecological indicators (statistics and flows, ecosystem maturity status and trophic indices) estimated by the Ecopath models of EAOR, NAOR, and NBS ecosystems.

Indicators	Acronym	EAOR	NAOR	NBS	Units
Statistics and flows					
Total system throughput	TST	12282.80	11086.12	4828.71	$t \cdot km^2 \cdot yr^{-1}$
Total production	TP	3387.68	3041.47	2065.29	$t \cdot km^2 \cdot yr^{-1}$
Total biomass	TB	471.49	379.92	54.47	$t \cdot km^2 \cdot yr^{-1}$
Total consumption/TST	TQ/TST	49.52	52.31	29.29	%
Total exports/TST	Ex/TST	2.72	2.29	21.63	%
Flows to detritus/TST	FD/TST	25.91	24.46	36.02	%
Total respiration/TST	TR/TST	21.84	20.94	13.05	%
Total production/TST	TP/TST	0.276	0.274	0.428	–
Total biomass/TST	TB/TST	0.038	0.034	0.011	–
Ecosystem maturity status					
Primary production/total respiration	PP/R	0.748	0.691	2.657	–
Primary production/total biomass	PP/B	4.257	4.223	30.734	–
Finn's cycling index	FCI	19.81	20.51	11.81	%
Finn's mean path length	FMPL	4.071	4.305	2.883	–
System omnivory index	SOI	0.161	0.150	0.130	–
Connectance index	CI	0.240	0.242	0.247	–
Ascendency/capacity	A/C	26.76	24.87	31.87	%
Overhead/capacity	O/C	73.24	75.13	68.13	%
Trophic indices					
Mean transfer efficiency	mTE	9.16	6.94	7.57	%
mTE from primary production	mTEpp	8.21	5.48	6.16	%
mTE from detritus	mTEd	9.57	7.70	8.42	%
Proportion of total flow from detritus	PFFD	62.28	59.59	52.38	%
Proportion of total flow from primary productors	PFFPP	37.72	40.41	47.62	%
Mean trophic level of the community	MTL	2.205	2.227	2.197	–
Mean ecotrophic efficiency	mEE	0.497	0.572	0.417	–

utilization in the EAOR and NAOR systems than in the NBS area. The TB/TST ratio in the three models showed the same trend (**Table 2**).

In the EAOR and NAOR systems, the TPP/TR ratios were < 1 (0.748 and 0.691, respectively), and the TPP/TB ratios were 4.257 and 4.223 (**Table 2**). In the NBS area, the TPP exceeded TR (2.657), and the PP/TB ratio was 30.734. The FCI and SOI displayed increasing tendencies in the order of EAOR > NAOR > NBS. However, the opposite trend was observed for the CI.

The development capacity (C) of the three models was 57,214, 54,175, and 16,675 flowbits in the EAOR, NAOR, and NBS ecosystems, respectively. The A/C and O/C ratios were 26.76 and 73.24% in the EAOR, 24.87 and 75.13% in the NAOR, and 31.87 and 68.13% in the NBS ecosystems (**Table 2**).

Mixed Trophic Impact and Key Functional Groups

Figure 5 shows the ε of each functional group in the three models determined based on the results of MTI analysis. In the EAOR ecosystem, cephalopods (0.832) and oysters (0.749) had the greatest ε on the ecosystem (**Table 3**), whereas pelagic fishes (0.072) and sea bass (0.042) had relatively low impacts. Cephalopods group had the highest KS value (–0.081) and thus was identified as the keystone functional group of the system. Oysters had the greatest KD value (–0.501) and acted as the structuring functional group of the system (**Table 3**).

In the NAOR system, other benthic fishes (1.203), cephalopods (0.946), and oysters (0.919) had the top three ε values. Sea bass (0.063), greenling (0.085), the fish *Platycephalus indicus* (0.075), and other macrobenthos (0.050) had relatively lower impacts on the whole system. Other benthic fishes and cephalopod groups were identified as the keystone groups of the system (KS values of 0.080 and –0.025, respectively). Oysters group with KD of –0.382 was recognized as the structuring group of the ecosystem (**Table 3**).

In the NBS system, mantis shrimp had the greatest total mixed ε value of 1.176. With a KS value of 0.067, it was regarded as the keystone group of the system. Large crabs (0.741) and bivalves (0.790) also had high ε values, but they were not identified as keystone groups. Phytoplankton with a KD of –0.677 was the structuring group of the ecosystem. Pelagic fishes (0.061) and flatfishes (0.093) had the lowest ε values in this ecosystem (**Table 3**).

Biological Carrying Capacities

According to the precondition of maintaining the balance and stability of the current marine ecosystems, the biomass of

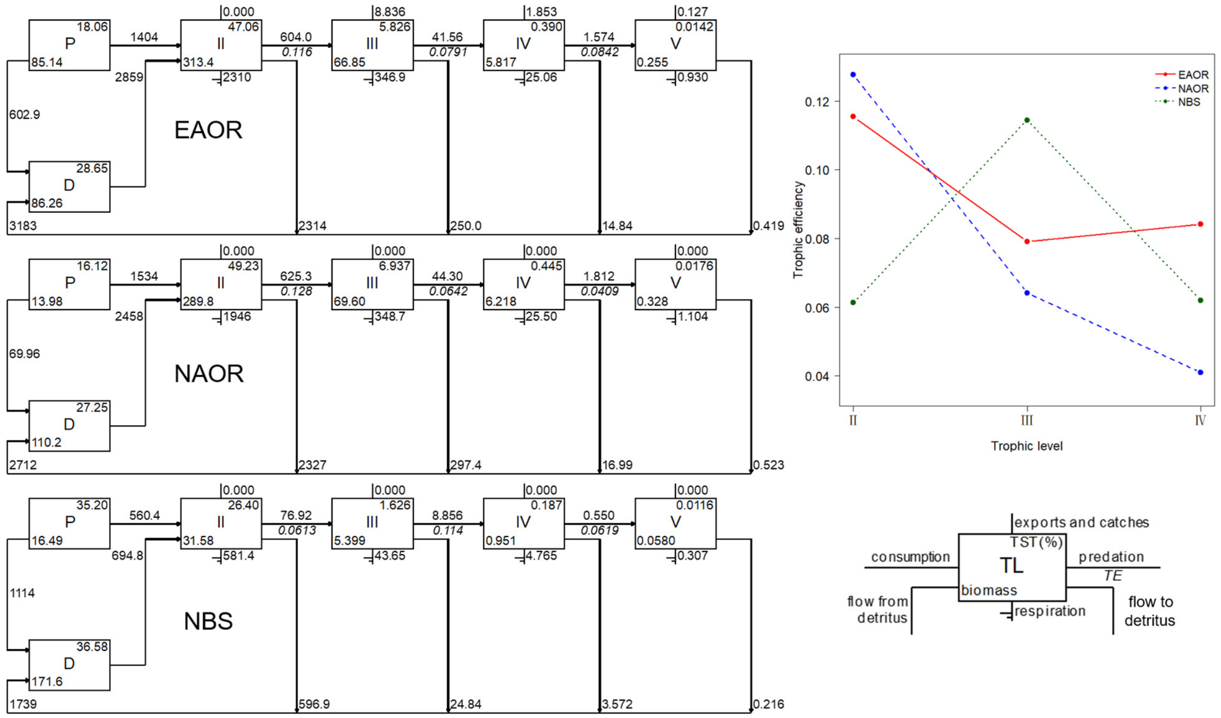

FIGURE 3 | Flow diagrams **(left)** and transfer efficiencies **(upper right)** between discrete trophic levels for the three models (EAOR, NAOR and NBS ecosystems).

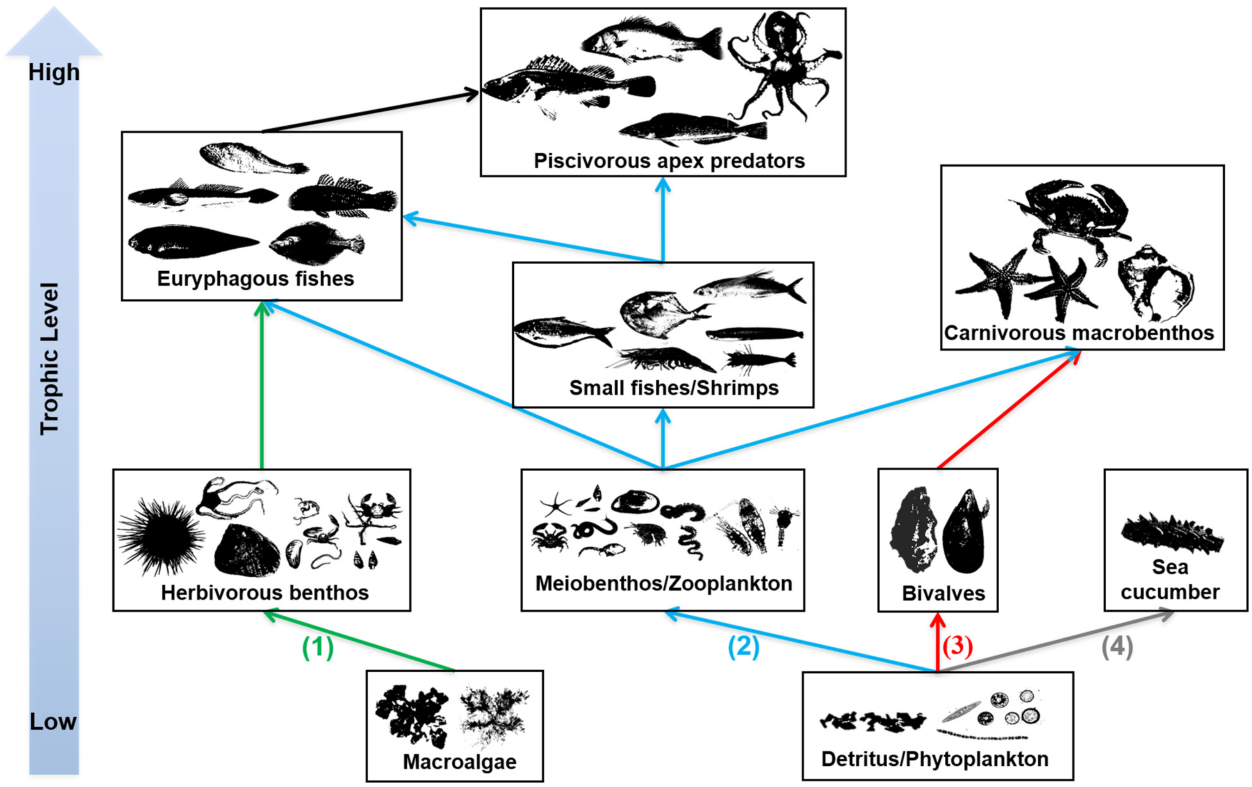

FIGURE 4 | Trophic pathways in EAOR ecosystem [(1)–(4)], NEOR ecosystem [(2)–(4)], and NBS ecosystem [only (2)–(3)].

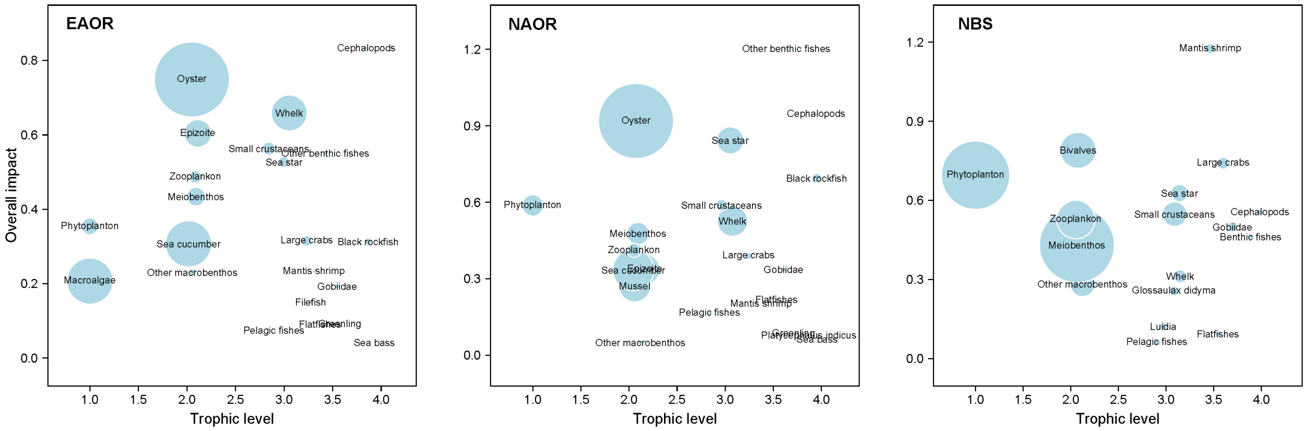

FIGURE 5 | Overall impact (ε) of each functional group in the three models (EAOR, NAOR, and NBS ecosystems). Circle size indicates the proportional biomass.

TABLE 3 | Keystone and structuring functional groups for the three ecosystems.

Ecosystem	Function group	ε	P	KS	KD	TD	TL	K/S
EAOR	Cephalopods	0.832	0.17%	–0.081	–2.843	97.58%	3.848	K
	Oyster	0.749	42.20%	–0.364	–0.501	65.25%	2.050	S
NAOR	Other benthic fishes	1.203	0.16%	0.080	–2.724	80.51%	3.635	K
	Cephalopods	0.946	0.10%	–0.025	–3.037	99.81%	3.945	K
	Oyster	0.919	45.20%	–0.298	–0.382	56.25%	2.073	S
NBS	Mintis shrimp	1.176	0.64%	0.067	–2.121	93.99%	3.462	K
	Phytoplankton	0.695	30.27%	–0.314	–0.677	9.80%	1.000	S

ε, its overall impact on other groups; P, biomass percentage; KS, keystoneness index; KD, dominance index; TD, top-down effect; TL, trophic level; K, keystone group; S, structuring/dominant group.

TABLE 4 | Biological carrying capacities (BCC) of ecological or economical important groups in the three models (EAOR, NAOR, and NBS ecosystems).

Group name	Biological carrying capacity (t·km^{-2}·yr^{-1})		
	EAOR	NAOR	NBS
Bivalves	208.600	218.180	86.300
Gobiidae	0.855	0.795	0.525
Cephalopods	0.864	0.427	0.226
Large crabs	4.260	1.705	0.671
Mantis shrimp	0.378	0.165	0.465
Whelk	83.400	65.000	0.834
Black rockfish	1.736	3.095	–
Greenling	0.540	0.333	–
Sea cucumber	84.800	86.900	–

Bivalves represent oyster group in EAOR, oyster and mussel groups in NAOR. "–" means no data available (There is no sea cucumber in NBS, and black rockfish and greenling are grouping into "Benthic fishes" due to their minimal biomass).

relevant economically and ecologically important organisms in the Ecopath model of the system was gradually increased until the EE value of any one group exceeded 1, and finally the biocapacities of these groups in the ecosystem were obtained (**Table 4**). For four of the six common groups, there were greater biological carrying capacities (BCCs) in the EAOR ecosystem than in the NAOR and NBS systems. However, mantis shrimp had a greater BCC in the NBS than in the other two ecosystems. As one of the most commercially important aquaculture species in northern China, sea cucumbers had the highest BCC among the functional groups in the EAOR and NAOR ecosystems, and they were principally sustained by detritus. The whelk *Rapana venosa* mostly benefited from the massive bivalves, had the second highest BCC, and had the most enhancement potential. As the critical structuring functional group of the reef ecosystems, the BCCs of bivalves were also evaluated. The NAOR area had the greatest bivalve BCC value among the three sites, followed by the EAOR and NBS ecosystems. Overall, the EAOR system had very similar but slightly better BCC values than the NAOR system, and both were much better than the NBS system. The reef systems could maintain greater biomass for top predator groups and economically important macrobenthos groups.

DISCUSSION

Because of the wide distribution of oysters, restoration work for oyster reefs can be carried out from temperate to tropical coastal regions in water depths of < 20 m. The deployment of artificial structures that can provide a suitable substrate for oyster larvae to settle on offers a kick-start for oyster reef establishment (Walters and Coen, 2006). The projects in Xiangyun Bay represent progress in artificial habitat construction from bare substratum to rocky reefs in the Bohai Sea nearshore zone. In this study, we conducted integrated analysis of the structure and function of reef and non-reef ecosystems using the Ecopath model to clarify the role of artificial oyster reefs in coastal ecological restoration. We explored the similarities and differences in biomass composition, trophic transfer, mixed trophic impact, total system characteristics, and ecosystem maturity and stability among three different ecosystem types, thereby providing a holistic and profound understanding of artificial oyster reefs in the Bohai Sea. Our results can further facilitate oyster reef restoration and preservation.

Key Functional Groups

Based on the description in Libralato et al. (2006) and Heymans et al. (2011), we identified keystone functional groups (i.e., with KS $\geq$ 0) and dominant/structuring functional groups (i.e., with KD $\geq$ –0.7) in each of the three ecosystems. The TL, biomass proportion, and top-down effects of keystone functional groups and structuring functional groups calculated from the three models were almost all within the reasonable ranges averaged for 105 models in Heymans et al. (2014), except for cephalopods in reef systems presenting stronger top-down effects than the average 67 $\pm$ 28%.

For the EAOR and NAOR ecosystems, cephalopods constituted the keystone functional group and oysters were the structuring functional group (**Table 3**). In the NBS system, the keystone and structuring groups were mantis shrimp and phytoplankton, respectively. Although keystone functional groups exhibited a clear prevalent top-down effect in each ecosystem, their trophic levels decreased from the EAOR to the NAOR to the NBS ecosystem. The oyster group in the EAOR and NAOR ecosystems exerted a moderate top-down effect, but phytoplankton in the NBS ecosystem exhibited a strong bottom-up effect. These differences between the three ecosystems demonstrated the presence of stronger top-down effects in artificial oyster reefs compared to the NBS ecosystem (Mcqueen et al., 2011). Rahman et al. (2019) also indicated the strong bottom-up dynamics in the entire Bohai Sea ecosystem.

In ecosystems, keystone functional groups usually had higher trophic level and mainly affected food webs through top-down effects, whereas structuring groups affected ecosystems mainly through bottom-up effects. However, researches referring to structuring functional group were scarce. Heymans et al. (2014) concluded that producers, especially benthic primary producers, were key structuring groups following method of Libralato et al. (2006). But those ecosystems were shallow water with depth < 10 m. In deeper waters, phytoplankton was identified as structuring functional group (NBS ecosystem in this study; Morales-Zárate et al., 2004). Ju et al. (2020) proposed that zooplankton, meiobenthos, and shrimp were the structuring functional groups based on their pelagic-benthic coupling effect in the ecosystem following Valls et al. (2015). In this study, we followed the calculation of Libralato et al. (2006). But the results of our reef ecosystems were differed from them, mainly due to different ecosystem structures. In EAOR and NAOR systems, the biomass proportions of oysters were 42.20 and 45.20%, and their flow to detritus took percentages of 45.07 and 44.39%. Their dominant role in ecosystem structure and energy flow made them the structuring groups of the systems. The ecological role of oysters might be even larger because of their non-predatory roles (Heymans et al., 2014). As the oyster population is quite vulnerable to various disturbances (Walles et al., 2016), long-term monitoring of environmental factors and protection strategies for the oyster populations need to be implemented.

Energy Utilization

The relative values of total system throughput (TST) of the three systems were 1.000, 0.903, and 0.393, respectively, indicating that the overall scales of the EAOR and NAOR were nearly comparable, but both were much greater than that of the NBS system. This result was consistent with that of reef and non-reef ecosystems reported by Feng et al. (2018). The TST scale of the EAOR and NAOR were of same magnitude as that of Lidao Island (Wu et al., 2016) and Jurien Bay (Lozano-Montes et al., 2011), but smaller than that of Tongyeong Bay (Lee and Zhang, 2018) and the Galapagos subtidal rocky reef (Okey et al., 2004), which are all characterized by reefs. Meanwhile, the scale of the NBS ecosystem was similar to that of Bohai Sea (Lin et al., 2009), Laizhou Bay (Ju et al., 2020) and the southern Yellow Sea (Lin et al., 2013), which represent non-reef large-scale systems. The ratios of allocation of TST in each system revealed the same utilization pattern for the EAOR and NAOR areas, with the most consumed and least exported. This pattern was in line with the natural reef ecosystem modeled in Zhang (2021). However, the NBS system showed a totally different pattern, with the most flows to detritus and the least to respiration, which was in agreement with results from Laizhou Bay and Haizhou Bay (Ju et al., 2020). These two diverse patterns were also consistent with the artificial reef system and its control area system studied by Feng et al. (2018) and Xu et al. (2019). Greater energy flows occurred in consumption and respiration activities in the EAOR and NAOR systems, whereas larger quantities of energy flowed into detritus and accumulated in the NBS system, which was also in agreement with the high TPP/TR ratio and low FCI index of the NBS system (**Table 2**).

In each of the three ecosystems, the energy of the system was mainly transferred through grazing and the detrital chain, but the latter played a more important role in the reef systems than in the bare substratum system. Simultaneously, the mTEd was greater than the mTEpp in the three models. Detritus-feeding activities increased with artificial oyster reef construction. The same conclusion was drawn from similar filter feeder-dominated ecosystems (Jiang and Gibbs, 2005; Pinkerton et al., 2008; Raoux et al., 2017). Raoux et al. (2017) suspected that the colonization by bivalves of the turbines of offshore wind farms would increase detritivory in the food web. In the field experiment conducted at Vanarna, on the west coast of Sweden, abundance and biomass of associated flora and fauna and their biodiversity increased because of mussels biodeposition (Norling and Kautsky, 2007). Increased numbers of bivalves improved the benthic-pelagic link by filtering organic matter out of the water column and depositing it on the seafloor, making it biologically available to benthic consumers (Newell, 2004; Wilhelmsson et al., 2006; Maar et al., 2009). The production of benthic organisms was enhanced by the sufficient food supply and thus improved the efficiency of energy recycling. In this process, bivalves ultimately initiated the shift from primary producer- and grazing-dominated food chains toward a more detritus-feeding community (Norling and Kautsky, 2007). Blomberg and Montagna (2014) also identified that 63–80% of total secondary production of ecosystems in Gulf of Mexico was supported by the benthic food chain than the pelagic food chain and with more efficiency in energy transfer.

Transfer Efficiency

The mean transfer efficiencies (mTEs) in the three ecosystems were all under the average of 10.1% of 48 global aquatic ecosystems (Pauly and Christensen, 1995) and 15% for temperate coastal ecosystems (Ryther, 1969), but they were comparable to values from systems shallower than 20 m (Heymans et al., 2014). However, these three systems exhibited different transfer patterns, indicating disparate functioning processes (**Figure 3**). For the EAOR and NAOR ecosystems, the TEs of TL II–III were 12.77 and 11.55%, but they rapidly decreased in the next two TL transfers. In the NBS system, the TE between TL III and IV was the highest (11.45%), while other transfers were ∼6%. These differences might be due to the high mean EEs of TL II in the EAOR and NAOR ecosystems. Prey groups were well utilized in TL III, but a large proportion of the biomass consisted of whelks, large crabs, and sea stars in TL III, which could not be consumed by top predators such as cephalopods, sea bass, and black rockfish. This contributed to the low TEs in the next TL transfers. In the NBS system, instead of carnivorous macroinvertebrates, fish functional groups constituted the larger percentage of the biomass in TL III, which can be exploited more efficiently by top predators. However, due to its lower biomass, herbivorous and detritivorous groups could not be utilized as well. Similar results could be seen in Daya Bay (Chen et al., 2015) and Haizhou Bay (Ju et al., 2020).

In EAOR and NAOR ecosystems, 67.73 and 71.00% of the energy flowing to TL II were consumed by oysters, respectively. As the zooplankton and meiobenthos mostly passed energy on to demersal or pelagic fishes, the bivalves efficiently deposited it to the macrobenthos through predation. In this way, the linear phytoplankton/detritus-oyster-carnivorous macrobenthos pathway developed and dominated and sustained highly efficient secondary production in oyster reefs. As the energy decreases by 90% with each increase of a discrete TL, a large amount of energy was dissipated through biological respiration and excretion, leading to a great reduction of biomass with increasing TL (Pauly and Christensen, 1995). However, ecosystems with massive numbers of oysters or other bivalves can effectively alter this situation (Blomberg and Montagna, 2014). Oysters or bivalves feed on phytoplankton and detritus of TL I and promptly transfer the energy to predators of TL III, such as whelks, large crabs, and sea stars. From the beginning to the end, the energy was transferred twice with about 1% of the energy of the fractional primary production conserved in TL III, thus it could support the large biomass of economically important macroinvertebrates. Compared with traditional grazing food chains flowing through zooplankton or meiobenthos, at least one energy transfer was shortened. Hence, the utilization of primary production became more efficient and was able to sustain the great biomass of carnivorous gastropods and crabs (Xu et al., 2019). Vander Zanden et al. (2006) and Blomberg and Montagna (2014) also found that benthic trophic pathways might be more efficient in their transfer compared to pelagic pathways. Therefore, we proposed that the artificial oyster reefs have produced carnivorous macrobenthos with high efficiency (Cresson et al., 2014, 2019). Considerable economic benefits can be generated through reasonable exploitation.

Ecosystem Maturity and Stability

As an ecosystem develops, its biomass, information, and complexity increase. However, when the ecosystem is affected by external disturbances, such as overfishing activities, it may show the opposite trend (Essington et al., 2006; Heymans and Tomczak, 2016). The TPP/TR and TPP/TB ratios are both significant parameters that reflect the maturity of an ecosystem (Odum, 1969; Christensen et al., 2005). When an ecosystem develops into maturity, the TPP/TR ratio approaches 1 and the TPP/TB ratio decreases. As an ecosystem becomes more mature, the food chains change from linear into web-like, and the TST, FCI, FMPL, CI, and SOI values increase (Ulanowicz, 1986; Libralato, 2013). The TPP/TR ratio of the NBS ecosystem was > 1 and was comparable to those of Laizhou Bay and Haizhou Bay (Ju et al., 2020), indicating their similar unmature ecosystem status. Large amounts of surplus primary production deposited or exported (Feng et al., 2018). In the EAOR and NAOR ecosystems, the TPP/TR ratio was < 1, which was different from values of many other ecosystems, except for the Galapagos rock reefs (Okey et al., 2004), Fuhan artificial reefs (Feng et al., 2018), and Laizhou Bay artificial reefs (Xu et al., 2019). The Galapagos ecosystem was characterized by large biomass of filter feeders, urchins, and herbivorous fish concentrated in TL II. The Fuhan and Laizhou Bay ecosystems had structural features similar to those of the EAOR and NAOR ecosystems, with large amounts of bivalves settled on the reefs. As the macroalgae could not be consumed directly (Krumhansl and Scheibling, 2012), and the phytoplankton and detritus in the oyster reef ecosystems could not support the massive consumption of oysters and other bivalves, these systems required nutrient input along with water exchange from other areas (Okey et al., 2004). Zhang et al. (2008) also discovered that suspended particle organic materials supporting massive biomass of scallop mainly coming from the water exchange. This might explain why most natural oyster reefs always occurred in estuaries (Kirby, 2004).

The FCI and FMPL indices of reef systems were comparable with the ratios of the 1–10 km^2 ecosystems described in Heymans et al. (2011), indicating that both systems had stability and energy flow diversity (Finn, 1976). The difference in FCI between the EAOR and NAOR systems and the NBS system supports the premise that strong recycling activity is linked to high bivalve biomass (Raoux et al., 2017, 2020). The SOI and CI were relatively low in all three models compared to the models listed in Wu et al. (2016) and to the SOI of reef ecosystems described in Heymans et al. (2011), demonstrating that the food webs of the three systems were simple and linear (Libralato, 2013). This might be strongly related to the increase of stenophagous oysters, whelks and sea cucumbers. The linear phytoplankton/ detritus-oysters-carnivorous macrobenthos and detritus-sea cucumbers pathways enhanced the energy utilization efficiency but decreased the complexity of food webs (Heymans et al., 2014).

System maturity also can be evaluated by the development capacity, A, and O (Ulanowicz, 1986; Monaco and Ulanowicz, 1997). The development capacities of the EAOR and NAOR ecosystems were much greater than that of the NBS system by factors of 2.431 and 2.249, respectively. The A/C ratio, which describes the system organization and efficiency, and the O/C ratio, which describes the system's resilience, were all moderate in the three systems compared with values reported for other reef models (Wu et al., 2016; Calderon-Aguilera et al., 2021). The higher O/C values in the NAOR and EAOR ecosystems (about 7.00 and 5.11% greater than that of the NBS system) suggested that the food webs in reefs were more stable than that of the NBS area (Pérez-España and ArreguìN-Sánchez, 2001), with a greater capacity to resist disturbances (Ulanowicz, 1986; Christensen, 1995). This scenario was confirmed by the current states of the reef ecosystems. The NAOR system is located farther from the coast and it is more vulnerable to illegal fishing and disturbed by freighters than the EAOR area. The EAOR ecosystem, however, is negatively impacted by nearby channel dredging. In contrast, the NBS ecosystem has become more specialized under generally intensive fishery pressures (Heymans and Tomczak, 2016). Its A/C and O/C ratios were comparable to those of Laizhou Bay described in Ju et al. (2020), demonstrating that these ecosystems gradually reorganized under various disturbances and easily return to equilibrium (Pezy et al., 2017; Raoux et al., 2020). Overfishing activities shifted the regime of the bare substratum ecosystem, and trapped it at the early development stages (Heymans and Tomczak, 2016; Sun and Zhang, 2018).

In short, all three ecosystems evaluated in this study were not yet mature, but the EAOR and NAOR ecosystems had more complicated trophic relationships and greater capacity to withstand perturbations compared to the NBS ecosystem. The differences could be attributed to the oyster reef construction and restoration, which enhanced the ecosystem complexity and diversity, and energy transfer efficiency. The nutrient input through water exchange would compensate the prey deficit of oysters and influence the maintenance of the system. Water exchange rate might be a critical factor in oyster reefs site selection and design.

Carrying Capacity and Management

The main economically important organisms in the study area include the rockfish *Sebastes schlegelii*, the greenling *Hexagrammos otakii*, gobies, cephalopods, and macroinvertebrates such as the crab *Charybdis japonica*, the mantis shrimp *Oratosquilla oratoria*, the whelk *R. apana venosa*, and sea cucumbers. The BCCs of the bivalves in the EAOR and NAOR ecosystems were comparable with those of Fuhan artificial reefs (Feng et al., 2018), Laoshan Bay (Liu et al., 2019), and Zhangzi Island (Xu et al., 2016). The BCCs of sea cucumbers in our study were relatively low in comparison with that of Lidao (Wu et al., 2013). Comparative analysis of the BCCs of functional groups between the artificial oyster reef ecosystems and the NBS ecosystem showed that the BCCs of the economically and ecologically important groups in the reef systems were much greater than those of the NBS system, which illustrated that the artificial oyster reef construction could sustain more massive biomass of organisms and benefit to resources conservation.

The BCC assessment could become one of the foundations of ecosystem-based management (Byron et al., 2011; Kluger et al., 2016; Yang, 2018). Results of BCC analysis could be a meaningful guidance for marine ranching and food web optimizing to enhance the utilization efficiency of organic matter and energy. In the EAOR and NAOR ecosystems, the biomass of whelks and sea cucumbers could be reasonably enhanced by feeding on oysters and detritus. Additionally, sea stars predation on oysters can be severe and they compete with whelks and large crabs, so they need to be eliminated in a timely manner. In the NBS system, however, the low EEs of phytoplankton and detritus were consistent with the enormous BCC of bivalves, indicating insufficient utilization of primary production and the potential to restore oyster reefs in such areas.

Keystone and structuring functional groups both have a strong overall effect on entire ecosystems (Power et al., 1996; Libralato et al., 2006). In our study, cephalopods and oysters were identified as the common keystone and structuring groups, respectively, in the reef ecosystems. A small change in their biomass would alter the structure and function of the systems. Therefore, both groups should be well preserved. Cephalopods are also important fishing targets, so they need to be carefully managed. Although it is not a fishery target in the local region, the oyster population is quite vulnerable to various disturbances (Kirby, 2004; Walles et al., 2016). Therefore, long-term monitoring of environmental factors and protection strategies for the oyster populations need to be implemented.

CONCLUSION

Numerous oyster reef restoration or preservation projects have been launched by governments and non-governmental organizations around the world in last few decades (La Peyre et al., 2014; Pogoda, 2019; Gillies et al., 2020; Mcafee et al., 2020). However, the restoration and construction of oyster reefs began more recently in China, and great knowledge gaps still exist (Quan et al., 2017; Yang et al., 2020). The results of this study could facilitate our understandings of oyster reef ecosystems. In artificial oyster reef ecosystem: (1) the oyster group was the structuring functional group and played a critical role in trophic structure; (2) the phytoplankton/detritus-oyster-carnivorous macrobenthos pathway developed and dominated, leading to highly efficient secondary production; (3) detritus-feeding activities increased with artificial oyster reef construction; (4) the TPP/TR ratio was < 1 and relied on nutrient inputs from adjacent ecosystems; and (5) there was great potential to resist disturbances.

The overall better ecosystem status of oyster reefs than the bare substratum indicates that artificial oyster reef restoration/construction provides great advantages to the ecosystem, such as habitat provisions and improved trophic structure, which can fundamentally alleviate the trend of seabed desertification and benefit coastal ecological restoration (Langlois et al., 2006; Gain et al., 2016). The high secondary productivity of the ecosystem is catering to the demand for aquatic products. Combined with marine ranching of commercial important species and recreational fishing, considerable economic benefits can be generated (Xu et al., 2019). This study also certifies its suitability and great potential for oyster reef restoration and construction in coastal waters shallower than 10 m. Besides, the NAOR ecosystem demonstrates the short temporal scales (1–2 years) for artificial oyster reef ecosystems evolving into a reasonable stage.

However, our study had some limitations. We failed to take the effects of water depth, temporal scale and ecosystem size into account. Offshore distance and water depth may influence the community composition and food webs (Giraldo et al., 2017; Wu et al., 2019; Cresson et al., 2020). Temporal scale is the main factor of community composition and biomass (Walters and Coen, 2006; Paxton et al., 2018; Cresson et al., 2019). Heymans et al. (2014) indicated that shallower systems had more flow to detritus and smaller systems usually had lower mean Ecotrophic Efficiencies. In this study, although with shorter constructed time, the NAOR ecosystem showed similar community composition and ecosystem structure with EAOR systems and artificial reefs reported in Feng et al. (2018) and Xu et al. (2019). The main difference between EAOR and NAOR ecosystem is the macroalgae influenced by depth. Further studies should focus on the detailed differences between these two ecosystems.

Besides, only 1 year of data was used in the modeling, resulting in static snapshots of the ecosystems. In the future, multi-year data should be used and dynamic simulations of the system should be performed. Then, the sampling and investigations were carried out only in artificial reef areas, and that the relationship with adjacent ecosystems and impacts of river inputs were not considered. Additionally, the artificial oyster reefs are still subject to severe anthropogenic impacts. More studies should focus on how these systems respond to external disturbances. Finally, additional models could be used, such as the Ecosim and Ecotroph modules, to help us better understand the ecosystems for better ecosystem-based management.

DATA AVAILABILITY STATEMENT

The raw data supporting the conclusions of this article will be made available by the authors, without undue reservation.

AUTHOR CONTRIBUTIONS

XW carried out the experiments, implemented the models and drafted the manuscript. JF and CL contributed to the design of the work and revised the manuscript. HL and YZ prepared materials and carried out the experiments. MC revised the manuscript. All authors contributed to the article and approved the final manuscript.

FUNDING

This work was supported by the National Key R&D Program of China (2019YFD0900800) and the National Natural Science Foundation of China (42030408).

SUPPLEMENTARY MATERIAL

The Supplementary Material for this article can be found online at: https://www.frontiersin.org/articles/10.3389/fmars.2022.829557/full#supplementary-material

REFERENCES

Baine, M. (2001). Artificial reefs: A review of their design, application, management and performance. *Ocean Coast. Manage* 44, 241–259. doi: 10.1016/S0964-5691(01)00048-5

Beck, M. W., Brumbaugh, R. D., Airoldi, L., Carranza, A., Coen, L. D., Crawford, C., et al. (2011). Oyster reefs at risk and recommendations for conservation, restoration, and management. *Bioscience* 61, 107–116. doi: 10.1525/bio.2011.61.2.5

Blomberg, B. N., and Montagna, P. A. (2014). Meta-analysis of Ecopath models reveals secondary productivity patterns across the Gulf of Mexico. *Ocean Coast. Manage* 100, 32–40.

Blomberg, B. N., Lebreton, B., Palmer, T. A., Guillou, G., Beseres Pollack, J., and Montagna, P. A. (2017). Does reef structure affect oyster food resources? A stable isotope assessment. *Mar. Environ. Res.* 127, 32–40. doi: 10.1016/j.marenvres.2017.03.003

Borsje, B. W., Van Wesenbeeck, B. K., Dekker, F., Paalvast, P., Bouma, T. J., Van Katwijk, M. M., et al. (2011). How ecological engineering can serve in coastal protection. *Ecol. Eng.* 37, 113–122. doi: 10.1016/j.ecoleng.2010.11.027

Byron, C., Link, J., Costa-Pierce, B., and Bengtson, D. (2011). Calculating ecological carrying capacity of shellfish aquaculture using mass-balance modeling: Narragansett Bay, Rhode Island. *Ecol. Model.* 222, 1743–1755. doi: 10.1016/j.ecolmodel.2011.03.010

Calderon-Aguilera, L. E., Reyes-Bonilla, H., Olán-González, M., Castañeda-Rivero, F. R., and Perusquía-Ardón, J. C. (2021). Estimated flows and biomass in a no-take coral reef from the eastern tropical Pacific through network analysis. *Ecol. Indic.* 123:107359. doi: 10.1016/j.ecolind.2021.107359

Chen, Z., Xu, S., and Qiu, Y. (2015). Using a food-web model to assess the trophic structure and energy flows in Daya Bay, China. *Cont. Shelf Res.* 111, 316–326. doi: 10.1016/j.csr.2015.08.013

Chowdhury, M. S. N., La Peyre, M., Coen, L. D., Morris, R. L., Luckenbach, M. W., Ysebaert, T., et al. (2021). Ecological engineering with oysters enhances coastal resilience efforts. *Ecol. Eng.* 169:106320. doi: 10.1016/j.ecoleng.2021.106320

Christensen, V. (1995). Ecosystem maturity — towards quantification. *Ecol. Model.* 77, 3–32. doi: 10.1016/0304-3800(93)E0073-C

Christensen, V., Walters, C., and Pauly, D. (2005). *Ecopath with Ecosim: A user's guide*. Vancouver: Fisheries Centre of University of British Columbia.

Christensen, V., and Walters, C. J. (2004). Ecopath with Ecosim: methods, capabilities and limitations. *Ecol. Model.* 172, 109–139. doi: 10.1016/j.ecolmodel.2003.09.003

Coen, L. D., Brumbaugh, R. D., Bushek, D., Grizzle, R., Luckenbach, M. W., Posey, M. H., et al. (2007). Ecosystem services related to oyster restoration. *Mar. Ecol. Prog. Ser.* 341, 303–307.

Cresson, P., Le Direach, L., Rouanet, E., Goberville, E., Astruch, P., Ourgaud, M., et al. (2019). Functional traits unravel temporal changes in fish biomass production on artificial reefs. *Mar. Environ. Res.* 145, 137–146. doi: 10.1016/j.marenvres.2019.02.018

Cresson, P., Ruitton, S., and Harmelin, M. (2014). Artificial reefs do increase secondary biomass production: Mechanisms evidenced by stable isotopes. *Mar. Ecol. Prog. Ser.* 509, 15–26. doi: 10.3354/meps10866

Cresson, P., Chouvelon, T., Bustamante, P., Bănaru, D., Baudrier, J., Le Loc'h, F., et al. (2020). Primary production and depth drive different trophic structure and functioning of fish assemblages in French marine ecosystems. *Prog. Oceanogr.* 186:102343. doi: 10.1016/j.pocean.2020.102343

Darwall, W. R. T., Allison, E. H., Turner, G. F., and Irvine, K. (2010). Lake of flies, or lake of fish? A trophic model of Lake Malawi. *Ecol. Model.* 221, 713–727. doi: 10.1016/j.ecolmodel.2009.11.001

Deng, J. Y., Jiang, W. M., Yang, J. M., and Li, J. (1997). Species interaction and food web of major predatory species in the Bohai Sea. *J. Fish. Sci. China.* 4, 2–8.

Essington, T. E., Beaudreau, A. H., and Wiedenmann, J. (2006). Fishing through marine food webs. *Proc. Natl. Acad. Sci. USA* 103:3171. doi: 10.1073/pnas.0510964103

Feng, J., Zhang, T., Li, H. Z., Jiang, H., Yang, H. S., Zhou, Y., et al. (2018). "Assessment of biocapacity and prediction of future biomass change in marine ranching area based on ecopath with ecosim model," in *The 3rd International Symposium on Modern Marine Ranching; 2018 Annual Conference of Fishery Resources and Environment Committee*, (Chinese Fisheries Society), 104.

Finn, J. T. (1976). Measures of ecosystem structure and function derived from analysis of flows. *J. Theor. Biol.* 56, 363–380. doi: 10.1016/S0022-5193(76)80080-X

Gain, I. E., Brewton, R. A., Reese Robillard, M. M., Johnson, K. D., Smee, D. L., and Stunz, G. W. (2016). Macrofauna using intertidal oyster reef varies in relation to position within the estuarine habitat mosaic. *Mar. Biol.* 164:8. doi: 10.1007/s00227-016-3033-5

Gillies, C. L., Castine, S. A., Alleway, H. K., Crawford, C., Fitzsimons, J. A., Hancock, B., et al. (2020). Conservation status of the oyster reef ecosystem of southern and eastern Australia. *Glob. Ecol. Conserv.* 22:e00988. doi: 10.1016/j.gecco.2020.e00988

Giraldo, C., Ernande, B., Cresson, P., Kopp, D., Cachera, M., Travers-Trolet, M., et al. (2017). Depth gradient in the resource use of a fish community from a semi-enclosed sea. *Limnol. Oceanogr.* 62, 2213–2226. doi: 10.1002/lno.10561

Gutiérrez, J., Jones, C., Strayer, D., and Iribarne, O. (2003). Mollusks as ecosystem engineers: The role of shell production in aquatic habitats. *Oikos* 101, 79–90. doi: 10.1034/j.1600-0706.2003.12322.x

Heymans, J., Coll, M., Libralato, S., and Christensen, V. (2011). "Ecopath theory, modeling, and application to coastal ecosystems," in *Treatise on estuarine and coastal science*, eds E. Wolanski and D. Mclusky (Oxford: Elsevier), 93–113.

Heymans, J., Coll, M., Libralato, S., Morissette, L., and Christensen, V. (2014). Global patterns in ecological indicators of marine food webs: A modelling approach. *PLoS One* 9:e95845. doi: 10.1371/journal.pone.0095845

Heymans, J. J., Coll, M., Link, J. S., Mackinson, S., Steenbeek, J., Walters, C., et al. (2016). Best practice in ecopath with ecosim food-web models for ecosystem-based management. *Ecol. Model.* 331, 173–184. doi: 10.1016/j.ecolmodel.2015.12.007

Heymans, J. J., and Tomczak, M. T. (2016). Regime shifts in the Northern Benguela ecosystem: Challenges for management. *Ecol. Model.* 331, 151–159. doi: 10.1016/j.ecolmodel.2015.10.027

Hoellein, T. J., Zarnoch, C. B., and Grizzle, R. E. (2015). Eastern oyster (Crassostrea virginica) filtration, biodeposition, and sediment nitrogen cycling at two oyster reefs with contrasting water quality in Great Bay Estuary (New Hampshire, USA). *Biogeochemistry* 122, 113–129. doi: 10.1007/s10533-014-0034-7

Jiang, W., and Gibbs, M. T. (2005). Predicting the carrying capacity of bivalve shellfish culture using a steady, linear food web model. *Aquaculture* 244, 171–185. doi: 10.1016/j.aquaculture.2004.11.050

Jin, X., Shan, X., Li, X., Wang, J., Cui, Y., and Zuo, T. (2013). Long-term changes in the fishery ecosystem structure of Laizhou Bay. *China. Sci. China Earth Sci.* 56, 366–374. doi: 10.1007/s11430-012-4528-7

Jin, X. S., and Deng, J. Y. (2000). Variations in community structure of fishery resources and biodiversity in the Laizhou Bay. *China. Biodivers. Sci.* 11, 65–72. doi: 10.17520/biods.2000009

Ju, P., Cheung, W. W. L., Chen, M., Xian, W., Yang, S., and Xiao, J. (2020). Comparing marine ecosystems of Laizhou and Haizhou Bays, China, using ecological indicators estimated from food web models. *J. Mar. Syst.* 202:103238. doi: 10.1016/j.jmarsys.2019.103238

Kirby, M. (2004). Fishing down the coast: Historical expansion and collapse of oyster fisheries along continental margins. *Proc. Natl. Acad. Sci. USA* 101, 13096–13099. doi: 10.1073/pnas.0405150101

Kluger, L. C., Taylor, M. H., Mendo, J., Tam, J., and Wolff, M. (2016). Carrying capacity simulations as a tool for ecosystem-based management of a scallop aquaculture system. *Ecol. Model.* 331, 44–55. doi: 10.1016/j.ecolmodel.2015.09.002

Krumhansl, K. A., and Scheibling, R. E. (2012). Production and fate of kelp detritus. *Mar. Ecol. Prog. Ser.* 467, 281–302. doi: 10.3354/meps09940

Langlois, T. J., Anderson, M. J., and Babcock, R. C. (2006). Inconsistent effects of reefs on different size classes of macrofauna in adjacent sand habitats. *J. Exp. Mar. Biol. Ecol.* 334, 269–282. doi: 10.1016/j.jembe.2006.02.001

La Peyre, M., Furlong, J., Brown, L. A., Piazza, B. P., and Brown, K. (2014). Oyster reef restoration in the northern Gulf of Mexico: Extent, methods and outcomes. *Ocean Coast. Manage.* 89, 20–28. doi: 10.1016/j.ocecoaman.2013.12.002

Latham, L. G. (2006). Network flow analysis algorithms. *Ecol. Model.* 192, 586–600. doi: 10.1016/j.ecolmodel.2005.07.029

Layman, C., and Allgeier, J. (2020). An ecosystem ecology perspective on artificial reef production. *J. Appl. Ecol.* 57:13748. doi: 10.1111/1365-2664.13748

Lee, M. O., Otake, S., and Kim, J. K. (2018). Transition of artificial reefs (ARs) research and its prospects. *Ocean Coast. Manage.* 154, 55–65. doi: 10.1016/j.ocecoaman.2018.01.010

Lee, S. I., and Zhang, C. I. (2018). Evaluation of the effect of marine ranching activities on the Tongyeong marine ecosystem. *Ocean Sci. J.* 53, 557–582. doi: 10.1007/s12601-018-0045-8

Li, X., Yang, W., Li, S., Sun, T., Bai, J., Pei, J., et al. (2020). Asymmetric responses of spatial variation of different communities to a salinity gradient in coastal wetlands. *Mar. Environ. Res.* 158:105008. doi: 10.1016/j.marenvres.2020.105008

Li, X., Yang, W., Sun, T., and Gaedke, U. (2021). Quantitative food web structure and ecosystem functions in a warm-temperate seagrass bed. *Mar. Biol.* 168:74.

Libralato, S. (2013). "System omnivory index," in *Encyclopedia of ecology*, eds S. E. Jørgensen and B. D. Fath (Oxford: Elsevier), 481–486. doi: 10.1007/s00227-021-03878-z

Libralato, S., Christensen, V., and Pauly, D. (2006). A method for identifying keystone species in food web models. *Ecol. Model.* 195, 153–171. doi: 10.1016/j.ecolmodel.2005.11.029

Lin, Q., Jin, X. S., Zhang, B., and Guo, X. (2009). Comparative study on the changes of the Bohai Sea ecosystem structure based on Ecopath model between ten years. *Acta Ecol. Sin.* 07, 3613–3620.

Lin, Q., Jin, X. S., and Zhang, B. (2013). Trophic interactions, ecosystem structure and function in the southern Yellow Sea. *Chin. J. Oceanol. Limnol.* 31:6. doi: 10.1007/s00343-013-2013-6

Link, J. S. (2010). Adding rigor to ecological network models by evaluating a set of pre-balance diagnostics: A plea for PREBAL. *Ecol. Model.* 221, 1580–1591. doi: 10.1016/j.ecolmodel.2010.03.012

Liu, H. Y., Yang, C. J., Zhang, P. D., Li, W. T., and Zhang, X. M. (2019). An Ecopath evaluation of system structure and function for the Laoshan Bay artificial reef zone ecosystem. *J. Ocean Univ. China* 39, 168–177.

Liu, Z., Yu, P., Chen, M., Cai, M., Fan, B., Lv, W., et al. (2018). Macrobenthic community characteristics and ecological health of a constructed intertidal oyster reef in the Yangtze Estuary, China. *Mar. Pollut. Bull.* 135, 95–104. doi: 10.1016/j.marpolbul.2018.07.019

Lozano-Montes, H., Loneragan, N., Babcock, R., and Jackson, K. (2011). Using trophic flows and ecosystem structure to model the effects of fishing in the Jurien Bay marine park, temperate western Australia. *Mar. Freshwat. Res.* 62, 421–431. doi: 10.1071/MF09154

Lv, X., Wang, X., Wu, Y., Jiang, W., Fang, J., Fang, J., et al. (2018). Effect of temperature on the energy budget of Arcuatula senhousei. *Prog. Oceanogr.* 39, 119–125. doi: 10.19663/j.issn2095-9869.20170420002

Maar, M., Bolding, K., Petersen, J. K., Hansen, J. L. S., and Timmermann, K. (2009). Local effects of blue mussels around turbine foundations in an ecosystem model of nysted off-shore wind farm, Denmark. *J. Sea Res.* 62, 159–174. doi: 10.1016/j.seares.2009.01.008

Mcafee, D., Mcleod, I. M., Boström-Einarsson, L., and Gillies, C. L. (2020). The value and opportunity of restoring Australia's lost rock oyster reefs. *Restor. Ecol.* 28, 304–314. doi: 10.1111/rec.13125

Mcqueen, D., Post, J., and Mills, E. (2011). Trophic relationships in freshwater pelagic ecosystems. *Can. J. Fish. Aquat. Sci.* 43, 1571–1581. doi: 10.1139/f86-195

Miller, W., Reynolds, A., Sobrino, C., and Riedel, G. (2009). Shellfish face uncertain future in high CO2 world: Influence of acidification on oyster larvae calcification and growth in estuaries. *PLoS One* 4:e5661. doi: 10.1371/journal.pone.0005661

Monaco, M. E., and Ulanowicz, R. E. (1997). Comparative ecosystem trophic structure of three U.S. Mid-Atlantic estuaries. *Mar. Ecol. Prog. Ser.* 161, 239–254. doi: 10.3354/meps161239

Morales-Zárate, M. V., ArreguìN-Sánchez, F., López-MartìNez, J., and Lluch-Cota, S. E. (2004). Ecosystem trophic structure and energy flux in the Northern Gulf of California, México. *Ecol. Model.* 174, 331–345.

Morissette, L. (2007). *Complexity, cost and quality of ecosystem models and their impact on resilience : A comparative analysis, with emphasis on marine mammals and the Gulf of St. Lawrence.* (Doctoral thesis). Vancouver: University of British Columbia, doi: 10.14288/1.0074903

Newell, R. I. E. (2004). Ecosystem influences of natural and cultivated populations of suspension-feeding bivalve molluscs: A review. *J. Shellfish Res.* 23, 51–61.

Norling, P., and Kautsky, N. (2007). Structural and functional effects of Mytilus edulis on diversity of associated species and ecosystem functioning. *Mar. Ecol. Prog. Ser.* 351, 163–175. doi: 10.3354/meps07033

Odum, E. P. (1969). The strategy of ecosystem development. *Science* 164, 262–270. doi: 10.1126/science.164.3877.262

Okey, T. A., Banks, S., Born, A. F., Bustamante, R. H., Calvopiña, M., Edgar, G. J., et al. (2004). A trophic model of a Galápagos subtidal rocky reef for evaluating fisheries and conservation strategies. *Ecol. Model.* 172, 383–401. doi: 10.1016/j.ecolmodel.2003.09.019

Ortiz, M., Berrios, F., Campos, L., Uribe, R., Ramirez, A., Hermosillo-Núñez, B., et al. (2015). Mass balanced trophic models and short-term dynamical simulations for benthic ecological systems of Mejillones and Antofagasta bays (SE Pacific): Comparative network structure and assessment of human impacts. *Ecol. Model.* 309-310, 153–162. doi: 10.1016/j.ecolmodel.2015.04.006

Ouyang, L. J., and Guo, X. W. (2010). Studies on the Q/B values and food consumption of major fishes in the East China Sea and the Yellow Sea. *Prog. Oceanogr.* 31, 23–29.

Parsons, T. R., Maita, Y., and Lalli, C. M. (1984). "Determination of chlorophylls and total carotenoids: Spectrophotometric method," in *A manual of chemical & biological methods for seawater analysis*, eds T. R. Parsons, Y. Maita, and C. M. Lalli (Pergamon: Amsterdam), 101–104. doi: 10.1016/b978-0-08-030287-4.50032-3

Pauly, D., and Christensen, V. (1995). Primary production required to sustain global fisheries. *Nature* 374, 255–257. doi: 10.1038/374255a0

Pauly, D., Christensen, V. V., Dalsgaard, J., Froese, R., and Torres, F. Jr. (1998). Fishing down marine food webs. *Science* 279, 860–863. doi: 10.1126/science.279.5352.860

Paxton, A. B., Revels, L. W., Rosemond, R. C., Van Hoeck, R. V., Lemoine, H. R., Taylor, J. C., et al. (2018). Convergence of fish community structure between a newly deployed and an established artificial reef along a five-month trajectory. *Ecol. Eng.* 123, 185–192. doi: 10.1016/j.ecoleng.2018.09.012

Pérez-España, H., and ArreguìN-Sánchez, F. (2001). An inverse relationship between stability and maturity in models of aquatic ecosystems. *Ecol. Model.* 145, 189–196. doi: 10.1016/S0304-3800(01)00390-8

Pezy, J.-P., Raoux, A., Marmin, S., Balay, P., Niquil, N., and Dauvin, J.-C. (2017). Before-after analysis of the trophic network of an experimental dumping site in the eastern part of the Bay of Seine (English Channel). *Mar. Pollut. Bull.* 118, 101–111. doi: 10.1016/j.marpolbul.2017.02.042

Piazza, B. P., Banks, P. D., and La Peyre, M. K. (2005). The potential for created oyster shell reefs as a sustainable shoreline protection strategy in Louisiana. *Restor. Ecol.* 13, 499–506. doi: 10.1111/j.1526-100X.2005.00062.x

Pinkerton, M. H., Lundquist, C. J., Duffy, C. A. J., and Freeman, D. J. (2008). Trophic modelling of a New Zealand rocky reef ecosystem using simultaneous adjustment of diet, biomass and energetic parameters. *J. Exp. Mar. Biol. Ecol.* 367, 189–203. doi: 10.1016/j.jembe.2008.09.022

Pogoda, B. (2019). Current status of european oyster decline and restoration in Germany. *Humanities* 8:9. doi: 10.3390/h8010009

Polovina, J. J. (1984). Model of a coral reef ecosystem. *Coral Reefs* 3, 1–11. doi: 10.1007/BF00306135

Power, M. E., Tilman, D., Estes, J. A., Menge, B. A., Bond, W. J., Mills, L. S., et al. (1996). Challenges in the quest for keystones: Identifying keystone species is difficult—but essential to understanding how loss of species will affect ecosystems. *Bioscience* 46, 609–620. doi: 10.2307/1312990

Powers, S. P., Peterson, C., Grabowski, J., and Lenihan, H. S. (2009). Success of constructed oyster reefs in no-harvest sanctuaries: Implications for restoration. *Mar. Ecol. Prog. Ser.* 389, 159–170. doi: 10.3354/meps08164

Quan, W. M., Feng, M., Zhou, Z., Wu, Z., Tang, F., Wang, Y., et al. (2017). Ecological assessment of the oyster Crassostrea sikamea population and associated benthic communities on restored oyster reefs along Jiangsu Province coast, China. *Acta Ecol. Sin.* 37, 1709–1718. doi: 10.5846/stxb201510102049

Rahman, M. F., Qun, L., Xiujuan, S., Chen, Y., Ding, X., and Liu, Q. (2019). Temporal changes of structure and functioning of the Bohai Sea ecosystem: Insights from ecopath models. *Thalassas* 35, 625–641. doi: 10.1007/s41208-019-00139-1

Raoux, A., Noémie, B., Pezy, J.-P., Balay, P., Lesourd, S., and Dauvin, J.-C. (2020). Evaluating ecosystem functioning of a long-term dumping site in the Bay of Seine (English Channel). *Ecol. Indic.* 115:106381. doi: 10.1016/j.ecolind.2020.106381

Raoux, A., Tecchio, S., Pezy, J.-P., Lassalle, G., Degraer, S., Wilhelmsson, D., et al. (2017). Benthic and fish aggregation inside an offshore wind farm: Which effects on the trophic web functioning? *Ecol. Indic.* 72, 33–46. doi: 10.1016/j.ecolind.2016.07.037

Rodriguez-Perez, A., James, M., Donnan, D. W., Henry, T. B., Møller, L. F., and Sanderson, W. G. (2019). Conservation and restoration of a keystone species: Understanding the settlement preferences of the European oyster (Ostrea edulis). *Mar. Pollut. Bull.* 138, 312–321. doi: 10.1016/j.marpolbul.2018.11.032

Ryther, J. H. (1969). Photosynthesis and fish production in the sea. *Science* 166, 72–76. doi: 10.1126/science.166.3901.72

Samonte, G., Ihde, T., and Lipton, D. (2020). *Estimating Ecological Benefits and Socio-Economic Impacts from Oyster Reef Restoration in the Choptank River Complex*. Chesapeake Bay: Morgan State University.

Sun, Y., and Zhang, Z. (2018). *Background environmental data analysis report of Xiangyun bay Marine Ranching and surrounding sea area in Tangshan city*. Qingdao: First Institute of Oceanography, Ministry of Natural Resources.

Tang, Q., Guo, X., Sun, Y., and Zhang, B. (2007). Ecological conversion efficiency and its influencers in twelve species of fish in the Yellow Sea ecosystem. *J. Mar. Syst.* 67, 282–291. doi: 10.1016/j.jmarsys.2006.04.013

Theuerkauf, S. J., Burke, R. P., and Lipcius, R. N. (2014). Settlement, growth and survival of eastern oysters on alternative reef substrates. *bioRxiv* 2014:010793. doi: 10.1101/010793

Tumbiolo, M. L., and Downing, J. A. (1994). An empirical model for the prediction of secondary production in marine benthic invertebrate populations. *Mar. Ecol. Prog. Ser.* 114, 165–174. doi: 10.3354/meps114165

Ulanowicz, R. E. (1986). *Growth and development: Ecosystems phenomenology*. New York, NY: Springer-Verlag.

Ulanowicz, R. E., and Puccia, C. J. (1990). Mixed trophic impacts in ecosystems. *Coenoses* 5, 7–16.

Valls, A., Coll, M., and Christensen, V. (2015). Keystone species: toward an operational concept for marine biodiversity conservation. *Ecol. Monogr.* 85, 29–47. doi: 10.1890/14-0306.1

Vander Zanden, J., Chandra, S., Park, S., Vadeboncoeur, Y., and Goldman, C. (2006). Efficiencies of benthic and pelagic trophic pathways in a subalpine lake. *Can. J. Fish. Aquat. Sci.* 63, 2608–2620. doi: 10.1139/F06-148

Walles, B., Troost, K., Ende, D., Nieuwhof, S., Smaal, A. C., and Ysebaert, T. (2016). From artificial structures to self-sustaining oyster reefs. *J. Sea Res.* 108, 1–9. doi: 10.1016/j.seares.2015.11.007

Walters, K., and Coen, L. (2006). A comparison of statistical approaches to analyzing community convergence between natural and constructed oyster reefs. *J. Exp. Mar. Biol. Ecol.* 330, 81–95. doi: 10.1016/j.jembe.2005.12.018

Wei, S., and Jiang, W. M. (1992). Study on food web of fishes in the Yellow Sea. *Oceanol. Limnol. Sin.* 23, 182–192.

Wilhelmsson, D., Malm, T., and Öhman, M. C. (2006). The influence of offshore windpower on demersal fish. *ICES J. Mar. Sci.* 63, 775–784. doi: 10.1016/j.icesjms.2006.02.001

Wu, Z., Tweedley, J. R., Loneragan, N. R., and Zhang, X. (2019). Artificial reefs can mimic natural habitats for fish and macroinvertebrates in temperate coastal waters of the Yellow Sea. *Ecol. Eng.* 139:105579. doi: 10.1016/j.ecoleng.2019.08.009

Wu, Z., Zhang, X., Lozano-Montes, H. M., and Loneragan, N. R. (2016). Trophic flows, kelp culture and fisheries in the marine ecosystem of an artificial reef zone in the Yellow Sea. *Estuar. Coast. Shelf Sci.* 182, 86–97. doi: 10.1016/j.ecss.2016.08.021

Wu, Z. X., Zhang, X. M., Zhang, L., Tong, F., and Liu, H. J. (2013). Predicting the ecological carrying of the lidao artificial reef zone of Shandong Province for the sea cucumber, *Apostichopus japonicus*, (Selenck) and the abalone, *Haliotis discus hannai*, using a linear food web model. *J. Fish. Sci. China.* 20, 327–337. doi: 10.3724/sp.j.1118.2013.00327

Xu, M., Qi, L., Zhang, L., Zhang, T., Yang, H., and Zhang, Y. (2019). Ecosystem attributes of trophic models before and after construction of artificial oyster reefs using ecopath. *Aquac. Environ. Interact.* 11, 111–127. doi: 10.3354/aei00284

Xu, M., Yang, X. Y., Song, X. J., Xu, K. D., and Yang, L. L. (2020). Seasonal analysis of artificial oyster reef ecosystems: Implications for sustainable fisheries management. *Aquacult. Int.* 29, 167–192. doi: 10.1007/s10499-020-00617-x

Xu, Y., and Ma, S. (2009). Effects of different diets on the growth and bioenergetics of swimming crab Portunus trituberculatus. *J. Ocean Univ. China* 39, 353–358. doi: 10.16441/j.cnki.hdxb.2009.s1.064

Xu, Z. X., Chen, Y., Tian, T., Liu, Y. H., Yin, Z. Q., and Liu, H. C. (2016). Structure and function of an artificial reef ecosystem in Zhangzi island based on ecopath model. *J. Dalian Ocean. Univ.* 31, 85–94. doi: 10.16535/j.cnki.dlhyxb.2016.01.015

Yang, H. S. (2018). *Monitoring and biocapacity evaluation of marine ranch ecosystem*. Beijing: Sciences Press.

Yang, H. S., Xu, S., Lin, C. G., Sun, J. C., and Zhang, L. B. (2020). Research progress and prospects of restoration and resource conservation in typical sea areas. *Oceanol. Limnol. Sin.* 51, 809–820.

Yang, J. M. (2001a). A study on food and trophic levels of Bohai Sea fish. *Mod. Fish. Inform.* 16, 10–19.

Yang, J. M. (2001b). A study on food and trophic levels of Bohai Sea invertebrates. *Mod. Fish. Inform.* 16, 8–16.

Yang, X. Y. (2019). *The community characteristics and ecological functions of artificial oyster reef at Xiangyun Bay marine ranching.* (Master's thesis). Qingdao: University of Chinese Academy of Sciences.

Yue, J., Zhang, B. H., Han, F., Zhao, X. T., Liu, D. Y., Duan, H. C., et al. (2012). Several oyster barrier reefs in the northernwest coast of Bohai Sea. *Acta Geogr. Sin.* 86, 1175–1187.

Zhang, B. (2018). Feeding ecology of fishes in the Bohai Sea. *Prog. Oceanogr.* 39, 11–22. doi: 10.19663/j.issn2095-9869.20171103001

Zhang, J., Fang, J., and Wang, S. (2008). Carryiny capacity for *Patinopecten yessoensis* in Zhang Zidao Island. *China. J. Fish. China.* 02, 236–241.

Zhang, R. L. (2021). *The comparative study of the food web structure and function between the artificial and natural reef s in the nearshore.* (Doctoral thesis). Yantai: University of Chinese Academy of Sciences.

Zhu, W., Sun, Y., Zhao, H., Yu, M., Guo, J., and Li, D. (2016). Effects of different diets on growth of shot arm octopus Octopus ocellatus. *Fish. Sci.* 35, 573–577. doi: 10.16378/j.cnki.1003-1111.2016.05.020

Zu Ermgassen, P. S. E., Grabowski, J. H., Gair, J. R., Powers, S. P., and Jones, J. (2015). Quantifying fish and mobile invertebrate production from a threatened nursery habitat. *J. Appl. Ecol.* 53, 596–606. doi: 10.1111/1365-2664.12576

Conflict of Interest: YZ was employed by Tangshan Marine Ranching Co., Ltd.

The remaining authors declare that the research was conducted in the absence of any commercial or financial relationships that could be construed as a potential conflict of interest.

frontiers | Frontiers in Marine Science

ORIGINAL RESEARCH
published: 14 June 2022
doi: 10.3389/fmars.2022.880453

Short-Term Response of Deep-Water Benthic Megafauna to Installation of a Pipeline Over a Depth Gradient on the Angolan Slope

Virginia Biede[1,2]*, Andrew R. Gates*[3]*, Simone Pfeifer*[1,3]*, Jane E. Collins*[1]*, Carmen Santos*[4,5] *and Daniel O. B. Jones*[3]*

[1] *University of Southampton, National Oceanography Centre, Southampton, United Kingdom,* [2] *Florida State University, Tallahassee, FL, United States,* [3] *National Oceanography Centre, European Way, Southampton, United Kingdom,* [4] *University Agostinho Neto, Luanda, Angola,* [5] *Academia de Pesca e Ciências do Mar do Namibe, Namibe, Angola*

Edited by:
Toyonobu Fujii,
Tohoku University, Japan

Reviewed by:
Sarah Henkel,
Oregon State University, United States
Dianne McLean,
Australian Institute of Marine Science (AIMS), Australia
Lene Buhl-Mortensen,
Norwegian Institute of Marine Research (IMR), Norway

***Correspondence:**
Daniel O. B. Jones
dj1@noc.ac.uk

Specialty section:
This article was submitted to Marine Ecosystem Ecology, a section of the journal Frontiers in Marine Science

Received: *21 February 2022*
Accepted: *11 May 2022*
Published: *14 June 2022*

Citation:
Biede V, Gates AR, Pfeifer S, Collins JE, Santos C and Jones DOB (2022) Short-Term Response of Deep-Water Benthic Megafauna to Installation of a Pipeline Over a Depth Gradient on the Angolan Slope. Front. Mar. Sci. 9:880453. doi: 10.3389/fmars.2022.880453

Large structures are introduced into deep-water marine environments by several industrial activities, including hydrocarbon exploitation. Anthropogenic structures can alter ecosystem structure and functioning in many marine ecosystems but the responses on continental margins are poorly known. Here, we investigate the short-term response of benthic megafauna to the installation of a 56 km-long 30 cm diameter pipeline on the Angolan Margin (Block 31) from 700 to 1800 m water depth using remotely operated vehicle imagery. Clear depth-related patterns exist in the density, diversity and community structure of megafauna observed in 2013 prior to pipeline installation. These patterns are altered in a subsequent survey in 2014, three-months after pipeline installation. Significant increases in density, particularly in mid-slope regions are observed. Diversity is generally, but not consistently, enhanced, particularly in the shallower areas in 2014. Clear changes are noted in community structure between years. These changes are primarily caused by increases in the abundance of echinoderms, particularly the echinoid *Phormosoma* sp. indet. There was no evidence of colonisation of the pipeline in three months by visible fauna. The few large anemones observed attached to the pipe may be able to move as adults. The pipeline appeared to trap organic material and anthropogenic litter, and may enhance available food resources locally as well as providing hard substratum. These results indicate complex and ecosystem-dependent responses to structure installation and caution against simplistic approaches to environmental management.

Keywords: deep-sea, benthic, succession, colonisation, oil and gas, West Africa, artificial structures, marine litter

INTRODUCTION

Artificial structures in the marine environment alter ecological structure and functioning (Gates et al., 2019). They provide habitat for threatened species (Bell and Smith, 1999), contribute reef habitat (Fowler et al., 2018), enhance recruitment of overfished species (Love et al., 2006), increase connectivity (Henry et al., 2018), often produce considerable fish biomass (Claisse et al., 2014) and provide foraging areas for large predators (Todd et al., 2016). Structures can also have negative effects, such as disturbing seabed habitats and causing increased levels of pollution (Cordes et al., 2016). These effects may vary over time, relating to environmental conditions and stage of ecological succession (Fujii, 2015; Gates et al., 2019; Todd et al., 2019). Consequently, artificial structures have a potential role in restoring degraded marine ecosystems such as coral reefs (Rinkevich, 2014), mollusc reefs (Walles et al., 2016), algal forests (Gianni et al., 2013) and historically trawled or degraded habitats (Bond et al., 2018a), and have been proposed for restoration of disturbed deep-sea habitats (Cuvelier et al., 2018).

Oil and gas industry infrastructure is an important source of artificial hard substratum on continental shelf and slope habitats globally (Fowler et al., 2018). Pipelines may provide long stretches of continuous hard substratum habitat that extend from the shore into the deep ocean (Cordes et al., 2016). There is an initial impact on the seafloor from pipeline construction but pipelines appear to be quickly colonised in shallow water (de Groot, 1982; Lewis et al., 2002; Todd et al., 2019). Colonisation follows clear ecological succession (Gates et al., 2019). The provision of hard substratum by pipelines contributes to elevated biomass and appears to enhance diversity, but these effects vary with depth (Love and York, 2005; McLean et al., 2017; Bond et al., 2018b). The presence of pipelines may act as a barrier to dispersal or as a trap for organic matter (Lebrato and Jones, 2009). These effects have been poorly studied in water deeper than 300 m, although other similar hard substrata are colonised in deeper water (Vinogradov, 2000; Mugge et al., 2019). Knowledge of the nature and duration of succession on artificial structures is valuable for our understanding of deep-sea communities in general but also for assessing the impact of anthropogenic activities in deep-sea environments. The information needed to make these assessments is routinely collected by the oil and gas industry, but is not always accessible to scientists (Macreadie et al., 2018).

The benthic megafauna and fishes of the Angolan margin appear abundant and diverse on a range of substrata (Vardaro et al., 2013; Jones et al., 2014; Jamieson et al., 2017). These organisms are important for the structure and functioning of ecosystems, for example rapidly processing sinking carbon, reworking sediments and increasing structural complexity. Megafaunal responses to changes in the environment vary, mobile species may respond rapidly but energy-limitation typically means colonisation and growth rates are slow (McClain et al., 2012). Quantifiable observations of growth and succession are rare in the deep-ocean (Mullineaux, 1988; Snelgrove et al., 1992) and few if any exist for the south Atlantic.

In this study, we investigate the short-term responses of benthic communities to the introduction of hard substratum in the deep sea. We use an extensive archive of seabed imagery obtained before and 3-months after the installation of a pipeline to determine if the introduction of a structure changes the density (e.g. through attraction), distribution, diversity or community structure of the benthic megafaunal assemblages characteristic of a range of continental slope depths. This will allow more effective assessment of the environmental impacts of structure installation as well as providing insight on the potential effects of introducing hard substratum for marine ecosystem restoration.

METHODS

Study Site

Angolan licence block 31 covers a 5,349 km^2 area of seafloor and became operational in 2012. To the north of the block is the Congo submarine canyon, which directly connects with the Congo River (Droz et al., 2003; Savoye et al., 2009). An estimated average of 55 x10^6 tonnes of suspended sediment, typically laden with particulate and dissolved organic matter, is released annually from the Congo River (Wetzel, 1993; Vangriesheim et al., 2009) and deposited on the seabed from surface-derived flux or diverted through the Congo canyon in episodic turbidity flows (Vangriesheim et al., 2009), with sedimentation rates within the canyon of around 36 cm ka^{-1} near Block 31 (Savoye et al., 2009). In the area of Block 31 the sediments are mostly hemi-pelagic in origin and sedimentation rates are lower at 20 cm ka^{-1} (Hill et al., 2010). The surface waters of Block 31 are characterised by high primary productivity, estimated to be over 200 gCm^{-2} yr^{-1} (Behrenfeld and Falkowski, 1997), driven by river-induced and coastal upwelling (van Bennekom and Berger, 1984; Schneider et al., 1994). The near-seabed water in the area of Block 31 appears to have typical temperatures (~5°C) and salinities (34.9 PSU), as well as high dissolved oxygen concentrations (230 µmol kg^{-1}) (Vangriesheim et al., 2009). Current speeds in Block 31 are low (0.02 to 0.12 m/s) (Hill et al., 2010; Jamieson et al., 2017). Regular and large turbidity currents in the nearby Congo canyon may suspend sediment and organic material into the water column, where they may be transported along the slope (Azpiroz-Zabala et al., 2017).

The benthic biology of the deep waters off Angola has received increasing attention (Sibuet et al., 1989; Vinogradova et al., 1990; Bianchi, 1992; Kröncke and Turkay, 2003; Arbizu and Schminke, 2005; Van Gaever et al., 2009; Jones et al., 2014) and has been the focus for a number of large international programmes with biological components including Latitudinal Gradients of Deep-Sea BioDIVersity in the Atlantic Ocean [DIVA] (Arbizu and Schminke, 2005), ZaiAngo (Savoye et al., 2009), BioZaire (Galéron et al., 2009; Vangriesheim et al., 2009), and Congolobe (Rabouille et al., 2017). These studies have mostly focussed on chemosynthetic systems in the deep bathyal (Sibuet and Olu-LeRoy, 2002; Sibuet and Vangriesheim, 2009) and abyssal (Sen et al., 2017) or deep-water coral reefs on the upper slope (Le Guilloux et al., 2009). Less scientific attention has been directed towards the bathyal (200 – 2000 m) depths of the margin, although this area has been the subject of many environmental assessments by the oil industry (Cazes et al., 2012). Access to the region through oil company activities has permitted some scientific investigations on the scavenging fishes in Block 18 and 31 (Jamieson et al., 2017) and on communities associated with asphalt mounds in Block 31 (Jones et al., 2014). Two permanent scientific observatory platforms were installed at Block 18 to the South East of Block 31 (Vardaro et al., 2013), which are bringing further insights into the deep-water biology of the region (Milligan et al., 2020).

Pipeline Installation and Survey

In February 2014 BP Angola installed a gas export pipeline off the coast of Angola, which extends a total of 56 km from a deep-water manifold in BPs Concession Block 31 (approximately 1800 m water depth, 6°15'S, 10°49'E) to a tie-in manifold in Block 15 (700 m water depth, 6°14'S, 11°17'E). Remotely operated vehicle (ROV) video surveys were carried out prior to installation in December 2013 and after installation in May 2014 (**Figure 1**).

A routine pre-lay inspection of the 56 km long swath of seafloor was recorded by ROV Hercules 18 operated from the pipelay support vessel (PLSV) *Seven Pacific* in December 2013. The ROV was outfitted with a single colour camera and a single black and white camera on a pan and tilt mounting enabling oblique angle viewing. Pre-pipeline installation video survey commenced on December 9th 2013; the last video collected on December 12th 2013. Transect videos were recorded in 30 minute files including position in Easting and Northing (coordinate system Camacupa_TM_11_30_SE), depth (meters), altitude (meters), heading, date, and time. All video was standard definition (720 x 576 pixels). The altitude varied as the ROV recorded above the seafloor and images were scaled using known acceptance angles of the camera (32°) following Jones et al. (2006). The average image width for the pre-pipeline survey was calculated at 2.90 m. Image width was also verified by travelling over objects of known size, such as a drink can, on the seafloor. The video was divided into sections representing 100 m depth intervals. Video from each depth band was segmented at random into three sample units each with 500 m transect length. The sample area was calculated from the average image width and transect length, averaging 1429.21 m^2 in the pre-pipeline survey.

After the installation of the pipeline (pipeline installation was completed on 23 February 2014), an initial inspection survey was done three months after completion in May of 2014 from the same vessel. The ROV travelled along the 304.8 mm (12 inch) diameter pipeline. The ROV remained at a consistent height from the seafloor as it moved on wheels in direct contact with the pipeline. The ROV had three cameras viewing obliquely: one was mounted on the front of the ROV viewing the pipeline ahead, while two were on either side of the ROV recording the sides of the pipeline. The video commenced on May 12th and was completed on May 26th. Transect videos were recorded in the same video format as the 2013 pre-pipeline survey. Images were scaled with reference to the known width of the pipeline. The average image width for the post-pipeline survey was calculated at 2.02 m. The same 500 m samples were selected where possible to the pre-pipeline survey. The area imaged was smaller (reduced altitude survey) averaging 939.76 m^2.

Pipelines were surveyed in a predominantly westerly direction (except in the 700 m depth zone, which were surveyed in an easterly direction) during the pre-installation surveys. The post-installation surveys were surveyed in the opposite direction (**Table 1**).

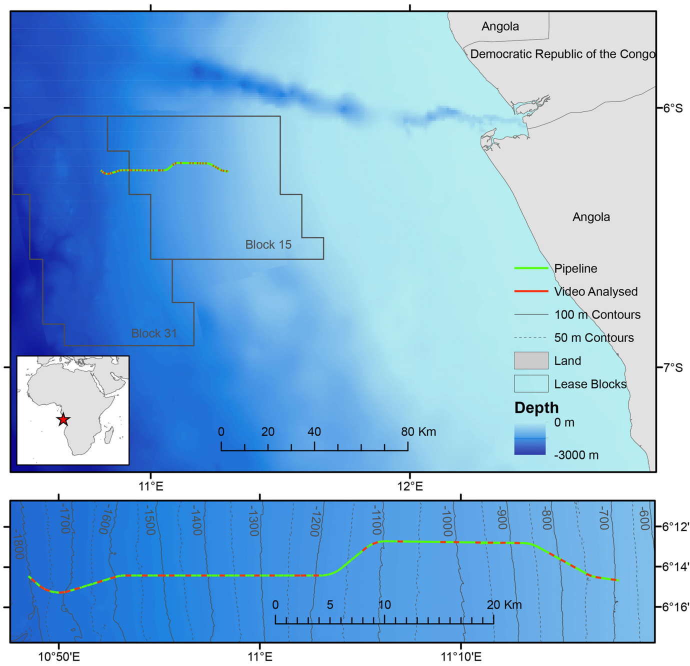

FIGURE 1 | Map showing the location of the survey area in Angola. Contours marked on lower detailed map. Red star on inset map indicates position of survey in west Africa.

Image Annotation

Image annotation was standardized between the two surveys. The order of assessment of individual 500 m transects was randomized to reduce the impact of sequence bias (Durden et al., 2016).

Video files were viewed using VLC Media Player (version 2.2.6, VideoLan Community). For the post-pipeline survey only video from the central camera was used for annotation, ensuring a similar approach to the pre-pipeline survey. The video from the side cameras were used on occasion to confirm identification of organisms. All organisms that were entirely within the field of view were counted and identified within each sample (Durden et al., 2016). Organisms were counted at a constant position near the base of the screen (at a line 150 pixels above the bottom of the frame in 2013 and at the level of laser line in 2014) to ensure observations were made with the highest resolution and best lighting.

An organism only partly within the frame was excluded. Every observation was noted with the time, position, depth, identification, and necessary measurements for area, as well as relative position of the organism from the centre of the field of view or pipeline. Measurements were made from the centre of the pipeline, or screen, to the centre of the organism using ImageJ software (version 1.51s 64-bit, National Institutes of Health). In 2014, when the pipeline was installed and visible in video, it was noted whether the pipeline was buried or exposed. It was also noted if organisms counted were directly on or under the pipeline.

Faunal identifications (morphotypes) were made following a standardised catalogue developed for the region (Pfeifer, 2021) that aligns with existing image-based literature from the area (Vardaro et al., 2013; Jones et al., 2014; Jamieson et al., 2017). Organisms were classified to lowest taxonomic level and named according to WoRMS (Horton et al., 2019). Open nomenclature identifiers (Horton et al., 2021) were used to indicate identifier confidence following the protocol set out for physical specimens (Sigovini et al., 2016).

Video resolution varied along transects (particularly prior to pipeline installation) because of suspended sediment, debris, or altitude variation. Poor quality sections of video were identified, removed from analysis and additional video was analysed at the end of each transect to bring the total length to 500 m. In all cases, any changes in transect location did not bring the data outside of the identified depth zone. A single annotator was used for all video analysis to minimize annotator bias (Durden et al., 2016). Only megafauna greater than 80 mm in maximum diameter were included in analysis to ensure consistent identifications could be made between surveys. Smaller fauna, including amphipods, squat lobsters and other small decapods were very abundant but were not included in analysis. Wholly benthopelagic organisms, such as scyphozoans and ctenophores were commonly observed, but were not included in analysis.

Data Analysis

A range of ecological parameters were calculated for each replicate transect (used as the sampling unit for all analysis). Numerical density (individuals m^{-2}) was calculated for the whole area examined as well as split between the area on the pipe and on the adjacent sediment. To assess the range of diversity characteristics, Hill's diversity numbers of order 0, 1, and 2 (Jost, 2006) standardised by individuals were calculated as morphospecies richness (S), the exponential form of the Shannon index (exp H′), and the inverse form of Simpson's index (1/D), using the 'vegan' package implemented in R (Oksanen et al., 2019). Hill numbers are a mathematically unified family of diversity indices that incorporate species richness and species relative abundances (Chao et al., 2014).

Generalized linear models (GLM) (Dobson and Barnett, 2008) were built to test whether statistically significant variation in biological parameters was apparent between years and 100 m depth bands, using the 'car' package (Fox and Weisberg, 2011) implemented in R (R Core Team, 2020). Models were fitted with quasi-Poisson errors in non-negative integer metrics (i.e. density, S) with over-dispersion (Gardner et al., 1995), and with normal errors applied to non-integer variables (i.e. exp Hí, 1/D) (Freund and Littell, 1981). Homogeneity of variance and normality assumptions were verified by visual inspection of model histograms and QQ plots. Statistical significance was reported for $p < 0.05$.

Differences in community composition between years and depth bands were tested using permutational multivariate analysis of variance (PERMANOVA) based on Bray-Curtis dissimilarity matrix of fourth-root transformed faunal densities, using the 'vegan' package implemented in R. Similarities were visualised using non-metric multi-dimensional scaling (nMDS).

RESULTS

Seabed Environment

The seabed observed prior to pipeline installation comprised soft sediments with abundant bioturbation (<100 mm width pits, tracks and mounds). No hard substratum was observed, apart from the pipeline and anthropogenic litter. Most litter (**Figure 2**) was observed after pipeline installation and over 1500 items were recorded in the 2014 survey (16 items total in the 2013 survey) comprising plastic bags, bottles, buckets and aluminium cans. Litter was relatively abundant (>0.1 litter items m^{-2}) in 2014 between 700 and 1400 m depth (max 0.24 litter items m^{-2} at 1300 -1400 m depth) and the amounts reduced below 1500 m depth (< 0.07 litter items m^{-2}; < 0.03 litter items m^{-2} at >1700 m). Terrigenous vascular plant and algal material was observed very occasionally (3 occurrences) prior to pipeline installation, but regularly observed near the pipeline after installation (>500 occurrences). Drifting particles in the water column showed that currents were predominantly from the north to the south. Most (79%) of the litter accumulated on the downstream (southern) side of the pipeline. However, organic material was approximately evenly distributed (56% on southern side) either side of the pipe.

Density of Megafauna

In both 2013 and 2014 megafaunal density varied significantly with depth (**Table 2**). Before the pipeline was installed megafaunal density was lowest at 1800 m (0.023 ind m^{-2}) and highest at 800 m (0.215 ind m^{-2}) with an additional peak in

TABLE 1 | Positions of remotely operated vehicle transects and approximate movement direction.

Survey	Transect	Survey date	Start Latitude	Start Longitude	End Latitude	End Longitude	Movement Direction
Pre	700C	09/12/2013	-6.24386	11.29090	-6.24448	11.29540	E
Pre	700B	09/12/2013	-6.24198	11.27840	-6.24273	11.28280	E
Pre	700A	09/12/2013	-6.23926	11.27070	-6.24104	11.27490	W
Pre	800C	09/12/2013	-6.23196	11.25760	-6.23418	11.26150	W
Pre	800B	09/12/2013	-6.22740	11.24940	-6.22956	11.25330	W
Pre	800A	10/12/2013	-6.22218	11.23990	-6.22437	11.24390	W
Pre	900C	10/12/2013	-6.21368	11.21110	-6.21376	11.21560	W
Pre	900B	10/12/2013	-6.21353	11.19930	-6.21358	11.20380	W
Pre	900A	10/12/2013	-6.21338	11.18900	-6.21345	11.19350	W
Pre	1000C	10/12/2013	-6.21325	11.17860	-6.21331	11.18310	W
Pre	1000B	10/12/2013	-6.21298	11.16070	-6.21305	11.16520	W
Pre	1000A	10/12/2013	-6.21286	11.14960	-6.21291	11.15410	W
Pre	1100C	10/12/2013	-6.21233	11.11410	-6.21241	11.11860	W
Pre	1100B	11/12/2013	-6.21454	11.09350	-6.21307	11.09780	W
Pre	1100A	11/12/2013	-6.22011	11.08510	-6.21731	11.08860	W
Pre	1200C	11/12/2013	-6.24053	11.04450	-6.24054	11.04900	W
Pre	1200B	11/12/2013	-6.24052	11.03390	-6.24052	11.03840	W
Pre	1200A	11/12/2013	-6.24051	11.02880	-6.24052	11.03330	W
Pre	1300C	11/12/2013	-6.24048	11.00790	-6.24048	11.01240	W
Pre	1300B	11/12/2013	-6.24046	10.99540	-6.24047	10.99990	W
Pre	1300A	11/12/2013	-6.24045	10.98340	-6.24045	10.98790	W
Pre	1300C	11/12/2013	-6.24042	10.96660	-6.24044	10.97110	W
Pre	1300B	11/12/2013	-6.24044	10.95140	-6.24044	10.95590	W
Pre	1400A	11/12/2013	-6.24043	10.93840	-6.24044	10.94290	W
Pre	1500C	11/12/2013	-6.24043	10.92470	-6.24043	10.92920	W
Pre	1500B	11/12/2013	-6.24040	10.91540	-6.24041	10.92200	W
Pre	1500A	11/12/2013	-6.24037	10.90230	-6.24038	10.90680	W
Pre	1600C	11/12/2013	-6.24039	10.88860	-6.24039	10.89320	W
Pre	1600B	12/12/2013	-6.24287	10.87610	-6.24156	10.88040	W
Pre	1600A	12/12/2013	-6.24620	10.86510	-6.24490	10.86940	W
Pre	1700C	12/12/2013	-6.25190	10.84640	-6.25055	10.85070	W
Pre	1700B	12/12/2013	-6.25409	10.83840	-6.25296	10.84280	W
Pre	1700A	12/12/2013	-6.25445	10.83340	-6.25415	10.83800	W
Pre	1800C	12/12/2013	-6.25150	10.82160	-6.25315	10.82580	W
Pre	1800B	12/12/2013	-6.25092	10.82050	-6.25141	10.82140	W
Pre	1800A	12/12/2013	-6.24299	10.81060	-6.24597	10.81400	W
Post	700C	26/05/2014	-6.24448	11.2954	-6.24386	11.29090	W
Post	700B	26/05/2014	-6.24274	11.2828	-6.24206	11.27840	W
Post	700A	26/05/2014	-6.24111	11.2749	-6.23927	11.27070	W
Post	800C	23/05/2014	-6.23197	11.2576	-6.23416	11.26150	E
Post	800B	23/05/2014	-6.22743	11.2493	-6.22960	11.25330	E
Post	800A	23/05/2014	-6.2222	11.2399	-6.22437	11.24390	E
Post	900C	23/05/2014	-6.21368	11.2111	-6.21374	11.21560	E
Post	900B	23/05/2014	-6.21353	11.1993	-6.21362	11.20380	E
Post	900A	22/05/2014	-6.21339	11.189	-6.21345	11.19340	E
Post	1000C	22/05/2014	-6.21324	11.1786	-6.21331	11.18310	E
Post	1000B	22/05/2014	-6.21298	11.1607	-6.21305	11.16520	E
Post	1000A	22/05/2014	-6.21285	11.1496	-6.21289	11.15410	E
Post	1100C	22/05/2014	-6.21232	11.1141	-6.21243	11.11860	E
Post	1100B	22/05/2014	-6.21453	11.0935	-6.21304	11.09780	E
Post	1100A	22/05/2014	-6.22011	11.0851	-6.21731	11.08860	E
Post	1200C	21/05/2014	-6.24053	11.0445	-6.24054	11.04890	E
Post	1200B	21/05/2014	-6.24051	11.0339	-6.24053	11.03840	E
Post	1200A	21/05/2014	-6.24048	11.0288	-6.24051	11.03330	E
Post	1300C	21/05/2014	-6.2405	11.0079	-6.24050	11.01240	E
Post	1300B	21/05/2014	-6.24049	10.9954	-6.24049	10.99990	E
Post	1300A	21/05/2014	-6.24046	10.9834	-6.24049	10.98790	E
Post	1300C	20/05/2014	-6.24042	10.9666	-6.24042	10.97110	E
Post	1300B	20/05/2014	-6.24043	10.9514	-6.24043	10.95590	E
Post	1400A	20/05/2014	-6.24043	10.9384	-6.24041	10.94290	E
Post	1500C	20/05/2014	-6.24042	10.9247	-6.24043	10.92910	E
Post	1500B	20/05/2014	-6.24041	10.9175	-6.24042	10.92190	E
Post	1500A	20/05/2014	-6.24037	10.9023	-6.24037	10.90680	E

(Continued)

TABLE 1 | Continued

Survey	Transect	Survey date	Start Latitude	Start Longitude	End Latitude	End Longitude	Movement Direction
Post	1600C	13/05/2014	-6.24039	10.8886	-6.23028	8.18299	E
Post	1600B	13/05/2014	-6.24286	10.8761	-6.24157	10.88030	E
Post	1600A	13/05/2014	-6.2462	10.8651	-6.24489	10.86940	E
Post	1700C	13/05/2014	-6.25189	10.8464	-6.25063	10.85050	E
Post	1700B	13/05/2014	-6.25409	10.8384	-6.25305	10.84260	E
Post	1700A	13/05/2014	-6.25445	10.8334	-6.25413	10.83820	E
Post	1800C	13/05/2014	-6.2515	10.8216	-6.25349	10.82670	E
Post	1800B	13/05/2014	-6.249	10.8176	-6.25140	10.82140	E
Post	1800A	13/05/2014	-6.24299	10.8106	-6.24593	10.81400	E

Coordinate system World Geodetic System 1984.

density at 1400-1500 m (**Figure 3**). There were significant differences between years (GLM: L-ratio = 12.03, d.f. = 1, $p < 0.001$), depths (L-ratio = 56.74, d.f. = 11, $p < 0.001$) and a significant interaction (L-ratio = 60.62, d.f. = 11, $p < 0.05$) – indicating that the pattern with depth changed between years. In 2014, when the pipeline was present, megafaunal density was significantly higher overall than the 2013 survey particularly at 900 – 1200 m and 1800 m depth.

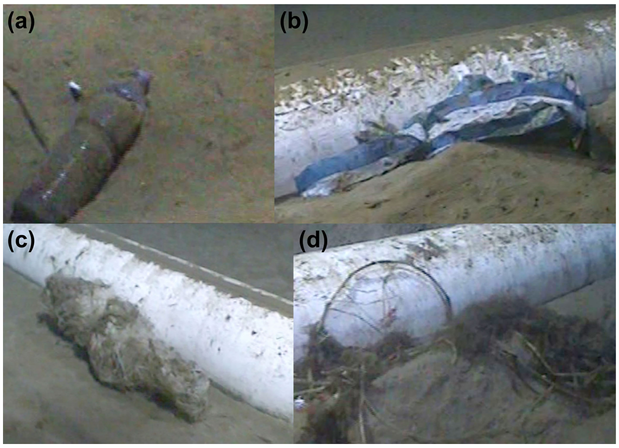

FIGURE 2 | Selected pipeline associations. **(A)** Plastic bottle c. 730 m; **(B)** Plastic bag c. 1333 m; **(C)** Fishing net c. 1696 m; **(D)** Plant debris c. 1768 m.

In 2013, the benthic megafauna (**Figure 4**) were evenly distributed across the width of the transect (**Figure 5**). After the installation of the pipeline, the distribution of animals changed. In 2014 a total of 132 individuals were observed on the pipeline itself (overall density = 0.02 ind m^{-2}) but there were not sufficient individuals to address patterns with depth. On the adjacent sediment a total of 5496 individuals were observed (overall density = 0.17 ind m^{-2}). The density was significantly higher than on the pipeline itself and the 2013 seabed once the depth variation had been accounted for (GLM: L-ratio = 87.95, d.f. = 2, $p<0.001$) but organisms were distributed close to the margin of the pipe (**Figures 4**, **5**).

Patterns in Individual Species

The most abundant organism was the echinoid *Phormosoma* sp. indet., almost all the individuals of this morphotype occurred between 800 and 1100 m depth and it was around an order of magnitude more abundant in 2014 than in 2013. *Phormosoma* sp. indet. (example image in **Figure 4D**) was particularly abundant at the edge of the pipeline. In 2014, densities tended to be several times higher on the north side of the pipeline, except at 1000 - 1100 m where abundances were nearly an order of

TABLE 2 | Depth-related patterns in density and morphospecies richness (number of morphospecies observed) both before (pre) and after (post) pipeline installation.

Depth, m	Density pre, no. m^{-2}	Density post off pipe, no. m^{-2}	Density post on pipe, no. m^{-2}	Total morphospecies pre	Total morphospecies post off pipe	Total morphospecies post on pipe	Area pre, m^2	Area post on pipe, m^2	Area post off pipe, m^2
700	0.116	0.155	0.052	26	33	10	4323	458	2536
800	0.215	0.180	0.033	29	27	10	4299	458	2623
900	0.054	0.188	0.028	24	30	8	4129	458	2612
1000	0.037	0.691	0.048	19	26	11	4622	458	2599
1100	0.074	0.327	0.026	26	32	5	4241	458	2600
1200	0.045	0.122	0.024	26	35	8	3569	458	2533
1300	0.042	0.067	0.015	33	30	5	4032	458	2526
1400	0.140	0.080	0.011	28	32	4	4429	458	2549
1500	0.091	0.061	0.024	30	23	9	3834	458	2602
1600	0.036	0.036	0.007	26	20	3	4098	458	2435
1700	0.034	0.052	0.009	25	20	2	4627	458	2428
1800	0.023	0.082	0.011	22	25	4	4693	458	2446

The data for after pipeline installation are split between the organisms observed living on and off the pipeline. The area of each set of observations made at each depth is recorded. The 2013 survey covered a greater area of seafloor (50,898 m^2) than the 2014 survey (34,940 m^2). A total of 3845 individual organisms were recorded in 2013 and 5391 individuals in 2014.

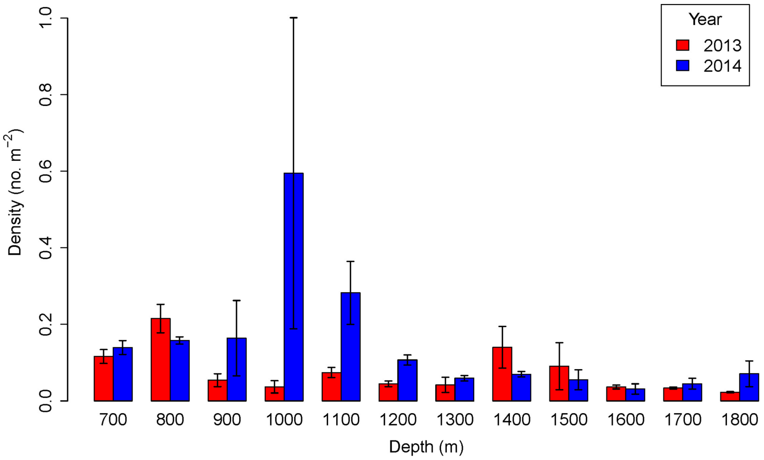

FIGURE 3 | Density variation with depth before (2013) and after (2014) pipeline installation. Error bars represent standard deviations.

magnitude higher on the south side. Although it was harder to detect an elevation in abundances close to the pipe in less abundant taxa, there is some evidence of increased abundances (approximately double the average frequency) of two large holothurians *Paelopatides* sp. indet. (most abundant >1200 m) and *Benthothuria* sp. indet. 1 (most abundant <1000 m, **Figure 4I**) adjacent to the pipe. Other echinoderms, such as ophiuroids and asteroids, were more evenly distributed with distance from the pipeline. Many taxa showed increased abundances at particular depth ranges, for example ophiuroids (second most abundant taxon - comprising several species) were almost exclusively found at 700 – 800 m and 1700 – 1800 m depth (see **Supplementary Table**). Many, but not all, taxa, for example asteroids, Bythitidae stet. and Zoarcids (Pachycara sp.

FIGURE 4 | Selected morphotypes visible in survey. **(A)** *Actinostolidae* gen. indet.; **(B)** *Actinoscyphia* sp. indet. 1; **(C)** *Actinoscyphia* sp. indet. 2; **(D)** *Polycheles* sp. indet. 1; **(E)** Lithodidae stet.; **(F)** Decapoda natant fam. indet. 2; **(G)** *Phormosoma* sp. indet.; **(H)** Ophiuroidea ord. indet.; **(I)** *Benthothuria* sp. indet. 1; **(J)** Holothuroidea ord. indet. 4; **(K)** Brisingida stet.; **(L)** Asteroidea ord. indet. 2; **(M)** *Pachycara* sp. indet.; **(N)** *Eurypharynx* sp. indet. 1; **(O)** Macrouridae gen. indet. 3; **(P)** Bythitidae stet.

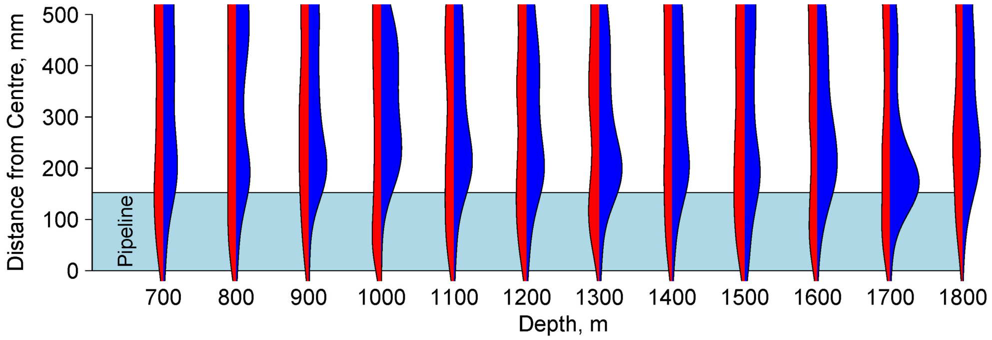

FIGURE 5 | Beanplot of density of megafauna prior to pipeline installation (red; left hand side of each plot) and after pipeline installation (blue; right hand side of each plot) relative to centre of the transect for each depth zone. In 2014 this was aligned with the pipeline axis. The extent of the pipeline (at 153 mm from the centre) is shown as a light blue polygon. The density trace is smoothed using a Gaussian smoother. The increased densities of megafauna close to the edge of the pipeline are visible at all depths after pipeline installation but not before.

indet.), had higher densities in 2014 than 2013 (**Figures 4M, P**). Notable exceptions, with higher densities in 2013, include ophiuroids, *Psychropotidae* indet. and *Peniagone* sp. indet.

Only 30 individual sessile animals were observed on the pipeline, these comprised *Actinoscyphia* sp. indet. 1 (12 individuals; 36% total observations; **Figure 4B**), Actinaria indet. 5 (9 individuals; 41% total observations), Anthozoa indet. 2 (4 individuals; 44% total observations), *Actinoscyphia* sp. indet. 2 (4 individuals; 21% total observations; **Figure 4C**) and Actinaria indet. 1 (1 individual; from a total of 53 individuals). These animals were large (Actinaria indet. 1, the largest, was up to 200 mm diameter) and were visibly attached to the pipe. When the anemones came into contact with the wheels that directed the ROV along the pipeline they were detached easily at the base of the column.

Diversity Patterns

There were significant differences in species richness between years (GLM: L-ratio = 10.64, d.f. = 1, p<0.01), depths (GLM: L-ratio = 61.33, d.f. = 11, p<0.001) and the interaction (GLM: L-ratio = 28.87, d.f. = 11, p<0.001). Species richness was generally higher in 2014, after the pipeline was installed (**Figure 6**), particularly at depths between 700 and 1100-1200 m. Deeper than 1200 m species richness was similar between the years. In 2013, species richness varied with depth with peaks at around 800 m and 1300 m depth. In 2014 species richness was approximately constant between 700 and 1200 m depth, decreasing at deeper depths.

Exponential Shannon diversity was not significantly different between years (GLM: L-ratio = 0.47, d.f. = 1, p = 0.5) but was different between depths (GLM: L-ratio: 68.73, d.f. = 11, p < 0.001). There was broadly higher diversity, as measured by exponential Shannon, at 1200 – 1800 m depth than shallower, although there was an exception at 1400 m in 2013 (**Figure 6**). Inverse Simpson diversity shows a very similar pattern to exponential Shannon diversity.

Community Structure

Overall, the community composition varied significantly between years (PERMANOVA: Pseudo-F=21.41, df = 1, p < 0.001), depths (Pseudo-F=8.12, df = 11, p < 0.001) and the interaction between year and depth (Pseudo-F = 2.40, df = 11, p < 0.001). The difference between the years is particularly striking, with clear dissimilarity between years (**Figure 7**). In both years, the multivariate community similarity shows a gradient of change with depth (**Figure 7**). Although the gradient is similar

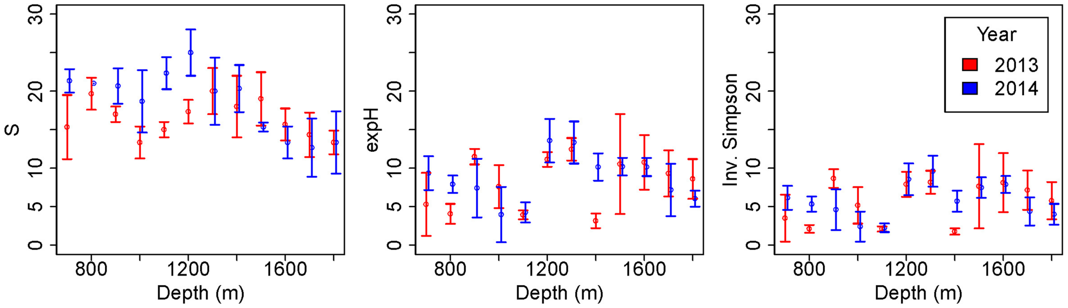

FIGURE 6 | Diversity variation with depth before (2013) and after (2014) pipeline installation. Error bars represent standard deviations. Diversity measured as species richness (S), exponential Shannon index (expH) and inverse Simpson index (Inv. Simpson) following Hill (Hill, 1973).

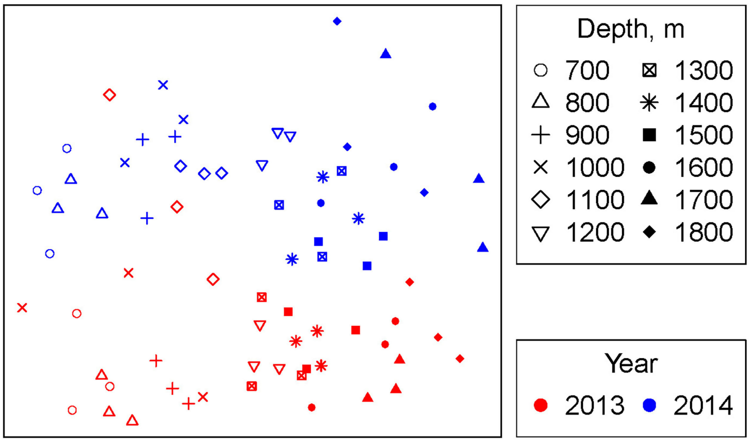

FIGURE 7 | Non-metric multidimensional scaling ordination. MDS stress = 0.23.

before and after pipeline installation the significant interaction indicates differences between the depth patterns in 2013 and 2014. The most distinct communities (by Bray-Curtis dissimilarity) were in the shallowest sites in 2013 (700-900 m) and the deepest in 2014 (1600-1800 m), although there was a gradual increase in dissimilarity with increasing depth difference between sites.

DISCUSSION

The introduction of a large pipeline structure into the deep-sea environment off Angola has likely resulted in changes in megabenthic communities, particularly at mid-slope depths. This is perhaps surprising as the pipeline had only been in place for three months. The effects of natural seasonal variability in benthic communities, as occur in fishes off Angola (Milligan et al., 2020), cannot be excluded. The pipeline appeared to cause elevated densities of many fauna, both at the broader scale (between surveys) and at a fine scale (more organisms were found nearer the pipe), which was a result of aggregations of motile fauna, potentially in response to the shelter provided or elevated organic material trapped by expected hydrodynamic changes induced by the pipeline. These hydrodynamic processes may have helped aggregate the fauna themselves, as likely occurred with the increased quantity of litter in 2014, although wide ranging movements are possible in many of the taxa observed (Miller and Pawson, 1990). Organic enrichment and faunal aggregation was also found associated with a pipeline on the margin of Ivory Coast (Lebrato and Jones, 2009), to the north of Angola. Despite the large geographic separation of > 2000 km between Ivory Coast and Angola, several similar morphospecies aggregated at the pipeline in both studies, notably the abundant *Phormosoma* sp. indet. echinoids (Lebrato and Jones, 2009). Benthic megafauna in the deep sea can respond rapidly to spatio-temporally variable food resources (Billett et al., 2001). There are also possible seasonal migrations of organisms in response to varying organic matter, as suggested for fishes very close to this site in Angola (Milligan et al., 2020). Some natural temporal variation in the fauna may be unrelated to the pipeline installation, but the only faunal time-series observations in this region show higher abundances of fishes in the austral summer (i.e. around the time of the pre-installation survey in December) than in the austral winter (at around the same time as the post-installation survey in May). This is the opposite trend to that observed in this study, possibly indicating that the elevations in density are happening in spite of natural variation rather than because of it.

There was little evidence of megafaunal colonisation on the pipeline. The few taxa found apparently attached to the pipeline are principally actiniarians, primarily of the genus *Actinoscyphia*. Some deep-sea actiniarians, including *Actinoscyphia*, are unattached and likely capable of movement to find optimal food resources (Aldred et al., 1979). Little recruitment would be expected in a three-month period. At a similar depth in the Pacific, introduced structures attracted new recruits of mostly meiofaunal taxa within weeks (Mullineaux, 1988). Even if new recruits were present, growth rates at comparable depths are typically too slow (Mercier et al., 2017; Girard et al., 2019) for individuals to reach a size that could be resolved in the ROV images in three months. It is also possible that recruitment would be higher on the hidden underside of the pipeline (where this was not covered in sediment) than the exposed top (Mullineaux, 1988), but that was not possible to detect in this study. The little available information on hard substrata on the Angolan margin shows a broad range of attached fauna and associated mobile fauna, with several species of mobile fauna common to this study (Le Guilloux et al., 2009; Jones et al., 2014).

The depth-related changes in megafaunal abundance, diversity and community composition observed here do not show any clear monotonic patterns, rather a mid-bathyal peak in abundance and possibly diversity, particularly in the 2014 survey. Depth-related patterns in the fauna of the Angolan margin appear to be typical, as in other areas (Carney, 2005), potentially related to transition zones between overlapping faunal components. The sediment-dwelling macrofauna in Angola show a similar mid-bathyal peak in abundance and species diversity (Cazes et al., 2012) to that found here. There was also high turnover with depth reported in the Angolan fishes, for example in Rajidae (Compagno and Ebert, 2009) and virtually no overlap (only the hagfish *Myxine ios*) in fishes collected at shallower below 800 m (277 species) (Tweddle and Anderson, 2008) compared to deeper (1297-2453 m) areas (Jamieson et al., 2017). Many of the fishes observed here, including the common Halosauridae, Macrouridae and Synaphobranchidae, appear to correspond to those found in these studies, but lack of species-level identification here prevents full comparison. Unlike for the other groups investigated, scavenging amphipods showed no clear difference with depth on the Angolan Margin (Duffy et al., 2016).

In conclusion, this study demonstrates that the installation of a pipeline may cause considerable changes in the fauna in some areas of the continental slope. These changes are very depth dependent and likely depend on both the nature of the community and the potential for trapping of organic matter by the pipeline. It is likely that the results presented here are only an early stage in a succession of ecological change resulting from installation of a pipeline in deep water, with later stages largely unknown. The sediment underlying the pipeline here was soft sediment and it is unknown if there were any disturbance related effects. In many areas, including deep-water areas, the damage of the seafloor created by pipeline installation may lead to more complex and more negative effects than observed here. The results presented here may provide some useful information for environmental managers assessing the potential impacts of pipeline installation and for those assessing the potential mitigation or restoration value of introducing structures into the deep sea. The complex ecological responses and dependency on the community and environmental conditions present suggest careful ecological assessment is needed to inform environmental management decisions.

DATA AVAILABILITY STATEMENT

The original contributions presented in the study are included in the article/**Supplementary Material**. Further inquiries can be directed to the corresponding author.

AUTHOR CONTRIBUTIONS

DJ and AG conceived the study and developed the approach. VB analysed video with the help of AG, SP, CS, JC and DJ. SP, DJ and CS helped identify megafauna. DJ and VB carried out data analysis. DJ wrote the original draft of this paper based on thesis written by VB and JC. All authors contributed to the article and approved the submitted version.

FUNDING

This project was supported through the European Union's Horizon 2020 Research and Innovation Program under the MERCES (Marine Ecosystem Restoration in Changing European Seas) project, grant agreement no. 689518. This work was also supported by the United Kingdom Natural Environment Research Council (NERC) grant "Advanced monitoring of marine infrastructure for decommissioning" reference NE/P016561/1, "Sustained Autonomous Monitoring of Offshore Oil and Gas" reference NE/S009426/1 and the NERC National Capability funding to the National Oceanography Centre, as part of the Climate Linked Atlantic Section Science (CLASS) program (Grant Number NE/R015953/1). SP was supported by the United Kingdom Natural Environmental Research Council (grant number NE/L002531/1), and a CASE studentship 'Collaborative Awards in Science and Engineering' with BP.

ACKNOWLEDGMENTS

We thank BP Angola for providing access to these data. We also thank Subsea 7 for facilitating access to data. The authors would like to thank Dr Mike Clare at the National Oceanography Centre for valuable discussions on the environment of the region.

SUPPLEMENTARY MATERIAL

The Supplementary Material for this article can be found online at: https://www.frontiersin.org/articles/10.3389/fmars.2022.880453/full#supplementary-material

REFERENCES

Aldred, R. G., Riemann-Zurneck, K., Thiel, H., and Rice, A. L. (1979). Ecological Observations on the Deep Sea Anemone *Actinoscyphia Aurelia*. *Oceanolog. Acta.* 2, 389–395.

Arbizu, P. M., and Schminke, H. K. (2005). DIVA-1 Expedition to the Deep Sea of the Angola Basin in 2000 and DIVA-1 Workshop in 2003. *Org. Divers. Evol.* 5 (Supplement 1), 1–2. doi: 10.1016/j.ode.2004.11.009

Azpiroz-Zabala, M., Cartigny, M. J. B., Talling, P. J., Parsons, D. R., Sumner, E. J., Clare, M. A., et al. (2017). Newly Recognized Turbidity Current Structure can Explain Prolonged Flushing of Submarine Canyons. *Sci. Adv.* 3 (10), e1700200. doi: 10.1126/sciadv.1700200

Behrenfeld, M. J., and Falkowski, P. G. (1997). Photosynthetic Rates Derived From Satellite-Based Chlorophyll Concentration. *Limnol. Oceanogr.* 42 (1), 1–20. doi: 10.4319/lo.1997.42.1.0001

Bell, N., and Smith, J. (1999). Coral Growing on North Sea Oil Rigs. *Nature* 402 (6762), 601–601. doi: 10.1038/45127

Bianchi, G. (1992). Demersal Assemblages of the Continental-Shelf and Upper Slope of Angola. *Marine Ecol-Progress Ser.* 81 (2), 101–120. doi: 10.3354/meps081101

Billett, D. S. M., Bett, B. J., Rice, A. L., Thurston, M. H., Galeron, J., Sibuet, M., et al. (2001). Long-Term Change in the Megabenthos of the Porcupine Abyssal Plain (NE Atlantic). *Prog. Oceanogr.* 50, 325–348. doi: 10.1016/S0079-6611(01)00060-X

Bond, T., Langlois, T. J., Partridge, J. C., Birt, M. J., Malseed, B. E., Smith, L., et al. (2018a). Diel Shifts and Habitat Associations of Fish Assemblages on a Subsea Pipeline. *Fish Res.* 206, 220–234. doi: 10.1016/j.fishres.2018.05.011

Bond, T., Partridge, J. C., Taylor, M. D., Cooper, T. F., and McLean, D. L. (2018b). The Influence of Depth and a Subsea Pipeline on Fish Assemblages and Commercially Fished Species. *PLos One* 13 (11), e0207703. doi: 10.1371/journal.pone.0207703

Carney, R. S. (2005). Zonation of Deep Biota on Continental Margins. *Oceanogr. Marine Biol. Annu. Rev.* 43, 211–278. doi: 10.1201/9781420037449.ch6

Cazes, L., Plisson-Saune, S., Canovas, S., Bamber, R., and Robbins, R. (2012). "Angola Biodiversity of Bathyal Sea Bottoms," in *International Conference on Health, Safety and Environment in Oil and Gas Exploration and Production*, September 2012. (Perth, Australia: Society of Petroleum Engineers), 11–13.

Chao, A., Chiu, C.-H., and Jost, L. (2014). Unifying Species Diversity, Phylogenetic Diversity, Functional Diversity, and Related Similarity and Differentiation Measures Through Hill Numbers. *Annu. Rev. Ecol. Evol. Syst.* 45 (1), 297–324. doi: 10.1146/annurev-ecolsys-120213-091540

Claisse, J. T., Pondella, D. J., Love, M., Zahn, L. A., Williams, C. M., Williams, J. P., et al. (2014). Oil Platforms Off California are Among the Most Productive Marine Fish Habitats Globally. *Proc. Natl. Acad. Sci.* 111 (43), 15462–15467. doi: 10.1073/pnas.1411477111

Compagno, L. J. V., and Ebert, D. A. (2009). "Southern African Skate Biodiversity and Distribution," in *Biology of Skates*. Eds. D. A. Ebert and J. A. Sulikowski (Dordrecht: Springer Netherlands), 19–39.

Cordes, E., Jones, D., Schlacher, T., Amon, D., Bernardino, A., Brooke, S., et al. (2016). Environmental Impacts of the Deep-Water Oil and Gas Industry: A Review to Guide Management Strategies. *Front. Environ. Sci.* 4(58). doi: 10.3389/fenvs.2016.00058

Cuvelier, D., Gollner, S., Jones, D. O. B., Kaiser, S., Arbizu, P. M., Menzel, L., et al. (2018). Potential Mitigation and Restoration Actions in Ecosystems Impacted by Seabed Mining. *Front. Marine Sci.* 5, 467. doi: 10.3389/fmars.2018.00467

de Groot, S. J. (1982). The Impact of Laying and Maintenance of Offshore Pipelines on the Marine Environment and the North Sea Fisheries. *Ocean Manage.* 8 (1), 1. doi: 10.1016/0302-184X(82)90011-7

Dobson, A. J., and Barnett, A. G. (2008). *An Introduction to Generalized Linear Models*. London: Chapman & Hall.

Droz, L., Marsset, T., Ondréas, H., Lopez, M., Savoye, B., and Spy-Anderson, F.-L. (2003). Architecture of an Active Mud-Rich Turbidite System: The Zaire Fan (Congo–Angola Margin Southeast Atlantic). *Aapg Bull.* 87 (7), 1145–1168. doi: 10.1306/03070300013

Duffy, G. A., Lawler, S. F., and Horton, T. (2016). Scavenging Amphipods of the Angolan Deep-Sea Habitat, With a Focus on (Birstein and Vinogradov 1960) (Amphipoda: Lysianassoidea). *J. Crustacean Biol.* 36 (4), 417–426. doi: 10.1163/1937240X-00002448

Durden, J. M., Schoening, T., Althaus, F., Friedman, A., Garcia, R., Glover, A., et al. (2016). Perspectives in Visual Imaging for Marine Biology and Ecology: From Acquisition to Understanding. *Oceanogr Marine Biol: Annu. Rev.* 54, 1–72. doi: 10.1201/9781315368597-2

Fowler, A. M., Jørgensen, A.-M., Svendsen, J. C., Macreadie, P. I., Jones, D. O. B., Boon, A. R., et al. (2018). Environmental Benefits of Leaving Offshore Infrastructure in the Ocean. *Front. Ecol. Environ.* 16 (10), 571–578. doi: 10.1002/fee.1827

Fox, J., and Weisberg, S. (2011). *An {R} Companion to Applied Regression. Second Edition*. Thousand Oaks CA: Sage.

Freund, R. J., and Littell, R. C. (1981). *SAS for Linear Models: A Guide to the ANOVA and GLM Procedures*. Cary, North Carolina: Sas Institute.

Fujii, T. (2015). Temporal Variation in Environmental Conditions and the Structure of Fish Assemblages Around an Offshore Oil Platform in the North Sea. *Marine Environ. Res.* 108, 69–82. doi: 10.1016/j.marenvres.2015.03.013

Galéron, J., Menot, L., Renaud, N., Crassous, P., Khripounoff, A., Treignier, C., et al. (2009). Spatial and Temporal Patterns of Benthic Macrofaunal Communities on the Deep Continental Margin in the Gulf of Guinea. *Deep Sea Res. Part II: Topical Stud. Oceanogr* 56 (23), 2299–2312. doi: 10.1016/j.dsr2.2009.04.011

Gardner, W., Mulvey, E. P., and Shaw, E. C. (1995). Regression Analyses of Counts and Rates: Poisson, Overdispersed Poisson, and Negative Binomial Models. *psychol. Bull.* 118 (3), 392–404. doi: 10.1037/0033-2909.118.3.392

Gates, A. R., Horton, T., Serpell-Stevens, A., Chandler, C., Grange, L. J., Robert, K., et al. (2019). Ecological Role of an Offshore Industry Artificial Structure. *Front. Marine Sci.* 6. doi: 10.3389/fmars.2019.00675

Gianni, F., Bartolini, F., Airoldi, L., Ballesteros, E., Francour, P., Guidetti, P., et al. (2013). Conservation and Restoration of Marine Forests in the Mediterranean Sea and the Potential Role of Marine Protected Areas. *Adv. Oceanogr Limnol* 4 (2), 83–101. doi: 10.4081/aiol.2013.5338

Girard, F., Cruz, R., Glickman, O., Harpster, T., and Fisher, C. R. (2019). *In Situ* Growth of Deep-Sea Octocorals After the Deepwater Horizon Oil Spill. *Elementa: Sci. Anthropocene* 7, 12. doi: 10.1525/elementa.349

Henry, L. A., Mayorga-Adame, C. G., Fox, A. D., Polton, J. A., Ferris, J. S., McLellan, F., et al. (2018). Ocean Sprawl Facilitates Dispersal and Connectivity of Protected Species. *Sci. Rep* 8, 11346. doi: 10.1038/s41598-018-29575-4

Hill, M. O. (1973). Diversity and Evenness: A Unifying Notation and Its Consequences. *Ecology* 54 (2), 427–432. doi: 10.2307/1934352

Hill, A. J., Southgate, J. G., Fish, P. R., and Thomas, S. (2010). "Deepwater Angola Part I," in *Frontiers in Offshore Geotechnics II*. Eds. S. Gourvenec and D. White (London: CRC Press), 209–214.

Horton, T., Kroh, A., Ahyong, S., Bailly, N., Boyko, C. B., Brandão, S. N., et al. (2019). World Register of Marine Species (WoRMS). *WoRMS Editorial Board*. Accessed 2022-05-23. doi: 10.14284/170

Horton, T., Kroh, A., Ahyong, S., Bailly, N., Boyko, C. B., Brandão, S. N., et al. *World Register of Marine Species*. Available at: https://www.marinespecies.org at VLIZ. (Accessed 2022-05-23).

Jamieson, A. J., Linley, T. D., and Craig, J. (2017). Baited Camera Survey of Deep-Sea Demersal Fishes of the West African Oil Provinces Off Angola: 1200-2500m Depth, East Atlantic Ocean. *Mar Environ. Res.* 129, 347–364. doi: 10.1016/j.marenvres.2017.05.009

Jones, D. O. B., Hudson, I. R., and Bett, B. J. (2006). Effects of Physical Disturbance on the Cold-Water Megafaunal Communities of the Faroe-Shetland Channel. *Marine Ecol. Prog. Ser.* 319, 43–54. doi: 10.3354/meps319043

Jones, D. O. B., Walls, A., Clare, M., Fiske, M. S., Weiland, R. J., O'Brien, R., et al. (2014). Asphalt Mounds and Associated Biota on the Angolan Margin. *Deep Sea Res. Part I: Oceanographic Res. Papers* 94, 124–136. doi: 10.1016/j.dsr.2014.08.010

Jost, L. (2006). Entropy and Diversity. *Oikos* 113 (2), 363–375. doi: 10.1111/j.2006.0030-1299.14714.x

Kröncke, I., and Turkay, M. (2003). Structural and Functional Aspects of the Benthic Communities in the Deep Angola Basin. *Marine Ecol. Prog. Ser.* 260, 43–53. doi: 10.3354/meps260043

Lebrato, M., and Jones, D. O. B. (2009). Mass Deposition Event of *Pyrosoma Atlanticum* Carcasses Off Ivory Coast (West Africa). *Limnol. Oceanogr.* 54 (4), 1197–1209. doi: 10.4319/lo.2009.54.4.1197

Le Guilloux, E., Olu, K., Bourillet, J. F., Savoye, B., Iglésias, S. P., and Sibuet, M. (2009). First Observations of Deep-Sea Coral Reefs Along the Angola Margin. *Deep Sea Res. Part II: Topical Stud. Oceanogr.* 56 (23), 2394–2403. doi: 10.1016/j.dsr2.2009.04.014

Lewis, L. J., Davenport, J., and Kelly, T. C. (2002). A Study of the Impact of a Pipeline Construction on Estuarine Benthic Invertebrate Communities. *Estuar Coastal Shelf Sci.* 55 (2), 213–221. doi: 10.1006/ecss.2001.0898

Love, M. S., Schroeder, D. M., Lenarz, W., MacCall, A., Bull, A. S., and Thorsteinson, L. (2006). Potential Use of Offshore Marine Structures in Rebuilding an Overfished Rockfish Species, Bocaccio (*Sebastes Paucispinis*). *Fish Bull.* 104 (3), 383–390.

Love, M. S., and York, A. (2005). A Comparison of the Fish Assemblages Associated With an Oil/Gas Pipeline and Adjacent Seafloor in the Santa Barbara Channel, Southern California Bight. *Bull. Marine Sci.* 77 (1), 101–117.

Macreadie, P. I., McLean, D. L., Thomson, P. G., Partridge, J. C., Jones, D. O. B., Gates, A. R., et al. (2018). Eyes in the Sea: Unlocking the Mysteries of the Ocean Using Industrial, Remotely Operated Vehicles (ROVs). *Sci. Total Environ.* 634, 1077–1091. doi: 10.1016/j.scitotenv.2018.04.049

McClain, C. R., Allen, A. P., Tittensor, D. P., and Rex, M. A. (2012). Energetics of Life on the Deep Seafloor. *Proc. Natl. Acad. Sci.* 109 (38), 15366–15371. doi: 10.1073/pnas.1208976109

McLean, D. L., Partridge, J. C., Bond, T., Birt, M. J., Bornt, K. R., and Langlois, T. J. (2017). Using Industry ROV Videos to Assess Fish Associations With Subsea Pipelines. *Continental Shelf Res.* 141 (Supplement C), 76–97. doi: 10.1016/j.csr.2017.05.006

Mercier, A., Baillon, S., Daly, M., Macrander, J., and Hamel, J.-F. (2017). Biology of a Deep-Water Sea Anemone (Anthozoa: Actiniidae) From Eastern Canada: Spawning, Development, and Growth. *Deep Sea Res. Part II: Topical Stud. Oceanogr.* 137, 359–367. doi: 10.1016/j.dsr2.2016.01.006

Miller, J. E., and Pawson, D. L. (1990). Swimming Sea Cucumbers (Echinodermata: Holothuroidea): A Survey, With Analysis of Swimming Behavior in Four Bathyal Species. *Smithsonian Contributions to Marine Sci.* 35, 1–18. doi: 10.5479/si.01960768.35.1

Milligan, R. J., Scott, E. M., Jones, D. O. B., Bett, B. J., Jamieson, A. J., O'Brien, R., et al. (2020). Evidence for Seasonal Cycles in Deep-Sea Fish Abundances: A Great Migration in the Deep SE Atlantic? *J. Anim. Ecol.* 89 (7), 1593–1603. doi: 10.1111/1365-2656.13215

Mugge, R. L., Brock, M. L., Salerno, J. L., Damour, M., Church, R. A., Lee, J. S., et al. (2019). Deep-Sea Biofilms, Historic Shipwreck Preservation and the Deepwater Horizon Spill. *Front. Marine Sci.* 6 (48). doi: 10.3389/fmars.2019.00048

Mullineaux, L. S. (1988). The Role of Settlement in Structuring a Hard-Substratum Community in the Deep Sea. *J. Exp. Marine Biol. Ecol.* 120 (3), 247–261. doi: 10.1016/0022-0981(88)90005-6

Oksanen, J., Blanchet, F. G., Kindt, R., Legendre, P., O'Hara, R. B., Simpson, G. L., et al. (2019). "Vegan: Community Ecology Package," in *R Package Version 2.5-6.* Available at: http://CRAN.R-project.org/package=vegan.

Pfeifer, S. (2021). Megabenthic Ecology of the Angolan Continental Slope. PhD Thesis. Southampton: University of Southampton.

Rabouille, C., Olu, K., Baudin, F., Khripounoff, A., Dennielou, B., Arnaud-Haond, S., et al. (2017). The Congolobe Project, a Multidisciplinary Study of Congo Deep-Sea Fan Lobe Complex: Overview of Methods, Strategies, Observations and Sampling. *Deep Sea Res. Part II: Topical Stud. Oceanogr* 142, 7–24. doi: 10.1016/j.dsr2.2016.05.006

R Core Team (2020). *R: A Language and Environment for Statistical Computing* (Vienna, Austria: R Foundation for Statistical Computing).

Rinkevich, B. (2014). Rebuilding Coral Reefs: Does Active Reef Restoration Lead to Sustainable Reefs? *Curr. Opin. Environ. Sustainability* 7, 28–36. doi: 10.1016/j.cosust.2013.11.018

Savoye, B., Babonneau, N., Dennielou, B., and Bez, M. (2009). Geological Overview of the Angola–Congo Margin, the Congo Deep-Sea Fan and its Submarine Valleys. *Deep Sea Res. Part II: Topical Stud. Oceanogr* 56 (23), 2169–2182. doi: 10.1016/j.dsr2.2009.04.001

Schneider, R. R., Müller, P. J., and Wefer, G. (1994). Late Quaternary Paleoproductivity Changes Off the Congo Deduced From Stable Carbon Isotopes of Planktonic Foraminifera. *Palaeogeogr Palaeoclimatol Palaeoecol.* 110 (3), 255–274. doi: 10.1016/0031-0182(94)90087-6

Sen, A., Dennielou, B., Tourolle, J., Arnaubec, A., Rabouille, C., and Olu, K. (2017). Fauna and Habitat Types Driven by Turbidity Currents in the Lobe Complex of the Congo Deep-Sea Fan. *Deep Sea Res. Part II: Topical Stud. Oceanogr.* 142, 167–179. doi: 10.1016/j.dsr2.2017.05.009

Sibuet, M., Lambert, C. E., Chesselet, R., and Laubier, L. (1989). Density of the Major Size Groups of Benthic Fauna and Trophic Input in Deep Basins of the Atlantic Ocean. *J. Marine Res.* 47 (4), 851–867. doi: 10.1357/002224089785076064

Sibuet, M., and Olu-LeRoy, K. (2002). "Cold Seep Communities on Continental Margins: Structure and Quantitative Distribution Relative to Geological and Fluid Venting Patterns," in *Ocean Margin Systems*. Eds. G. Wefer, D. Hebbeln, B. B. Jorgensen and T. Van Weering (Berlin: Springer), 235–251.

Sibuet, M., and Vangriesheim, A. (2009). Deep-Sea Environment and Biodiversity of the West African Equatorial Margin. *Deep Sea Res. Part II: Topical Stud. Oceanogr.* 56 (23), 2156–2168. doi: 10.1016/j.dsr2.2009.04.015

Sigovini, M., Keppel, E., and Tagliapietra, D. (2016). Open Nomenclature in the Biodiversity Era. *Methods Ecol. Evol.* 7 (10), 1217–1225. doi: 10.1111/2041-210X.12594

Snelgrove, P. V. R., Grassle, J. F., and Petrecca, R. F. (1992). The Role of Food Patches in Maintaining High Deep-Sea Diversity - Field Experiments With Hydrodynamically Unbiased Colonization Trays. *Limnol Oceanogr.* 37 (7), 1543–1550. doi: 10.4319/lo.1992.37.7.1543

Todd, V. L. G., Warley, J. C., and Todd, I. B. (2016). Meals on Wheels? A Decade of Megafaunal Visual and Acoustic Observations From Offshore Oil & Gas Rigs and Platforms in the North and Irish Seas. *PLos One* 11 (4), e0153320. doi: 10.1371/journal.pone.0153320

Todd, V. L. G., Williamson, L. D., Cox, S. E., Todd, I. B., and Macreadie, P. I. (2019). Characterizing the First Wave of Fish and Invertebrate Colonization on a New Offshore Petroleum Platform. *ICES J. Marine Sci.* 77 (3), 1127–1136. doi: 10.1093/icesjms/fsz077

Tweddle, D., and Anderson, M. E. (2008). A Collection of Marine Fishes From Angola, With Notes on New Distribution Records. *Smithiana Bull.* 8, 3–24.

van Bennekom, A. J., and Berger, G. W. (1984). Hydrography and Silica Budget of the Angola Basin. *Netherlands J. Sea Res.* 17, 149–200. doi: 10.1016/0077-7579(84)90047-4

Van Gaever, S., Galéron, J., Sibuet, M., and Vanreusel, A. (2009). Deep-Sea Habitat Heterogeneity Influence on Meiofaunal Communities in the Gulf of Guinea. *Deep Sea Res. Part II: Topical Stud. Oceanogr* 56 (23), 2259–2269. doi: 10.1016/j.dsr2.2009.04.008

Vangriesheim, A., Pierre, C., Aminot, A., Metzl, N., Baurand, F., and Caprais, J.-C. (2009). The Influence of Congo River Discharges in the Surface and Deep Layers of the Gulf of Guinea. *Deep Sea Res. Part II: Topical Stud. Oceanogr.* 56 (23), 2183–2196. doi: 10.1016/j.dsr2.2009.04.002

Vardaro, M. F., Bagley, P. M., Bailey, D. M., Bett, B. J., Jones, D. O. B., Milligan, R. J., et al. (2013). A Southeast Atlantic Deep-Ocean Observatory: First Experiences and Results. *Limnol. Oceanogr-Methods* 11, 304–315. doi: 10.4319/lom.2013.11.304

Vinogradov, G. M. (2000). Growth Rate of the Colony of a Deep-Water Gorgonarian Chrysogorgia Agassizi: *In Situ* Observations. *Ophelia* 53 (2), 101–103. doi: 10.1080/00785236.2000.10409439

Vinogradova, N. G., Galkin, S. W., Kamenskaja, O. E., Levenstein, R. Y., and Romanov, V. N. (1990). The Distribution of the Deep Sea Bottom Fauna in the Transoceanic Section in the South Atlantic Ocean Along 31° 30'. *Trans. P. P. Shirshov. Inst. Oceanol.* 126, 7–19.

Walles, B., Troost, K., van den Ende, D., Nieuwhof, S., Smaal, A. C., and Ysebaert, T. (2016). From Artificial Structures to Self-Sustaining Oyster Reefs. *J. Sea Res.* 108, 1–9. doi: 10.1016/j.seares.2015.11.007

Walls, A. H., Clarke, J., Bagley, P. M., and Bazika Sangolay, B. (2010). Deepwater Environmental Long-Term Observatory System (DELOS). *Soc. Petroleum Engineers J.*, 126642. doi: 10.2118/126642-MS

Wetzel, A. (1993). The Transfer of River Load to Deep-Sea Fans: A Quantitative Approach. *Aapg Bull.* 77 (10), 1679–1692.

Conflict of Interest: The authors declare that the research was conducted in the absence of any commercial or financial relationships that could be construed as a potential conflict of interest.

frontiers | Frontiers in Marine Science

TYPE Original Research
PUBLISHED 26 August 2022
DOI 10.3389/fmars.2022.960496

OPEN ACCESS

EDITED BY
Andrew James Guerin,
McMaster University, Canada

REVIEWED BY
Ilana Rosental Zalmon,
State University of the North Fluminense Darcy Ribeiro, Brazil
James Smith,
University of California, Santa Cruz, United States

*CORRESPONDENCE
Dianne McLean
d.mclean@aims.gov.au

SPECIALTY SECTION
This article was submitted to Marine Ecosystem Ecology, a section of the journal Frontiers in Marine Science

RECEIVED 03 June 2022
ACCEPTED 26 July 2022
PUBLISHED 26 August 2022

CITATION
McLean D, Speed CW, Birt MJ, Colquhoun J, Case M, Stowar M, Bond T, Ierodiaconou D, Whitmarsh SK, Taylor MD, Wines S, Booth DJ, Fowler AM and Vaughan BI (2022) Habitat value of subsea wells and pipelines for fishery target species in Australia. *Front. Mar. Sci.* 9:960496. doi: 10.3389/fmars.2022.960496

Habitat value of subsea wells and pipelines for fishery target species in Australia

Dianne McLean[1,2]*, Conrad W. Speed[1], Matthew Jon Birt[1], Jamie Colquhoun[1], Mark Case[1], Marcus Stowar[3], Todd Bond[2,4], Daniel Ierodiaconou[5], Sasha K. Whitmarsh[5], Michael D. Taylor[2,4], Sam Wines[5], David John Booth[6], Ashley M. Fowler[6,7] and Brigit I. Vaughan[1]

[1]Australian Institute of Marine Science, Indian Ocean Marine Research Centre, Perth, WA, Australia, [2]Oceans Institute, The University of Western Australia, Indian Ocean Marine Research Centre, Perth, WA, Australia, [3]Australian Institute of Marine Science, Cape Cleveland, QLD, Australia, [4]School of Biological Sciences, The University of Western Australia, Perth, WA, Australia, [5]School of Life and Environmental Sciences, Deakin University, Warrnambool, VIC, Australia, [6]School of Life Sciences, University of Technology Sydney, Sydney, NSW, Australia, [7]New South Wales Department of Primary Industries, Sydney Institute of Marine Science, Mosman, NSW, Australia

Subsea pipelines and wells installed to support the oil and gas industry represent some of the most extensive and numerous anthropogenic structures throughout global marine ecosystems. There remains a paucity of information on the habitat value of these structures for fishery target species and, as a result, little understanding of how decommissioning should be conducted to minimise impacts to populations of these economically and socially important species. We assess the diversity and abundance of species that are targets of recreational and commercial fisheries on 33 subsea wells and 17 pipelines across the tropical northwest and temperate southeast marine regions of Australia. We examine relationships between fish identity and abundance and a range of environmental (e.g., depth, location), infrastructure-specific (e.g., pipeline position, diameter, age, length of pipeline, height of well, position on well), and biological (% cover of epibiota) variables using video filmed by remotely operated vehicles during their routine offshore inspection and maintenance campaigns. A total of 100 fishery target species were observed across subsea well and pipeline infrastructure, 56 species uniquely observed on pipelines and nine unique to wells. The families Lutjanidae (snapper), Serranidae (rock cods, groupers, perch), and Carangidae (trevallies) were most common and abundant on both wells and pipelines. In the northwest, lutjanids were most abundant around the base of wells, in shallow depths, on shorter wells, and where pipelines spanned the seafloor. A greater number of fishery target species and abundance of ocean perch (*Helicolenus* spp.) were also associated with pipelines that spanned the seafloor in temperate southeast Australia. The combined biomass of three species of snapper on wells in the northwest was 1,270 kg, with production levels for these species on each well estimated to be 105.2 g m^2 $year^{-1}$. The present study serves as an important reference point for informing decommissioning decisions for pipeline and well infrastructure and demonstrates the utility of industry-held data for science. We suggest that key predictor variables identified here be incorporated into comprehensive before-after-control-impact scientific studies for specific fields/assets to enable the prediction of potential impacts of decommissioning scenarios on marine communities present and quantification of such impacts after the decommissioning activity has occurred.

KEYWORDS

fisheries, oil and gas infrastructure, fish production, subsea pipeline, subsea well, decommissioning

1 Introduction

Globally, there is a paucity of knowledge on the influence of subsea wells and pipelines on marine ecosystems. Fundamental to understanding the roles that these structures have in our oceans is insight into the marine communities that interact with them. While, for ~100 years, the oil and gas (O&G) industry has installed structures in the oceans to extract resources (Gourvenec et al., 2022), it is only in recent decades that scientists have been able to access and/or research these structures. Science has traditionally been hampered, to various extents in different regions, by restrictions on access to structures, logistical challenges, and high costs. Yet the science is critically needed to ensure that impacts on marine communities are minimised as these structures are decommissioned.

O&G infrastructure provides additional hard substrata in marine ecosystems that can increase the diversity and abundance of fishes important for recreational and commercial fisheries (Szedlmayer and Shipp, 1994; Gallaway et al., 2009; Bond et al., 2018a; Bond et al., 2018b). Studies documenting high densities of fishery target species on O&G platforms have led to "rigs to reefs" programs where some infrastructure is left in place as habitat for target fishes after decommissioning (e.g., Gulf of Mexico; Love et al., 2003; Kaiser, 2006; Jorgensen, 2009; Cowan and Rose, 2016). A different form of reefing is to repurpose decommissioned O&G structures into artificial reef complexes that incorporate purpose-built reef structures (e.g., King Reef, Exmouth, Western Australia). In addition to platforms, subsea pipelines have been found to possess higher abundances of important fishery species relative to surrounding sand-dominated ecosystems (Love and York, 2005; Bond et al., 2018a; Bond et al., 2018b; McLean et al., 2021a). The concentration of fishery target species on subsea pipelines in northwest (NW) Australia has influenced commercial trap fishing in the region with fishing effort on pipelines ~11.4 times greater per km^2 than effort in the rest of the area of the Pilbara Trap Managed Fishery (Bond et al., 2021). Interactions between fisheries and pipelines (positive and negative) have also been examined in the North Sea for different fishing practices (Rouse et al., 2018; Rouse et al., 2020). For these reasons, it is important to understand the mechanisms that promote a high abundance of fishery target species on O&G infrastructure to inform new developments and decommissioning. This knowledge also has implications for structures deployed in the marine renewable energy sector (e.g., wind and tidal power) and purpose-built artificial reefs.

For decades, scientists have sought to understand the extent to which O&G structures create new productivity for fisheries or simply attract/redistribute existing biomass (Lindberg, 1997). Platforms off the coast of California have been found to be among the most productive marine fish habitats globally (Claisse et al., 2014), with most secondary production (80%) associated with fish biomass around the base of these platforms (Claisse et al., 2015). This was linked to shell mounds that housed abundant and diverse communities of fishes and invertebrates that in turn supported predatory fishes (Claisse et al., 2015). It is not known whether platforms in other regions around the world have similar shell mound features that might also generate high productivity. Smith et al. (2016) conducted assessments of a purpose-built artificial reef for fishing off Sydney, Australia, and found evidence for high production of fish communities but considered also "new" production, noting that the productivity measured may not greatly augment net overall productivity due to the contribution of a high number of "visitor" species. Fish production on subsea pipelines is much harder to quantify owing to the nature of these structures (long, narrow corridors), and to our knowledge, no research programs have attempted such analyses. Similarly, there has been no published research that has documented fish production on subsea wells, despite the hundreds of thousands of structures that exist in our oceans and consequently the high proportion of the costs of decommissioning they require (Oil and Gas UK, 2016; CODA, 2021). In Australia, there has been relatively little research on the extent to which O&G structures promote fish production, and this remains a clear knowledge gap.

Important fishery target species can occupy diverse ecological niches that will influence the extent and way in which they associate with O&G structures. For example, pelagic mackerels (Scombridae) and trevallies (Carangidae) are known to be attracted to floating and mid-water fish-attracting devices (FADs) *via* the provision of structure in open water (a reference point) and associated prey (Dempster and Taquet, 2004). Large schools of these species have been observed around offshore O&G platforms that span the water column and are well lit (Franks, 2000; Simonsen, 2013), suggesting that these structures, particularly when situated in the open ocean, serve a similar function to FADs. Habitat complexity is another important driver of community structure and abundance (Menge and Sutherland, 1976; Martin-Smith, 1993), with complex habitats providing more attachment points for sessile organisms (Hauser et al., 2006) that in turn support more individuals than less complex habitats in their vicinity (Hall and Kingsford, 2021; Kovalenko et al., 2012). Some fishes associate with caves or overhangs, and pipeline spans, well overhangs, and platform beam junctions may be places where these species occur (e.g., Love et al., 2019). Such relationships help explain why higher abundances of demersal fishery species have been observed on subsea pipelines compared to surrounding sand-dominated communities (Bond et al., 2018a; Bond et al., 2018b; McLean et al., 2021a). However, these associations may not necessarily be permanent, as the habitat requirements of fish may change as they grow and mature. Some species may only utilise O&G structures during specific ontogenetic stages (Fujii, 2015; Munnelly et al., 2021). For example, red snapper (*Lutjanus campechanus*) utilise O&G platforms when young but migrate to less vertically complex structures as they mature (Gallaway et al., 2009). Understanding how species associate with particular structural features of O&G infrastructure is essential for predicting the potential influence that different decommissioning options may have on fish communities and, in turn, commercial fisheries (e.g., plugging and abandonment of wells, removal of pipelines).

The present study analyses videos of subsea wells and pipelines collected using remotely operated vehicle (ROV) deployed by industry in Australia to investigate how a range of environmental and structural variables may influence the diversity and abundance of fishery target species. Furthermore, we provide the first estimates of secondary fish production for important fishery target species on wells globally and for O&G structures in Australia. We predict positive relationships between fishery target species abundance and the complexity of colonising benthic communities and the availability of shelter (i.e., pipeline spans, well height). Furthermore, we expect secondary fish production to be high on subsea wells. With the projected global extent of artificial structures increasing (Bugnot et al., 2021; Gourvenec et al., 2022), the results of this research will not only inform decommissioning of O&G structures but also advise reefing of structures, the creation of new artificial reefs, and the design of new infrastructure for O&G and marine renewable energy industries. With a focus on subsea wells and pipelines, the present study provides insights into fish communities on these globally understudied O&G structures.

2 Methods

Using ROV imagery obtained by industry during routine offshore inspection and maintenance works, we were able to document and describe the diversity and abundance of important fishery target species present on subsea wells and pipelines in the NW and southeast (SE) marine regions of Australia. As we utilised existing imagery, we were limited in our ability to examine the potential influence of certain structural elements of wells and pipelines on fishery species abundance, as replication, stratification, and standardisation in sampling were not possible. As illustrated in Table S1 and Table S2, there was high variability in surveys, e.g., surveys performed in different years, differences in lengths of surveys. Furthermore, there were differences in ROV field of view (FOV), altitude, speed, resolution of imagery, etc. Considering these inconsistencies and limitations, we report on patterns in fishery target species abundance in response to features quantifiable from this imagery such as the extent of burial of pipelines, certain areas of subsea wells (Christmas tree, tree cap assembly, etc.), and the percent cover of particular biota on these structures.

2.1 Study sites and infrastructure descriptions

The present study analysed data from ROV imagery collected by the O&G industry during routine offshore inspection, maintenance, and repair campaigns for subsea pipelines and wells in NW and SE Australian waters (Figure 1). Additional data were included from five independent studies (McLean et al., 2017; Bond et al., 2018c; McLean et al., 2018; McLean et al., 2020; Ierodiaconou et al., 2021) that each varied in the way in which the imagery of structures was analysed for ecological data, detailed in sections that follow (Tables S1, S2).

For subsea wells, we analysed imagery collected from a single point in time (one survey period) from 31 wells in the NW in depths of 74–155 m and two wells in the SE in 128- and 155-m depths (Table S1). For subsea pipelines, we analysed imagery from seven pipelines in the NW and 10 pipelines in the SE, again from ROV surveys conducted at one point in time (Figure 1). As very few target species were observed at depths below 400-m depth, this provided a depth limit for video analysis (Table S2).

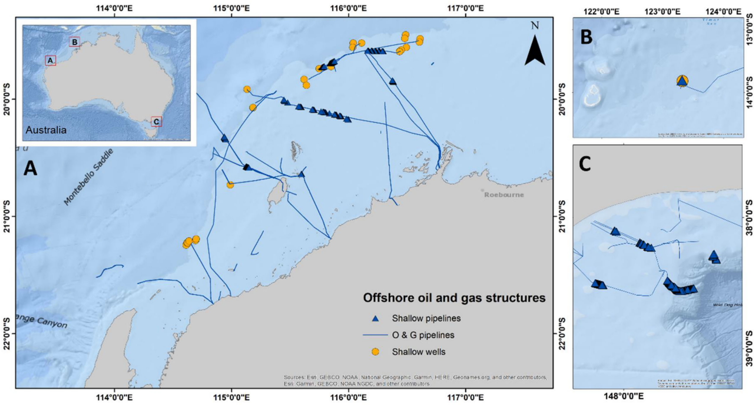

FIGURE 1
Location of wells (<150 m NW and<160 m SE) and pipelines (<400 m) surveyed for abundance of species targeted by fisheries in **(A)** NW, **(B)** NW (Browse), and **(C)** SE marine regions of Australia. NW = north-west, SE = south-east.

2.2 Remotely operated vehicle (ROV) imagery analysis

All analyses of colonising epibiotic communities used the specialised software program TransectMeasure (SeaGIS, 2020a). "Virtual" quadrats were placed on the ROV imagery (photographs taken from the video), overlapping infrastructure, with 20 points overlaid on each quadrat in a 5 × 4 grid layout. Benthic biota underneath each point was identified using an adaptation of the Collaborative and Annotation Tools for Analysis of Marine Imagery (CATAMI) classification scheme (Althaus et al., 2015). Identification was to the lowest taxonomic resolution possible, and relevant morphological characteristics were noted (e.g., encrusting, complex or taller erect forms). Due to the range in the quality of the images, we pooled categories of epibiota to broad groups (e.g., sponges, soft corals) to facilitate analyses across all structures. Percent cover data were therefore obtained for each broad group observed from these points. In addition to this percent cover data, for each quadrat, we also recorded the complexity of the epibenthic community by estimating the height of the benthic biota for the entire quadrat as 0, negligible; 1, low (0–20 cm); 2, medium (20–40 cm); and 3, high (>40 cm) and density (percent cover of quadrat) as 0, none; 1,<25%; 2, 25%–75%; 3, >75%. Epibiota height was estimated using the known dimensions of structures as a reference.

Analyses of species that were fishery targets used the specialised software program EventMeasure Stereo (SeaGIS, 2020b). Where fish could not be reliably identified to species level, they were recorded to the next lowest taxonomic level possible (typically genus or family). Target species were defined as those that are retained by recreational and commercial fisheries that operate in the NW and SE regions (Butler et al., 2002; Gaughan and Santoro, 2021) and were also identified from online fishing sources (e.g., West resource; East resource) and knowledge of the authors. A full list of these species is provided for wells in Table S3 and pipelines in Table S4. The size (fork length–distance from snout to fork of tail) of all individuals that were abundant target species was estimated in 10-cm-size bins using the known sizes of components of wells and pipelines as a visual reference for size. Methods for analysing the abundance of fishery target species differed for wells and pipelines and are described in sections that follow.

2.2.1 Analysis of ROV imagery of subsea wells

Ten non-overlapping FOV images were obtained in each of the six sections of each well: tree cap assembly, Christmas tree general, flow base, seafloor around structure, seafloor beneath structure, and water column around structure (Figure 2A). It was not possible to standardise the size of these FOV images due to high variability in ROV movements relative to the wells; however, the point classification enabled quantification of percent cover data of the benthic community from these images (Table 1) using the methods described *in ROV imagery analysis*.

Abundance counts of fishes and other mobile fauna were obtained by counting the maximum number of each species present within the FOV at a single frame of the ROV video (MaxN). This conservative measure prevents repeated counts of the same individuals leaving and reentering the FOV (Cappo et al., 2007). In addition to an overall MaxN measure, we obtained separate MaxN measures for each target species from the six different sections of the well shown in Figure 2A. We acknowledge that MaxN measures do typically underestimate measures of actual abundance, and this may very well be the case here, but we predict that this difference would be quite conservative given the relatively small size of the structures. It

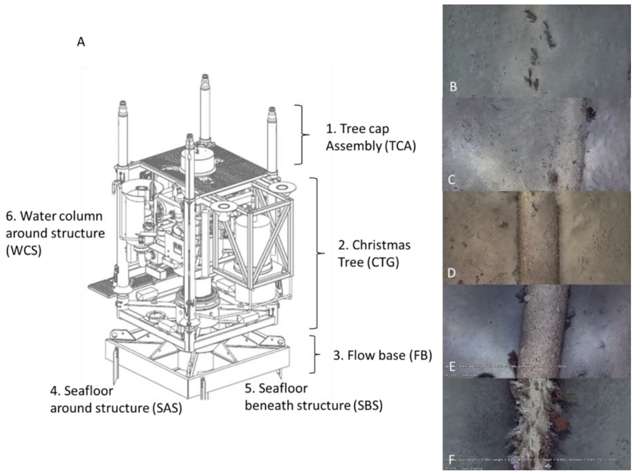

FIGURE 2
(A) Schematic of a subsea well (adapted from McLean et al., 2018) indicating the different sections for which separate measures of epibiota and abundance of fishery target species were measured. The total abundance of all fish species was also obtained for the entire well (highest MaxN across the sections). **(B–F)** Features of pipelines assessed from ROV imagery including the extent of burial/spanning ("pipeline position") ranging from completely buried (0 = A) to more than half buried (1 = B), resting on seafloor (2 = C), underside of pipeline not touching seafloor (3 = D), and pipeline span >0.5 m above seafloor (4 = E).

was not possible to use the historical imagery of wells to attempt to count all fish species present given the nature of the surveys that often stopped and started again, focused on particular sections for extended periods, etc.

The length of ROV well surveys varied from rapid general visual inspections (<15 min) to detailed structural assessments (>2 h; Table S1), and as such, "survey time" (among other variables) was included as a variable in statistical analyses (see *Data analysis*).

The data set analysed here (n = 13 wells) was supplemented with the addition of fish and benthic data obtained from independent studies (n = 20 wells; Ierodiaconou et al., 2021; McLean et al., 2018.). Cooper Energy wells were analysed using the same methods described in *Analysis of ROV imagery of subsea wells* with the exception that epibenthic community height and density were not recorded for these wells. For wells operated by Woodside, only a total MaxN for each well was recorded (McLean et al., 2018). Percent cover of benthic biota and complexity were estimated for each side of these wells (McLean et al., 2018) rather than by the use of the quadrat method. Given the small size of these structures (Table S1), we assumed that the data obtained for percent cover and complexity of benthos were comparable across all types of wells.

2.2.2 Analysis of ROV imagery of pipelines

The position of pipelines relative to the seafloor (pipeline position) was scored following McLean et al. (2020) with the following: 0, completely buried; 1, pipeline showing above sediment but more than halfway buried; 2, pipeline touching the seafloor but making a closed crevice; 3, underside of pipeline not touching the seafloor (spanning); and 4, pipeline >0.5 m above the seafloor (Figure 2). This pipeline position information was recorded every *ca.* 10 m along each pipeline. For analysis of the effects of pipeline position, benthic biota, time of day, depth, etc., on abundance and diversity of fishery target species, data was split into 50-m video "transects" each separated by a 10-m gap.

Benthic biota type, complexity, and cover were analysed from quadrats as described in *ROV imagery analysis* (although refer to *Using independent ecological data on subsea pipelines* for other data included in the project). For pipelines, each "virtual" quadrat was of approximately 1.5 m^2 (~30 cm × ~50 cm, depending on ROV altitude), placed on a freeze-framed image taken every 10 m along each pipeline, spanning the pipeline and seafloor to either side. All fish and other mobile fauna encountered in each 50-m transect were identified to the lowest taxonomic level possible, and their abundances were summed to give a total abundance per transect.

2.2.2.1 Using independent ecological data on subsea pipelines

To supplement the data available for the present study, we included four additional pipeline data sets from independent studies: Cooper flowlines and umbilicals (seven; Ierodiaconou et al., 2021), Echo Yodel (Bond et al., 2018c), 2TL (McLean et al., 2017), and Pluto pipelines (McLean et al., 2020; see Table S2). Cooper pipelines were surveyed in the same manner as is

TABLE 1 List of variables recorded to examine relationships with fish communities observed on different infrastructure.

	Variables	Wells	Pipelines
Environmental and structural (see also Table S1, Table S2)	Easting	x	x
	Northing	x	x
	Depth of survey (m)	x	x
	Structure age at time of survey (years)	x	x
	Structure height (m)	x	
	Time of day (decimal hours)	x	
	Survey duration (min)	x	
	Pipeline position		x
	Diameter of pipe (mm)		x
	Total length of pipeline (km)		x
	Number of transects per pipeline (sampling effort)		x
	Distance along pipeline		x
	Distance to closest O&G structure		x
Benthic variables	Macroalgae % cover	x	x
	Other (could not be identified) % cover	x	x
	Anemones % cover	x	
	Sponge % cover		x
	Turf algae % cover		X
	Bare structure/biofilm % cover	x	X
	Hard corals % cover	x	X
	Soft corals % cover	x	X
	Gorgonian % cover		x
	Barnacles % cover	x	x
	Rubble % cover	x	
	Sand % cover	x	x
	Epibenthic height (categorical)		x
	Epibenthic density (categorical)		x
	*Invertebrate % cover		x

*This variable included combined cover for hard and soft corals and sponges. This variable was used where data were rare and distributions were highly skewed and unsuitable for inclusion independently in models.

described in *Analysis of ROV imagery of pipelines*. Echo Yodel and 2TL were surveyed using 5-m transect lengths, whereas Pluto used 10-m transects. To make these transects comparable with the 50-m transects used for all other locations, sets of adjacent shorter transects were pooled to create 50-m transects. All pipeline surveys were conducted during daylight hours; therefore, only the daytime imagery from these additional independent data sets was included. Data from the additional pipelines also recorded epibenthic communities as a single combined score for epibenthic height and density (McLean et al., 2017; McLean et al., 2020), which was different to the approach used for the present study. Consequently, these measures were considered separately for these pipelines. Furthermore, analysis of epibenthic communities on Echo Yodel, 2TL, and Pluto focused only on the pipeline and did not include the adjacent seabed (McLean et al., 2017; Bond et al., 2018c; McLean et al., 2020); thus, the benthic category “sand” was likely to be underrepresented in the data. These independent studies also did not estimate fork lengths of selected target species.

2.3 Data analysis

We recorded environmental, structural, and biological variables to examine their influence on the diversity and abundance of species targeted by fisheries (Table 1). However, we note that ROV imagery was not collected by industry with the goal of hypothesis-testing, so it did not include balanced sampling designs. Thus, our interpretations of outcomes cannot exclude confounding effects. For example, the deepest pipeline (Jansz) was also one of the most recently deployed, so any patterns in fish abundance and diversity could have been due to either depth or age or some combination of the two variables. This is discussed further in *Discussion*. Additionally, our ability to identify epibenthic communities was constrained by the quality of imagery, which required pooling of biota into broad categories (e.g., sponges, soft corals) for analysis. This meant that we were unable to perform detailed analyses to examine patterns in the distribution and abundance of these colonising communities. With only two wells surveyed in the SE, we were limited to presenting the total fishery target species list for each well and component of each well.

2.3.1 Multivariate analyses of fishery target species abundance

Multivariate tests were used to explore patterns in fishery target species across depths. Prior to analyses, we used a PERMDISP analysis (Anderson, 2004) to test the null hypothesis of no difference in dispersion among depths. The test is a multivariate analogue to a Levene's test (Levene, 1960). Dispersion of the data did not differ for the different depth categories examined for NW wells [p(perm) = 0.47] but did for NW pipelines [p(perm)< 0.01] and SE pipelines [p(perm)< 0.01]. Multivariate dispersion was examined visually using a principal coordinate (PCO) analysis (Anderson et al., 2008) in the software PRIMER V7 (Clarke and Gorley, 2015). Unconstrained patterns in abundance were analysed using a Bray–Curtis dissimilarity matrix. Individual species or benthic habitat types that were likely responsible for any of the observed differences were identified using Pearson correlations of their abundance with the canonical axes. These relationships are shown as vectors displayed on the PCO plot. Prior to running the PCO analysis, a draftsman plot was produced to examine correlations among Table 1. For wells, only easting and northing were correlated (0.95), with the former removed from the data prior to running the PCO analysis. For NW pipelines, easting and northing were correlated with distance measures and epibenthic density and complexity, whereas epibenthic density and complexity were correlated with a range of epibiota categories. For this reason, easting, northing, distance along pipeline, distance to closest O&G structure, epibenthic density, and epibenthic height were removed prior to PCO analysis.

2.3.2 Univariate analyses of richness and abundance of fishery target species

The influence of variables listed in Table 1. on fish richness and abundance on NW wells and pipelines was investigated using generalised additive models (GAMs; Table 3; Hastie and Tibshirani, 1986; Fisher et al., 2018). Because of a strong collinearity, a full subset approach was used to fit all combinations of predictor variables up to a maximum of two (to prevent overfitting and ensure models remained ecologically interpretable). Some benthic variables were combined due to rarity and highly skewed distributions. Time of day was treated as a circular variable using the function (bs='cc') in mgcv (Wood, 2011). Predictor variables with correlations greater than 0.28 were included in the model set but were not included in the same model. The best model had the fewest variables (most parsimonious) and was the one with lowest Akaike information criterion corrected for small sample sizes (AICc). These best models were also within two AICc units of the lowest AICc value (Burnham and Anderson, 2003; Symonds and Moussalli, 2011). As recommended by O'Hara and Kotze (2010), we used untransformed abundance metrics as our response variables. Models were fitted using a Tweedie error distribution (Tweedie, 1984). A Tweedie model is an extension of a compound Poisson model derived from the stochastic process where a gamma distribution is used for the counted or measured objects (i.e., number of fishes) and has an advantage over delta-type two-step models by handling the zero data in a unified way. All GAM modelling and plots used the R language for statistical computing (R Development Core Team, 2019) with the package mgcv (Wood, 2011) and ggplot2 (Wickham, 2016) and based on the scripts found in Fisher et al. (2018).

2.3.3 Fish production estimates for subsea wells

Estimates were obtained for wells in the NW for three snapper species that had sufficient data on abundance and life history traits and ecology. These included *Lutjanus argentimaculatus* (mangrove jack), *Lutjanus malabaricus* (saddletail snapper), and *Lutjanus russellii* (Moses' snapper). Wells were chosen for this modelling over pipelines as the ROV imagery covered most, if not all, of the structure and therefore was most likely to provide an accurate estimate of total abundance (and therefore density and biomass) for these species. To facilitate estimates of production, we first had to calculate the volume of "reef" habitat for wells. The average height of wells surveyed here was 6.5 m (data provided from industry; Table S1), and from imagery, we estimated dimensions to be 4 m × 4 m (seabed footprint). However, as we included fish observed within ~2 m of the well structure, we extended the area of well habitat sampled to 8 m × 8 m (seabed footprint m^2) × 6.5 m height of well to a volume of 416 m^3.

To estimate fish production, we followed the method of Smith et al. (2016), which assumes a steady-state population structure. This allowed us to assume that relative production (i.e., the production to biomass ratio) was equal to the instantaneous total mortality of an organism (Dickie, 1972; Mertz and Myers, 1998; Randall and Minns, 2000), an assumption at the basis of much ecosystem modelling (Christensen and Pauly, 1992). Here, $P_i = B_i \times Z_i$, with P_i being production (kg per year), B_i is fish biomass on a structure, and Z_i is the instantaneous total mortality rate. Total mortality includes the sum of natural (M) and fishing (F) mortality rates ($Z_i = M_i + F_i$). In this instance, fishing mortality is assumed to be zero as commercial fishing activities in these zones are negligible and they are too remote for access by recreational fishers.

We were interested to determine production that was new (P_{new}) by incorporating time into the equation such that new production accounted for the proportion of a year that a particular species spent on a structure $P_{new}=P_i \times t_{prop}$. In this way, P_{new} equated to the local production that would be lost if the structure was to be removed during decommissioning. The proportion of time likely spent on wells (residency) by *L. malabaricus* and *L. russellii* was estimated based on diel observations of the presence of these species on a pipeline in this region (Bond et al., 2018c) and estimated for *L. argentimaculatus* based on publications on the behaviour of this species (Table 2). One limitation of our estimate of t_{prop} was that it did not account for potential seasonal movements of species away from structure.

To estimate biomass (B_i), we first required an estimate of the average length of each species on wells. This "average" was calculated from the mean length of individuals that were measured from stereo-video imagery obtained from subsea pipelines and platforms in the NW region (Pradella et al., 2014; Bond et al., 2018a; Bond et al., 2018b; McLean et al., 2020; McLean et al., 2021a). Average lengths (499 mm, *L. argentimaculatus*; 429.4 mm, *L. malabaricus*; 337 mm, *L. russellii*) were converted into biomass using the equation $B_i=aL^b$ (Table 2). Here, a was a parameter describing body shape and condition, L was length, and b was allometric growth in body proportions. We note that the use of MaxN here is likely to underestimate the total abundance of fishery target species for these structures, and therefore, measures derived from the use of MaxN (e.g., Production) may likewise be underestimates.

3 Results

3.1 Fishery target species on subsea wells

A total of 42 target species were observed on subsea wells, with 35 in the NW and 7 on wells in the SE regions (Table S3). The most speciose families were Serranidae (n = 12; rockcods/groupers/perch), Lutjanidae (n = 10 snapper species), and Carangidae (n = 8 trevally species). Examples of fishery target species associating with subsea wells are shown in Figure S1. The wells with the highest richness of fishery target species were AP2 and PER01 (14 spp. each), then AP3, WA7, and BAL08 (13 spp. each) (Table 3). Those with the least were Scindian2XT (n = 4 spp., 9 individuals) and 4-Well (4 species, 31 individuals).

The most abundant species observed on wells in the NW were *L. russellii* (Moses' snapper; n = 1,192; Table 3), *L. vitta* (brownstripe snapper; n = 321), *Seriola dumerili* (amberjack; n = 158), and *L. argentimaculatus* (mangrove jack; n = 151; Table 3) (Table S3). In the SE, the most abundant target species were *Nemadactylus macropterus* (jackass morwong; n = 16, 4-well only), *Helicolenus* spp. (ocean perch; n = 15, 2-Well, 4-Well), and *Pseudophycis* spp. (cod; n = 9, 2-Well, 4-Well) (Table S3). The highest abundance of target species (493 individuals) occurred on LN2, the shallowest surveyed well, followed by the similarly shallow LOW1. Most of these fishes were *L. russellii*, with 480 individuals observed on LN2 and 448 on LOW1 (Table 3). PER02 in 130-m depths had the next highest abundance of fishery target species with 154.

The most ubiquitous fishery target species on subsea wells in the NW were *L. russellii* (90% wells), *L. argentimaculatus* (90%), *Cephalopholis sonnerati* (tomato rockcod; 90%), and *S. dumerili* (84%). *L. malabaricus* was also included in modelling of fish production, as it was a common species occurring at 58% of wells (Table 3).

The greatest number of fishery target species (richness) occurred on the seafloor both around and under the structure, followed by the main Christmas tree structure (Figure 3). The total abundance of target species was greatest on the seafloor around the structure followed by the seafloor beneath the structure (Figure 3). The lowest abundance occurred in the water column around the structure and in the tree cap assembly. The two most abundant and common families of target species on wells in the NW exhibited slightly different patterns in spatial distribution around wells. Serranidae (groupers) were more abundant on the seafloor beneath the structure and within the Christmas tree of the well, whereas Lutjanidae (snappers) were most abundant on the seafloor around the structure (Figure 3).

There was an overlap in the composition and abundance of fish communities on wells in depths of (Figure 4), suggesting

TABLE 2 Estimated mortality (natural M and fishing F), level of residency (t_{prop}), and biomass metrics.

Species	 ***Lutjanus argentimaculatus***	 ***Lutjanus malabaricus***	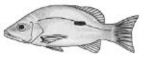 ***Lutjanus russellii***
M (year^{-1})	0.13 [d]	0.115 [a]	0.152 [g]
F (year^{-1})	0	0	0
t_{prop}	0.6	0.5 [f]	0.75 [f]
a	0.02647 [b]	0.2348 [a]	0.01856 [g]
b	2.92 [b]	2.9279 [a]	2.889 [g]
L	49.9 [e]	42.9 [c]	33.7 [c]

[a] Newman (2002a), [b] Piddocke et al. (2015), [c] Mean lengths obtained from Bond et al., (2018a); Bond et al., (2018b) and McLean et al., (2021a), [d] Pember et al. (2005), [e] Pradella et al. (2014) and McLean et al. (2019), [f] Bond et al., (2018c), [g] Newman (2002b).

TABLE 3 Total relative abundance (sum of MaxNs) of all fishery target species and three of the most common and abundant snapper (Lutjanus) species observed on remotely operated vehicle imagery of subsea wells.

Well	Depth (m)	# fishery target species	Total abundance	MaxN for*L. argentimaculatus* 	MaxN for*L. malabaricus* 	MaxN for*L. russellii* 
LN2	74.5	7	493	1	0	480
WA1	78	11	31	2	1	8
AP3	80	13	108	3	2	9
CK4	80	10	46	9	1	4
WA7	80	13	116	2	1	2
WA6	84	9	83	3	0	2
AP2	85	14	89	4	19	12
LOW1	87	9	475	3	0	448
EastSpar6	96	12	58	0	12	0
LB5	117	6	6	1	1	1
GWN6	125	11	40	11	5	6
4-Well	**128**	**4**	**31**	**N/A**	**N/A**	**N/A**
L6	128	9	20	6	3	4
Chinook1XT	130	11	60	3	0	2
GRIFFIN1XT	130	7	12	0	1	2
GRIFFIN2XT	130	8	17	2	1	1
GRIFFIN3XT	130	12	32	1	10	3
GRIFFIN4XT	130	8	42	1	0	11
GRIFFIN5XT	130	7	21	2	0	2
GRIFFIN6XT	130	7	29	4	0	3
GRIFFIN8XT	130	5	8	1	0	0
GRIFFIN9XT	130	5	16	0	0	3
Scindian2XT	130	4	9	1	0	0
Scindian3XT	130	11	49	1	8	3
Scindian4XT	130	12	50	3	5	4
PER02	130	8	154	1	0	90
EY3	134	7	34	1	0	18
EY4	134	10	99	47	7	12
BAL05	135	11	77	12	6	11
BAL08	135	13	51	1	8	20
CP1	135	8	56	23	1	16
PER01	135	14	34	2	0	15
2-Well	**155**	**6**	**14**	**N/A**	**N/A**	**N/A**

SE wells indicated in green, the remainder are in the NW. Wells listed in order of shallowest to deepest.

that the distinction between these depths is not clear. A few patterns were evident, however, with *Glaucosoma buergeri* (pearl perch) associated with wells at >100-m depths (Table S3; n = 59 vs. 0 in<100 m) where rubble, sand, and hard cover were also more prevalent. Conversely, some species of Epinephelidae (groupers; *E. chlorostigma*, *E. multinotatus*, *C. sonnerati*, *E. coioides*) were correlated with wells<100 m in depth (Figure 4; Table S3). *L. russellii* (Moses' snapper), *Seriola rivoliana* (highfin amberjack), and *S. dumerili* (amberjack) were each correlated with shorter wells and higher percent cover of barnacles (Figure 4).

Depth, well height, and the percent cover of bare structure or structure covered in a thin biofilm of unidentifiable biota were the most commonly identified important predictors (Table 4; Figure S2). Fishery target species richness increased as the percent of bare structure or cover of biofilm increased, as did the abundance of Serranidae (Figure 5); however, both relationships were weak, as indicated by relatively low R^2 values (Table 4). Serranidae also increased in abundance with increasing percent cover of "other" (unidentified epibiota), while fishery target species richness was highest where barnacle coverage was lowest. The total abundance of fishery target

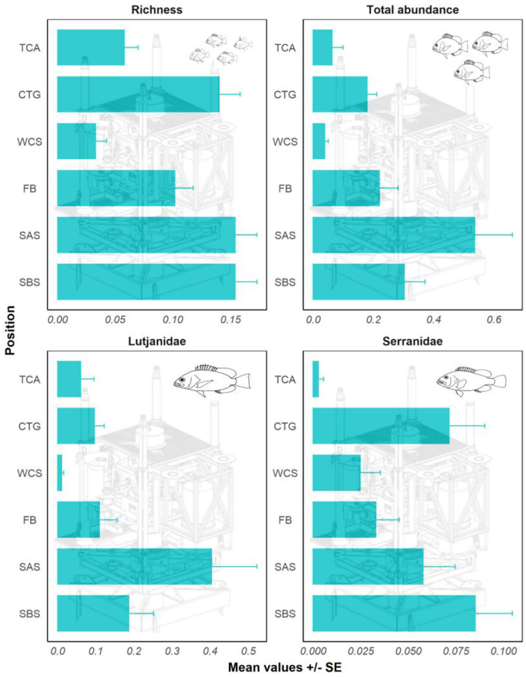

FIGURE 3
Fishery species richness, total abundance of fishery target species (sum all MaxNs), and the abundance of Lutjanidae (snappers) and Serranidae (groupers) on different sections of NW wells. TCA, tree cap assembly; CTG, Christmas tree; WCS, water column around structure; FB, flow base; SAS, seafloor around structure; SBS, seafloor beneath structure, NW = north-west, SE = south-east.

species and the abundance of Lutjanidae and Serranidae declined with increasing depth (Figure 5). A similar relationship was evident for well height, with taller wells possessing fewer fishery target individuals and lutjanids.

The size structures of *L. argentimaculatus* and *L. malabaricus* were very similar on wells in the NW (Table S1) with most (93%, 98%, respectively) 40–50 cm in length (Figure 6). *L. russellii* were smaller, with 45% 20–30 cm and 47% 30–40 cm in length. Slightly smaller individuals were observed on pipelines (Figure 6; see *Structural components of subsea pipelines that promote fishery target species abundance*).

3.2 Fish production on wells in north-west Australia

The estimated biomass of targeted snapper species on wells in the NW was 130.06 kg for *L. malabaricus* (18 wells), 777 kg for *L. russellii* (28 wells), and 363.2 kg for *L. argentimaculatus* (28 wells) (Table 5). Assuming a well volume of 416 m^3, this equated to an average standing stock biomass at each well of ~17.4 g m^{-3} for *L. malabaricus*, ~66.7 g m^{-3} for *L. russellii*, and ~31.2 g m^{-3} for *L. argentimaculatus*.

Local production P at wells ranged from 0.83 ± 0.05 kg $year^{-1}$ per well for *L. malabaricus* to 1.69 ± 0.65 kg $year^{-1}$ per well for *L. argentimaculatus* and 4.22 ± 2.08 kg $year^{-1}$ per well for *L. russellii* (Table 5). Considering a seabed footprint of 64 m^2, this equates to "per well" estimates of 13 g m^{-2} $year^{-1}$ for *L. malabaricus*, 26.3 g m^{-2} for *L. argentimaculatus*, and 66 g m^{-2} *L. russellii* with a summed per well total of 105.23 g m^{-2} $year^{-1}$ for the three species. New production P_{new} is an estimate of that which would be lost from the ecosystem (not just the specific wells) if they were to be removed (Table 5). Our estimates of t_{prop} produced a total P_{new} value of 7.48 kg $year^{-1}$ for *L. malabaricus*, 28.33 kg $year^{-1}$ for *L. argentimaculatus*, and 88.56 kg $year^{-1}$ for *L. russellii*.

3.3 Structural components of subsea pipelines that promote fishery target species abundance

A total of 90 target species were recorded on subsea pipelines with 67 observed from the seven pipelines in the NW and 23 from the 10 pipelines in the SE marine regions (Table S4). The most speciose families were the same as those observed on wells; Serranidae (n = 18; rockcod/grouper/perch species), Lutjanidae (n = 14 snapper species), and Carangidae (n = 9 trevally species). Examples of fishery target species associating with subsea pipelines are shown in Figure S3. Pipelines with the highest richness of fishery target species were Jansz (36 spp.), Pluto (32

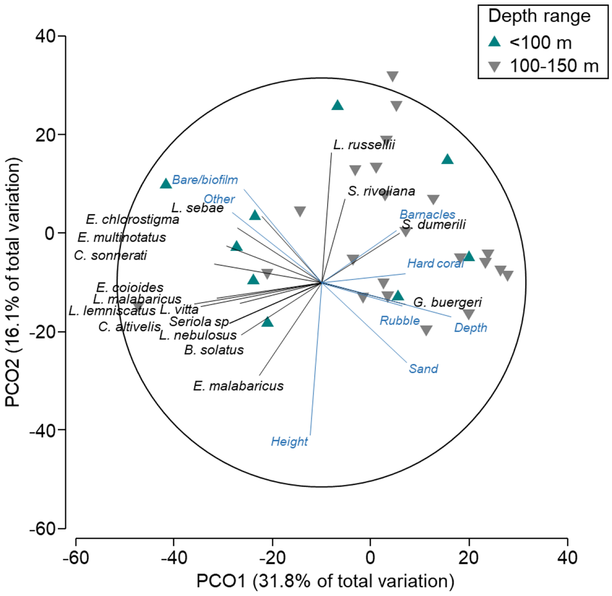

FIGURE 4
Principal coordinates ordination (PCO) on fishery target species only in depths <150 m (north-west wells). Vectors are displayed and show fish species and explanatory variables with Pearson's correlations of |R|>0.3 to one or more axes. Vectors indicate the direction of the relationship, and their length indicates the strength of their effect on the assemblage of fishery target species.

spp.), and 2TL (26 spp.) in the NW and Blackback to Mackerel (15 spp.) and MarlinA to Shore (9 spp.) in the SE (Table 6).

The most abundant species observed on pipelines in the NW were *L. vitta* (brownstripe snapper, n = 2,900), *L. russellii* (Moses' snapper; n = 1,810), *L. quinquelineatus* (five-line snapper, n = 1,735) (Table 6, Figure 7), *Glaucosoma buergeri* (northern pearl perch, n = 1,540; Figure S3), and *Epinephelus areolatus* (areolate grouper, n = 1,160) (Table S4). In the SE, the most abundant fishery target species were *Helicolenus* spp. (ocean perch; n = 2,015; Table S3), *N. macropterus* (jackass morwong; n = 1,038; Figure S3), *Arripis trutta* (eastern Australian salmon, n = 250) (Table 6, Figure 7), and *Centroberyx affinis* (redfish, n = 119) (Table S4). The pipeline with the highest total abundance of fishery target species was Jansz (n = 3,734), followed by Pluto (n = 3,624), then Echo Yodel (n = 2,501) (Table 6), with total abundances likely linked to sampling effort (Table S2).

In the NW, pipelines in depths<100 m had a larger diameter and were longer than deeper pipelines and also had a distinct fish community that was composed of 11 species targeted by fisheries from a range of families including the Serranidae, Lutjanidae, and Labridae (Figure 8). Pipelines in depths >100 m in this region tended to have a higher percent cover of sand, sponges, and soft corals and were characterised by abundances of *Pristipomoides multidens* (goldband snapper) and *Epinephelus latifasciatus* (striped grouper) (Figure 8, Table S4). In the SE, four distinct clusters were evident, potentially reflecting differences in fish assemblages with depth, percent cover of sponges, and sampling effort (Figure 8). *Helicolenus* spp. were correlated with depth, with higher abundance on deep pipelines in this region.

TABLE 4 Generalised additive mixed models (GAMs) for predicting fishery target species richness, total fishery target species abundance (sum of MaxNs for all species), and the total abundance of Lutjanidae and Serranidae families observed on subsea wells in <150 m in the north-west, within 2 Akaike information criterion of the top model.

Response	Model	R^2	ΔAICc	*w*AICc	AICc	edf
Richness	Bare/Biofilm + Barnacles	0.21	0.00	0.31	153.32	3
Total abundance	Depth + Well height	0.82	0.00	0.91	306.39	3
Lutjanidae	Depth + Well height	0.85	0.00	0.90	296.43	3
Serranidae	**Bare/Biofilm + Other**	**0.26**	**0.00**	**0.32**	**152.02**	**3**
	Bare/Biofilm + Depth	0.22	1.46	0.15	153.48	3

Where there was more than one model evident, the best model ranked using wAICc is indicated in bold.

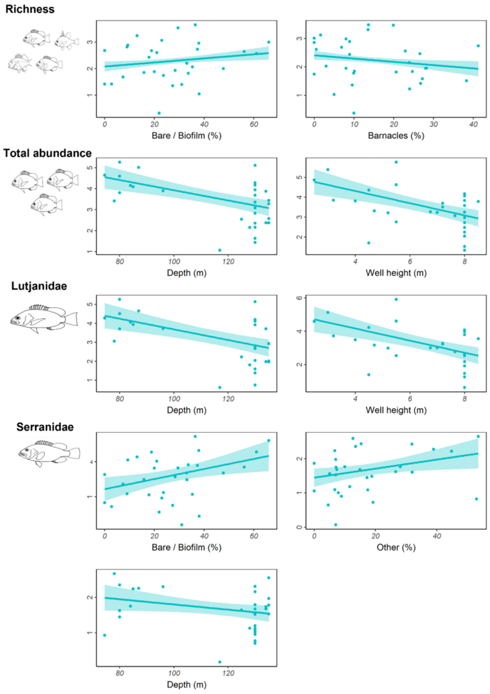

FIGURE 5
Total residual abundance of fishery target species, richness and residual abundance of the two most abundant fishery target families on wells in <150 m depth in the north-west. Residual abundances are plotted relative to their most important explanatory variables (Table 4; Figure S2). Models were fitted using Generalised additive models. The solid line represents the estimated smoothing curve, and dashed lines represent ±2 × south-east of the estimate.

Older pipelines possessed a higher number of fishery target species and high abundances of Lethrinidae (Table 7, Figure 9, Figure S2). As depth increased, the number of fishery target species declined as did the abundance of Lethrinidae, yet this latter relationship was quite weak (low R^2; Table 7, Figure 9). Total abundance of fishes increased on pipelines in depths<400 m in the NW and with increased pipeline exposure (reduced burial of the pipeline by sediment) (Table 7, Figure 9, Figure S2). Although sponges were identified as a key factor by the GAM, the relationship with total fish abundance was not clear (Figure 9) and was characterised by high variability. Serranidae increased in abundance along pipelines with moderate (middle of the range) sampling effort and where the percent cover of bare pipeline or pipeline covered in a thin biofilm was greatest, this latter relationship mirroring that found on subsea wells in this region (Figure 9).

For pipelines in the SE, the most important predictor variables for richness and abundance of fishery target species and abundances of *Helicolenus* spp. and *N. macropterus* are shown in Table 8 and Figure S5. Fishery target species richness was highest on the smallest-diameter pipelines and increased with pipeline exposure (less buried, more spanning) (Figure 10). Total abundance of fishery target species increased with increasing depth and total pipeline length (Figure 10). *Helicoloenus* spp. tended to be present in slightly higher abundance where the underside of the pipeline was not touching the seafloor, yet despite this relationship with pipeline exposure was also more abundant in areas with increasing percent cover of sand (Figure 10). *N. macropterus* peaked in abundance on pipelines in mid-depth ranges of 200–300 m and were least abundant on shallow pipelines in depths<100 m; however, this relationship was particularly weak (Table 8). This species was also most abundant on the longest pipelines in this region (Figure 10), potentially an artefact of sampling with a higher likelihood of encountering species when a greater area is covered.

In the NW, most *L. quinquelineatus* and *L. russellii* were estimated to be 20–30 cm in size (58%). Approximately 36% of *L. quinquelinatus* are smaller than this at 10–20 cm, and 29% of *L. russellii* are larger at 30–40 cm (Figure 11). *L. vitta* were smaller, with the vast majority being 10–20 cm in length. In the SE, almost all *N. macropterus* were 20–30 cm (95%), while *Helicolenus* spp. were typically small, with 42% being<10 cm and 55% being 10–20 cm in length (Figure 11). Sizes of *A. trutta* were not obtained from imagery.

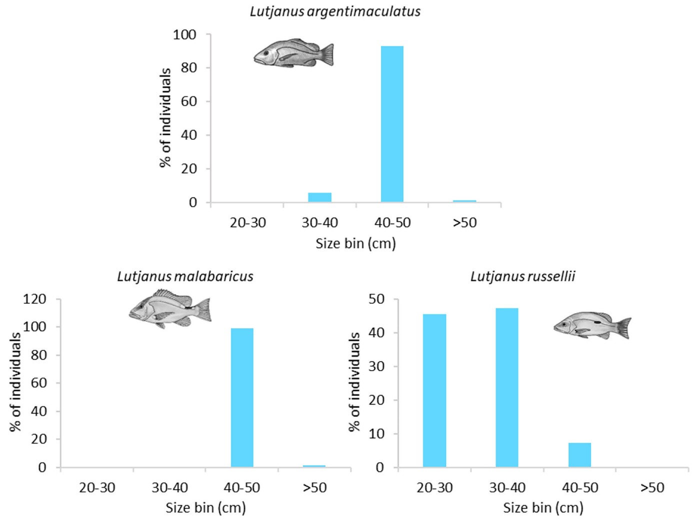

FIGURE 6
Size frequency of abundant fishery target species observed on subsea wells. Sizes estimated from imagery in 10-cm bins.

4 Discussion

4.1 Fishery target species on subsea wells in Australia

A total of 49 species that are targets of fisheries was observed in ROV video from 33 subsea wells (31 in the NW, two in the SE), with >60% of these representatives of Serranidae, Lutjanidae, and Carangidae. Only six target species were observed on video from the two wells sampled in the Bass Strait region of SE Australia. This limited sampling means that additional work will be required to understand relationships between fish communities and well infrastructure in this region (noting the slightly larger data set for wells in this region in Ierodiaconou et al., 2021). For wells in the NW, the abundance of fishery target species was greatest on the seafloor around the structure and right at the seafloor–structure interface, a phenomenon primarily driven by high abundances of demersal snappers and groupers. Such species favour habitats under ledges and overhangs (Figure S1), and as many are ambush predators (e.g., *L. argentimaculatus*, *C. sonnerati*), this position may facilitate feeding in addition to providing shelter. Absence or low abundance of pelagic species at this seafloor–structure interface does not necessarily mean that they are not found in these sections but could very well reflect their transient nature or behaviour to the ROV (Bond et al., 2022).

Wells in the shallowest depths and those that were among the shortest in height were associated with high abundances of fishery target species (Figure 5). For well height, this result seems somewhat

TABLE 5 Total and mean (±SE) abundance (from MaxN), biomass B_i), and production estimates for subsea wells on the northwest shelf, Western Australia.

Species	 ***Lutjanus argentimaculatus***	 ***Lutjanus malabaricus***	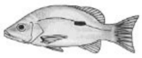 ***Lutjanus russellii***
# Wells observed	28	18	28
Depth range of wells	74.5–135	78–135	74.5–135
Total # individuals	151	92	1192
Mean # ± SE per well	5.39 ± 1.7	5.11 ± 1.17	42.57 ± 21.2
Total B_i (kg)	363.23	130.1	776.8
Mean ± SE B_i per well (kg)	12.97 ± 4.9	7.23 ± 0.4	27.74 ± 13.7
Total P (P kg year^{1})	47.22	14.96	118.08
Mean P per well (P kg year^{1} per well)	1.69 ± 0.65	0.83 ± 0.05	4.22 ± 2.08
Total P_{new} (P_{new} kg year^{1})	28.33	7.48	88.56
Mean P_{new} per well (P_{new} kg year^{1} per well)	1.01 ± 0.39	0.42 ± 0.02	3.16 ± 1.56

= number.

TABLE 6 Abundance of all fishery target species on remotely operated vehicle imagery of subsea pipelines. Ordered by region then approximately by depth.

		Depth range	**# Fishery target species**	**Total abundance**	***Lutjanus vitta*** 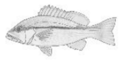	***Lutjanus russellii*** 	***Lutjanus quinquelineatus*** 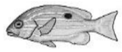
North-west	Tanker Loading Line	5–15	7	43	6	0	0
	2TL	60–80	26	1427	145	58	391
	Pluto	60–80	32	3624	1026	436	460
	Jansz	67–1,320	36	3734	466	770	288
	Wanaea Cossack	108–123	15	2176	1255	209	251
	Echo Yodel	120–140	18	2501	2	337	345
	Prelude	239–240	3	10	0	0	0
South-east					*Helicolenus* spp. 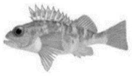	*Nemadactylus macropterus* 	*Arripis trutta* 
	MarlinA to Shore	45.4–55	9	928	53	445	250
	BreamB to BreamA	58–61	3	21	2	0	0
	Blackback to Mackerel	92–390	15	1669	919	580	0
	Flowline 2	132–138	4	153	145	5	0
	Flowline 5	141–152	1	131	131	0	0
	Flowline 6	142–153	4	427	408	5	0
	Flowline 9	226–270	6	134	94	1	0
	Flowline 1 (umbilical)	131–261	4	98	80	1	0
	Flowline 4 (umbilical)	141–152	4	107	102	1	0
	Flowline 8 (umbilical)	145–261	4	105	81	0	0

counterintuitive, as the surface area of structures and fish abundance are typically positively related. For example, Wilhelmsson et al. (2006) reported highest fish densities with greater vertical relief of offshore wind turbines. The complexity or surface area of artificial structures has also been found to have a positive relationship with abundances of fishes and epifauna (Bohnsack et al., 1994; Mintz et al., 1994; Hackradt et al., 2011). This abundance–well height relationship was likely driven by the particularly high abundance of fish on LN2 and LOW1, the two shallowest wells surveyed (Table S1). A potential reason for the negative relationship we found between well height and fishery target species abundance may be the overarching influence of depth. This variable was a strong predictor of abundance of target species (including lutjanids and serranids) with numbers declining as depth increased. Depth has also been shown to be a strong predictor of fish communities in natural ecosystems of this region (Abdul Wahab et al., 2018; Currey-Randall et al., 2021). In this case, shorter wells were found in the shallowest depths, which may have confounded the relationship between surface area and abundance.

Interestingly, fishery target species richness and Serranidae abundance increased with the percent cover of bare structure or wells coated in a thin “biofilm” of unidentifiable encrusting epibiota. The relationships were not strong (Figure 4) and for serranids occur in tandem with a high percent cover of “other” epibiota. Rather than suggest that wells relatively bare of epifauna promote the abundance of target species, this relationship is likely masking some other unmeasured, and therefore untested, variable that influences abundance. This might be revealed if the quality of imagery collected by ROVs was improved to allow better assessment of epibenthic communities. Furthermore, collection of such imagery could facilitate three-dimensional modelling and produce improved estimates of biofouling community weight that can be used to assist industry prepare for decommissioning.

For wells, we focused on three target snapper species that were particularly abundant and common on these structures in the NW and for which sufficient biological information existed to facilitate production modelling. Extraordinarily high abundances of *L. russellii* on LN2 (480) and LOW1 (448),

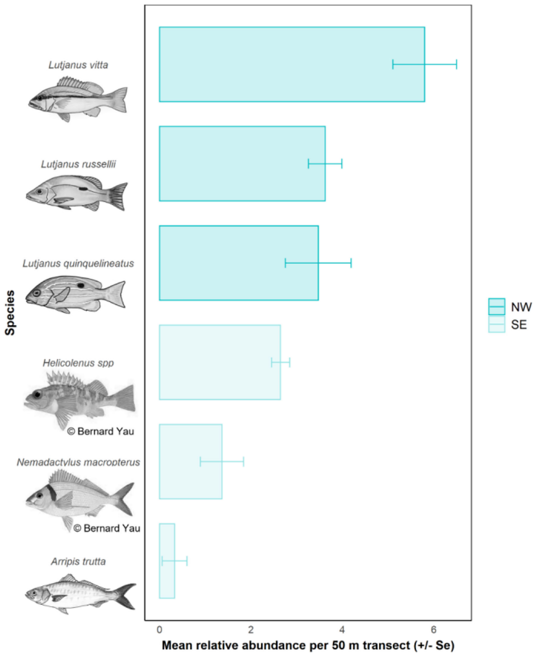

FIGURE 7
Top three most abundant fishery target species observed on pipelines in each region.

wells that were reasonably close together (6 km), suggested that the position of these on the North West Shelf may be of significance for this species. Both wells were in a similar depth (75–87 m) and were surveyed at the same time of year (late January 2018), coinciding with a full moon. The high abundance of these species we observed may be due to the presence of spawning schools of *L. russellii*. Although we could find no published works documenting the spawning location and timing for this species, spawning for other species in the family Lutjanidae occurs around new and full moon periods elsewhere (e.g., Russell and McDougall, 2008, for *L. argentimaculatus* off the coast of northeastern Australia). As *L. russellii* is long-lived (~20 years) with rapid growth toward asymptotic length, the species may be vulnerable to overfishing

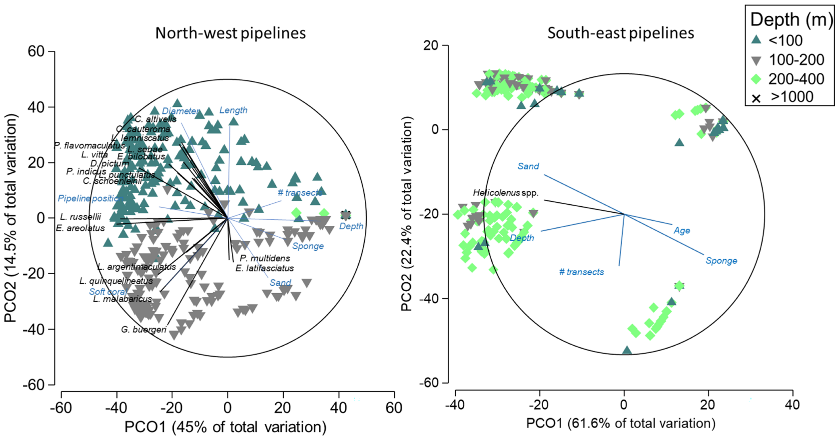

FIGURE 8
Principal component ordination (PCO) on fishery target species abundance on pipelines in the north-west and south-east marine regions. Vectors are displayed and show fish species and explanatory variables with Pearson's correlations of |R|>0.3 to one or more axes. Vectors indicate the direction of the relationship, and their length indicates the strength of their effect on the assemblage of fishery target species.

TABLE 7 Generalised additive models (GAMs) for predicting total fishery target species abundance, fishery target species richness, and the total abundance of Lutjanidae, Lethrinidae, and Serranidae observed on pipelines in depths <400 m in the north-west, within 2 Akaike information criterion of the top model.

Response	Model	R^2	ΔAICc	*w*AICc	AICc	edf
Richness	Age + Depth	0.34	0.00	0.97	1891.06	4.89
Total abundance	**Pipeline position + Sponge**	**0.26**	**0.00**	**0.68**	**3378.08**	**4.69**
	Other + Pipeline position	0.25	1.76	0.28	3379.85	3.83
Lutjanidae	Pipeline position + Sponge	0.19	0.00	0.94	2950.65	4.69
Lethrinidae	**Age + Depth**	**0.04**	**0.00**	**0.66**	**656.15**	**3.28**
	Length + Other	0.04	1.89	0.26	658.04	3.81
Serranidae	Bare/Biofilm + Transect (n)	0.76	0.00	0.92	1827.12	4.98

Where there was more than one model, the best model ranked using wAICc is indicated in bold.

(Newman, 2002b). Further research should seek to verify whether subsea wells are facilitating spawning of these target species in the NW, and if this proves to be the case, management measures (e.g., temporary closures) could be instigated to protect these locations. It is worth also noting that the abundances of *L. russellii* on these two wells were more than half the total annual catch of this species by the recreational and charter sector for WA (n = 753 in 2017/2018; Gaughan and Santoro, 2021). Of the 114 species/groups of taxa caught by commercial fisheries in WA, *L. russellii* is ranked 20th in terms of catch tonnage (67 tonnes in 2018/2019; Gaughan and Santoro, 2021).

The total average biomass of the three species we examined (*L. russellii*, *L. malabaricus*, *L. argentimaculatus*) was 47.94 kg per well or 115.24 g m^{-3} per well. The total biomass (1,270 kg) represents only a tiny fraction of the tonnage obtained across commercial and recreational fisheries in this region (approximately 1,170 tonnes in 2019/2020; Gaughan and Santoro, 2021). However, this value is higher than demersal species observed on a larger Sydney artificial reef (Table 2 in Smith et al., 2016). Our estimate of local production of fish per well was 105.2 g m^2 $year^{-1}$, and while lower than assemblage-level studies [e.g., 384 g m^{-2} $year^{-1}$, Smith et al. (2016); 105–887 g m^{-2} $year^{-1}$, Claisse et al. (2014)], it is still

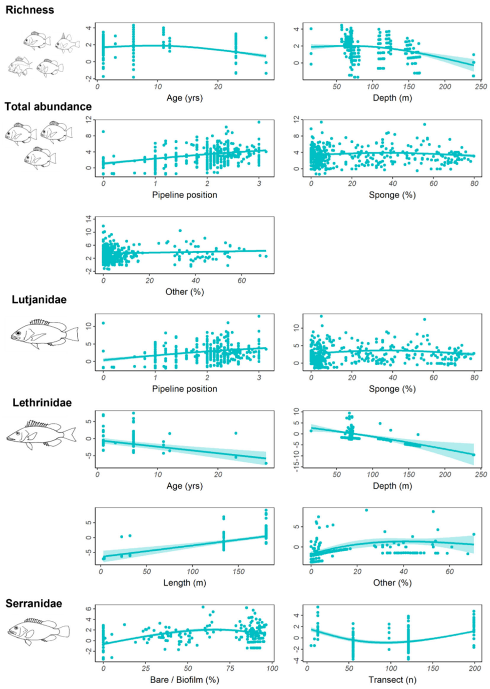

FIGURE 9
Total residual abundance of fishery target species, richness and residual abundance of the three most abundant fishery target families on pipelines in <400 m depth in the north-west. Residual abundances are plotted relative to their most important explanatory variables (Table 7, Figure S2). Models were fitted using Generalised additive models. The solid line represents the estimated smoothing curve, and dashed lines represent ±2 × SE of the estimate.

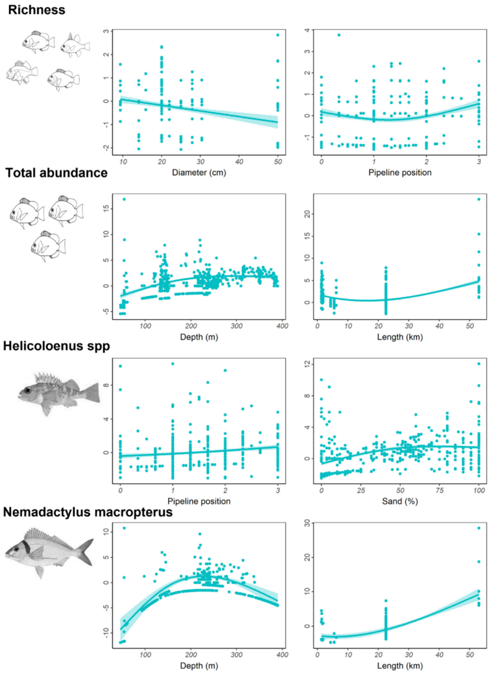

FIGURE 10
Total residual abundance of fishery target species, richness and residual abundance of the two most common fishery target species on pipelines in<400 m depth in the south-east. Residual abundances are plotted relative to their most important explanatory variables (Table 8, Figure S5). Models were fitted using Generalised additive models. The solid line represents the estimated smoothing curve, and dashed lines represent ±2 × south-east of the estimate.

similar to some oil platforms listed in Claisse et al. (2014). A lower production value here compared to these studies is not surprising given that our estimate reflects only three species (18 in Smith et al., 2016), species that are each relatively long-lived with low mortality and quite reef-affiliated and the conservative nature of "MaxN." Smith et al. (2016) also used a video method to sample fish, but instead of using the highest MaxN across sections of the artificial reef (as was done here), they summed each separate measure of relative abundance from the different areas of the reef. While the subsea wells surveyed here are approximately half the size of the Sydney artificial reef surveyed by Smith et al. (2016), our method would likely still have underestimated the abundances of species observed. Levels of production for each lutjanid species were within the range of those reported for demersal fish species on a shallow coral reef in Moorea (e.g., *Sargocentron microstroma*; Galzin, 1987) and coastal artificial reefs off southern California (e.g., *Embioloca jacksoni*; Johnson et al., 1994). In calculating this overall production, we averaged the total production across all wells where individuals were observed. If wells were considered on their own, production could be as little as zero where no individuals were observed or much higher, such as on LN2 where 480 *L. russellii* were observed, giving a total production value for this one species of 742.9 g m^2 $year^{-1}$ on this well. This highlights the importance and value of including multiple survey periods (e.g., long-term monitoring) in

TABLE 8 Generalised additive models (GAMs) for predicting total fishery target species abundance, fishery target species richness, and the total abundance of *Helicolenus* spp. *and Nemadactylus macropterus* on pipelines in depths < 400 m in the south-east, within 2 Akaike information criterion of the top model.

Response	Model	R^2	ΔAICc	*w*AICc	AICc	edf
Richness	**Age + Pipeline position**	**0.09**	**0.00**	**0.82**	**711.15**	**4.40**
	Diameter + Pipeline position	0.07	3.07	0.18	714.22	3.95
Total abundance	Depth + Length	0.01	0.00	1.00	3720.79	4.98
Helicolenus spp.	Pipeline position + Sand	0.21	0.00	1.00	2773.97	4.75
N. macropterus	Depth + Length	0.02	0.00	1.00	1455.81	4.95

Where there was more than one model evident, the best model ranked using wAICc is indicated in bold.

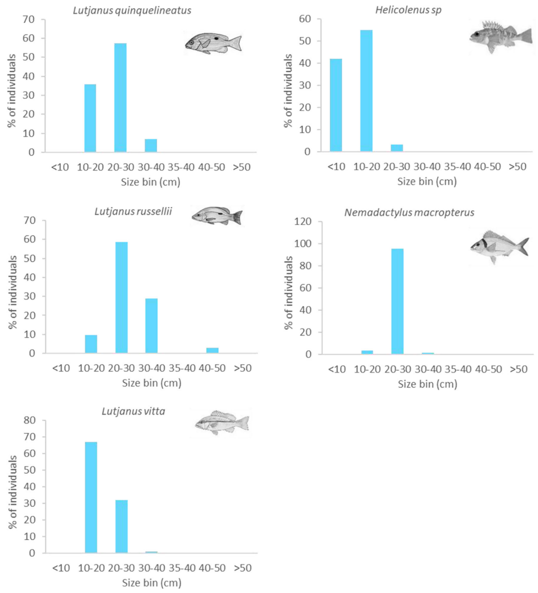

FIGURE 11
Size frequency of abundant fishery target species observed on subsea pipelines. Sizes estimated from imagery in 10-cm bins.

production estimates to obtain measures that more accurately encompass temporal variability in fish abundances. Without accounting for temporal variability in abundances, our production estimates reflect production for the period in which these structures were surveyed.

New production refers to the production that will be lost from the entire ecosystem (not just specific wells) if wells were to be removed. Here, our estimates of t_{prop} resulted in a total P_{new} across all wells (summed) of 124 kg year^{-1} (mean of 4.6 kg year^{-1} per well), which is ~69% of total local production. This result contrasts that of Smith et al. (2016) who found that new production was only 4% of total production per year. The result of Smith et al. (2016) was likely due to the high number of visitor species in their study compared to the comparatively more resident species surveyed here (Table 2). This result demonstrates that production measures can be higher for more resident reef-associated species, particularly when on structures in oligotrophic ecosystems where natural reef environments are lacking, such as those surveyed here. However, these results are based on a single survey period and, as stated, really need repeat surveys to better understand how resident or otherwise these species are on these structures and therefore to validate the accuracy of measures presented here.

4.2 Fishery target species on subsea pipelines in Australia

Many more target species were observed along subsea pipelines (90 spp.) than on well infrastructure (49 spp.), yet assemblages were similarly dominated by lutjanids, serranids, and carangids (total 46% species in these families). These families are known to be ubiquitous in natural reef ecosystems across the NW (McLean et al., 2016; Abdul Wahab et al., 2018; Currey-Randall et al., 2021) and, excluding tropical snappers, also in the SE marine region (Williams and Bax, 2001; Butler et al., 2002). As richness and abundance counts are intrinsically linked to sampling effort, and with disproportionate sampling effort across pipelines (Table S2), it is not possible to compare these measures across pipelines. However, we can describe the fish communities we observed and link this abundance to epibenthic communities and environmental and pipeline-specific variables, noting that (similar to wells) it is not possible to account for the likely influence of other unmeasured variables.

The most abundant taxa observed on pipelines in the SE was *Helicolenus* spp. (ocean perch), which is likely to include the two species that were indistinguishable in imagery (*H. barathi*—offshore and *H. percoides*—inshore). These species are targeted by the southern and eastern scalefish and shark fishery *via* bottom trawl and Danish seine with 189.2 tonnes landed in 2020–2021 (Patterson et al., 2021) and 304 tonnes permitted for the 2021–2022 season. Here, this species was most abundant in depths of 100–400 m, averaged 2.64 ± 0.2 individuals per 50-m transect, and was most abundant on Blackback (BKA) to Mackerel (MKA) (noting our caveat on sampling effort above). The abundance of *Helicolenus* spp. increased with increasing pipeline exposure and sand cover, suggesting that the species may be attracted to the pipeline as shelter in the absence of complex biota. Similar relationships between fish abundance and pipeline spans have been reported previously in the NW (McLean et al., 2017; Bond et al., 2018a; Schramm et al., 2021) and the North Sea (Redford et al., 2021). This pattern may also reflect known associations of this species with rocky habitat during the adult phase and soft habitat in the juvenile phase (Seiler et al., 2012). Here, the majority of this species were small (<20 cm; 96%) and as such are likely to be juveniles at ~5 years of age (Paul and Horn, 2009). Their observation on pipelines that were exposed but surrounded by soft sediment communities suggests both an affiliation with soft habitat and benefit derived from shelter that an exposed pipeline may offer.

The second most abundant target species observed in the SE region was *N. macropterus* (morwong), which, like *Helicolenus* spp., is a demersal fish found in continental waters of southern Australia (Jordan, 2001; Patterson et al., 2021). Targeted by the same fishery as ocean perch, 97.6 tonnes were landed in 2020–2021 (Patterson et al., 2021). Nearly all individuals we observed were estimated to be 20–30 cm in length, approximately the size at which this species attains maturity (23–29 cm; Jordan, 1998). Interestingly, 580 individuals of *N. macropterus* were observed on Blackback to Mackerel and 445 on MarlinA to Shore, yet none were observed on BreamB (BMB) to BreamA (BMA) pipeline and very few (0–5) on all other flowlines (Table 6). We are unsure why this might be the case, but note that it is unlikely due to imagery quality, depth, nor pipeline size, with these metrics similar to at least one other pipeline surveyed. The strongest environmental predictor for this species abundance in our models was depth, which indicated a peak around 200–300 m and therefore not too dissimilar for the depth at which peak catch rates occur in Tasmania (150–200 m) (Lyle and Ford, 1993).

The eastern Australian salmon (*A. trutta*) were abundant only on MarlinA to Shore (n = 250 individuals) but were observed on two transects, i.e., schools of individuals passing within view of the ROV. This species contributes significantly to the commercial fishery in SE Australia as well as being a prized recreational sportfish (Hughes, 2012; Hughes et al., 2017). After *A. trutta*, redfish (*Centroberyx affinis*), an endemic species to SE Australia, were the fourth most abundant fishery target species on pipelines in the SE, with all observations occurring in a single transect on MarlinA–Shore in<100-m depth. This species is presently classed as “overfished” by the southern and eastern scalefish and shark fishery (Patterson et al., 2021).

Lutjanids were the most abundant target species on subsea pipelines in NW Australia. Of these, *L. vitta* were the smallest in size and most abundant, averaging 5.8 ± 0.7 individuals per 50-m transect. This demersal reef-associated species is known to form schools (Newman et al., 2000) and is an important component of the northern demersal scalefish fishery, ranking #7 in terms of gross tonnage (Newman et al., 2020). Fetching a similar price to *L. vitta* ($3.93 kg), *L. quinquelineatus* were slightly larger and observed in similar abundances across pipelines in the NW region. This species is reported to be the most abundant lutjanid species on the Great Barrier Reef (Newman, 1995). Also particularly abundant, *L. russellii* are slightly larger-bodied lutjanids not known to form large schools (although see *Fishery target species on subsea wells in Australia* above). High abundance of lutjanids along pipelines supports previous research on pipelines in this region (Bond et al., 2018a; Bond et al., 2018b; Bond et al., 2018c; McLean et al., 2021a). The value of pipelines as habitat for lutjanids appears closely linked to the provision of shelter, with a higher abundance of these species where pipelines are less buried and span the seafloor (Figure 9).

A range of serranids and lethrinids were also abundant on subsea pipelines (Table S4), and although relationships with pipeline spanning were not evident at the level of family, some other factors relating to pipelines as structures did. A higher abundance of lethrinids on younger, shallower, longer pipelines suggests an abundance of these species on particular pipelines (or sections of pipelines), namely, Jansz and Pluto. Serranids tended to be present in higher abundance where pipelines were bare or coated in a thin biofilm of unidentified encrusting biota, a result similar to that observed to wells but suspected to be an artefact of imagery quality. There is potentially an undetected relationship with epibiotic communities for this species that requires higher-resolution imagery to resolve. There is perhaps also the potential that serranids may predate upon fauna that have a strong relationship with soft sediment communities (e.g., crabs, prawns). Examination of dietary studies of these species utilising O&G infrastructure would provide an improved understanding of the habitat value for these key fishery species.

5 Conclusion

The provision of hard surfaces configured with complexity that includes crevices and overhangs near the seafloor (e.g., near flow base of wells, under pipeline spans) appears to benefit the abundance of many demersal species that are targets of fisheries. Although industry seeks to minimise pipeline spans due to the increased prevalence of vortex vibrations and risks to pipeline integrity they can pose, this would likely reduce their value as habitat for these species. As previous research has shown, some fish may in fact maintain or even increase the size of such spans (Leckie et al., 2016). Other pipeline features such as concrete mattresses that add additional habitat complexity *via* increased surface area and crevices also have positive relationships with fish abundance (Rouse et al., 2019; Redford et al., 2021—North Sea) yet do not appear to be used as often in Australia perhaps due to lower incidences of trawl fishery interactions with pipelines. Although complex structure near the seabed is important for fishery target species, vertical relief that includes complexity (e.g., tree cap assembly on subsea wells) provides important habitat for non-fishery target species (McLean et al., 2021b). As many smaller-bodied non-target species are likely prey of larger (primarily predatory) fishery target species, structures that incorporate vertical height above the seafloor may provide habitat for a broader representation of species across trophic groups.

Research should build upon our first estimates of fish production for wells and assess such metrics for entire fish communities on offshore platforms, a feat that would require sampling an entire jacket structure to ensure accuracy in abundance estimates. All such analyses are based on a good understanding of the biology of species and for many species in remote regions such as the far NW and SE, such information is still to be acquired. Here, it is not possible to state whether the production and biomass of fish on subsea wells are significant relative to natural reefs or potential fishery contribution. Comparable surveys and fish production estimates across natural habitats are required in addition to temporal studies to better quantify variability in fish abundances at these structures.

In summary, our conclusions are as follows:

1. Every structure possesses a fish community seemingly shaped by a unique combination of environmental, structural, and biological relationships. As such, the impact of decommissioning on communities present and the broader ecological processes that they are a part of will need to be considered on a case-by-case basis.
2. Existing industry-held ROV imagery, while useful for documenting larger more mobile fauna and observing unique behaviours, range extensions, interactions, etc. (Macreadie et al., 2018; Todd et al., 2020), is typically not sufficient for quantifying epibenthic communities. An exception is the recent use of super High definition autonomous underwater vehicle (HD AUV) imagery (e.g., Cooper Energy flowlines, Wanaea Cossack pipeline). Imagery not fit for purpose limits our understanding of relationships between epibenthic communities and fishery species.
3. An understanding of the role that O&G structures play in marine ecosystems will require quantification of ecological phenomena such as connectivity, trophic relationships, and levels of residency (e.g., Fowler and Booth, 2012; Fowler et al., 2015). This will require dedicated and expanded sampling of offshore structures and surrounds. Until such quantitative data are obtained, studies rely heavily on estimates (e.g., residency rates here), and as such, queries or unanswered questions regarding their findings remain.
4. Before-after-control-impact studies with sufficient replication (spatially, temporally) are required to inform decommissioning. Such studies will enable not only better prediction of environmental impacts that may arise under different decommissioning options (informing comparative assessments) but also quantification of such impacts. A comparison of fish production on structures and in natural ecosystems before and after their decommissioning, in tandem with fishery spatial operations and catch per unit effort data, would improve our understanding of how this infrastructure contributes to fisheries and fish stocks generally in this region. This information is essential for decisions to be made that minimise environmental impacts and inform Australia's decommissioning journey ahead.

Data availability statement

The original contributions presented in the study are included in the article/Supplementary Material. Further inquiries can be directed to the corresponding author.

Ethics statement

Ethical review and approval was not required for the animal study because visual *in situ* observations only.

Author contributions

DM led the project. DM, CS, MB, JC, MC, MS, and BV undertook detailed video and statistical analysis. DM, CS, MB produced graphics. TB, DI, SWi, MT, and SWh provided additional data that was incorporated into the study. All authors contributed to writing of the manuscript. All authors contributed to the article and approved the submitted version.

Acknowledgments

We thank the National Decommissioning Research Initiative (NDRI) for coordinating the funding for this project, in addition to managing all contributing industry partners, namely Shell Australia Pty Ltd, Esso Australia Pty Ltd, Chevron Australia Pty Ltd, BHP Petroleum Pty Ltd, Woodside Energy Ltd, Santos Ltd, Vermillion Oil and Gas Australia Ltd, Cooper Energy Ltd. We thank Andrew Taylor for his tireless efforts as the founding Director and most recently, Sam Jarvis as the new Director. We thank the NDRI science advisory board, in particular Prof Peter Macreadie and Prof Iain Suthers for their ideas and guidance along the way. We also thank industry representatives for their advice and positive engagement throughout the project. Assistance in refining the production metrics for important commercially fished species was provided by Dr Stephen Newman (Department of Primary Industries and Region Development) for which we are grateful.

We acknowledge Douglas Reeves who commenced analysis of Bass Strait infrastructure for his masters, before moving on to employment. We thank Dr Mark Meekan and Dr Karen Miller for their review of our writings. AIMS acknowledges the Traditional Owners of the Country adjacent to where this research was undertaken. We recognise their ongoing spiritual and physical connection to Country and pay our respects to their Elders past, present and emerging.

Conflict of interest

The authors declare that the research was conducted in the absence of any commercial or financial relationships that could be construed as a potential conflict of interest.

Publisher's note

Supplementary material

The Supplementary Material for this article can be found online at: https://www.frontiersin.org/articles/10.3389/fmars.2022.960496/full#supplementary-material

References

Abdul Wahab, M. A., Radford, B., Cappo, M., Colquhoun, J., Stowar, M., Depczynski, M., et al. (2018). Biodiversity and spatial patterns of benthic habitat and associated demersal fish communities at two tropical submerged reef ecosystems. *Coral Reefs* 37 (2), 327–343. doi: 10.1007/s00338-017-1655-9

Althaus, F., Hill, N., Ferrari, R., Edwards, L., Przeslawski, R., Schönberg, C. H. L., et al. (2015). A standardised vocabulary for identifying benthic biota and substrata from underwater imagery: The CATAMI classification scheme. *PloS One* 10, e0141039–e0141039. doi: 10.1371/journal.pone.0141039

Anderson, M. J. (2004). *PERMDISP: a FORTRAN computer program for permutational analysis of multivariate dispersions (for any two-factor ANOVA design) using permutational tests* (New Zealand: Department of Statistics, University of Auckland).

Anderson, M., Gorley, R., and Clarke, K. (2008). *PERMANOVA+ for PRIMER: Guide to software and statistical methods* (Plymouth, UK: PRIMER-E Ltd).

Bohnsack, J. A., Harper, D. E., McClellan, D. B., and Hulsbeck, M. (1994). Effects of reef size on colonization and assemblage structure of fishes at artificial reefs off southeastern Florida, U.S.A. *Bull. Mar. Sci.* 55 (2-3), 796–823.

Bond, T., Langlois, T. J., Partridge, J. C., Birt, M. J., Malseed, B. E., Smith, L., et al. (2018c). Diel shifts and habitat associations of fish assemblages on a subsea pipeline. *Fish. Res.* 206, 220–234. doi: 10.1016/j.fishres.2018.05.011

Bond, T., McLean, D. L., Prince, J., Taylor, M. D., and Partridge, J. C. (2022). Baited remote underwater video sample less site attached fish species along a subsea pipeline compared to a remotely operated vehicle. *Mar. Freshw. Res* 73 (7), 915–930. doi: 10.1071/MF21261

Bond, T., McLean, D. L., Wakefield, C., Partridge, J., Prince, J., White, D., et al. (2021). Quantifying fishing activity targeted subsea pipelines by commercial trap fishers. *Rev. Fish Biol. Fish.* 31, 1009–1023. doi: 10.1007/s11160-021-09686-4

Bond, T., Partridge, J. C., Taylor, M. D., Cooper, T. F., and McLean, D. L. (2018a). The influence of depth and a subsea pipeline on fish assemblages and commercially fished species. *PloS One* 13, e0207703. doi: 10.1371/journal.pone.0207703

Bond, T., Partridge, J. C., Taylor, M. D., Langlois, T. J., Malseed, B. E., Smith, L. D., et al. (2018b). Fish associated with a subsea pipeline and adjacent seafloor of the north West shelf of Western Australia. *Mar. Environ. Res.* 141, 53–65. doi: 10.1016/j.marenvres.2018.08.003

Bugnot, A. B., Mayer-Pinto, M., Airoldi, L., Heery, E. C., Johnston, E. L., Critchley, L. P., et al. (2021). Current and projected global extent of marine built structures. *Nat. Sustain.* 4, 33–41. doi: 10.1038/s41893-020-00595-1

Burnham, K. P., and Anderson, D. R. (2003). *Model selection and multimodel inference: A practical information-theoretic approach* (New York: Springer New York). doi: 10.1007/b97636

Butler, A., Althaus, F., Furlani, D., and Ridgway, K. (2002). Assessment of the conservation values of the bass strait sponge beds area. *CSIRO Mar. Res. Rep. Environ. Aust.*, 64.

Cappo, M., Harvey, E., and Shortis, M. (2007). "Counting and measuring fish with baited video techniques – an overview," in *Proceedings of the 2006 Australian society of fish biology conference and workshop cutting edge technologies in fish and fisheries science*. Eds. J. M. Lyle, D. M. Furlani and C. D. Buxton (Hobart: ASFB, Hobart).

Christensen, V., and Pauly, D. (1992). ECOPATH II–a software for balancing steady-state ecosystem models and calculating network characteristics. *Ecol. Model.* 61, 169–185. doi: 10.1016/0304-3800(92)90016-8

Claisse, J. T., Pondella, D. J.II, Love, M., Zahn, L. A., Williams, C. M., and Bull, A. S. (2015). Impacts from partial removal of decommissioned oil and gas platforms on fish biomass and production on the remaining platform structure and surrounding shell mounds. *PloS One* 10, e0135812. doi: 10.1371/journal.pone.0135812

Claisse, J. T., Pondella, D. J., Love, M., Zahn, L. A., Williams, C. M., Williams, J. P., et al. (2014). Oil platforms off California are among the most productive marine fish habitats globally. *Proc. Natl. Acad. Sci.* 111, 15462–15467. doi: 10.1073/pnas.1411477111

Clarke, K., and Gorley, R. (2015). *PRIMER v7: User Manual/Tutorial* (Plymouth, UK: PRIMER-E Ltd).

CODA (2021). "A baseline assessment of australia's offshore oil and gas decommissioning liability," in *Summary of an advisian study commissioned by the centre of decommissioning Australia (CODA).*

Cowan, J. H., and Rose, K. A. (2016). "O&G platforms in the gulf of Mexico: their relationship to fish and fisheries. chapter 5," in *Fisheries and aquaculture in the modern world*. Ed. H. Mikkola (London: IntechOpen).

Currey-Randall, L. M., Galaiduk, R., Stowar, M., Vaughan, B. I., and Miller, K. J. (2021). Mesophotic fish communities of the ancient coastline in Western Australia. *PloS One* 16 (4), e0250427. doi: 10.1371/journal.pone.0250427

Dempster, T., and Taquet, M. (2004). Fish aggregation device (FAD) research: gaps in current knowledge and future directions for ecological studies. *Rev. Fish Biol. Fish.* 14, 21–42. doi: 10.1007/s11160-004-3151-x

Dickie, L. (1972). Food chains and fish production. *Int. Comm. Northwest Atl. Fish. Spec. Publ.* 8, 201–219.

Fisher, R., Wilson, S. K., Sin, T. M., Lee, A. C., and Langlois, T. J. (2018). A simple function for full-subsets multiple regression in ecology with r. *Ecol. Evol.* 8, 6104–6113. doi: 10.1002/ece3.4134

Fowler, A. M., and Booth, D. J. (2012). Evidence of sustained populations of a small reef fish on artificial structures. does depth affect production on artificial reefs? *J. Fish Biol.* 80, 613–629. doi: 10.1111/j.1095-8649.2011.03201.x

Fowler, A. M., Macreadie, P. I., Bishop, D. P., and Booth, D. J. (2015). Using otolith microchemistry and shape to assess the habitat value of oil structures for reef fish. *Mar. Environ. Res.* 106, 103–113. doi: 10.1016/j.marenvres.2015.03.007

Franks, J. S. (2000). A review: pelagic fishes at petroleum platforms in the northern gulf of mexico; diversity, interrelationships, and perspectives. *Pêche Thonière Dispositifs Concentration 21oisons Caribbean-Martinique*, 502–515.

Fujii, T. (2015). Temporal variation in environmental conditions and the structure of fish assemblages around an offshore oil platform in the north Sea. *Mar. Environ. Res.* 108, 69–82. doi: 10.1016/j.marenvres.2015.03.013

Gallaway, B. J., Szedlmayer, S. T., and Gazey, W. J. (2009). A life history review for red snapper in the gulf of Mexico with an evaluation of the importance of offshore petroleum platforms and other artificial reefs. *Rev. Fish. Sci.* 17, 48–67. doi: 10.1080/10641260802160717

Galzin, R. (1987). Potential fisheries yield of a moorea fringing reef (French Polynesia) by the analysis of three dominant fishes. *Atoll Res. Bull.* 305, 1–21. doi: 10.5479/si.00775630.305.1

Gaughan, D. J., and Santoro, K. (2021). *Status reports of the fisheries and aquatic resources of Western Australia 2019/20: The state of the fisheries* (Western Australia: Department of Primary Industries and Regional Development).

Gourvenec, S., Sturt, F., Reid, E., and Trigos, F. (2022). Global assessment of historical, current and forecast ocean energy infrastructure: Implications for marine space planning, sustainable design and end-of-engineered-life management. *Renewable Sustain. Energy Rev.* 154, 111794. doi: 10.1016/j.rser.2021.111794

Hackradt, C. W., Félix-Hackradt, F. C., and García-Charton, J. A. (2011). Influence of habitat structure on fish assemblage on an artificial reef in southern Brazil. *Mar. Environ. Res.* 72 (5), 235–247. doi: 10.1016/j.marenvres.2011.09.006

Hall, A. E., and Kingsford, M. J. (2021). Habitat type and complexity drive fish assemblages in a tropical seascape. *J. Fish Biol.* 99 (4), 1364–1379. doi: 10.1111/jfb.14843

Hastie, T., and Tibshirani, R. (1986). Generalized additive models. *Stat. Sci.* 1, 297–310. doi: 10.1214/ss/1177013604

Hauser, A., Attrill, M., and Cotton, P. A. (2006). Effects of habitat complexity on the diversity and abundance of macrofauna colonising artificial kelp holdfasts. *Mar. Ecol. Prog. Ser.* 325, 93–100. doi: 10.3354/meps325093

Hughes, J. M. (2012). *The biology and population structure of eastern Australian salmon (Arripis trutta) in south-eastern Australia* (The University of New South Wales).

Hughes, J. M., Stewart, J., Lyle, J. M., McAllister, J., Stocks, J. R., and Suthers, I. M. (2017). Influence of latitudinal variation in environmental gradients and population structure on the demography of a widespread pelagic fish, *Arripis trutta* (Forster 1801). *Environ. Biol. Fish* 11, 121–135. doi: 10.1007/s10641-016-0565-y

Ierodiaconou, D., McLean, D., Birt, M., Bond, T., Whitmarsh, S., Wines, S., et al. (2021). Industry remotely operated video imagery for assessing marine communities associated with subsea oil and gas infrastructure in south-east Australia.

Johnson, T. D., Barnett, A. M., DeMartini, E. E., Craft, L. L., Ambrose, R. F., and Purcell, L. J. (1994). Fish production and habitat utilization on a southern California artificial reef. *Bull. Mar. Sci.* 55 (2-3), 709–723.

Jordan, A. R. (1998) *The life -history ecology of platycephalus bassensis and nemadactylus macropterus*. Available at: https://eprints.utas.edu.au/16414/2/jordon_whole.pdf.

Jordan, A. R. (2001). Spatial and temporal variations in abundance and distribution of juvenile and adult jackass morwong, *Nemadactylus macropterus*, in south-eastern Tasmania. *Mar. Freshw. Res.* 52 (4), 661–670. doi: 10.1071/MF99156

Jorgensen, D. (2009). An oasis in a watery desert? discourses on an industrial ecosystem in the gulf of Mexico rigs-to-Reefs program. *Hist Technol.* 25 (4), 343–364. doi: 10.1080/07341510903313030

Kaiser, M. J. (2006). The Louisiana artificial reef program. *Mar. Policy* 30, 605–623. doi: 10.1016/j.marpol.2005.04.005

Kovalenko, K. E., Thomaz, S. M., and Warfe, D. M. (2012). Habitat complexity: Approaches and future directions. *Hydrobiologia* 685 (1), 1–17. doi: 10.1007/s10750-011-0974-z

Leckie, S., Mohr, H., Draper, S., McLean, D., White, D., and Cheng, L. (2016). Sedimentation-induced burial of subsea pipelines: observations from field data and laboratory experiments. *Coast. Eng.* 114, 137–158. doi: 10.1016/j.coastaleng.2016.04.017

Levene, H. (1960). "Robust tests for equality of variances," in *Contributions to probability and statistics: Essays in honor of Harold hotelling*. Eds. I. Olkin, H. Hotelling, et al (Palo Alto, CA: Stanford University Press), 278–292.

Lindberg, W. J. (1997). Can science resolve the attraction-production issue? *Fisheries* 22, 10–13.

Love, M. S., Kui, L., and Claisse, J. (2019). The role of jacket complexity in structuring fish assemblages in the midwaters of two California oil and gas platforms. *Bull. Mar. Sci.* 95 (4), 597–615. doi: 10.5343/bms.2017.1131

Love, M. S., Schroeder, D. M., and Nishimoto, M. M. (2003). "The ecological role of O&G production platforms and natural outcrops on fishes in southern and central California: a synthesis of information," U. S. Department of the Interior, United States Geological Survey, Biological Resources Division, Seattle, Washington, 98104, OCS Study MMS 2003-032.

Love, M. S., and York, A. (2005). A comparison of the fish assemblages associated with an oil/gas pipeline and adjacent seafloor in the Santa Barbara channel, southern California bight. *Bull. Mar. Sci.* 77, 101–118.

Lyle, J. M., and Ford, W. B. (1993). *Review of trawl research 1979-1987: With summaries of biological information for the major species* (Tasmania. Division of Sea: Department of Primary Industry and Fisheries).

Macreadie, P. I., McLean, D. L., Thomson, P. G., Partridge, J. C., Jones, D. O. B., Gates, A. R., et al. (2018). Eyes in the sea: Unlocking the mysteries of the ocean using industrial, remotely operated vehicles (ROVs). *Sci. Total Environ.* 634, 1077–1091. doi: 10.1016/j.scitotenv.2018.04.049

Martin-Smith, K. M. (1993). Abundance of mobile epifauna: The role of habitat complexity and predation by fishes. *J. Exp. Mar. Biol. Ecol.* 174 (2), 243–260. doi: 10.1016/0022-0981(93)90020-O

McLean, D. L., Birt, M., Speed, C., Case, M., Colquhoun, J., Galaiduk, R., et al. (2021b). Marine communities of australia's oil and gas infrastructure. *Draft Rep. Rev. A Natl. Decommissioning Res. Initiat. RP1:Pro1.*, 133.

McLean, D., Cure, K., Abdul Wahab, M. A., Galaiduk, R., Birt, M., Vaughan, B., et al. (2021a). A comparison of marine communities along a subsea pipeline with those in surrounding seabed areas. *Cont. Shelf Res.* 219, 104394. doi: 10.1016/j.csr.2021.104394

McLean, D., Langlois, T. J., Bond, T., Birt, M. J., Bornt, K. R., Collins, D. L., et al. (2016). Distribution, abundance, diversity and habitat associations of fishes across a dynamic bioregion experiencing rapid coastal development. *Estuar. Coast. Shelf Sci.* 178, 36–47. doi: 10.1016/j.ecss.2016.05.026

McLean, D. L., Partridge, T. J. C., Bond, T., Birt, M. J., Bornt, K. R., and Langlois, T. J. (2017). Using industry ROV videos to assess fish associations with subsea pipelines. *Cont. Shelf Res.* 141, 76–97. doi: 10.1016/j.csr.2017.05.006

McLean, D. L., Taylor, M. D., Giraldo Ospina, A., and Partridge, J. C. (2019). An assessment of fish and marine growth associated with an oil and gas platform jacket using an augmented remotely operated vehicle. *Cont. Shelf Res.* 179, 66–84. doi: 10.1016/j.csr.2019.04.006

McLean, D. L., Taylor, M. D., Partridge, J. C., Gibbons, B., Langlois, T. J., Malseed, B. E., et al. (2018). Fish and habitats on wellhead infrastructure on the north west shelf of Western Australia. *Cont. Shelf Res.* 164, 10–27. doi: 10.1016/j.csr.2018.05.007

McLean, D. L., Vaughan, B. I., Malseed, B. E., and Taylor, M. D. (2020). Fish-habitat associations on a subsea pipeline within an Australian marine park. *Mar. Environ. Res.* 153, 104813. doi: 10.1016/j.marenvres.2019.104813

Menge, B. A., and Sutherland, J. P. (1976). Species diversity gradients: synthesis of the roles of predation, competition, and temporal heterogeneit. *Am. Nat.* 110 (973), 351–369. doi: 10.1086/283073

Mertz, G., and Myers, R. A. (1998). A simplified formulation for fish production. *Canadian Journal of Fisheries and Aquatic Sciences* 55, 478–484.

Mintz, J. D., Lipcius, R. N., Eggleston, D. B., and Seebo, M. S. (1994). Survival of juvenile Caribbean spiny lobster: effects of shelter size, geographic location and conspecific abundance. *Mar. Ecol. Prog. Ser.* 112, 255–266. doi: 10.3354/meps112255

Munnelly, R. T., Reeves, D. B., Chesney, E. J., and Baltz, D. M. (2021). Spatial and temporal influences of nearshore hydrography on fish assemblages associated with energy platforms in the northern Gulf of Mexico. *Estuaries and Coasts* 44, 269–285.

Newman, S. J. (1995). *Spatial variability in the distribution, abundance, growth, mortality and age structures of tropical snappers (Pisces: Lutjanidae) in the central great barrier reef, Australia* (Townsville: James Cook University of North Queensland), 325.

Newman, S. J., Cappo, M., and Williams, D. M. B. (2000). Age, growthand mortality of the stripey, Lutjanus carponotatus (Richardson), and the brown-stripe snapper, L. vitta (Quoy andGaimard), from the central Great Barrier Reef, Australia. *Fish. Res.* 48, 263–275. doi: 10.1016/S0165-7836(00)00184-3

Newman, S. J. (2002a). Growth rate, age determination, natural mortality and production potential of the scarlet seaperch, lutjanus malabaricus Schneider 1801, off the pilbara coast of north-Western Australia. *Fish. Res.* 58, 215–225. doi: 10.1016/S0165-7836(01)00367-8

Newman, S. J. (2002b). Growth, age estimating and preliminary estimates of longevity and mortality in the Moses perch, *Lutjanus russellii* (Indian ocean form), from continental shelf waters off north-Western Australia. *Asian Fish. Sci.* 15, 283–294. doi: 10.33997/j.afs.2002.15.3.009

Newman, S., Wakefield, C., Skepper, C., Boddington, D., and Steele, A. (2020). "North coast demersal resource status report 2020," in *Status reports of the fisheries and aquatic resources of Western Australia 2019/20: The state of the fisheries*. Eds. D. J. Gaughan and K. Santoro (Western Australia: Department of Primary Industries and Regional Development), 156–165.

O'Hara, R. B., and Kotze, D. J. (2010). Do not log-transform count data. *Methods Ecol. Evol.* 1, 118–122. doi: 10.1111/j.2041-210X.2010.00021.x

Oil and Gas UK (2016) *Decommissioning insight report*. Available at: https://cld.bz/bookdata/jb05Hxr/basic-html/page-4.html.

Patterson, H., Bromhead, D., Galeano, D., Larcombe, J., Woodhams, J., and Curtotti, R. (2021). *Fishery status reports 2021, Australian bureau of agricultural and resource economics and sciences, Canberra*. doi: 10.25814/vahf-ng93

Paul, L. J., and Horn, P. L. (2009). Age and growth of sea perch (*Helicolenus percoides*) from two adjacent areas off the east coast of south island, new Zealand. *Fish. Res.* 95, 169–180. doi: 10.1016/J.FISHRES.2008.08.011

Pember, M. B., Newman, S. J., Hesp, S. A., Young, G. C., Skepper, C. L., Hall, N. G., et al. (2005). "Biological parameters for managing the fisheries for blue and king threadfins, estuary rockcod, malabar grouper and mangrove jack in north-western Australia," in *Final report to the fisheries research and development corporation* (Murdoch, Western Australia, Australia: Centre for Fish and Fisheries Research, Murdoch University), PIddic172.

Piddocke, T. P., Butler, G. L., Butcher, P. A., Stewart, J., Bucher, D. J., and Christidis, L. (2015). Age and growth of mangrove red snapper *Lutjanus argentimaculatus* at its cool-water-range limits. *J. Fish Biol.* 86, 1587–1600. doi: 10.1111/jfb.12665

Pradella, N., Fowler, A. M., Booth, D. J., and Macreadie, P. I. (2014). Fish assemblages associated with oil industry structures on the continental shelf of north-western Australia. *J. Fish Biol.* 84, 247–255. doi: 10.1111/jfb.12274

R Development Core Team (2019). R: A Language and Environment for Statistical Computing. R Foundation for Statistical Computing, Vienna, Austria.

Randall, R. G., and Minns, C. K. (2000). Use of fish production per unit biomass ratios for measuring the productive capacity of fish habitats. *Can. J. Fish. Aquat. Sci.* 57, 1657–1667. doi: 10.1139/f00-103

Redford, M., Rouse, S., Hayes, P., and Wilding, T. A. (2021). Benthic and fish interactions with pipeline protective structures in the north Sea. *Front. Mar. Sci.* 8, 417. doi: 10.3389/fmars.2021.652630

Rouse, S., Hayes, P., and Wilding, T. A. (2020). Commercial fisheries losses arising from interactions with offshore pipelines and other oil and gas infrastructure and activities. *ICES J. Mar. Sci.* 77 (3), 1148–1156. doi: 10.1093/icesjms/fsy116

Rouse, S., Kafas, A., Hayes, P., and Wilding, T. A. (2018). Offshore pipeline decommissioning: scale and context. *Mar. pollut. Bull.* 129, 241–244. doi: 10.1016/j.marpolbul.2018.02.041

Rouse, S., Lacey, N. C., Hayes, P., and Wilding, T. A. (2019). Benthic conservation features and species associated with subsea pipelines: considerations for decommissioning. *Front. Mar. Sci.* 6. doi: 10.3389/fmars.2019.00200

Russell, D. J., and McDougall, A. J. (2008). Reproductive biology of mangrove jack (*Lutjanus argentimaculatus)* in northeastern Queensland, Australia. *New Z. Mar. Freshw. Res.* 42, 219–232. doi: 10.1080/00288330809509950

Schramm, K. D., Marnane, M. J., Elsdon, T. S., Jones, C. M., Saunders, B. J., Newman, S. J., et al. (2021). Fish associations with shallow water subsea pipelines compared to surrounding reef and soft sediment habitats. *Sci. Rep.* 11, 6238. doi: 10.1038/s41598-021-85396-y

SeaGIS (2020a). *TransectMeasure* (Bacchus Marsh: SeaGIS Pty Ltd). Available at: http://www.seaGIS.com.au.

SeaGIS (2020b). *EventMeasure (Stereo) (version 5.22)* (Bacchus Marsh: SeaGIS Pty Ltd). Available at: http://www.seaGIS.com.au.

Seiler, J., Williams, A., and Barrett, N. (2012). Assessing size, abundance and habitat preferences of the ocean perch *Helicolenus percoides* using an AUV-borne stereo camera system. *Fish. Res.* 129, 64–72. doi: 10.1016/j.fishres.2012.06.011

Simonsen, K. A. (2013). *Reef fish demographics on Louisiana artificial reefs: the effects of reef size on biomass distribution and foraging dynamics* (Louisiana State University: Dissertation).

Smith, J. A., Lowr, M. B., Champion, C., and Suthers, I. M. (2016). A designed artificial reef is among the most productive marine fish habitats: new metrics to address 'production versus attraction'. *Mar. Biol.* 163, 188. doi: 10.1007/s00227-016-2967-y

Szedlmayer, S. T., and Shipp, R. L. (1994). Movement and growth of red snapper, *Lutjanus campechanus*, from an artificial reef area in the northeastern gulf of Mexico. *Bull. Mar. Sci.* 55, 887–896.

Symonds, M. R. E., and Moussalli, A.. (2011). A brief guide to model selection, multimodel inference and model averaging in behavioural ecology using Akaike's information criterion. *Behavioral Ecology and Sociobiology* 65 (1), 13–21. doi: 10.1007/s00265-010-1037-6

Todd, V. L. G., Lazar, L., Williamson, L. D., Peters, I. T., Hoover, A. L., Cox, S. E., et al. (2020). Underwater visual records of marine megafauna around offshore anthropogenic structures. *Front. Mar. Sci.* 7, 230. doi: 10.3389/fmars.2020.00230

Tweedie, M. (1984). "An index which distinguishes between some important exponential families," in *In 'Statistics: Applications and new directions: Proc. Indian statistical institute golden jubilee international conference'*, pp. 579–604.

Wickham, H. (2016). *ggplot2: Elegant graphics for data analysis* (New York, NY, Springer). doi: 10.1007/978-0-387-98141-3

Wilhelmsson, D., Malm, T., and Öhman, M. C. (2006). The influence of offshore windpower on demersal fish. *ICES J. Mar. Sci.* 63, 775–784. doi: 10.1016/j.icesjms.2006.02.001

Williams, A., and Bax, N. (2001). Delineating fish-habitat associations for spatially-based management: an example from the south-eastern Australian continental shelf. *Mar. Freshw. Res. Mar. Freshw. Res.* 52 (4), 513–536. doi: 10.1071/MF00017

Wood, S. N. (2011). Fast stable restricted maximum likelihood and marginal likelihood estimation of semiparametric generalized linear models. *J. R. Stat. Soc. Ser. B: Stat. Method.* 73, 3–36. doi: 10.1111/j.1467-9868.2010.00749.x

frontiers | Frontiers in Marine Science

TYPE Original Research
PUBLISHED 14 September 2022
DOI 10.3389/fmars.2022.980384

Check for updates

OPEN ACCESS

EDITED BY
Daniel Joseph Pondella,
Occidental College, United States

REVIEWED BY
Ilana Rosental Zalmon,
State University of the North Fluminense Darcy Ribeiro, Brazil
Tim Glasby,
New South Wales Department of Primary Industries, Australia

*CORRESPONDENCE
Avery B. Paxton
avery.paxton@noaa.gov

†PRESENT ADDRESS
D'amy N. Steward,
University of Guam Marine Laboratory,
Mangilao, GU, United States

SPECIALTY SECTION
This article was submitted to Marine Ecosystem Ecology, a section of the journal Frontiers in Marine Science

RECEIVED 28 June 2022
ACCEPTED 18 August 2022
PUBLISHED 14 September 2022

CITATION
Steward DN, Paxton AB, Bacheler NM, Schobernd CM, Mille K, Renchen J, Harrison Z, Byrum J, Martore R, Brinton C, Riley KL, Taylor JC and Kellison GT (2022) Quantifying spatial extents of artificial versus natural reefs in the seascape.
Front. Mar. Sci. 9:980384.
doi: 10.3389/fmars.2022.980384

Quantifying spatial extents of artificial versus natural reefs in the seascape

D'amy N. Steward[1†], Avery B. Paxton[2*], Nathan M. Bacheler[3], Christina M. Schobernd[3], Keith Mille[4], Jeffrey Renchen[4], Zach Harrison[5], Jordan Byrum[5], Robert Martore[6], Cameron Brinton[7], Kenneth L. Riley[2], J. Christopher Taylor[2] and G. Todd Kellison[3]

[1]Duke University Marine Lab, Duke University, Beaufort, NC, United States, [2]National Centers for Coastal Ocean Science, National Ocean Service, National Oceanic and Atmospheric Administration, Beaufort, NC, United States, [3]Southeast Fisheries Science Center, National Marine Fisheries Service, National Oceanic and Atmospheric Administration, Beaufort, NC, United States, [4]Division of Marine Fisheries Management, Florida Fish and Wildlife Conservation Commission, Tallahassee, FL, United States, [5]North Carolina Division of Marine Fisheries, North Carolina Department of Environmental Quality, Morehead City, NC, United States, [6]Marine Resources Division, South Carolina Department of Natural Resources, Charleston, SC, United States, [7]Coastal Resources Division, Georgia Department of Natural Resources, Brunswick, GA, United States

With increasing human uses of the ocean, existing seascapes containing natural habitats, such as biogenic reefs or plant-dominated systems, are supplemented by novel, human-made habitats ranging from artificial reefs to energy extraction infrastructure and shoreline installments. Despite the mixture of natural and artificial habitats across seascapes, the distribution and extent of these two types of structured habitats are not well understood but are necessary pieces of information for ocean planning and resource management decisions. Through a case study, we quantified the amount of seafloor in the southeastern US (SEUS; 103,220 km^2 in the Atlantic Ocean; 10 – 200 m depth) covered by artificial reefs and natural reefs. We developed multiple data-driven approaches to quantify the extent of artificial reefs within state-managed artificial reef programs, and then drew from seafloor maps and published geological and predictive seafloor habitat models to develop three estimates of natural reef extent. Comparisons of the extent of natural and artificial reefs revealed that artificial reefs account for substantially less habitat (average of two estimates 3 km^2; <0.01% of SEUS) in the region than natural reefs (average of three estimates 2,654 km^2; 2.57% of SEUS) and that this pattern holds across finer regional groupings (e.g., states, depth bins). Our overall estimates suggest that artificial reef coverage is several orders of magnitude less than natural reef coverage. While expansive seafloor mapping and characterization efforts are still needed in SEUS waters, our results fill information gaps regarding the extent of artificial and natural reef habitats in the region, providing support for ecosystem-based management, and demonstrating an approach applicable to other regions.

KEYWORDS

artificial reef, habitat distribution, natural reef, seascape ecology, seafloor habitat, structured habitat

Introduction

Artificial habitats are increasingly prevalent in marine environments, where human uses of the coastal oceans are often accompanied by installations of artificial or engineered structures and other materials, a phenomenon sometimes referred to as ocean sprawl (Firth et al., 2016) or marine urbanization (Dafforn et al., 2015). The global extent of artificial structures was estimated to be at least 32,000 km^2 in 2018 and is projected to increase to 39,400 km^2 by 2028 (Bugnot et al., 2021). These structures include artificial reefs, energy extraction infrastructure, and shoreline installments (Heery et al., 2017). Artificial reefs, for example, are deployed for a variety of purposes, such as enhancing or supplementing existing habitat, restoring degraded habitat, providing opportunities for fishing and diving recreation, or mitigating environmental impacts (Seaman, 2007; Becker et al., 2018; Lee et al., 2018; Ramm et al., 2021). Energy extraction infrastructure includes structures, such as wind turbines, tidal power extraction devices, and current hydrokinetic energy, that extract renewable energy (Miller et al., 2013), as well as infrastructure required for oil and gas production (Claisse et al., 2014). Human-made shoreline structures that afford habitat values and ecosystem services include structures, such as piers, jetties, breakwaters, and groins (Dugan et al., 2011).

With increased marine urbanization, natural biogenic reefs (e.g., rocky reefs, coral reefs, oyster reefs) and plant-dominated systems (e.g., seagrass or mangroves) in the seascape are supplemented by, or in some cases – replaced by, artificial, human-made structures. Artificial structures added to seascapes already containing natural habitats form novel habitats whose function may differ from those of their natural counterparts. For instance, the introduction of human-made structures alters ecosystem connectivity (Bishop et al., 2017), especially in circumstances where artificial reefs are deployed near existing natural structured habitats, such as rocky reefs (Rosemond et al., 2018) or coral reefs (Stone et al., 1979). Artificial structures have the potential to facilitate invasions (Bulleri and Airoldi, 2005) and range expansions (Cannizzo and Griffen, 2019), by providing support for species at their range edges (Paxton et al., 2019b) and for highly-migratory species, such as sharks and large predators (Paxton et al., 2020). Some artificial structures (e.g., oil platforms) have been estimated to be among the most productive marine fish habitats (Claisse et al., 2014) and these novel human-made habitats (van Elden et al., 2019) support high degrees of zooplanktivory (Champion et al., 2015) and enhance epifaunal invertebrate biomass and associate macrofauna (Gates et al., 2019).

Despite the mixture of natural and artificial habitats that occur across the seascape, the relative distribution and extent of these two structured habitat types is not well understood. Given the increasing number of artificial structures in the marine environment and the often-distinct ecological role of artificial habitats, quantifying the extent of artificial versus natural habitats would provide information useful for guiding ocean planning decisions. Here, we quantify the extent of natural versus artificial reefs through a case study in the southeastern US (SEUS, Atlantic Ocean). Artificial reefs are defined as structures intentionally sunk by state-managed artificial reef programs and do not include historic shipwrecks or oil and gas infrastructure (Figures 1A, B). We focus on the SEUS because its continental shelf contains naturally occurring reefs that are now joined by artificial reefs deployed through state-managed artificial reef programs and intended to enhance existing natural habitat and provide sites for fishers and divers to use. The extent of artificial reefs in the SEUS has not, to our knowledge, been previously quantified.

Natural reefs in the region are patchy (Powles and Barans, 1980; Parker et al., 1983; Schobernd and Sedberry, 2009) and highly variable in size, structure, and composition, ranging from high-relief rocky ledges and outcrops to flat pavement sometimes covered by a veneer of sand (Barans and Henry, 1984; Parker Jr. and Mays, 1998) (Figures 1C, D). Because of their patchy and variable nature, natural reef extent has rarely been estimated in the SEUS and seafloor coverage estimates using limited data range from 3% to 30%. The most comprehensive study to estimate the extent of natural reefs in the SEUS used a stratified random sampling design and estimated that 30% of the seafloor between Cape Fear, North Carolina, and Cape Canaveral, Florida (27–101 m deep), was

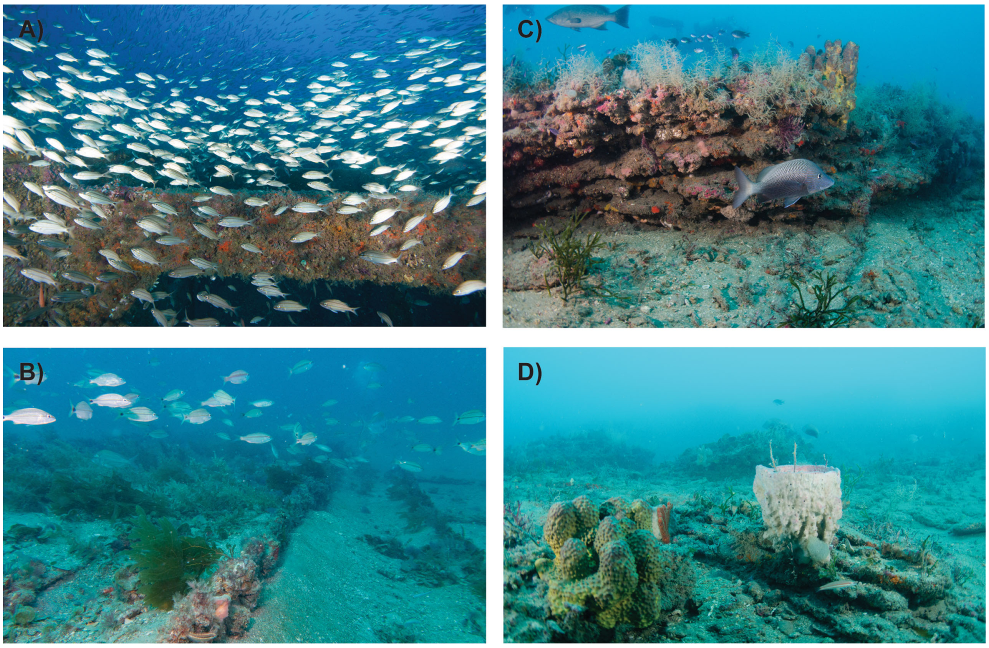

FIGURE 1
Underwater images of artificial reefs **(A, B)** and natural reefs **(C, D)** on the southeast US continental shelf. **(A)** Artificial reef created by a ship. **(B)** Artificial reef formed from a train boxcar. **(C)** High-relief rocky reef. **(D)** Low-relief rocky reef. Photos by John McCord/Coastal Studies Institute **(A)**, Cory Ames/NCCOS **(B)**, Dave Sybert **(C, D)**.

composed of natural reefs, and that natural reef coverage varied geographically with less coverage (14% of the seafloor) between Cape Hatteras and Cape Fear, North Carolina (Parker et al., 1983). Others have informally estimated that 10% of the SEUS continental shelf constitutes natural reef habitat (Hedgpeth, 1957; Struhsaker, 1969), and Parker et al. (1983) cite various personal communications that estimated 3–5% of various parts of the SEUS seafloor were covered by natural reefs. Regardless of their extent, it is well documented that these natural reefs provide substrate for various species of attached biota, such as sponges, soft corals, and algae, and together these natural reefs with attached biota provide important habitat for a diverse reef-associated fish community (Bacheler et al., 2019).

We develop and implement a reproducible and easily standardized approach for estimating the extent of artificial and natural reefs in the SEUS. Additionally, we compare the resulting reef extent estimates by reef type (artificial versus natural) and examine patterns in reef extent over the entire SEUS region, by state, and by depth. For artificial reefs, specifically, we also examine reef coverage by the material from which the artificial reef is constructed. While our case study was conducted for reefs in the SEUS, this approach is translatable to other large marine ecosystems to help better understand the relative coverage and spatial distribution of habitats, with implications for marine spatial planning and ecosystem-based fisheries management.

Materials and methods

Geographic scope

We compared artificial and natural reef extent in the SEUS (Figure 1), which we defined as bounded to the north by Cape Hatteras, NC (35.25° N latitude) and to the south by Port St. Lucie, FL (27.10° N latitude; Figure S1). Port St. Lucie was the southern boundary of our comparison because the transition from hard-bottom or rocky reefs to reef-building corals generally occurs south of this location. Depth was constrained to the continental shelf and upper slope between 10 m and 200 m for the comparison. Ten meters was selected as the shallowest extent for our analysis because current fishery sampling assessments for reef associated species and associated natural reef habitat begin at 10 m. Two hundred meters was selected as the deepest depth cutoff as this is the generally accepted limit of the upper continental slope off the SEUS (Wenner and Barans, 2001).

We developed multiple approaches, as described below, for quantifying the extent of artificial and natural reefs in the SEUS region, by state (North Carolina (NC), South Carolina (SC), Georgia (GA), Florida (FL)), and by depth bins (Figure S1). We defined state boundaries based on the Bureau of Ocean Energy Management (BOEM) administrative boundaries established for offshore energy planning and development (https://www.boem.

]

gov/oil-gas-energy/mapping-and-data/map-gallery/administrative-boundaries, accessed 12/9/21). We binned depth at a fine resolution (10 m) for depths 10 m to 100 m and at a coarser resolution (100 m) for depths 100 m to 200 m, past the shelf break.

Artificial reefs

Data acquisition

Artificial reef data from four SEUS states – NC, SC, GA, FL – were obtained from the NC Division of Marine Fisheries, SC Department of Natural Resources, GA Department of Natural Resources – Coastal Resources Division, and FL Division of Marine Fisheries Management – Artificial Reef Program. Two data types were provided: 1) data on permitted artificial reef zones and 2) data on reef structures that occur in these zones.

Artificial reef plots

Data on permitted artificial reef zones or plots, which are areas in the coastal ocean officially designated through the permitting process as locations where artificial reefs can be deployed, included the reef plot coordinates (decimal degrees), depth (m), minimum permitted vertical clearance above the artificial reef (m), plot area (km^2), deployment date, and special management zone (SMZ) designation, if applicable. We collated plot data from each state into one SEUS regional dataset such that all data were in standardized formats necessary for extent calculations. All data cleaning, collation, and analysis were conducted using ArcGIS Pro (ESRI, 2021) and R (R Development Core Team, 2021).

Artificial reef structures

Artificial reef structures deployed within permitted plots include items such as ships, concrete pipes, and concrete modules. Data for each structure included the permitted plot that the structure was deployed within, as well as the coordinates of the structure deployment. In some cases, we received depth information on the structures, but in most cases, we used depth collected at the level of the permitted plot and applied it to each structure within the plot. Data on the quantity of structure deployed, including the count (e.g., 100 units), tonnage, and for vessels, the vessel length (m), were provided for most structures, but unavailable for others. Each structure was also categorized more broadly (e.g., concrete pipes, steel vessel, train boxcars, bridge pieces, unknown) and sometimes accompanied by a more qualitative description (e.g., 330 ft barge, 75 Reef Balls, 925 tons of concrete pipe). We standardized and collated structure data from each state into one regional structures dataset.

There were 137 unique structure classifications across the four SEUS states. We categorized each of the 137 unique structure classifications into 25 broad categories to streamline the diverse structure types and nomenclature across states (Table S1). Each structure category reflected a combination of material (metal, concrete, rubber, wood, plastic, rock, fiberglass, unknown), structure (e.g., secondary use, modules, bridges, unspecified, vessels, tires, aircraft), and in some cases a subtype further describing the structure attributes (e.g., long and skinny shaped, squat and block shaped, large vs. small, vessel size category). We also assigned each structure as low relief (< 2 m height) or high relief (> 2 m height) and as having a low, medium, or high rate of degradation.

Footprint calculation

Three data-driven approaches were developed to quantify the extent or footprint of artificial reefs within the SEUS artificial reef programs. Multiple approaches were necessary as each state had differing levels of information on artificial reefs. For example, NC conducted high-resolution habitat mapping of their artificial reefs and had precise estimates of artificial reef footprint, whereas others had not conducted habitat mapping but had quantity data for some structures.

Plot extent (all SEUS states)

We calculated the area of permitted artificial reef plots using the *raster* package (Hijmans, 2020) in R. The plot areas represent the total possible coverage of artificial reefs since no plots are fully covered by artificial reef structures.

Structure extent - measured (NC)

When artificial reef data included accurate measurements of the amount of area covered by structures in each plot, we used these measurements to calculate artificial reef extent. This approach, which we refer to as the "measured extent" method, was applicable when states had conducted habitat mapping surveys of artificial reefs using instruments, such as multibeam echosounders or side-scan sonar, that permitted delineation of artificial reef structures to calculate footprints. We applied the measured extent method to NC artificial reefs because NC artificial reefs had been mapped using side-scan sonar following an extensive multi-year mapping effort by the NC Artificial Reef Program, from which artificial reef structures were manually delineated for area calculations.

Structure extent - plot percentage (SC, GA, FL)

When measured structure footprints were unavailable, we estimated the extent of artificial reef structures as a percentage of the permitted plot area. This approach, which we refer to as the "plot percentage" method, used NC data to extrapolate to other states. We calculated the mean (0.57%), minimum (0.005%), and maximum (4.07%) percentage of artificial reef plots covered by artificial reef structures. We applied the mean, minimum, and maximum structure extents to permitted plots in SC, GA, and FL by multiplying the artificial reef plot sizes in each state by the NC mean, minimum, and maximum values to obtain an estimated mean, minimum, and maximum coverage value for each SEUS plot.

Structure extent - classified structures (SC, GA, FL)

The third approach for estimating structure extent, called the "classified structures" method, was based upon the footprint of particular structures, such as concrete pipes or large metal vessels. For each of the 25 broad structure categories (Table S1), we estimated footprints as follows. Structures from NC and some from FL were associated with measured footprint values. Some additional structures in FL had model-predicted footprints from a generalized linear model using a power-link function. This model was developed by the FL Artificial Reef Program and used the tonnage of material deployed as a parameter to predict the artificial reef footprint. These measured and modeled values provided footprints for discrete deployments of artificial reef structures. In cases where dimensions (e.g., 20 ft x 20 ft) but not footprints were provided, we used dimensions to calculate footprint. Some of the footprint values also had quantity data, either counts (e.g., a deployment of 500 concrete pipe), tons (a deployment of 100 tons of concrete pipe), or in some cases both count and tonnage values, associated with them. We used these footprint and quantity data to calculate unit footprint as m^2/count or m^2/ton and then to calculate the unit footprint minimum, mean, and maximum across deployments for each structure type. When quantity (count, tons) but not footprint data were available, we applied the minimum, mean, and maximum unit footprint values and multiplied them by the reported quantity. Footprints per count were preferred and used when available, otherwise we used footprints per ton. When neither quantity nor footprint values were provided for a structure deployment, we obtained footprint estimates from artificial reef managers or found the minimum, mean, and maximum footprints of all deployments (not per unit) of the same structure type across states and applied those values to estimate footprint. For structures with no measured values in the SEUS or manager-estimated footprint values, values were obtained from outside the SEUS from other artificial reef data. Calculating the mean, minimum, and maximum footprint values in a hierarchical fashion (e.g., first for structures with quantity, prioritizing count vs. ton, etc.) helped estimate uncertainty since there were likely variations in structures within each category (e.g., secondary-use concrete with long or skinny shapes included pipes, pilings, and culverts).

Natural reefs

The seafloor of the SEUS mostly consists of sand or mud, but patches of natural reef habitats occur throughout the region (Powles and Barans, 1980; Parker et al., 1983; Schobernd and Sedberry, 2009). Given the large discrepancies in previous estimates of natural reef extent in the SEUS that range from 3% to 30%, we provide updated estimates of the extent of natural reefs in the SEUS using three approaches: 1) polygon delineation, 2) regional synthesis, and 3) predictive model.

Polygon delineation

We delineated polygons corresponding to natural reefs using a spatial dataset of sonar mapping, survey data, and information from fishers in the SEUS (Text S2). Two coauthors (CMS, NMB) independently delineated estimated boundaries of natural reefs in ArcGIS Pro. In most cases, the size and shape of natural reef areas were obvious from the multiple data source layers (e.g., dozens of fishing points on top of a clear natural reef from the multibeam sonar map). In some cases, however, there were sparse points from fishers and no other correlating evidence of natural reefs in an area, so coauthors used their best judgment (independently) to determine if these points indicated a natural reef.

Because natural reefs are patchy and often occur as a matrix of rock and sand, drawing a polygon around this matrix of natural reef and sand would likely overestimate the amount of natural reef inside of the polygons. Low profile or pavement type reefs face exposure and burial by sediment movement influencing their detectability (Renaud et al., 1997). In addition, by drawing polygons around only obvious natural reefs, patches of natural reef habitat would likely be missed outside of the polygons. Thus, we estimated the extent of natural reefs in the SEUS region, by state, and by depth bin using three scenarios. The first scenario was designed as a low estimate of the extent of natural reef, assuming only 50% of the area inside and 0% outside of polygons was natural reef. The second scenario was designed as our best approximation of the extent of natural reefs, assuming 50% of the area inside and 1% outside of polygons was natural reef. Our third scenario was designed as a high estimate of natural reef, assuming 100% of the area inside and 2% of the area outside of polygons was natural reef. This approach resulted in six total estimates of natural reef extent in each stratum using the polygon delineation approach: estimates from two people and three scenarios. From these six estimates, we calculated mean and variance of the extent of natural hard-bottom for the overall SEUS, as well as by state and depth strata.

Regional synthesis - TNC synthesis

The second broad approach to estimate the extent of natural reefs in the SEUS used previously published thematic seafloor habitat classification maps from a regional synthesis conducted by The Nature Conservancy (TNC), called the South Atlantic Bight Marine Assessment (SABMA). SABMA is a synthesis and assessment of publicly available data and literature review on depth, seafloor complexity, geology, and sediments that classifies and defines seafloor habitats from tidal estuary to the outer continental shelf from the NC-VA state boundary to FL Keys (Conley et al., 2017). To quantify the distribution of natural reef habitats we restricted selection of habitat classes in the dataset to "hard-bottom slope" and "shelf upper slope" and only considered polygons that had confidence rankings from the review process of "probable", "high confidence", and "very high confidence" and omitted confidence rankings of "possible" and "potential". The resulting polygons were converted and gridded into a raster layer with square cell dimensions of 90 m. The habitat classes were then reclassified to a binary value, where hard-bottom is 1 and no hard-bottom is 0.

Predictive habitat model - NCCOS model

The third natural reef estimation method was a hard-bottom likelihood map of the SEUS region from a predictive habitat model that was described in Pickens and Taylor (2020). We refer to this model as the NCCOS (NOAA National Centers for Coastal Ocean Science) model. The NCCOS model uses a spatially-explicit likelihood-based approach with derivatives of seafloor complexity as predictor variables and a Maximum Entropy model using bootstrapping to assess accuracy. Observations from fishery-independent surveys and compilations from sediment sampling databases were used to validate model predictions (Pickens and Tayor, 2020). The model output was a raster grid with cell resolution of 90 m by 90 m. We applied a threshold of likelihood values >0.63, which represented an accuracy of greater than 90% at predicting the occurrence of hard-bottom within the grid cell and a <5% false positivity rate. This threshold was used to reclassify into a binary raster with cell resolution 90 m by 90 m.

We also assessed another predictive model for hard-bottom distribution in the SEUS from Dunn and Halpin (2009) but did not include this model in our estimation approaches because it exhibited biases (Text S1).

Results

Multiple data-driven approaches quantifying the amount of seafloor in the SEUS covered by artificial and natural reefs revealed that artificial reefs account for several orders of magnitude less habitat than natural reefs (Figures 2, 3; Table 1). Of the entire SEUS region (103,220 km^2), permitted artificial reef zones comprise 705 km^2 (0.68%) of the seafloor (Figure S2). Permitted extent of artificial reef zones is an overestimate of the amount of seafloor covered by artificial reefs because the zones are not completely covered with artificial reef structures (Table 1). Estimates of structure extent based on percent coverage of permitted zones (plot percentage method) indicated that 4.02 km^2 (<0.01%) of the SEUS seafloor is covered by artificial reefs (Figure 3A; Tables 1; S2). When we estimated artificial reef coverage based on different structure classifications (e.g., concrete pipes, metal vessels), our calculations suggested that a smaller area, 1.98 km^2 (<0.01%), of the SEUS is covered with artificial reef structures (Figure 3A; Tables 1, S2). Averaging results from the plot percentage and classified structures approaches resulted in an estimate of 3.00 km^2 (<0.01%) of the SEUS seafloor covered by artificial reefs.

Estimates of natural reef extent, in contrast, far exceeded those of artificial reef extent in the SEUS. The three natural reef extent methods predicted an average of 2,654 km^2 (2.57%) of the SEUS covered by natural reefs (Figure 3B; Tables 1, S3). The TNC synthesis model suggested the highest coverage (3,602.0 km^2, 3.49%), followed by expert drawn polygons (2,852.59 km^2, 2.76%), and the NCCOS maximum entropy model (1,506.00 km^2, 1.46%; Figure 3B; Tables 1, S3).

The pattern of artificial reefs covering orders of magnitude less seafloor than natural reefs held across each of the four SEUS states (Figure 4; Table 1). While measured footprints based on seafloor mapping provided the best estimate of artificial reef extent in NC, we also calculated extent based on plot percentage and classified structures as a means of validating these two methods before applying to SC, GA, and FL (Figure 4A; Tables 1, S2). Coverage estimates based on plot percentages consistently exceeded estimates based on classified structures in SC, GA, and FL. For natural reefs, the TNC synthesis predicted the highest coverage for FL, whereas the NCCOS model predicted the highest coverage in SC and the polygon method predicted the highest in NC (Figure 4B; Tables 1, S3). Each artificial reef estimation method was several orders of magnitude less than its respective natural reef estimation.

Natural reef coverage surpassed that of artificial reefs across SEUS depths ranging from 10 m to 200 m (Figure 5). The deepest artificial reef documented in our study rests in 90 - 100 m, and most occur shallower than 60 m (Figure 5A; Table S2). In contrast, natural reefs were more widely distributed across the continental shelf up to the 200 m cut-off of the study, representing the upper continental slope (Figure 5B; Table S3). The three estimates of natural reef coverage exhibited different patterns. In the NCCOS model, natural reefs were concentrated in shallower depths, whereas in the TNC synthesis the opposite trend was observed. In the expert-based polygon approach, natural reefs were more universally distributed across the depth range.

Analysis of the types of artificial reef structures in the SEUS revealed a diversity of structure materials (e.g., concrete, metal) and types (e.g., bridges, modules) (Table S1). Throughout the SEUS, secondary-use concrete structures with a long-skinny shape, such as concrete pipes, were deployed most frequently (449 deployments), followed by medium-sized metal vessels (249

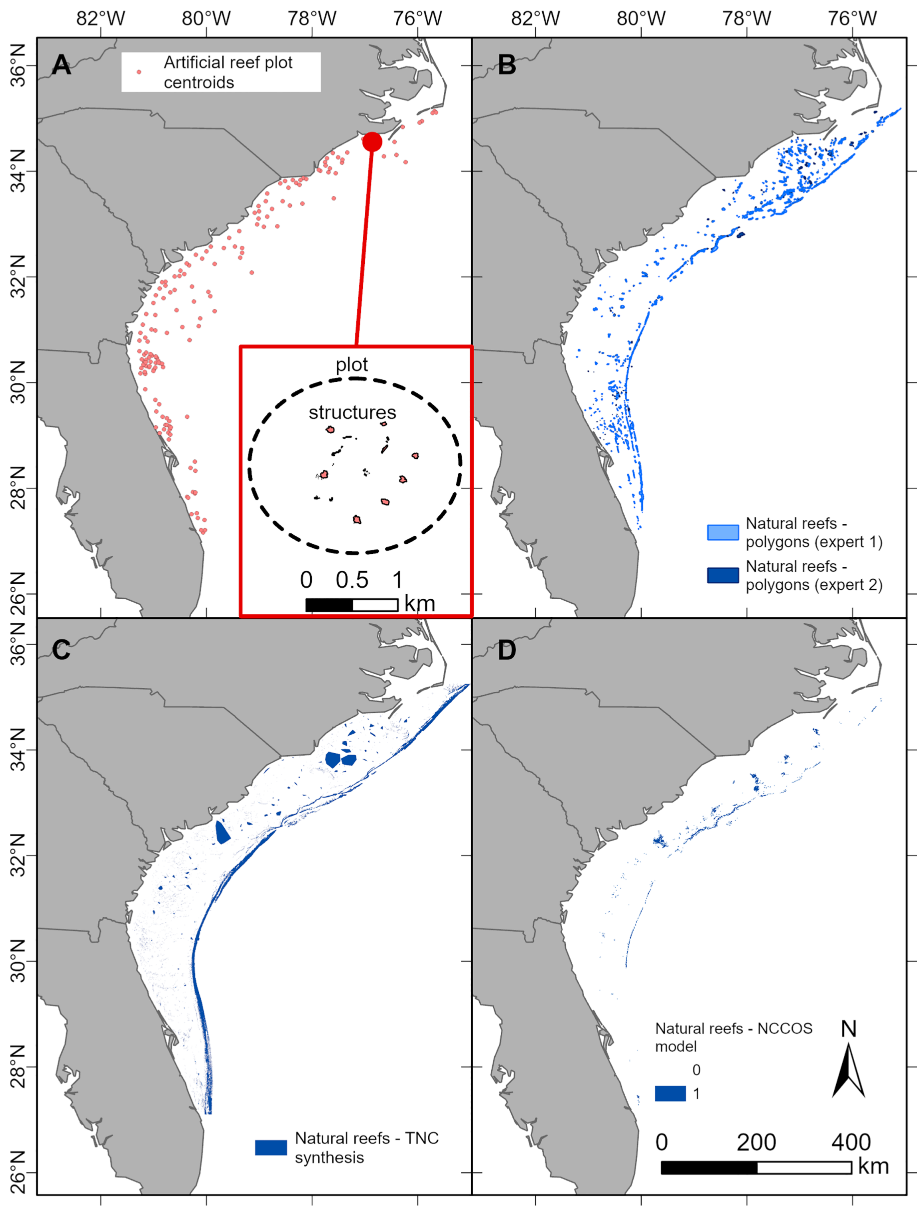

FIGURE 2
Locations of artificial reefs **(A)** and natural reefs **(B–D)** along the southeastern US continental shelf. **(A)** Artificial reef locations correspond to centroids of permitted artificial reef plots, and the size of the artificial reef dots corresponding to each plot is not to scale. The inset in panel A depicts one NC artificial reef permitted plot (dashed line) and the artificial reef structures (red polygons) within. **(B)** Natural reefs delineated by expert-drawn polygons. **(C)** Natural reefs predicted by the TNC synthesis. **(D)** Natural reefs predicted by the NCCOS model (likelihood >0.63).

deployments), trains and containers (220 deployments), small concrete modules (199 deployments), and long-lived metal vehicles (146 deployments; Figure S3; Table S1). The structures with the largest regional footprint were secondary-use concrete structures with a long-skinny shape (0.78 km^2), followed by concrete bridges (0.34 km^2), unspecified concrete (0.27 km^2), small concrete modules (0.12 km^2), and secondary-use concrete structures with a squat-block shape (0.10 km^2; Figure S3; Table S1).

Discussion

Our evaluation of artificial versus natural reef extent indicates that the amount of seafloor covered by artificial reefs in the SEUS is several orders of magnitude less than that of natural reefs. Across the SEUS region (103,220 km^2), artificial reef extent (3 km^2, averaged across methods) was 885 times less than natural reef extent (2,654 km^2). This pattern of more

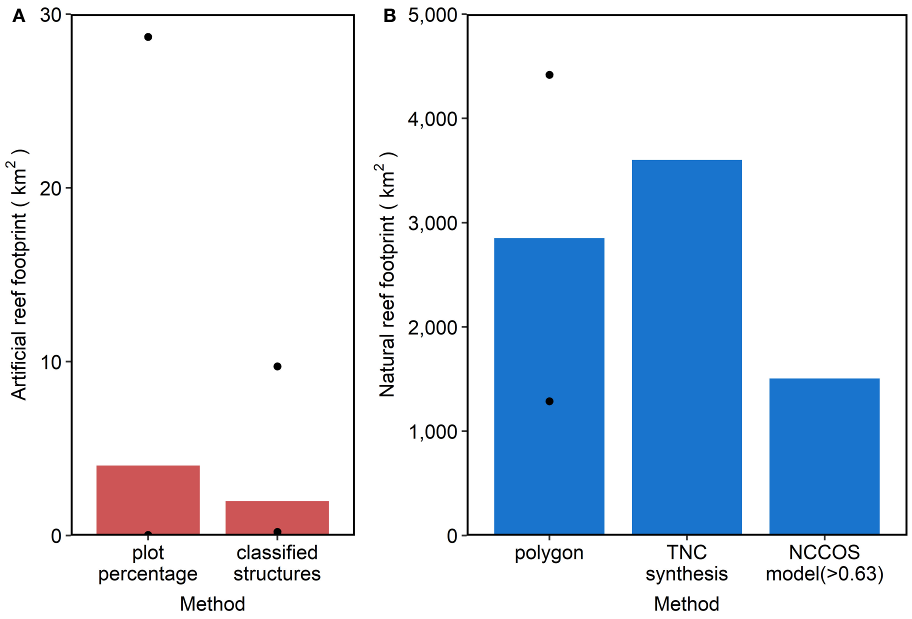

FIGURE 3
Extent of artificial reefs (**A**, red) and natural reefs (**B**, blue) for the entire SEUS region. Measured approach for artificial reef footprint not shown because only applied to NC. Black circles represent the maximum and minimum extent values for applicable methods. Note different y-axis scales.

extensive natural reef extent was consistent across state and depth groupings. To our knowledge, ours is the first estimate of artificial reef extent in the SEUS. Prior estimates of natural reefs in the region vary dramatically from 3% to 30% (Hedgpeth, 1957; Struhsaker, 1969; Parker et al., 1983). Our estimates based on seafloor maps and published geological and predictive seafloor habitat models suggest that natural reef coverage is less than previous estimates at 2.57% (average of our three approaches) of the SEUS seafloor.

Our SEUS regional estimates suggesting that artificial reefs are a “drop in the bucket” compared to natural reefs are similar to estimates of reef type extent in other geographic regions. A recent synthesis of seafloor mapping data on the eastern Gulf of Mexico (GOM) continental shelf extrapolated that 2.6% of the

TABLE 1 Approaches for and corresponding estimates of artificial and natural reef extents.

Reef type	Category	Method	Description	NC (km^2)	SC (km^2)	GA (km^2)	FL (km^2)	SEUS (km^2)	SEUS (%)
artificial	permitted extent	NA	permitted area of artificial reef zones or plots in which artificial reef structures can be deployed; total possible area of artificial reefs	31.64	95.80	297.29	280.52	705.25	0.68
artificial	structure extent	measured	sonar-derived areas of artificial reef structures	0.30	–	–	–	–	–
artificial	structure extent	plot percentage	estimate of artificial reef structure area as percent of permitted plot	0.18*	0.55	1.69	1.60	4.02	<0.01
artificial	structure extent	classified structures	estimate of artificial reef structure area based on footprint of different structure types (e.g., pipes, ship)	0.41*	0.32	0.28	0.97	1.98	<0.01
natural	polygon	NA	expert-drawn polygons corresponding to natural reefs from sonar, survey, and fisher data	1197.61	620.46	243.73	790.79	2852.59	2.76
natural	model	TNC synthesis	synthesis of thematic habitat classification maps (Conley et al., 2017)	1318.00	498.00	175.00	1611.00	3602.00	3.49
natural	model	NCCOS model	maximum entropy model predicting natural reefs (Pickens and Tayor, 2020)	532.00	745.00	79.00	151.00	1506.00	1.46

*For NC artificial reefs whose extents were measured, we used measured values to verify two other methods (structure extent - plot percentage; structure extent - classified structures) and used the estimated values for plot percentage (0.18 km^2) and classified structure (0.41 km^2) methods to calculate extent in the entire SEUS. The entire SEUS study area is 103,220 km^2.
NA, not applicable.

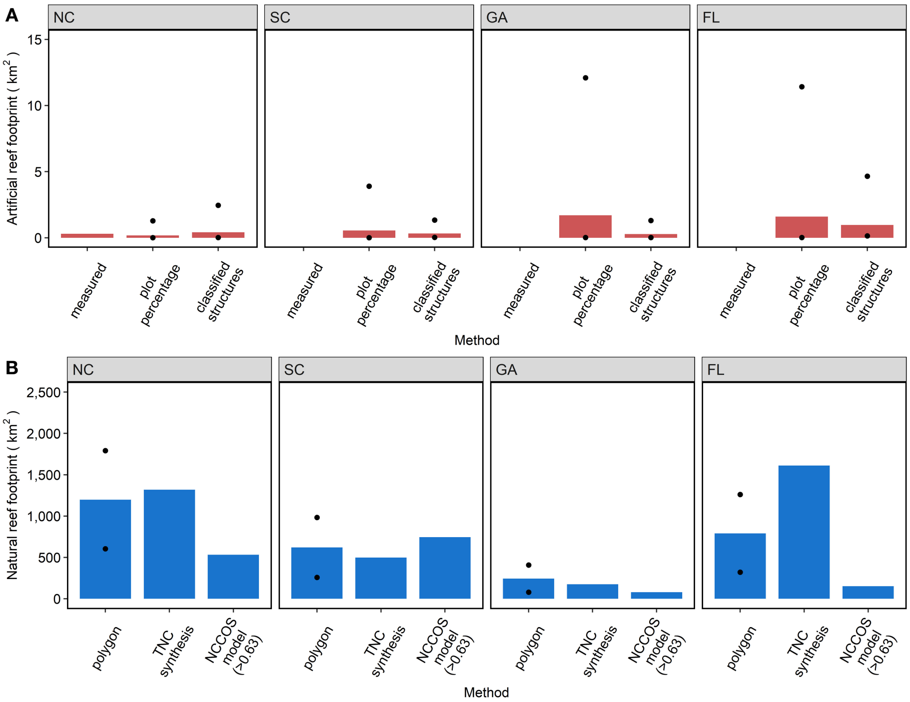

FIGURE 4
Footprint (km^2) of artificial reefs (**A**, red) and natural reefs (**B**, blue) by state (columns). Measured approach for artificial reef footprint was only available in NC. Black circles represent the maximum and minimum extent values for applicable methods. Note different y-axis scales between panels **(A, B)**.

seafloor is covered in natural reefs (Keenan et al., 2022), which similarly helped refine previous natural reef coverage estimates that ranged from 13% (Jaap, 2015) based on Rohmann et al. (2005) to 38% (Parker et al., 1983). While Keenan et al. did not extrapolate artificial reef coverage across the eastern GOM, they did delineate both artificial and natural reefs from their seafloor mapping dataset that covered a subset of the eastern GOM. These non-extrapolated seafloor mapping data interpretations demonstrated that artificial reefs are several orders of magnitude less than natural reefs (2.2 km^2 artificial reefs versus 226.2 km^2 natural reefs delineated) in the eastern GOM. Likewise, in a small portion of the Florida Reef Tract (Martin County, FL), habitat mapping data identified that 0.66% of the region was artificial structure whereas 4.13% was colonized pavement and coral reefs (Walker and Gilliam, 2013).

Patterns in artificial versus natural reef extent observed over the SEUS region translated to finer groupings of states and depth zones. While artificial and natural reef extent estimates varied based on the estimation method, all states exhibited substantially less seafloor covered by artificial reefs than by natural reefs. In NC, for example, the measured footprint of artificial reefs was four orders of magnitude less than each natural reef extent estimate. The same pattern of heightened natural reef coverage applied across depth bins. Artificial reefs had greater proportional coverage in shallower depths, likely reflecting artificial reef deployment goals, which often include providing fishing and diving sites that are easily accessible by stakeholders and thus close to shore in shallower depths (Becker et al., 2018; Paxton et al., 2022). Natural reefs, however, are more widespread across depth gradients and are susceptible to burial and exposure with sediment movement, reflecting the underlying geology of the SEUS region (Parker et al., 1983; Riggs et al., 1996; Renaud et al., 1997; Riggs et al., 1998).

Despite their relatively small footprint (<0.01% of seafloor) in the SEUS, these artificial reefs play key ecological roles within the seascape. Within the SEUS region, for example, artificial reefs have been shown to host high abundances of tropical and subtropical reef fish at their poleward climate range edges (Paxton et al., 2019b) and high densities of large predators (Paxton et al., 2020), potentially provide stepping stones or connectivity corridors for large predator movement (Paxton et al., 2019a), and form hotspots for economically valuable fish species (Paxton et al., 2021). The fish communities on artificial reefs differ from those of nearby natural reefs (Paxton et al., 2017; Rosemond et al., 2018; Lemoine et al., 2019) and this translates to differences in species-specific feeding ecology (Lindquist et al., 1994; Pike and Lindquist, 1994). Additionally, findings outside of the SEUS in shallow urbanized estuaries

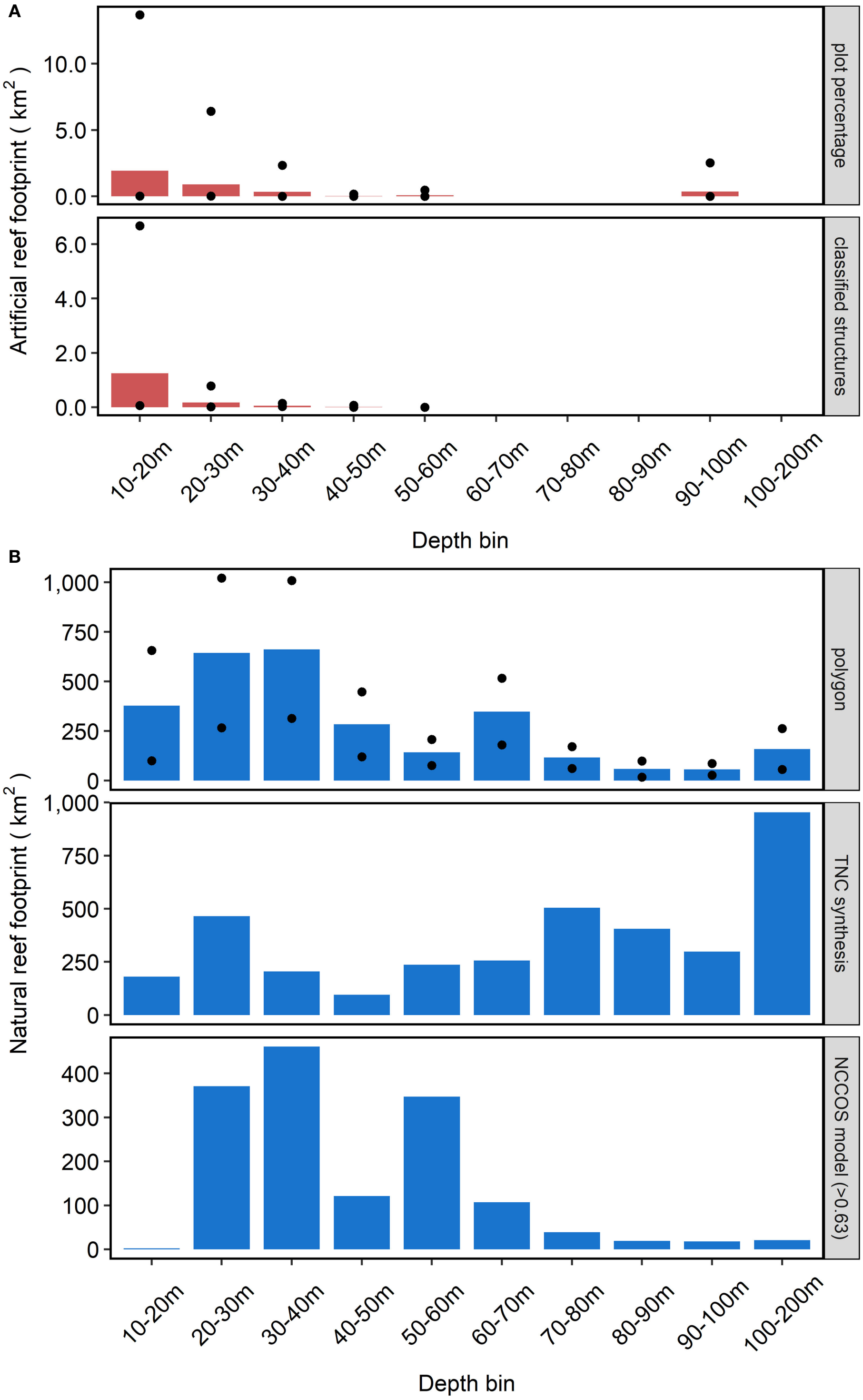

FIGURE 5
Extent of artificial reefs **(A)** and natural reefs **(B)** by depth bin. Measured approach for artificial reef footprint not shown because only applied to NC. Twelve artificial reefs did not have assigned values, so these artificial reefs permitted plots and structures are not represented in this figure. Black circles represent the maximum and minimum extent values for applicable methods. Note different y-axis scales between panels **(A, B)**.

indicate that artificial reefs have the potential to exacerbate the spread of invasive species (Dafforn et al., 2012; Airoldi et al., 2015) and pose other risks, such as aggregating fish away from natural reefs (Bohnsack, 1989; Layman et al., 2016). Given the ecological functions of artificial reefs, they have the potential to drive change by affecting ecosystem patterns and processes (Bulleri and Chapman, 2010; Dafforn et al., 2015; Bishop et al., 2017; Heery et al., 2017) and by hosting fish communities that differ long-term from those on nearby natural reefs (Becker et al., 2022). Potential ecological ramifications, including both benefits and risks, of artificial reef placement in the seascape cement a future research need to incorporate footprint estimations into ecological projections of artificial reef effects.

There are numerous economically and ecologically important fish species that associate with natural and artificial reefs in the SEUS (Bacheler et al., 2019), and knowing the extent and spatial arrangement of natural reefs can improve their management in several ways. For instance, estimating the total abundance of reef-associated fish species precisely and accurately would be beneficial for reef fish management, as evidenced by the millions of dollars of recent federal funding to estimate red snapper (*Lutjanus campechanus*; (Stunz et al., 2021); https://www.scseagrant.org/sc-sea-grant-award-red-snapper-count/) and greater amberjack (*Seriola dumerili*; https://masgc.org/news/article/team-selected-to-estimate-abundance-of-greater-amberjack-in-south-atlantic) absolute abundance in the SEUS and the GOM. With detailed knowledge of the extent of natural and artificial reefs, fish densities could be estimated more accurately and also incorporated into long-term studies, similar to Becker et al. (2022). Another benefit of knowing the spatial arrangement of natural reef habitats in the SEUS is in guiding marine spatial planning, including marine protected area placement and placement of future artificial reefs in the region, since artificial reefs are often installed to supplement existing natural reefs.

Fish are known to concentrate at artificial reefs, but there is disagreement about whether they might add or subtract fish biomass from natural reefs (Bohnsack, 1989; Powers et al., 2003). Artificial reefs may attract fish away from natural reefs ("attraction hypothesis"), which would increase abundance at artificial reefs at the expense of natural reefs and facilitate exploitation by fishers (Grossman et al., 1997). In contrast, artificial reefs may support additional fish production ("production hypothesis"), which would not reduce biomass in natural reefs (Folpp et al., 2020). Regardless of whether aggregation, production, or a blend of both occurs on artificial reefs, artificial reefs are often deployed to enhance fish habitat, forming locations for recreational fishing. Fishing pressure at artificial reefs has not been well-quantified in the SEUS; however, findings from the FL GOM coast suggest high fishing pressure occurs on artificial reefs. For example, recreational reef fish angler surveys revealed that 46% of angler trips seeking reef fish targeted artificial reefs (Cross et al., 2018). Additionally, recreational anglers anecdotally perceive that artificial reefs experience high fishing pressure based on observations of recreational vessel congestion. Given our finding that artificial reefs cover a relatively small amount of SEUS seafloor compared to natural reefs, if heightened fishing pressure on artificial reefs manifests across the SEUS, then small, island-like artificial reefs could be receiving a disproportionate amount of recreational fishing pressure. The designation of artificial reefs in federal waters as Special Management Zones (SMZs), which already existed off SC and have recently been completed and codified in NC through the South Atlantic Fishery Management Council, could prevent inequitable fishing by restricting high-efficiency gears. Directing fishing pressure to artificial reefs instead of natural reefs has ecological implications, potentially establishing natural reefs as refugia from fishing pressure while depleting fish populations at artificial reefs (Solonsky, 1985; Addis et al., 2016). With these scenarios in mind, region-wide reef fish sampling programs could consider sampling artificial reefs concurrently with sampled natural reefs to quantify reef-associated fish communities and potential effects from differential fishing pressure on these two types of structured habitat.

Estimating the extent of artificial reefs was challenging because it involved synthesizing disparate data across a broad geographic region. The methods we developed effectively standardized artificial reef data across states, enabling region-wide analysis, and ultimately comparison with natural reef data. When we validated the plot percentage estimate by performing the estimation in NC and comparing it to the measured NC footprint, we found that the plot percentage approach underestimated the artificial reef footprint. However, when extrapolated to SC, GA, and FL, this method likely overestimated coverage, as NC permitted zones were typically filled with a higher portion of structures than those in the other states. This discrepancy likely reflects different artificial reef development strategies between states. For example, NC rarely established new artificial reef plots, preferring to continue to develop within existing permitted zones, which could explain the inflated artificial reef estimates for reefs in other states. And, in some states, sandy habitat within permitted plots is intentionally left devoid of artificial reef structures to provide foraging grounds for select fish species. When we validated the classified structure method in NC, it overpredicted NC coverage compared to the measured footprint. Despite the overprediction in NC, the structure classification estimate accounted for the diversity of artificial reef structure types deployed on the SEUS seafloor and in general estimated a smaller footprint than the plot percentage method. The true coverage of artificial reefs likely falls between the plot percentage and classified structure estimates. In the future, additional habitat mapping efforts following artificial reef deployment would allow delineation of the footprint of deployed artificial reef structures and could help streamline this approach and refine estimates.

The three approaches to estimating natural reef extent had respective strengths and weaknesses. First, the polygon approach resulted in natural reef extent estimates that were between those predicted by the other two methods, the TNC synthesis and NCCOS model, in all states except GA. Second, the TNC synthesis predicted the highest NR extent compared to the other methods in NC and FL and predicted high natural reef coverage between 100-200 m depths. Third, the NCCOS maximum entropy model predicted the lowest NR extent in all states except SC. This model seemingly underpredicted natural reef extent in the shallowest and deepest depth groupings. This could be explained by the considerable change in relative seafloor complexity from the relatively flat, shallow shelf waters, through the steep slope of the shelf edge to the lower slope of the continental shelf. The true coverage of natural reefs likely falls within the three natural reef estimation approaches. More extensive and concentrated habitat mapping and ground-truthing approaches along the SEUS continental shelf will help improve natural reef extent estimates.

This study fills gaps in and establishes baseline understanding of artificial and natural reef coverage on the SEUS seafloor by generating the first estimate of artificial reef footprint in the SEUS and simultaneously refining previous regional natural reef extent estimates. It also identified gaps, such as the need for more expansive, but also finer scale, seafloor mapping and characterization efforts for both artificial and natural reefs along with a more standardized approach to recording and managing quantitative information on artificial reef deployments. With projected increases in artificial structures globally, including slated offshore wind energy development, and potential reef-related impacts from climate change, the reproducible approach that we developed for quantifying reef footprint is applicable to other geographic regions and ultimately provides support for regional marine spatial planning needs and accompanying ecosystem-based management.

Data availability statement

The original contributions presented in the study are included in the article/Supplementary Material. Further inquiries can be directed to the corresponding authors.

Author contributions

GK, AP, NB, and JT conceived of this research. KM and JR provided Florida artificial reef data. ZH and JB provided North Carolina artificial reef data. RM and CB provided South Carolina and Georgia artificial reef data, respectively. DS and AP processed artificial reef data. NB and CS delineated natural reef polygons and performed associated calculations. JT acquired natural reef habitat synthesis and predictive models and calculated the extent of natural reefs from these. DS and AP conducted comparative analyses for artificial and natural reef extents and created figures and tables. DS, AP, and NB drafted the manuscript. All authors contributed to the article and approved the submitted version.

Funding

CSS-Inc was not involved in the study design, collection, analysis, interpretation of data, the writing of this article or the decision to submit it for publication.

Acknowledgments

We thank the NOAA National Centers for Coastal Ocean Science for supporting this synthesis. DS was supported by Duke University Rachel Carson Scholars Program. AP was partially supported by CSS-Inc. under NOAA/NCCOS Contract #EA133C17BA0062. We thank M. Burton for thoughtful reviews of the manuscript. The views and conclusions contained in this document are those of the authors and should not be interpreted as representing the opinions or policies of the US Government, nor does mention of trade names or commercial products constitute endorsement or recommendation for use.

Conflict of interest

AP received partial support from CSS-Inc.

The remaining authors declare that the research was conducted in the absence of any commercial or financial relationships that could be construed as a potential conflict of interest.

Publisher’s note

Supplementary material

The Supplementary Material for this article can be found online at: https://www.frontiersin.org/articles/10.3389/fmars.2022.980384/full#supplementary-material

References

Addis, D. T., Patterson, W. F., and Dance, M. A. (2016). The potential for unreported artificial reefs to serve as refuges from fishing mortality for reef fishes. *North Am. J. Fisheries Manage.* 36, 131–139. doi: 10.1080/02755947.2015.1084406

Airoldi, L., Turon, X., Perkol-Finkel, S., and Rius, M. (2015). Corridors for aliens but not for natives: Èffects of marine urban sprawl at a regional scale. *Diversity Distributions* 21, 755–768. doi: 10.1111/ddi.12301

Bacheler, N. M., Schobernd, Z. H., Gregalis, K. C., Schobernd, C. M., Teer, B. Z., Gillum, Z., et al. (2019). Patterns in fish biodiversity associated with temperate reefs on the southeastern US continental shelf. *Mar. Biodiversity* 49, 2411–2428. doi: 10.1007/s12526-019-00981-9

Bacheler, N. M., and Shertzer, K. W. (2020). Catchability of reef fish species in traps is strongly affected by water temperature and substrate. *Mar. Ecol. Prog. Ser.* 642, 179–190. doi: 10.3354/meps13337

Barans, C. A., and Henry, V. J. (1984). A description of the shelf edge groundfish habitat along the southeastern united states. *Northeast Gulf Sci.* 7, 77–96. doi: 10.18785/negs.0701.05

Becker, A., Taylor, M. D., Folpp, H., and Lowry, M. B. (2018). Managing the development of artificial reef systems: The need for quantitative goals. *Fish Fisheries* 19, 740–752. doi: 10.1111/faf.12288

Becker, A., Taylor, M., Folpp, H., and Lowry, M. (2022). Revisiting an artificial reef after 10 years: What has changed and what remains the same? *Fisheries Res.* 249. doi: 10.1016/j.fishres.2022.106261

Bishop, M. J., Mayer-Pinto, M., Airoldi, L., Firth, L. B., Morris, R. L., Loke, L. H. L., et al. (2017). Effects of ocean sprawl on ecological connectivity: Impacts and solutions. *J. Exp. Mar. Biol. Ecol.* 492, 7–30. doi: 10.1016/j.jembe.2017.01.021

Bohnsack, J. A. (1989). Are high densities of fishes at artificial reefs the result of habitat limitation or behavioral preference? *Bull. Mar. Sci.* 44, 631–645.

Bugnot, A. B., Mayer-Pinto, M., Airoldi, L., Heery, E. C., Johnston, E. L., Critchley, L. P., et al. (2021). Current and projected global extent of marine built structures. *Nat. Sustainability* 4, 33–41. doi: 10.1038/s41893-020-00595-1

Bulleri, F., and Airoldi, L. (2005). Artificial marine structures facilitate the spread of a non-indigenous green alga, *Codium fragile* ssp. *tomentosoides*. *North Adriatic Sea. J. Appl. Ecol.* 42, 1063–1072. doi: 10.1111/j.1365-2664.2005.01096.x

Bulleri, F, and Chapman, M. G. (2010). The introduction of coastal infrastructure as a driver of change in marine environments. *J. Appl. Ecol.* 47, 26–35. doi: 10.1111/j.1365-2664.2009.01751.x

Cannizzo, Z. J., and Griffen, B. D. (2019). An artificial habitat facilitates a climate-mediated range expansion into a suboptimal novel ecosystem. *PloS One* 14, e0211638. doi: 10.1371/journal.pone.0211638

Champion, C., Suthers, I. M., and Smith, J. A. (2015). Zooplanktivory is a key process for fish production on a coastal artificial reef. *Mar. Ecol. Prog. Ser.* 541, 1–14. doi: 10.3354/meps11529

Christiansen, H. M., Switzer, T. S., Brodie, R. B., Solomon, J. J., and Paperno, R. (2020). *Indices of abundance for red snapper (Lutjanus campechanus) from the FWC fish and wildlife research institute (FWRI) repetitive timed drop survey in the U.S. south Atlantic* (North Charleston, SC:SEDAR).

Claisse, J. T., Pondella, D. J., Love, M., Zahn, L. A., Williams, C. M., Williams, J. P., et al. (2014). Oil platforms off California are among the most productive marine fish habitats globally. *Proc. Natl. Acad. Sci.* 111, 15462–15467. doi: 10.1073/pnas.1411477111

Conley, M. F., Anderson, M. G., Steinberg, N., and Barnett, A. (2017). The South Atlantic bight marine assessment: Species, habitats and ecosystems. *Nat. Conservancy Eastern Conserv. Sci*, 496 pp.

Cross, T. A., Sauls, B., Germeroth, R., and Mille, K. (2018). Methods to quantify recreational angling effort on artificial reefs off florida's gulf of Mexico coast. *Am. Fisheries Soc. Symposium* 86, 265–277.

Dafforn, K. A., Glasby, T. M., Airoldi, L., Rivero, N. K., Mayer-Pinto, M., and Johnston, E. L. (2015). Marine urbanization: An ecological framework for designing multifunctional artificial structures. *Front. Ecol. Environ.* 13, 82–90. doi: 10.1890/140050

Dafforn, K. A., Glasby, T. M., and Johnston, E. L. (2012). Comparing the invasibility of experimental "reefs" with field observations of natural reefs and artificial structures. *PloS One* 7, e38124. doi: 10.1371/journal.pone.0038124

Development Core Team, R. (2021). *R: A language and environment for statistical computing* (Vienna, Austria: R Foundation for Statistical Computing).

Dugan, J. E., Airoldi, L., Chapman, M. G., Walker, S. J., and Schlacher, T. (2011). Estuarine and coastal structures: Environmental effects, a focus on shore and nearshore structuresE. Wolanski and D. S. McLusky . *Treatise Estuar. Coast. Sci.* 8, pp 17–41. Waltham:Academic Press. doi: 10.1016/B978-0-12-374711-2.00802.0

Dunn, D. C., and Halpin, P. N. (2009). Rugosity-based regional modeling of hard-bottom habitat. *Mar. Ecol. Prog. Ser.* 377, 1–11. doi: 10.3354/meps07839

ESRI (2021). *ArcGIS pro. redlands, California, USA. environmental systems research institute* (Redlands, California, USA: Environmental Systems Research Institute).

Firth, L. B., Knights, A. M., Bridger, D., Evans, A. J., Mieszkowska, N., Moore, P., et al. (2016). Ocean sprawl: Challenges and opportunities for biodiversity management in a changing world. *Oceanography Mar. Biol.: Annu. Rev.* 54, 189–262. doi: 10.1201/9781315368597-5

Folpp, H. R., Schilling, H. T., Clark, G. F., Lowry, M. B., Maslen, B., Gregson, M., et al. (2020). Artificial reefs increase fish abundance in habitat-limited estuaries. *J. Appl. Ecol.* 57, 1752–1761. doi: 10.1111/1365-2664.13666

Gates, A. R., Horton, T., Serpell-Stevens, A., Chandler, C., Grange, L. J., Robert, K., et al. (2019). Ecological role of an offshore industry artificial structure. *Front. Mar. Sci.* 6. doi: 10.3389/fmars.2019.00675

Grossman, G. D., Jones, G. P., and Seaman, W. J.Jr. (1997). Do artificial reefs increase regional fish production? A review of existing data. *Fisheries* 22, 17–23. doi: 10.1577/1548-8446(1997)022<0017:DARIRF>2.0.CO;2

Harter, S. L., Ribera, M. M., Shepard, A. N., and Reed, J. K. (2008). Assessment of fish populations and habitat on oculina bank, a deep-sea coral marine protected area off eastern Florida. *Fishery Bull.* 107, 195–206.

Hedgpeth, J. W. (1957). Treatise on marine ecology and paleoecology. *Geological Soc. America Memoir* 1, 1296.

Heery, E. C., Bishop, M. J., Critchley, L. P., Bugnot, A. B., Airoldi, L., Mayer-Pinto, M., et al. (2017). Identifying the consequences of ocean sprawl for sedimentary habitats. *J. Exp. Mar. Biol. Ecol.* 492, 31–48. doi: 10.1016/j.jembe.2017.01.020

Hijmans, R. J. (2020). Raster: Geographic data analysis and modeling. https://CRAN.R-project.org/package=raster

Jaap, W. C. (2015). Stony coral (Milleporidae and scleractinia) communities in the eastern gulf of Mexico: A synopsis with insights from the hourglass collections. *Bull. Mar. Sci.* 91, 207–253. doi: 10.5343/bms.2014.1049

Keenan, S. F., Switzer, T. S., Knapp, A., Weather, E. J., and Davis, J. (2022). Spatial dynamics of the quantity and diversity of natural and artificial hard bottom habitats in the eastern gulf of Mexico. *Continental Shelf Res.* 233. doi: 10.1016/j.csr.2021.104633

Layman, C. A., Allgeier, J. E., and Montaña, C. G. (2016). Mechanistic evidence of enhanced production on artificial reefs: A case study in a Bahamian seagrass ecosystem. *Ecol. Eng.* 95, 574–579. doi: 10.1016/j.ecoleng.2016.06.109

Lee, M. O., Otake, S., and Kim, J. K. (2018). Transition of artificial reefs (ARs) research and its prospects. *Ocean Coast. Manage.* 154, 55–65. doi: 10.1016/j.ocecoaman.2018.01.010

Lemoine, H. R., Paxton, A. B., Anisfeld, S. C., Rosemond, R. C., and Peterson, C. H. (2019). Selecting the optimal artificial reefs to achieve fish habitat enhancement goals. *Biol. Conserv.* 238. doi: 10.1016/j.biocon.2019.108200

Lindquist, D. G., Cahoon, L. B., Clavijo, I. E., Posey, M. H., Bolden, S. K., Pike, L. A., et al. (1994). Reef fish stomach contents and prey abundance on reef and sand substrata associated with adjacent artificial and natural reefs in onslow bay, north Carolina. *Bull. Mar. Sci.* 55, 308–318.

Miller, R. G., Hutchison, Z. L., Macleod, A. K., Burrows, M. T., Cook, E. J., Last, K. S., et al. (2013). Marine renewable energy development: Assessing the benthic footprint at multiple scales. *Front. Ecol. Environ.* 11, 433–440. doi: 10.1890/120089

Mitchell, W. A., Kellison, G. T., Bacheler, N. M., Potts, J. C., Schobernd, C. M., and Hale, L. F. (2014). Depth-related distribution of postjuvenile red snapper in southeastern U.S. Atlantic ocean waters: Ontogenic patterns and implications for management. *Mar. Coast. Fisheries* 6, 142–155. doi: 10.1080/19425120.2014.920743

Parker, R., Colby, D., and Willis, T. (1983). Estimated amount of reef habitat on a portion of the U.S. *South Atlantic Gulf Mexico Continental Shelf. Bull. Mar. Sci.* 33, 935–940.

Parker, R. O. Jr., and Mays, R. W. (1998). *Southeastern u. s. deepwater reef fish assemblages, habitat characteristics, catches, and life history summaries.* NOAA Technical Report, NMFS 138, 41

Paxton, A. B., Blair, E., Blawas, C., Fatzinger, M. H., Marens, M., Holmberg, J., et al. (2019a). Citizen science reveals female sand tiger sharks (*Carcharias taurus*) exhibit signs of site fidelity on shipwrecks. *Ecology* 100, e02687. doi: 10.1002/ecy.2687

Paxton, A. B., Harter, S. L., Ross, S. W., Schobernd, C. M., Runde, B. J., Rudershausen, P. J., et al. (2021). Four decades of reef observations illuminate deep-water grouper hotspots. *Fish Fisheries* 22, 749–761. doi: 10.1111/faf.12548

Paxton, A. B., Newton, E. A., Adler, A. M., Van Hoeck, R. V., Iversen, E. S.Jr., Taylor, J. C., et al. (2020). Artificial habitats host elevated densities of large reef-associated predators. *PloS One* 15, e0237374. doi: 10.1371/journal.pone.0237374

Paxton, A. B., Peterson, C. H., Taylor, J. C., Adler, A. M., Pickering, E. A., and Silliman, B. R. (2019b). Artificial reefs facilitate tropical fish at their range edge. *Commun. Biol.* 2, 168. doi: 10.1038/s42003-019-0398-2

Paxton, A. B., Pickering, E. A., Adler, A. M., Taylor, J. C., and Peterson, C. H. (2017). Flat and complex temperate reefs provide similar support for fish: evidence for a unimodal species-habitat relationship. *PloS One* 12, e0183906. doi: 10.1371/journal.pone.0183906

Paxton, A. B., Steward, D. N., Harrison, Z. H., and Taylor, J. C. (2022). Fitting ecological principles of artificial reefs into the ocean planning puzzle. *Ecosphere* 13. doi: 10.1002/ecs2.3924

Pickens, B. A., and Tayor, J. C. (2020). *Regional essential fish habitat geospatial assessment and framework for offshore sand features* (Sterling, VA: US Department of the Interior, Bureau of Ocean Energy Management).

Pike, L. A., and Lindquist, D. G. (1994). Feeding ecology of spottail pinfish. *Bull. Mar. Sci.* 55, 363–374.

Powers, S., Grabowski, J., Peterson, C., and Lindberg, W. (2003). Estimating enhancement of fish production by offshore artificial reefs: Uncertainty exhibited by divergent scenarios. *Mar. Ecol. Prog. Ser.* 264, 265–277. doi: 10.3354/meps264265

Powles, H., and Barans, C. A. (1980). Groundfish monitoring in sponge-coral areas off the southeastern united states. *Mar. Fisheries Rev.* 42, 21–35.

Ramm, L. A. W., Florisson, J. H., Watts, S. L., Becker, A., and Tweedley, J. R. (2021). Artificial reefs in the anthropocene: A review of geographical and historical trends in their design, purpose, and monitoring. *Bull. Mar. Sci.* 97, 699–728. doi: 10.5343/bms.2020.0046

Renaud, P. E., Riggs, S. R., Ambrose, W. G.Jr., Schmid, K., and Snyder, S. W. (1997). Biological-geological interactions: Storm effects on macroalgal communities mediated by sediment characteristics and distribution. *Continental Shelf Res.* 17, 37–56. doi: 10.1016/0278-4343(96)00019-2

Riggs, S. R., Ambrose, W. G.Jr., Cook, J. W., Snyder, S. W., and Snyder, S. W. (1998). Sediment production on sediment-starved continental margins: The interrelationship between hardbottoms, sedimentological and benthic community processes, and storm dynamics. *J. Sedimentary Res.* 68, 155–168. doi: 10.2110/jsr.68.155

Riggs, S. R., Snyder, S. W., Hine, A. C., and Mearns, D. L. (1996). Hardbottom morphology and relationship to the geologic framework: Mid-Atlantic continental shelf. *J. Sedimentary Res.* 66, 830–846. doi: 10.1306/D4268419-2B26-11D7-8648000102C1865D

Rohmann, S. O., Hayes, J. J., Newhall, R. C., Monaco, M. E., and Grigg, R. W. (2005). The area of potential shallow-water tropical and subtropical coral ecosystems in the united states. *Coral Reefs* 24, 370–383. doi: 10.1007/s00338-005-0014-4

Rosemond, R. C., Paxton, A. B., Lemoine, H. R., Fegley, S. R., and Peterson, C. H. (2018). Fish use of reef structures and adjacent sand flats: Implications for selecting minimum buffer zones between artificial reefs and existing reefs. *Mar. Ecol. Prog. Ser.* 587, 187–199. doi: 10.3354/meps12428

Rudershausen, P. J., Williams, E. H., Buckel, J. A., Potts, J. C., and Manooch, C. S. (2008). Comparison of reef fish catch per unit effort and total mortality between the 1970s and 2005-2006 in onslow bay, north Carolina. *Trans. Am. Fisheries Soc.* 137, 1389–1405. doi: 10.1577/T07-159.1

Schobernd, C. M., and Sedberry, G. R. (2009). Shelf-edge and upper-slope reef fish assemblages in the south Atlantic bight: Habitat characteristics, spatial variation, and reproductive behavior. *Bull. Mar. Sci.* 84, 67–92.

Seaman, W. (2007). Artificial habitats and the restoration of degraded marine ecosystems and fisheries. *Hydrobiologia* 580, 143–155. doi: 10.1007/s10750-006-0457-9

Solonsky, A. C. (1985). Fish colonization and the effect of fishing activities on two artificial reefs in Monterey bay, California. *Bull. Mar. Sci.* 37, 336–347.

Stone, R. B., Pratt, H. L., Parker, R. O.Jr., and Davis, G. E. (1979). A comparison of fish populations on an artificial and natural reef in the Florida keys. *Mar. Fisheries Rev.*, 1–11. September 1979

Struhsaker, P. (1969). Demersal fish resources: Composition, distribution, and commercial potential of the continental shelf stocks off southeastern united states. *Fish. Ind. Res.* 4, 261–300.

Stunz, G. W., Patterson, W. F. III, Powers, S. P., Cowan, J. H. Jr, Rooker, J. R., Ahrens, R. A., et al. (2021). *Estimating the absolute abundance of age-2+ red snapper (Lutjanus campechanus) in the U.S. Gulf of Mexico* (Mississippi-Alabama Sea Grant Consortium, NOAA Sea Grant), 408.

van Elden, S., Meeuwig, J. J., Hobbs, R. J., and Hemmi, J. M. (2019). Offshore oil and gas platforms as novel ecosystems: A global perspective. *Front. Mar. Sci.* 6. doi: 10.3389/fmars.2019.00548

Walker, B. K., and Gilliam, D. S. (2013). Determining the extent and characterizing coral reef habitats of the northern latitudes of the Florida reef tract (Martin county). *PloS One* 8, e80439. doi: 10.1371/journal.pone.0080439

Wenner, E. L., and Barans, C. A. (2001). Benthic habitats and associated fauna of the upper- and middle-continental slope near the Charleston bump. *Am. Fisheries Soc. Symposium* 25, 161–175.

Whitfield, P. E., Muñoz, R. C., Buckel, C. A., Degan, B. P., Freshwater, D. W., and Hare, J. A. (2014). Native fish community structure and indo-pacific lionfish *Pterois volitans* densities along a depth-temperature gradient in onslow bay, north Carolina, USA. *Mar. Ecol. Prog. Ser.* 509, 241–254. doi: 10.3354/meps10882

frontiers | Frontiers in Marine Science

TYPE Original Research
PUBLISHED 16 September 2022
DOI 10.3389/fmars.2022.980388

EDITED BY
Victoria Louise Georgia Todd,
Ocean Science Consulting Ltd.,
United Kingdom

REVIEWED BY
Magnus Wahlberg,
University of Southern Denmark,
Denmark
Jonas Teilmann,
Aarhus University, Denmark

*CORRESPONDENCE
Oihane Fernandez-Betelu
oihane.fernandez@abdn.ac.uk

SPECIALTY SECTION
This article was submitted to
Marine Ecosystem Ecology,
a section of the journal
Frontiers in Marine Science

RECEIVED 28 June 2022
ACCEPTED 05 September 2022
PUBLISHED 16 September 2022

CITATION
Fernandez-Betelu O, Graham IM and Thompson PM (2022) Reef effect of offshore structures on the occurrence and foraging activity of harbour porpoises.
Front. Mar. Sci. 9:980388.
doi: 10.3389/fmars.2022.980388

Reef effect of offshore structures on the occurrence and foraging activity of harbour porpoises

Oihane Fernandez-Betelu*, Isla M. Graham and Paul M. Thompson

Lighthouse Field Station, School of Biological Sciences, University of Aberdeen, Cromarty, United Kingdom

With increasing numbers of offshore structures being installed and decommissioned, a better understanding of their effect on marine predators is timely. There is some evidence that oil and gas platforms may attract marine mammals, acting as artificial reefs. However, it is unclear whether different man-made structure designs have similar effects or whether artificial structures modify the diel patterns of occurrence and foraging of marine mammals. Here, we used passive acoustics to investigate the occurrence and foraging activity of harbour porpoises (*Phocoena phocoena*) around four artificial structures of different age and complexity. We deployed an array of echolocation click detectors (CPODs) in 2021, along a gradient of distances to these structures and assessed the extent to which porpoises were attracted to them and their effect on porpoises' diel patterns of occurrence and foraging activity. The probability of porpoise occurrence and foraging activity decreased with distance from offshore structures. A significant increase in porpoise occurrence and foraging was detected during night-time compared to daytime around all four offshore structures (< 200 m). Comparing pre- and post-installation porpoise detections, the daily patterns of occurrence and foraging activity shifted from a weak diel pattern before the structure was installed, to a strong nocturnal pattern when the structure was present. These findings provide evidence that marine mammals are attracted to man-made structures and that porpoises modify their diel patterns of occurrence and foraging activity around them. This research suggests that offshore structures play an important role as foraging areas for some marine mammals and provides key information for decommissioning considerations and the planning of decommissioning activities.

KEYWORDS

artificial reefs, oil and gas industry (O&G), offshore renewable energy installations, marine mammal, passive acoustic monitoring (PAM), diel patterns, foraging behaviour

Introduction

Increasing numbers of oil and gas (O&G) structures are coming to the end of their operational life, and there is ongoing debate about the best ecological approaches to their removal or re-use (Bull and Love, 2019; Fortune and Paterson, 2020; Lemasson et al., 2021). In parallel, the rapid growth of offshore wind energy is leading to the installation of many new fixed artificial structures in shelf seas. Assessments of the biological costs and benefits of installing and decommissioning these structures are complicated by uncertainties over the importance of offshore artificial structures for many mobile species (Fortune and Paterson, 2020). In some regions, this constrains policy decisions over re-use of O&G structures as artificial reefs (Bull and Love, 2019). In others, policy decisions already require removal of structures (Lemasson et al., 2021), but the required EIAs are not mandated to consider effects on marine biota adhering to or dependent on the structure (Fortune and Paterson, 2020).

It is recognised that marine mammals may be attracted to artificial offshore structures in certain situations (Russell et al., 2014; Clausen et al., 2021), but the generality of these findings is less clear. This is partly because studies have focused on a limited number of the many designs of structure currently installed offshore, but also because research has been conducted only in a few ecological regions. In common with studies of many aspects of artificial structures, the lack of baseline data can hinder the assessment of decommissioning effects (Fortune and Paterson, 2020).

Harbour porpoises are abundant and widely distributed across the North Sea (Hammond et al., 2013). Given their known sensitivity to anthropogenic disturbance, they are considered key receptors within EIAs underpinning extensive offshore energy activities across this region (Thomsen et al., 2011). Future assessments will need, first, to consider the extent to which attraction to redundant structures may affect local densities during decommissioning activities. Second, mitigation measures will require an understanding of how local densities vary in time to identify periods when these receptors may be more, or less, sensitive to disturbance.

To date, just one study has demonstrated that harbour porpoises are locally attracted to O&G structures. In this case, within the Danish sector of the North Sea, porpoise echolocation activity was up to twofold higher within 800m of an operational O&G platform compared to reference sites (Clausen et al., 2021). As demonstrated in earlier work from a jack-up barge around a gas platform in the German sector of the North Sea, porpoise echolocation activity was also highest during the night (Todd et al., 2009). Similar diel patterns of activity in prey (Fujii and Jamieson, 2016) and avian predators (Ronconi et al., 2015) have been observed around active O&G platforms. However, it is not known whether such diel patterns in predator-prey interactions are driven by the physical presence of artificial structures or through attraction of prey to lights and flares on operational platforms (Todd et al., 2009; Clausen et al., 2021).

Here, using passive acoustic monitoring (PAM), we studied the occurrence and foraging activity of harbour porpoises around a cluster of redundant artificial structures within Scottish shelf waters. First, we assessed the extent to which porpoises were attracted to structures of different age and complexity. Secondly, we explored whether observed increased levels of nocturnal occurrence and foraging were also evident around platforms that have been abandoned, with lighting reduced to levels required for navigational safety. Finally, we used pre-installation baseline data at one site (Thompson et al., 2010) to provide a direct assessment of how the presence of structures affected diel patterns of occurrence and foraging activity of porpoises.

Material and methods

The study was carried out around the Smith Bank, within the Moray Firth, NE Scotland. The area has been subject to O&G exploration and production for several decades (Addy, 1987), and has more recently seen the development of demonstration (Thompson et al., 2010) and commercial (Graham et al., 2019) offshore wind energy. Several marine mammal species occur across the area, but harbour porpoises are the most abundant and widespread of these, providing a model species for understanding interactions between wildlife and offshore energy activities (Thompson et al., 2010; Thompson et al., 2013; Benhemma-Le Gall et al., 2021).

Acoustic deployments

In August 2021, an array of 23 click detectors (V.0 and V.1 CPODs; www.chelonia.co.uk) was deployed along a gradient of distances to four offshore structures on the Smith Bank: Jacky Wellhead platform, Beatrice Bravo O&G platform and the two Beatrice Demonstrator turbines (Figure 1 and detailed information on these offshore structures in Supplementary Material Table S1).

Jacky Wellhead O&G platform, installed in 2008, is a monopile structure with three suction piles (jacket weight: 596 t). Beatrice Bravo O&G platform was installed in 1983 and has 10 leg piles and 4 skirt-piles (total jacket weight: 2,946 t). Oil production from the Beatrice field began in 1981 and ceased in 2015. Jacky started production in 2009 and stopped in 2014. The Beatrice Demonstrator turbines were installed in 2007 on a 4 skirt-pile jacket design (jacket weight: 804 t each). All four structures are unmanned, and their lighting is reduced to the minimum required to comply with national and international regulations on aviation and shipping navigation.

Two CPODs were located in close proximity to each of the structures (< 200 m), hereafter *Structure CPODs*. The remaining 15 CPODs were deployed at distances between 373 and 2700 m from the structures, hereafter *Non-structure CPODs* (detailed information in Supplementary Material Table S2). All CPODs were set to record continuously, with a 20 kHz High pass filter.

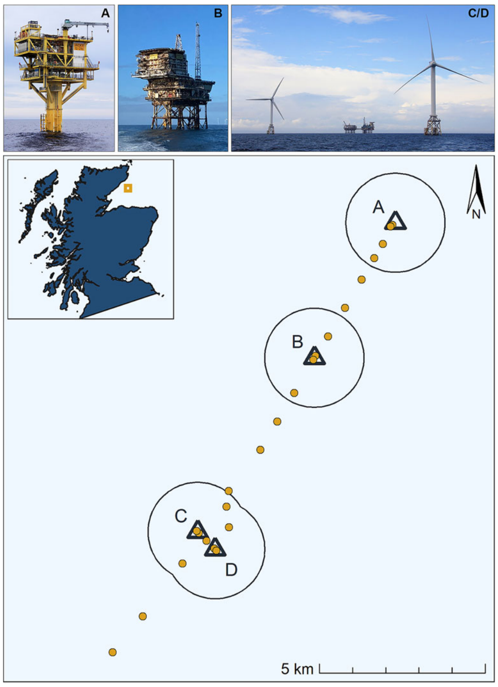

FIGURE 1
CPOD deployments (yellow circles) and offshore structures (black triangles) with a 1500 m buffer around them (black empty circles). **(A)** Jacky Wellhead O&G platform (© Stephen Hurrel), **(B)** Beatrice Bravo O&G platform (© Repsol Sinopec Resources UK LTD), **(C, D)** Beatrice Demonstrator turbines (© Stephen Hurrel).

Data from these recent studies were compared with historic baseline data from one of the contemporary sites. In August 2005, two TPODs (v.4 TPODs; www.chelonia.co.uk) were deployed between the locations where the Beatrice Demonstrator turbines were planned to be installed to collect baseline data from the pre-installation period (Thompson et al., 2010). TPODs were configured to detect the presence of echolocation clicks from harbour porpoises following the set up and analysis methods described by Bailey et al. (2010). TPODs were the analogue predecessors of CPODs and, although TPODs had a less sophisticated detection algorithm than their successors, they were a well-established tool to study variation in the occurrence of harbour porpoises (Carlstrom, 2005; Thomsen et al., 2005; Todd et al., 2009).

Data processing

CPOD data were downloaded and processed using CPOD custom software (cpod.exe v. 2.044). Following the manufacturer's manual, only echolocation clicks classified as high or moderate quality by the built-in "KERNO" classifier were included in the analyses.

To save CPOD memory in noisy environments, a maximum number of recorded clicks per minute (scan limit) can be set. When the scan limit is reached, CPODs stop recording for the rest of the minute and start again at the next one. We set 19 CPODs to record a maximum of 4096 clicks min^{-1} while the remaining 4 CPODs did not have any scan limit (Supplementary Material Table S2). To minimise false-negative detections, CPOD data days when the scan limit was reached in more than 1% of the total minutes were excluded from the analyses.

CPOD data were first used to assess variation in porpoise occurrence, with those hours containing echolocation clicks being defined as detection positive hours (Brookes et al., 2013; Williamson et al., 2016). We then identified the presence of buzzes within each of these hours by modelling the variation in harbour porpoise inter-click intervals (ICIs). To do so, we extracted high and moderate quality click details of porpoise origin and we fitted a Gaussian mixture-model to log transformed ICIs (Pirotta et al., 2014b). We set the number of component distributions *k* to three, dividing ICIs into three groups: inter-train, regular and buzzes. The first and second groups included ICIs between distinct click trains and ICIs within regular click trains, respectively. The third group included click trains with high repetition rate, known as buzzes. Porpoises use buzzes for both foraging activity and social communication (Clausen et al., 2011; Sørensen et al., 2018). Since it is not possible to distinguish between these two behaviours, in line with previous work (Pirotta et al., 2014a; Williamson L. et al., 2017; Benhemma-Le Gall et al., 2021) we assumed that all the identified buzzes could be used as a proxy for foraging.

Variation in harbour porpoise occurrence and foraging activity linked to offshore structures

To investigate the effect of offshore structures on harbour porpoise occurrence and foraging activity, we performed four generalized linear mixed-effects models (GLMM; Bolker et al., 2009).

First, to assess the extent to which porpoises were attracted to offshore structures we modelled the proportion of detection positive hours (DPH) and buzz positive hours (BPH) per day as a function of distance to the closest offshore structure. Proportion of detection positive hours per day was defined as the ratio between the number of hours when porpoises were detected and the total number of hours of the day (Brookes et al., 2013; Williamson et al., 2016). Proportion of buzz positive hours per day was defined as the ratio between the number of hours in which at least one buzz was detected and the number of hours in which porpoises were detected in that day (Pirotta et al., 2014b). For these models we considered the complete CPOD array.

Second, to investigate whether increased levels of nocturnal occurrence and foraging persisted around offshore structures with low levels of lighting, we divided the day into two diel phases (day/night) based on local sunrise and sunset times. We then summarised the proportion of DPH and BPH per diel phase and modelled them as a function of the interaction between the CPOD group (two levels: *Structure/Non-structure CPODs*), the closest offshore structure (three levels: *Jacky/ Beatrice Bravo/Beatrice Demonstrators*) and the diel phase (two levels: *day/night*). Tukey Honestly Significant Difference tests (Tukey HSD; Tukey, 1991) were conducted as a post-hoc test to identify significant differences between group means. In this analysis, we only considered the CPODs deployed within 1500 m of an offshore structure.

All GLMMs were fitted with a binomial family distribution (probit link function) and included a unique identifier for CPOD, to account for variation in device sensitivity, and Julian day as random effects.

Comparison of harbour porpoise diel patterns of occurrence and foraging before and after installation of offshore structures

To assess whether the presence of structures affected diel patterns of occurrence and foraging activity of harbour porpoises, the hourly presence/absence of porpoise detections and buzzes were modelled as a function of the interaction between the hour of the day (*0-24h*) and the presence of the structure (two levels: *Present/Absent*). We fitted generalised additive models (GAMs; Wood, 2006) with a binomial distribution and a logit link. In this analysis, we only considered one site, located between the Beatrice Demonstrator turbines (< 375 m; Supplementary material Table S2), where pre-installation baseline data were available from a previous study (Thompson et al., 2010).

Results

Harbour porpoises were detected every day throughout the 31-day study period for an average of 17 hours day^{-1}. The complete dataset comprised 636 data days from 22 CPOD deployments, with only 23 data days (< 4%) needing to be excluded from further analyses due to excessive background noise (Supplementary Material Table S2).

Variation in harbour porpoise occurrence and foraging activity linked to offshore structures

The probability of both porpoise occurrence (Figure 2A) and foraging activity (Figure 2B) decreased significantly with distance from offshore structures (porpoise occurrence: GLMM X^2 = 16.01, df = 1, P < 0.001; porpoise foraging activity: GLMM X^2 = 14.59, df = 1, P < 0.001). Porpoise occurrence decreased from 0.76 (95% CI: 0.73-0.79) around structures (< 200 m) to 0.63 (95% CI: 0.58-0.68) further away (2500 m). The probability of foraging activity decreased from 0.55 (95% CI: 0.49-0.60) around structures (< 200 m) to 0.36 (95% CI: 0.31-0.44) further away (2500 m).

Variation in both occurrence (Figure 3A) and foraging activity (Figure 3B) were best explained by the interaction between CPOD group, closest structure and diel phase (porpoise occurrence: GLMM X^2 = 24.3, df = 2, P < 0.001; porpoise foraging activity: GLMM X^2 = 45.8, df = 2, P < 0.001). The nature and extent of changes in occurrence varied slightly between structures. However, there was a stronger and more consistent pattern in variation in foraging activity across all three structure levels (Figure 3).

Around structures (< 200 m), harbour porpoise occurrence was significantly higher during night-time compared to daytime at both Beatrice Bravo and Beatrice Demonstrator turbines (Tukey HSD: P < 0.001), while no significant variation in diel occurrence was observed at Jacky (Tukey HSD: P > 0.05; Figure 3A and Supplementary Table S3). At Beatrice Bravo, the probability of occurrence around structures increased from 0.69 during daytime (95% CI: 0.60-0.77) to 0.87 during night-time (95% CI: 0.78-0.92). At Beatrice Demonstrator turbines, the probability of occurrence around structures increased from 0.74 during daytime (95% CI: 0.69-0.78) to 0.83 during night-time (95% CI: 0.79-0.86). In contrast, away from structures (200-1500 m), porpoise occurrence was significantly lower during night-time compared to daytime around Jacky and Beatrice Bravo (Tukey HSD: P < 0.001), while no significant variation in diel occurrence was detected around the Beatrice Demonstrator turbines (Tukey HSD: P > 0.05).

An increase in foraging activity during night-time compared to daytime was observed around all offshore structures (< 200 m; Figure 3B and Supplementary Table S4). At Jacky, the

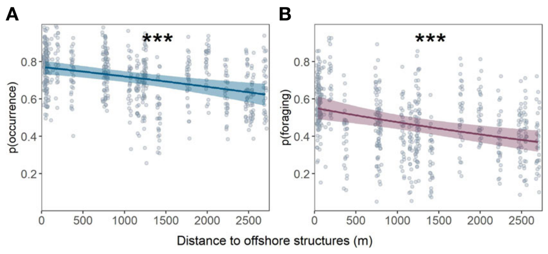

FIGURE 2
Predicted probability of harbour porpoise occurrence **(A)** and foraging activity **(B)** in relation to distance from offshore structures including raw data points (circles). Shaded areas are the 95% confidence intervals for the fixed effects only. Significance of the explanatory variable indicated at the top: ***P < 0.001.

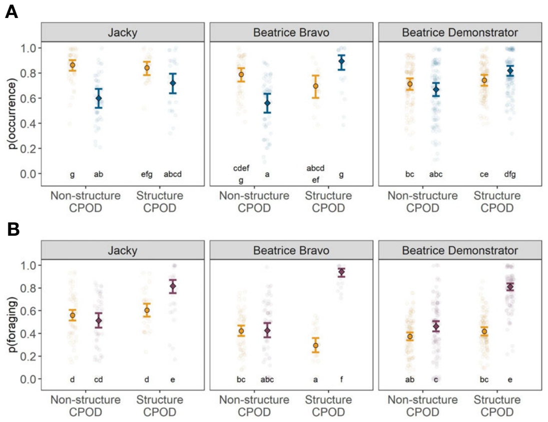

FIGURE 3
Predicted probability of harbour porpoise occurrence **(A)** and foraging activity **(B)** around Structure and Non-structure CPODs at each of the structures during the day (error bars with yellow circles) and during the night (error bars with diamonds) including raw data points (translucid circles). Unlike letters denote groups that differed statistically from each other in Tukey post-hoc test (e.g. a and b: P < 0.05; a and ab: P > 0.05).

probability of foraging activity increased from 0.52 during daytime (95% CI: 0.47-0.58) to 0.78 during night-time (95% CI: 0.71-0.83). At Beatrice Bravo, foraging activity increased from 0.29 during daytime (95% CI: 0.23-0.35) to 0.94 during night-time (95% CI: 0.90-0.97). At the Beatrice Demonstrator turbines, foraging activity increased from 0.39 during daytime (95% CI: 0.36-0.43) to 0.79 at night (95% CI:0.75-0.82). During night-time, the foraging activity was significantly higher around all structures (< 200 m) compared to distances further away (200-1500 m; Figure 3B and Supplementary Table S4).

Comparison of harbour porpoise diel patterns of occurrence and foraging before and after installation of offshore structures

There was a marked change in diel patterns of occurrence and foraging activity when comparing our 2021 data around the Beatrice demonstrators with baseline data collected in 2005 prior to the installation of these structures (Figure 4).

GAM model results confirmed that the presence of the structure had a significant effect on the diel patterns of both harbour porpoise occurrence (Figure 4A) and foraging activity (Figure 4B). In the baseline year, neither porpoise occurrence nor foraging activity changed with the diel cycle. However, in 2021, the probability of both harbour porpoise occurrence and foraging activity increased significantly during night-time.

Discussion

An extensive PAM array around four offshore structures revealed that harbour porpoise occurrence and foraging activity was higher around structures and that this effect was explained by an increase in occurrence and foraging at night. Further, we showed a change in the diel pattern of porpoise occurrence linked to the presence of an offshore structure.

Consistent with previous work (Russell et al., 2014; Clausen et al., 2021), our results provide further evidence that offshore structures attract some species of marine mammals, which use these structures to forage. A previous study found an increase in harbour porpoise activity within an operating windfarm compared to reference sites further away but raised uncertainty about the drivers of attraction as the windfarm was also subject to restricted fishing and vessel activity (Scheidat et al., 2011). Here, we also found a significant increase in harbour porpoise occurrence and foraging activity near isolated offshore structures compared to locations further away. Similarly, Clausen et al. (2021) detected an increase in porpoise occurrence within 800 m of an O&G platform compared to more distant areas. Marine artificial structures create artificial reefs that are colonised by epifaunal communities which, in turn, cause an increase in shallow- and mid-water pelagic species (Stanley and Wilson, 2000; Degraer et al., 2020). O&G platforms have been described as highly productive areas that support high fish density (Claisse et al., 2014; Love et al., 2019a). Therefore, one possible explanation for the observed increase in porpoise occurrence and foraging activity closer to the structures is that they provide more foraging opportunities. Alternatively, porpoises may perceive offshore structures as more complex areas to navigate and, since they use echolocation both to navigate and communicate (Clausen et al., 2011; Sørensen et al., 2018), the increase in occurrence and foraging activity detected in this study could

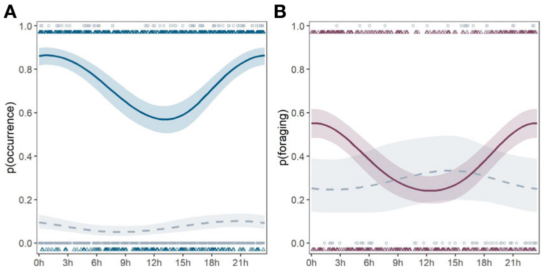

FIGURE 4
Predicted probability of harbour porpoise occurrence **(A)** and foraging activity **(B)** per hour when Beatrice demonstrator turbines were absent (dashed line) and present (solid line) including raw data points (circles: structure absent; triangles: structure present). Shaded areas are the 95% CI.

partly be explained by changes in echolocation behaviour around structures. However, the attraction to man-made structures has also been detected in seals, which also use these areas to forage (Russell et al., 2014; Arnould et al., 2015). Furthermore, the increase in bentho-pelagic communities around man-made structures is well documented in the literature (Gates et al., 2019; Perry and Heyman, 2020). Therefore, we suggest that the enhanced foraging opportunities around offshore structures is the most plausible explanation for the observed increase in porpoise detections.

Our analyses showed strong diel patterns in the occurrence and foraging activity of harbour porpoises around offshore structures (< 200 m). Porpoise occurrence was significantly higher at night compared to daytime around three of four structures investigated here, while foraging activity was significantly higher at night around all four of them. Similar nocturnal increases in porpoise occurrence and foraging activity near man-made structures were found in previous studies (Todd et al., 2009; Brandt et al., 2014; Clausen et al., 2021). However, in those studies the authors highlighted that any influence of physical structures on predator-prey interactions could be confounded by the lighting on these structures attracting prey species at night (Todd et al., 2009; Clausen et al., 2021). In our study, lighting on all four structures had been reduced to minimum levels required to comply with national and international regulations on aviation and shipping navigation. Consequently, it is likely to be the physical presence of structures that shape these foraging patterns. The precise mechanisms underlying this nocturnal increase in foraging remain unclear, but it seems likely to be related to diel movements of prey or changes in their activity or schooling behaviour (Todd et al., 2009; Brandt et al., 2014; Clausen et al., 2021). Further research to directly investigate activity patterns of fish (Williamson B. J. et al., 2017) in relation to porpoise movements (e.g. Gillespie et al., 2020) are now required to better understand the drivers of porpoise activity around offshore structures.

Importantly, our study also provides direct evidence of a change in harbour porpoise diel patterns in relation to the introduction of an offshore structure. Although baseline data were available from only one of our sites, this analysis demonstrated a clear difference in nocturnal patterns of occurrence and foraging activity when the structure was present compared to the year before the structure was installed (Figure 4). It should be noted that, for this comparison, we used data sets obtained with different devices: CPODs, when the offshore structure was present, and their predecessors TPODs, when the structure was absent (Thompson et al., 2010). Current CPODs include a more sophisticated detection algorithm, which results in a lower false positive rate compared to TPODs. Therefore, the absolute differences in levels of porpoise occurrence and foraging activity cannot be directly compared. Nevertheless, the difference in the diel patterns within each of these data sets should be robust to device-specific differences in detection probability. Additionally, the larger contemporary dataset also demonstrated a clear increase in nocturnal occurrence and foraging around the structures (< 200 m) compared to locations further away (Figure 3). Together, these two datasets provide strong support for the hypothesis that the change in diel patterns of porpoise occurrence and foraging are linked to the presence of structures. Future studies using similar devices before and after the installation of a man-made structure could investigate this further.

While a significant increase in nocturnal foraging was detected around all four offshore structures studied here, the highest increase was detected around Beatrice Bravo (from 0.29 during daytime to 0.94 during night-time; Figure 3B). More complex subsea structures exhibit higher fish density and greater species richness (Love et al., 2019b). Furthermore, species diversity also increases with the age of the artificial reef (Perkol-Finkel and Benayahu, 2005). Beatrice Bravo is both the oldest and the most complex structure among those investigated here, and, in line with those studies, our results suggest that higher foraging opportunities may exist around it compared to simpler structures, such as the Jacky monopile. Nevertheless, our findings are based only on individual (Beatrice Bravo & Jacky) or pairs (Beatrice Demonstrator) of similar offshore structures, where other factors could confound patterns of predator occurrence and foraging activity. Furthermore, all the structures that we studied had been in the water for at least 12 years, and we could not determine the age at which they started becoming attractive to porpoises. A recent study in the Southern North Sea found no evidence of attraction to a gas production platform in its first five years of operation (Todd et al., 2022), perhaps suggesting that it may take several years for prey communities to develop to levels at which they influence predator activity. Additionally, Clausen et al. (2021) found seasonal variability in porpoise activity around O&G platforms. Previous work in our study area has also shown seasonal changes in porpoise occurrence, with a peak in August, when the present study was conducted (Graham et al., 2019). Whether our observed attraction to structures during this month remains consistent throughout other seasons remains unclear. Further research of larger groups of similar man-made structures throughout their life cycle is now required to investigate how structure age, complexity and seasonality influence the occurrence and foraging activity of marine predators.

In conclusion, our analyses showed that harbour porpoises are attracted to isolated offshore structures and that porpoises use these structures to forage, especially at night. These findings suggest that offshore structures play an important role as foraging areas for some marine mammals, filling a key gap in the ecological understanding of offshore decommissioning in the North Sea (Fowler et al., 2020). These findings now provide important baseline to support the assessment and mitigation of future decommissioning projects.

Data availability statement

The datasets presented in this study can be found in online repositories. The names of the repository/repositories and accession number(s) can be found below: https://doi.org/10.5061/dryad.mpg4f4r2p

Ethics statement

Ethical review and approval was not required for the animal study because it was a non-invasive, acoustic observational study of harbour porpoise activity around offshore structures. No animals were captured or tagged during this study and no research or animal ethical assessments were required. Harbour porpoise activity was determined using remote passive acoustic devices on seabed moorings licensed for scientific use by Marine Scotland and consented by the Crown Estate. Moorings were deployed and recovered using vessels with appropriate certification, accreditation, and endorsements.

Author contributions

OF-B: Conceptualization, data curation, formal analysis, funding acquisition, methodology, visualization, writing – original draft. IG: Conceptualization, data curation, funding acquisition, methodology, supervision, writing – review & editing. PT: Conceptualization, funding acquisition, methodology, project administration, resources, supervision, writing – review & editing. All authors contributed to the article and approved the submitted version.

Funding

This study was funded by the UK Department for Business, Energy & Industrial Strategy (BEIS) Offshore Energy Strategic Environmental Assessment research programme under contracts OESEA-20-125 and OESEA-21-133, using equipment previously purchased by UK Department of Energy and Climate Change, Scottish Government, Oil and Gas UK, COWRIE and Moray Offshore Renewables Ltd. Funding for the 2005 baseline studies was provided by the EU DOWNVinD Project and Talisman Energy (UK) Ltd., who were not involved in the study design, collection, analysis, interpretation of data, the writing of this article, or the decision to submit it for publication.

Acknowledgments

We would like to thank Bill Ruck, Moray First Marine and colleagues from the University of Aberdeen for assistance with the data collection, and John Hartley for his support through the project and for his comments on the manuscript. We are very grateful to Ithaca Energy (UK) Limited, Repsol Sinopec Resources UK Limited and SSE Generation Limited for allowing access to the Jacky platform, Beatrice Bravo platform and Beatrice wind demonstrator turbine sites.

Conflict of interest

The authors declare that the research was conducted in the absence of any commercial or financial relationships that could be construed as a potential conflict of interest.

Publisher's note

Supplementary material

The Supplementary Material for this article can be found online at: https://www.frontiersin.org/articles/10.3389/fmars.2022.980388/full#supplementary-material

References

Addy, J. M. (1987). Environmental monitoring of the Beatrice oilfield development. *Philos. Trans. R. Soc. London B Biol. Sci.* 316 (1181), 655–668. doi: 10.1098/rstb.1987.0044

Arnould, J. P., Monk, J., Ierodiaconou, D., Hindell, M. A., Semmens, J., Hoskins, A. J., et al. (2015). Use of anthropogenic Sea floor structures by Australian fur seals: Potential positive ecological impacts of marine industrial development? *PloS One* 10 (7), e0130581. doi: 10.1371/journal.pone.0130581

Bailey, H., Clay, G., Coates, E. A., Lusseau, D., Senior, B., and Thompson, P. M. (2010). Using T-PODs to assess variations in the occurrence of coastal bottlenose dolphins and harbour porpoises. *Aquat. Conservation: Mar. Freshw. Ecosyst.* 20, 150–158. doi: 10.3354/meps08789

Benhemma-Le Gall, A., Graham, I. M., Merchant, N. D., and Thompson, P. M. (2021). Broad-scale responses of harbor porpoises to pile-driving and vessel activities during offshore windfarm construction. *Front. Mar. Sci.* 8, 735. doi: 10.3389/fmars.2021.664724

Bolker, B. M., Brooks, M. E., Clark, C. J., Geange, S. W., Poulsen, J. R., Stevens, M. H. H., et al. (2009). Generalized linear mixed models: a practical guide for ecology and evolution. *Trends Ecol. Evol.* 24 (3), 127–135. doi: 10.1016/j.tree.2008.10.008

Brandt, M. J., Hansen, S., Diederichs, A., and Nehls, G. (2014). Do man-made structures and water depth affect the diel rhythms in click recordings of harbor porpoises (*Phocoena phocoena*)? *Mar. Mammal Sci.* 30 (3), 1109–1121. doi: 10.1111/mms.12112

Brookes, K. L., Bailey, H., and Thompson, P. M. (2013). Predictions from harbor porpoise habitat association models are confirmed by long-term passive acoustic monitoring. *J. Acoust. Soc. America* 134 (3), 2523–2523. doi: 10.1121/1.4816577

Bull, A. S., and Love, M. S. (2019). Worldwide oil and gas platform decommissioning: A review of practices and reefing options. *Ocean Coast. Manage.* 168, 274–306. doi: 10.1016/j.ocecoaman.2018.10.024

Carlstrom, J. (2005). Diel variation in echolocation behavior of wild harbor porpoises. *Mar. Mammal Sci.* 21 (1), 1–12. doi: 10.1111/j.1748-7692.2005.tb01204.x

Claisse, J. T., Pondella, D. J.2nd, Love, M., Zahn, L. A., Williams, C. M., Williams, J. P., et al. (2014). Oil platforms off California are among the most productive marine fish habitats globally. *Proc. Natl. Acad. Sci.* 111 (43), 15462–15467. doi: 10.1073/pnas.1411477111

Clausen, K. T., Teilmann, J., Wisniewska, D. M., Balle, J. D., Delefosse, M., and Beest, F. M. (2021). Echolocation activity of harbour porpoises, *Phocoena phocoena*, shows seasonal artificial reef attraction despite elevated noise levels close to oil and gas platforms. *Ecol. Solutions Evid.* 2 (1), e12055. doi: 10.1002/2688-8319.12055

Clausen, K. T., Wahlberg, M., Beedholm, K., Deruiter, S., and Madsen, P. T. (2011). Click communication in harbour porpoises *Phocoena phocoena*. *Bioacoustics* 20 (1), 1–28. doi: 10.1080/09524622.2011.9753630

Degraer, S., Carey, D. A., Coolen, J. W. P., Hutchison, Z. L., Kerckhof, F., Rumes, B., et al. (2020). Offshore wind farm artificial reefs affect ecosystem structure and functioning - a synthesis. *Oceanography* 33 (4), 48–57. doi: 10.5670/oceanog.2020.405

Fortune, I. S., and Paterson, D. M. (2020). Ecological best practice in decommissioning: a review of scientific research. *ICES J. Mar. Sci.* 77 (3), 1079–1091. doi: 10.1093/icesjms/fsy130

Fowler, A. M., Jørgensen, A. M., Coolen, J. W. P., Jones, D. O. B., Svendsen, J. C., Brabant, R., et al. (2020). The ecology of infrastructure decommissioning in the north Sea: what we need to know and how to achieve it. *ICES J. Mar. Sci.* 77 (3), 1109–1126. doi: 10.1093/icesjms/fsz143

Fujii, T., and Jamieson, A. J. (2016). Fine-scale monitoring of fish movements and multiple environmental parameters around a decommissioned offshore oil platform: A pilot study in the north sea. *Ocean Eng.* 126, 481–487. doi: 10.1016/j.oceaneng.2016.09.003

Gates, A. R., Horton, T., Serpell-Stevens, A., Chandler, C., Grange, L. J., Robert, K., et al. (2019). Ecological role of an offshore industry artificial structure. *Front. Mar. Sci.* 6. doi: 10.3389/fmars.2019.00675

Gillespie, D., Palmer, L., Macaulay, J., Sparling, C., and Hastie, G. (2020). Passive acoustic methods for tracking the 3D movements of small cetaceans around marine structures. *PloS One* 15 (5), e0229058. doi: 10.1371/journal.pone.0229058

Graham, I. M., Merchant, N. D., Farcas, A., Barton, T. R., Cheney, B., Bono, S., et al. (2019). Harbour porpoise responses to pile-driving diminish over time. *R. Soc. Open Sci.* 6 (6), 190335. doi: 10.1098/rsos.190335

Hammond, P. S., Macleod, K., Berggren, P., Borchers, D. L., Burt, L., Cañadas, A., et al. (2013). Cetacean abundance and distribution in European Atlantic shelf waters to inform conservation and management. *Biol. Conserv.* 164, 107–122. doi: 10.1016/j.biocon.2013.04.010

Lemasson, A. J., Knights, A. M., Thompson, M., Lessin, G., Beaumont, N., Pascoe, C., et al. (2021). Evidence for the effects of decommissioning man-made structures on marine ecosystems globally: a systematic map protocol. *Environ. Evid.* 10 (1), 4. doi: 10.1186/s13750-021-00218-y

Love, M. S., Claisse, J. T., and Roeper, A. (2019a). An analysis of the fish assemblages around 23 oil and gas platforms off California with comparisons with natural habitats. *Bull. Mar. Sci.* 95 (4), 477–514. doi: 10.5343/bms.2018.0061

Love, M. S., Kui, L., and Claisse, J. T. (2019b). The role of jacket complexity in structuring fish assemblages in the midwaters of two California oil and gas platforms. *Bull. Mar. Sci.* 95 (4), 597–616. doi: 10.5343/bms.2017.1131

Perkol-Finkel, S., and Benayahu, Y. (2005). Recruitment of benthic organisms onto a planned artificial reef: shifts in community structure one decade post-deployment. *Mar. Environ. Res.* 59 (2), 79–99. doi: 10.1016/j.marenvres.2004.03.122

Perry, R. L., and Heyman, W. D. (2020). Considerations for offshore wind energy development effects on fish and fisheres in the united states. *Oceanography* 33 (4), 28–37. doi: 10.5670/oceanog.2020.403

Pirotta, E., Brookes, K. L., Graham, I. M., and Thompson, P. M. (2014a). Variation in harbour porpoise activity in response to seismic survey noise. *Biol. Lett.* 10 (May), 5–5. doi: 10.1098/rsbl.2013.1090

Pirotta, E., Thompson, P. M., Miller, P. I., Brookes, K. L., Cheney, B., Barton, T. R., et al. (2014b). Scale-dependent foraging ecology of a marine top predator modelled using passive acoustic data. *Funct. Ecol.* 28 (1), 206–217. doi: 10.1111/1365-2435.12146

Ronconi, R. A., Allard, K. A., and Taylor, P. D. (2015). Bird interactions with offshore oil and gas platforms: Review of impacts and monitoring techniques. *J. Environ. Manage.* 147, 34–45. doi: 10.1016/j.jenvman.2014.07.031

Russell, D. J. F., Brasseur, S., Thompson, D., Hastie, G. D., Janik, V. M., Aarts, G., et al. (2014). Marine mammals trace anthropogenic structures at sea. *Curr. Biol.* 24 (14), R638–R639. doi: 10.1016/j.cub.2014.06.033

Sørensen, P. M., Wisniewska, D. M., Jensen, F. H., Johnson, M., Teilmann, J., and Madsen, P. T. (2018). Click communication in wild harbour porpoises (*Phocoena phocoena*). *Sci. Rep.* 8 (1), 9702. doi: 10.1038/s41598-018-28022-8

Scheidat, M., Tougaard, J., Brasseur, S., Carstensen, J., van Polanen Petel, T., Teilmann, J., et al. (2011). Harbour porpoises (*Phocoena phocoena*) and wind farms: a case study in the Dutch north sea. *Environ. Res. Lett.* 6 (2), 025102. doi: 10.1088/1748-9326/6/2/025102

Stanley, D. R., and Wilson, C. A. (2000). Variation in the density and species composition of fishes associated with three petroleum platforms using dual beam hydroacoustics. *Fisheries Res.* 47 (2-3), 161–172. doi: 10.1016/S0165-7836(00)00167-3

Thompson, P. M., Brookes, K. L., Graham, I. M., Barton, T. R., Needham, K., Bradbury, G., et al. (2013). Short-term disturbance by a commercial two-dimensional seismic survey does not lead to long-term displacement of harbour porpoises. *Proc. R. Soc. B: Biol. Sci.* 280 (1771), 20132001–20132001. doi: 10.1098/rspb.2013.2001

Thompson, P. M., Lusseau, D., Barton, T., Simmons, D., Rusin, J., and Bailey, H. (2010). Assessing the responses of coastal cetaceans to the construction of offshore wind turbines. *Mar. pollut. Bull.* 60 (8), 1200–1208. doi: 10.1016/j.marpolbul.2010.03.030

Thomsen, F., McCully, S. R., Weiss, L. R., Wood, D. T., Warr, K. J., Barry, J., et al. (2011). Cetacean stock assessments in relation to exploration and production industry activity and other human pressures: Review and data needs. *Aquat. Mammals* 37 (1), 1–93. doi: 10.1578/AM.37.1.2011.1

Thomsen, F., van Elk, N., Brock, V., and Piper, W. (2005). On the performance of automated porpoise-click-detectors in experiments with captive harbor porpoises (*Phocoena phocoena*). *J. Acoust. Soc. Am.* 118 (1), 37–40. doi: 10.1121/1.1937347

Todd, V. L. G., Pearse, W. D., Tregenza, N. C., Lepper, P. A., and Todd, I. B. (2009). Diel echolocation activity of harbour porpoises (*Phocoena phocoena*) around north Sea offshore gas installations. *ICES J. Mar. Sci.* 66 (4), 734–745. doi: 10.1093/icesjms/fsp035

Todd, V. L. G., Williamson, L. D., Couto, A. S., Todd, I. B., and Clapham, P. J. (2022). Effect of a new offshore gas platform on harbor porpoises in the dogger bank. *Mar. Mammal Sci.* 1–14 doi: 10.1111/mms.12949

Tukey, J. W. (1991). The philosophy of multiple comparisons. *Stat. Sci.*, 100–116. doi: 10.1214/ss/1177011945

Williamson, L., Brookes, K. L., Scott, B. E., Graham, I. M., Bradbury, G., Hammond, P. S., et al. (2016). Echolocation detections and digital video surveys provide reliable estimates of the relative density of harbour porpoises. *Methods Ecol. Evol.* 77, 762–769 doi: 10.1111/2041-210X.12538

Williamson, L., Brookes, K. L., Scott, B. E., Graham, I. M., and Thompson, P. M. (2017). Diurnal variation in harbour porpoise detection – potential implications for management. *Mar. Ecol. Prog. Ser.* 570, 223–232. doi: 10.3354/meps12118

Williamson, B. J., Fraser, S., Blondel, P., Bell, P. S., Waggitt, J. J., and Scott, B. E. (2017). Multisensor acoustic tracking of fish and seabird behavior around tidal turbine structures in Scotland. *IEEE J. Oceanic Eng.*, 1–18. doi: 10.1109/JOE.2016.2637179

Wood, S. N. (2006). Low rank scale invariant tensor product smooths for generalized additive mixed models. *Biometrics* 62 (4), 1025–1036. doi: 10.1111/j.1541-0420.2006.00574.x

frontiers | Frontiers in Marine Science

TYPE Original Research
PUBLISHED 29 September 2022
DOI 10.3389/fmars.2022.1010303

OPEN ACCESS

EDITED BY
Stelios Katsanevakis,
University of the Aegean, Greece

REVIEWED BY
Caitlin Blain,
The University of Auckland,
New Zealand
Gilda Savonitto,
University of Trieste, Italy
Davide Agnetta,
Istituto Nazionale di Oceanografia e di
Geofisica Sperimentale), Italy

*CORRESPONDENCE
Jonathan P. Williams
jonwilliams@oxy.edu

SPECIALTY SECTION
This article was submitted to
Marine Ecosystem Ecology,
a section of the journal
Frontiers in Marine Science

RECEIVED 02 August 2022
ACCEPTED 15 September 2022
PUBLISHED 29 September 2022

CITATION
Williams JP, Williams CM,
Pondella DJII and Scholz ZM (2022)
Rebirth of a reef: As-built description
and rapid
returns from the Palos Verdes Reef
Restoration Project.
Front. Mar. Sci. 9:1010303.
doi: 10.3389/fmars.2022.1010303

Rebirth of a reef: As-built description and rapid returns from the Palos Verdes Reef Restoration Project

Jonathan P. Williams*, Chelsea M. Williams,
Daniel J. Pondella II and Zoe M. Scholz

Department of Biology, Vantuna Research Group, Occidental College, Los Angeles, CA, United States

Palos Verdes Reef (PVR) is an artificial reef designed to restore rocky-reef associated marine species by directly restoring rocky-reef habitat that has been impacted by scour, sedimentation, and burial in the shallow subtidal portion of the Palos Verdes Peninsula in Los Angeles County, California, USA. The restoration reef provides high-quality habitat that is contiguous with the natural reef and allows for rapid succession. This project is a unique endeavor as restoring lost habitat *in situ* and has not been attempted in a temperate rocky reef and kelp forest community. While the primary design criteria for PVR is fish production in an area where already-limited hard substrate had been lost, it is also designed to be resilient to ongoing sedimentation and turbidity challenges on the peninsula. Following over a decade of design, planning, outreach, site surveying, and permitting, PVR was built in 2020 as 18 discrete modules using 52,729 tons of quarry rock placed approximately 8–80 m from existing, unburied rocky-reef habitat. There was no significant accumulation or scouring of sediment due to the placement of the reef and temperature data shows that internal tides regularly inundate the reef with cool, nutrient rich water. Rocky-reef associated taxa rapidly recruited to the restoration site, with visible changes occurring within just a few months post-construction. PVR modules showed rapid, significantly positive responses in fish density, fish biomass, kelp density, and biotic benthic cover less than 18 months after reef placement with a general pattern of succession in giant kelp growth from nearshore to offshore resulting in an established, thick canopy, in the nearshore, shallow modules. The newly available, high-quality habitat was quickly colonized and already shows late successional patterns with respect to fish and benthic communities. This restoration reef will produce large amounts of biomass over the long-term, though future surveys of multiple restored, adjacent, and reference sites will determine if high biomass at PVR is a result of new secondary production or attraction from nearby reefs.

KEYWORDS

rocky reef, restoration, giant kelp, biomass, fish, ecological succession, sedimentation

Introduction

The shallow subtidal portion of the Palos Verdes Peninsula in Los Angeles County, California, USA, is a nearly unbroken stretch of more than 20 km of rocky reef habitat, one of the largest continuous segments of rocky reef in the Southern California Bight. Rocky reefs and associated giant kelp (*Macrocystis pyrifera*) forests form three-dimensional habitats that support nearly one-quarter of California's marine organisms (Graham, 2004). This ecosystem is economically and ecologically valuable but is adjacent to a highly populated and altered coastline and subject to multiple ecological stressors including pollution, overharvesting (Pondella, 2009), and the formation of persistent urchin barrens (Williams et al., 2021). In addition, this geologically active peninsula is also the location of several recent anthropogenically induced (or reactivated) landslides (Kayen et al., 2002). Though issues of pollution, overharvesting, and urchin barrens have all been addressed to some degree and landslides have slowed appreciably in recent years due to major infrastructure improvements, there is continued turbidity and scour associated with previously deposited sediment. Furthermore, the 18th hole of what is now Trump National Golf Club slid into the ocean and onto the rocky reefs below in 1999, and long-term reef burial has been noted in all surveys since (e.g., Pondella et al., 2015; Pondella et al., 2018). Much of the historic low-lying reef continues to be impacted by chronic sedimentation due to reef burial, scour, and associated turbidity, significantly decreasing the amount of habitable rocky reef habitat in the area.

The purpose of the Palos Verdes Reef Restoration Project is to restore rocky-reef associated marine species by directly restoring rocky-reef habitats that were lost due to sedimentation. Developing a subtidal rocky reef restoration project of this type is a unique endeavor, as restoring lost habitat *in situ* has not been attempted in a temperate rocky reef and kelp forest community. Artificial structures have been placed on the seafloor throughout the Southern California Bight with various goals and varying degrees of success, often with limited monitoring and capacity for experimental analysis. Artificial reefs were built to enhance fishing (Lewis and McKee, 1989) and scuba opportunities (Ilieva et al., 2019), mitigate for lost kelp bed habitat (Reed et al., 2006), and enhance habitat in estuaries (Pondella et al., 2006). Additionally, infrastructure needs often incidentally create habitat ('secondary reefs'), including breakwaters and jetties (Stephens et al., 1994) and oil and gas platforms (Claisse et al., 2014).

Our goal was to develop a restoration plan that maximizes the biological benefits to this ecosystem while balancing economic, physical, and engineering constraints. As a heavily utilized region for commercial and recreational harvest (Pondella, 2009), natural rocky reefs in the area are almost certainly not at their carrying capacities for any native fish species, and low-quality habitat is less conducive to fish production (Zellmer et al., 2019). Therefore, a key aspect of this reef design is not to just provide *more* habitat for rocky-reef associated fishes, but to provide *better* habitat (Bohnsack, 1989). For over a decade, we examined the potential efficacy of fishery production enhancement reefs in this region by establishing an intensive biological and physical sampling program throughout subtidal areas of Palos Verdes Peninsula (Pondella et al., 2018). We developed a secondary production model that specifically analyzes the production of fish biomass to evaluate reef performance (Pondella et al., 2019) and utilizes stacked-species distribution modeling to predict an optimal site for restoration (Zellmer et al., 2019). Notable among all survey locations was KOU Rock, a relatively high relief (~5 m) area of reef within the sediment impacted area that consistently had the highest fish biomass density anywhere on the peninsula, including non-sediment impacted areas and reefs inside marine protected areas (Pondella et al., 2018; Figure 1). The high structural relief prevents sediment accumulation, scour, and subsequent reef burial while allowing for high biotic benthic cover, and this natural feature ultimately served as the example for the design of the quarry rock reef modules that together form the restoration reef.

Palos Verdes Reef (PVR) was constructed in 2020 using 52,729 tons of quarry rock and is unique in terms of both design and location. It was designed as a series of high-relief modules to provide essential habitat for fishes and substrate for giant kelp, other marine algae, and marine invertebrates to become attached to. The intention was to create a productive rocky-reef ecosystem in an area with limited hard substrate that had previously been lost. PVR was built on top of previously existing, but recently buried (< 1 m burial depth) rocky reef and is directly adjacent to existing, exposed, natural rocky reef and kelp forests (8–80 m) and the edge of the continental shelf (< 2 km). This manuscript serves as an 'as-built' description of the newly constructed restoration reef, as well as a summary of the rapid and notable responses in the fish and benthic communities in the first 12-18 months post-construction.

Methods

Construction and general as-built description

PVR was designed with submodules (1-4 m in height) staggered within modules, with the higher-relief (3-4 m) submodules placed at the ends of each module to buffer any potential sedimentation of the 1-m relief submodules in the middle of each module (Figure 2). Modules were placed at 16.7–21.1 m seafloor depth (MLLW), maintain connectivity with existing natural reefs, were oriented similarly to natural features, and were placed on a maximum of 1 m sediment depth to limit long-term burial/sinking (Figure 1). Within each group of modules, or block, we incorporated 10-20 m sand

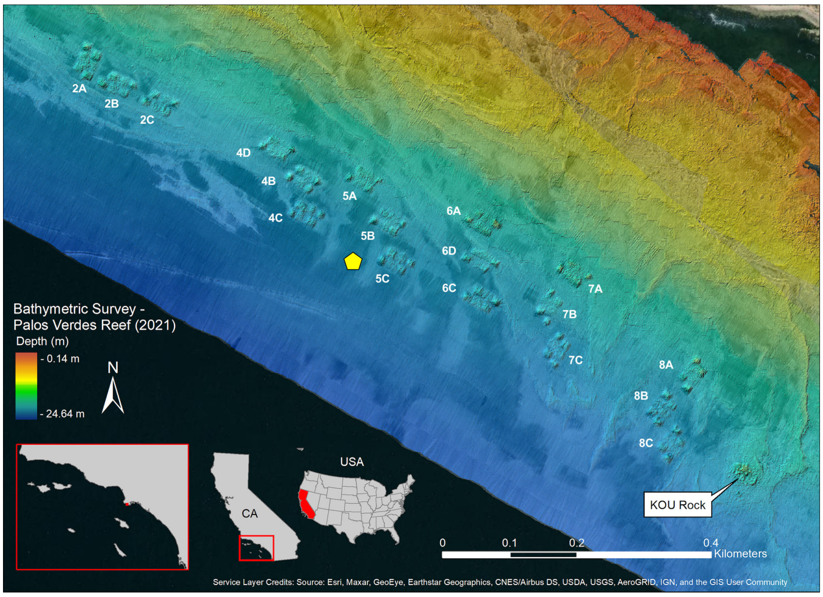

FIGURE 1
Finalized design of Palos Verdes Restoration Reef including bathymetry shaded relief and processed backscatter. Backscatter data are shown as a grayscale overlay where lighter areas indicate soft substrate and darker areas indicate either hard substrate or lightly buried hard substrate. Yellow pentagon indicates the position of the Spotter Buoy.

channels between modules to permit space for the movement of sediment.

Quarry mining, rock transportation, and reef construction were all performed by Connolly-Pacific Co. Quarry rock boulders of a variety of sizes (estimated mean = 0.36 MT, range ≈ 0.04–1.20 MT; Figure 3) were mined from Empire Quarry on Santa Catalina Island, California, and passed independent testing for specific gravity, absorption, and abrasion resistance. The reef was constructed in two phases to accommodate quarry rock demand, concurrent projects, and complications from the COVID-19 pandemic. The first phase was 8 May 2020 – 4 June 2020 and the second phase was 29 August 2020 – 23 September 2020 (Table 1). The quarry rock was transported across Catalina Channel to the restoration site on a flat rock barge towed by a tugboat where the rock barge was secured to a derrick barge with wire ropes. A front-end track loader placed boulders over the edge of the rock barge along engineered gridlines, and when each gridline was completed, the derrick barge was re-positioned so that the edge of the rock barge was aligned along the next gridline, and the process was repeated until the module was completed. Periodically during rock placement, handheld leadline soundings were taken to verify compliance with the required placement specifications. To verify the rock quantity placed, the net weight of the material was calculated using barge displacement measures and tables. Upon completion of a module, the derrick barge moved anchors and positioned itself and the rock barge on the next module.

Geophysical and oceanographic monitoring

High-resolution multibeam bathymetry data were collected from Bunker Point to KOU Rock, Palos Verdes, prior to deployment in October 2019, and again after the reefs were constructed in May 2020, August/September 2020, and December 2021 using an Edgetech 6205 MultiPhase EchoSounder pole mounted to a 6.5–7.5-m research vessels. Each survey consisted of parallel transects, spaced 30 m apart to assure 100% coverage of the reef area, with most areas having 200% coverage. This coverage helped to avoid false soundings and increased resolution. Sound velocity profiles were collected at the start and end of each survey day using a SeaBird SBE 19plus V2 SeaCAT profiler CTD and were applied to the data by matching the cast closest in time to the survey line. Boat position was obtained by an SBG Ekinox survey grade dual-frequency global navigation satellite system (GNSS) receiver with real-time kinematic and dynamic positioning provided by the California Real Time Network, a multipurpose statewide GNSS network. This system is capable of 8-cm resolution with a depth accuracy of 2 cm and a horizontal position accuracy of less than 3 cm. Data were collected using SonarWiz 7 and EdgeTech's Discover software. All multibeam data were cleaned and processed in SonarWiz 7 software and ArcGIS ArcMap 10.8 and used to produce annual bathymetric shaded relief images and differential depth comparisons over time.

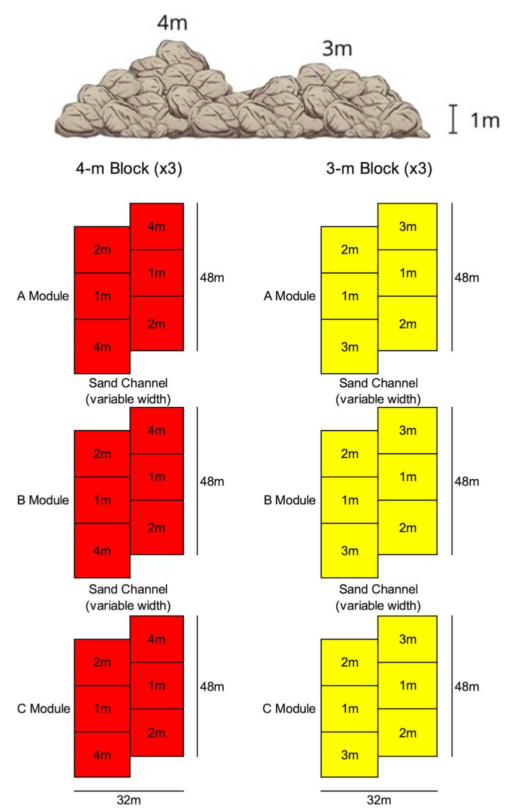

FIGURE 2
Basic schematic diagram of the restoration reef blocks.

On 2 June 2021, we deployed a Sofar Ocean (https://www.sofarocean.com/) Spotter Buoy and Smart Mooring approximately 50 m west of Module 5C (33.72054° N, 118.34584° W, Figure 1). The buoy was purchased and donated by Aqualink (https://www.aqualink.org/) and registered as a Private Aid to Navigation with the United States Coast Guard and Department of Homeland Security. This buoy system is entirely solar powered and monitors the geographic position of the buoy, the sea temperature at both 1 m and 18 m below the surface (near the seafloor), as well as wind speed/direction, significant wave height, and wave period/direction. Data are transmitted *via* Iridium satellite every ten minutes and historical and real-time data are publicly available. The buoy system was temporarily out of commission after a boat strike severed the mooring/data cable on 13 July 2021. The buoy and cable were repaired, and the system was reinstalled on 20 October 2021. Though use of this data thus far has mainly been exploratory, we paired buoy data with water level data from the nearest NOAA tide gauge (Los Angeles, CA – Station ID: 9410660) to illustrate the relationship between surface/seafloor temperatures and tidal cycles.

Biological monitoring

Our biological monitoring approach includes diver surveys, protocols for which are described in detail by Zahn et al. (2016) and Pondella et al. (2019). Briefly, each pre-construction reef footprint and restoration reef module was characterized using 3 survey types: (1) 30-m × 2-m band transects to estimate species-specific fish density and size distribution along the reef surface, in the midwater, and through the kelp canopy when it was present; (2) 30-m × 2-m band transects to estimate density of macroinvertebrates and stipitate algae (kelp) on the reef; and (3) uniform point contact surveys to determine percent cover of primary reef placeholders, including sessile invertebrates, algae, and abiotic features (e.g. bare sand, bare rock, shell hash). The reef footprints were surveyed twice prior to construction (2019 and 2020) and the reef modules were surveyed twice post-construction (2020 and 2021). Each of the 18 reef footprints/modules were sampled independently and transects covered approximately equal areas of each submodule height. Two of the reef footprints were not surveyed in 2019 due to late-stage changes in reef placement.

Prior to analysis, pelagic and highly mobile fish species that are not characteristic inhabitants of rocky reef habitats were excluded from the data, and young-of-the-year fishes were removed prior to density (but not biomass) calculations because they could numerically dominate the assemblage at some sites sampled early during the sampling season but decline later in the year due to natural mortality. Total length (TL) estimates were converted to biomass using standard

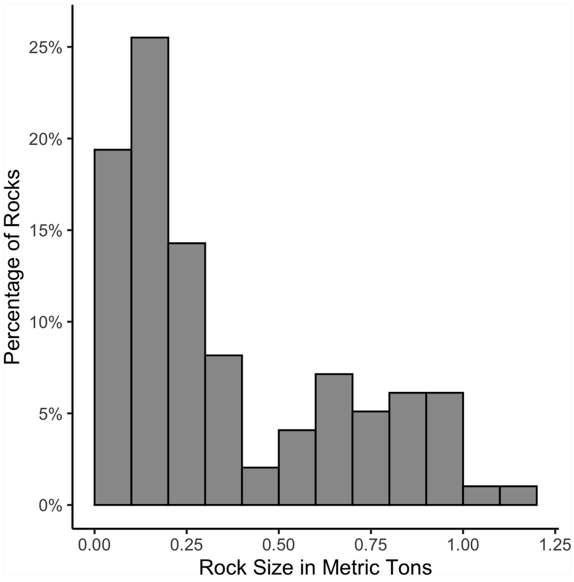

FIGURE 3
Results of rock gradation testing (n=98) from Empire Quarry.

TABLE 1 Start and end of construction dates for each Palos Verdes Reef module.

Block	Module	Start Date	Completed	Latitude (°)	Longitude (°)	Tonnage
2	A	8-May-2020	11-May-2020	33.72311	-118.34993	3,645.3
	B	11-May-2020	22-May-2020	33.72281	-118.34943	3,346.7
	C	12-May-2020	21-May-2020	33.72257	-118.34875	2,250.3
4	D	23-May-2020	28-May-2020	33.72198	-118.34686	2,919.2
	B	23-May-2020	29-May-2020	33.72157	-118.34644	2,585.0
	C	29-May-2020	30-May-2020	33.72111	-118.34639	3,121.0
5	A	1-Jun-2020	2-Jun-2020	33.72158	-118.34547	2,666.0
	B	2-Jun-2020	3-Jun-2020	33.72100	-118.34506	2,672.8
	C	3-Jun-2020	31-Aug-2020	33.72048	-118.34491	2,667.9
6	A	2-Sep-2020	10-Sep-2020	33.72102	-118.34353	2,860.5
	D	1-Sep-2020	2-Sep-2020	33.72050	-118.34356	2,447.9
	C	31-Aug-2020	1-Sep-2020	33.71998	-118.34353	3,298.3
7	A	5-Sep-2020	11-Sep-2020	33.72037	-118.34206	2,968.5
	B	11-Sep-2020	11-Sep-2020	33.71990	-118.34245	2,418.4
	C	11-Sep-2020	14-Sep-2020	33.71933	-118.34232	3,126.8
8	A	14-Sep-2020	16-Sep-2020	33.71901	-118.34015	3,246.3
	B	16-Sep-2020	18-Sep-2020	33.71855	-118.34062	3,037.3
	C	18-Sep-2020	22-Sep-2020	33.71808	-118.34046	3,450.4

Blocks 1 and 3 were not constructed as planned after identifying sensitive habitat within the proposed footprints. 'D' modules replaced initially planned modules to avoid sensitive habitat.

species-specific length-weight conversions from the literature (e.g., Williams et al., 2013). Density and biomass (separately) were then summed across all three portions (bottom, midwater, and canopy) of each transect. All densities were scaled to number or grams per 100 m^2, and benthic cover was calculated as a percentage.

Statistical analyses

All analyses were performed using R version 4.1.2 (R Core Team, 2021). One-way repeated measures ANOVAs were performed using the 'anova_test' function in the *rstatix* package to identify the extent and magnitude of changes in biotic cover, giant kelp density, fish density, and fish biomass between the pre-construction restoration reef footprints and post-construction reef modules. All data met the assumption of normality and Greenhouse-Geisser corrections were applied when within-subjects factors violated the assumption of sphericity. Differences between sampling events among individual years were identified using *post-hoc* Tukey tests. For visualization, means and 95% confidence intervals were calculated by performing bootstrapping (1,000 permutations) using the 'smean.cl.boot' function in the *Hmisc* package.

Results

Geophysical and oceanographic monitoring

We produced bathymetric shaded relief images of the restoration reef (Figure 1) and differential depth comparisons from annual bathymetric surveys. The addition of the reef was the most obvious change from 2019 to 2020, and from 2020 to 2021 we saw what appears to be slight settling at several modules resulting in a net loss in elevation, plus an increase in sub-canopy macroalgae that resulted in a net gain in elevation – specifically at the shallower modules (Figure 4). We saw no evidence of any large quarry rocks being dislodged from any module or large-scale scouring or buildup of sediment around the modules.

The dual temperature probes of the Spotter Buoy/Smart Mooring system provide insight into the frequency and degree of water column mixing and show that, though seasonally variable and highly influenced by storm activity, the thermocline appears to cross the reef modules at least once each day. Seafloor temperatures typically spike at or soon after low tides while surface temperatures often decrease slightly. Therefore, differences between the surface and bottom temperatures are typically highest during higher tides when the thermocline rises above the depth of the reef modules (Figure 5), though this

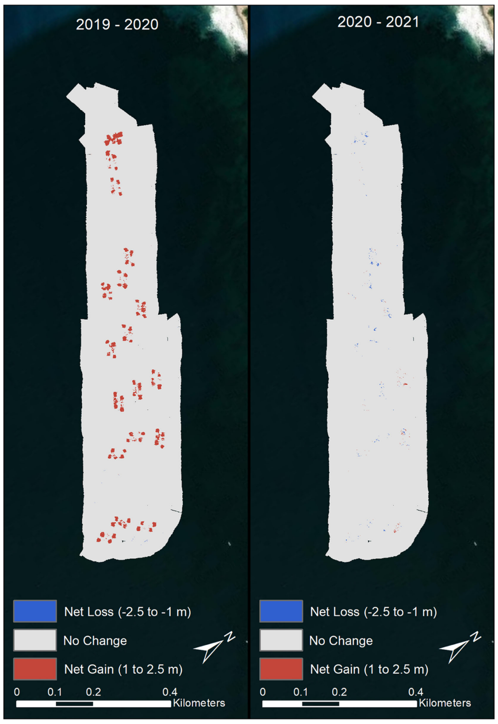

FIGURE 4
Year-to-year difference in bathymetry of the restoration area, including the 18 modules of Palos Verdes Reef. Blue and red indicate deeper and shallower seafloor, respectively, as compared to the previous year. Gray areas indicate a change of less than 1 m.

pattern is not absolute and degrades during winter months as sea surface temperatures drop.

Biological monitoring

Rocky-reef associated taxa recruited to the restoration site rapidly, with visible changes occurring within just a few months post-construction (Figure 6) and statistically significant changes all occurring in less than 18 months. The restoration reef benthos was initially colonized largely by hydroids, bryozoans (e.g. *Diaperoforma californica*), and brown turf algae, with kelp (both understory and canopy-forming), colonial tubeworms (e.g. *Salmacina tribranchiata*), and red turf algae succeeding the brown turf algae and filling in remaining bare rock spaces the following year. These are all common taxa in natural high-relief reefs in the region suggesting that benthic cover is quickly reaching a late-successional state. The new reef habitat was also quickly colonized by planktivores including Blacksmith (*Chromis punctipinnis*) and Señorita (*Oxyjulis californica*), followed the next year by several species of surfperches (Embiotocidae), Kelp Bass (*Paralabrax clathratus*), Barred Sand Bass (*P. nebulifer*), California Sheephead (*Bodianus pulcher*), Opaleye (*Girella nigricans*), and Halfmoon (*Medialuna californiensis*) – all common members of long-existing kelp forest communities.

Biotic benthic cover, giant kelp density, fish density, and fish biomass were all significantly higher post-construction than pre-construction (Table 2). In all cases, the 2019 and 2020 pre-construction surveys were not significantly different ($p \geq 0.999$; Figure 7). For all cases (Figures 7A, C, D) except giant kelp density

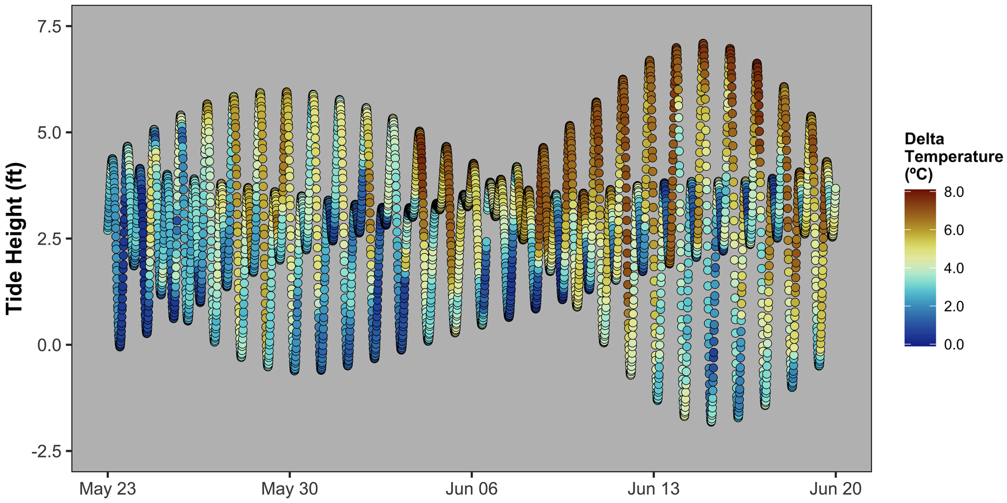

FIGURE 5
Tide height over an example lunar month (2022 May 23 – 2022 June 20), colored the difference between sea surface temperature and seafloor temperature.

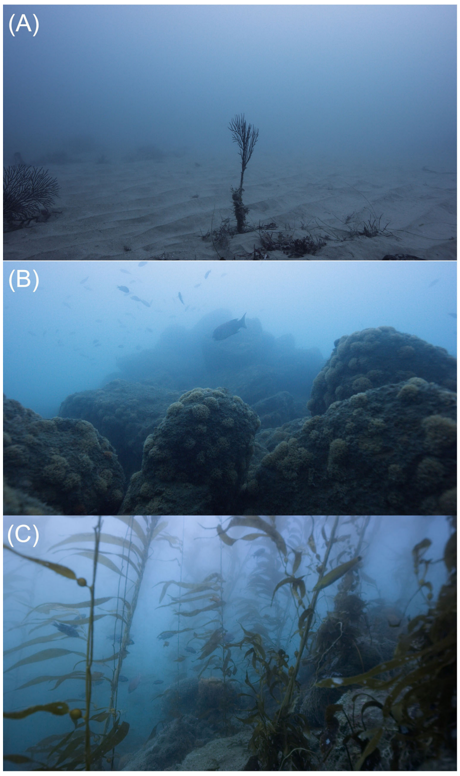

FIGURE 6
(A) A dead gorgonian attached to buried reef, **(B)** bryozoans covering Module 2A in February 2021 (eight months post-construction), and **(C)** giant kelp growing on Module 5A in November 2021 (18 months post-construction). Still images taken with permission from the short film "Rebirth of a Reef", by Shaun Wolfe of Shaun Wolfe Photography.

(Figure 7B), values from each post-construction survey were significantly higher than either pre-construction survey ($p < 0.001$), and values were not significantly different between post-construction surveys ($p = 0.125–0.187$). Giant kelp density in the 2021 post-construction survey was significantly higher than in each of the three previous surveys (including the 2020 post-construction survey; $p < 0.001$) which were not significantly different from each other ($p > 0.999$). Giant kelp was recorded on transect at 15 of the 18 reef modules by 2021. There is a general pattern of succession from nearshore to offshore and the kelp is already creating a thick canopy on some shallower modules (Figure 7B).

Discussion

This unique restoration effort – directly replacing lost rocky reef habitat *in situ* – presented many unusual challenges and limitations (e.g., avoiding existing functional reef, reef reburial, seafloor lease boundaries, cost), but also provided an opportunity to focus our efforts on a subtidal area with many dynamic features. The chosen location and depth of the restoration reef was partly defined by the location having been negatively affected by landslides and sedimentation. However, the area is also subject to positive physical forcing and many beneficial geologic and oceanographic factors that were accounted for in the reef placement and design. In fact, species distribution (Zellmer et al., 2019) and reef performance modeling (Pondella et al., 2019) had identified this area as a high potential location for many commercially, recreationally, and ecologically important species assuming reef habitat was properly designed.

This restoration reef not only provides more habitat for rocky-reef associated species but also provides higher quality habitat – highly rugose, steeply sloped, and heterogenous, versus the relatively flat, low relief nearby reef that is under continuous sedimentation pressure. PVR was built at a location directly adjacent (< 2 km) to a continental shelf break and in an upwelling zone with high primary production and frequent temperature fluctuations. The specific placement depth of the reef modules may prove particularly fortuitous, as water temperature data from the on-site Spotter Buoy appears to show internal tides inundating the modules with cool, nutrient rich water with some frequency – often twice a day at high tide.

TABLE 2 Mean values ± 95% CI for pooled pre- and post-construction metrics with repeated measures ANOVA results.

Metric	Pre-construction (n = 34) (mean ± 95% CI)	Post-construction (n = 36) (mean ± 95% CI)	df	F	*p*
biotic benthic cover (% cover)	19.0% ± 5.3%	50.7% ± 5.9%	3, 45	24.9	< 0.001
giant kelp density (No./100 m^2)	0.17 ± 0.14	21.0 ± 11.1	1, 15	14.1	0.002
fish density (No./100 m^2)	5.18 ± 2.90	94.7 ± 15.0	1.6, 24.6	32.1	< 0.001
fish biomass (kg/100 m^2)	0.84 ± 0.33	6.11 ± 0.79	2.2, 33.1	33.9	< 0.001

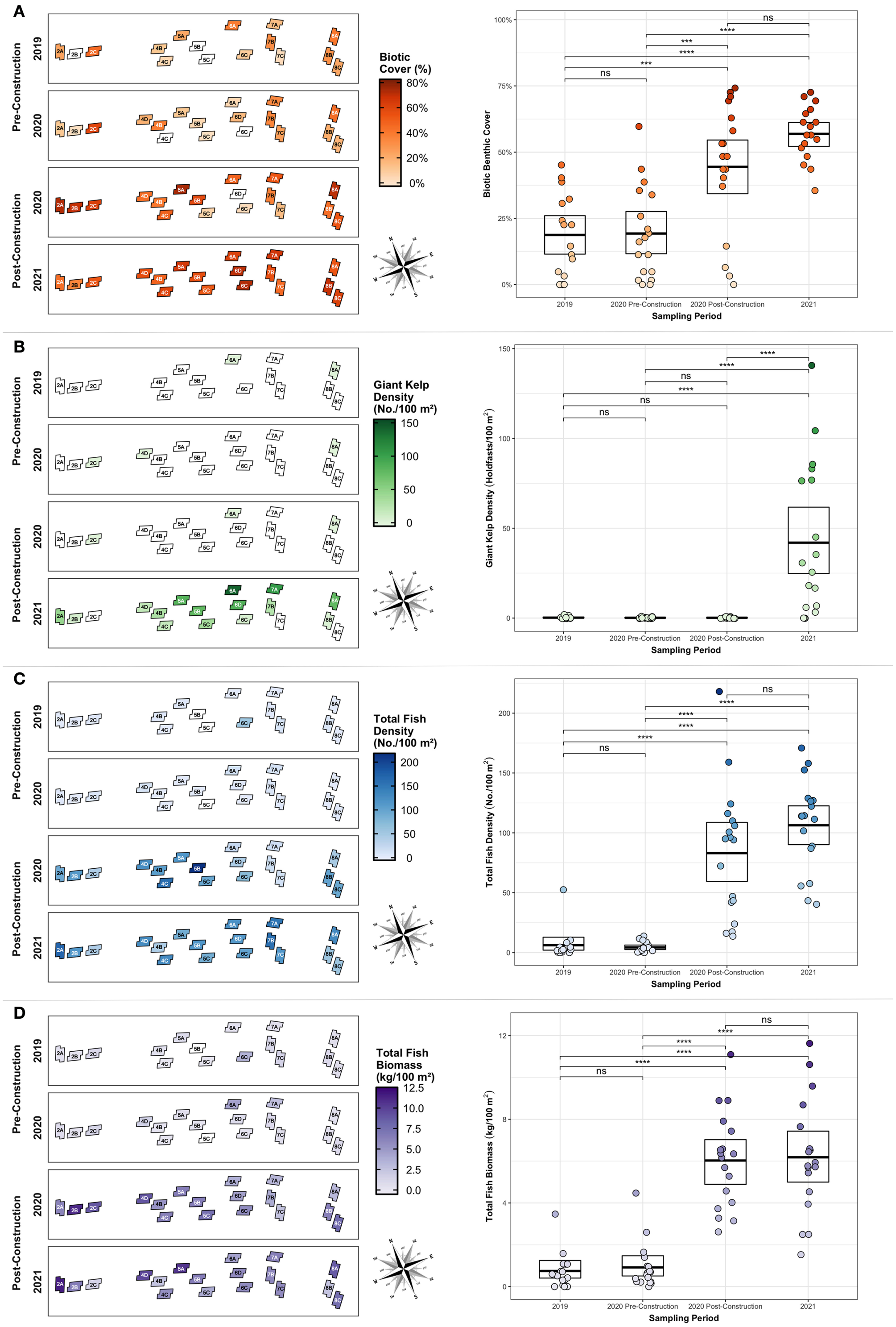

FIGURE 7
(A) Biotic cover, **(B)** giant kelp holdfast density, **(C)** total fish density, and **(D)** total fish biomass for each sampling period displayed geographically (left) and statistically (right). Notations above brackets indicates significance level between bracketed sampling periods; 'ns', non-significant ($p > 0.05$), *** = $p < 0.01$, **** = $p < 0.001$.

While the primary design criteria for PVR was fish production, the steep-slope design is also resilient to sedimentation and turbidity challenges on the peninsula. All reef aspects have a minimum of 1 m relief, placing them above the sediment scour zones documented in the area. Additionally, placing rock on existing but buried hard substrate provided a small maximum depth the modules can settle and subside into the sediment, avoiding a pitfall of past reefing efforts in the region (Ambrose and Anderson, 1990).

PVR modules showed rapid, significantly positive responses in fish density, fish biomass, kelp density, and biotic benthic cover following reef construction. It appears that this high relief feature, coupled with immediate proximity to the natural reefs that support giant kelp, created a substrate that was optimal for kelp recruitment and a unique opportunity to examine rapid succession as it attracted a wide array of taxa almost immediately. One common concern regarding artificial reefs is the potential for the new structure to simply attract individuals from other areas rather than produce new individuals and increase overall populations (Bohnsack, 1989). This prospect of attracting mobile organisms from other areas is particularly strong at PVR given the proximity of existing reefs. The present study does not address this concern, but we believe the higher quality habitat that is now available will result in an increase in secondary production for many initially-attracted taxa over the long-term, and the taxa utilizing the new habitat indicate that the restoration reef is already in the later stages of succession.

In addition to surveys of the restoration reef footprint and modules, we surveyed multiple restored, adjacent, and reference sites annually for several years prior to reef construction and continue to do so annually post-construction. Our surveys will ultimately utilize a progressive-change multiple before-after control-impact design (PCmBACI; Williams et al., 2021) to describe the pattern, extent, and magnitude of changes to communities. This type of analysis would suggest that positive changes in the restored and adjacent areas versus reference areas are a result of new secondary production rather than attraction from nearby reefs (Osenberg et al., 2002). With only two surveys performed post-construction thus far, these studies are in their infancy and most results cannot yet be reported with great statistical confidence. This large-scale, long-term biological study, coupled with annual sonar surveys and continuous oceanographic monitoring, will provide bountiful information about succession, usage, and response for numerous taxa, as well as sediment interaction with the restoration reef and more fine-scale assessments of our reef design.

Data availability statement

The raw data supporting the conclusions of this article will be made available by the authors, without undue reservation.

Ethics statement

Ethical review and approval was not required for the animal study because the study was observational only.

Author contributions

JW and DP developed the study approach. JW performed the analyses and wrote the manuscript. DP, CW, and ZS revised the manuscript. CW and ZS performed the sonar surveys and processed the sonar data. All authors performed the biological field surveys, contributed to the article, and approved the final manuscript.

Funding

California State Coastal Conservancy Grant Agreement # 19-019; NOAA Restoration Center Community-based Restoration Program Project Awards #2008-0073-010 and #2008-0073-046; National Fish and Wildlife Foundation Grant IDs #8006.13.040016 and # 3002.15.049578 under the Damage Assessment, Remediation, and Restoration Program (DARRP) Settlement Restoration Program Cooperative Agreement funded by National Oceanic and Atmospheric Administration Fund # NA12NMF4630196.

Acknowledgments

The authors would like to thank their partners in making this project a success, including the Montrose Settlements Restoration Program and its Trustees (National Oceanic and Atmospheric Administration, National Park Service, U.S. Fish and Wildlife Service, California Department of Fish and Wildlife, California State Lands Commission, California State Parks), The Bay Foundation, California State Coastal Conservancy, and the National Fish and Wildlife Foundation. We would specifically like to thank David Witting and Jennifer Boyce (NOAA) for their commitment to and support of this project for nearly two decades. We'd also like to thank those whose help was invaluable in field work, construction, and permitting: Tom Ford (The Bay Foundation); Justin Chin Wong, Steve Schryver, and Mike Ellis (Connolly-Pacific Co.); Cassidy Teufel, Kate Huckelbridge, Jonna Engel, John Dixon (California Coastal Commission); Bonnie Rogers, Lia Protopapadakis, Steve Estes (Department of the Army); Kelly Keen and Sarah Mongano (California State Lands Commission); Valerie Carrillo Zara, Celine Gallon, Melissa Lane, Serena Stumpf, Hope Sexton, L.B. Nye (Los Angeles Regional Water Quality Control Board); Chris Kroll (California State Coastal Conservancy); Carrie Wolfe, Sam Soule, Mark Loos, Darrell Montague, Sam Corder Lee, Adriana Stowell (Southern California Marine Institute); Bill Power (Los Angeles County Sanitation Districts); Matt Robart, Erin Jaco, Jeremy Claisse (Vantuna Research Group). This manuscript greatly benefitted from the help of three reviewers.

Conflict of interest

The authors declare that the research was conducted in the absence of any commercial or financial relationships that could be construed as a potential conflict of interest.

Publisher's note

References

Ambrose, R. F., and Anderson, T. W. (1990). Influence of an artificial reef on the surrounding infaunal community. *Mar. Biol.* 107, 41–52. doi: 10.1007/bf01313240

Bohnsack, J. A. (1989). Are high densities of fishes at artificial reefs the result of habitat limitation or behavioral preference? *Bull. Mar. Sci.* 44 (2), 631–645.

Claisse, J. T., Pondella, D. J.II, Love, M., Zahn, L. A., Williams, C. M., Williams, J. P., et al. (2014). Oil platforms off California are among the most productive marine fish habitats globally. *Proc. Natl. Acad. Sci. United States America* 111 (43), 15462–15467. doi: 10.1073/pnas.1411477111

Graham, M. H. (2004). Effects of local deforestation on the diversity and structure of southern California giant kelp forest food webs. *Ecosystems* 7 (4), 341–357. doi: 10.1007/s10021-003-0246-6

Ilieva, I., Jouvet, L., Seidelin, L., Best, B. D., Aldabet, S., da Silva, R., et al. (2019). A global database of intentionally deployed wrecks to serve as artificial reefs. *Data Brief* 23, 103584. doi: 10.1016/j.dib.2018.12.023

Kayen, R. E., Lee, H. J., and Hein, J. R. (2002). Influence of the Portuguese Bend landslide on the character of the effluent-affected sediment deposit, Palos Verdes Margin, southern California. *Continental Shelf Res.* 22, 911–922. doi: 10.1016/s-0278-4343(01)00111-x

Lewis, R. D., and McKee, K. K. (1989). A guide to the artificial reefs of southern California. (Sacramento, California: California Department of Fish and Game).

Osenberg, C. W., St. Mary, C. M., Wilson, J. A., and Lindberg, W. J. (2002). A quantitative framework to evaluate the attraction-production controversy. *ICES J. Mar. Sci.* 598, S214–S221. doi: 10.1006/jsmc.2002.1222

Pondella, D. J. II (2009). Science based regulation: California's marine protected areas. *Urban Coast.* 1, 33–36.

Pondella, D. J. II, Allen, L. G., Craig, M. T., and Gintert, B. (2006). Evaluation of eelgrass mitigation and fishery enhancement structures in San Diego Bay, California. *Bull. Mar. Sci.* 78 (1), 115–131.

Pondella, D. J. II, Piacenza, S. E., Claisse, J. T., Williams, C. M., Williams, J. P., Zellmer, A. J., et al. (2019). Assessing drivers of rocky reef fish biomass density from the Southern California Bight. *Mar. Ecol. Prog. Ser.* 628, 125–140. doi: 10.3354/meps13103

Pondella, D. J.II, Williams, J. P., Claisse, J. T., Schaffner, R., Ritter, K., and Schiff, K. (2015). The physical and biological characteristics of nearshore rocky reefs in the Southern California Bight. *Bull. South. California Acad. Sci.* 114 (3), 105–122. doi: 10.3160/soca-114-03-105-122.1

Pondella, D. J.II, Williams, J. P., Williams, C. M., Claisse, J. T., and Witting, D. (2018). "Restoring a nearshore rocky reef ecosystem in the challenge of an urban setting," in *Marine Artificial Reef Research and Development: Integrating fisheries management objectives*, vol. 86 . Ed. S. A. Bortone (Bethesda, MD: American Fisheries Society, Symposium), 165–186.

R Core Team (2021). "A language and environment for statistical computing." (Vienna, Austria: R Foundation for Statistical Computing).

Reed, D. C., Schroeder, S. C., and Huang, D. (2006). An experimental investigation of the use of artificial reefs to mitigate the loss of giant kelp forest habitat. a case study of the San Onofre Nuclear Generating Station's artificial reef project. *California SeaGrant Univ. California San Diego (T-058).*

Stephens, J. S., Morris, P. A., Pondella, D. J. II, Koonce, T. A., and Jordan, G. A. (1994). Overview of the dynamics of an urban artificial reef fish assemblage at King Harbor, California, USA 1974-1991 - a recruitment driven system. *Bull. Mar. Sci.* 55 (2-3), 1224–1239.

Williams, C. M., Williams, J. P., Claisse, J. T., Pondella, D. J.II, Domeier, M. L., and Zahn, L. A. (2013). Morphometric relationships of marine fishes common to central California and the Southern California Bight. Bulletin of the Southern California Academy of Sciences. 112(3), 217–227. doi: 10.3160/0038-3872-112.3.217

Williams, J. P., Claisse, J. T., Pondella, D. J., Williams, C. M., Robart, M. J., Scholz, Z., et al. (2021). Sea Urchin mass mortality rapidly restores kelp forest communities. *Mar. Ecol. Prog. Ser.* 664, 117–131. doi: 10.3354/meps13680

Zahn, L. A., Claisse, J. T., Williams, J. P., Williams, C. M., and Pondella, D. J.II (2016). The biogeography and community structure of kelp forest macroinvertebrates. *Mar. Ecol.* 37, 770–785. doi: 10.1111/maec.12346

Zellmer, A. J., Claisse, J. T., Williams, C. M., Schwab, S., and Pondella, D. J.II (2019). Predicting optimal sites for ecosystem restoration using stacked-species distribution modeling. *Front. Mar. Sci.* 6. doi: 10.3389/fmars.2019.00003

Frontiers in Marine Science

TYPE Original Research
PUBLISHED 30 September 2022
DOI 10.3389/fmars.2022.954974

EDITED BY
Daniel Joseph Pondella,
Occidental College, United States

REVIEWED BY
Edward Mager,
University of North Texas,
United States
Allen Mensinger,
University of Minnesota Duluth,
United States

*CORRESPONDENCE
Kelly S. Boyle
ksboyle@uno.edu

†PRESENT ADDRESSES
Kelly S. Boyle,
Department of Biological Sciences,
University of New Orleans, New
Orleans, LA, United States
T. Reid Nelson,
Potomac Environmental Research and
Education Center, Department of
Environmental Science and Policy,
George Mason University, Fairfax, VA,
United States

SPECIALTY SECTION
This article was submitted to
Marine Ecosystem Ecology,
a section of the journal
Frontiers in Marine Science

RECEIVED 27 May 2022
ACCEPTED 07 September 2022
PUBLISHED 30 September 2022

CITATION
Boyle KS, Hightower CL, Nelson TR
and Powers SP (2022) Diel, temporal,
and spatial patterns of biotic
soundscapes among Alabama artificial
reefs in late spring and summer.
Front. Mar. Sci. 9:954974.
doi: 10.3389/fmars.2022.954974

Diel, temporal, and spatial patterns of biotic soundscapes among Alabama artificial reefs in late spring and summer

Kelly S. Boyle[1,2*†], Crystal L. Hightower[1,2], T. Reid Nelson[1,2†] and Sean P. Powers[1,2]

[1]School of Marine and Environmental Sciences, University of South Alabama, Mobile, AL, United States, [2]Dauphin Island Sea Lab, Dauphin Island, AL, United States

Passive acoustic monitoring (PAM) in a variety of marine habitats has revealed distinct spatial and temporal variation of fish sounds that are predicted to vary in association with species composition and abundance, as well as diel and seasonal influences. Reefs in the Alabama Artificial Reef Zone (AARZ) in the northern Gulf of Mexico (nGOM) have an associated fish fauna composed of warm-temperate and tropical reef associated species. AARZ reefs are made of different structures (e.g. bridge rubble, concrete pyramids, etc.) and as a result, their fish species composition is predicted to vary. We used PAM to describe fish sounds on 18 shallow slope (20-33 m) AARZ reefs in 2017 and 2018. We detected calls from unknown sources, as well as sounds from leopard toadfish *Opsanus pardus*, cocoa damselfish *Stegastes variabilis*, and cusk-eels (Ophidiidae). We developed semi-automated screening methods to detect specific sound types and described diel and spatial patterns. Sound detection rates varied widely among reefs, but not by reef type. Number of sound types increased with species richness, but detection rates of specific sounds differed on reefs with similar species composition. Our results indicate that many frequently occurring sounds may not be associated with visually conspicuous fishes. Further research is needed to determine source species and associated behavior for common sounds in these habitats. Soundscape variability among nGOM artificial reefs may be a consideration for management, as biological sound can provide an acoustic cue for reef location by some larval and adult fish species.

KEYWORDS

passive acoustic monitoring (PAM), reef fish, northern Gulf of Mexico, artificial reefs, fish sounds

Introduction

Many teleost fish produce sounds for communication (Amorim, 2006; Fine and Parmentier, 2015). Such sounds are often associated with specific behaviors like courtship, spawning, parental care, and territoriality (Myrberg, 1981; Ladich, 2004). In addition, fish sounds that are emitted frequently for some species are hypothesized to be contact calls (i.e., a group cohesion cue that facilitates the maintenance of schools and shoals) (Radford et al., 2015), and detection of such sounds may provide an indication of the presence of such fish in a specific area. Fish sounds contribute to the overall soundscape in many habitats and because sounds are distinctive among species, they may be associated with specific behaviors and activities (Tricas and Boyle, 2014; Mueller et al., 2020; Tricas and Boyle, 2021). As a result, soundscape recordings have the potential to reveal patterns associated with fish species presence and abundance, and to indicate the potential behavior (e.g., spawning, nesting) of some species (Luczkovich et al., 1999; Fine and Thorson, 2008).

Fish and Mowbray (1970) described and documented sounds from many western Atlantic fish species. This effort greatly increased the awareness of the importance of sound to many marine fishes. The amount of data available from this effort for some fish species is not extensive and sometimes limited to sounds elicited from manual or electrical stimulation, yet these first observations indicate the potential for the role of sound in communication for a variety of species. Sound production for some fish species is known only from certain behavioral contexts (Boyle and Tricas, 2011; Tricas and Boyle, 2014). Thus, there may be many additional vocal fish species for which sound production has yet to be observed. Passive acoustic monitoring [PAM] has the potential to reveal new sound types and to show when and where different sounds occur in the field.

PAM has been used in a variety of north American marine temperate habitats to test for temporal and spatial variation of biological sound (Wall et al., 2012; Wall et al., 2013; Van Hoeck et al., 2020; Butler et al., 2021). Recently, PAM was used to document soundscapes in the eastern Gulf of Mexico (Wall et al., 2012; Wall et al., 2013). Soundscapes of temperate natural and artificial reef communities were also recently described on two natural and two artificial reefs in North Carolina (Van Hoeck et al., 2020). These studies revealed a variety of distinctive sound types that varied temporally and spatially and were attributed to fishes but in some cases from unknown source species.

The Alabama Artificial Reef Zone is a large (>2600 km^2) area of permitted and pre-permitted artificial reefs off coastal Alabama (Powers et al., 2018). Many artificial reefs in this system form relatively small reef structures: concrete and steel pyramids, re-purposed poultry transport cages ('chicken coops'), bridge rubble, and sunken M1 U.S. Army tanks (Minton and Heath, 1998; Jaxion-Harm and Szedlmayer, 2015). These relatively small hard-structure habitats are separated by larger expanses of soft-bottom habitat and each may have a limited resident fish fauna. Thus, these artificial reefs present an opportunity to examine soundscape characteristics associated with different reefs and their fish assemblages.

Overall, the purpose of our current study was to lay the foundation for future utility of passive acoustic monitoring of artificial reefs in the northern Gulf of Mexico to document changes in fish abundance, species composition, and behavior. Therefore, the goals of our study were to (1) describe the major types of observed biological sounds on shallow slope 20-33 m artificial reefs off coastal Alabama, (2) test for temporal patterns of sound occurrence over diel cycles, (3) test for associations of sound types with observed species, (4) test for an association between observed fish species diversity and diversity of sounds, and (5) to determine if soundscapes differed among artificial reefs and reef types. To achieve these goals, we developed and tested semi-automated sound detection methods to locate sounds in large acoustic datasets.

Materials and methods

Recorder deployments

PAM devices used in this study were three 'SNAP recorders' (Loggerhead Instruments, www.loggerhead.com, Sarasota, FL). Recordings were sampled at 44.1 kHz and stored as.wav format files. In 2017 (31 May – 16 August), the SNAP recorders were programmed for continuous recording stored as separated five-minute duration.wav files, which allowed for up to eight-day continuous recordings: a total of 2252.75 hours from 51 days. In 2018 (25 June – 6 August), the SNAP recorders were programmed for a duty cycle of 60 s recordings every five minutes. This duty cycle allowed for up to 40 days of recording. Scuba divers deployed recorders, which were placed on reefs by means of a ratchet strap and cable ties tied to the reef or immediately adjacent to the reef on a sand screw (<3 m away). The hydrophone end of the recorder was oriented opposite of the sea floor. Sites in 2017 included two bridge reefs (Br1, recorded 30 May – 07 June and Br2 from 10-17 July), two chicken coops (Cp2 from 10-18 July and Cp3 from 18-26 June), seven pyramid modules (Py3 from 08-13 August, Py4 from 01-05 August, Py5 from 01-08 August, Py6 from 10-16 July, Py7 from 18-26 June, Py8 from 18-23 June, and Py9 from 30 May to 07 June), and three M1 army tank reefs (Tk1 from 30 May to 07 June, Tk2 from 18-22 July, and Tk3 from 8 -16 August) (Figure 1). In 2018, we recorded from one chicken coop (Cp1 from 16-22 July), two pyramid modules (Py1 from 25 – 30 June and Py2 from 25 June to 06 August), and one M1 army tank (Tk4 from 25 June to 06 August) (Figure 1).

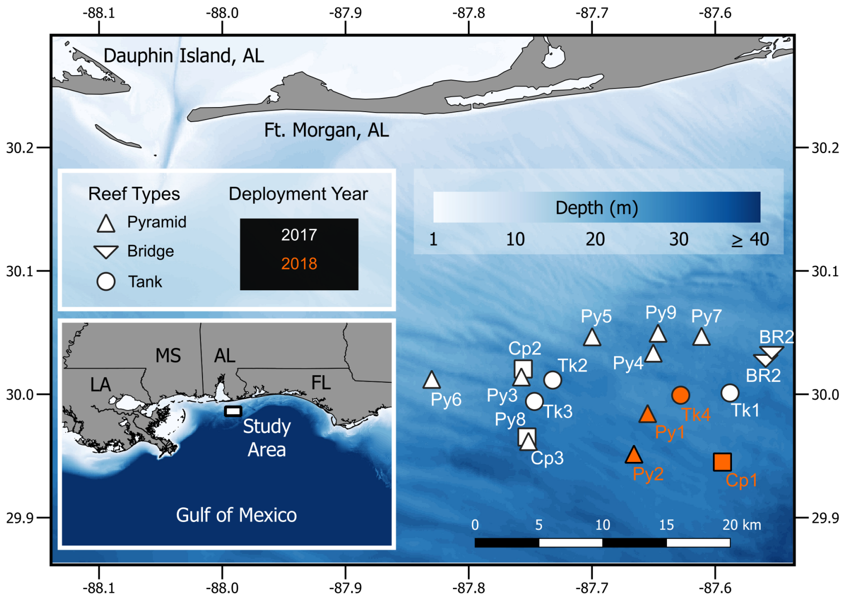

FIGURE 1
Alabama artificial reef sites where passive acoustic monitoring devices were deployed in 2017 (white) and 2018 (orange).

Reef fish composition

Video was taken during deployment and recovery dives using a GoPro Hero 3 camera. Video included the attachment or detachment of the recorder, a swim around the reef structure and examination of enclosed spaces. Video durations ranged from 4.5 to 17.4 minutes (10.1 ± 3.5 mean ± SD). All recovery dives took place within 59 days of the last recording. Fish species were identified from video frames and the local abundance of each species was estimated by taking the maximum number of individuals (MAXNO) of a species visible within a single video frame (Ellis and Demartini, 1995; Reeves et al., 2018). This conservative approach was chosen so that fish would not be repeatedly counted. For each reef, MAXNO values were averaged between the deployment and recovery dive for all identifiable species. Dense schools of small forage fishes, possibly round scad, *Decapterus punctatus*, were estimated to the nearest 100 individuals. For each reef, an average relative abundance was taken by averaging the MAXNO values from deployment and recovery videos at each reef. On some deployments, divers removed invasive red lionfish during deployments and recoveries. On the occasions when lionfish were removed during deployment dives, we estimated lionfish relative abundance from recovery dive videos only because lionfish observed in deployment videos may have been subsequently speared. On recovery dives when lionfish were speared, it was possible to count all speared lionfish observed on video and these numbers were used instead of the MAXNO value.

Similarity in species composition among reefs was assessed using Bray-Curtis (dis)similarity of presence-absence values using the package 'vegan' (Oksanen et al., 2020) in R (R Core Team, 2021). Species predicted to be transient near artificial reefs were not included in this analysis of species composition (Table 1). Two-dimensional non-metric multidimensional scaling (nMDS) plots were used to assess the pattern of reef fish composition similarity among reefs. In addition, we calculated species richness of reef fishes for each reef, excluding species assumed to be transient as described above.

Description of fish sounds

Raw sound data from reefs were examined aurally and with spectrograms in Adobe Audition v. 3.0. Sound types were examined qualitatively and described based on the waveform of sounds, train like features for sounds that had repeating pulses or other elements, and the spectral qualities of sounds. Several sound types have been described from previous research, including leopard toadfish calls (Wall et al., 2012; Wall et al., 2013), harmonic sounds ('365 Hz Harmonic' sound of Wall et al., 2012; Wall et al., 2013), and cusk-eel sounds (Mann et al., 1997; Kever et al., 2015; Mooney et al., 2016).

Semi-automatic detection of sounds

We attempted to use semi-automated screening methods to detect sound types that we characterized from raw data. For each sound type, we first tried to use a time domain cross correlation

(TDXC) technique. For each attempted sound type screening, a single representative pulse from train like sounds that have silent interpulse intervals, or a representative single sound from non-train like sounds was used as a template. Silence (0.25 s duration) was added before and after the sound template and a custom Matlab routine was used to screen through the directory of raw sound data from each artificial reef. Each raw sound data file (5 min files in 2017, 1 min files in 2018) was divided into segments of the length of the sound template and the maximum cross correlation of each segment with the sound template was calculated using the XCORR function. Values were scaled relative to the autocorrelation value of the template (between

TABLE 1 Sound types and detection method, number of detections, normalized detections, correlation level used, false positive rate, repeat detections, repeat detection rate, and performance relative to similar detection methods.

Sound Types and template or method used	Total detections (raw)	*Detections (normalized for effort)	Corr. level used	% False positive	No.repeat detect-ions removed	% Repeat detect-ions	% Time other similar templates out performed
Pop-like sounds							
P1	1520	1941.7	90%	0%	0	0%	
P2	4075	5130.9	80%	0%	0	0%	P4: 5.12% P1: 4.90% P3: 0.02%
P3	1456	1818.2	80%	3%	0	0%	P1: 4.58% P2: 0.26%
P4	418	485.4	90%	0%	0	0%	P1: 1.83% P2: 0.26%
Chirp-like sound							
CL	8	8.2	37%	68%	0	0%	
Grunt-like sound							
G1	44	96.0	30%	21%	0	0%	G2: 2.17% G5: 2.17%
G2	124	157.6	45%	34%	0	0%	
G3	22	22.0	50%	4%	0	0%	
G4	67	90.9	32%	43%	0	0%	
G5	61	93.5	32%	20%	0	0%	G2: 8.70% G4: 2.90%
Low f sounds, non-stereotyped							
LF1	194	496.9	35%	8%*	0	0%	LF2: 0.51%
LF2	128	280.7	65%	2%*	0	0%	
LF3	452	863.0	65%	1%*	0	0%	LF2: 3.62%
LF4	142	384.5	70%	0%*	0	0%	
Low frequency pulse sound							
LFP	132	189.3	86%	5%	0	0%	
Thud sounds custom thud script	1054	2504.1	custom routine	37% 35% - are knock trains	16	2%	
Knock train *via* thud script	561	1173.8	custom routine		179	24%	
Knock train custom knock train script	149	338.4	custom routine	38%	28	16%	
Harmonic sweep T_{HS}	83	116.5	36%	22% for all other sites 83% including Tk1	0	0%	
Leopard Toadfish	3187	4767.3	85% Pearson corr. of frequency domain	3%	1,699	35%	

*Detections are the number of sound events thought to most closely resemble the template sound. This number does not include false positives, repeat detections, or co-detections from other templates that had a higher correlation level.

-1 and 1). Sound phase was then ignored by taking the absolute value of the correlation. Thus, correlation values varied between 0 and 1, with 0 being the most dissimilar and 1 being an identical waveform (100% correlation) or identical inverted waveform. We qualitatively tested these techniques for different sounds by examining screening performance against sound files that were aurally screened to look for false positives and false negatives. We then chose a correlation threshold value for each screened sound with the goal of high reliability in avoiding false positives and to also detect a substantial number of sound events. Automatic detections were predicted to provide diel, temporal, and spatial patterns of sound production, even if they underestimate the absolute number of total sound events. Thus, absolute numbers of detections from this method are not directly comparable among sounds because of differences in the efficacy of the technique and the arbitrary choice of threshold values. However, objective comparisons of relative occurrence across diel cycles, days, and among reef locations within a sound type are possible because the same semi-automatic scanning technique was used within comparisons of the same sound type.

For most sound types scanned by TDXC, we aurally screened all putative hits in order to identify false positives. For several sound types, for which there were many putative detections we randomly subsampled screening of false positives. In cases when all putative detections were not aurally screened, we indicate the number of subsampled screens in the results. TDXC scanning was not effective for some sound types, and in these cases, we created custom alternative scanning routines that are detailed in the results.

For several kinds of sound types (pop sounds, grunt-like sounds, low frequency), we created multiple templates from different sounds and scanned them independently. This was done to capture more potential variation and because we were open to the possibility that these templates were similar, but from potentially different sources that would show differences in temporal and spatial abundance. Because the templates of these sounds were similar, it was not possible to identify potential co-detections with other similar templates from aural scanning (as is possible with other false positives). Thus, we identified all cases where different templates detected the same sound.

Before analyzing diel, temporal, and spatial patterns of detected sounds, we removed any detected false positives and only included sound events that were co-detected by multiple templates with the sound template type that had the highest TDXC threshold (i.e., detections were not double counted as multiple sound types). We report the rate of false positives (% of total putative detections or total subsampled putative detections that were aurally screened) and the rate of co-detections for all templates (% of all putative detections). For each sound type, we calculated the mean hourly detection rate among reefs over the diel cycle. In addition, we calculated the average daily sound detection rate for each reef and sound type. For mean hourly detection rate, estimated among reefs, we report the estimated standard error (SE) and for daily detection rates for each reef we report the standard deviation (SD). Sounds for figures were plotted from.wav files (sampling rate 4kHz) with oscillograms and spectrograms using the ‘spectro’ function in the ‘seewave’ package in R (Sueur, 2018; Sueur et al., 2018) with a Hanning window, length 128 samples, 75% overlap.

Associations of fish species presence and fish sounds

To qualitatively ascertain the co-occurrence of sound types with fish species, we calculated Pearson correlation values for presence/absence data of fish sounds on reefs and presence/ absence of fish species on reefs from video data. We then reported the fish species with the greatest correlation. To test for an overall association between daily fish sound emission similarity among reefs and reef similarity based on fish composition, we used a BIOENV procedure and Mantel test. To calculate fish sound similarity among reefs, we used the daily sound detection rate for each sound type. We used daily detections of knock trains calculated from the thud detection script and we used the average daily detection rate for similar sound types (see Results): pops (average of P1, P2, P3, P4), grunts (average of G1, G2, G3, G4, G5), and non-intentional low frequency sounds (average LF1, LF2, LF3, LF4).

We then conducted a BIOENV test to identify the fish sound(s) with the greatest association with reef similarity in fish species composition. Fish sound similarity among reefs was assessed using Euclidean distance and fish species composition was assessed with Bray-Curtis dissimilarity of presence/absence data and the BIOENV procedure assessed correlation using the Spearman method. We used a Mantel permutation procedure to determine if the association between the best subset of fish sounds among reefs and fish compositions was greater than would be expected by chance ($p < 0.05$). These procedures were conducted with the R package vegan (Oksanen et al., 2020).

Measuring the association of call diversity with fish species richness among artificial reefs

The diversity of call types (call richness) at each reef was estimated by counting the number of call types examined in the study at each reef. Pop-like sounds, detected with templates P1, P2, P3, and P4, were assumed to be the same type of call and were considered one call type. We tested for an association between call type diversity and fish species richness among reefs using Pearson correlation tests.

Reef noise and power spectral density over time

We examined spatial and temporal patterns of overall (root mean square sound pressure level [SPL_{RMS}]) and spectrum level noise values (dB re: $1\mu Pa/Hz^2$) at specific frequencies (200, 800, 1200, and 5000 Hz), which were chosen because they represent peaks of low frequency fish sound (200 Hz), pop sounds (800 Hz), cusk-eel chatter (1200 Hz), and evening biophonic tonal noise (5000 Hz). For each sound recording.wav file, we estimated SPL_{RMS} levels in ten second intervals using the 'rms' function in the 'seewave' package in R (Sueur, 2018; Sueur et al., 2018) and used the reported calibration of each snap recorder hydrophone and gain to calculate SPL_{RMS} dB re: $1\mu Pa$. We then calculated the average SPL over five minutes for the 2017 data or over one minute for 2018 (i.e., the average for the full.wav file). In addition, because intense, non-biophonic noise can occur for brief periods of time, we calculated the median and 95th percentiles of SPL_{RMS} noise levels for day and night-time hours for each reef and an average of these values among all reefs. We calculated spectrum level noise values in one-minute intervals by using the full.wav file for data from 2018 and dividing.wav files into one-minute intervals in 2017. We used the 'meanspec' function from the 'seewave' package (Sueur et al., 2018) and then extracted values for the specific frequencies described above.

Correlation of sound pressure level with fish species richness and boat presence

We tested for among-reef correlations between SPL_{RMS} (day and night, median and 95th percentiles) fish species richness. In addition, because vessels can contribute anthropogenic noise to the soundscape, we tested for correlations between idling boat detections, which were obtained from our study on fishing effort from vessel sounds using the same PAM recordings (Boyle et al., 2022), and SPL_{RMS} (day and night, median and 95th percentiles). We used Pearson correlation tests and the average daily boat detection rate for these analyses.

Results

Description and diel cycles of major sound types

Pop sounds

Several sound types were identified by aural screening and used to produce semi-automated scanning routines to compare diel, temporal, and spatial patterns. Pop-like sounds with a peak frequency between 500 and 1000 Hz occurred in series with irregular interpulse intervals (Figures 2A, B, S1). Four pop-like templates were used to scan for pops using TDXC (Table 1). These templates were made from four individual pops with a duration (mean ± SD) of 24 ± 6.8 ms and peak frequency of 681 + 87 Hz. This method was highly effective for finding pop events in raw recording data and because of the high number of putative detections, we randomly subsampled aural screening of putative detections: 65 aural screenings – P1, 70 – P2, 60 – P3, and 44 – P4. False positive rates for TDXC of pop like sounds at the chosen thresholds were low ¾ 3% (Table 1). Similarity in the pop like templates resulted in co-detection of some sounds between some templates of up to 5% of putative detections (Table 1).

Pop sounds were far more common in evening hours (Figures 2C , S1). For detections with all pop templates, there was a strong peak associated in most cases around 20h (Figures 2C, S1). There were also high levels of detections in early morning hours before sunrise, particularly for detections using P1 (Figure 2C), to a lesser degree for P2 and P3 (Figure S1C, F), but not for P4 (Figure S1I).

Chirp-like sounds

A chirp-like sound, similar to previous descriptions of damselfish chirps (Steinberg et al., 1965; Myrberg et al., 1993), with repeating pulse units, usually not separated by complete silence, was observed among artificial reef sound recordings (Figures 2D, E). This sound had a duration of 0.578 s, peak frequency of 645 Hz, and a pulse rate of 15.6 pulses s^{-1}. A template (CL) of this sound was created and used to screen reefs for similar sounds. Detection rates of this sound were modest and occurred in crepuscular, early-morning and late-afternoon hours, with the highest peak in the morning (Figure 2F).

Grunt-like sounds

Five templates of grunt-like sounds were created. These sounds were somewhat similar to the chirp-like sound described above, with repeating pulse units and little-to-no silence during the interpulse interval (Figures 2G, H, J, K, S2). These sounds ranged from 0.130-0.250 s duration (mean ± SD: 0.175 + 0.047), peak frequency from 270-539 Hz (mean ± SD: 270-539 Hz), and pulse rate from 32.0-43.0 pulses s^{-1} (mean ± SD: 36.1 ± 4.6 pulses s^{-1}). These templates varied in effectiveness and thus different threshold values for TDXC were used (Table 1). We aurally screened all putative detections except for template G2 at the Br1 site which had many putative detections and we screened a subsample (n=19, n=32 for all sites). Detection rates for these sounds were far more modest than for pop sounds and false positive rates were high for all grunt-like sound templates except G5 (Table 1). There was some co-detection of grunt-like sounds among templates, with G3 being the only grunt-like template that did not share co-detections with other templates (Table 1).

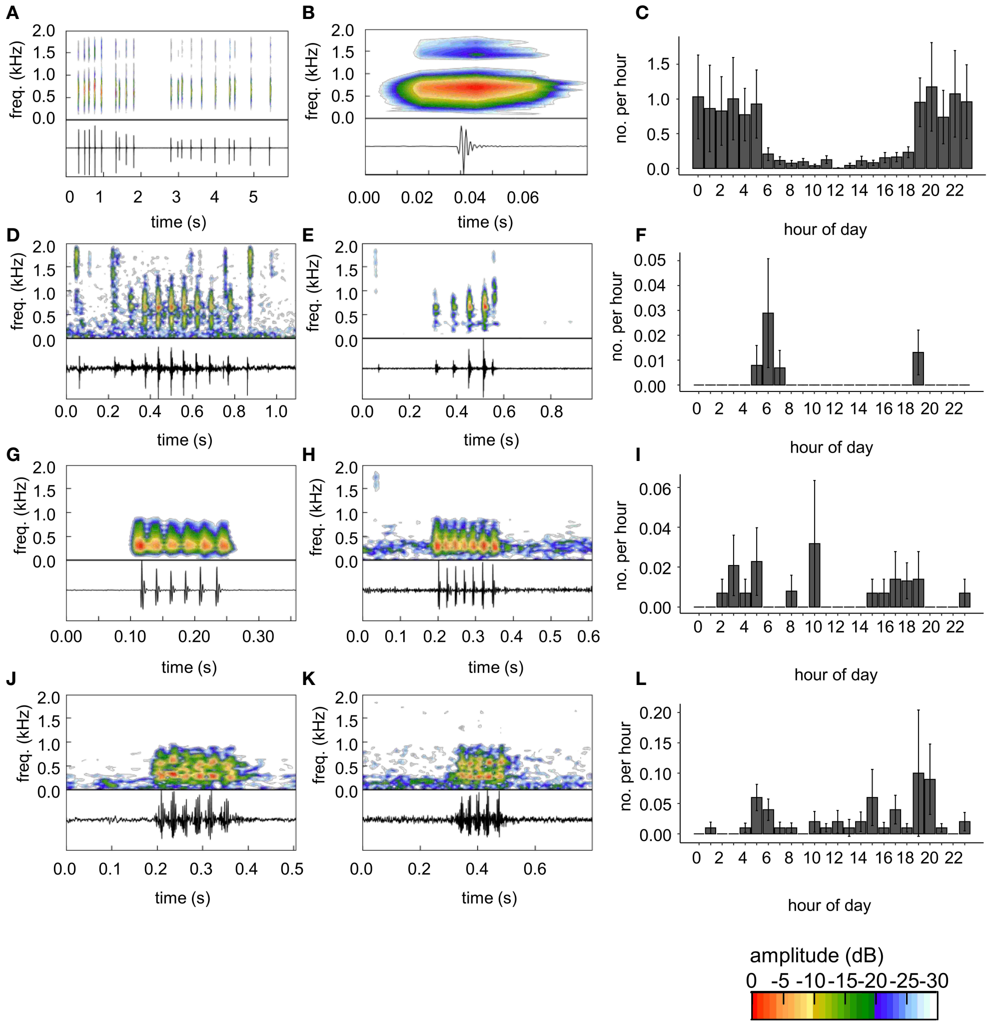

FIGURE 2
Sound types and diel cycles of sounds automatically detected. Oscillograms and spectrograms of sounds are shown for each sound. **(A)** Pop-sounds and **(B)** close-up view of a single pop, which was the first of the series shown in **(A)**. **(B)** The pop in **(B)** was used to create template P1 to automatically detect pop sounds. **(C)** Diel detection rate from template P1. **(D, E)** Damselfish chirp-like sounds **(F)** and diel detection rates chirp-like sounds detected by template CL. **(G)** Grunt-like sound used as template G3. **(H)** Grunt-like sound detected by template G3. **(I)** Diel detection rate of sounds using template G3. **(J)** Grunt-chirp like sound used as template G4. **(K)** Grunt-chirp like sound detected by template LFP. **(L)** Diel detection rate of sounds using template G4 as a template. Diel detection rates **(C, F, I, L)** are the mean ± SE hourly detection rate among all reefs (2017 and 2018) from each template. Note differences in time scales for sound figure panels. Color scale bar shows relative amplitude (dB) of frequencies depicted on the spectrogram.

Unlike what was observed for pop sounds, detections of grunt-like sounds varied over the diel cycle depending on the template (Figures 2I, L, S2C, F, I). Thus, it is possible these template sounds represent different kinds of sounds or at least tend to detect different kinds of sounds. Template G4 and G5 had similar times of peak activity to CL but showed additional activity mainly during diurnal hours (Figures 2L, S2I).

Low frequency sounds

Several occurrences of low frequency sounds were observed while aural screening raw data (Figures 3, S3). Templates were made from five low frequency sound events: LF1 (Figure 3A), LF2 (Figure S3A), LF3 (Figure S3D), LF4 (Figure 3D), and LFP (Figure 3G). Four of these low frequency sounds (LF1, LF2, LF3, and LF4) did not appear very stereotyped based on a lack of observed sounds with similar waveforms from aural screening of raw data (Figures 3, S3). These four non-stereotyped sounds ranged from 0.050 to 0.731 s duration (mean ± SD 0.2834 ± 0.304 s) and 121 to 168 Hz peak frequency (mean ± SD 142 + 21 Hz). TDXC screening with templates from these sounds found a wide array of low frequency sounds that varied in waveform shape and duration. Thus, we used these four templates to find generic low frequency sounds, which may be non-intentional sounds from fish. Correlation levels chosen were varied based on the number of putative detections (Table 1). LF1 had fewer putative detections and thus a lower threshold was used and all putative detections were aurally screened. For templates LF2, LF3, and LF4, even at a higher threshold, there were many putative detections and we thus subsampled aural screening: LF2 – 95 sounds screened, LF3 – 80 sounds screened, LF4 – 55 sounds screened. False positives (Table 1) for these generic low frequency sounds tended to be from boats and recognized fish sound types. The LF2 template detected some of the same sounds as the LF1 and LF3 templates, but at higher correlations (Table 1).

The low frequency pulse used to produce template LFP appeared stereotyped (Figures 3G, H). Some pulses detected by LFP had opposite polarity to the examples shown in Figures 3J, N, but all were characterized by a lower amplitude half cycle (negative in Figures 3G, H), immediately followed by a higher amplitude half cycle (positive in Figures 3G, H). The sound used to produce template LFP had a duration of 0.136 s and peak frequency of 74 Hz. At a chosen threshold of 86%, TDXC with template LFP showed a relatively low rate of false positives (Table 1).

Most non-stereotyped sounds occurred with similar frequency across all hours of the day, with a decrease at 8h (Figures 3C, S3C, F), decreasing the signal-noise ratio and potentially making detection more difficult. The non-stereotyped low frequency template LF4 tended to have the most detections at 22h (Figure 3F). The stereotyped low frequency pulse LFP had the highest levels of detections during diurnal hours (Figure 3I).

Thud sounds

Thud like sounds that occurred in trains (Figures 4A, B) were observed in aural screening of raw data. These sounds (Figures 4A, B) had a peak frequency (mean ± SD) of 162 ± 14 Hz and a pulse rate of 5.1 ± 1.4 pulses s^{-1}. Initial attempts to automatically detect these sounds using TDXC proved difficult because of many false positives and false negatives. One of the suspected challenges was the variable interpulse interval of this

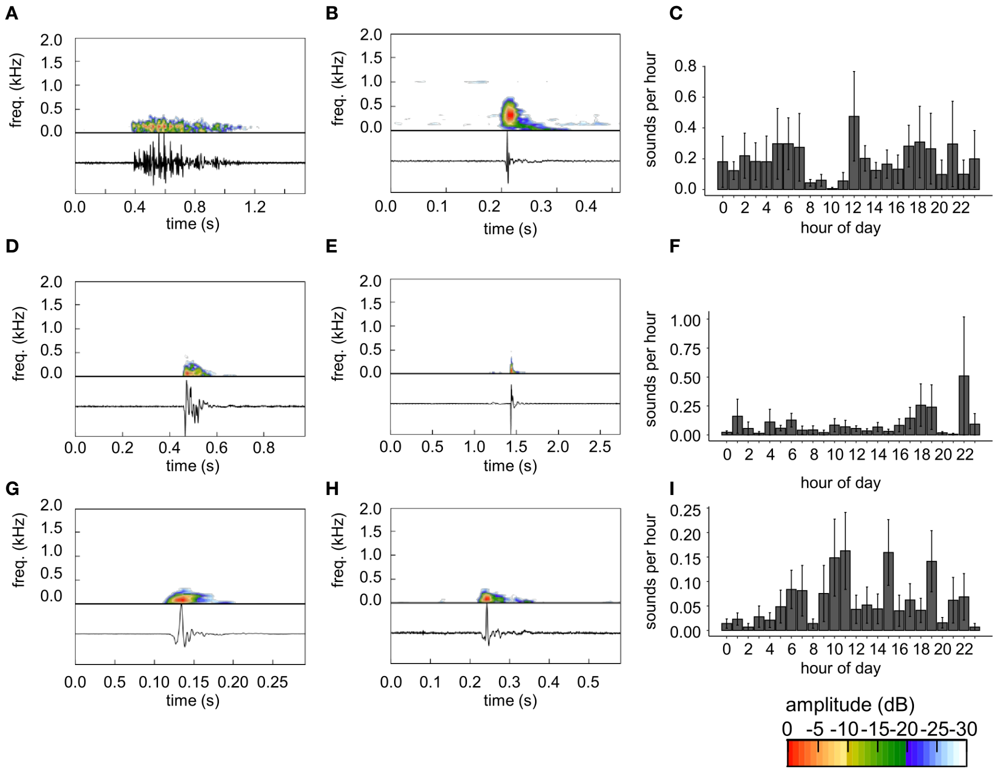

FIGURE 3
(A, B, D, E, G, H) Low frequency sounds and **(C, F, I)** diel detection rates of low frequency sounds. Oscillograms and spectrograms of sounds are shown in the panels in the left and middle columns. Low frequency sounds used as templates: **(A)** LF1, **(D)** LF4, **(G)** LFP. Low-frequency sounds detected by **(B)** LF1, **(E)** LF4, and **(H)** LFP. Note low frequency sounds in **(A)** and **(D)** do not appear to be a common stereotyped sound and **(B, E)** sounds with the highest detections are not similar sounds. In contrast, **(G)** template 27 detects similar, **(H)** stereotyped low frequency pulses. Diel detections (mean hourly detections ± SE) from **(C)** template LF1, **(F)** LF4, and **(I)** LFP. Diel detection rates **(C, F, I)** are the mean ± SE hourly detection rate among all reefs (2017 and 2018) from each template. Note differences in time scales for sound figure panels. Color scale bar shows relative amplitude (dB) of frequencies depicted on the spectrogram.

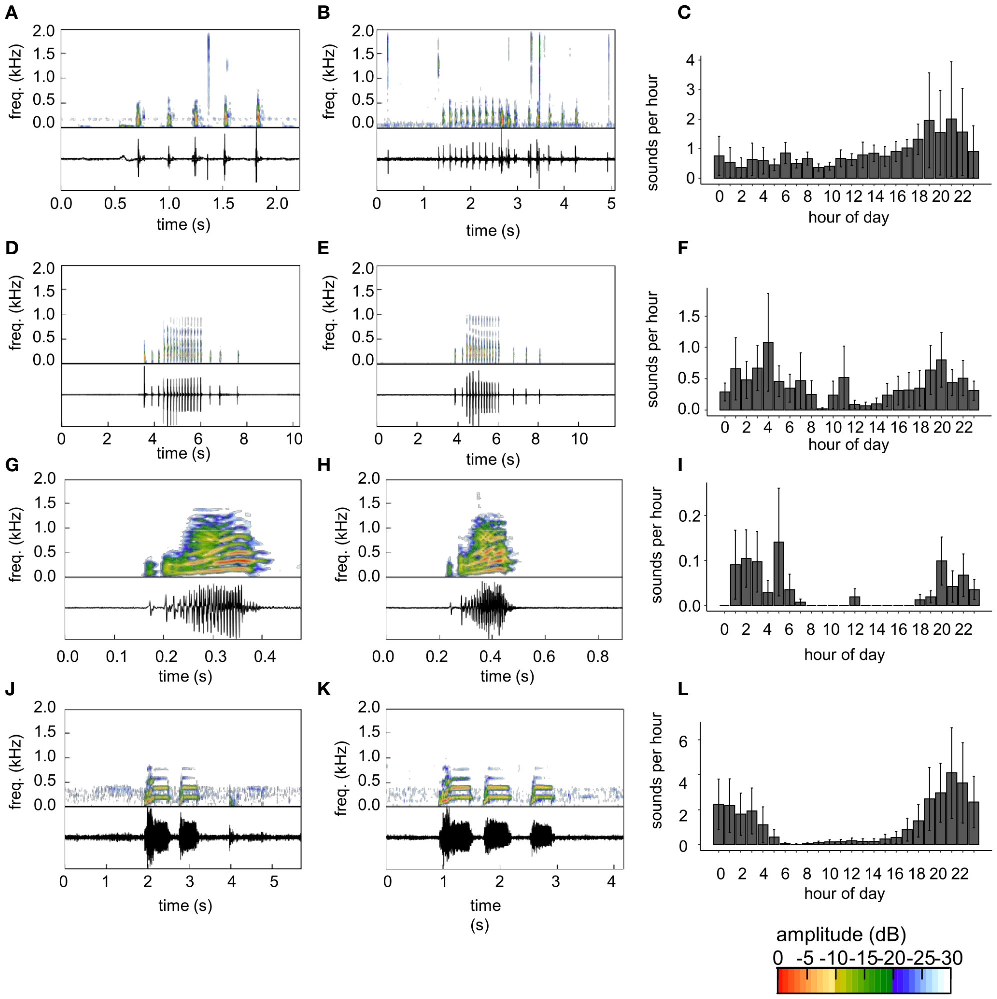

FIGURE 4

(A, B) Thud sounds, **(D, E)** knock train sounds, **(G, H)** harmonic sounds, **(J, K)** toadfish boatwhistles, and **(C, F, I, L)** diel detection of rates these sound types. Oscillograms and spectrograms of sounds are shown in the panels in the left and middle columns. A custom detection routine was used to detect thud sounds. The highest and second highest correlations with this routine are shown in **(A, B)**, respectively. **(D, E)** Knock-trains were also detected by the thud train routine. Harmonic sounds were detected with a template produced from the sound shown in **(G)** and an example detection is shown in **(H)** Toadfish boatwhistles were detected with a custom routine with a template in the frequency domain. Toadfish detections with the highest correlation are shown in **J** and **(K)** Diel detection rates **(C, F, I, L)** are the mean ± SE hourly detection rate among all reefs (2017 and 2018) from each template. Color scale bar shows relative amplitude (dB) of frequencies depicted on the spectrogram.

sound type. An initial template attempt with a single thud pulse detected many single sound events that were suspected to be of various different sound types and non-intentional sounds. Thus, we created a custom routine to detect these thud trains. The detection routine examined two seconds of raw data at a time and used a single thud with 40 ms of silence before and after as a template. The thud train from which the pulse template was created is shown in Figure 4A. The criteria for detection required six cases with a TDXC threshold of 50% within the two-second scanned portion. This routine detected many thud train sounds, but also had a high number of false positives (Table 1). Most of the false positives were detections of knock train sounds (described below). In addition, this method sometimes detected portions of the same sound train twice (Table 1). Thud sounds were detected at all hours of the day, but highest activity occurred from hour 19 to23 (Figure 4C).

Knock train sounds

Knock train sounds were observed that have a characteristic, stereotyped train of knock-like sounds in which some of the knocks, typically within the middle of a call, have a higher frequency component that extends from about 500-1000 Hz (Figures 4D, E, S4A, B, D, E). These sounds (Figures 4D, E) had an overall pulse rate (mean ± SD) of 4.3 ± 0.5 pulses s^{-1}, with a higher pulse rate of 7.5 ± 0.3 pulses s^{-1} during the higher frequency component in the center of the call. In these calls, lower frequency pulses had a peak frequency of 172 ± 5.5 pulses s^{-1}, while higher frequency pulses in the center of the call had a peak frequency of 240 ± 91 pulses s^{-1}. This higher frequency component, which occurs in rapid succession, distinguishes these knocks from thud train sounds (Figures 4D, E). Many knock train sounds were accidentally detected by the thud sound detection routine as false positives (Table 1). In addition, a large percentage of the accidental detections were of a different portion of the same knock train (double detections) (Table 1). We also attempted to screen for thud train sounds directly (on purpose) using TDXC with one or several knocks from a train. Initial attempts were ineffective because of high false negatives and false positives. Thus, we created a custom routine that scanned a one second sound portion using a single knock as a template with 40 ms of silence before and after the knock. The routine calculated TDXC values of the template within the one second screened portion and criteria for detection was a minimum of five correlations of 50% or more within that period. This custom routine was moderately effective at detecting knock trains, but also had a high false positive rate and moderate rate of double detections (Table 1). Surprisingly, the rate of knock-train detection was higher using the thud sound routine (as an accidental by-product) than it was for our knock train routine (Table 1). Eighty-two knock trains were detected by both methods. Both methods of semi-automated detection indicated increased knock train activity during nocturnal hours, with a pre-dawn peak at 4h, peaks near sunset (20h) and sustained activity throughout the evening (Figures 4F, S4C).

Harmonic sounds

Brief sounds with continuous oscillation, a harmonic structure, and slight frequency modulation were observed in aural screening of raw data. These sounds, which we termed harmonic sounds (Figures 4G, H) are similar to the '365 Hz Harmonic sound' of Wall et al. (2012, 2013). This sound (Figures 4G, H) had a duration of 0.205 s and peak frequency of 293 Hz. We screened for harmonic sounds with TDXC. All putative detections were screened aurally, except for Tk1, which had a high number of putative detections (n=368) that appeared to all be false positives with leopard toadfish boatwhistle sounds. Thus, we randomly screened a portion (n=138) of these sounds at Tk1, all of which were leopard toadfish calls and it was assumed that no harmonic sounds were detected at that site. False positives were modestly high among most sites, but appeared exceptionally high when Tk1 was included (Table 1). All Tk1 putative detections, based on subsampled aural screening, were assumed to be false positives from leopard toadfish and these high levels of false positives substantially increase the estimated false positive rate (Table 1). Harmonic sounds were detected mainly during evening and crepuscular hours with a peak at 5h (Figure 4I).

Leopard toadfish boatwhistles

Aural screening of raw data indicated many leopard toadfish boatwhistle sounds (Figures 4J, K). These sounds were very similar to descriptions in Wall et al. (2012, 2013) and the generation of a boatwhistle sound occurred once while a leopard toadfish was visually observed on a deployment dive at site (Tk 4). TDXC of the tonal boatwhistle sounds from leopard toadfish was not very effective because of false positives that were often associated with tonal sounds of running boats and false negatives. Thus, we produced a custom routine with trial and error to improve efficacy. We made a template file from the central portion of a single toadfish boatwhistle, which often occurred in threes; the portion after the beginning part of the boatwhistle which tends to increase and vary in amplitude and has frequency modulation. This tonal portion of the boatwhistle was 182 ms long, had a dominant frequency of 188 Hz, a higher intensity harmonic at 396 Hz and additional harmonics at 563, 750, 945, and 1130 Hz. No silent portion was used in construction of the template and the routine used the frequency domain to identify putative toadfish boatwhistles. The routine divided raw sound data into 182 ms intervals and calculated a power spectrum (1024 pt FFT, Hanning window) of the screened portion of the sound and the template boatwhistle. The similarity of the two power spectra were compared with a Pearson correlation and 85% correlation was used as a threshold. This method was highly effective, with over 3,000 detections, and large variation among sites and time periods when detections and putative detections occurred (Table 1). Thus, we aurally screened putative detections from all sites except Br1 and Tk1, which had very high numbers of putative detections. We randomly subsampled 560 putative detections at Br1 and 25 putative detections at Tk1. False positive rates from this screening routine were low (Table 1) and were mainly from boat noise. The leopard toadfish boatwhistle scanning routine was subject to a high rate of repeat detections of the same boatwhistle call series (Table 1). Because aural screening of putative detections of Br1 and Tk1 were subsampled, we automatically considered any putative detections occurring within three consecutive seconds to be repeat detections.Leopard toadfish boatwhistles were detected at all hours and showed a strongly nocturnal bias (Figure 4L). Leopard toadfish boatwhistle sounds peaked at 21h, began to drop off sharply at 4 and 5h and remained low until about 17h (Figure 4L).

Spatial patterns of sounds among reefs

Pop-like sounds

Daily detections of pop-like sounds varied greatly among reefs (Figures 5A, B, S5). The Br1 site, for example, had an average of over 100 detections for templates P1, P2, and P3,

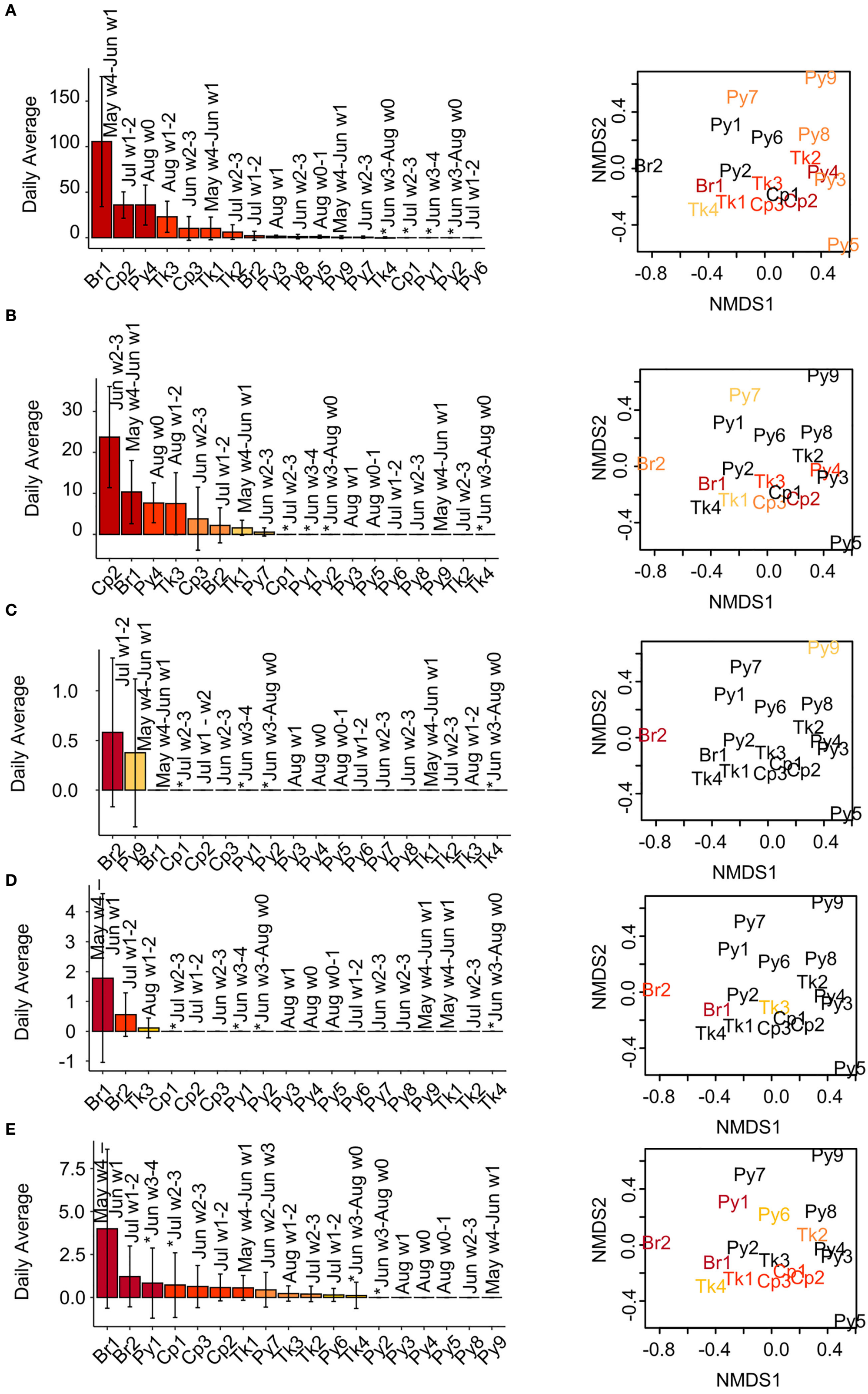

FIGURE 5 (Continued)

FIGURE 5 (Continued)
Daily call rates (average ± SD) among reefs and call rate associations with fish species abundance and composition. **(A, B)** Pop-like, **(C)** chirp, and **(D, E)** grunt sound call rates. Calls detected by templates **(A)** P1, **(B)** P4, **(C)** CL, **(D)** G3, and **(E)** G4. Month and week number (1-4) of the month the reef is sampled are indicated above the bars. Reefs sampled in 2018 are indicated on the month of sampling with an asterisk. nMDS plots of (dis)similarity of fish species presence/absence among reefs based are shown right (stress = 0.166), with reef abbreviations in colors indicating reefs in which this sound type was detected. Plots are repeated for each row (sound type) with colors assigned for that sound type. Colored bars and text from dark red to yellow indicate the relative call rates among reefs with > 0 calls, from high to low. Dark red = call rates in 100-75th percentile, red-orange = call rates from 50-74.9th percentile, orange = call rates from 25-49.9th percentile, yellow = call rates from 0-24.9th percentile, black = no calls detected on that reef.

while some sites had no detections (Figures 5A, B, S5). Pop-like sounds were detected on all reef types and showed high abundance on Br1, Cp1, and Tk1 (Figures 5A, B, S5). A distinct association between fish composition and abundance at reefs and pop-like sound detection was not apparent. Several sites, Br1, Tk1, Tk3, and Cp2, showed similar fish species composition and had high average pop-like sound detections for multiple templates (Figures 5A, B, S5). However, the Cp1 coop reef was very similar to these reefs in terms of fish species composition but had no pop sound detections (Figures 5A, B and S5). Notably, Cp1 recordings were from 2018 when very few pop-like sounds were detected. Also, most but not all reefs with high detections in 2017 were recorded from late May to early July, while most reefs recorded in late July and August had lower pop sound rates.

Chirp-like sounds

Chirp-like sounds detected by template CL were observed on only two reefs, Br2 and Py9 (Figure 5C). This sound type appears similar to previously described damselfish chirps (Steinberg et al., 1965; Myrberg et al., 1993), occurred within diurnal hours as would be predicted from damselfish sounds (Steinberg et al., 1965), and was detected on reefs where cocoa damselfish were observed (Table 2) near the PAM recorder. Notably, however, though damselfish are the suspected sound source, their contribution to the composition and abundance of fishes observed from video at these two sites is low, and the sites are relatively divergent in terms of overall fish composition (Figure 5C nMDS plots) despite sharing these sound types.

Grunt-like sounds

Daily detections of grunt-like sounds (templates G1, G2, G3, G4, and G5) (Figures 5D, E, S6) varied by template, with some template sources detected on more reefs. For all these sound types, however, the Br1 site had the most detections. For these five sounds, some of the associated reefs show evidence of similarity in fish abundance and composition, as evidenced by clustering of some reefs with detections on the nMDS plots, but also detections on some dissimilar reefs (Figures 5D, E, S6).

Low frequency sounds

Non-stereotyped low frequency sound events were detected on most reefs (Figures 6A, B, S7). These non-stereotyped low frequency sounds were never detected on Cp1 reef and only some templates were detected on Py2, Py3, Py8, and Cp3 (Figures 6A, B, S7). These low frequency sound events were associated with reefs with disparate patterns of fish composition (Figures 6A, B, S7). Stereotyped low-frequency pulses from LFP were detected on 11 different reefs, but were most common among reefs with similar species composition (Figure 6C).

Thud train sounds

Thud train sounds were detected on all reefs (Figure 7A). Reefs with the highest average daily detections tended to have similar patterns of fish abundance (Figure 7C, left nMDS plot) and presence/absence (Figure 7C, right nMDS plot).

Knock train sounds

Knock train sounds were not detected on all reefs (Figure 7B and S8). Both knock train detection methods detected similar relative occurrences among reefs, though accidental detections from the thud train detection routine localized a greater absolute number of events (as described previously). Knock-trains were detected on all tank and bridge reefs sampled, but just one coop (Cp2) and one pyramid (Py3). Knock-train detection occurred on reefs with variability in (dis)similarity of fish abundance patterns (Figure 7B, S8: left nMDS panels). Reefs with knock trains, however, were similar in terms of presence/absence, moderate to low scores on nMDS axis 2 (Figures 7B, S8: right nMDS panels). However, some reefs with similar fish composition lacked knock-train detections: Cp1, Cp3, Py2, and Py4 (Figures 7B, S8).

Harmonic sounds

Harmonic sounds were detected on all reef types, but only on seven reefs (Figure 7C). Reefs where harmonic sounds were detected were not very similar in terms of fish abundance or presence/absence (Figure 7C).

Leopard toadfish boatwhistles

Leopard toadfish boatwhistle sounds were detected on all reef types and eight reefs (Figure 7D). Detection rates among reefs were quite variable, with far more detections on Br1 (Figure 7D). In addition, there were relatively high detections on Tk1 and Tk4 (Figure 7D). Some of the detections on recordings from other reefs appeared to be much lower amplitude, and perhaps

TABLE 2 Fish abundance on reefs (MAXNO, maximum number of fish observed in a single video frame, ranked from highest estimated relative abundance 1, to lowest), fish species richness, fish species diversity, fish sound call richness, and fish sound call diversity.

	Rank of each species abundance relative to other reefs																	
Species	**Py1**	**Py2**	**Py3**	**Py4**	**Py5**	**Py6**	**Py7**	**Py8**	**Py9**	**Br1**	**Br2**	**Tk1**	**Tk2**	**Tk3**	**Tk4**	**Cp1**	**Cp2**	**Cp3**
forage fish[1]			100	5		50	100	500							50			
red snapper	8.5	13	5.5	8	15.5	21	12	29.5	3.5	15.5		9.5	16	14	6.5	9.5	24	22
tomtate			20	0.5	13.5	6.5		0.5		2.5	24.5	36.5	22	7.5	0.5	10.5	3.5	69
lionfish	7	1		11	3	1.5	7	3	3	3.5	3	4	1	1	6	5	0.5	5
gray triggerfish	2	2	4	0.5		3	2	2	3	2.5	1.5	6.5	1.5	3.5	12.5	3.5	2	1
greater amberjack	3	4.5				2				3		1		1.5	5	3.5	0.5	4.5
Atlantic spadefish		7				3		0.5		1	9							
regal damselfish											2				15	1.5		
whitespotted soapfish	2	1	0.5				4.5			1	0.5	3.5	1		1	2		0.5
cubbyu		0.5	0.5	2	1.5					1		1		1	1	2.5	2	2.5
gray snapper	1	1.5				2.5	0.5			0.5	0.5	1		0.5	2.5			1
blue runner															3			6
blue angelfish		0.5								3	2	1			2			
cocoa damselfish									2	0.5	1	1.5			2			
sheepshead						0.5	1			2				0.5	0.5			
spotfin butterflyfish										2	0.5	1.5						
bank sea bass					1.5													2
rainbow runner*															3.5			
reef sharks*									1	1.5		0.5						
almaco jack										0.5	2							
french angelfish							1				1							
vermillion snapper												1			1			
jackknife fish											1.5							
gag grouper	0.5																0.5	
goliath grouper							0.5								0.5			
goldface toby	1																	
leopard sea robin															1			
scamp												1						
slippery dick											1							
nurse shark*			1															
blackbar drum										0.5								
highhat									0.5									
leopard toadfish															0.5			
rock sea bass					0.5													
king and Spanish mackerels*									0.5									
spotted scorpionfish						0.5												
SPECIES RICHNESS	8	9	6	6	6	10	9	6	5	15	14	13	5	8	18	8	7	10
CALL RICHNESS	6	7	4	8	7	9	9	6	9	14	15	10	11	14	13	4	11	9

*Species assumed to be transient that were not used in the nMDS analysis of relative abundance among reefs or included in species richness estimates. [1]Forage fish, like round scad were not possible to count directly and were estimated to the nearest 50 individuals. Br, bridge rubble reefs; Cp, chicken coop reefs; Py, pyramid module reefs; Tk, M1 Army tank reefs.
Scientific names of fish species are given in Table 3.

were detections of reefs from a great distance. Detections of leopard toadfish boatwhistle sounds were higher early in the summer (May and June) (Figure 7D). Leopard toadfish boatwhistles were detected on reefs that varied in terms of fish species abundance and composition (Figure 7D). This observation demonstrates that this common sound, which averaged over 300 occurrences per day on Br1, comes from a source that was rarely observed (only one time at Tk4, Table 2)

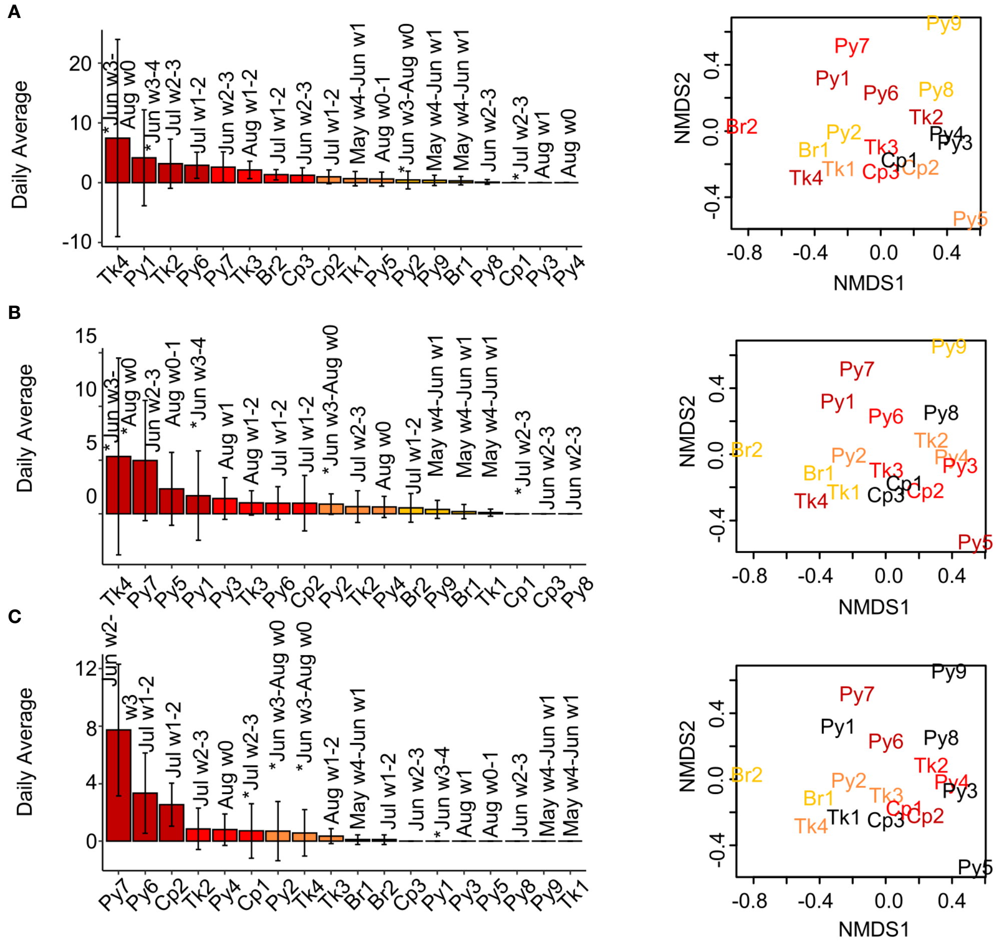

FIGURE 6
Daily low-frequency sound rates (average ± SD) among reefs and sound rate associations with fish species abundance and composition. Sounds detected by templates **(A)** LF1, **(B)** LF4, and **(C)** LFP. Month and week number (1-4) of the month the reef is sampled are indicated above the bars. Reefs sampled in 2018 are indicated on the month of sampling with an asterisk. nMDS plots of (dis)similarity of fish species presence/ absence among reefs based are shown right (stress = 0.166), with reef abbreviations in colors indicating reefs in which this sound type was detected. Plots are repeated for each row (sound type) with colors assigned for that sound type. Colored bars and text from dark red to yellow indicate the relative call rates among reefs with > 0 calls, from high to low. Dark red = call rates in 100-75th percentile, red-orange = call rates from 50-74.9th percentile, orange = call rates from 25-49.9th percentile, yellow = call rates from 0-24.9th percentile, black = no calls detected on that reef.

and thus does not directly contribute to patterns of fish composition and abundance (unless there are associations of leopard toadfish presence with other fish species that are not cryptic). The single leopard toadfish video observation in this study was accompanied by a typical boatwhistle which confirmed the source sound type hypothesized by Wall et al. (2012, 2013).

Fish associated with reefs

Thirty-six fish species were observed among reefs over the course of the study (Table 3). The top ten most abundant species (most-to-least) based on MaxNO relative abundance estimates were forage fishes (like round scad), red snapper, tomtate, lionfish, gray triggerfish, greater amberjack, Atlantic spadefish, regal damselfish, whitespotted soapfish, and cubbyu (Table 3). The relative abundance and occurrence of species, however, was variable among reefs (Table 2). The top nine most frequently observed fish species based on presence absence were red snapper, lionfish, gray triggerfish, tomtate, whitespotted soapfish, cubbyu, greater amberjack, gray snapper, and forage fish. After those species, Atlantic spadefish, blue angelfish, cocoa damselfish, and sheepshead were all observed with equal frequency.

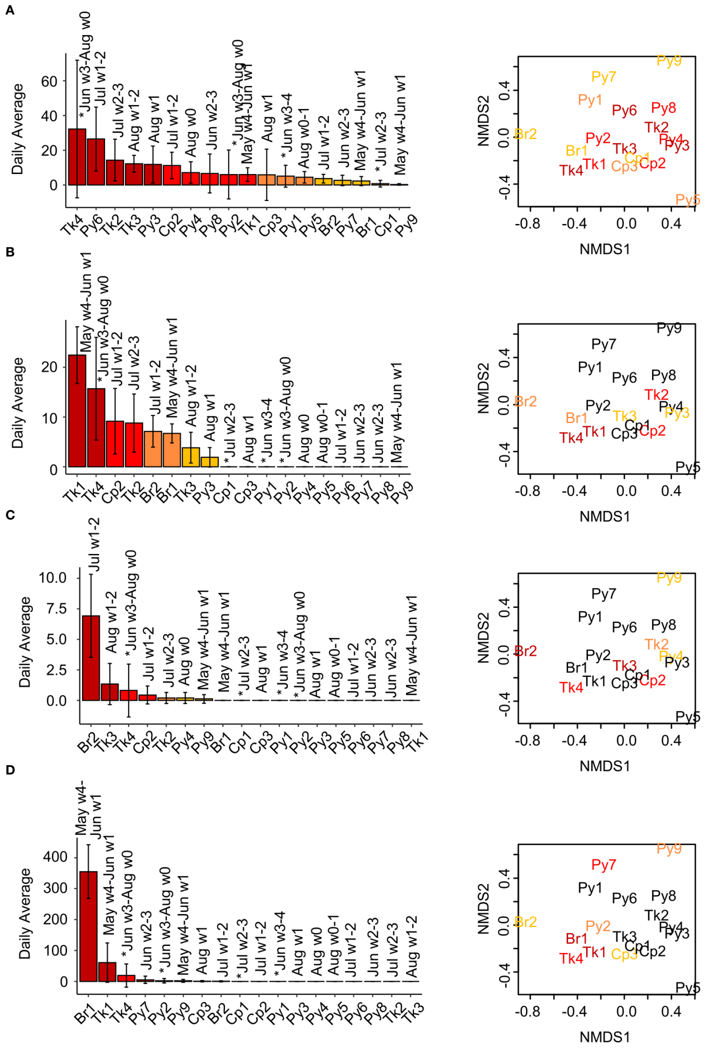

FIGURE 7
Daily call rates (average ± SD) among reefs and call rate associations with fish species abundance and composition. **(A)** Thud sound, **(B)** knock-train sound, **(C)** Harmonic sound, and **(D)** leopard toadfish boatwhistle call rates. **(B)** Daily averages of knock-trains come from accidental detections using a custom routine intended to detect thud sounds. Month and week number (1-4) of the month the reef is sampled are indicated above the bars. Reefs sampled in 2018 are indicated on the month of sampling with an asterisk. nMDS plots of (dis)similarity of fish species presence/absence among reefs based are shown right (stress = 0.166), with reef abbreviations in colors indicating reefs in which this sound type was detected. Plots are repeated for each row (sound type) with colors assigned for that sound type. Colored bars and text from dark red to yellow indicate the relative call rates among reefs with > 0 calls, from high to low. Dark red = call rates in 100-75th percentile, red-orange = call rates from 50-74.9th percentile, orange = call rates from 25-49.9th percentile, yellow = call rates from 0-24.9th percentile, black = no calls detected on that reef.

Association of fish species presence with sound detection rates

Correlations between sound detection rates among reefs and species presence do not appear to indicate the source of sounds (Table 4). For example, for some sound types in which multiple templates were used for detections (pop-like sounds, grunt-like sounds), templates differed in which species had the highest correlation with detections (Table 4). For known sound types, chirp-like damselfish sounds and leopard toadfish boatwhistles, detections were correlated with other species (Table 4). Thus, caution is needed when considering fish species presence from video for generating sound source species hypotheses. Such an association in this case is either from chance or because blue angelfish and cocoa damselfish were often observed on structurally complex artificial reefs that also had leopard

TABLE 3 Fish species estimated relative abundance (MAXNO, maximum number of fish observed in a single video frame) among artificial reef sites.

Common name	Scientific name	Previous descriptions of sound production and context	Total MAXNO	
			Ave	SE
forage fish[†]	*Decapterus punctatus*, etc.		44.7	27.9
red snapper	*Lutjanus campechanus*		13.0	1.8
Tomtate	*Haemulon aurolineatum*	grunts MS[1], knocks ES[5], grunts MS[9]	12.1	4.2
Lionfish	*Pterois* sp.	repetitive pulse calls SPO[1], hums S[1]	3.6	0.7
gray triggerfish	*Balistes capriscus*	grunt, scrape, toothy grunts MS[5], CF[5], S[5], thumps ES[5]	2.9	0.7
greater amberjack	*Seriola dumerili*	Knocks, Thuds F[5]	1.6	0.4
Atlantic spadefish	*Chaetodipterus faber*	drumbeats & grunts CF[5], tooth scrape MS[5], thumps & knocks ES[5]	1.2	0.6
regal damselfish	*Neopomacentrus cyanomos*		1.0	0.8
whitespotted soapfish	*Rypticus maculatus*	congeners produce knocks ES[5]	1.0	0.3
Cubbyu	*Pareques umbrosus*		0.9	0.2
gray snapper	*Lutjanus griseus*	thumps, knocks, growls, MS[5] & ES[5] in larvae: knocks, growls S[11]	0.6	0.2
blue runner	*Caranx crysos*	thump ES[1], grunt MS[5]	0.5	0.4
blue angelfish	*Holacanthus bermudensis*	thump ES[1], grunt MS[5]	0.5	0.2
cocoa damselfish	*Stegastes variabilis*	in a congener: chirps T[12], CF[10]	0.4	0.2
Sheepshead	*Archosargus probatocephalus*	feeding crunch sounds[5]	0.3	0.1
spotfin butterflyfish	*Chaetodon ocellatus*	thumps, knocks ES[5]	0.2	0.1
bank sea bass	*Centropristis ocyurus*	in congener: weak grunts MS[5] & ES[5], knocks ES[5]	0.2	0.1
rainbow runner*	*Elagatis bipinnulata*	grunts ESC[5]	0.2	0.2
reef sharks	*Carcharhinus* sp.*		0.2	0.1
almaco jack	*Seriola rivoliana*		0.1	0.1
French angelfish	*Pomacanthus paru*	thump,knock ES[5]	0.1	0.1
vermillion snapper	*Rhomboplites aurorubens*	thump,knock ES[5]	0.1	0.1
jackknife fish	*Equeus lanceolatus*		0.1	0.1
gag grouper	*Mycteroperca microlepis*	thumps, MS[5]	0.1	0.0
goliath grouper	*Epinephelus itajara*	booms, burst, MS[5], S[5], booms SPA[7,8]	0.1	0.0
goldface toby	*Canthigaster jamestyleri*		0.1	0.1
leopard sea robin	*Prionotus scitulus*	sonic muscles described in this species[4], in congeners: Bursts, Barks SPO[5], calls - S, SPO[3]	0.1	0.1
Scamp	*Mycteroperca phenax*	in congener: thumps, MS[5]	0.1	0.1
slippery dick	*Halichoeres bivittatus*	burst-like pulses S[12], stridulatory – F[12] knocks, thumps ES[5]	0.1	0.1
nurse shark*	*Ginglymostoma cirratum*		0.1	0.1
blackbar drum	*Pareques iwamotoi*	thumps, knocks MS[5], ES[5], scratches MS[5]	<0.1	0.0
Highhat	*Pareques acuminatus*	thumps, knocks MS & ES scratches MS[5]	<0.1	0.0
leopard toadfish	*Opsanus pardus*	boatwhistle[13,14], in congener boatwhistle SPA[6]	<0.1	0.0
rock sea bass	*Centropristis philadelphica*	in congener: weak grunts MS[5] & ES[5], knocks ES[5]	<0.1	0.0
king and Spanish mackerels	*Scomberomorus* sp.*		<0.1	0.0
spotted scorpionfish	*Scorpaena plumieri*	grunt, growl –reported as questionable, AI[5] in congener: Kwa sound T[2]	<0.1	0.0

*Species assumed to be transient that were not used in the nMDS analysis of fish species presence/absence among reefs. [†]Forage fish, like round scad (*Decapterus punctatus*) were not possible to directly count, so estimates are given.

Abbreviations of context or mechanism of eliciting sound from previous studies: AI, agonistic interaction; CF, sounds elicited in response to fish in a container; ES, electrical stimulation; ESC, escape sounds; F, Feeding;

MS, manual stimulation; S, startled; SPA, spawning and reproduction; SPO, spontaneous; T, territoriality.

References: [1]Beattie et al. (2017), [2]Bolgan et al. (2019), [3]Connaughton (2004), [4]Evans (1973), [5]Fish and Mowbray (1970), [6]Gray and Winn (1961), [7]Malinowski et al. (2019), [8]Mann et al. (2009), [9]Millot et al. (2021), [10]Myrberg et al. (1993), [11]Staaterman et al. (2014), [12]Steinberg et al. (1965), [13]Wall et al. (2012), [14]Wall et al. (2013)

TABLE 4 Associations between sound types among reefs and species presence (Pearson correlation).

Sound types and template	Species with the highest Pearson correlation	Correlation – level
Pop-like Sounds		
P1	tomtate	35%
P2	lionfish	45%
P3	spotfin butterflyfish	32%
P4	spotfin butterflyfish	50%
Chirp-like Sound		
CL	jackknife fish, highhat, and slippery dick	all 69%
Grunt-like Sound		
G1	tomtate	60%
G2	blackbar drum	54%
G3	almaco jack	79%
G4	gray snapper and greater amberjack	both 55%
G5	gray snapper and greater amberjack	both 44%
Low f sounds, non-stereotyped		
LF1	leopard sea robin and leopard toadfish	both 76%
LF2	lionfish	54%
LF3	lionfish	69%
LF4	blue angelfish, cocoa damselfish, and sheepshead	all 28%
Low frequency pulse sound		
LFP	sheepshead	49%
Thud Sounds	correlation tests not possible because sounds were present on all reefs	
Knock Train	spotfin butterflyfish	50%
Harmonic Sweep	leopard sea robin, leopard toadfish, highhat, jackknife fish, and slippery dick	all 30%
Leopard Toadfish Boatwhistle	blue angelfish and cocoa damselfish	both 69%

Correlations between species presence and sound occurrence do not reliably predict source. Pop-like sounds correlate with presence of three different species depending on the template. Chirp-like sounds from damselfish correlate equally with three non-damselfish species. Low frequency, non-stereotyped sounds correlate with many different species. The harmonic sound correlates equally with many different species. Leopard toadfish boatwhistle sound occurrence correlate equally with two non-toadfish species.

toadfish. Low-frequency, non-stereotyped sound templates had highest associations with six different species (Table 4), but because the templates produced from sounds that showed low repeatability, they were not expected to be associated with a single source species. Because thud train sounds were present on all reefs, correlation analysis between the presence/absence data of sounds and fish was not possible. The highest number of thud trains was observed at Tk4, which had a high number of gray triggerfish observed. The site with the second highest gray triggerfish observed, Tk1, however, did not have exceptionally high numbers of thuds and thus it is not clear that this is an obvious candidate for this sound type.

Overall association of fish sound emission similarity and fish species composition a0mong reefs

The BIOENV procedure indicated that non-stereotyped, low-frequency sounds were the sound type most associated with fish composition among reefs (Mantel correlation r = 0.233, permutation test P = 0.035).

Association of call diversity with fish species diversity among artificial reefs

Among reefs, fish species richness and call type richness (Table 2) were positively correlated (r = 0.59, t = 2.93, df = 16, p = 0.010). Shannon-Wiener indices of species and call diversity among reefs, however, did not correlate greater than would be expected by chance (r = 0.25, t = 1.05, df = 16, p = 0.312).

Longer-term patterns of sound production in 2018

Longer-term deployments of recorders at two reefs in 2018 provided the opportunity to examine temporal changes in call occurrence for several calls at two sites (Figure 8). These observations indicate variation in temporal patterns of call detection at sites. Over the 43-day period, leopard toadfish calls varied considerably, with detections at Tk4 peaking in early July, then ceasing until late July when they were detected sporadically on one day and then in a three-day

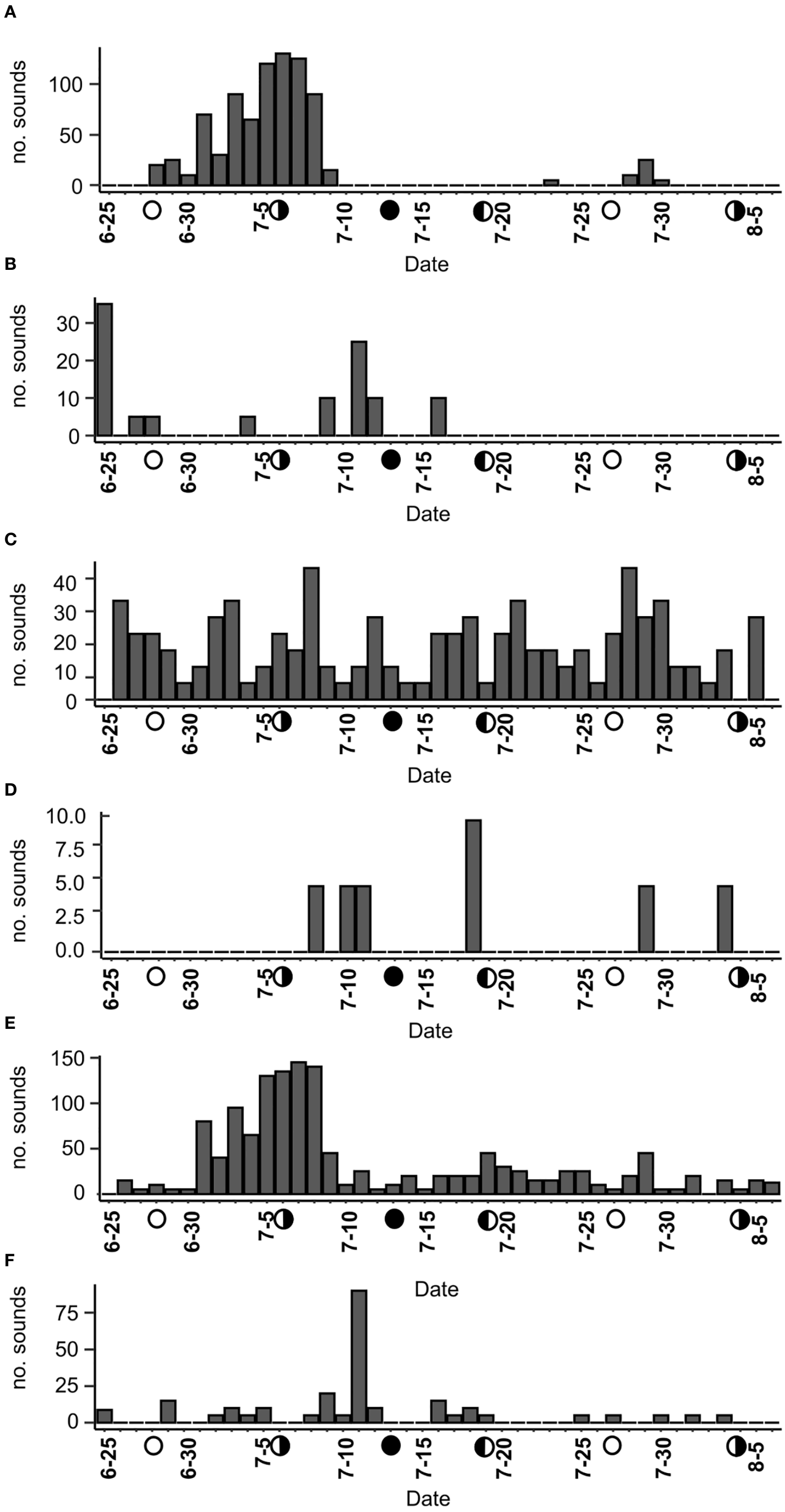

FIGURE 8 (Continued)

FIGURE 8 (Continued)
Longer term daily sound events from two sites in 2018. **(A)** Leopard toadfish boatwhistles from Tk4, **(B)** leopard toadfish from (Py2), **(C)** knock trains from Tk4, **(D)** Harmonic sounds from Tk4, **(E)** thud sounds from Tk4, and **(F)** thud sounds from Py2. Detections are adjusted for duty cycle and incomplete days on deployment. Lunar phase is shown with symbols on X-axes.

cluster from 28-30 July (Figure 8A). Notably, leopard toadfish call detection was much lower over the same period at Py2, but also followed a different pattern with detections peaking on the 25 June deployment date, with little activity until a slight increase after the peak of leopard toadfish activity was observed at Tk4 (Figures 8A, B). In addition, there were few detections of sounds at the Py2 site in comparison to Tk4, and the sound intensity of leopard toadfish sounds at Py2 indicate that the fish may have been located at a distance from the reef. Peak activity of leopard toadfish calls at either site did not follow a lunar pattern (Figures 8A, B). Knock trains at Tk4 showed a relatively steady rate of detection over the 43-day period, with no obvious lunar periodicity (Figure 8C). Harmonic sounds at Tk4 showed only a few sporadic detections from July to August (Figure 8D). Thud sounds were detected throughout the 43 day period at Tk4 (Figure 8E), but with much greater frequency around the last quarter moon in the beginning of July, over roughly the same period as when leopard toadfish calls were most abundant at that site (Figure 8A). Thud sounds, however, did not occur with high frequency in early August with the next last quarter moon (Figure 8E) and, at Py2, thud sounds were less frequent and peaked before the new moon on 11 July (Figure 8F).

Temporal and spatial variation of sound pressure levels

Sound pressure levels at reefs were highest in the evening, with a peak that tended to occur just after dusk (Figure 9; Table S1). On average, the median SPL levels in the day were approximately three dB below evening median SPL levels (Table S1). SPL levels among reefs varied by over 20 dB (Table S1). Notably, SPL levels were highest in 2018 with all four reefs (Tk4, Py2, Py1, Cp1) being higher than all reefs recorded in 2017 (Figure 9; Table S1). Sites Py8 and Br2 in 2017, also had high SPL levels (Figure 9; Table S1). Intense SPL is evident on 20 June 2017, especially at Py8, where rain and thunder could be heard on evening recordings. Intense rain also occurred at Py4 and Py5 on 03 August 2017 (Figures 9, S9-12). High frequency, 5000 Hz, was typically higher in intensity than lower frequencies at night, as evidenced from median PSD values (Figure S12). A 5000 Hz band of evening noise was evident and similar to the 6 kHz sound observed in the northern Gulf of Mexico (Wall et al., 2013).

Correlation of sound pressure level with fish species richness and boat presence

Day and night-time SPL_{RMS} levels were positively correlated with fish species richness, except for night-time SPL_{RMS} 95th percentile values, (Table 5). Vessel presence was also positively correlated with day and night-time SPL_{RMS} values.

Cusk-eel chatter

Chatter of sounds that appeared similar to cusk-eels (Mann et al., 1997; Kever et al., 2015; Mooney et al., 2016) was evident in the evenings from 01 August 2017 to 15 August 2017, with a strong peak at dusk and continued activity from PSD values of 1200 Hz. We were not successful using TDXC detection algorithms for choruses of this sound type (Figure 10A). In the evening, initial isolated calls quickly appear to form complex choruses (Figure 10B) from multiple sounds. These sounds were evident at sites Py4, Py5, Py3, Tk3 and especially intense at Py3 and Tk3 (Figure S11).

Discussion

Our study described complex biological soundscapes on artificial reefs in the nGOM during late spring and summer. Sounds include stereotyped signals and non-distinctive low-frequency sounds that vary over the diel cycle. Rates of sound detection varied among artificial reefs, which is predicted to be related in part to differences in the composition and abundance of soniferous fishes. We observed a positive correlation between the number of sound types detected among reefs and observed fish species richness. For sound types from both known and unknown sources, however, attempting to identify sound source species based on the co-occurrence between species and sounds among reefs was not reliable. Some of the observed sounds are consistent with previous descriptions of sounds (leopard toadfish, damselfish *Stegastes* spp., and cusk-eels [Ophidiidae]), however, the sources for many of the sounds that were common on some reefs remain unknown.

Several stereotyped sound types observed in this study showed strong nocturnal biases: pops, knock trains, harmonic sounds, leopard toadfish boatwhistle sounds, and putative cusk-eel chatter sounds. Oyster toadfish (*Opsanus tau*) in Maryland, U.S.A. also showed peak activities prior to sunrise and after

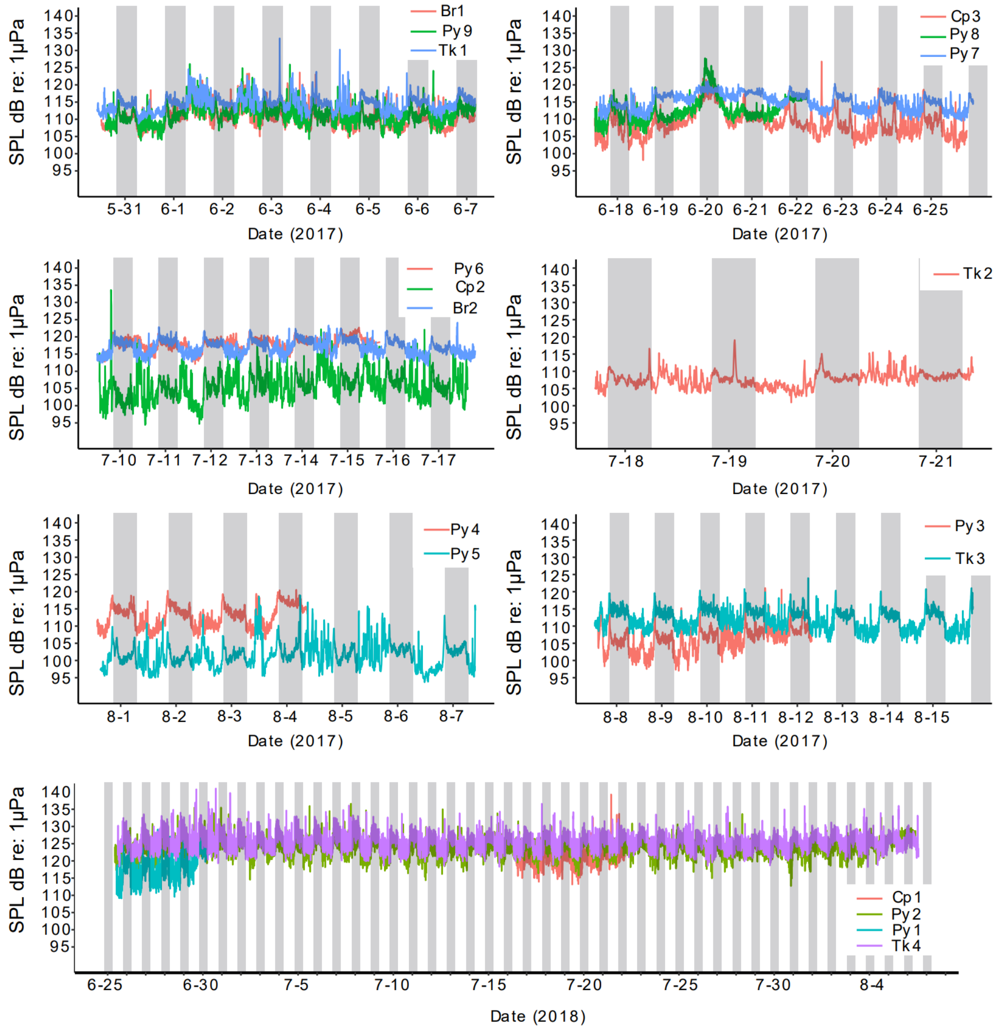

FIGURE 9
Sound intensity (SPL_{RMS} dB re 1μPa) over time at artificial reef study sites. Reefs recorded during the same period are shown on the same subplot. Gray bars indicate evening hours.

TABLE 5 Pearson correlation tests between SPL_{RMS} (median and 95th percentiles) and fish species richness among reefs and between SPL_{RMS} and vessel presence [daily detections of idling boats among reefs from Boyle et al. (2022)] among reefs.

		Reefs			
SPL		**Fish species richness**		**Vessel detections**	
		a	*P*	Corr.	*P*
Night	95%	0.436	0.070	**0.519**	**0.027**
	median	**0.472**	**0.048**	**0.584**	**0.011**
Day	95%	**0.515**	**0.029**	**0.600**	**0.008**
	median	**0.486**	**0.041**	**0.601**	**0.008**

Corr. = Pearson correlation coefficient
Correlation coefficients and *P*-values ¾ 0.05 are shown in bold.

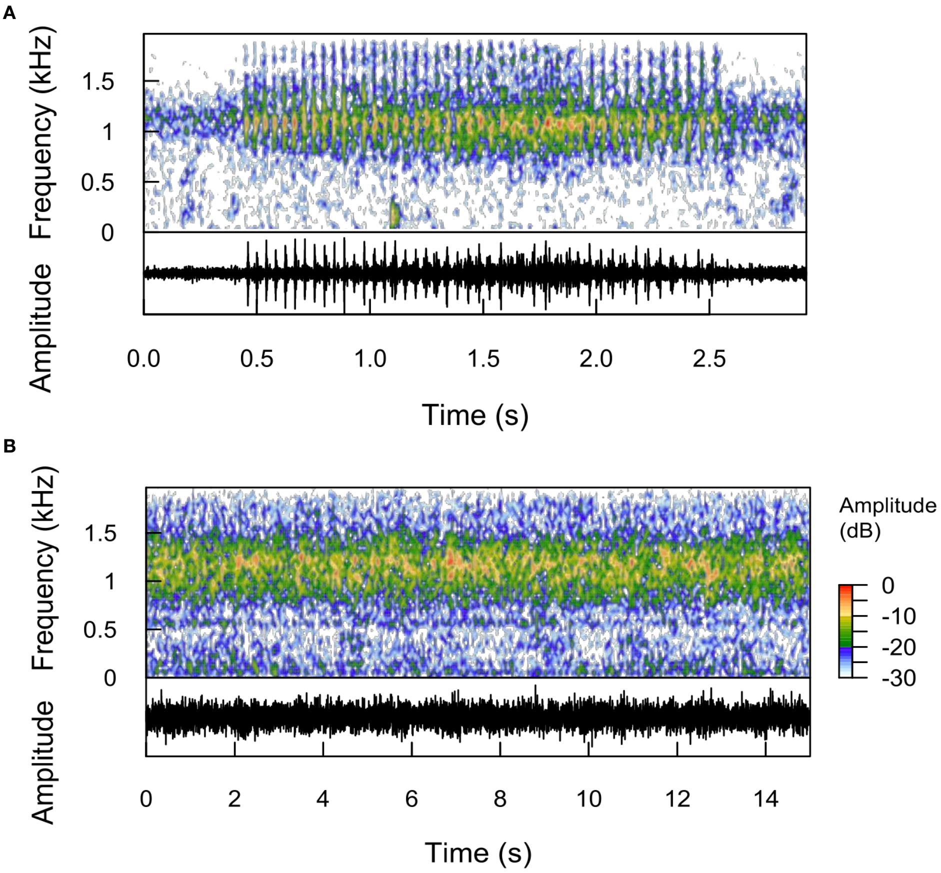

FIGURE 10
Putative cusk-eel **(A)** chatter calls and **(B)** chorus. Spectrogram and corresponding oscillograms are shown. Putative cusk-eel chatter sounds have many high frequency pulses (~25 per second). **(A)** Two putative calls, overlapping and in succession. At ca. 1.9 s, the second call, with lower pulse amplitudes and pulses that do not extend as high in frequency are evident. After sunset, **(A)** isolated calls quickly begin to overlap in time and form a **(B)** chorus with most energy concentrated between 900-1500 Hz. Chorus intensity began to wane at ca. 22h.

sunset (Ricci et al., 2017), however, leopard toadfish detections in this study showed a stronger nocturnal bias. Toadfish grunt sounds were not observed in this study. Grunt sounds have been attributed to agonistic behavior and unknown contexts based on spontaneous occurrences in oyster toadfish (Gray and Winn, 1961; Maruska and Mensinger, 2009). In gulf toadfish (*O. beta*), grunts have been interpreted as an agonistic call and can also occur at the beginning of a boatwhistle (Thorson and Fine, 2002). In a previous study, initial grunts at the beginning of boatwhistles were observed for *O. beta* but not *O. pardus* (Wall et al., 2013). It is possible that grunts occurred during our study and were not identified in subsampled data or that grunt-like sounds produced by leopard toadfish are one of our presently unidentified sound types. At this time, however, grunt sound descriptions for *O. pardus* are lacking.

The preponderance of several unknown sound types (pops, knock trains, harmonic sounds) during evening hours suggests nocturnal behavior for the source species of these sounds. Sources of these sounds remain unknown. Thus, sound emission could be part of a nocturnal behavior of fish that are typically diurnally active or, alternatively, may occur during peak activity for nocturnal and cryptic reef fishes. Activity of cryptic fish or nocturnal fish that shelter during daytime may explain the lack of association between abundance of fish species from visual observations with sound occurrence among reefs.

Other sound types showed more diurnal affinities. Dawn and dusk peaks were evident for the chirp-like sounds (template CL) predicted from cocoa damselfish, *Stegastes variabilis*. Grunt sounds were hypothesized to be from one or several different source species and showed a less pronounced dawn-dusk pattern. For example, sound detections by G3 occurred in pre-dawn and dawn hours and several hours over the afternoon but also some late evening detections. Sound detections from the grunt-like template G1 occurred in all hours but showed much higher variation in the evening hours. The stereotyped low frequency pulse sound was detected most often diurnally, but occurred at all hours and continued at a relatively high rate until two hours post-sunset. Thud sounds showed a fairly unique diel pattern relative to other sound types, with similar rates of occurrence in the late evening and pre-dawn hours until late afternoon, in which sound detections increased hourly and then remained steady and high until 22h.

Lunar periodicity was not evident in our study in the available data from longer-term recordings from two sites in 2018. Sound production correlates with lunar cycles in some fish species (Schärer et al., 2014; Radford et al., 2015; Monczak et al., 2017; Caiger et al., 2020). In a South Carolina estuary, lunar phase was found to be associated with both spotted seatrout (*Cynoscion nebulosus*) and oyster toadfish calling behavior (Monczak et al., 2017), unlike what was observed for the congener *O. pardus* (leopard toadfish) in our study.

Many low frequency sounds were observed among sites appeared biological but did not show stereotypy. We expected that these brief sounds were likely from incidental activity of fishes, like movement of swimming fish, but not produced from specialized sonic organs that result in a stereotyped sound (Fine and Parmentier, 2015). To quantify the relative occurrence of these sounds, we used example low frequency sounds as non-specific templates. This approach identified other low-frequency sounds that were clearly not-identical sounds, but still appeared consistent with our prediction of incidental sounds. Non-stereotyped low-frequency sounds detected with this approach tended to occur with similar frequency at most hours of the day, with the exception of sounds detected with template LF4, which showed a notably higher detection rate at 22h. The lack of apparent diel pattern for most of these non-stereotyped sounds is not surprising, as incidental sounds are expected to occur from a variety of potential source species that may vary in times of peak activities.

Sound types occurring diurnally may be expected to be produced by fish species more likely to be observed in visual fish surveys. Damselfish chirps, however, were the only mainly diurnal sound type detected from a known source. Chirps were only observed on artificial reefs in which cocoa damselfish were observed. Because these fish were a low portion of total fish species abundance on artificial reefs, and because damselfish chirps were only detected on two of the five artificial reefs for which cocoa damselfish were observed visually, the correlation of the frequency of sound detections with this species was relatively low. Only one individual leopard toadfish was observed visually during the study, yet the leopard toadfish boatwhistle sound was observed on eight reefs. Further, average detections of leopard toadfish on one reef exceeded 300 hundred per day despite no observations of this species on this reef on deployment and recovery dives. These observations highlight that correlations between specific soundscape features and overall abundance, diversity, or composition of visually surveyed fish species may be poor because the propensity and ability to produce stereotyped sounds varies among species and nocturnal and cryptic species (e.g., leopard toadfish) may call more often than diurnal, conspicuous fishes. Further study is needed with multiple fish species abundance survey methods (e.g., Plumlee et al., 2020) in conjunction with passive acoustic surveys to determine how specific sounds correlate with source species. Further, non-reef associated sound sources, such as cusk-eel sounds may contribute to part of the overall soundscape of artificial reefs. At least some cusk-eel species are buried in soft sediment during diurnal hours and thus are unlikely to be observed by video surveys.

Spatial patterns

A goal of this study was 1) to determine if occurrence of specific fish sounds rates varied among artificial reefs and reef types and 2) to determine if differences in sound type occurrence was correlated with differences in the composition of fish species observed on artificial reefs. In our study, call richness among reefs correlated with fish species richness. In a recent study of temperate rocky reefs in the Mediterranean Sea, fish species diversity was also associated with acoustic diversity (Desiderà et al., 2019). It is possible that species richness of non-vocal conspicuous reef fishes and vocal cryptic species are correlated because of similar habitat preferences or other factors. Such an indirect association could explain observed correlations between visually observed species richness and call richness. Our results showed large differences in the rate of specific sound detections on reefs, which is predicted to be associated with variable species composition and abundance on reefs. Yet, for many sound types identified in our study, obvious correlations with fish composition as observed by visual surveys on recorder deployment and recovery dives were lacking.

Some fish sounds appeared to be more associated with reef similarity as assessed by fish species presence/absence. For example, pop-like sounds tended to be abundant at Br1, Tk1, Cp2, Cp3, and Py4 sites, which were sites with relatively similar species composition patterns. However, pop-like sounds were never detected at Cp1 and Py2 sites, which also were similar in terms of species composition. Notably, however, the Cp1 and Py2 sites were recorded in 2018 and pop sounds were rarely detected in 2018 (only at site Tk4). The reefs with the highest pop sound rates varied depending on which template (P1, P2, P3, P4) was used for screening. As a result, despite being similar sounds that we predict are from the same source(s), different fish species had the highest associations with these sounds. Thus, correlating fish species presence and sound occurrence among reefs does not seem like a reliable method for determining potential sound sources among these artificial reefs. Of potential candidate species, spotfin butterflyfish seem the least likely, as they are conspicuous and were not observed on most of the reefs in which pop sounds occurred. Lionfish were observed on many reefs with pop sounds and high-frequency sounds (862

Hz) have been observed in captive specimens (Beattie et al., 2017). Lionfish, however, were also present on reefs that lacked pop sounds in this study. Tomtate were observed on most reefs with pop sounds and thus could be expected to be a candidate source species for this sound. However, the relatively narrow band and stereotyped pop waveform differs from the broadband and well-documented stridulatory sound of pharyngeal teeth associated with tomtate and other haemulids (Fish and Mowbray, 1970; Bertucci et al., 2014; Millot et al., 2021). Cubbyu did not have the highest association with pop sound detection rate among reefs with any of the templates. However, cubbyu were not observed on several pyramid reefs Py6, Py7, Py8, and Py9 that tended to have low or no pop sound detections and thus this species, which is from a highly soniferous family (Sciaenidae), deserves further investigation. Sounds from cubbyu that were elicited from mechanical and electrical stimulation (Fish and Mowbray, 1970), however, do not resemble these pop sounds. These brief reported observations do not preclude the possibility of the production of other sound types in this species. It is difficult to predict the source of many common sounds on reefs, particularly those emitted at night, without observations from captive fish. Some artificial reefs may have similar species composition because of abiotic and biotic features that make them attractive or suitable for the same suite of fishes. Further, these features may be suitable for a subset of soniferous species that may not be as abundant or conspicuous as the overall fish assemblage and thus result in spurious correlations between conspicuous species and sound type diversity. Spurious associations of species composition and sound detection rate were shown in this study with leopard toadfish boatwhistles, in which some reefs with detections were similar in terms of species composition (Br1, Py2, Tk1, Tk4), but leopard toadfish were only observed on one of those reefs (Tk4). Overall, non-intentional low frequency fish sounds, which we predict could be produced by multiple species because of their non-stereotyped waveforms, had the greatest association with fish species composition among reefs. Thus, such generalized low-frequency soundscape features may still provide a useful indicator of reef fish species composition.

Trends across summer

Longer-term recordings at two sites in 2018 demonstrated notable variation in sound detection patterns over the summer for some, but not all sounds. Leopard toadfish sound detections at Tk4 occurred mainly for a 12-day period beginning in late June and peaked on day nine. Boatwhistle calls in the related oyster toadfish (*Opsanus tau*) showed a period of approximately one month with increased calling activity in a study in Massachusetts (Van Wert and Mensinger, 2019). The brief period of increased detection in our study could correspond with some of the courtship and calling predicted to occur for a fish before or perhaps while nesting. In Maryland, oyster toadfish were observed spending a long time post-spawning guarding eggs (5-12 d), cling young (6-19 d), and free young (5-18 d) (Gray and Winn, 1961) and thus further study is required to determine the timing of these events in leopard toadfish and when calling occurs relative to care. Lower rates of leopard toadfish detections occurred on Py2 and mainly on different days during the same study period. Detections on Py2 seemed to be distant calls and may represent multiple fish from other reefs or off-reef locations, while detections on Tk4 were all high signal-to-noise ratio and likely from the same reef (perhaps a single fish). Thud sounds on Tk4 were detected throughout the period in which the recorder was active, but also over a remarkably similar period as leopard toadfish on the same reef. By contrast, knock train detections at the same reef remained relatively steady over the entire period. Further study is needed to determine the causes of such temporal variation, which may represent changes in behavior among fish present at a site, and such research can improve the potential utility of passive acoustics for monitoring change and ecosystem function on artificial reefs.

Overall and frequency specific noise levels among reefs

Most reefs tended to have higher (5-10 dB) sound pressure levels in the evening, particularly immediately after sunset, as part of the overall biophony. Intermittent boat noise at some days and sites, e.g. Cp2, Cp3, Tk2, and Py5 often exceeded evening sound pressure levels for some periods during the day. Such intense periods of anthropogenic noise deserve further consideration as a pollutant with potential negative consequences (stressor, masking communication, etc.) on artificial reefs in this area (Slabbekoorn et al., 2010; Radford et al., 2014a). Further study is needed to determine if vessel noise pollution has significant impacts on spawning behavior or other aspects (e.g., growth) of economically valuable fish species like red snapper and grouper. Anthropogenic noise has been shown to have negative impacts for several families of reef associated fishes. In Batrachoididae, boat noise interferes with communication space by masking calls (Alves et al., 2021) and experiments with simulated boat noise cause plainfin midshipman (*Porichthys notatus*) to respond with greater call amplitudes and shifts in fundamental frequency (Brown et al., 2021). Vessel noise appears likely to mask calls of sciaenids (Smott et al., 2018; Vieira et al., 2021). Damselfish (Pomacentridae) show behavioral responses, such as decreases in boldness and fleeing distance from predators (Holmes et al., 2017; Leduc et al., 2021), reduction in parental care behaviors (McCloskey et al., 2020) and succumb to increased predation (Simpson et al., 2016). Vessel noise is also predicted to reduce communication space for rocky-reef associated bigeyes

(*Pempheris adspersa*) (Putland et al., 2018). A study on movement and behavior of reef fishes exposed to intense seismic survey noise in the North West Shelf of Australia, however, did not observe adverse impacts from noise (Meekan et al., 2021). The Meekan et al. (2021) study included species from families that are also well-represented on Alabama artificial reefs (Lutjanidae, Sparidae, Balistidae, Pomacentridae, Epinephelidae), but it is possible that anthropogenic noise has subtle deleterious effects that were not observed in their study, as well as potential negative impacts on acoustic communication.

Overall SPL levels at night and day were positively correlated with fish species richness on reefs. However, SPL levels were also positively correlated with vessel presence and are a source of intense sound pressure. Therefore, it is not possible to determine if SPL results from higher fish species richness or simply because more vessels were present at reefs with higher richness. In addition to vessels, storm events (e.g., 20 June 2017) were a source of intense noise from rain and thunder. These sources of noise may have some influence on the likelihood of sound detection because of decreased signal-noise. Overall levels of sound intensity among reefs appeared to vary, with some reefs at substantially lower intensities. For example, the median sound level at night at Cp2 was 13-15 dB lower than the other two reefs (Py6, Br2) that were sampled at the same time (Figures 9, S1). Notably, however, at 200 Hz at night, the differences among these reefs is far more modest, with Cp2 5dB lower than Br2 and equal to Py6. Boat noise was less prevalent in night hours and 200 Hz is within the main frequency component of many observed fish sounds in the study. Among all reefs and time points in our study, the median night time intensity at 200 Hz only varied by 10 dB (Table S1). By contrast, 800 Hz, which was near the peak frequency of many pop sounds, varied among reefs by as much as 14 dB (Table S1). However, the reef with the lowest observed evening intensity at 800 Hz, Cp2, had high rates of pop sound detections. Further reef Br1, which had modest overall evening intensity at 800 Hz also had high pop sound detections and the site with the greatest 800 Hz intensity, Py3, had very few pop sound detections. In fact, the highest median intensities at 800 Hz and 1200 Hz were observed at Py3 and Tk3 (Figures S11, S12), which were deployed concurrently and these high intensities appear to be from intense choruses of putative cusk-eel sounds that began at dusk and remained intense for approximately 2 hours after sunset. Differences in intensity at 5 kHz among reefs at night were associated with differences in intensity of a tonal like sound that occurred at 5-6kHz nightly. This sound was observed previously in the eastern Gulf of Mexico and reported by Wall et al. (2012, 2013) and referred to as the '6kHz sound'. The source of the sound is unknown but is hypothesized to be of biological origin and occurring beyond small, relatively isolated artificial reefs. Our approach of scanning for specific sound types, found differences in relative rates of sound occurrence among reefs that would not be evident from just analyzing intensity at specific frequency over time. Some reefs with greater intensity at frequencies that overlap specific fish sounds of interest, appear to have fewer incidents of such sounds compared to reefs that are quieter overall at these frequencies. For example, Br1 reef, which had the greatest leopard toadfish detection rate, had median evening intensities at 200 Hz (near the peak of leopard toadfish boatwhistles) that were 4 dB quieter than Py9, yet the Br1 site had an average daily detection rate of toadfish boatwhistles that was 158 times greater than the Py9 site. This observation is important because it underscores that some quantitative comparisons of power spectral density, or other soundscape features, can still miss differences in specific sounds types that may correspond to differences in fish species present or differences in the behavioral state (e.g. spawning behavior, nesting) among reefs.

Considerations for screening for particular fish call types on artificial reefs

Our approach using semi-automated detection appeared promising for some sound types and situations but was less effective and feasible for others. Grunt and chirp-like sounds, which have multiple pulses in rapid succession, tended to have high false positive rates with TDXC. Sounds with distinctive pulses and in-consistent interpulse intervals, like the pop-sounds tended to have low-false positive rates. Producing an effective routine to detect thud-train sounds was challenging because the individual thud pulses appeared less stereotyped than some sounds and interpulse-intervals between thuds were variable. Knock-train sounds were difficult because the number and rate of the higher frequency broadband knocks that occurred in the middle of such calls were variable. Trial and error analyses with different approaches indicated that the best detection method in the time-domain for thud sounds detected more overall knock-trains than our original method designed to detect knock-trains. Tonal toadfish boatwhistle sounds were effectively screened in the frequency domain. This approach, however, while having a low false-positive rate often detected different portions of the same call. We found that substantial aural observation of putative detections with these semi-automated methods is required to reduce false positives or sort more generic detections into specific sound types. After detailed screening putative detections, however, it is possible to make quantitative comparisons of the relative rate of occurrence of specific sound events over temporal and spatial scales because the same methods are employed throughout the study.

Conclusion

Our study found substantial diel and temporal variation among artificial reefs off coastal Alabama. Differences among reefs were not clearly associated with reef structure. This study confirmed that artificial reefs in this area produce a range of biological sound. Such acoustic cues are known to attract and provide settlement cues for some larval reef fishes (Leis et al., 2002; Leis et al., 2003) and could also be a potential cue for adult fishes (Simpson et al., 2008) to return to reefs or find new reef habitats in the absence of other available cues (e.g., when above current from chemical cues and in low visibility). Soundscape recordings from our study and others may also benefit habitat restoration, given that playback of healthy reefs encourages larval settlement and retention in degraded habitats (Gordon et al., 2019). However, further research is needed to determine if such acoustic cues are important for navigation to reefs by larval and adult reef fish species commonly found on Alabama artificial reefs. Some evidence indicates that the distance in which reef noise may be an effective cue is more limited than has been widely assumed (Mann et al., 2007; Raick et al., 2021). Nevertheless, acoustic cues from limited distances could help fish detect reefs in low visibility environments and differences in soundscapes among reefs observed in this study and others (Radford et al., 2014b) may be predicted to vary the attractiveness of reefs for some species (Simpson et al., 2008; Gordon et al., 2019).

We hypothesize that differences in fish sounds among reefs are related, in part to which species are present on reefs. However, our results indicate that differences among visually conspicuous fish appear to contribute little to the overall observed differences among these reefs. Research is needed to identify the source species of many of these sounds and such data will improve the utility of passive acoustic data in these systems. Further study characterizing soundscapes of reef fish communities on artificial and natural reefs in the northern Gulf of Mexico relative to soft-bottom benthic habitats will help elucidate the potential role of this system.

Resource identification initiative

To take part in the Resource Identification Initiative, please use the corresponding catalog number and RRID in your current manuscript. For more information about the project and for steps on how to search for an RRID, please click here.

Data availability statement

The original contributions presented in the study are included in the article/Supplementary Material. Further inquiries can be directed to the corresponding author.

Author contributions

KB, CH, TN, and SP conceived of the study. KB, CH, and TN led field efforts. KB conducted initial analyses and wrote the first draft manuscript and figures. KB, CH, TN, and SP revised the final manuscript. All authors contributed to the article and approved the submitted version.

Funding

Financial support for this study was provided by the Alabama Department of Conservation and Natural Resources, Marine Resources Division to SP.

Acknowledgments

We thank Mark Albins, Reagan Coutorie, Erin Cox, Jacob Eagleton, Tom Guoba, Matt Jargowski, Grant Lockridge, Justin McDonald, Locke Revels, Sarah Schmid, and Jonathan Wittmann for field assistance. Financial support for this study was provided by the Alabama Department of Conservation and Natural Resources, Marine Resources Division.

Conflict of interest

Publisher's note

Supplementary material

The Supplementary Material for this article can be found online at: https://www.frontiersin.org/articles/10.3389/fmars.2022.954974/full#supplementary-material

References

Alves, D., Vieira, M., Amorim, M. C. P., and Fonseca, P. J. (2021). Boat noise interferes with lusitanian toadfish acoustic communication. *J. Exp. Biol.* 224, jeb234849. doi: 10.1242/jeb.234849

Amorim, M. C. P. (2006). "Diversity of sound production in fish," in *Communication in fishes*. Eds. F. Ladich, S. P. Collin, P. Moller and B. G. Kapoor (Enfield: Science Publishers), 71–104.

Beattie, M., Nowacek, D. P., Bogdanoff, A. K., Akins, L., and Morris, J. A.Jr. (2017). The roar of the lionfishes pterois volitans and *Pterois miles*. *J. Fish Biol.* 90, 2488–2495. doi: 10.1111/jfb.13321

Bertucci, F., Ruppe, L., Van Wassenbergh, S., Compere, P., and Parmentier, E. (2014). New insights into the role of the pharyngeal jaw apparatus in the sound-producing mechanism of *Haemulon flavolineatum* (Haemulidae). *J. Exp. Biol.* 217, 3862–3869. doi: 10.1242/jeb.109025

Bolgan, M., Soulard, J., Di Iorio, L., Gervaise, C., Lejeune, P., Gobert, S., et al. (2019). Sea Chordophones make the mysterious /Kwa/ sound: identification of the emitter of the dominant fish sound in Mediterranean seagrass meadows. *J. Exp. Biol.* 222, jeb196931. doi: 10.1242/jeb.196931

Boyle, K. S., Hightower, C. L., Nelson, T. R., and Powers, S. P. (2022). Use of passive acoustic monitoring to estimate fishing effort on artificial reefs in Alabama during the recreational red snapper fishing season. *Fish. Res.* 249, 106262. doi: 10.1016/j.fishres.2022.106262

Boyle, K. S., and Tricas, T. C. (2011). Sound production in the longnose butterflyfishes (genus *Forcipiger*): cranial kinematics, muscle activity and honest signals. *J. Exp. Biol.* 214, 3829–3842. doi: 10.1242/jeb.062554

Brown, N. A. W., Halliday, W. D., Balshine, S., and Juanes, F. (2021). Low-amplitude noise elicits the Lombard effect in plainfin midshipman mating vocalizations in the wild. *Anim. Behav.* 181, 29–39. doi: 10.1016/j.anbehav.2021.08.025

Butler, J., Pagniello, C. M. L. S., Jaffe, J. S., Parnell, P. E., and Širović, A. (2021). Diel and seasonal variability in kelp forest soundscapes off the southern California coast. *Front. Mar. Sci.* 8. doi: 10.3389/fmars.2021.629643

Caiger, P. E., Dean, M. J., DeAngelis, A. I., Hatch, L. T., Rice, A. N., Stanley, J. A., et al. (2020). A decade of monitoring Atlantic cod *Gadus morhua* spawning aggregations in Massachusetts bay using passive acoustics. *Mar. Ecol. Prog. Ser.* 635, 89–103. doi: 10.3354/meps13219

Connaughton, M. A. (2004). Sound generation in the searobin (*Prionotus carolinus*), a fish with alternate muscle contraction. *J. Exp. Biol.* 207, 1643–1654. doi: 10.1242/jeb.00928

Desiderà, E., Guidetti, P., Panzalis, P., Navone, A., Valentini-Poirrier, C., Boissery, P., et al. (2019). Acoustic fish communities: sound diversity of rocky habitats reflects fish species diversity. *Mar. Ecol. Prog. Ser.* 608, 183–197. doi: 10.3354/meps12812

Ellis, D. M., and Demartini, E. E. (1995). Evaluation of a video camera technique for indexing abundances of juvenile pink snapper, *Pristipomoides filamentosus*, and other Hawaiian insular shelf fishes. *Fish. Bull.* 93, 67–77.

Evans, R. R. (1973). The swimbladder and associated structures in Western Atlantic sea robins (Triglidae). *Copeia* 1973, 315–321. doi: 10.2307/1442970

Fine, M. L., and Parmentier, E. (2015). "Mechanisms of fish sound production," in *Sound communication in fishes*. Eds. F. Ladich (New York: Springer), 77–126.

Fine, M. L., and Thorson, R. F. (2008). Use of passive acoustics for assessing behavioral interactions in individual toadfish. *Trans. Am. Fish. Soc* 137, 627–637. doi: 10.1577/T04-134.1

Fish, M. P., and Mowbray, W. H. (1970). *Sounds of Western north Atlantic fishes* (Baltimore, MD: Johns Hopkins Press).

Gordon, T. A. C., Radford, A. N., Davidson, I. K., Barnes, K., McCloskey, K., Nedelec, S. L., et al. (2019). Acoustic enrichment can enhance fish community development on degraded coral reef habitat. *Nat. Commun.* 10, 5414. doi: 10.1038/s41467-019-13186-2

Gray, G.-A., and Winn, H. E. (1961). Reproductive ecology and sound production of the toadfish, *Opsanus tau*. *Ecology* 42, 274–282. doi: 10.2307/1932079

Holmes, L. J., McWilliam, J., Ferrari, M. C. O., and McCormick, M. I. (2017). Juvenile damselfish are affected but desensitize to small motor boat noise. *J. Exp. Mar. Biol. Ecol.* 494, 63–68. doi: 10.1016/j.jembe.2017.05.009

Jaxion-Harm, J., and Szedlmayer, S. T. (2015). Depth and artificial reef type effects on size and distribution of red snapper in the northern gulf of Mexico. *North Am. J. Fish. Manage.* 35, 86–96. doi: 10.1080/02755947.2014.982332

Kever, L., Boyle, K. S., and Parmentier, E. (2015). Effects of seawater temperature on sound characteristics in *Ophidion rochei* (Ophidiidae). *J. Fish. Biol.* 87, 502–509. doi: 10.1111/jfb.12730

Ladich, F. (2004). "Sound production and acoustic communication," in *The senses of fish*. Eds. G. von der Emde, J. Mogdans and B. G. Kapoor (New Delhi: Narosa Publishing House), 210–230.

Leduc, A. O. H. C., Nunes, J. A. C. C., de Araújo, C. B., Quadros, A. L. S., Barros, F., Oliveira, H., et al. (2021). Land-based noise pollution impairs reef fish behavior: A case study with a Brazilian carnival. *Biol. Conserv.* 253, 108910. doi: 10.1016/j.biocon.2020.108910

Leis, J. M., Carson-Ewart, B. M., and Cato, D. H. (2002). Sound detection *in situ* by the larvae of a coral-reef damselfish (Pomacentridae). *Mar. Ecol. Prog. Ser.* 232, 259–268. doi: 10.3354/meps232259

Leis, J. M., Carson-Ewart, B. M., Hay, A. C., and Cato, D. H. (2003). Coral-reef sounds enable nocturnal navigation by some reef-fish larvae in some places and at some times. *J. Fish Biol.* 63, 724–737. doi: 10.1046/j.1095-8649.2003.00182.x

Luczkovich, J. J., Sprague, M., Johnson, S. E., and Pullinger, C. (1999). Delimiting spawning areas of weakfish *Cynoscion regalis* (Family sciaenidae) in pamlico sound, north Carolina using passive hydroacoustic surveys. *Bioacoustics* 10, 143–160. doi: 10.1080/09524622.1999.9753427

Malinowski, C., Coleman, F., Koenig, C., Locascio, J., and Murie, D. (2019). Are Atlantic goliath grouper, *Epinephelus itajara*, establishing more northerly spawning sites? evidence from the northeast gulf of Mexico. *Bull. Mar. Sci.* 95, 371–391. doi: 10.5343/bms.2018.0062

Mann, D. A., Bowers-Altman, J., and Rountree, R. A. (1997). Sounds produced by the striped cusk-eel *Ophidion marginatum* (Ophidiidae) during courtship and spawning. *Copeia* 1997, 610–612. doi: 10.2307/1447568

Mann, D. A., Casper, B. M., Boyle, K. S., and Tricas, T. C. (2007). On the attraction of larval fishes to reef sounds. *Mar. Ecol. Prog. Ser.* 338, 307–310. doi: 10.3354/meps338307

Mann, D. A., Locascio, J. V., Coleman, F. C., and Koenig, C. C. (2009). Goliath Grouper *Epinephelus itajara* sound production and movement patterns on aggregation sites. *End. Species Res.* 7, 229–236. doi: 10.3354/esr00109

Maruska, K. P., and Mensinger, A. F. (2009). Acoustic characteristics and variations in grunt vocalizations in the oyster toadfish *Opsanus tau*. *Environ. Biol. Fish.* 84, 325–337. doi: 10.1007/s10641-009-9446-y

Meekan, M. G., Speed, C. W., McCauley, R. D., Fisher, R., Birt, M. J., and Currey-Randall, L. M. (2021). A large-scale experiment finds no evidence that a seismic survey impacts a demersal fish fauna. *Proc. Natl. Acad. Sci.* 118:e2100869118. doi: 10.1073/pnas.2100869118

McCloskey, K. P., Chapman, K. E., Chapuis, L., McCormick, M. I., Radford, A. N., and Simpson, S. D. (2020). Assessing and mitigating impacts of motorboat noise on nesting damselfish. *Environ. pollut.* 266, 115376. doi: 10.1016/j.envpol.2020.115376

Millot, M., Bertucci, F., Lecchini, D., Smeets, S., René-Trouillefou, M., and Parmentier, E. (2021). Characteristics of sound production and associated pharyngeal jaws in the tomtate grunt *Haemulon aurolineatum* (Cuvie) in Caribbean reefs. *Belg. J. Zool.* 151, 43–56. doi: 10.26496/bjz.2021.84

Minton, R., and Heath, S. (1998). Alabama's artificial reef program: building oases in the desert. *Gulf Mex. Sci.* 16, 105–105. doi: 10.18785/goms.1601.14

Monczak, A., Berry, A., Kehrer, C., and Montie, E. W. (2017). Long-term acoustic monitoring of fish calling provides baseline estimates of reproductive timelines in the may river estuary, southeastern USA. *Mar. Ecol. Prog. Ser.* 581, 1–19. doi: 10.3354/meps12322

Mooney, T., Kaplan, M., Izzi, A., Lamoni, L., and Sayigh, L. (2016). Temporal trends in cusk eel sound production at a proposed U.S. wind farm site. *Aquat. Biol.* 24, 201–210. doi: 10.3354/ab00650

Mueller, C., Monczak, A., Soueidan, J., McKinney, B., Smott, S., Mills, T., et al. (2020). Sound characterization and fine-scale spatial mapping of an estuarine soundscape in the southeastern USA. *Mar. Ecol. Prog. Ser.* 645, 1–23. doi: 10.3354/meps13373

Myrberg, A. A.Jr. (1981). "Sound communication and interception in fishes," in *Hearing and sound communication in fishes*. Eds. W. N. Tavolga, A. N. Popper and R. R. Fay (New York: Springer), 395–425.

Myrberg, A. A., Ha, S. J., and Shamblott, M. J. (1993). The sounds of bicolor damselfish (*Pomacentrus partitus*): Predictors of body size and a spectral basis for individual recognition and assessment. *J. Acoust. Soc Am.* 94, 3067–3070. doi: 10.1121/1.407267

Oksanen, J., Blanchet, F. G., Friendly, M., Kindt, R., Legendre, P., McGlinn, D., et al. (2020) *Vegan (R package version 2.5-7)*. Available at: https://cran.r-project.org/package=vegan.

Plumlee, J. D., Dance, K. M., Dance, M. A., Rooker, J. R., TinHan, T. C., Shipley, J. B., et al. (2020). Fish assemblages associated with artificial reefs assessed using multiple gear types in the northwest gulf of Mexico. *Bull. Mar. Sci.* 96, 655–677. doi: 10.5343/bms.2019.0091

Powers, S. P., Drymon, J. M., Hightower, C. L., Spearman, T., Bosarge, G. S., and Jefferson, A. (2018). Distribution and age composition of red snapper across the inner continental shelf of the north-central gulf of Mexico. *Trans. Am. Fish. Soc* 147, 791–805. doi: 10.1002/tafs.10081

Putland, R. L., Merchant, N. D., Farcas, A., and Radford, C. A. (2018). Vessel noise cuts down communication space for vocalizing fish and marine mammals. *Glob. Change Biol.* 24, 1708–1721. doi: 10.1111/gcb.13996

Radford, C. A., Ghazali, S., Jeffs, A. G., and Montgomery, J. C. (2015). Vocalisations of the bigeye *Pempheris adspersa*: characteristics, source level and active space. *J. Exp. Biol.* 218, 940–948. doi: 10.1242/jeb.115295

Radford, A. N., Kerridge, E., and Simpson, S. D. (2014a). Acoustic communication in a noisy world: can fish compete with anthropogenic noise? *Behav. Ecol.* 25, 1022–1030. doi: 10.1093/beheco/aru029

Radford, C., Stanley, J., and Jeffs., A. (2014b). Adjacent coral reef habitats produce different underwater sound signatures. *Mar. Ecol. Prog. Ser.* 505, 19–28. doi: 10.3354/meps10782

Raick, X., Di Iorio, L., Gervaise, C., Lossent, J., Lecchini, D., and Parmentier, E. (2021). From the reef to the ocean: revealing the acoustic range of the biophony of a coral reef (Moorea island, French Polynesia). *J. Mar. Sci. Eng.* 9, 420. doi: 10.3390/jmse9040420

R Core Team (2021). *R: A language and environment for statistical computing* (Vienna, Austria: R Foundation for Statistical Computing). Available at: https://www.r-project.org/.

Reeves, D. B., Chesney, E. J., Munnelly, R. T., Baltz, D. M., and Marx, B. D. (2018). Abundance and distribution of reef-associated fishes around small oil and gas platforms in the northern gulf of mexico's hypoxic zone. *Estuaries Coasts.* 41, 1835–1847. doi: 10.1007/s12237-017-0349-4

Ricci, S. W., Bohnenstiehl, D. R., Eggleston, D. B., Kellogg, M. L., and Lyon, R. P. (2017). Oyster toadfish (*Opsanus tau*) boatwhistle call detection and patterns within a large-scale oyster restoration site. *PloS One* 12, e0182757. doi: 10.1371/journal.pone.0182757

Schärer, M. T., Nemeth, M. I., Rowell, T. J., and Appeldoorn, R. S. (2014). Sounds associated with the reproductive behavior of the black grouper (*Mycteroperca bonaci*). *Mar. Biol.* 161, 141–147. doi: 10.1007/s00227-013-2324-3

Simpson, S. D., Jeffs, A., Montgomery, J. C., McCauley, R. D., and Meekan, M. G. (2008). Nocturnal relocation of adult and juvenile coral reef fishes in response to reef noise. *Coral Reefs* 27, 97–104. doi: 10.1007/s00338-007-0294-y

Simpson, S. D., Radford, A. N., Nedelec, S. L., Ferrari, M. C. O., Chivers, D. P., McCormick, M. I., et al. (2016). Anthropogenic noise increases fish mortality by predation. *Nat. Commun.* 7, 10544. doi: 10.1038/ncomms10544

Slabbekoorn, H., Bouton, N., van Opzeeland, I., Coers, A., ten Cate, C., and Popper, A. N. (2010). A noisy spring: the impact of globally rising underwater sound levels on fish. *Trends Ecol. Evol.* 25, 419–427. doi: 10.1016/j.tree.2010.04.005

Smott, S., Monczak, A., Miller, M. E., and Montie, E. W. (2018). Boat noise in an estuarine soundscape – a potential risk on the acoustic communication and reproduction of soniferous fish in the may river, south Carolina. *Mar. pollut. Bull.* 133, 246–260. doi: 10.1016/j.marpolbul.2018.05.016

Staaterman, E., Paris, C. B., and Kough, A. S. (2014). First evidence of fish larvae producing sounds. *Biol. Lett.* 10, 20140643. doi: 10.1098/rsbl.2014.0643

Steinberg, J. C., Cummings, W. C., Brahy, B. D., and MacBain (Spires), J. Y. (1965). Further bio-acoustic studies off the west coast of north bimini, Bahamas. *Bull. Mar. Sci.* 15, 942–963.

Sueur, J. (2018). *Sound analysis and synthesis with r. cham* (Switzerland: Springer International Publishing).

Sueur, J., Aubin, T., Brown, E. C., Depraetere, M., Desionqueres, C., Fabianek, F., et al. (2018) *Seewave. (R package version 3.4.6)*. Available at: https://cran.r-project.org/web/packages/seewave.

Thorson, R. F., and Fine, M. L. (2002). Acoustic competition in the gulf toadfish *Opsanus beta*: Acoustic tagging. *J. Acoust. Soc Am.* 111, 2302–2307. doi: 10.1121/1.1466865

Tricas, T. C., and Boyle, K. S. (2014). Acoustic behaviors in Hawaiian coral reef fish communities. *Mar. Ecol. Prog. Ser.* 511, 1–16. doi: 10.3354/meps10930

Tricas, T. C., and Boyle, K. S. (2021). Parrotfish soundscapes: implications for coral reef management. *Mar. Ecol. Prog. Ser.* 666, 149–169. doi: 10.3354/meps13679

Van Hoeck, R. V., Paxton, A. B., Bohnenstiehl, D. R., Taylor, J. C., Fodrie, F. J., Nowacek, D. P., et al. (2020). Soundscapes of natural and artificial temperate reefs: similar temporal patterns but distinct spectral content. *Mar. Ecol. Prog. Ser.* 649, 35–51. doi: 10.3354/meps13434

Van Wert, J. C., and Mensinger, A. F. (2019). Seasonal and daily patterns of the mating calls of the oyster toadfish, *Opsanus tau*. *Biol. Bull.* 236, 97–107. doi: 10.1086/701754

Vieira, M., Beauchaud, M., Amorim, M. C. P., and Fonseca, P. J. (2021). Boat noise affects meagre (*Argyrosomus regius*) hearing and vocal behaviour. *Mar. pollut. Bull.* 172, 112824. doi: 10.1016/j.marpolbul.2021.112824

Wall, C. C., Lembke, C., and Mann, D. A. (2012). Shelf-scale mapping of sound production by fishes in the eastern gulf of Mexico, using autonomous glider technology. *Mar. Ecol. Prog. Ser.* 449, 55–64. doi: 10.3354/meps09549

Wall, C. C., Simard, P., Lembke, C., and Mann, D. A. (2013). Large-Scale passive acoustic monitoring of fish sound production on the West Florida shelf. *Mar. Ecol. Prog. Ser.* 484, 173–188. doi: 10.3354/meps10268

frontiers | Frontiers in Marine Science

TYPE Original Research
PUBLISHED 06 October 2022
DOI 10.3389/fmars.2022.988158

OPEN ACCESS

EDITED BY
Bernardo Antonio Perez Da Gama,
Fluminense Federal University, Brazil

REVIEWED BY
Anthony Fowler,
South Australian Research and Development Institute, Australia
Sahar Fahmy Mehanna,
National Institute of Oceanography and Fisheries (NIOF), Egypt

*CORRESPONDENCE
Chelsea M. Williams
cmunoz@oxy.edu

SPECIALTY SECTION
This article was submitted to Marine Ecosystem Ecology, a section of the journal Frontiers in Marine Science

RECEIVED 07 July 2022
ACCEPTED 09 September 2022
PUBLISHED 06 October 2022

CITATION
Williams CM, Eagleton JL, Pondella DJ II and Claisse JT (2022) Habitat type and environmental conditions influence the age and growth of a temperate marine damselfish. *Front. Mar. Sci.* 9:988158. doi: 10.3389/fmars.2022.988158

Habitat type and environmental conditions influence the age and growth of a temperate marine damselfish

Chelsea M. Williams[1,2]*, Jacob L. Eagleton[2], Daniel J. Pondella II[1] and Jeremy T. Claisse[1,2]

[1]Vantuna Research Group, Department of Biology, Occidental College, Los Angeles, CA, United States, [2]Department of Biological Sciences, California State Polytechnic University, Pomona, CA, United States

Life history parameters for fishes have generally been applied to species across their entire range, however, different ecological and environmental conditions and processes (e.g., sea surface temperature, habitat, primary productivity, fishing mortality, resource availability) influence life history patterns at smaller spatial scales. By focusing on a historically protected species, we determined how environmental and ecological factors shape patterns in growth and longevity, without the impact of fishing. The Garibaldi (*Hypsypops rubicundus)* is a territorial marine damselfish native to the shallow rocky reefs of southern California. Garibaldi were collected from five mainland locations and five Channel Islands throughout the Southern California Bight. Paired natural reef and artificial reef habitats (i.e., breakwaters and jetties) in each mainland location were sampled. Otolith-based ageing and biological data from these populations were used to assess how age and growth vary by location, reef type (natural/artificial), island or mainland, mean annual sea surface temperature, and/or sex. The annual formation of growth increments in otoliths was validated *in-situ* using tetracycline mark-recapture methods to confirm that increments are formed annually. Garibaldi grew significantly larger on artificial reefs than on natural reefs but tended to live longer on paired natural reefs. Regionally, growth and longevity followed mean annual sea surface temperature gradients, consistent with Bergmann's rule. Garibaldi exhibited clear sexual size dimorphism; males grew larger, which is uncharacteristic for both damselfish and other marine fishes from the southern California. The Garibaldi collected for this study had a maximum age of 57 years, which makes this the longest lived damselfish species by two decades.

KEYWORDS

artificial reefs, southern California, fish life history, growth patterns, spatial variation, Garibaldi, *Hypsypops rubicundus*

Introduction

Marine fish life history strategies (i.e., the allocation of limited resources to the competing demands of growth, reproduction, and survival) and demographic parameters can provide insight into population and community-level processes and ecological patterns. They are typically assumed to be consistent for a species across its entire range (King and McFarlane, 2003; Fonseca and Cabral, 2007). However, several recent studies concluded that different ecological and environmental conditions result in intraspecific spatial variation in fish life history patterns. This variation has been attributed to multiple factors including: differences in mean annual, inter-annual, or range in sea surface temperature (Trip et al., 2014; Trip et al., 2016; Tanner et al., 2019); habitat (DeMartini et al., 1989; DeMartini et al., 1994; Love et al., 2007; Granneman and Steele, 2014); primary productivity (Ruttenberg et al., 2005; Tanner et al., 2019); fishing mortality (Robertson et al., 2005; Hamilton et al., 2007; Hsieh et al., 2009; Hamilton et al., 2011; Taylor, 2013; Taylor et al., 2015); differing environmental conditions during larval/juvenile growth (Atkinson, 1994; Atkinson, 1996; Fonseca and Cabral, 2007; Williams et al., 2007); food resource availability (Hjelm et al., 2000); and density-dependent interactions (Figueira et al., 2007). Understanding the complexities of species-specific life histories for marine fishes is essential for informing ecosystem-based fisheries management (Jennings and Dulvy, 2008).

The Southern California Bight (SCB) spans 3.5° of latitude of the ocean from Point Conception, CA in the north to the United States-Mexico border in the south. The SCB encompasses 1,198 km of coastline that includes the mainland and an eight-island archipelago, known as the California Channel Islands (Pondella et al., 2015b). Roughly 26% of the nearshore (<30 m depth) habitat is composed of rocky reefs with the remainder dominated by soft substrata, exhibiting fragmented distributions of rocky reef habitat. The SCB has a unique surface current circulation pattern where the year-round, dominant California Current brings cool water to the region from the north. South of Point Conception, the flow of the California Current is disrupted by the Channel Islands and branches shoreward and poleward where it forms the Southern California Countercurrent, drawing warmer water from the south and creating a large eddy that circulates counterclockwise throughout the Bight (Hickey, 1992). This current pattern, when coupled with the complex bathymetry, results in strong abiotic gradients such as sea surface temperature (Figure 1) and diverse habitats that support various assemblages of fish fauna. This provides a prime opportunity to study how variability in environment and habitat type shape life history patterns (Engle, 1993; Allen and Pondella, 2006; Pondella et al., 2015a; Pondella et al., 2015b). Prior studies of spatial differences in growth patterns and demographic parameters for fishes in the SCB have concentrated on commercially and recreationally exploited species (Love et al., 1990; Love et al., 2007; Granneman, 2011; Hamilton et al., 2011; Granneman and Steele, 2014). Size-selective fishing mortality on larger, older members of a population can influence fish life history patterns including rapid growth to asymptotic size, early maturity, reduced reproductive output, skewed sex ratios, and age- and size-truncation of exploited populations, which can have evolutionary consequences (Robertson et al., 2005; Hamilton et al., 2007; Hsieh et al., 2009; Caselle et al., 2011; Hamilton et al., 2011; Taylor, 2013; Audzijonyte et al., 2016).

In addition to natural rocky reefs, artificial or anthropogenic structures also provide habitat for reef-associated fishes in the SCB. Over the last 50 years, the population of southern California has nearly doubled and is one of the most densely populated areas in the United States, currently supporting roughly 24 million people. In addition, nearly 25% of the entire nation's coastal population lives in the four counties bordering the shoreline of the SCB (Schiff et al., 2000; Wilson and Fischetti, 2010). The artificial structures in the SCB were primarily built as coastal infrastructure (e.g., breakwaters and jetties, oil and gas platforms, and outfall and discharge pipes) to support this urbanization. In addition, rapid population growth has put stress on marine resources through the discharge of pollutants, loss of habitat, and overfishing. In 1958, California Department of Fish and Game (currently California Department of Fish and Wildlife) began the Nearshore Sportfish Habitat Enhancement Program, which focused on restoring and enhancing fish habitat through the implementation of purpose-built artificial reefs in southern California (Lewis and McKee, 1989). The function of artificial structures, both infrastructure and purpose-built, as fish habitat is well-studied within the Bight (Ambrose and Swarbrick, 1989; DeMartini et al., 1989; DeMartini et al., 1994; Pondella and Stephens, 1994; Stephens et al., 1994; Pondella et al., 2002; Stephens and Pondella, 2002; Claisse et al., 2014; Granneman and Steele, 2015; Claisse et al., 2019; Love et al., 2019; Barilotti et al., 2020; Burns et al., 2020), however relatively few studies have compared the ecological performance of fish on artificial reefs to natural reefs (Love et al., 2007; Granneman and Steele, 2014).

The Garibaldi (*Hypsypops rubicundus*) is a territorial marine damselfish endemic to the shallow reefs of southern California and Baja California, Mexico. Out of 385 species of damselfish (Family: Pomacentridae), Garibaldi is the largest, reaching up to 35 cm in length (Limbaugh, 1964; Clarke, 1970; Allen, 1991; Nelson et al., 2016). Their bright orange adult coloration, with spots of iridescent blue as juveniles, makes them the most conspicuous reef fish in southern California (Kritzler et al., 1950). Once an intense target of collection for the aquarium trade, as the State Marine Fish of California, this species has been fully protected in the United States since 1995. Although

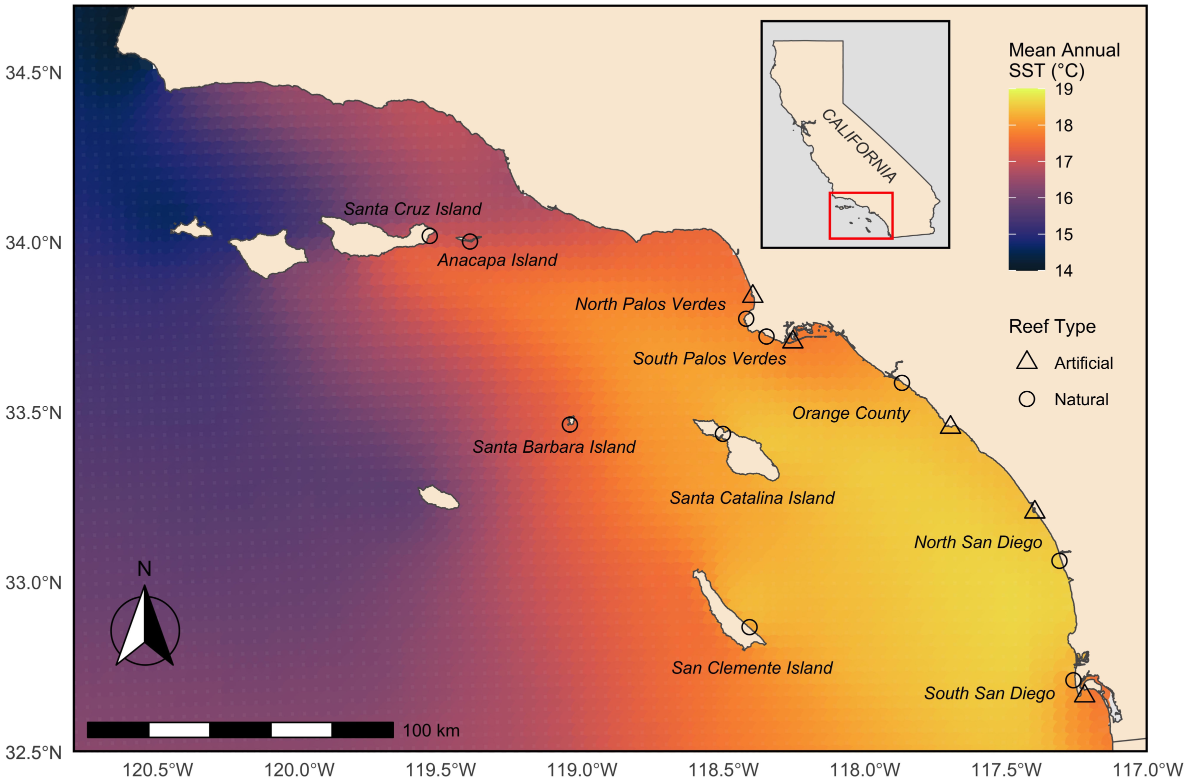

FIGURE 1
Map of sampled Garibaldi (*Hypsypops rubicundus)* populations (locations) in the Southern California Bight. Reef type is indicated by shape – triangles for artificial rocky reefs (i.e., breakwaters and jetties) and circles for natural rocky reefs. Mean annual sea surface temperature (SST;°C) values for January 2002-December 2018 are from merged 1 km resolution data.

predation on young-of-the-year Garibaldi by Kelp Bass (*Paralabrax clathratus*) (Cook, 2011), adult Garibaldi have very few known natural predators (Kritzler et al., 1950; Clarke, 1970) and are currently unfished. Unlike other damselfish where males guard nest sites only during the mating season, both male and female adult Garibaldi typically defend year-round territories of approximately 3-10 m^2, demonstrating high site fidelity (Limbaugh, 1964; Clarke, 1970; Foster, 1972; Sikkel, 1988; Sikkel, 1989; Alcalay and Sikkel, 1994). A territory includes a shelter hole, foraging area, and for adult males, a nest site comprised of perennial patches of red algae cultivated by the male. Females are allowed into the territory to deposit eggs into the nest during spawning season (April through September), the timing of which varies within and among populations (Clarke, 1970; Clarke, 1971; Sikkel, 1988). The eggs are guarded by the male until young hatch, and disperse into the plankton (Clarke, 1970). In early summer to early fall, juveniles settle on shallow rocky reefs on exposed or semi-protected coasts (Limbaugh, 1964; Clarke, 1970; Alcalay and Sikkel, 1994). Vagility is only through the larval stage making this taxon optimal for describing site-specific growth characteristics. Previous life history studies on Garibaldi are limited primarily to the San Diego, CA area and/or prior to 1995, when their protected status was implemented. Clarke (1970) reported that Garibaldi achieve adult coloration at around 5 years, sexual maturity at 6 years, and a maximum age of 17 years. However, Clarke's study used scale-based ageing, which can drastically underestimate the ages of fish (Francis and Francis, 1992; Beamish and McFarlane, 1995; Campana, 2001), and was conducted prior to the implementation of protected status. During the period from when that study was conducted in 1965 to 2010, Garibaldi densities more than doubled at Clarke's study sites (Cook, 2011), indicating that the status of Garibaldi populations have changed considerably over time. By focusing on a historically protected species with high site fidelity, like the Garibaldi, we can determine how habitat type, environmental, and ecological factors shape patterns in growth and longevity at distinct locations within the SCB.

For this study, otolith-based ageing was used to assess how life history patterns vary by reef type (natural/artificial), mean annual sea surface temperature, sex, island or mainland geographies, and/or location for Garibaldi populations throughout the SCB. The periodicity of increment formation in otoliths was assessed using *in-situ* tetracycline mark-recapture methods to confirm that increments form annually rather than conforming to some other periodicity (e.g., seasonality, lunar cycles) (Campana, 2001). Accounting for patterns in variation of fish life history observed in previous studies, the following predictions were made:

1. Garibaldi from artificial reef habitats will grow larger and faster than Garibaldi from natural reef habitats. Within the SCB, juvenile (young-of-the-year) Blue Rockfish (*Sebastes mystinus)* were found to have faster daily growth rates at oil platforms compared to nearby natural reefs (Love et al., 2007). Garibaldi were collected from breakwaters because they were consistent in habitat structure and presence in each mainland location. Breakwaters and jetties are built to protect coastal infrastructure and are made up of large (1-2 m) quarry rock boulders, providing a complex and ideal fish habitat with several open spaces to provide refuge and for Garibaldi to maintain territories (Stephens et al., 1994).

2. Garibaldi will be larger, slower-growing, and longer-lived at cooler locations, and smaller, faster-growing, and shorter-lived at warmer locations. Ectotherms tend to be larger and live longer in colder environments due to a trade-off between metabolism and longevity (Atkinson and Sibly, 1997; Mangel and Abrahams, 2001). In addition, fish populations in colder waters often have shorter reproductive seasons and therefore may allocate less of their annual energy budgets to reproduction, which results in larger and older fish in these populations (Ruttenberg et al., 2005).

3. Male Garibaldi will grow larger than female Garibaldi. Although previous Garibaldi life history studies found no apparent differences between growth rates for males and females, they did find that males lived longer and grew larger (Clarke, 1970). In addition, Sikkel (1988; 1989) determined that male size was positively correlated with female nest preference and posited that male size may be correlated with nest quality. Further, large males may be more successful in the defense of their nesting sites.

Methods

Study area

Garibaldi were collected from ten locations in the SCB (Figure 1). Locations were selected based on two criteria: they supported at minimum 100 Garibaldi per hectare (Pondella et al., 2015a); and were ecologically and environmentally distinct and geographically distant (Engle, 1993; Pondella et al., 2015b). Five locations were in the California Channel Islands of Santa Cruz Island, Anacapa Island, Santa Barbara Island, Santa Catalina Island, and San Clemente Island and the other five locations were on the mainland coast in Northern and Southern Palos Verdes, Orange County, and Northern and Southern San Diego. For locations on the mainland, paired natural rocky reefs and artificial or human-built rocky reefs (e.g., breakwaters and jetties at harbors nearby or adjacent to natural reef sites) were sampled. This investigated the influence of differences in habitat type under similar environmental conditions.

Fish collections

From 2013-2019, 1,111 Garibaldi were collected from the ten study locations (Figure 1) by scientific divers using pole spears. Divers attempted to collect a representative size sample of the fish present at each location. Upon collection, fish were transported to the laboratory where they were weighed to the nearest gram and measured head (HL), standard (SL), fork (FL), and total lengths (TL) to the nearest millimeter. The digestive tract and gonads were removed, weighed, and preserved for future studies. Sex was determined macroscopically, if possible. Macroscopic sex determination was difficult outside of the spawning season, especially in smaller male individuals, therefore sex was determined through histological preparations when necessary. Sagittal otoliths were extracted and stored dry. This study was reviewed and approved by the Institutional Care and Use Committees at both Cal Poly Pomona and Occidental College, and fish were collected under California Department of Fish and Wildlife Scientific Collecting Permits.

Otolith processing and age determination

Sagittal otoliths were used for ageing. Annual periodicity of sagittal otolith increment formation was validated using standard methods (Cappo et al., 2000) including *in-situ* tetracycline mark-recapture at Flat Rock in North Palos Verdes (Section 1 in Supplementary Material). Each whole sagittal otolith was weighed to the nearest 0.0001 g. One otolith from each fish was mounted on a glass slide using thermoplastic resin and sectioned using a 1200 grit diamond flat lap on a grinding wheel following Taylor and McIlwain (2010) to produce a thin transverse section. Next, otoliths were covered in resin and heated on a hotplate to 260 °C, to improve readability. This increased the contrast between alternating translucent and opaque annual zones producing results similar to the "break and burn method" (Forsberg, 2001). When the transverse sections were viewed under a stereomicroscope with reflected light, each displays a central, dense, opaque region (pre-settlement) and alternating translucent and opaque zones (annuli) (Figure S2 in Supplementary Material). Annuli were counted along a path from the center towards the tip of the inner face next to the sulcus, where annual growth increments are clearly defined (García-Mederos et al., 2016). Readings were done by a single reader (C. M. Williams) a minimum of two times. The final age (in years) of an individual was determined when two or more counts agree (Choat and Axe, 1996; Claisse et al., 2009). If at least two counts did not agree after three readings, the otolith was excluded from age-based analyses (1.1% of otoliths).

Age and growth analyses

All age and growth analyses were performed in R (R Core Development Team, 2021) and are reported in relation to fish total length (TL; mm). Growth patterns were evaluated by fitting the von Bertalanffy growth function (VBGF) using maximum likelihood using the 'mle2' function in the *bbmle* package (Bolker and R Core Development Team, 2020), which models the mean TL (L_t, in mm) at age (t, in years) following:

$$L_t = L_\infty[1 - e^{-k(t-t_0)}]$$

where L_∞ is mean asymptotic length, k describes the rate at which L_t reaches L_∞ (with units of yr^{-1}), and t_0 is the theoretical age at 0 mm in length. Since fish often demonstrate rapid initial growth, it is important to include small, young fish to obtain accurate estimations of mean size-at-age for early life stages when modeling growth (Kritzer et al., 2001; Berumen, 2005; Claisse, 2009). Therefore, for immature individuals where sex was unidentifiable *via* macroscopic identification and histological preparation, sex was assigned randomly following a 1:1 sex ratio. Additionally, because there were few individuals of age 0-3 within each distinct grouping, t_0 was fixed to a value of -2.1 years which was determined by fitting the von Bertalanffy growth function to the global population.

The longevity of fishes is typically assessed using three methods: (1) the maximum age, or oldest individual in the population (T_{max}) (Beverton and Holt, 1959), (2) as the mean age of the oldest 25% of fish collected ($T_{max\ 25\%}$) (Choat and Robertson, 2002), and (3) as the mean age of the oldest 10% of fish collected ($T_{max\ 10\%}$) (Trip et al., 2008). All three metrics were calculated for males and females for each location and reef type, and for the global population.

Environmental data

Measures of environmental variables were derived from remotely sensed data. Mean annual sea surface temperature (SST; °C) values were derived from merged MODIS 1 km resolution data from MODIS-Aqua and MODIS-Terra sensors composited over each month from January 2002- December 2018. This period was used to best represent the average conditions that fish experienced during their lifetime, with the data available from MODIS, which spans 2002-present. Surface chlorophyll-a (Chl-a; g C m^{-3}) values for each location were derived using satellite data from MODIS-Aqua, MODIS-Terra, VIIRS-NPP, SeaWiFS, MERIS and OLCI sensors composited over each month during the same time period. Data were merged using simple pixel-wise averaging of valid pixel values to increase coverage and composited by the California Current Ecosystem Long-Term Ecological Research program based at Scripps Institution of Oceanography. Full-resolution 1 km data sets were downloaded in HDF5 format, clipped to the study area then converted to a data frame table format for plotting specific points using R (R Core Development Team, 2021). Values for mean annual SST and Chl-a were calculated by averaging the annual means. Because nearshore values for both Chl-a and SST often contain erroneous values due to some cells containing a portion of land, these data were then imported into ArcGIS, the cells that overlapped with land were deleted, and then the layers were converted to a 4 km raster using the Point to Raster tool (ESRI ArcMap 10.8.1 Spatial Analyst) and assigned a value using the average values of all the points within the cell. Cell values for SST and Chl-a for each study location were then extracted using the Extract Values to Points tool.

Age and growth model selection and confidence interval estimation

The level of evidence for effects of sex, reef type, island/mainland, and location on growth patterns was investigated using model selection. We used the corrected Akaike Information Criterion (AICc), which adds a correction for bias due to small sample size, effectively penalizing complex models with small data sets (Burnham and Anderson, 2002; Anderson, 2008). Akaike weights (w_i) were calculated to assess the relative likelihood of each model in the set and were interpreted as the weight of evidence in favor of the model. Parameter estimates are reported for the highest ranked model, as indicated by w_i, and 95% confidence intervals were produced using random bootstrap resampling with replacement (5,000 bootstraps) using the 'bootstraps' function in the *rsample* package (Silge et al., 2021) and mapped to the grouped data using the 'map' function in the *purrr* package (Henry and Wickham, 2020). Sampling with replacement assumes that the variation in the sampled group is representative of the population as a whole, and any additional fish collected would fall within the bounds of the sampled group (Kritzer et al., 2001). For models fit to data subsets with small sample sizes where bootstrap confidence intervals produced unrealistic values, the 95% confidence intervals from the likelihood profile are reported.

In total, 1,027 fish were used in the final data set for model selection. The sampled population from Anacapa Island was small (n = 55) so it was grouped with the sampled population from Santa Cruz Island (n = 101) for geographic analyses. Anacapa Island and Santa Cruz Island sites were close to each other and had similar environmental conditions and habitat types (Table 1 and Figure 1). Surface Chl-a was strongly

TABLE 1 Garibaldi (*Hypsypops rubicundus*) collection locations, environmental and geographic information including mean annual sea surface temperature (SST; °C) and mean annual Chlorophyll-a (Chl-a, g C m^{-3}) from January 2002- December 2018.

Location	Reef type	Latitude	Longitude	Mean annual SST (°C)	Mean annual Chl-a (g C m^{-3})	Dates sampled
Santa Cruz Island	Natural	34.01926	-119.53821	17.05	1.233	Aug 2015*, Aug 2017
Anacapa Island	Natural	34.00289	-119.39580	17.15	0.992	Aug 2017
Santa Barbara Island	Natural	33.46439	-119.04280	17.51	0.654	Jan 2019
Santa Catalina Island	Natural	33.43702	-118.50201	18.24	0.607	Aug 2013**, Jul 2014
North Palos Verdes	Natural	33.77567	-118.41960	17.63	2.405	Aug 2013, Jun/Jul 2014, Dec 2015, Nov 2019
King Harbor Breakwater	Artificial	33.84133	-118.39630			Aug/Sept 2013, Mar 2014, Jun 2015, Jan 2016, Mar 2017
South Palos Verdes	Natural	33.72333	-118.34780	17.87	2.166	Oct 2013, Dec 2015
Port of Los Angeles Breakwater	Artificial	33.70726	-118.25460			Jun 2016
Orange County	Natural	33.58706	-117.86900	18.30	1.820	Sept 2018
Dana Point Harbor Breakwater	Artificial	33.45614	-117.69730			Aug 2015, Jun 2018
San Clemente Island	Natural	32.86839	-118.40780	18.25	0.434	Feb 2019
North San Diego	Natural	33.06349	-117.31230	18.48	2.133	May 2018
Oceanside Harbor Breakwater	Artificial	33.20677	-117.39940			May 2018
South San Diego	Natural	32.71210	-117.26300	17.81	2.947	Jun 2018
Zuniga Jetty	Artificial	32.66584	-117.22320			Jun 2018

*Collected by Ben Grime, Kelp Forest Monitoring Program, U.S. National Park Service.
**Collected by Dr. Scott Hamilton, Moss Landing Marine Laboratories, San José State University.
All collections were made by the Vantuna Research Group unless otherwise noted.

correlated with the island/mainland categorization, likely due to localized upwelling events common at island sites (Kilpatrick et al., 2018) and terrestrial runoff at mainland sites (Schiff et al., 2000), so only island/mainland was used as a variable with the understanding that mainland sites often have significantly higher primary productivity than island sites.

Results

There is strong evidence that Garibaldi age and growth patterns vary by sex, reef type, mean annual sea surface temperature, and location within the SCB. The highest ranked model, where model parameters were fitted separately for each sex at each reef type within each location (Table 2; Figure S5 in Supplementary Material), was also the most complex model and received 100% of total Akaike weight (w_i) (Table S4 in Supplementary Material).

Garibaldi demonstrated clear sexual dimorphism in body length with males exhibiting greater mean asymptotic total length (L_∞) than females at each location for each reef type, with only one exception, the artificial reef sampled in North San Diego, Oceanside Harbor Breakwater (Table 2; Figures 2A, S5 in Supplementary Material). In most instances, male-female pairwise L_∞95% confidence intervals did not overlap (Table 2). When data from all reef types and locations were pooled, mean asymptotic length (L_∞) was significantly higher for males (271 mm, 95% CI: 267 to 274 mm) than females (247 mm, 95% CI: 243 to 250 mm), with adult males being 24 mm larger than females on average (Table S5; Figure S8 in Supplementary Material). The greatest difference in L_∞ between sexes was observed at the natural reef site in Orange County, where L_∞ for males was 42 mm larger than for females. In contrast, the L_∞ values between sexes were most similar at the artificial reef in South Palos Verdes, the Port of Los Angeles Breakwater, which differed by only 2 mm (Table 2).

Garibaldi grew significantly larger on artificial reefs than on paired natural reefs across the mainland locations, with females being 26 mm larger (95% CI: 20 to 32 mm) and males 15 mm larger (95% CI: 10 to 20 mm) on average, when data from all sites were pooled (pairwise differences in L_∞; Figure 2B). For the smaller location-specific samples, there were significant pairwise differences (95% CIs did not include 0) for females at all but one location, (mean pairwise difference range: 18 to 36 mm), and males exhibited positive, albeit smaller and not significant pairwise differences at all but one mainland location (mean pairwise difference range: -2 to 24 mm). Female L_∞values from all but one of the artificial reefs were also higher than any natural reef populations including fish from Anacapa and Santa Cruz Islands, which was the northernmost and coolest location sampled (Figure 3). Additionally, the L_∞ of females from the South Palos Verdes artificial reef (i.e., the Los Angeles Harbor breakwater) was still higher than those from almost all natural reefs. In general, males exhibited a similar, but less distinct pattern, interrupted by males from the artificial reef in South Palos Verdes exhibiting relatively low L_∞ and males from natural reef in Orange County and South San Diego exhibiting relatively high L_∞ values (Figure 3).

TABLE 2 Garibaldi (*Hypsypops rubicundus*) von Bertalanffy growth function parameters (bold) for the highest ranked (and most complex) model with bootstrapped 95% confidence intervals.

Population					**Parameters and 95% Confidence Intervals**					
Location	**Reef type**	**Sex**	**n**	**Size (TL mm)**	**L_∞ (mm)**	**95% CI**	**k (yr^{-1})**	**95% CI**	**σ**	**95% CI**
Anacapa & Santa Cruz Islands	Natural	M	65	98 - 307	**280**	274 - 286	**0.18**	0.17 - 0.20	**24**	19 - 28
		F	87	18 - 290	**264**	259 - 269	**0.22**	0.20 - 0.24	**26**	21 - 30
Santa Barbara Island	Natural	M	32	139 - 283	**269**	260 - 277	**0.17**	0.16 - 0.19	**14**	10 - 18
		F	37	122 - 261	**248**	235 - 257	**0.20**	0.18 - 0.24	**23**	18 - 26
Santa Catalina Island	Natural	M	70	29 - 285	**266**	262 - 273	**0.15**	0.13 - 0.16	**18**	15 - 20
		F	77	29 - 278	**247**	243 - 253	**0.17**	0.15 - 0.19	**17**	14 - 19
North Palos Verdes	Natural	M	34	119 - 273	**258**	244 - 270	**0.18**	0.15 - 0.22	**19**	14 - 23
		F	46	107 - 284	**241**	236 - 248	**0.20**	0.18 - 0.23	**17**	11 - 21
	Artificial	M	35	116 - 298	**301**	243 - 315	**0.18**	0.15 - 0.21 *	**20**	14 - 57
		F	17	121 - 275	**279**	234 - 299	**0.20**	0.16 - 0.25 *	**19**	12 - 40
South Palos Verdes	Natural	M	16	180 - 270	**259**	241 - 276	**0.23**	0.20 - 0.28 *	**12**	7 - 23
		F	30	77 - 250	**238**	234 - 242	**0.23**	0.19 - 0.27	**14**	9 - 17
	Artificial	M	32	98 - 278	**258**	233 - 268	**0.27**	0.23 - 0.31 *	**15**	11 - 31
		F	25	103 - 256	**256**	249 - 265	**0.22**	0.19 - 0.25	**16**	11 - 20
Orange County	Natural	M	26	127 - 286	**277**	265 - 297	**0.10**	0.08 - 0.12	**15**	11 - 19
		F	31	118 - 253	**235**	225 - 246	**0.15**	0.13 - 0.18	**15**	11 - 18
	Artificial	M	41	120 - 296	**290**	282 - 301	**0.13**	0.11 - 0.15	**18**	14 - 21
		F	24	132 - 277	**271**	265 - 277	**0.14**	0.13 - 0.15	**8**	6 - 8
San Clemente Island	Natural	M	33	148 - 247	**242**	233 - 254	**0.19**	0.15 - 0.24	**19**	12 - 24
		F	38	126 - 241	**234**	229 - 239	**0.17**	0.15 - 0.20	**13**	9 - 17
North San Diego	Natural	M	19	130 - 254	**255**	240 - 266	**0.16**	0.13 - 0.21	**21**	11 - 29
		F	40	118 - 240	**242**	237 - 249	**0.16**	0.15 - 0.18	**11**	9 - 14
	Artificial	M	32	123 - 276	**269**	231 - 287	**0.19**	0.14 - 0.25 *	**28**	18 - 37
		F	25	142 - 273	**273**	246 - 303	**0.17**	0.13 - 0.24	**24**	17 - 29
South San Diego	Natural	M	25	132 - 286	**278**	267 - 287	**0.14**	0.12 - 0.16	**15**	9 - 19
		F	23	122 - 243	**253**	245 - 271	**0.15**	0.13 - 0.18	**13**	9 - 15
	Artificial	M	45	135 - 287	**282**	274 - 286	**0.12**	0.11 - 0.15	**14**	11 - 17
		F	22	134 - 288	**274**	259 - 269	**0.13**	0.11 - 0.14	**12**	8 - 15

L_∞ is mean asymptotic total length in mm, k describes the yearly rate at which mean TL approaches L_∞, σ is the standard deviation of total length at a given age.
t_0 was not reported because it was fixed to a value of -2.1 years which was determined by fitting the von Bertalanffy growth function to the global population. Bootstrap 95% confidence intervals were reported except in cases where they were unrealistic (noted with an asterisk *), in which case the likelihood profile 95% CIs are reported.

The negative relationship between mean asymptotic total length (L_∞) and mean annual SST was much stronger for natural reefs (male $R^2 = 0.22$, slope = -12.9 mm/°C, 95% CI: -34.6 to 8.8 mm/°C ; female $R^2 = 0.49$, slope = -14.8 mm/°C, 95% CI: -28.4 to -1.3 mm/°C) than at artificial reefs (male $R^2 = 0.09$, slope = -14.2 mm/°C, 95% CI: -97.1 to 68.8 mm/°C; female R^2 =< 0.01, slope = -1.55 mm/°C, 95% CI: -47.9 to 44.9 mm/°C) for both sexes (Figure 3). Among the Channel Islands, growth patterns followed both a latitudinal and SST gradient (Figure 3). Garibaldi from Anacapa and Santa Cruz Islands, the northernmost and coolest location, had the largest L_∞ for both sexes at any island (male L_∞ = 280 mm, female L_∞ = 264 mm) whereas at the southernmost and warmest channel island, San Clemente Island, L_∞ was the smallest at any island for both sexes (male L_∞ = 242 mm, female L_∞ = 234 mm). Mainland sites spanned a smaller range in both latitude and mean annual SST and the patterns were less distinct. The largest L_∞ for Garibaldi from mainland natural reefs was in South San Diego (Point Loma) for both males and females (male L_∞ = 278 mm, female L_∞ = 253 mm). The main difference was for males from natural reefs in Orange County, which were similarly large (L_∞ = 277 mm), while the females were the smallest (L_∞ = 235 mm). Patterns in the growth coefficient (k) are generally more difficult to interpret than those for L_∞ because they are dependent on L_∞ in the von Bertalanffy growth model. However, when k and L_∞ are plotted together, there was also a positive relationship with temperature for both males and females at natural reefs and a less distinct pattern for artificial reefs (Figure S7 in Supplementary Material).

Longevity (T_{max}) exhibited a similar pattern with mean annual SST as observed for L_∞ (Figure 4). Among natural reefs, maximum age (T_{max}) was negatively correlated with mean annual SST (male $R^2 = 0.36$ slope = -14.9 yrs/°C, 95% CI: -32.8 to 3.0 yrs/°C; female R^2 = 0.46, slope = -12.9 yrs/°C, 95% CI: -25.3 to -0.4 yrs/°C). This

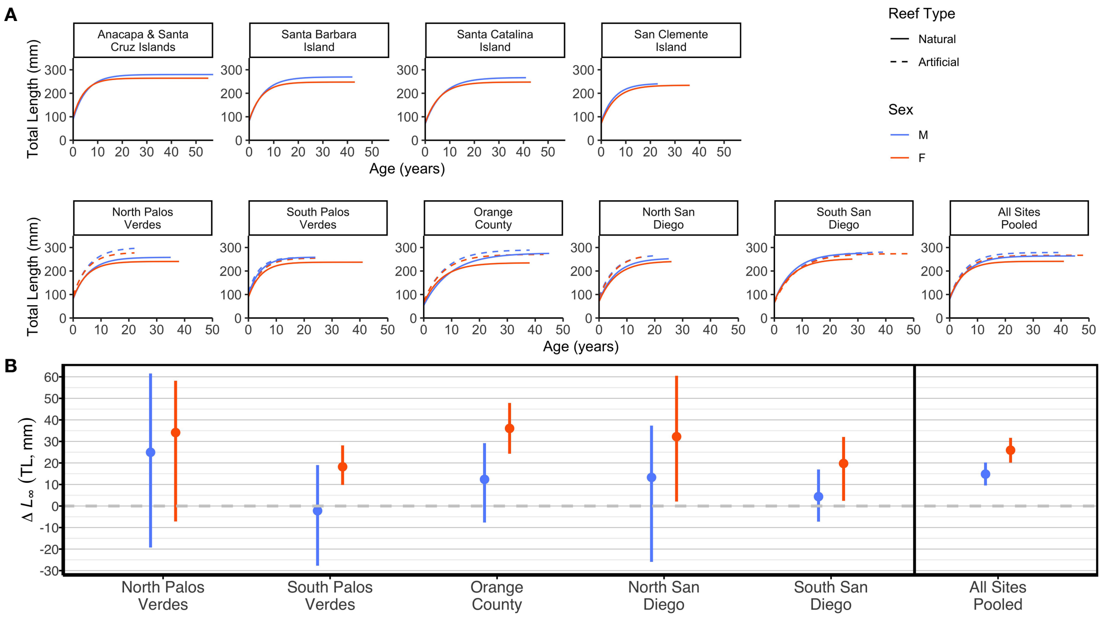

FIGURE 2

(A) Von Bertalanffy growth curves for Garibaldi (*Hypsypops rubicundus)* by sex (color) and reef type (dashed/solid line) for each location (Channel Islands on top and mainland locations below), and all mainland locations pooled fitted using maximum likelihood estimation. **(B)** Mean pairwise difference in L_∞ values by sex (color) between artificial and natural rocky paired sites, and for all mainland sites pooled with bootstrapped 95% confidence intervals. The dashed line at $\Delta L_\infty = 0$ represents no difference between the paired artificial and natural reef sites, with a positive difference indicating adult Garibaldi were larger on the artificial reefs.

supported the hypothesis that fish live longer in colder locations, while there was no relationship for fish from artificial reefs (male $R^2 =< 0.01$, slope = 1.31 yrs/°C, 95% CI: -51.5 to 54.1 yrs/°C; female $R^2 = 0.01$, slope = -4.5 yrs/°C, 95% CI: -76.8 to 67.8 yrs/°C) (Figure 4). The maximum ages of Garibaldi in this study were 57 years for males and 55 years for females (Figures 2, 4; Figures S5, S6, and Table S5 in Supplementary Material). Both fish were collected from Santa Cruz Island, the northernmost location with the coldest mean annual SST. Within locations, fish lived longer on natural reefs compared with their paired artificial reefs, except for the South San Diego population (Table S4 in Supplementary Material). There was no apparent difference in longevity between sexes (Figures S5, S6, and Table S6 in Supplementary Material), although the relationship between mean annual SST and maximum age was stronger for females than for males (Figure 4).

Discussion

Spatial and habitat variability in the life history of Garibaldi is apparent at the relatively small spatial scale of this study with growth patterns differing by reef type, location, and sex. Garibaldi exhibited clear sexual size dimorphism; males grew larger than females in all populations. Garibaldi grew significantly larger on artificial quarry rock reefs (i.e., breakwaters and jetties) compared to natural rocky reefs, but tended to live longer on natural reefs. Regionally, growth and longevity patterns followed gradients in mean annual sea surface temperature, consistent with the hypothesis that Garibaldi are larger and live longer in cooler locations than in warmer locations. Sex-specific average adult asymptotic size (L_∞) was greater for most artificial reef sites than the coldest natural reef sites, indicating, at least across the temperature range sampled, that habitat can have a greater effect than environmental conditions on this life history parameter, particularly for females. The Garibaldi collected for this study had a maximum age of 57 years, which makes them the longest lived of any species of damselfish by two decades (Tzioumis and Kingsford, 1999). Annual otolith increment formation was validated using the *in-situ* tetracycline mark-recapture method which is an ideal technique for age validation for species with high site fidelity (Campana, 2001). This technique is uncommon for fish life history studies conducted in temperate marine systems.

Sexual dimorphism in size was observed within all populations of Garibaldi and agreed with Clarke's (1970) observation that males achieve larger body size than females. This appears to be an unusual trait for damselfish species (Dulčić and Kraljević, 1995; Kim et al., 2016) and nearshore dioicous reef-associated fish in southern California (Love and Westphal,

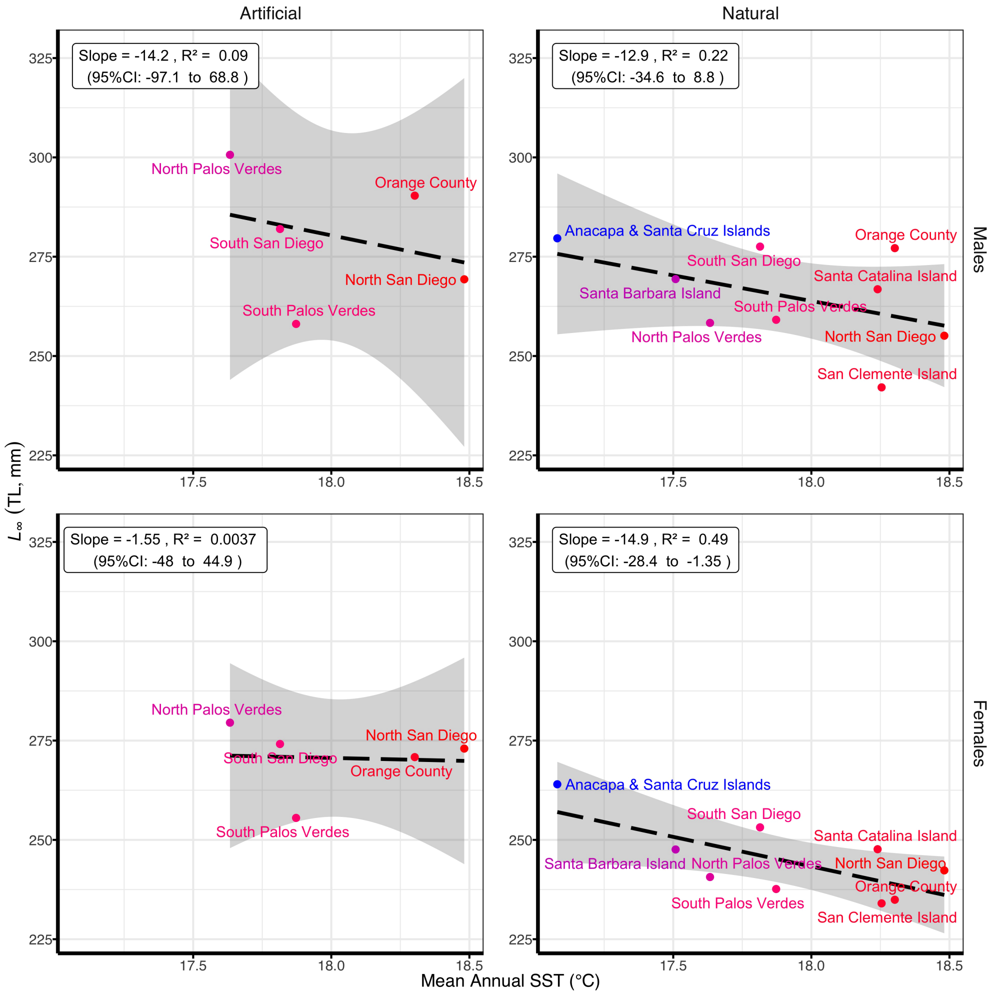

FIGURE 3
Relationship between mean asymptotic total length (L_∞) of Garibaldi (*Hypsypops rubicundus)* from the highest ranked (and most complex) model (Table 2) and mean annual sea surface temperature (SST; °C) for January 2002-December 2018. Locations are colored from a scale of blue (cold) to red (warm).

1981; Love et al., 1987; MacNair et al., 2001; Laidig et al., 2003; Pondella et al., 2008; Grebel and Cailliet, 2010; Williams et al., 2012; Miller et al., 2014), where adult females are typically larger. Only one other damselfish species, the Canary Damsel (*Similiparma lurida*) from the northeastern Atlantic (García-Mederos et al., 2016), shows the same pattern of males growing larger than females. Other than average body size, there are no visually discernable phenotypic sexually dimorphic traits for Garibaldi, as researchers were unable to distinguish between sexes both underwater and in the laboratory. In addition, length-weight relationships were very similar between sexes (Figure S4 in Supplementary Material), which demonstrates that males simply grow larger than females, but there are no apparent body shape or weight differences when at similar lengths. Garibaldi exhibit polygyny, where multiple females sequentially lay eggs in one male's nest site. Females visit multiple nest sites before selecting one for spawning, and tend to prefer nests that have a high percentage of dense turf algae and contain eggs in the early phase of development (i.e., another female had deposited eggs there less than 5 days prior) (Sikkel, 1988; Sikkel, 1989; Sikkel, 1994; Sikkel, 1995). Sikkel 1988; 1989 also found that male size was correlated with female nest preference, and posited that male size is correlated with nest quality, although the relationship between the two variables was not strong. Further, large males may be more successful in the defense of their nesting sites (Sikkel, 1995), suggesting that females are choosing mates based on size.

For mainland locations, Garibaldi grew larger on average (L_∞) at artificial reefs than at paired natural reefs. The breakwater and jetty artificial reefs sampled in this study were primarily built to protect coastal infrastructure and were made up of large (1-2 m) quarry rock boulders, providing a complex

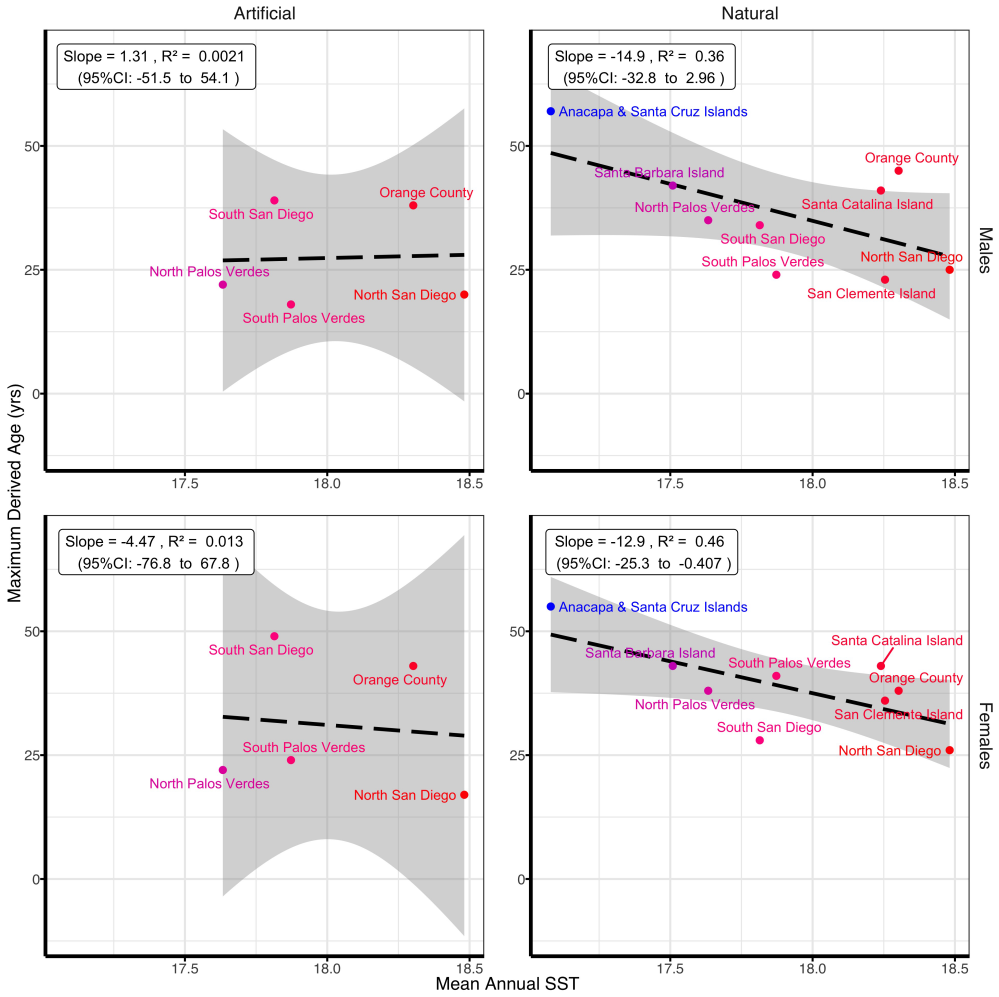

FIGURE 4
Relationship between maximum derived age (life span) of Garibaldi (*Hypsypops rubicundus)* and mean annual sea surface temperature (SST; °C) for January 2002-December 2018. Locations are colored from a scale of blue (cold) to red (warm).

and ideal habitat with vertical rock surfaces and several open spaces for Garibaldi to maintain territories (Stephens et al., 1994; Cook, 2011). Natural rocky reefs within the SCB, although much larger in area, characteristically have lower vertical relief and less habitat complexity than breakwaters (Pondella et al., 2015b). For rocky reefs within the SCB, vertical relief and variation in vertical relief is correlated with increased fish density, biomass, and production (Ambrose and Swarbrick, 1989; Pondella et al., 2002; Pondella et al., 2018; Pondella et al., 2019) indicating that more complex reefs are more productive than homogenous habitats. Garibaldi from artificial reefs grew significantly larger, on average, than fish on natural reefs (sexes pooled, artificial L_∞ = 276, 95% CI: 271 to 281 mm; natural L_∞ = 252; 95% CI: 249 to 255 mm) (Table S7 and Figure S10 in Supplementary Material). However, the largest Garibaldi were from natural reefs at Anacapa & Santa Cruz Islands (290 mm TL for females, 307 mm TL for males). This may be due to not sampling artificial habitats in coolest locations, where fish tend to be larger overall, and sampling effort being greater overall for natural reefs (n = 732) than for artificial reefs (n = 298).

Garibaldi from South Palos Verdes and South San Diego did not exhibit as strong of a difference in growth patterns between natural and artificial habitats as the other mainland locations. Both the natural and artificial reefs at South Palos Verdes are degraded habitats, which may have affected growth. The natural rocky reef (Bunker Point) is characterized by low structural relief and is impacted by sedimentation from ongoing landslides from 1956 to present, resulting in reef burial, scour, and chronic turbidity (Pondella et al., 2018). Scour and sedimentation affect benthic sessile invertebrate communities (e.g., sponges, anemones), the primary component in the diet of Garibaldi, interfering with filter and suspension feeding, or by denuding or burying the reef and eliminating sessile invertebrates entirely in severe instances (Figurski et al., 2016). In addition, the reduction in light intensity due to persistent turbidity limits benthic algal recruitment and growth (Airoldi and Virgilio, 1998; Gibson and Atkinson, 2003), which is necessary for successful nest-building (Sikkel, 1995). The South Palos Verdes artificial reef (Port of Los Angeles breakwater) borders the busiest harbor in the United States. In South San Diego, both natural (Point Loma) and artificial (Zuniga Jetty) reefs are adjacent to San Diego Bay, a highly urbanized estuary and home to the Port of San Diego. Point Loma is an expansive shelf of natural reef characterized by low relief bedrock with minimal slope and lacking boulders that would provide hiding spaces and good habitat for Garibaldi. Unlike the other breakwaters sampled, Zuniga Jetty is often fully submerged and Garibaldi typically recruit to rocky reefs depths of less than 5m (Clarke, 1970). The distance from the shallow subtidal to the reef where fish were collected at Point Loma, compounded with the relatively high density of adult Garibaldi (Cook, 2011) and skewed sex ratio (2/3 of fish were male) at Zuniga Jetty could explain why natural and artificial reefs in South San Diego are performing similarly in relation to Garibaldi growth patterns.

Growth and longevity patterns followed gradients in mean annual sea surface temperature with fish getting larger and living longer in cooler environments than in warmer environments, particularly for females from natural reefs. This is a common intraspecific pattern in damselfishes and marine fishes in general and has been observed on spatial scales larger and smaller than the present study (Meekan et al., 2001; Choat and Robertson, 2002; Choat et al., 2003; Ruttenberg et al., 2005; Hamilton et al., 2011; Trip et al., 2014; Taylor et al., 2019). Within the SCB, this pattern of fish growing larger at cooler locations has also been observed in the California Sheephead (*Bodianus pulcher*), a fished protogynous hermaphroditic wrasse (Hamilton et al., 2011) and in recreationally and commercially targeted conspecific rockfish species (Scorpaenidae: *Sebastes*) (Love et al., 1990). Further, California Halibut (*Paralichthys californicus*) grew larger in the cooler waters of central California than in southern California (MacNair et al., 2001). The pattern in the present study was not as strong as in other studies, likely due to the mean annual SST values throughout the SCB varying by only ~ 1.5°C. Further, sample sizes were relatively small for a given location, especially when grouping populations by sex, which can increase variability in estimates of L_∞ and T_{max} (Kritzer et al., 2001). The relationship between age and growth and SST was not present for Garibaldi from artificial reefs, but these reefs spanned a lower temperature range than natural reefs. Further, annual and seasonal temperature patterns in the SCB are dynamic (Dong et al., 2009; Kim and Cornuelle, 2015) and long-term annual SST means over the relatively small spatial scale may not be indicative of the environmental conditions that influence Garibaldi life history at local scales. Finally, fish were collected opportunistically over a six-year period, with some locations only being visited once and others being visited multiple times. Differences in sample dates across some sites could mean that the younger fish in a sample may have experienced different environmental conditions during their early faster growth years prior to when they were collected, possibly confounding temporal and spatial effects on growth. However, this was unlikely to affect the major results of our study. Most natural-artificial reef pairs were collected in the same or similar sets of years. Further, we focused our comparisons mostly on estimates of L_∞, and for the long-lived Garibaldi, this parameter is going to primarily be determined by the 10- to 40-year-old fish in our sample which would not be impacted by the relatively small differences in collection dates.

Garibaldi have a much longer lifespan than has previously been reported. The next longest lifespan for a Pomacentrid is for the White-Ear Scalyfin (*Parma microlepis*) endemic to Eastern Australia at 37 years maximum age (Tzioumis and Kingsford, 1999), and most damselfishes considered to be "long-lived" live to be only 10-20 years old (Fowler, 1990; Fowler and Doherty, 1992; Kohda, 1996; Meekan et al., 2001; Schwamborn and Ferreira, 2002; Ruttenberg et al., 2005). Maximum age for both sexes was negatively correlated with mean annual SST for natural reefs, supporting the hypothesis that fish live longer in colder locations. There was also no apparent difference in longevity between sexes although the relationship between mean annual SST and maximum age was stronger for females than for males. The oldest 55-year-old female and 57-year- old male were from the highest latitude and the coolest Santa Cruz Island location. It is important to note that mean annual SST and latitude do not follow the same pattern within the SCB due to the complex current system. The furthest south location, South San Diego had the second oldest female fish (49 years) and is cooler than locations that are further north due to the Southern California Countercurrent (Table 1; Figure 1). There were consistently multiple fish around 40 years old collected from many sites (Table S4, Figure S6 in Supplementary Material). The long lifespan of this species and relatively small sample sizes for each site and sex, make it less likely to collect very old fish and thus limits the ability to make precise longevity comparisons across sites.

This study has demonstrated that habitat and environmental conditions can have a substantial effect on localized age and growth patterns in the absence of fishing effects. Our results contribute to the growing body of evidence that age and growth patterns for marine fish vary spatially and among habitats, even at small geographical scales. In addition, this study provided location-, habitat- and sex-specific parameters enabling researchers to effectively apply appropriate life history traits for specific localities to estimate secondary production (e.g., Claisse et al., 2014, Granneman and Steele, 2014) and as a basis to further investigate differences in habitat quality. The effects of habitat and temperature on both age and growth patterns were stronger for female Garibaldi than for males.

Behavioral factors such as sexual selection and competition amongst males for apparently preferable nesting sites (Sikkel, 1988; Sikkel, 1989; Sikkel, 1995) may play a larger role in shaping the localized life history patterns for male Garibaldi than for females. Additional variability in male growth rates and longevity could result from variability in energy expenditures for territoriality, courting behaviors, nest defense, and/or differences in habitat quality at the scale of individual male territories. That adult female Garibaldi grow significantly larger on artificial reefs is a potential indicator of habitat quality and may have regional population-level implications. Estimates of total reproductive-energy output (i.e., combining fecundity, egg size, egg energy content) per spawn scaled hyperallometrically with body size for Garibaldi and other demersal spawning damselfish species, and therefore larger mothers contribute disproportionately to population replenishment (Barneche et al., 2018). The amount of human-built structures in the marine environment is expected to increase in the coming decades with the continued expansion of marine infrastructure associated with activities such as port construction, marine aquaculture, sea level rise adaptation, and marine renewable energy development (Tickell et al., 2019; Bugnot et al., 2020), and with the growing interest to design artificial reefs for reef habitat restoration and mitigation (e.g., Pondella et al., 2006; Reed et al., 2006; Pondella et al., 2018; Komyakova et al., 2019) and/or for fisheries enhancement (e.g., Polovina and Sakai, 1989; Santos et al., 2011; Roa-Ureta et al., 2019). Fish life history studies that compare ecological performance across habitat types, such as this one, are essential to inform the design and assessment of these future reefing projects.

Data availability statement

The raw data supporting the conclusions of this article will be made available by the authors, without undue reservation.

Ethics statement

The animal study was reviewed and approved by Institutional Care and Use Committees at both Cal Poly Pomona and Occidental College.

Author contributions

CW envisioned the project, managed and contributed to field work and dissections, performed computational analyses, and wrote the manuscript. JE contributed to field work and dissections, prepared histological preparations of gonads and performed microscopic determination of sex. DP contributed to field work and writing. JC envisioned the project, contributed to field work, and oversaw writing and data analysis. All authors contributed to the article and approved the submitted version.

Funding

Funding for this project was provided by the Vantuna Research Group at Occidental College, the Claisse Lab at Cal Poly Pomona, the Southern California Academy of Sciences, the American Society of Ichthyologists and Herpetologists, the Department of Biological Sciences at Cal Poly Pomona, the Western Society of Naturalists, and CSU Council on Ocean Affairs, Science & Technology (COAST) and the University of Southern California Sea Grant Program through a Sea Grant Traineeship to C. M. Williams.

Acknowledgments

This project, particularly the field component, was an immense undertaking and would not have been completed without the help of several people. Thanks to those who participated in field collections, dissections, and gonad histological preparations, particularly J. Williams, M. Robart, M. Hansler, B. Power, B. Grime, A. Pyles, J. Eagleton, Z. Scholz, S. Schwab, A. Obaza, C. Pollock, D. Erana, K. Lau, E. Jaco, S. Soule, A. Sugimoto, A. Roeper, C. Pollock, G. Coogan, H. Hoefs, M. Winston, N. Myers, R. Stokes, S. Moffly, S. Akiyama, S. Ashey, S. D'Orazio, S. Franck, E. Liang, G. Yang, J. Sturges, and B. Calderon. Several Garibaldi were collected from Catalina Island by Dr. S. Hamilton at Moss Landing Marine Laboratories. J. Davis, C. Dobbins, K. Walker at California Department of Fish and Wildlife provided ship time to collect Garibaldi at Santa Cruz and Anacapa Islands. We thank the anonymous reviewers for their careful reading, insightful comments, and suggestions that improved the quality of this manuscript. The content of this manuscript was previously published as a master's thesis (Williams, 2021) and benefitted greatly from the guidance of committee members A. Zellmer, A. Bonisoli-Alquati, and Á. Valdés.

Conflict of interest

The authors declare that the research was conducted in the absence of any commercial or financial relationships that could be construed as a potential conflict of interest.

Publisher's note

All claims expressed in this article are solely those of the authors and do not necessarily represent

Supplementary material

The Supplementary Material for this article can be found online at: https://www.frontiersin.org/articles/10.3389/fmars.2022.988158/full#supplementary-material

References

Airoldi, L., and Virgilio, M. (1998). Responses of turf-forming algae to spatial variations in the deposition of sediments. *Mar. Ecol. Prog. Ser.* 165, 271–282. doi: 10.3354/meps165271

Alcalay, O. M., and Sikkel, P. C. (1994). Diel periodicity of hatching of demersal eggs in the temperate damselfish, *Hypsypops rubicundus*. *Bull. Mar. Sci.* 54 (2), 565–569.

Allen, G. R. (1991). *Damselfishes of the world* (Melle, Germany: MERGUS Publishers).

Allen, L. G., and Pondella II, D. J. (2006). "Ecological Classification," in *The ecology of marine fishes: California and adjacent waters*. Eds. L. G. Allen, D. J. Pondella II and M. Horn (Los Angeles, CA: University of California Press), 81–113.

Ambrose, R. F., and Swarbrick, S. L. (1989). Comparison of fish assemblages on artificial and natural reefs off the coast of southern California. *Bull. Mar. Sci.* 44, 718–733.

Anderson, D. R. (2008). *Model based inferences in the life sciences: A primer on evidence* (New York, New York, USA: Springer Science + Business Media, LLC).

Atkinson, D. (1994). Temperature and organism size - a biological law for ectotherms? *Adv. Ecol. Res.* 25, 1–58. doi: 10.1016/0306-4565(94)00028-H

Atkinson, D. (1996). "Ectotherm life-history responses to developmental temperature," in *Animals and temperature: Phenotypic and evolutionary adaptation*. Eds. I. A. Johnston and A. F. Bennett (New York: Cambridge University Press), 183–204.

Atkinson, D., and Sibly, R. M. (1997). Why are organisms usually bigger in colder environments? making sense of a life history puzzle. *Trends Ecol. Evol.* 12 (6), 235–239. doi: 10.1016/S0169-5347(97)01058-6

Audzijonyte, A., Fulton, E., Haddon, M., Helidoniotis, F., Hobday, A. J., Kuparinen, A., et al. (2016). Trends and management implications of human-influenced life-history changes in marine ectotherms. *Fish Fish.* 7, 1005–1028. doi: 10.1111/faf.12156

Barilotti, A. A., White, C. F., and Lowe, C. G. (2020). Are fishes attracted to piers? Movements and association of marine fishes to a public fishing pier within a commercial harbor. *Bulletin South. Cal. Acad. Sci.* 119 (1), 18–34. doi: 10.3160/0038-3872-119.1.18

Barneche, D. R., Robertson, D. R., White, C. R., and Marshall, D. J. (2018). Fish reproductive-energy output increases disproportionately with body size. *Science* 360 (6389), 642–645. doi: 10.1126/science.aao6868

Beamish, R. J., and McFarlane, G. A. (1995). "A discussion of the importance of aging errors, and an application to walleye pollock: the world 's largest fishery," in *Recent developments in fish otolith research*. Eds. D. H. Secor, J. M. Dean and S. E. Campana (Columbia: University of South Carolina Press).

Berumen, M. L. (2005). The importance of juveniles in modelling growth: butterflyfish at lizard island. *Environ. Biol. Fish.* 72 (4), 409–413. doi: 10.1007/s10641-004-2595-0

Beverton, R. J. H., and Holt, S. J. (1959). "A review of the lifespans and mortality rates of fish in nature, and their relation to growth and other physiological characteristics," in *Ciba foundation symposium - the Lifespan of animals, colloquia on aging*. (Boston, MA: Little, Brown), 142–180.

Bolker, B., R Core Development Team (2020). *Bbmle: Tools for general maximum likelihood estimation. R package version 1.0.23.1*.

Bugnot, A. B., Mayer-Pinto, M., Airoldi, L., Heery, E. C., Johnston, E. L., Critchley, L. P., et al. (2020) Current and projected global extent of marine built structures. *Nat. Sustain.* doi: 10.1038/s41893-020-00595-1

Burnham, K. P., and Anderson, D. R. (2002). *Model selection and multimodel inference, a practical information-theoretic approach* (New York, New York, USA: Springer Science + Business Media, LLC).

Burns, E. S., Clevenstine, A. J., Logan, R. K., and Lowe, C. G. (2020). Evidence of artificial habitat use by a recovering marine predator in southern California. *J. Fish Biol.* 97 (6), 1857–1860. doi: 10.1111/jfb.14539

Campana, S. E. (2001). Accuracy, precision and quality control in age determination, including a review of the use and abuse of age validation methods. *J. Fish Biol.* 59, 197–242. doi: 10.1111/j.1095-8649.2001.tb00127.x

Cappo, M., Eden, P., Newman, S. J., and Robertson, S. (2000). A new approach to validation of periodicity and timing of opaque zone formation in the otoliths of eleven species of *Lutjanus* from the central great barrier reef. *Fish. Bull.* 98, 474–488.

Caselle, J. E., Hamilton, S. L., Schroeder, D. M., Love, M. S., Standish, J. D., Rosales-Casian, J. A., et al. (2011). Geographic variation in density, demography, and life history traits of a harvested, sex-changing, temperate reef fish. *Can. J. Fish. Aquat. Sci.* 68 (2), 288–303. doi: 10.1139/f10-140

Choat, J. H., and Axe, L. M. (1996). Growth and longevity in fishes of the family scaridae. *Mar. Ecol. Prog. Ser.* 145, 33–41. doi: 10.3354/meps145033

Choat, J. H., and Robertson, D. R. (2002). "Age-based studies," in *Coral reef fishes: dynamics and diversity in a complex ecosystem* (San Diego, California, USA: Academic Press), 57–80.

Choat, J. H., Robertson, D. R., Ackerman, J. L., and Posada, J. M. (2003). An age-based demographic analysis of the Caribbean stoplight parrotfish *Sparisoma viride*. *Mar. Ecol. Prog. Ser.* 246, 265–277. doi: 10.3354/meps246265

Claisse, J. T. (2009). *The life history and movements of yellow tang, Zebrasoma flavescens, with implications for fisheries management using protected areas* (Manoa: University of Hawaii).

Claisse, J. T., Kienzle, M., Bushnell, M. E., Shafer, D. J., and Parrish, J. D. (2009). Habitat- and sex-specific life history patterns of yellow tang *Zebrasoma flavescens* in Hawaii, USA. *Mar. Ecol. Prog. Ser.* 389, 245–255. doi: 10.3354/meps08114

Claisse, J. T., Love, M. S., Meyer-Gutbrod, E. L., Williams, C. M., Pondella, D. J. II, and Daniel, J. (2019). Fishes with high reproductive output potential on California offshore oil and gas platforms. *Bull. Mar. Sci.* 95 (4), 515–534. doi: 10.5343/bms.2019.0016

Claisse, J. T., Pondella, D. J. II, Love, M., Zahn, L. A., Williams, C. M., Williams, J. P., et al. (2014). Oil platforms off California are among the most productive marine fish habitats globally. *Proc. Natl. Acad. Sci. USA* 111 (43), 15462–15467. doi: 10.1073/pnas.1411477111

Clarke, T. A. (1970). Territorial behavior and population dynamics of a pomacentrid fish, the Garibaldi *Hypsypops rubicunda*. *Ecol. Soc. America* 40 (2), 189–212. doi: 10.2307/1942295

Clarke, T. A. (1971). Territory boundaries, courtship, and social behavior in the garibaldi, *Hypsypops rubicunda* (Pomacentridae). *Copeia* 1971, 295–299. doi: 10.2307/1442830

Cook, G. S. (2011). *Rocky reef fish connectivity: Patterns, processes, and population dynamics* (San Diego: University of California).

DeMartini, E. E., Barnett, A. M., Johnson, T. D., and Ambrose, R. F. (1994). Growth and production estimates for biomass-dominant fishes on a southern California artificial reef. *Bull. Mar. Sci.* 55, 484–500.

DeMartini, E. E., Roberts, D. A., and Anderson, T. W. (1989). Contrasting patterns of fish density and abundance at an artificial rock reef and a cobble-bottom kelp forest. *Bull. Mar. Sci.* 44 (2), 881–892.

Dong, C., Idica, E. Y., and McWilliams, J. C. (2009). Circulation and multiple-scale variability in the Southern California Bight. *Prog. Oceanogr.* 82 (3), 168–190. doi: 10.1016/j.pocean.2009.07.005

Dulčić, J., and Kraljević, M. (1995). Age, growth and mortality of damselfish (*Chromis chromis* l.) in the eastern middle Adriatic. *Fish. Res.* 22 (3-4), 255–264. doi: 10.1016/0165-7836(94)00318-Q

Engle, J. (1993). "Distribution patterns of rocky subtidal fishes around the California islands," in *Third California islands symposium: recent advances in research on the California islands* (Santa Barbara, California, USA: Santa Barbara Museum of Natural History), 475–484.

Figueira, W. F., Lyman, S. J., Crowder, L. B., and Rilov, G. (2007). Small-scale demographic variability of the biocolor damselfish, *Stegastes partitus*, in the Florida keys USA. *Environ. Biol. Fish.* 81 (3), 297–311. doi: 10.1007/s10641-007-9201-1

Figurski, J. D., Freiwald, J., Lonhart, S. I., and Storlazzi, C. D. (2016). Seasonal sediment dynamics shape temperate bedrock reef communities. *Mar. Ecol. Prog. Ser.* 552, 19–29. doi: 10.3354/meps11763

Fonseca, V., and Cabral, H. (2007). Are fish early growth and condition patterns related to life-history strategies? *Rev. Fish Biol. Fish.* 17 (4), 545–564. doi: 10.1007/s11160-007-9054-x

Forsberg, J. E. (2001). "Aging manual for pacific halibut: procedures and methods used at the International pacific halibut commission", in *International Pacific Halibut Commission Technical Report 46.* (Seattle, WA).

Foster, M. S. (1972). "The algal turf community in the nest of the ocean goldfish, *Hypsypops rubicunda*," in *Proceedings of the 7th international seaweed symposium.* Ed. K. Nisizawa (Japan: University of Tokyo Press), 55–60.

Fowler, A. J. (1990). Validation of annual growth increments in the otoliths of a small, tropical coral reef fish. *Mar. Ecol. Prog. Ser. Oldendorf* 64 (1), 25–38. doi: 10.3354/meps064025

Fowler, A. J., and Doherty, P. J. (1992). Validation of annual growth increments in the otoliths of two species of damselfish from the southern great barrier reef. *Mar. Freshw. Res.* 43 (5), 1057–1068. doi: 10.1071/MF9921057

Francis, M. P., and Francis, R. I. C. C. (1992). Growth rate estimtes for new Zealand rig (*Mustelus lenticulatus*). *Aust. J. Freshw. Res.* 43, 1157–1176. doi: 10.1071/MF9921157

García-Mederos, A. M., Tuya, F., and Tuset, V. M. (2016). Life-history strategies of a conspicuous reef fish, the canary damsel *Similiparma lurida* (Pomacentridae) in the northeastern Atlantic. *Sci. Mar.* 8 (1), 57–68. doi: 10.3989/scimar.04343.28A

Gibson, R. N., and Atkinson, R. J. A. (2003). The effects of sedimentation on rocky coast assemblages. *Oceanogr. Mar. Biol.: an Annu. Rev.* 41, 161–236. doi: 10.1201/9780203180570-23

Granneman, J. E. (2011). *A comparison of fish production on artifical and natural reefs in southern California* (Northridge: California State University).

Granneman, J. E., and Steele, M. A. (2014). Fish growth, reproduction, and tissue production on artificial reefs relative to natural reefs. *ICES J. Mar. Sci.* 71 (9), 2494–2504. doi: 10.1093/icesjms/fsu082

Granneman, J. E., and Steele, M. A. (2015). Effects of reef attributes on fish assemblage similarity between artificial and natural reefs. *ICES J. Mar. Sci.* 72 (8), 2385–2397. doi: 10.1093/icesjms/fsv094

Grebel, J. M., and Cailliet, G. M. (2010). Age, growth, and maturity of cabezon (*Scorpaenichthys marmoratus*) in California. *Cal. Fish Game* 96 (1), 36–52.

Hamilton, S. L., Caselle, J. E., Standish, J. D., Schroeder, D. M., Love, M. S., Rosales-Casian, J. A., et al. (2007). Size-selective harvesting alters life histories of a temperate sex-changing fish. *Ecol. Appl.* 17 (8), 2268–2280. doi: 10.1890/06-1930.1

Hamilton, S. L., Wilson, J. R., Ben-Horin, T., and Caselle, J. E. (2011). Utilizing spatial demographic and life history variation to optimize sustainable yield of a temperate sex-changing fish. *PloS One* 6 (9), e24580. doi: 10.1371/journal.pone.0024580

Henry, L., and Wickham, H. (2020). *Purrr: Functional programming tools. R package version 0.3.4.*

Hickey, B. M. (1992). Circulation over the Santa Monica-San Pedro basin and shelf. *Prog. Oceanogr.* 30 (1-4), 37–115. doi: 10.1016/0079-6611(92)90009-O

Hjelm, J., Persson, L., and Christensen, B. (2000). Growth, morphological variation and ontogenetic niche shifts in perch (*Perca fluviatilis*) in relation to resource availability. *Oecologia* 122(2):190–199. doi: 10.1007/PL00008846

Hsieh, C.-h., Yamauchi, A., Nakazawa, T., and Wang, W.-F. (2009). Fishing effects on age and spatial structures undermine population stability of fishes. *Aquat. Sci.* 72(2):165–178. doi: 10.1007/s00027-009-0122-2

Jennings, S., and Dulvy, N. K. (2008). Beverton and Holt's insights into life history theory: Influence, application and future use. *Adv. Fish. Sci.* 50, 434–450. doi: 10.1002/9781444302653.ch18

Kilpatrick, T., Xie, S. P., Miller, A. J., and Schneider, N. (2018). Satellite observations of enhanced chlorophyll variability in the Southern California Bight. *J. Geophys. Res.: Ocean.* 123 (10), 7550–7563. doi: 10.1029/2018JC014248

Kim, S. Y., and Cornuelle, B. D. (2015). Coastal ocean climatology of temperature and salinity off the Southern California Bight: Seasonal variability, climate index correlation, and linear trend. *Prog. Oceanogr.* 138, 136–157. doi: 10.1016/j.pocean.2015.08.001

Kim, H., Na, J., and Oh, C. W. (2016). Age and growth of damselfish *Chromis notata* (Temminck & schlegel 1843), Jeju Island, Korea. *J. Appl. Ichthyol.* 32 (6), 1179–1185. doi: 10.1111/jai.13137

King, J., and McFarlane, G. (2003). Marine fish life history strategies: applications to fishery management. *Fish. Manage. Ecol.* 10 (4), 249–264. doi: 10.1046/j.1365-2400.2003.00359.x

Kohda, M. (1996). A damselfish living for more than 15 years: a longevity record for small reef fishes. *Ichthyol. Res.* 43 (4), 459–462. doi: 10.1007/BF02347643

Komyakova, V., Chamberlain, D., Jones, G. P., and Swearer, S. E. (2019). Assessing the performance of artificial reefs as substitute habitat for temperate reef fishes: Implications for reef design and placement. *Sci. Total Environ.* 668, 139–152. doi: 10.1016/j.scitotenv.2019.02.357

Kritzer, J. P., Davies, C. R., and Mapstone, B. D. (2001). Characterizing fish populations: effects of sample size and population structure on the precision of demographic parameter estimates. *Can. J. Fish. Aquat. Sci.* 58 (8), 1557–1568. doi: 10.1139/cjfas-58-8-1557

Kritzler, H., Fox, D. L., Hubbs, C. L., and Crane, S. C. (1950). Carotenoid pigmentation of the pomacentrid fish *Hypsypops rubicunda*. *Copeia* 1950 (2), 125–138. doi: 10.2307/1438955

Laidig, T. E., Pearson, D. E., and Sinclair, L. L. (2003). Age and growth of blue rockfish (*Sebastes mystinus)* from central and Northern California. *Fish. Bull.* 101 (4), 800–808.

Lewis, R. D., and McKee, K. K. (1989). A guide to the artificial reefs of southern California. *Dep. Fish Game Sacramento Cal.* 73, 1–67.

Limbaugh, C. (1964). Notes on the life history of two Californian pomacentrid: Garibaldis, *Hypsypops rubicunda* (Girard), and blacksmiths, *Chromis punctipinnis* (Cooper). *Pac. Sci.* 18, 41–50.

Love, M. S., Axell, B., Morris, P., Collins, R., and Brooks, A. (1987). Life history and fishery of the California scorpionfish, *Scorpaena guttata*, within the Southern California Bight. *Fish. Bull.* 85 (1), 99–116.

Love, M. S., Brothers, E. B., Schroeder, D., and Lenarz, W. H. (2007). Ecological performance of young-of-the-year blue rockfish (*Sebastes mystinus)* associated with oil platforms and natural reefs in California as measured by daily growth rates. *Bull. Mar. Sci.* 80 (1), 147–157.

Love, M. S., Claisse, J. T., and Roeper, A. (2019). An analysis of the fish assemblages around 23 oil and gas platforms off California with comparisons with natural habitats. *Bull. Mar. Sci.* 95 (4), 477–514. doi: 10.5343/bms.2018.0061

Love, M. S., Morris, P., McCrae, M., and Collins, R. (1990). Life history aspects of 19 rockfish species (Scorpaenidae: *Sebastes*) from the Southern California Bight. *NOAA Tech. Rep. NMFS* 827, 1–38.

Love, M. S., and Westphal, W. V. (1981). Growth, reproduction, and food habits of olive rockfish, *Sebastes serranoides*, off central California. *Fish. Bull.* 79, 533–543.

MacNair, L. S., Domeier, M. L., and Chun, C. S. (2001). Age, growth, and mortality of California halibut, *Paralichthys californicus*, along southern and central California. *Fish. Bull.* 99 (4), 588–601.

Mangel, M., and Abrahams, M. V. (2001). Age and longevity in fish, with consideration of the ferox trout. *Exp. Gerontol.* 36 (4-6), 765–790. doi: 10.1016/S0531-5565(00)00240-0

Meekan, M., Ackerman, J., and Wellington, G. (2001). Demography and age structures of coral reef damselfishes in the tropical eastern pacific ocean. *Mar. Ecol. Prog. Ser.* 212, 223–232. doi: 10.3354/meps212223

Miller, E. F., Pondella, D. J., and Goldberg, S. (2014). Life history and historic trends in salema (*Haemulon californiensis*) in Southern California. *Cal. Coop. Ocean. Fish. Invest. Prog. Rep.* 55, 144–157.

Nelson, J. S., Grande, T. C., and Wilson, M. V. H. (2016). *Fishes of the world. 5th edition* (Hoboken, New Jersey: John Wiley & Sons, Inc).

Polovina, J. J., and Sakai, I. (1989). Impacts of artificial reefs on fishery production in Shimamaki, Japan. *Bull. Mar. Sci.* 44 (2), 997–1003.

Pondella, D. J. II, Allen, L. G., Craig, M. T., and Gintert, B. (2006). Evaluation of eelgrass mitigation and fishery enhancement structures in San Diego Bay, California. *Bull. Mar. Sci.* 78 (1), 115–131.

Pondella, D. J. II, Caselle, J. E., Claisse, J. T., Williams, J. P., Davis, K., Williams, C. M., et al. (2015a). "Baseline characterization of the shallow rocky reef and kelp forest ecosystems of the south coast study region," in *South coast baseline program final report: Kelp and shallow rock ecosystems. SCMPA-27.*

Pondella, D. J. II, Froeschke, J. T., Wetmore, L. S., Miller, E., Valle, C. F., and Medeiros, L. (2008). Demographic parameters of yellowfin croaker, *Umbrina roncador* (Perciformes: Sciaenidae), from the Southern California Bight. *Pac. Sci.* 62 (4), 555–568. doi: 10.2984/1534-6188(2008)62[555:DPOYCU]2.0.CO;2

Pondella, D. J. II, Piacenza, S. E., Claisse, J. T., Williams, C. M., Williams, J. P., Zellmer, A. J., et al. (2019). Assessing drivers of rocky reef fish biomass density from the Southern California Bight. *Mar. Ecol. Prog. Ser.* 628, 125–140. doi: 10.3354/meps13103

Pondella, D. J. II, and Stephens, J. S. (1994). Factors affecting the abundance of juvenile fish species on a temperate artificial reef. *Bull. Mar. Sci.* 55 (2-3), 1216–1223.

Pondella, D. J. II, Stephens, J. S., and Craig, M. T. (2002). Fish production of a temperate artificial reef based on the density of embiotocids (Teleostei: Perciformes). *ICES J. Mar. Sci.* 59, S88–S93. doi: 10.1006/jmsc.2002.1219

Pondella, D. J. II, Williams, J. P., Claisse, J. T., Schaffner, R., Ritter, K., and Schiff, K. (2015b). The physical characteristics of nearshore rocky reefs in the Southern

California Bight. *Bull. South. Cal. Acad. Sci.* 114 (3), 105–122. doi: 10.3160/soca-114-03-105-122.1

Pondella, D. J. II, Williams, J. P., Williams, C. M., Claisse, J.T., and Witting, D (2018). “Restoring a nearshore rocky reef ecosystem in the challenge of an urban setting,”S Bortone Marine Artificial Reef Research and Development: Integrating Fisheries Management Objectives Location: Bethesda, MD:American Fisheries Society Symposium. 86, 165–186

R Core Development Team (2021). “R: A language and environment for statistical computing,” in *R foundation for statistical computing* (Vienna, Austria: R Core Development Team 2021). Available at: http://www.R-project.org.

Reed, D. C., Schroeter, S. C., Huang, D., Anderson, T. W., and Ambrose, R. F. (2006). Quantitative assessment of different artificial reef designs in mitigating losses to kelp forest fishes. *Bull. Mar. Sci.* 78 (1), 133–150.

Roa-Ureta, R. H., Santos, M. N., and Leitão, F. (2019). Modelling long-term fisheries data to resolve the attraction versus production dilemma of artificial reefs. *Ecol. Model.* 407, 1–12. doi: 10.1016/j.ecolmodel.2019.108727

Robertson, D. R., Choat, J. H., Posada, J. M., Pitt, J., and Ackerman, J. L. (2005). Ocean surgeonfish *Acanthurus bahianus.* II. Fishing effects on longevity, size and abundance? *Mar. Ecol. Prog. Ser.* 295, 245–256. doi: 10.3354/meps295245

Ruttenberg, B. I., Haupt, A. J., Chiriboga, A. I., and Warner, R. R. (2005). Patterns, causes and consequences of regional variation in the ecology and life history of a reef fish. *Oecologia* 145 (3), 394–403. doi: 10.1007/s00442-005-0150-0

Santos, M. N., Monteiro, C. C., and Leitão, F. (2011). The role of artificial reefs in the sustainability of artisanal fisheries. *Artificial reefs in fisheries management* (New York:Taylor and Francis Group), 221–237 edited by. SA Bortone, FP Brandini, G Fabi and S Otake

Schiff, K. C., Allen, M. J., Zeng, E. Y., and Bay, S. M. (2000). Southern California. *Mar. Pollut. Bull.* 41 (1-6), 76–93. doi: 10.1016/S0025-326X(00)00103-X

Schwamborn, S. H., and Ferreira, B. P. (2002). Age structure and growth of the dusky damselfish, *Stegastes fuscus*, from tamandare reefs, Pernambuco, Brazil. *Environ. Biol. Fish.* 63 (1), 79–88. doi: 10.1023/A:1013851532298

Sikkel, P. C. (1988). Factors influencing spawning site choice by female garibaldi, *Hypsypops rubicundus* (Pisces: Pomacentridae). *Copeia* 1988, 710–718. doi: 10.2307/1445392

Sikkel, P. C. (1989). Egg presence and developmental stage influence spawning-site choice by female garibaldi. *Anim. Behav.* 38 (3), 447–456. doi: 10.1016/S0003-3472(89)80038-7

Sikkel, P. C. (1994). Why female garibaldi prefer males with young eggs: A test of the parental investment hypothesis. *Ethol. Ecol. Evol.* 6 (2), 191–211. doi: 10.1080/08927014.1994.9522994

Sikkel, P. C. (1995). Effects of nest quality on male courtship and female spawning-site choice in an algal-nesting damselfish. *Bull. Mar. Sci.* 57 (3), 682–689.

Silge, J., Chow, F., Kuhn, M., and Wickham, H. (2021). in *Rsample: General resampling infrastructure. R package version 0.0.9.*

Stephens, J. S., Morris, P. A., Pondella, D. J., Koonce, T. A., and Jordan, G. A. (1994). Overview of the dynamics of an urban artificial reef fish assemblage at King Harbor, California, USA 1974-1991: A recruitment driven system. *Bull. Mar. Sci.* 55 (2-3), 1224–1239.

Stephens, J. S., and Pondella, D. J. II (2002). Larval productivity of a mature artificial reef: the ichthyoplankton of King Harbor, California 1974-1997. *ICES J. Mar. Sci.* 59, S51–S58. doi: 10.1006/jmsc.2002.1189

Tanner, S. E., Vieira, A. R., Vasconcelos, R. P., Dores, S., Azevedo, M., Cabral, H. N., et al. (2019). Regional climate, primary productivity and fish biomass drive growth variation and population resilience in a small pelagic fish. *Ecol. Indic.* 103, 530–541. doi: 10.1016/j.ecolind.2019.04.056

Taylor, B. M. (2013). Drivers of protogynous sex change differ across spatial scales. *Proc. R. Soc. B: Biol. Sci.* 281 (1775), 20132423. doi: 10.1098/rspb.2013.2423

Taylor, B. M., Choat, J. H., DeMartini, E. E., Hoey, A. S., Marshell, A., Priest, M. A., et al. (2019). Demographic plasticity facilitates ecological and economic resilience in a commercially important reef fish. *J. Anim. Ecol.* 88 (12), 1888–1900. doi: 10.1111/1365-2656.13095

Taylor, B. M., Lindfield, S. J., and Choat, J. H. (2015). Hierarchical and scale-dependent effects of fishing pressure and environment on the structure and size distribution of parrotfish communities. *Ecography* 38 (5), 520–530. doi: 10.1111/ecog.01093

Taylor, B. M., and McIlwain, J. L. (2010). Beyond abundance and biomass: effects of marine protected areas on the demography of a highly exploited reef fish. *Mar. Ecol. Prog. Ser.* 411, 243–258. doi: 10.3354/meps08672

Tickell, S., Sáenz-Arroyo, A., and Milner-Gulland, E. J. (2019). Sunken worlds: The past and future of human-made reefs in marine conservation. *BioScience* 69 (9), 725–735. doi: 10.1093/biosci/biz079

Trip, E. D. L., Choat, J. H., Wilson, D. T., and Robertson, D. R. (2008). Inter-oceanic analysis of demographic variation in a widely distributed indo-pacific coral reef fish. *Mar. Ecol. Prog. Ser.* 373, 97–109. doi: 10.3354/meps07755

Trip, E. D. L., Clements, K. D., Raubenheimer, D., and Choat, J. H. (2014). Temperature-related variation in growth rate, size, maturation and life span in a marine herbivorous fish over a latitudinal gradient. *J. Anim. Ecol.* 83 (4), 866–875. doi: 10.1111/1365-2656.12183

Trip, E. D. L., Clements, K. D., Raubenheimer, D., and Choat, J. H. (2016). Temperate marine herbivorous fishes will likely do worse, not better, as waters warm up. *Mar. Biol.* 163, 24. doi: 10.1007/s00227-015-2790-x

Tzioumis, V., and Kingsford, M. J. (1999). Reproductive biology and growth of the temperate damselfish *Parma microlepis. Copeia* 1999, 348–361. doi: 10.2307/1447480

Williams, C. M. (2021). *Spatial and habitat variation in life history of the Garibaldi, Hypsypops rubicundus, including validation of annual growth increments* (Pomona: California State Polytechnic University).

Williams, J. P., Allen, L. G., Steele, M. A., and Pondella, D. J. (2007). El Niño periods increase growth of juvenile white seabass (*Atractoscion nobilis*) in the Southern California Bight. *Mar. Biol.* 152 (1), 193–200. doi: 10.1007/s00227-007-0673-5

Williams, J. P., Claisse, J. T., Pondella, D. J., Medeiros, L., Valle, C. F., and Shane, M. A. (2012). Patterns of life history and habitat use of an important recreational fishery species, spotfin croaker, and their potential fishery implications. *Mar. Coast. Fish.* 4 (1), 71–84. doi: 10.1080/19425120.2012.661392

Wilson, S. G., and Fischetti, T. R. (2010). “Coastline population trends in the United States: 1960-2008,” in *United States Census Bureau current population report*, P25–1139 (Washington D.C).

frontiers | Frontiers in Marine Science

TYPE Review
PUBLISHED 20 October 2022
DOI 10.3389/fmars.2022.983253

EDITED BY
Ibon Galparsoro,
Technological Center Expert in Marine and Food Innovation (AZTI), Spain

REVIEWED BY
Daniel Ierodiaconou,
Deakin University, Australia
Gladwin Asir,
Suganthi Devadason Marine Research Institute (SDMRI), India

*CORRESPONDENCE
Daniel J. Pondella II
pondella@oxy.edu

SPECIALTY SECTION
This article was submitted to Marine Ecosystem Ecology, a section of the journal Frontiers in Marine Science

RECEIVED 30 June 2022
ACCEPTED 29 September 2022
PUBLISHED 20 October 2022

CITATION
Pondella DJ II, Claisse JT and Williams CM (2022) Theory, practice, and design criteria for utilizing artificial reefs to increase production of marine fishes.
Front. Mar. Sci. 9:983253.
doi: 10.3389/fmars.2022.983253

Theory, practice, and design criteria for utilizing artificial reefs to increase production of marine fishes

Daniel J. Pondella II[1]*, Jeremy T. Claisse[1,2] and Chelsea M. Williams[1]

[1]Department of Biology, Vantuna Research Group, Occidental College, Los Angeles, CA, United States, [2]Department of Biological Sciences, California State Polytechnic University, Pomona, Pomona, CA, United States

Increasing the production of marine fishes is a tractable goal with wide socioeconomic and ecological appeal. Ecosystem restoration projects that increase the amount of suitable habitat in an area and/or habitat quality enhance both fishery production and ecosystem services. Fortuitously, there are a wealth of studies documenting the specific examples of restoring these services from successful artificial reef deployments. Considering the need to create future structures in a variety of scenarios and locations, it is salient to summarize the mechanisms through which increased secondary production occurs and the design considerations. To achieve this objective maximizing ecological processes including the provisioning of planktonic and epibenthic food resources and related trophic pathways, and those associated with life-stage specific habitat use (e.g., recruitment, juvenile survival, reproductive output) are critical mechanisms of productive reefs. We synthesized this information by addressing the structural and ecological theory of artificial reef design based upon physical attributes such as complexity, vertical relief, habitat heterogeneity, and spatial scale. Within this framework we summarized the mechanisms that may be used to increase secondary fish production and propose a general theory for optimization of these variables.

KEYWORDS

secondary fish production, habitat restoration, shelter, habitat complexity, habitat heterogeneity, trophic pathways, ecosystem services

Introduction

There is no debate that marine resources are crucial for current and future socioeconomic processes. Unfortunately, these resources have declined over time due to a variety of stressors including the depletion of species at higher trophic levels, habitat loss, pollution, and climate change, dramatically impacting marine ecosystems worldwide

(Jackson et al., 2001; Worm et al., 2006). Reduced fishery stocks and deterioration or loss of habitat, compounded by the increasing socioeconomic need to access marine resources highlights the theory that current secondary (fish) production and services were below the potential, and certainly historical potential, for marine ecosystems. While this theory is generally not tested directly (i.e., manipulation and/or calculation of a maximum versus current production potential), it has been indirectly demonstrated and is at the core of a variety of fishery management actions to improve stock sizes and sustainability (Knowlton, 2021). Well-designed ecosystem restoration projects increase the amount of suitable habitat area and/or quality, enhancing both fishery production and ecological services. Similarly, marine protected areas increase fishery stock biomass within their boundaries (Claudet et al., 2008; Edgar and Stuart-Smith, 2009), supporting this fundamental concept: current production is less than potential production in marine ecosystems.

Ongoing macroscale alterations of marine habitats and the implementation of infrastructure projects challenge us from a variety of perspectives. For thousands of years 'human-made', or as the literature primarily refers to them 'artificial' reefs, were installed to enhance marine habitats and there are continuous proposals for future implementation (Whitmarsh et al., 2008; Seaman, 2019; Tickell et al., 2019; Bugnot et al., 2020). Optimal artificial reef design is salient for deploying these structures to adequately restore lost ecosystem services. Herein, we delineate the theory and applicability of reversing or offsetting these losses, synthesizing the current empirical evidence for contributions of artificial reef habitats to local and regional ecosystems worldwide and the mechanisms supporting this goal. These theoretical constructs are essential for establishing design and evaluation criteria for utilizing reefing technology to improve ecosystem health and associated services.

Artificial reefs deployments have resulted in substantial increases of local and regional fish and invertebrate production. Johnson et al. (1994) found the rate of secondary production for a reef fish assemblage on a quarry rock artificial reef in southern California, USA was nine times greater than the sand-bottom fish assemblage the artificial reef replaced (i.e., was constructed on top of). Similarly, artificial reef habitat in Delaware Bay, USA supported up to two orders of magnitude higher secondary production (benthic macrofauna) per unit area than the comparable soft bottom habitat it replaced (Steimle et al., 2002). Large-scale artificial reef deployment assessments provide evidence for regional increases of production in fishes and invertebrates. In Japan, analyses of catch data revealed regional increases in octopus production in response to approximately 50,000 m^3 of artificial reef habitat construction (Polovina and Sakai, 1989). Following the deployment of an artificial reef complex in Algarve, southern Portugal, Roa-Ureta et al. (2019) analyzed 27 years of landings data to estimate the regional carrying capacity (K) of two-banded seabream, *Diplodus vulgaris*, increased by 35% (an additional 895 tons). This large-scale reefing effort comprised over 21,500 concrete modules (small 3 m^3 or large 174 m^3) covering an area of 43 km^2 (Santos et al., 2011). The Algarve artificial reef design focused on adding habitat for high-value (€12–18/kg in 2011) juvenile and adult fishes, which were targets of an artisanal fishery, to a soft bottom area where this habitat was previously rare (Santos et al., 2011). An economic analysis found revenues from fishing the areas around this artificial reef complex was greater than at control sites and catch rates and associated revenues had risen consistently over a 15 year period following deployment of the reef (Whitmarsh et al., 2008). Additionally, the artificial reef in Algarve relieved pressure from natural reefs in the region by redistributing fishing effort across a larger area (Leitao et al., 2009). These researchers also emphasized the need for additional fishery management regulations to prevent overfishing (Santos et al., 2011; Roa-Ureta et al., 2019). Thus, increased regional secondary production is achievable, but necessitates holistic design strategies that incorporate local and regional ecological processes, proper spatial scale and location, and socioeconomic factors such as management.

Impacts of a given artificial reef project were typically species- or taxa-specific (or even specific to a life-stage within a species), because responses to artificial reef habitats depend on species-specific functional attributes (e.g., diet, habitat use, life history) (Leitão, 2013; Smith et al., 2015; Cresson et al., 2019). Impacts were so diverse across taxa that predicting potential effects for entire assemblages was difficult and therefore a 'case-by-case' approach was generally more accurate (Brickhill et al., 2005). In paired comparisons between natural rocky or coral reefs and nearby artificial habitats (e.g., artificial reefs, shipwrecks, energy infrastructure), fish density, biomass and richness were often similar, demonstrating that artificial reefs have the potential to mimic natural reefs, if that is the objective (Paxton et al., 2020b). Most assessments of artificial reef designs examining specific objectives concentrated on important focal species (e.g., fishery or keystone species) and/or functional groups (e.g., those with specific trophic roles or habitat use patterns). Similarly, comparing reef success across ecosystems was highly context-specific and necessitates an understanding of regional goals as well as fine-scale biological and physical processes. The goal of increasing local and/or regional production is feasible, but a "one size fits all" approach is not advised (Komyakova et al., 2019; Paxton et al., 2020b; Blount et al., 2021).

Thus, a substantial amount of literature documented specific effects of individual artificial reef deployments, the mechanisms through which increased production occurred, and design considerations for achieving these objectives. Recently there has been more focus in the literature on the specific mechanisms, sometimes referred to as "enhanced ecological functions" (Glarou et al., 2020), that lead to increased secondary production of fish on artificial reefs, even above rates observed on natural reefs (e.g., Cresson et al., 2014a;

Glarou et al., 2020; Rouse et al., 2020; Puckeridge et al., 2021). These mechanisms provide benefits to individual species, typically through provision of shelter and/or food supporting survival or growth. While in some instances data were not available to directly quantify regional or local secondary production of fishes, evidence of these mechanisms, often in the context of a focal species' life history and behavioral ecology, support an assumption that reefs were contributing to secondary production. Yet, across ecosystems, there were consistent elements in artificial reef design that support increased secondary production and these criteria are useful for planning, evaluation, and design of current and future projects and have the potential to increase production on a regional scale. We posit that the most tractable metric to evaluate ecological services across habitats is secondary production.

Ecological process considerations of reef design

Planktonic and epibenthic food resources

A sizable proportion of the secondary production of fishes and invertebrates in artificial reef systems is fueled through planktonic resources, with a lesser proportion being supported by macroalgae or detritus. In a stable isotope and diet study of the largest artificial reef complex in the Mediterranean Sea (RECIFS PRADO program), organic matter of pelagic origin (i.e., phytoplankton and zooplankton) was the primary source supporting the system through artificial reef resident fishes feeding on sessile filter feeding invertebrates or directly on zooplankton (Cresson et al., 2014a; Cresson et al., 2014b). Similarly, a study of trophic pathways of fishes on a natural reef system in Australia observed that planktonic resources supported 60% of fishes, compared to approximately 30% by macroalgae and 10% by detritus (Truong et al., 2017). Current flow that delivers the associated flux of plankton and nutrients are critical factors supporting secondary production and thus are essential for overall performance. Therefore, understanding trophic bottlenecks and maximizing planktonic flux is necessary for increasing secondary production.

Zooplanktivorous fishes on artificial reefs are often the key trophic link between zooplankton and the larger reef-associated community (Bray et al., 1981; Cresson et al., 2014a; Holland et al., 2021; Puckeridge et al., 2021). Schooling water column and zooplanktivorous fishes were in greater abundance above higher relief purpose-built artificial reefs in temperate Australia (Puckeridge et al., 2021) and wrecks off of North Carolina, USA (Lemoine et al., 2019), when compared to lower relief natural reefs within each region. An Australian study directly documented the trophic link between Bluespotted Flathead (*Platycephalus caeruleopunctatus*), a resident benthic ambush predator, feeding on pelagic forage fish above the high relief artificial reef modules (Holland et al., 2021). This mechanism has also involved nutrient transfer, such as the case with diurnal planktivorous pomacentrids in California that increase overall reef production with their metabolic byproducts being used by algae (Bray et al., 1981). Many artificial reef systems are therefore more productive than natural reefs because they provide sufficient habitat for zooplanktivorous fishes (Champion et al., 2015; Pondella et al., 2018; Holland et al., 2021).

With this in mind, flux of planktonic resources and even inducing upwelling to increase primary productivity (e.g., Itosu et al., 1995; Otake et al., 1995) are important considerations. Further, for reefs that receive higher current flow, such has offshore oil and gas platforms in California, this translated to increased growth rates for mussels (*Mytilus* spp.), a dominant filter feeding invertebrate, and the planktivorous Blue Rockfish (*Sebastes mystinus*) than individuals in nearby natural nearshore habitats (Page and Hubbard, 1987; Blanchette et al., 2007; Love et al., 2007). Similarly, a study of an experimental artificial reef off of Scotland demonstrated the importance of water flow for the secondary production of a suspension feeding bryozoan both on the outer-facing reef surfaces and into internal reefs spaces, with higher secondary invertebrate production found on reefs with more complex designs and larger internal reef spaces (Rouse et al., 2020). Clearly in order to maximize secondary production, optimizing both benthic and pelagic food resources is essential.

Shelter

Proper shelter allows fishes to maximize the acquisition of planktonic and epibenthic food resources while minimizing the amount of energy needed to maintain themselves. In a system with underutilized food resources, the increase of shelter and associated use by various life history stages of fishes theoretically results in greater production. Beyond increasing appropriate habitat where it is limited or lost, properly designed habitats provide a direct survival and metabolic benefit to the fish sheltering on them. In Atlantic Cod, metabolic rates associated with reef habitat (as compared to sand) were lower, suggesting that the energy saved by sheltering contributed to increased somatic growth and thus production rates (Schwartzbach et al., 2020). Reef holes and cavities (i.e., void spaces) provide refuges, and hole size was often positively associated with the body sizes of fishes found sheltering in them (Hixon and Beets, 1993; Beets and Hixon, 1994; Friedlander and Parrish, 1998). For example, smaller reef fishes had higher survival rates on reefs with smaller hole sizes compared to similar sized fish on reefs with larger holes (Hixon and Beets, 1993). Some reef designs utilized models to predict hole/crevice size and number based on the rock size (Barry and Wickins, 1992), suggesting the possibility of designing reefs with appropriate hole sizes for a specific taxa or life history stages (e.g., Glarou et al., 2020). Survival and growth of fishes is a function of both predator avoidance and the reduced energy associated with sheltering from current flow in appropriately sized holes. Productive reefs have shelter characteristics enabling fishes to minimize their energy expenditures from flow regimes and predator avoidance while allowing them to maximize the flux of energy from the plankton and epibenthic prey. Theoretically increasing shelter increases the secondary production a reef supports. This is ulitmately limited by the carrying capacity of the system (e.g, food availability, species and life-stage specific survival rates) in a density dependent manner resulting in an asymptotic relationship between shelter and production (Figure 1).

Recruitment and juvenile survivorship

The function of artificial reefs as shelter for recruitment, survivorship, and growth of young-of-year and juvenile reef-associated fishes is another essential component for increasing local and regional production. Recruitment and juvenile success, the hallmarks of fishery models (Ricker, 1975), are a critical factor for stock management. There are multiple examples of artificial reefs providing habitat for newly settled and/or juvenile fish, which increased recruitment rates and cohort success, which in turn increased ecosystem-wide services. High prevalence of newly recruited and/or juvenile fishes on artificial reefs was common (e.g., Santos et al., 2011; Reubens et al., 2014; Granneman and Steele, 2015; Krone et al., 2017). Fish assemblages on more complex, larger-scale artificial reefs supported a higher proportion of smaller juvenile fishes (e.g., Santos et al., 2011; Granneman and Steele, 2015; Love et al., 2019) suggesting these patterns documented on small experimental reefs (cm^2 to m^2) are scalable to larger systems (10’s to 100’s of m^2). Additionally, Komyakova et al. (2019) found in temperate southern Australia that the location relative to larger reefs, either natural rocky reefs or large breakwaters, had a greater influence on fish densities at smaller artificial reef modules. This was attributed to increased recruitment of young-of-the-year fishes to these larger reefs and subsequent movement of those fishes to the artificial reef modules. Undoubtedly, incorporation of a nursery design is a key component for successful reefing programs.

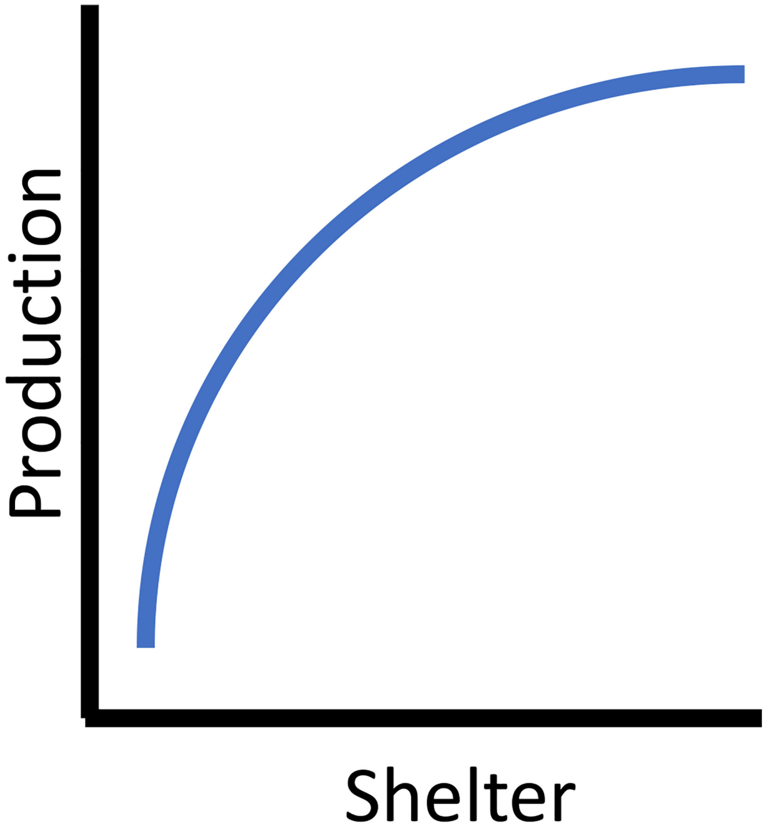

FIGURE 1
The asymptotic theoretical relationship between available shelter and secondary (fish) production.

In a variety of ecosystems, increasing habitat for juvenile fish resulted in corresponding production increases. Windmill artificial reefs (WARs), consisting of monopile offshore wind turbines surrounded by quarry rock scour protection and deployed in largely soft bottom regions of the North Sea, supported high abundances of juvenile fishes. Specifically, they were suitable feeding grounds for juvenile Atlantic Cod (*Gadus morhua*) and Pouting (*Trisopterus luscus*), which fed upon epifaunal invertebrate prey and showed high seasonal site fidelity (De Troch et al., 2013; Reubens et al., 2014). Juvenile Atlantic Cod sheltered on WARs between dawn and dusk (crepuscular) feeding periods, suggesting sheltering from predators provides a survival advantage (Reubens et al., 2014), in addition to metabolic energy savings (Schwartzbach et al., 2020). In passive acoustic tracking of Atlantic Cod, these patterns were consistent over 2-5 month periods, with fish sheltering on the same WAR reef daily (Reubens et al., 2014). While these increases were in local production and regional-scale increases had not yet been observed, these juvenile fish likely emigrated as they matured, benefitting commercial fisheries. Similarly, in a mark-recapture study, juvenile Gag Grouper (*Mycteroperca microlepis*) had high site fidelity (average 300 days) on an experimental concrete artificial reef off Florida. Adults then moved further offshore where they became part of the broader fished stock, with two fish being recaptured on other side of the Gulf of Mexico in Texas and Mexico (Lindberg et al., 2006). In the Algarve artificial reef complex, which was designed to specifically provide shelter for juvenile fishes of fishery importance (Santos et al., 2011), this juvenile sheltering effect made an important contribution to the increases in regional carrying capacity (K) and production of Two-Banded Seabream (Roa-Ureta et al., 2019). Up to 88% of the fish assemblage associated with the Algarve reef modules were juveniles, with consistent recruitment of young-of-the-year fishes observed for some species. Juveniles were also documented as sheltering in the structure and feeding directly on the benthic macrofauna or in the water column near the structures (Leitao et al., 2009; Santos et al., 2011). These examples illustrate the progression necessary for increasing production: creating habitat where appropriate, documenting the density of critical life stages and their associated habitat use, then linking this to regional production. Clearly, reducing habitat and recruitment limitations by increasing nursery areas has significant benefits.

Reproductive output

In addition to providing a nursery function and sheltering juvenile fishes with high rates of somatic production, a frequently overlooked component in artificial reef studies is reproductive output, or gonadal production. Reproductive output is a function of the number of larger adult fishes residing on a reef, and is a "major component of energy flow through the fishes in [a] reef system" (Demartini et al., 1994). In this study, fish gonadal production on artificial reefs was equivalent to, or a large multiple of, the somatic production estimates. For territorial species, reefs with more suitable habitat have a corresponding greater number of potential feeding and mating territories (Hixon, 1980), which can lead to increased secondary production compared to less complex natural reefs (Pondella et al., 2002). These concepts are frequently incorporated in fisheries management and conservation network designs, such as MPA connectivity, with the overall goal of increasing localized spawning stock biomass and exporting it throughout the ecosystem (Russ et al., 2004; Pérez-Ruzafa et al., 2008; Almany et al., 2009; Botsford et al., 2009; Cudney-Bueno et al., 2009; Foley et al., 2010; Berumen et al., 2012; Schmiing et al., 2017; Baetscher et al., 2019; Marshall et al., 2019). Further, since most fishes have a pelagic larval stage, understanding gonadal production was a critical feature in modeling connectivity and the link between biomass density and recruitment (Pondella et al., 2015). Particularly well-studied for fishes, gonadal production and egg quality is a function of female size and age. Larger females have higher fecundity and allocate more energy for egg production, and in some instances, produce more fit larvae than smaller females (Berkeley et al., 2004). Importantly, this relationship was not linear, instead being hyperallometric with size (Barneche et al., 2018), and supported the idea that the protection and production of larger females disproportionately and positively affects stock structure. Larger adults have lower annual somatic production but theoretically are a major link to regional increases, especially if habitats are not limiting recruitment. Thus, habitat design and/or management actions taking this into account (e.g., the implementation of MPAs or fishery management practices such as slot limits and protection of spawning aggregations) have a greater impact on recovery due to increased gonadal production and potentially more fit larvae (Claudet et al., 2008; Edgar and Stuart-Smith, 2009; Marshall et al., 2019). Habitat characteristics that optimize spawning aggregations, generating larval sources throughout an ecosystem were also important considerations (Schmiing et al., 2017). Some studies identified larval production as a key management action for fishery replenishment (Kough et al., 2019). Higher quality habitats also support greater densities of large individuals, magnifying this effect.

Physical considerations of reef design

Structural complexity

Increasing reef complexity, both externally (rugosity) and internally (void space), improves secondary production (Blount et al., 2021). Simply increasing the complexity of reef modules in the

French Mediterranean doubled overall fish species richness, increased density by ten times, and increased biomass by forty times (Charbonnel et al., 2002). Experimental artificial reefs across a broad geographic range consistently found increased fish density, biomass, and/or species diversity associated with more complex structures (North Carolina, USA : Potts and Hulbert, 1994, South Carolina, USA: Kellison and Sedberry, 1998, Gulf of Mexico, Florida, USA: Sherman et al., 2002, Mediterranean, Italy: Relini et al., 2007, Scotland, UK: Hunter and Sayer, 2009, temperate southern Australia: Komyakova et al., 2019). Often fish density and size structure have a greater impact on rates of secondary production than relative differences in individual growth rates. For example, Granneman and Steele (2014) compared somatic growth rates, estimated from otolith back-calculation, on paired artificial and adjacent natural reefs in southern California, USA. When combined with observed density and size structure of the fish assemblage, they found secondary production rates on quarry rock artificial reefs were similar to or greater than natural reefs, and positively correlated with habitat characteristics (i.e., the abundance of larger boulders on artificial reefs). The authors also found that size-specific differences in fish density made a large contribution to the differences in production, while growth rates among sites were similar. The general mechanism discussed for this phenomenon relates direct sheltering opportunities for a variety of sizes of fishes provided by the increased number and diversity of sizes of holes and crevices in the reefs. Further, more rugose reefs are more suitable for attachment of both algae and sessile invertebrates (Harlin and Lindbergh, 1977; Walters and Wethey, 1996). As such, there is a positive relationship between complexity and production. In addition, three-dimensional complexity adds increased surface area, elevating the overall abundance of benthic forage resources, which results in increased fish density, an integral factor in secondary production models. Theoretically, this relationship asymptotes with increasing complexity (Figure 2). While increasing complexity adds structural elements that correspond to species-specific functional attributes (e.g., diet, habitat use, life history) of the fish assemblage, similar to within reef habitat heterogeneity, this is ultimately limited by the surface area to volume structural relationship and the availability of internal spaces of a reef of a given size (Kim et al., 1994; Lemoine et al., 2019; Rouse et al., 2020). Thus, increasing complexity to maximize production is a theoretical and practical design consideration.

Vertical relief

Vertical relief (i.e., height above the seafloor) is another commonly investigated factor in reef design and artificial reefs

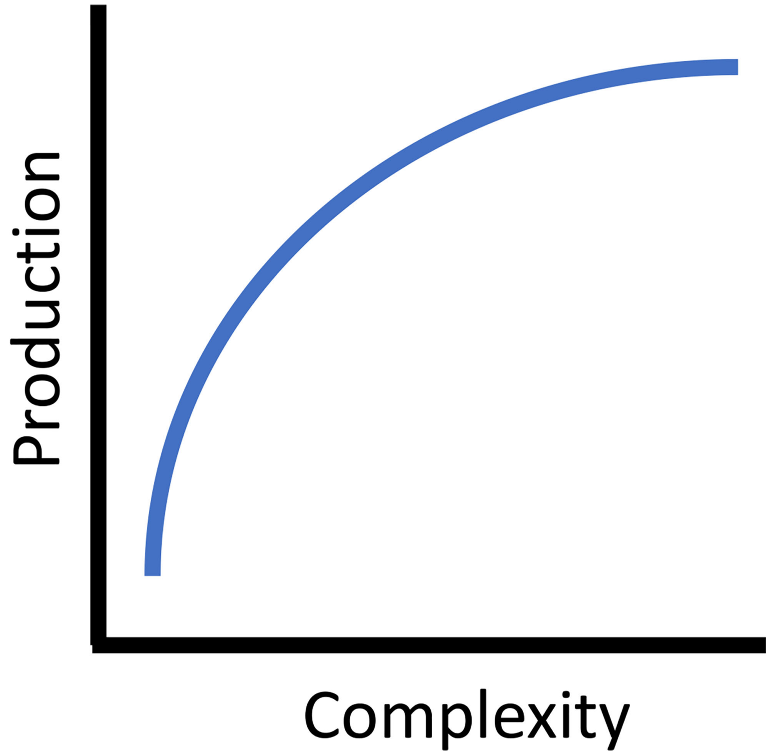

FIGURE 2
The asymptotic theoretical relationship between reef complexity and secondary (fish) production.

that provide sufficient vertical relief support greater taxonomic diversity (Ogawa, 1967; Molles and Manuel, 1978; Bohnsack et al., 1994). Positive relationships between vertical relief and fish density and/or biomass were documented at quarry rock artificial reefs in California, USA (e.g., Ambrose and Swarbrick, 1989; Pondella et al., 2006; Granneman and Steele, 2015). Studies comparing fish assemblages on shipwrecks (i.e., high-relief artificial reefs) with natural reefs and/or concrete artificial reefs found higher-relief wrecks have higher mean densities of fishes (northeast Pacific: Bulger et al., 2019, North Carolina, USA: Lemoine et al., 2019; Paxton et al., 2020a), as well as differences in trophic guilds. Similarly, Paxton et al. (2020a) observed wrecks had higher densities of transient predators (e.g., jacks, mackerel, barracuda, sharks) than concrete and natural reefs, and their review of the artificial reef literature suggested this pattern of more high trophic level (i.e., predatory, typically transient) fishes on artificial reefs than natural reefs was a global pattern. Yet, shipwrecks were not necessarily adequate surrogates for natural reefs (Medeiros et al., 2021). This is representative of a general pattern of predators being more common on artificial reefs globally, with transient predators being observed in higher densities on taller structures (Paxton et al., 2020a). While there were numerous objective and anecdotal observations of this phenomenon, salient are the mechanisms and their potential utility in reef design.

Reefs with greater relief perform better than low relief reefs. At the spatial scale of typical reefs (meters), theoretically this will asymptote (Figure 3). While many species of fish orient to high relief structures for feeding purposes (as described previously) they also utilize them for spawning sites. Such spawning aggregations were often associated with the highest relief components within a reef and in some taxa optimal spawning sites were favored. Additionally, adults return to traditional spawning sites based upon a learned response, yet in the absence of this learning, they chose new sites based upon reef features implying there was an optimization of assessed reef features to maximize spawning success (Warner, 1988). Interestingly, on newly deployed reefs adult fishes sometimes within hours, but certainly within days orient to these structures, which, since they were just placed in the water, do not yet have epibenthic resources (Turner et al., 1969). Over the long term, large predatory fishes migrate and orient to these vertical features (Barilotti et al., 2020; Burns et al., 2020; Paxton et al., 2020a). However, very high-relief reefs, particularly those with an intertidal component (i.e., breakwaters, some shipwrecks, and oil platforms), had increased ecosystem heterogeneity and

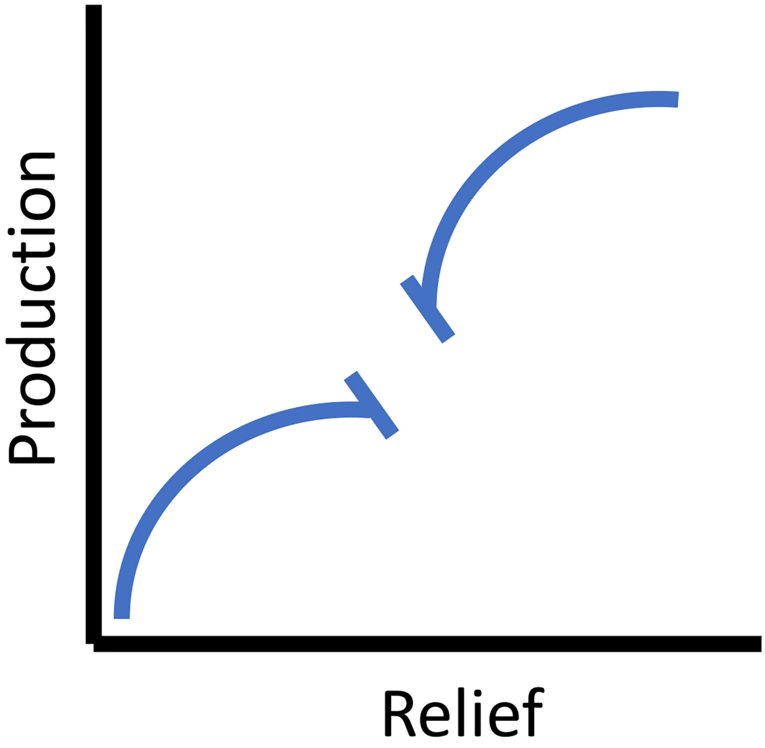

FIGURE 3
The theoretical relationship between vertical relief and secondary (fish) production. For the scale of typical reefs (meters) the relationship asymptotes (left side on x-axis), and then for very high relief reefs (10's of meters) and those that include an intertidal component (e.g., breakwaters, some shipwrecks, and oil platforms) the relationship is extended until it asymptotes again (right side on x-axis).

associated production (e.g., Stephens et al., 1994; Claisse et al., 2014). For example, breakwaters incorporate the intertidal zone, increasing habitat heterogeneity and have high rates of secondary production (Pondella et al., 2002). These processes are consistent with the inclusion of kelp, whereby a three-dimensional relief component is extended to the surface by a canopy providing habitat heterogeneity and trophic resources that support an increased suite of life stages and species (Graham, 2004). Structures with these high-relief components also act as fish aggregating devices (FADs) for more transient pelagic fishes. This attraction can occur on a non-random consistent basis, resulting in increased overall production through the inclusion of planktivores into the system (Smith et al., 2016). Relief is an attraction mechanism of adults and larval fishes, potential spawning sites, and food resources. On a typical reef module without an intertidal component, production as a function of relief asymptotes (especially if resource dependent), then adding an additional three-dimensional FAD/kelp/intertidal component increases production to a theoretical maximum (Figure 3).

Habitat heterogeneity, reef size, and spacing

In many systems, nursery areas are often decoupled from adult habitats. Thus, increasing habitat heterogeneity (i.e., variability of habitat types across a given landscape area) (Wedding and Yoklavich, 2015), is a critical step towards optimizing habitat for multiple life stages. Fishes, either through ontogenetic changes or during specific life history stages, often use various habitats within an ecosystem. For many reef associated species this includes foraging in surrounding soft-bottom areas. A "halo effect" documented around artificial and natural reef structures that were surrounded by soft-bottom habitat largely refers to direct and secondary effects of the organic enrichment of these sediments. These halo effects were due to complex processes. Hydrodynamic changes from the increased vertical relief of an artificial reef directly affected the composition and size of sediments, and created a plume of detritus and waste generated by reef inhabitants (e.g., filter feeding invertebrates, planktivorous fishes, macroalgae) organically enriching sediments at scales of meters to tens of meters around an artificial reef (Heery et al., 2017; Bugnot et al., 2020). Changes in the composition and densities of sediment infauna (e.g., polychaetes and amphipods) at these scales [e.g., out to 30 m in Reeds et al. (2018) and out to 80 m in Bortone et al. (1998)], were a result of being fed by the additional organic material and increased predation from reef-associated fishes and crabs. These soft-bottom foraging grounds were important in supporting the diets (i.e., production) of many species that shelter in reefs. Many taxa utilize these reef/soft bottom ecotones, emphasizing the importance of the halo effects. Multiple studies have focused on assessing the foraging distance of fishes from artificial reefs (Bortone et al., 1998; Brandt and Jackson, 2013) to minimize the overlap of foraging areas in reef design (Champion et al., 2015; Rosemond et al., 2018), which has the potential to limit growth and reef productivity (e.g., Lindberg et al., 2006). Johnson et al. (1994) found 20-25% of reef associated fish diets on a California artificial quarry rock reef derived from sand-rock ecotone habitats. These ecotones in southern California support increased densities of a commercial serranid, Barred Sandbass (*Paralabrax nebulifer*) (Anderson et al., 1989). Pondella et al. (2018) increased the amount of ecotone habitat by designing a reef with offset modules to increase the reef perimeter. Rosemond et al. (2018) found that reef-associated fish species were mostly foraging in the soft-bottom habitat up to 30 m away from a variety of artificial reef types (e.g., concrete pipes, metal ships) off North Carolina, USA. Reeds et al. (2018) documented reef fish foraging at elevated densities only out to 15 m from a steel fishery enhancement, but because the reef had a relatively small footprint (12 m x 16 m), they calculated that reef associated fishes were using an area 15 times greater that the reef footprint itself, demonstrating that for some species, a relatively large area of these surrounding sediments play an important ecological role. In the Adriatic Sea, Tyrrhenian Sea, and southern California, physical factors associated with artificial reef proximity outweighed the influence of predators (Ambrose and Anderson, 1990; Danovaro et al., 2002; Fabi et al., 2002) illustrating the importance of these 'halos'.

Extending the 'halo effect' by incorporating the utilization of planktonic resources is conceptually a 'dome effect', as reefs extend three-dimensionally up into the water column. Multiple studies have taken a mechanistic approach in examining how the amount of shelter a reef provides interacts with the trophic processes of artificial reef residents who feed in adjacent habitats (e.g., water column, soft bottom, or a mix of soft bottom and natural reef). These studies suggested there is a trade-off (and potentially thresholds) between providing shelter for more individuals within the artificial reef and competition among those individuals for planktonic (Champion et al., 2015) or benthic food resources in the surrounding habitats (Lindberg et al., 2006; Brandt and Jackson, 2013), or both (Lindquist et al., 1994). Champion et al. (2015) empirically derived the amount of zooplankton that flowed across an artificial reef in Australia and the amount consumed per day by individuals of a resident fish species (*Atypichthys strigatus*, a smaller Kyphosidae). They modeled thresholds at which reefs were able to shelter more fish than the zooplankton flow could support, suggesting an optimal reef size exists to balance this tradeoff. They also noted that reef shape was important. Lindberg et al. (2006) found that growth was density-dependent in larger juvenile and young adult Gag Grouper (*Mycteroperca microlepis*) sheltering in concrete artificial reefs off Florida, USA and attributed it to competition for food in the surrounding feeding grounds. When also factoring in the potential for increased fishing mortality, if fish were in higher densities, the authors argued that most positive effect on stocks was achieved through widely scattered patch reefs with appropriately sized cavities, as that should increase growth rates of individual fish while they were residing in the reefs. It is also important to note that this species used these reefs during an older juvenile/younger adult stage prior to moving further offshore, again emphasizing that habitat use patterns associated with artificial reefs are species and life stage dependent. For example, adult wrasses (Labridae) shelter nocturnally in sand proximate to reefs. Some wrasses on coral reefs have a post-settlement stage where they shelter in the sand prior to recruitment to the reef (Hamilton et al., 2008). For overall fish productivity, there are tradeoffs between distance between reef modules, size, spacing, and maximization of the halo and ecotone effects, as these effects are synergistic to overall performance (Figure 4). But adding more structure without optimizing spacing criteria may have diminishing returns. As such, in a particular reef system, the heterogeneity of subhabitats has a maximum (Figure 4). Theoretically, each increase in subhabitat type theoretically increases the production to a maximum.

Construction logistics, available funding, engineering, regulation restrictions or boundaries, and costs constrain reef size and associated local and regional effects (Lan and Hsui, 2006). Often it is necessary to weigh the benefits of one or a few larger reefs versus many smaller reefs optimizing the use of limited resources (e.g., Pondella et al., 2018). Some studies that have directly addressed reef size suggested intermediate sizes were most productive (reef volumes from 400-4000 cubic meters, (Ogawa et al., 1977), as cited and discussed in Glarou (et al. 2020). For example, on reefs constructed with concrete cubes with holes in Taiwan, the biomass of resident fish species increased sigmoidally when compared to reef size, indicating that intermediate sizes produced the best ratio of standing stock biomass to construction cost (Jan et al., 2003). Further, reefs that are too large will reduce habitat heterogeneity and ultimately reduce production for the suite of species that depend on these varied resources (Figure 5) The trade-offs between costs and design criteria are important considerations for maximizing fish production with available resources.

Additional considerations for realizing benefits

There are species-specific timescales for expected fishery benefits, based on life history and behavioral ecological traits. These benefits follow periods of good larval survival and

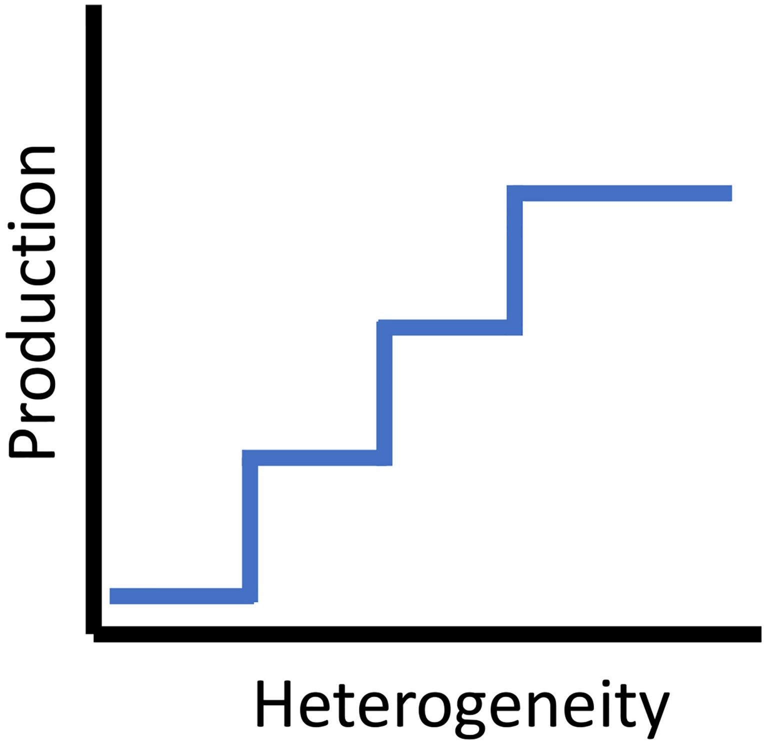

FIGURE 4
The theoretical step relationship between habitat heterogeneity and secondary (fish) production.

recruitment. In Algarve, the Seabream fishery regional carrying capacity increased by 35% eight years post construction (construction took five years) as new production attributed to the artificial reef spilled over to the surrounding continental shelf. It followed multiple strong recruitment years, and then a four year lag for the species to enter the fishery (Roa-Ureta et al., 2019). An earlier economic analysis for the initial pilot-scale deployments of artificial reefs in this region also demonstrated fishery value (i.e., revenue) per unit effort slowly increased over a 15 year period following reef deployment and was higher near artificial reef modules when compared to fishing near control areas (Whitmarsh et al., 2008). These are consistent with timelines reported for maturity in Marine Protected Areas (MPA). Typically, post-closure fish densities and biomass asymptote at an interval of at least 15-20 years with older reserves outperforming younger reserves (Abesamis and Russ, 2005; Claudet et al., 2006). These time frames for maximizing reef contribution on both local and regional scales parallel typical age at maturity, the significantly greater gonadal output for larger females, and overall longevity for many focal species.

The installation of an artificial reef complex took pressure off natural reefs in the region by redistributing fishing effort across a larger area (Leitao et al., 2009). As such, spacing and connectivity to other reefs are important design criteria. In some instances, reef development and spacing protect soft-bottom species by acting as barriers to bottom trawling (Guillen et al., 1994). Shallow anthropogenic seafloor structures influence the foraging of marine mammals (Arnould et al., 2015; Todd et al., 2020). The interplay among the potential to redistribute and/or enhance mammal populations as well as attracting these predators to artificial reefs (Fernandez-Betelu et al., 2022) is an open question necessitating further investigation as these predators could increase the natural mortality of fish and invertebrate populations. Determining mechanisms for (or direct evidence of) increased survival or growth of fishes also provided evidence that artificial reef systems are not functioning as ecological traps (Reubens et al., 2014). In such traps, an organism is attracted to and settles preferably in a habitat with suboptimal conditions relative to other available and more suitable habitats (Robertson and Hutto, 2006). If an ecological trap occurs, growth, recruitment and survival rates are lower than at reference habitats, as was recently described for Reef Ball reefs in Australia (Komyakova et al., 2021). Although better alternative habitats are available, the suboptimal habitat is unfortunately chosen, resulting in reduced production. While there are few examples of this in the literature, demonstrating a net benefit to a species with certain characteristics (e.g., life history, habitat use or movement patterns, trophic traits/groups) is critical. There is also the potential for artificial reefs to support or expand the

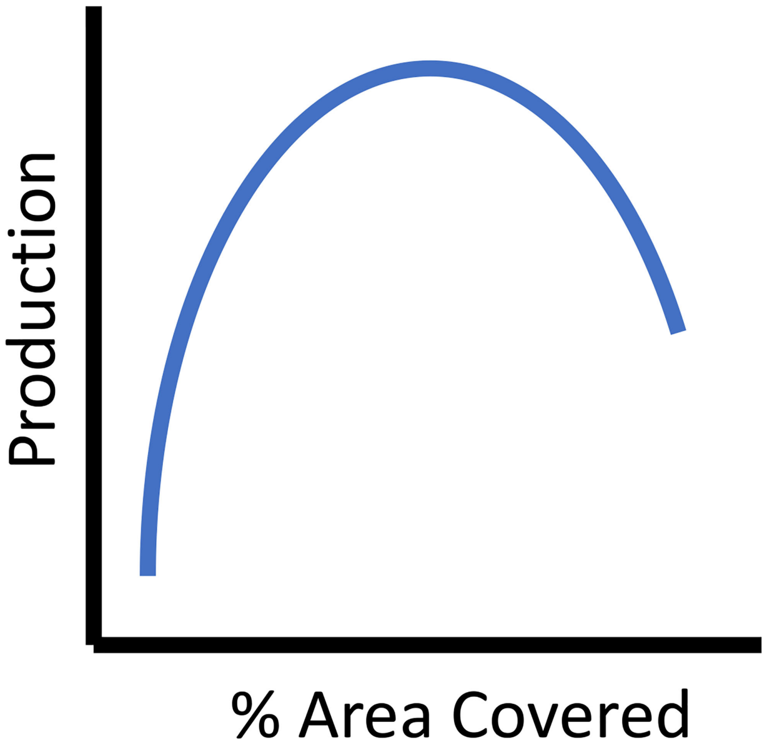

FIGURE 5
The theoretical relationship between percent of area covered, as a metric of reef spacing criteria and secondary (fish) production.

range of invasive species (Dahl and Patterson, 2014; Dafforn, 2017; Schulze et al., 2020). In heavily overfished populations (i.e., the current standing stock is not producing enough reproductive output to begin with), adding additional, even higher quality, habitat will not realize increased production if recruitment levels are low (Powers et al., 2003). In these cases, considering larger location-specific integrative coastal management approaches (Komyakova et al., 2019; Paxton et al., 2020b) and additional fishery management is necessary to achieve or sustain positive outcomes (Powers et al., 2003; Whitmarsh et al., 2008; Roa-Ureta et al., 2019).

Artificial reefs have a long history of use in fishery management (Bortone et al., 2011). An emerging concern in the literature was the consideration of artificial reefs as part of larger location-specific integrative coastal management approaches (Komyakova et al., 2019; Paxton et al., 2020b) and the potential necessity of additional fishery management for achieving or sustaining positive outcomes (Powers et al., 2003; Whitmarsh et al., 2008; Santos et al., 2011; Roa-Ureta et al., 2019). While not a concern when artificial reefs are primarily providing a nursery function to life stages with sizes below those targeted by fisheries (e.g., oyster reef restoration in estuaries in southeastern USA: Peterson et al., 2003, WARs in the North Sea: Reubens et al., 2014), this was a consideration when artificial reefs are being used by adult stages of species targeted heavily in local fisheries. On one hand, if an artificial reef or complex is relatively large (with respect to natural reefs in the area), then it may take pressure off natural reefs in the region by redistributing fishing effort across a larger total area reef habitat (Leitao et al., 2009). There are complex interactions within habitats, for instance reviews cite many studies where artificial reefs essentially stop bottom trawling in the area and may have positive impacts for soft bottom species (Relini et al., 2007; Brandini, 2014; Heery et al., 2017; Glarou et al., 2020). However, if the artificial reefs instead aggregated existing biomass in the region making target species easier to exploit (the goal of Fish Aggregating Devices [FADs]), and if this fishing mortality was not counter-balanced with a proportional increase in localized production (Lindberg et al., 2006; Smith et al., 2015), essentially the crux of the 'attraction vs production' debate (Osenberg et al., 2002), then consideration of additional fisheries management actions is prudent. In the case where an artificial reef serves as a spawning aggregation site (Schmiing et al., 2017), this necessitates potential permanent or reproductive season fishing closures. Balancing this against the potential secondary production increases due to increasing gonadal production are the challenges managers face. More broadly though, if objectives include amplifying regional impacts of deploying an artificial habitat (e.g., population recovery or increasing regional carrying capacity), then considerations including additional management actions focused on spawning stock biomass recovery, and particularly the protection of larger/older individuals, like in the implementation of MPAs and size limits, were practical (Claudet et al., 2008; Edgar and Stuart-Smith, 2009; Barneche et al., 2018; Marshall et al., 2019). Thus, incorporating an ecosystem-wide approach in reef design is necessary.

Overall successful reefing projects optimize all these discussed criteria (shelter, complexity, heterogeneity, relief and spacing) to maximize reproductive output and recruitment success. These parameters are ecosystem- and taxa- specific; thus, wherever possible a thorough and understanding of the geographical, ecological, and socioeconomic context is necessary.

Author contributions

All authors listed have made a substantial, direct, and intellectual contribution to the work and approved it for publication.

Funding

Funding for this study was provided by Chevron Technical Center, a division of Chevron USA Inc., under Service Order No. 0015115104.

Acknowledgments

We would like to thank Travis Elsdon, Gary Wolinsky, and William Gala for their feedback during initial project development and manuscript preparation.

Conflict of interest

This paper is the result of a study funded by Chevron Technical Center, a division of Chevron USA Inc., which supported the core project team to conduct a literature review on factors influencing secondary production on artificial reef structures. The funder was not involved in the study design, literature review, interpretation of data, the writing of this article or the decision to submit it for publication. This funding source has not influenced the authors' objectivity. The authors have no further potential conflicts of interest to disclose.

Publisher's note

References

Abesamis, R. A., and Russ, G. R. (2005). Density-dependent spillover from a marine reserve: long-term evidence. *Ecol. Appl.* 15, 1798–1812. doi: 10.1890/05-0174

Almany, G., Connolly, S., Heath, D., Hogan, J., Jones, G., McCook, L., et al. (2009). Connectivity, biodiversity conservation and the design of marine reserve networks for coral reefs. *Coral reefs* 28, 339–351. doi: 10.1007/s00338-009-0484-x

Ambrose, R. F., and Anderson, T. W. (1990). Influence of an artifical reef on the surrounding infaunal community. *Mar. Biol.* 107, 41–52. doi: 10.1007/BF01313240

Ambrose, R. F., and Swarbrick, S. L. (1989). Comparison of fish assemblages on artificial and natural reefs off the coast of southern California. *Bull. Mar. Sci.* 44, 718–733.

Anderson, T. W., DeMartini, E. E., and Roberts, D. A. (1989). The relationship between habitat structure, body size and distribution of fishes at a temperate artificial reef. *Bull. Mar. Sci.* 44, 681–697.

Arnould, J. P. Y., Monk, J., Ierodiaconou, D., Hiindell, M. A., Semmens, J., Hoskins, A. J., et al. (2015). Use of anthropogenic sea floor structures by Australian fur seals: potential positive ecological impacts of marine industrial development? *PloS One* 107, e0130581. doi: 10.1371/journal.pone.0130581

Baetscher, D. S., Anderson, E. C., Gilbert-Horvath, E. A., Malone, D. P., Saarman, E. T., Carr, M. H., et al. (2019). Dispersal of a nearshore marine fish connects marine reserves and adjacent fished areas along an open coast. *Mol. Ecol.* 28, 1611–1623. doi: 10.1111/mec.15044

Barilotti, A. A., White, C. F., and Lowe, C. G. (2020). Are Fishes Attracted to Piers? Movements and Association of Marine Fishes to a Public Fishing Pier within a Commercial Harbor. *Bulletin, Southern California Academy of Sciences* 119 (1):18–34

Barneche, D. R., Robertson, D. R., White, C. R., and Marshall, D. J. (2018). Fish reproductive-energy output increases disproportionately with body size. *Science* 360, 642–645. doi: 10.1126/science.aao6868

Barry, J., and Wickins, J. F. (1992). A model for the number and sizes of crevices that can be seen on the exposed surface of submerged rock reefs. *Environmetrics* 3, 55–69. doi: 10.1002/env.3170030104

Beets, J., and Hixon, M. A. (1994). Distribution, persistence, and growth of groupers (Pisces: Serranidae) on artificial and natural patch reefs in the virgin islands. *Bull. Mar. Sci.* 55, 470–483.

Berkeley, S. A., Hixon, M. A., Larson, R. J., and Love, M. S. (2004). Fisheries sustainability *via* protection of age structure and spatial distribution of fish populations. *Fisheries* 29, 23–32. doi: 10.1577/1548-8446(2004)29[23:FSVPOA]2.0.CO;2

Berumen, M. L., Almany, G. R., Planes, S., Jones, G. P., Saenz-Agudelo, P., and Thorrold, S. R. (2012). Persistence of self-recruitment and patterns of larval connectivity in a marine protected area network. *Ecol. Evol.* 2, 444–452. doi: 10.1002/ece3.208

Blanchette, C. A., Helmuth, B., and Gaines, S. D. (2007). Spatial patterns of growth in the mussel, *Mytilus californianus*, across a major oceanographic and biogeographic boundary at point conception, California, USA. *J. Exp. Mar. Biol. Ecol.* 340, 126–148. doi: 10.1016/j.jembe.2006.09.022

Blount, C., Komyakova, V., Barnes, L., Smith, M. L., Zhang, D., Reeds, K., et al. (2021). Using ecological evidence to refine approaches to deploying offshore artificial reefs for recreational fisheries. *Bull. Mar. Sci.* 97, 665–698. doi: 10.5343/bms.2020.0059

Bohnsack, J. A., Harper, D. E., McClellan, D. B., and Hulsbeck, M. (1994). Effects of reef size on colonization and assemblage structure of fishes at artificial reefs off southeastern Florida, USA. *Bull. Mar. Sci.* 55, 796–823.

S. A. Bortone, F. P. Brandini, G. Fabi and S. Otake (Eds.) (2011). *Artificial reefs in fishery management* (Boca Raton, Florida: CRC Press, Taylor & Francis Group).

Bortone, S. A., Cody, R. P., Turpin, R. K., and Bundrick, C. M. (1998). The impact of artificial-reef fish assemblages on their potential forage area. *Ital. J. Zool.* 65, 265–267. doi: 10.1080/11250009809386830

Botsford, L., White, J. W., Coffroth, M.-A., Paris, C., Planes, S., Shearer, T., et al. (2009). Connectivity and resilience of coral reef metapopulations in marine protected areas: matching empirical efforts to predictive needs. *Coral reefs* 28, 327–337. doi: 10.1007/s00338-009-0466-z

Brandini, F. (2014). Marine biodiversity and sustainability of fishing resources in Brazil: a case study of the coast of paraná state. *Regional Environ. Change* 14, 2127–2137. doi: 10.1007/s10113-013-0458-y

Brandt, J. R., and Jackson, D. C. (2013). Influences of artificial reefs on juvenile red snapper along the Mississippi gulf coast. *Mar. Coast. Fisheries* 5, 1–10. doi: 10.1080/19425120.2012.736445

Bray, R. N., Miller, A. C., and Geesey, G. G. (1981). The fish connection: A trophic link between planktonic and rocky reef communities? *Science* 214, 204–205. doi: 10.1126/science.214.4517.204

Brickhill, M. J., Lee, S. Y., and Connolly, R. M. (2005). Fishes associated with artificial reefs: attributing changes to attraction or production using novel approaches. *J. Fish Biol.* 67, 53–71. doi: 10.1111/j.0022-1112.2005.00915.x

Bugnot, A. B., Mayer-Pinto, M., Airoldi, L., Heery, E. C., Johnston, E. L., Critchley, L. P., et al. (2020). Current and projected global extent of marine built structures. *Nat. Sustain*, 33–41. doi: 10.1038/s41893-020-00595-1

Bulger, D. S., Volpe, J. P., and Fisher, J. T. (2019). Differences in fish communities on natural versus artificial temperate reefs, groundfish conservation applications in British Columbia. *Mar. Environ. Res.* 152, 104788. doi: 10.1016/j.marenvres.2019.104788

Burns, E. S., Clevenstine, A. J., Logan, R. K., and Lowe, C. G. (2020). Evidence of artificial habitat use by a recovering marine predator in southern California. *J. Fish Biol* 97, 1857–1860. doi: 10.1111/jfb.14539

Champion, C., Suthers, I. M., and Smith, J. A. (2015). Zooplanktivory is a key process for fish production on a coastal artificial reef. *Mar. Ecol. Prog. Ser.* 541, 1–14. doi: 10.3354/meps11529

Charbonnel, E., Serre, C., Ruitton, S., Harmelin, J.-G., and Jensen, A. (2002). Effects of increased habitat complexity on fish assemblages associated with large artificial reef units (French Mediterranean coast). *ICES J. Mar. Sci.* 59, S208–S213. doi: 10.1006/jmsc.2002.1263

Claisse, J. T., Pondella II, D. J., Love, M., Zahn, L. A., Williams, C. M., Williams, J. P., et al. (2014). Oil platforms off California are among the most productive marine fish habitats globally. *Proc. Natl. Acad. Sci. U.S.A.* 111, 15462–15467. doi: 10.1073/pnas.1411477111

Claudet, J., Osenberg, C. W., Benedetti-Cecchi, L., Domenici, P., García-Charton, J.-A., Pérez-Ruzafa, Á., et al. (2008). Marine reserves: size and age do matter. *Ecol. Lett.* 11, 481–489. doi: 10.1111/j.1461-0248.2008.01166.x

Claudet, J., Pelletier, D., Jouvenel, J., Bachet, F., and Galzin, R. (2006). Assessing the effects of marine protected area (MPA) on a reef fish assemblage in a northwestern Mediterranean marine reserve: identifiying community-based indicators. *Biol. Conserv.* 130, 349–369. doi: 10.1016/j.biocon.2005.12.030

Cresson, P., Le Direach, L., Rouanet, E., Goberville, E., Astruch, P., Ourgaud, M., et al. (2019). Functional traits unravel temporal changes in fish biomass production on artificial reefs. *Mar. Environ. Res.* 145, 137–146. doi: 10.1016/j.marenvres.2019.02.018

Cresson, P., Ruitton, S., and Harmelin-Vivien, M. (2014a). Artificial reefs do increase secondary biomass production: mechanisms evidenced by stable isotopes. *Mar. Ecol. Prog. Ser.* 509, 15–26. doi: 10.3354/meps10866

Cresson, P., Ruitton, S., Ourgaud, M., and Harmelin-Viivien, M. (2014b). Contrasting perception of fish trophic level from stomach content and stable isotope analyses: A Mediterranean artificial reef experience. *J. Exp. Mar. Biol. Ecol.* 452, 54–62. doi: 10.1016/j.jembe.2013.11.014

Cudney-Bueno, R., Lavín, M. F., Marinone, S. G., Raimondi, P. T., and Shaw, W. W. (2009). Rapid effects of marine reserves *via* larval dispersal. *PloS One* 4, e4140. doi: 10.1371/journal.pone.0004140

Dafforn, K. A. (2017). Eco-engineering and management strategies for marine infrastructure to reduce establishment and dispersal of non-indigenous species. *Manage. Biol. Invasions* 8, 153–161. doi: 10.3391/mbi.2017.8.2.03

Dahl, K. A., and Patterson, W. F.III (2014). Habitat-specific density and diet of rapidly expanding invasive red lionfish, *Pterois volitans*, populations in the northern gulf of Mexico. *PloS One* 9, e105852. doi: 10.1371/journal.pone.0105852

Danovaro, R., Gambi, C., Mazzola, A., and Mirto, S. (2002). Influence of artificial reefs on the surrounding infauna: analysis of meiofauna. *ICES J. Mar. Sci.* 59, S356–S362. doi: 10.1006/jmsc.2002.1223

Demartini, E. E., Barnett, A. M., Johnson, T. D., and Ambrose, R. F. (1994). Growth and production estimates for biomass-dominant fishes on a southern California artificial reef. *Bull. Mar. Sci.* 55, 484–500.

De Troch, M., Reubens, J. T., Heirman, E., Degraer, S., and Vincx, M. (2013). Energy profiling of demersal fish: A case-study in wind farm artificial reefs. *Mar. Environ. Res.* 92, 224–233. doi: 10.1016/j.marenvres.2013.10.001

Edgar, G. J., and Stuart-Smith, R. D. (2009). Ecological effects of marine protected areas on rocky reef communities–a continental-scale analysis. *Mar. Ecol. Prog. Ser.* 388, 51–62. doi: 10.3354/meps08149

Fabi, G., Luccarini, F., Panfili, M., Solustri, C., and Spagnolo, A. (2002). Effects of an artificial reef on the surrounding soft-bottom community (central Adriatic Sea). *ICES J. Mar. Sci.* 59, S343–S349. doi: 10.1006/jmsc.2002.1308

Fernandez-Betelu, O., Graham, I. M., and Thompson, P. M. (2022). Reef effect of offshore structures on the occurrence and foraging activity of harbour porpoises. *Front. Mar. Sci.* 9. doi: 10.3389/fmars.2022.980388

Foley, M. M., Halpern, B. S., Micheli, F., Armsby, M. H., Caldwell, M. R., Crain, C. M., et al. (2010). Guiding ecological principles for marine spatial planning. *Mar. Policy* 34, 955–966. doi: 10.1016/j.marpol.2010.02.001

Friedlander, A. M., and Parrish, J. D. (1998). Temporal dynamics of fish communities on an exposed shoreline in Hawaii. *Environ. Biol. Fishes* 53, 1–18. doi: 10.1023/A:1007497210998

Glarou, M., Zrust, M., and Svendsen, J. C. (2020). Using artificial-reef knowledge to enhance the ecological function of offshore wind turbine foundations: Implications for fish abundance and diversity. *J. Mar. Sci. Eng.* 8:1–25. doi: 10.3390/jmse8050332

Graham, M. H. (2004). Effects of local deforestation on the diversity and structure of southern California giant kelp forest food webs. *Ecosystems* 7, 341–357. doi: 10.1007/s10021-003-0245-6

Granneman, J. E., and Steele, M. A. (2014). Fish growth, reproduction, and tissue production on artificial reefs relative to natural reefs. *ICES J. Mar. Sci.* 71, 2494–2504. doi: 10.1093/icesjms/fsu082

Granneman, J. E., and Steele, M. A. (2015). Effects of reef attributes on fish assemblage similarity between artificial and natural reefs. *ICES J. Mar. Sci.* 72, 2385–2397. doi: 10.1093/icesjms/fsv094

Guillen, J. E., Ramos, A. A., Martinez, L., and Sanchez Lizaso, J. L. (1994). Antitrawling reefs and the protection of *Posidonia oceanica* (L.) delile meadows in the Western Mediterranean Sea: demand and aims. *Bull. Mar. Sci.* 55, 645–650.

Hamilton, S. L., Regetz, J., and Warner, R. R. (2008). Postsettlement survival linked to larval life in a marine fish. *Proc. Natl. Acad. Sci.* 105, 1561–1566. doi: 10.1073/pnas.0707676105

Harlin, M. M., and Lindbergh, J. M. (1977). Selection of substrata by seaweeds: Optimal surface relief. *Mar. Biol.* 40, 33–40. doi: 10.1007/BF00390625

Heery, E. C., Bishop, M. J., Critchley, L. P., Bugnot, A. B., Airoldi, L., Mayer-Pinto, M., et al. (2017). Identifying the consequences of ocean sprawl for sedimentary habitats. *J. Exp. Mar. Biol. Ecol.* 492, 31–48. doi: 10.1016/j.jembe.2017.01.020

Hixon, M. A. (1980). Comparative interactions between California reef fishes of the genus *Embiotoca*. *Ecology* 61, 918–931. doi: 10.2307/1936761

Hixon, M. A., and Beets, J. P. (1993). Predation, prey refuges, and the structure of coral-reef fish assemblages. *Ecol. Monogr.* 63, 77–101. doi: 10.2307/2937124

Holland, M. M., Becker, A., Smith, J. A., Everett, J. D., and Suthers, I. M. (2021). Fine-scale spatial and diel dynamics of zooplanktivorous fish on temperate rocky and artificial reefs. *Mar. Ecol. Prog. Ser.* 674, 221–239. doi: 10.3354/meps13831

Hunter, W. R., and Sayer, M. D. J. (2009). The comparative effects of habitat complexity on faunal assemblages of northern temperate artificial and natural reefs. *Ices J. Mar. Sci.* 66, 691–698. doi: 10.1093/icesjms/fsp058

Itosu, C., Otake, S., and Nakamura, M. (1995). "Excess energy of separated eddies due to its spin-down and upwelling," in *ECOSET '95 international conference on ecological system enhancement technology for aquatic environments* (Tokyo, Japan: Japan Internationa Marine Science and Technology Federation), 251–256.

Jackson, J. B. C., Kirby, M. X., Berger, W. H., Bjorndal, K. A., Botsford, L. W., Bourque, B. J., et al. (2001). Historical overfishing and the recent collapse of coastal ecosystems. *Science* 293, 629–638. doi: 10.1126/science.1059199

Jan, R.-Q., Liu, Y.-H., Chen, C.-Y., Wang, M.-C., Song, G.-S., Lin, H.-C., et al. (2003). Effects of pile size of artificial reefs on the standing stocks of fishes. *Fisheries Res.* 63, 327–337. doi: 10.1016/S0165-7836(03)00081-X

Johnson, T. D., Barnett, A. M., DeMartini, E. E., Craft, L. L., Ambrose, R. F., and Purcell, L. J. (1994). Fish production and habitat utilization on a southern California artificial reef. *Bull. Mar. Sci.* 55, 709–723.

Kellison, T. G., and Sedberry, G. R. (1998). The effects of artificial reef vertical profile and hole diameter on fishes off south Carolina. *Bull. Mar. Sci.* 62, 763–780.

Kim, C. G., Lee, J. W, and Park, J. S (1994). Artificial reef designs for Korean coastal waters. *Bulletin Mar. Sci.*, 55(2–3), 858–866.

Knowlton, N. (2021). Ocean optimism: moving beyond the obituaries in marine conservation. *Annu. Rev.* 13, 2.1–2.21. doi: 10.1146/annurev-marine-040220-101608

Komyakova, V., Chamberlain, D., Jones, G. P., and Swearer, S. E. (2019). Assessing the performance of artificial reefs as substitute habitat for temperate reef fishes: Implications for reef design and placement. *Sci. Total Environ.* 668, 139–152. doi: 10.1016/j.scitotenv.2019.02.357

Komyakova, V., Chamberlain, D., and Swearer, S. E. (2021). A multi-species assessment of artificial reefs as ecological traps. *Ecol. Eng.* 171, 106394. doi: 10.1016/j.ecoleng.2021.106394

Kough, A. S., Belak, C. A., Paris, C. B., Lundy, A., Cronin, H., Gnanalingam, G., et al. (2019). Ecological spillover from a marine protected area replenishes an over-exploited population across an island chain. *Conserv. Sci. Pract.* 1, e17. doi: 10.1111/csp2.17

Krone, R., Dederer, G., Kanstinger, P., Kramer, P., Schneider, C., and Schmalenbach, I. (2017). Mobile demersal megafauna at common offshore wind turbine foundations in the German bight (North Sea) two years after deployment - increased production rate of cancer pagurus. *Mar. Environ. Res.* 123, 53–61. doi: 10.1016/j.marenvres.2016.11.011

Lan, C.-H., and Hsui, C.-y. (2006). Insight from complexity: a new approach to designing the deplyment of artificial reef communities. *Bull. Mar. Sci.* 78, 21–28.

Leitão, F. (2013). Artificial reefs: from ecological processes to fishing enhancement tools. *Braz. J. Oceanogr.* 61, 77–81. doi: 10.1590/S1679-87592013000100009

Leitao, F., Santos, M. N., Erzini, K., and Monteiro, C. C. (2009). *Diplodus* spp. assemblages on artificial reefs: importance for near shore fisheries. *Fisheries Manage. Ecol.* 16, 88–99. doi: 10.1111/j.1365-2400.2008.00646.x

Lemoine, H. R., Paxton, A. B., Anisfeld, S. C., Rosemond, R. C., and Peterson, C. H. (2019). Selecting the optimal artificial reefs to achieve fish habitat enhancement goals. *Biol. Conserv.* 238:1–9. doi: 10.1016/j.biocon.2019.108200

Lindberg, W. J., Frazer, T. K., Portier, K. M., Vose, F., Loftin, J., Murie, D. J., et al. (2006). Density-dependent habitat selection and performance by a large mobile reef fish. *Ecol. Appl.* 16, 731–746. doi: 10.1890/1051-0761(2006)016[0731:DHSAPB]2.0.CO;2

Lindquist, D. G., Cahoon, L. B., Clavijo, I. E., Posey, M. H., Bolden, S. K., Pike, L. A., et al. (1994). Reef fish stomach contents and prey abundance on reef and sand substrata associated with adjacent artificial and natural reefs in onslow bay, North Carolina. *Bull. Mar. Sci.* 55, 308–318.

Love, M. S., Brothers, E., Schroeder, D. M., and Lenarz, W. H. (2007). Ecological performance of young-of-the-year blue rockfish (*Sebastes mystinus*) associated with oil platforms and natural reefs in California as measured by daily growth rates. *Bull. Mar. Sci.* 80, 147–157.

Love, M. S., Claisse, J. T., and Roeper, A. (2019). An analysis of the fish assemblages around 23 oil and gas platforms off California with comparisons with natural habitats. *Bull. Mar. Sci.* 95, 477–514. doi: 10.5343/bms.2018.0061

Marshall, D. J., Gaines, S., Warner, R., Barneche, D. R., and Bode, M. (2019). Underestimating the benefits of marine protected areas for the replenishment of fished populations. *Front. Ecol. Environ.* 17, 407–413. doi: 10.1002/fee.2075

Medeiros, A. P., Ferreira, B. P., Betancur-R, R., Cardoso, A. P., Matos, M. R., and Santos, B. A. (2021). Centenary shipwrecks reveal the limits of artificial habitats in protecting regional reef fish diversity. *J. Appl. Ecol.* 59, 286–299. doi: 10.1111/1365-2664.14053

Molles, J., and Manuel, C. (1978). Fish species diversity on model and natural reef patches: experimental insular biogeography. *Ecol. Monogr.* 48, 289–305. doi: 10.2307/2937232

Ogawa, Y. (1967). Experiments on the attractiveness of artificial reefs for marine fishes. *VII. Attraction Fishes to Various Sizes Model. Reefs. Bull. Jap. Soc Sci. Fish* 33, 801–811. doi: 10.2331/suisan.33.801

Ogawa, Y., Takeuchi, S., and Hattori, A. (1977). An estimate for the optimum size of artificial reef. *Bull. Japanese Soc. Fisheries Oceanogr. (Japan)* 30, 39–45.

Osenberg, C. W., St, C. M., Wilson, J. A., and Lindberg, W. J. (2002). A quantitative framework to evaluate the attraction-production controversy. *ICES J. Mar. Sci.* 598, S214–S221. doi: 10.1006/jmsc.2002.1222

Otake, S., Itosu, C., and Nakamura, M. (1995). "Artificial upwelling due to parallel walls," in *ECOSET '95 international conference on ecological system enhancement technology for aquatic environments* (Tokyo, Japan: Japan Internationa Marine Science and Technology Federation), 245–250.

Page, H. M., and Hubbard, D. M. (1987). Temporal and spatial patterns of growth in mussels *Mytilus edulis* on an offshore platform: relationships to water temperature and food availability. *J. Exp. Mar. Biol. Ecol.* 111, 159–179. doi: 10.1016/0022-0981(87)90053-0

Paxton, A. B., Newton, E. A., Adler, A. M., Van Hoeck, R. V., Iversen, E. S.Jr., Taylor, J. C., et al. (2020a). Artificial habitats host elevated densities of large reef-associated predators. *PloS One* 15, e0237374. doi: 10.1371/journal.pone.0237374

Paxton, A. B., Shertzer, K. W., Bacheler, N. M., Kellison, G. T., Riley, K. L., and Taylor, J. C. (2020b). Meta-analysis reveals artificial reefs can be effective tools for fish community enhancement but are not one-Size-Fits-All. *Front. Mar. Sci.* 7. doi: 10.3389/fmars.2020.00282

Pérez-Ruzafa, A., Martín, E., Marcos, C., Zamarro, J. M., Stobart, B., Harmelin-Vivien, M., et al. (2008). Modelling spatial and temporal scales for spill-over and biomass exportation from MPAs and their potential for fisheries enhancement. *J. Nat. Conserv.* 16, 234–255. doi: 10.1016/j.jnc.2008.09.003

Peterson, C. H., Grabowski, J. H., and Powers, S. P. (2003). Estimated enhancement of fish production resulting from restoring oyster reef habitat:

quantitative valuation. *Mar. Ecol. Prog. Ser.* 264, 249–264. doi: 10.3354/meps264249

Polovina, J. J., and Sakai, I. (1989). Impacts of artificial reefs on fishery production in Shimamaki, Japan. *Bull. Mar. Sci.* 44, 997–1003.

Pondella II, D. J., Allen, L. G., Craig, M. T., and Gintert, B. (2006). Evaluation of eelgrass mitigation and fishery enhancement structures in San Diego bay, California. *Bull. Mar. Sci.* 78, 115–131.

Pondella II, D. J., Stephens, J. S., and Craig, M. T. (2002). Fish production of a temperate artificial reef based on the density of embiotocids (Teleostei: Perciformes). *ICES J. Mar. Sci.* 59, S88–S93. doi: 10.1006/jmsc.2002.1219

Pondella II, D. J., Williams, J. P., Williams, C. M., Claisse, J. T., and Witting, D. (2018). "Restoring a nearshore rocky reef ecosystem in the challenge of an urban setting," in *Marine artificial reef research and development: Integrating fisheries management objectives* (Bethesda, Maryland, USA: American Fisheries Society), 165–186.

Pondella II, D. J., Zahn, L. A., Love, M. S., Siegel, D., and Bernstein, B. B. (2015). Modeling fish production for southern California's petroleum platforms. *Integrated Environ. Assess. Manage.* 11, 584–593. doi: 10.1002/ieam.1689

Potts, T. A., and Hulbert, A. W. (1994). Structural influences of artificial and natural habitats on fish aggregations in onslow bay, North Carolina. *Bull. Mar. Sci.* 55, 609–622.

Powers, S. P., Grabowski, J. H., Peterson, C. H., and Lindberg, W. J. (2003). Estimating enhancement of fish production by offshore artificial reefs: uncertainty exhibited by divergent scenarios. *Mar. Ecol. Prog. Ser.* 264, 265–277. doi: 10.3354/meps264265

Puckeridge, A. C., Becker, A., Taylor, M. D., Lowry, M. B., McLeod, J., Schilling, H. T., et al. (2021). Foraging behaviour and movements of an ambush predator reveal benthopelagic coupling on artificial reefs. *Mar. Ecol. Prog. Ser.* 666, 171–182. doi: 10.3354/meps13691

Reeds, K. A., Smith, J. A., Suthers, I. M., and Johnston, E. L. (2018). An ecological halo surrounding a large offshore artificial reef: Sediments, infauna, and fish foraging. *Mar. Environ. Res.* 141, 30–38. doi: 10.1016/j.marenvres.2018.07.011

Relini, G., Relini, M., Palandri, G., Merello, S., and Beccornia, E. (2007). History, ecology and trends for artificial reefs of the Ligurian sea, Italy. *Hydrobiologia* 580, 193–217. doi: 10.1007/s10750-006-0453-0

Reubens, J. T., Degraer, S., and Vincx, M. (2014). The ecology of benthopelagic fishes at offshore wind farms: a synthesis of 4 years of research. *Hydrobiologia* 727, 121–136. doi: 10.1007/s10750-013-1793-1

Ricker, W. E. (1975). Computation and interpretation of biological statistics of fish populations. *Bull. Fisheries Res. Board Canada* 191, 382.

Roa-Ureta, R. H., Santos, M. N., and Leitão, F. (2019). Modelling long-term fisheries data to resolve the attraction versus production dilemma of artificial reefs. *Ecol. Model.* 407:1–12. doi: 10.1016/j.ecolmodel.2019.108727

Robertson, B. A., and Hutto, R. L. (2006). A framework for understanding ecological traps and an evaluationn of existing evidence. *Ecology* 87, 1075–1085. doi: 10.1890/0012-9658(2006)87[1075:AFFUET]2.0.CO;2

Rosemond, R. C., Paxton, A. B., Lemoine, H. R., Fegley, S. R., and Peterson, C. H. (2018). Fish use of reef structures and adjacent sand flats: implications for selecting minimum buffer zones between new artificial reefs and existing reefs. *Mar. Ecol. Prog. Ser.* 587, 187–199. doi: 10.3354/meps12428

Rouse, S., Porter, J. S., and Wilding, T. A. (2020). Artificial reef design affects benthic secondary productivity and provision of functional habitat. *Ecol. Evol.* 10 (4), 2122–2130. doi: 10.1002/ece3.6047

Russ, G. R., Alcala, A. C., Maypa, A. P., Calumpong, H. P., and White, A. T. (2004). Marine reserve benefits local fisheries. *Ecol. Appl.* 14, 597–606. doi: 10.1890/03-5076

Santos, M. N., Monteiro, C. C., and Leitão, F. (2011). "The role of artificial reefs in the sustainability of artisanal fisheries," in *Artificial reefs in fisheries management* (New York: Taylor and Francis Group), 221–237.

Schmiing, M., Fontes, J., and Afonso, P. (2017). Predictive mapping of reproductive fish habitats to aid marine conservation planning. *Can. J. Fisheries Aquat. Sci.* 74, 1016–1027. doi: 10.1139/cjfas-2015-0538

Schulze, A., Erdner, D. L., Grimes, C. J., Holstein, D. M., and Miglietta, M. P. (2020). Artificial reefs in the northern gulf of Mexico: Community ecology amid the "Ocean sprawl". *Front. Mar. Sci.* 7, 447. doi: 10.3389/fmars.2020.00447

Schwartzbach, A., Behrens, J. W., and Svendsen, J. C. (2020). Atlantic Cod gadus morhua save energy on stone reefs: implications for the attraction versus production debate in relation to reefs. *Mar. Ecol. Prog. Ser.* 635, 81–87. doi: 10.3354/meps13192

Seaman, W. (2019). "Artificial reefs," in *Encyclopedia of ocean sciences, 3rd edition*, vol. 1 . Eds. J.K Cochran, H. Bokuniewicz and L. P. Yager, Elsevier: Amsterdam, Netherlands 662–670.

Sherman, R. L., Gilliam, D. S., and Spieler, R. E. (2002). Artificial reef design: void space, complexity, and attractants. *ICES J. Mar. Sci.* 59, S196–S200. doi: 10.1006/jmsc.2001.1163

Smith, J. A., Lowry, M. B., Champion, C., and Suthers, I. M. (2016). A designed artificial reef is among the most productive marine fish habitats: new metrics to address 'production versus attraction'. *Mar. Biol.* 163, 1–8. doi: 10.1007/s00227-016-2967-y

Smith, J. A., Lowry, M. B., and Suthers, I. M. (2015). Fish attraction to artificial reefs not always harmful: a simulation study. *Ecol. Evol.* 5, 4590–4602. doi: 10.1002/ece3.1730

Steimle, F., Foster, K., Kropp, R., and Conlin, B. (2002). Benthic macrofauna productivity enhancement by and artificial reef in Delaware Bay, USA. *ICES J. Mar. Sci.* 59, S100–S105. doi: 10.1006/jmsc.2002.1268

Stephens, J. S., Morris, P. A., Pondella II, D. J., Koonce, T. A., and Jordan, G. A. (1994). Overview of the dynamics of an urban artificial reef fish assemblage at king Harbor, California, USA, 1974-1991: A recruitment driven system. *Bull. Mar. Sci.* 55, 1224–1239.

Tickell, S. C., Sáenz-Arroyo, A., and Milner-Gulland, E. J. (2019). Sunken worlds: The past and future of human-made reefs in marine conservation. *BioScience* 69, 725–735. doi: 10.1093/biosci/biz079

Todd, V. L. G., Lazar, L., Williamson, L. D., Peters, I. T., Hoover, A. L., Cox, S. E., et al. (2020). Underwater visual records of marine megafauna around offshore anthropogenic structures. *Front. Mar. Sci.* 7, 230. doi: 10.3389/fmars.2020.00230

Truong, L., Suthers, I. M., Cruz, D. O., and Smith, J. A. (2017). Plankton supports the majority of fish biomass on temperate rocky reefs. *Mar. Biol.* 164:1–12. doi: 10.1007/s00227-017-3101-5

Turner, C. H., Ebert, E. E., and Given, R. R. (1969). *Fish Bulletin 146. Man-Made Reef Ecology.* (UC San Diego: Library – Scripps Digital Collection). *Retrieved from https://escholarship.org/uc/item/2s55m47r*

Walters, L. J., and Wethey, D. S. (1996). Settlement and early post-settlement survival of sessile marine invertebrates on topographically complex surfaces: the importance of refuge dimensions and adult morphology. *Mar. Ecol. Prog. Ser.* 137, 161–171. doi: 10.3354/meps137161

Warner, R. R. (1988). Traditionality of mating-site preferences in a coral reef fish. *Nature* 335, 719–721. doi: 10.1038/335719a0

Wedding, L., and Yoklavich, M. M. (2015). Habitat-based predictive mapping of rockfish density and biomass off the central California coast. *Mar. Ecol. Prog. Ser.* 540, 235–250. doi: 10.3354/meps11442

Whitmarsh, D., Santos, M. N., Ramos, J., and Monteiro, C. C. (2008). Marine habitat modification through artificial reefs off the Algarve (southern Portugal): An economic analysis of the fisheries and the prospects for management. *Ocean Coast. Manage.* 51, 463–468. doi: 10.1016/j.ocecoaman.2008.04.004

Worm, B., Barbier, E. B., Beaumont, N., Duffy, J. E., Folke, C., Halpern, B. S., et al. (2006). Impacts of biodiversty loss on ocean ecosystem services. *Science* 314, 787–790. doi: 10.1126/science.1132294

frontiers | Frontiers in Marine Science

TYPE Original Research
PUBLISHED 28 October 2022
DOI 10.3389/fmars.2022.979987

OPEN ACCESS

EDITED BY
Toyonobu Fujii,
Tohoku University, Japan

REVIEWED BY
Astrid Brigitta Leitner,
Monterey Bay Aquarium Research Institute (MBARI), United States
Felipe Torquato,
Qatar University, Qatar

*CORRESPONDENCE
Ronen Galaiduk
r.galaiduk@aims.gov.au

SPECIALTY SECTION
This article was submitted to Marine Ecosystem Ecology, a section of the journal Frontiers in Marine Science

RECEIVED 28 June 2022
ACCEPTED 11 October 2022
PUBLISHED 28 October 2022

CITATION
Galaiduk R, Radford B, Case M, Bond T, Taylor M, Cooper T, Smith L and McLean D (2022) Regional patterns in demersal fish assemblages among subsea pipelines and natural habitats across north-west Australia. *Front. Mar. Sci.* 9:979987. doi: 10.3389/fmars.2022.979987

Regional patterns in demersal fish assemblages among subsea pipelines and natural habitats across north-west Australia

Ronen Galaiduk[1,2*], Ben Radford[1,2], Mark Case[1], Todd Bond[2,3], Michael Taylor[2,3], Tim Cooper[2,4], Luke Smith[2,5] and Dianne McLean[1,2]

[1]Australian Institute of Marine Science, Indian Ocean Marine Research Centre (IOMRC), Perth, WA, Australia, [2]Oceans Institute, The University of Western Australia, Perth, WA, Australia, [3]School of Biological Sciences, The University of Western Australia, Perth, WA, Australia, [4]BHP, Perth, WA, Australia, [5]Woodside Energy, Perth, WA, Australia

Regional patterns of fish diversity, abundance, distribution, and assemblage composition are driven by a combination of biotic and abiotic conditions in the marine environment, but these conditions can be altered through anthropogenic activities, such as those associated with oil and gas extraction. The present study utilises data on fish relative abundance and diversity obtained from 1546 baited remote underwater video deployments conducted between 2004 – 2019 in depths of 9 – 170 m across 2000 km of coastline in north-west Australia on natural habitats and subsea pipelines to understand the influence of oil and gas infrastructure on fish assemblages. A total of 450 fish taxa from 56 families was observed, with populations dominated by generalist and invertebrate carnivore taxa. At the regional scale, subsea pipelines had lower diversity (lower taxonomic richness) than natural environments, but possessed a higher abundance of piscivorous and herbivorous fish taxa. Clear patterns in fish assemblage composition were observed in multivariate analyses, reflecting the proximity of oceanic shoals and banks, depth, and to a lesser extent, oil and gas infrastructure. Shallow-water and close to shoals assemblages were characterised by a diversity of site-attached (e.g., wrasses, tuskfish), reef-associated taxa (e.g., emperors). Mesophotic fish assemblages were characterised by commercially important (e.g., goldband snapper), wide-ranging (e.g., sharks) and sand-affiliated (e.g., toadfish, threadfin bream) taxa. Proximity to pipelines and platforms ranked low as predictors in the multivariate analyses suggesting a negligible regional influence of these structures on fish communities in comparison to depth and shoal habitats. Local-scale influences of subsea infrastructure, however, may be important for some fish species (infrastructure *vs.* immediate surrounds). Our study highlights the influence of abiotic factors on regional-scale patterns in fish assemblage structure across north-west Australia.

KEYWORDS

multivariate regression trees (MRT), subsea oil and gas infrastructure, decommissioning, north-west Australia, species richness

Introduction

Fish-habitat relationships can govern assemblage structure and vary spatially, with such variability manifesting in contrasting patterns of ecosystem functioning and values across a region (Underwood et al., 2000; Bradley et al., 2021). This can lead to diverging perceptions of the importance of different habitats for fish and the impact that their loss or modification may have on species survival and community maintenance (Zanini et al., 2009; Randin et al., 2020). While the underlying mechanisms for variation in fish assemblage structure are often unclear (Bradley et al., 2021), at fine spatial scales, they likely reflect population processes (e.g. competition, predation, settlement, recruitment mortality; Hyndes et al., 1996; Hyndes et al., 2003; Willis & Anderson, 2003; Almany, 2004; Hixon & Jones, 2005; Galaiduk et al., 2013) and at broader spatial scales may reflect environmental factors (e.g. depth, temperature, complexity; Gratwicke & Speight, 2005; Tuya et al., 2011; Langlois et al., 2012; Galaiduk et al., 2017a; Bradley et al., 2021). Understanding the processes that influence fish assemblage structure from fine scale to those that occur across seascapes is required to disaggregate population processes and environmental drivers, with this information also key to informing conservation and resource management.

A challenge for fisheries and conservation managers is to understand the status and trend of fish assemblages, not only considering population processes and environmental drivers, but the multiple natural and anthropogenic pressures that fish assemblages may face such as climate change (Pratchett et al., 2011) and cyclones (Gilmour et al., 2019). Another type of anthropogenic influence in the marine environment globally, is the presence and operation of offshore oil and gas (O&G) infrastructure. These structures are placed strategically on continental shelfs (Claisse et al., 2014; Fujii, 2015) where crude oil and natural gas pockets are identified (van Elden et al., 2019) and typically comprise pipelines, wells, platforms or floating facilities with substantial additional subsea infrastructure (e.g. umbilicals, flowlines, etc) deployed to support these activities. The addition and subsequent removal (e.g., through the decommissioning of O&G infrastructure) of this prominent artificial habitat is likely to have a substantial impact on marine communities (Meyer-Gutbrod et al., 2019), including fish (Claisse et al., 2015), yet such impact assessment research is missing from published literature (but see Coolen et al., 2020; Meyer-Gutbrod et al., 2020).

The fish assemblages of natural shallow marine ecosystems across north-west (NW) Australia have been relatively well studied (Wilson et al., 2012; Evans et al., 2014; McLean et al., 2016), particularly in comparison to those present in mesophotic depths and beyond (Currey-Randall et al., 2021; Saunders et al., 2021; Wellington et al., 2021). Unique and diverse fish communities exist across the inshore shallow coral reefs, offshore emergent oceanic reefs, oceanic banks and shoals of the region (Heyward et al., 2012; Moore et al., 2014; Wilson et al., 2014; Moore et al., 2017) with lower fish diversity in sand-dominated regions offshore (Currey-Randall et al., 2021; McLean et al., 2021). The NW supports a number of commercial finfish fishery operations such as Northern Demersal Scalefish Managed Fishery, Pilbara Demersal Scalefish Fisheries and Northern Territory Demersal fishery as well as several others throughout this region (Newman et al., 2020; Gaughan & Santoro, 2021). Habitat, depth and latitude have a strong influence on fish assemblage structure across this region (McLean et al., 2016) and fish species richness declines with increasing latitude (Wellington et al., 2021). In recent years, research into fish-habitat relationships in the NW has extended to O&G infrastructure with the goal of quantifying communities that exist on previously unstudied structures. This region possesses a significant O&G precinct valued at $37 billion (DMIRS, 2021) with construction, operation and decommissioning activities all potentially interacting with diverse marine ecosystems in this region. A diversity of fish assemblages have been observed to associate with subsea wells (Cummings et al., 2011; Fowler et al., 2015; McLean et al., 2018), pipelines (McLean et al., 2017; Bond et al., 2018a; Bond et al., 2018b; McLean et al., 2020) and platforms (Pradella et al., 2014; McLean et al., 2019; Thomson et al., 2021). Few studies have compared local fish assemblages on subsea structures to those in natural ecosystems (Bond et al., 2018a; Bond et al., 2018b; McLean et al., 2021; Schramm et al., 2021), with a lack of comparable data from infrastructure and natural ecosystems remaining one of the biggest drawbacks to understanding the influence of O&G structures on marine communities.

The present study represents the first large-scale investigation of the relative influence of environmental predictors including O&G infrastructure in structuring fish assemblages in NW Australia. Utilising comparable data from subsea pipelines and natural habitats, we aimed to: i) compare fish abundance and species richness on subsea pipelines to those observed in neighbouring natural seabed environments, ii) investigate the relative influence of environmental predictors in structuring fish assemblages in NW Australia and, iii) understand how proximity to oil and gas infrastructure (platform jackets and pipelines) may influence these fish assemblages.

Methods

Study locations

The study focussed on three subsea pipelines (Griffin, Echo Yodel and Bayu-Undan) located within natural habitats in

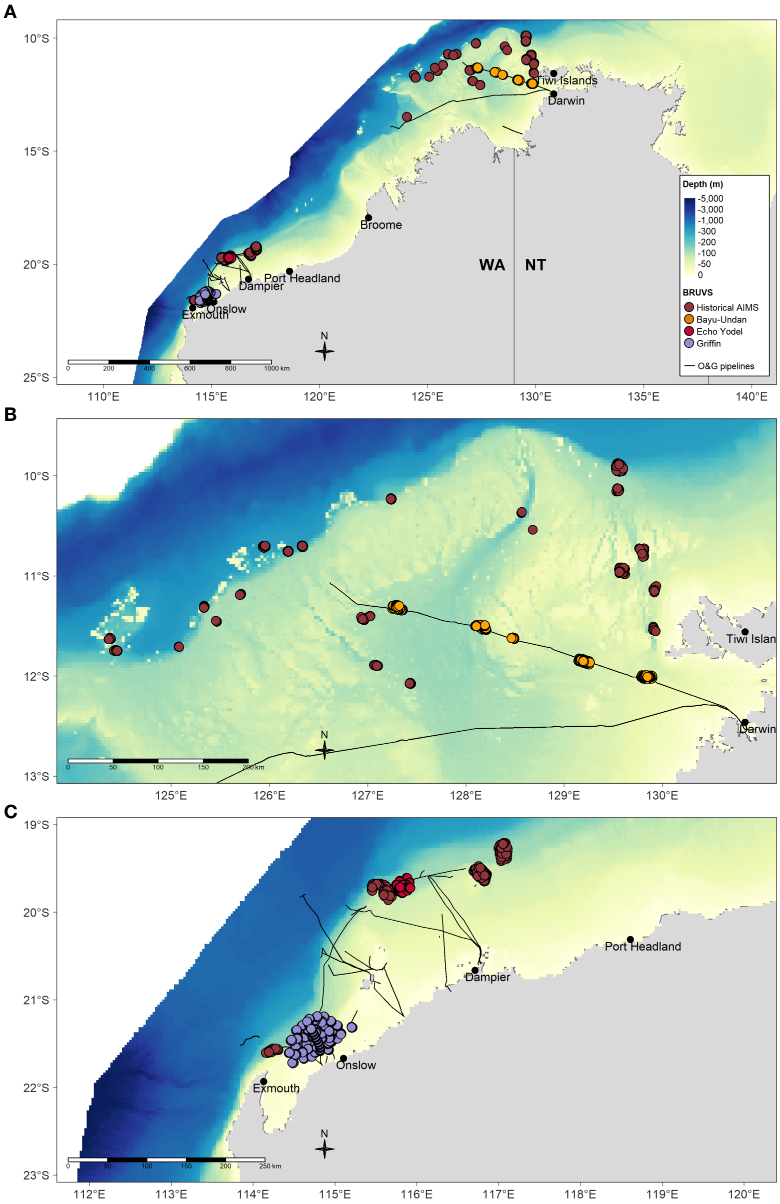

FIGURE 1
Location of individual BRUV deployments for which data were included in the present study from **(A)** across the region, **(B)** in the north and including the Bayu-Undan pipeline and, **(C)** in the north-west including Griffin and Echo Yodel pipelines and from historical AIMS BRUVs deployments in natural habitats. The studies for which the BRUVs data were collected are documented in Table 1. Depth raster sourced from Geoscience Australia 250 m bathymetry grid (Whiteway, 2009).

Australia's NW marine estate (Figure 1). Data for pipelines and surrounding ecosystems were contributed by three independent studies, namely Bond et al., 2018a (Griffin), Bond et al., 2018b (Echo Yodel) and McLean et al., 2021 (Bayu-Undan), which was combined with historical data collected by the Australian Institute of Marine Science (AIMS) on the fish faunas occupying a range of natural habitats across the NW shelf (Table 1).

Fish surveys

All surveys used baited remote underwater video systems (BRUVs) to sample fish communities according to standard protocols (Langlois et al., 2020). This included daytime surveys (one hour after sunrise to one hour before sunset), spacing of neighbouring deployments by at least 400 m, seabed filming times of 60 minutes and the use of ~1 kg of crushed pilchards

(*Sardinops* sp.) as bait. EventMeasure software (www.seagis.com.au) was used to annotate individual fish within 8 m from the camera system, identify each fish to the finest taxonomic unit possible, and to obtain measures of relative abundance which was expressed as MaxN (the greatest abundance of each taxonomic unit record in a single frame of a deployment; Priede et al., 1994). Where fish could not be identified reliably to species level, they were recorded to the next lowest taxonomic level possible (typically genus or family, e.g., *Nemipterus* spp.). Use of BRUVs provides information on carnivorous fish species without precluding sampling of herbivores or prey species, yet tends to under-sample (as do other visual methods) very cryptic and small-bodied fishes such as Gobiidae (Watson et al., 2005; Harvey et al., 2007). Fishery target species were defined as those that are retained by commercial fisheries that operate in the NW region (Gaughan and Santoro, 2021). An additional range of fish metrics was recorded to facilitate investigation of how the trophic roles of species and assemblages compared across different habitats in the region. All species were assigned to feeding guilds based on dietary information obtained from Fishbase (Froese and Pauly, 2021a; Froese and Pauly, 2021b).

Environmental predictors

A range of environmental predictors considered to be potential ecological drivers for fish diversity and abundance were measured in order to examine their potential to predict the observed patterns in the fish assemblage structure across NW Australia.

Distance to natural and artificial features

We calculated proximity in metres between individual BRUV deployments and each of the nearest neighbour of a range of natural and artificial features: i) inshore shallow coral reefs (hereinafter reef; Kordi et al., 2016; UNEP-WCMC et al., 2021), ii) emergent oceanic reefs, oceanic banks, and oceanic shoals (hereinafter shoal; Moore et al., 2017; Heyward & Radford, 2019), as well as oil and gas iii) platform and iv) pipeline using the Euclidean distance tool in ArcGIS Pro 2.8.

Sea surface temperature

Daily sea surface temperature (SST) data were acquired for all BRUV deployments from Modis Aqua Level 3 product satellite imagery with a spatial resolution of 500 m. The average SST for each historical campaign is indicated in Table 1. The nearest neighbour pixel extraction approach was used for deployments where SST data were not directly available using the NASA Appears application programming interface. This was necessary because data may not be available for a myriad of reasons (e.g., clouds, refraction and reflection, etc). The Level 3 product is geometrically and radiometrically corrected and cleaned to remove cloud artefacts with the SST calculated from surface reflectance bands using the algorithm outlined in Brown et al. (1999). Daily SST values from the time-series (2004-2019) were then averaged for each BRUV deployment location.

Depth and geomorphology gradients

Seafloor depth and structural complexity were extracted and estimated for each BRUV deployment. Structural complexity variables (such as the mean or slope) were calculated from a 250 m resolution bathymetry raster (Whiteway, 2009) using ArcGIS Pro 2.8, custom-written code in Python, and terrain analysis techniques (Holmes et al., 2008). These techniques quantify the relationships among depth values in small neighbourhoods to reveal textural differences. Calculations are run on a small number of neighbourhood cells surrounding each pixel and the value assigned to the central cell in the output, thus creating a derivative dataset (see Cure et al., 2021; Currey-Randall et al., 2021; McLean et al., 2021) for additional information on secondary rasters). This produced a set of 23 secondary rasters that describe the structure and complexity of the seafloor (Supplementary Data Table S1). We then used a principal component analysis (PCA; Fung & LeDrew, 1987) and a geomorphic gradient isoclassification (Isoclass; Richards & Jia, 2006) to reduce the dimensionality of the secondary rasters and combine them into geomorphic clusters based on increasing levels of seafloor complexity (see Galaiduk et al., 2019; McLean et al., 2021 for additional details on geomorphic gradient analysis). We classified the seafloor complexity into three categories: 'pipeline', to represent the pipeline artificial habitat which was assigned based on *a priori* allocation of BRUV deployment locations from the sampling designs for each study; 'low complexity off pipeline' which consisted of the bottom two geomorphic clusters from the Isoclass analysis derived for natural habitats; and 'high complexity off pipeline' which included the top two geomorphic clusters of the natural seafloor complexity from the Isoclass analysis (hereafter pipeline, low and high complexity, respectively). All 'off pipeline' deployments are those >400 m away from subsea pipelines while 'pipeline' deployments were those specifically targeted at pipelines *via* either vessel's echo sounder, GPS coordinates or visual observation in the camera systems, often with high accuracy (see Bond et al., 2018a; Bond et al., 2018b; McLean et al., 2021).

Data analyses

To test for differences among seafloor complexity categories and the relative abundance of feeding guilds of fish (summed MaxN's for each deployment into six feeding guilds) we used a one way PERMANOVA analysis in PRIMER 7 with

TABLE 1 A description of BRUVs data used and its source.

Data	Survey year	# BRUV deployments	Depth range (m)	Mean SST (°C)	Reference
Griffin pipeline & surrounds	Mar-Apr 2017	269	9-135	25.85 ± 0.01	Bond et al., 2018a
Echo Yodel pipeline & adjacent	Apr 2017	69	108-140	26.98 ± 0.002	Bond et al., 2018b
Bayu-Undan pipeline & surrounds	Sept-Oct 2019	198	22-121	29.03 ± 0.005	McLean et al., 2021
Historical AIMS data					
Oceanic Shoals: biodiversity assessment	Jan-Feb 2004	192	21-120	28.94 ± 0.05	Unpublished AIMS data
ATSEA Timor Sea shoals	Jun-Jul 2011	84	19-43	29.01 ± 0.01	Da Silva & Luis Pereira, 2011
NERP: Oceanic shoals CMR	Sep-Oct 2012	47	31-76	28.94 ± 0.04	Nichol et al., 2013; Przeslawski et al., 2013
Rankin Bank & Glomar shoal	Nov 2013	142	19-90	26.96 ± 0.02	AIMS, 2014
NW shoals	May 2014	76	23-158	28.86 ± 0.04	Heyward et al., 2015
Barossa environmental program	Sep-Oct 2015	95	16-88	28.54 ± 0.02	Heyward et al., 2017
Rankin GWF	Nov-Jan 2017	211	19-91	26.96 ± 0.02	Currey-Randall et al., 2019
Conoco Barossa environmental study	Sep-Oct 2017	63	27-77	28.74 ± 0.09	AIMS, 2016
Ancient coastline KEF	May-Oct 2019	100	62-170	26.86 ± 0.63	Currey-Randall et al., 2021
Range/total	**2004-2019**	**1546**	**9-170**	**25.8-29**	

Bold text refers to range/total of the column. SST refers to sea surface temperature.

PERMANOVA extension (Anderson et al., 2008). We applied dispersion-based weighting first on the raw MaxN data to down weight the effects of highly abundant, schooling and clustered species (Clarke et al., 2006). We subsequently performed the PERMANOVA analysis which accounts for an unbalanced design (Anderson et al., 2008) using unrestricted permutation of the down-weighted data based on Bray-Curtis distance matrix with 9999 permutation and type III sum of squares. A *post-hoc* pairwise comparison was completed to investigate significant statistical results of the PERMANOVA. In addition, we ran individual PERMANOVA tests on each feeding guild separately (using the same method described above) to investigate guild-specific patterns.

To examine whether variation in fish assemblage composition could be predicted by a range of environmental variables, we performed two different tests, 1) distance-based linear model (DISTLM; McArdle and Anderson, 2001) and 2) multivariate regression tree (MRT) analysis (De'ath, 2002; Ouellette et al., 2012).

Distance-based linear model

A DISTLM was used to partition multivariate variability in fish abundance that is explained by the environmental predictors included in the model (seafloor complexity, depth, mean SST, distance to platform, distance to pipeline, distance to shoal, distance to reef), with the best model visualised *via* distance-based redundancy analysis (dbRDA; McArdle & Anderson, 2001; Anderson et al., 2008) using the PRIMER-E statistical software package. Seafloor complexity was a categorical variable in the analysis and therefore assigned numerical values with 1 = low, 2 = high and 3 = pipe. Prior to undertaking the DISTLM analysis, a draftsman plot was produced to detect multicollinearity. This resulted in the removal of latitude and longitude from the analysis as each was unsurprisingly correlated with mean SST. The best model was selected using a stepwise procedure in which the relative contribution of each predictor in explaining fish abundance was assessed for 1) statistical significance using marginal tests (from 9999 permutations) and 2) percentage contribution of the variance explained (R^2) of each set of variables (Anderson et al., 2008). Adjusted R^2 was used as the selection criterion as it considers predictor variables with different numbers of levels.

Multivariate regression tree

MRT is a type of constrained clustering that recursively partitions the dataset into homogenous clusters using explanatory environmental variables, is robust to the co-variation in explanatory variables and is well-suited for modelling complex linear and nonlinear relationships (De'ath & Fabricius, 2000; De'ath, 2002). After excluding rare species (those that occurred less than five times in the dataset), fourth root transformed MaxN fish abundance was the response variable in the MRT with all available environmental variables, including the seafloor complexity variables (low, high, pipe), used as predictors. Rare species tend to amplify the importance of rare habitat types and so by removing them we avoided biasing results based on a shared common absence of rare species, instead concentrating specifically on common conditions found throughout the region (Gust et al., 2001).

In each split of the MRT, the machine learning algorithm considered all explanatory variables and selected the variable that maximised the reduction in group heterogeneity. The most parsimonious tree (i.e. the simplest possible tree given the data) was selected using cross-validation and the 1-SE rule (De'ath & Fabricius, 2000). To identify representative species in each community derived from the MRT, Dufrêne-Legendre index (DLI) values were calculated for all species across all leaves of the tree (Dufrene and Legendre, 1997). Each species was assigned to the terminal node (leaf) of the tree where its DLI value was highest. Species with the highest DLI values are considered representative of that assemblage, and the spatial extent of the assemblage indicated the region where the species was predominantly found (DeVantier et al., 2006). This analysis was performed in R statistical software (R Core Team, 2019), using the packages *mvpart* (De'ath, 2011), *vegan* (Oksanen et al., 2013) and *labdsv* (Roberts & Roberts, 2016).

Species diversity on pipelines and in natural habitats

To make a broad comparison of alpha diversity (i.e., species richness) between fish communities on pipelines and those observed in natural habitats, individual BRUV deployments were grouped by habitat type (low/high complexity seafloor and pipeline). We derived species rarefaction and extrapolation sampling curves for the observed species richness in each habitat type using iNEXT package in R (Hsieh et al., 2016). The species richness was calculated based on observed cumulative number of individuals and unique species for the three habitat types. This approach allowed for an unbiased comparison of species richness across assemblages irrespective of sample size or sampling effort (Colwell et al., 2012; Chao et al., 2014).

Results

The 1546 BRUV deployments detected a total of 90,435 individual fishes from 450 taxa spanning 56 families. The most ubiquitous taxa across the region were *Nemipterus* spp. (threadfin bream; present on 37% of BRUV deployments), *Abalistes stellatus* (starry triggerfish; 28% of BRUVs), *Carangoides coeruleopinnatus* (onion trevally; 27%), *Lethrinus rubrioperculatus* (spotcheek emperor; 27%) and *Sufflamen fraenatum* (bridled triggerfish; 25%) (Supplementary Data Table S2). The most numerically abundant fishes were *Parupeneus heptacanthus* (opalescent goatfish; n = 5253), *Nemipterus* spp. (n = 3015), *Scarus dimidiatus* (bluebridled parrotfish; n = 2712), *Pomacentrus nagasakiensis* (blue-scribble damsel; n = 2598), *Caranx sexfasciatus* (bigeye trevally; n = 2315) and *Lutjanus fulviflamma* (blackspot snapper; n = 2083) (Supplementary Data Table S2). The most abundant and commonly observed feeding guild of fishes was generalist carnivores (n = 30,238 individuals on 99% BRUVs) followed by invertebrate carnivores (n = 24,754 on 80% BRUVs). While zooplanktivores were the next most abundant (n = 23,053 on 40% BRUVs), piscivores were the third most ubiquitous feeding guild across the samples (n = 2329 on 51% of BRUVs) (Supplementary Data Table S2).

Mean abundance of specific feeding guilds varied significantly among seafloor complexity categories (PERMANOVA: MS = 4734.9, Pseudo-F = 9.85, *P(perm)* = 0.0001), but not for zooplanktivores, invertebrate carnivores, and generalist carnivores ($P_{(\mathrm{pairwise})}$ = 0.12, 0.85, 0.35, respectively). The mean abundance of piscivores differed between all seafloor complexities (all $t > 2.4$, all $P_{(\mathrm{pairwise})} < 0.02$), largely due to being most abundant on pipelines and least abundant on low complexity seafloor (Figure 2). Piscivores (see Supplementary Data Table S2) typically included large-bodied taxa such as sharks, barracuda, groupers, and tuna. The abundance of algae/invertebrate consumers was greater on high complexity seafloor than low complexity ($t = 2.46$, $P_{(\mathrm{pairwise})} = 0.016$) (Figure 2). Herbivore abundance was similar on low and high complexity seafloor ($P_{(\mathrm{pairwise})}= 0.95$) but higher on pipelines (both $t > 3.9$, $P_{(\mathrm{pairwise})} < 0.001$) with this group represented by many parrotfish and surgeonfish species.

Marginal tests from DISTLM suggested a significant relationship between the variation in fish assemblages (all $p < 0.01$) and all the potential environmental predictors. Depth explained the greatest amount of variation in fish abundance (5%). The variables that increased the value of adjusted R^2 after depth were distance to shoal (3%, 8% cumulative), mean SST (2%, 10% cumulative), distance to pipeline (2%, 11.9% cumulative), distance to platform (1%, 13% cumulative), distance to reef (0.8%, 13.8% cumulative) and then seafloor complexity (0.7%, 14.6% cumulative). All conditional tests associated with these sequential additions were significant ($p < 0.01$). The best solution in the stepwise model included all seven variables and explained 14% of the variation in fish relative abundance (Figure 3). The first two dbRDA axes captured ~63.5% of the variability in the fitted model (primarily along axis 1 - horizontal) and 9.2% of total variation in the data (Figure 3). The dbRDA plot clearly illustrates separation in fish assemblages across the sampling region (north = offshore Broome, Darwin; south = Pilbara, Dampier; Figure 1), reflecting these relationships with depth, distance to shoals, mean SST and other factors, with patterns across the different habitats (structural complexity of seafloor) less clear.

Fish communities in the southern end of the sampling region were distinct from those in the north, but there was little distinction between fish communities according to seafloor complexity (Figure 3A). The spread of data in the DISTLM plot suggests the fish community is more variable on low and high seafloor complexities and more uniform on pipelines. A number of sand-affiliated taxa were associated with deep BRUV deployments, including *Saurida undosquamis* (largescale saury), *Lagocephalus lunaris* (rough golden toadfish), *Argyrops notialis* (Australian soldierbream) and an important fishery species *Pristipomoides multidens* (goldband snapper;

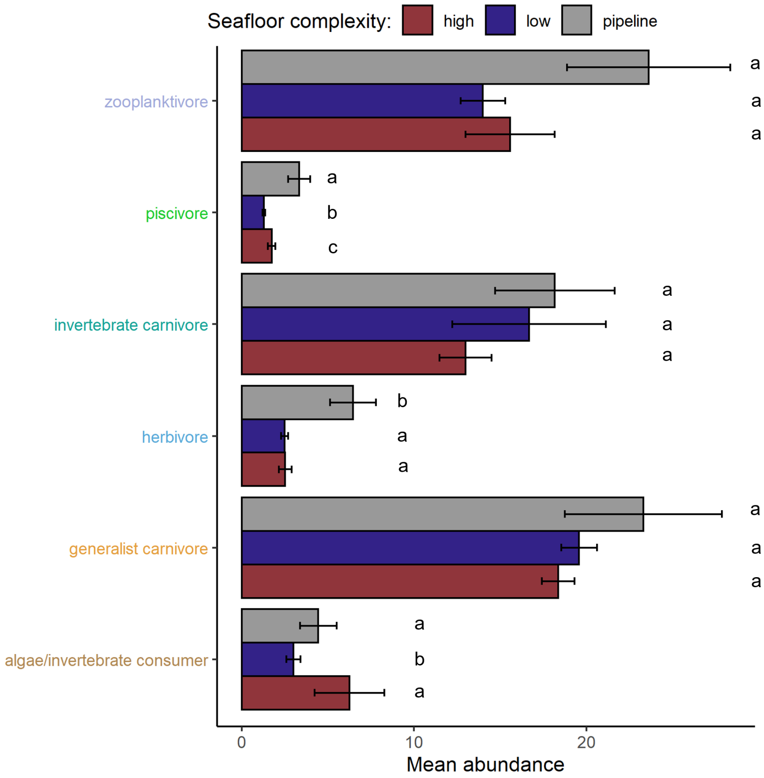

FIGURE 2
Mean (± SE) abundance fish per BRUV deployment for fish six feeding guilds represented on the vertical axis and between seafloor complexities: pipelines, low complexity natural habitat and high complexity natural habitat. Statistically similar means are indicated by the same letter (e.g., a/b/c).

Figures 3B, C). A range of fish taxa were most abundant in shallow depths including *Oxychelinus digramma* (violetline Maori wrasse), *Lethrinus semisinctus* (blackspot emperor) and *Balistapus undulatus* (orangestripe triggerfish). Also abundant in the shallows but close to shoals and pipelines were several triggerfish (*S. fraenatum, Pseudobalistes fuscus)* and some fishery target generalist/invertebrate carnivores (*Variola louti, L. rubrioperculatus, Lethrinus atkinsoni)*, in addition to triggerfish (*P. fuscus, S. fraenatum)* and the pigfish *Bodianus bilunulatus* (Figures 3B, C).

The MRT explained approximately 13% of the variation in fish abundance data with the most parsimonious community structure defined by five terminal nodes (where membership to each group is as 'pure' as possible given the data variation) and constrained by three environmental predictors with distance to shoal and depth as primary predictors (Figure 4). The primary split in the MRT separated fish communities far from shoals (≥11.6 km) from those located closer to shoals. Subsequently, the fish community was split by depth with a terminal node identifying a shallow-water assemblage (depth <18.7 m) and mesophotic assemblage (depth ≥ 18.7 m). The shallow water assemblage occurred primarily offshore of Onslow in the southern Pilbara with a small number of sites west of Tiwi Islands attributed to this assemblage (Figures 5A–C). This assemblage included many invertebrate and generalist carnivore taxa, dominated by indicator taxa within the families Labridae (wrasses, tuskfish), Nemipteridae (monocle breams, threadfin bream) and Lethrinidae (emperors) (Table 2). It was characterised by the second lowest proportion of BRUV deployments (6.7%) but had the third highest proportion of indicator taxa (15.5% of DLI taxa).

The mesophotic fish assemblage (Figure 4) occurred both in the southern (offshore Pilbara; Figures 5A, C, D) and the northern (west of Tiwi Islands and offshore from Darwin; Figures 5A, B) parts of the NW region. This assemblage was characterised by the highest proportion of BRUV deployments (n = 592 or 38.3%) and second lowest proportion of indicator taxa (8.2%) with a majority of high DLI taxa being generalist carnivore taxa from the ubiquitous Nemipteridae and Carcharhinidae (requiem sharks) families (Table 2). This assemblage also had a high proportion of taxa listed on the IUCN threatened species list (IUCN, 2021), especially sharks from the genus *Carcharhinus* and critically endangered scalloped hammerhead shark (*Sphyrna lewini*).

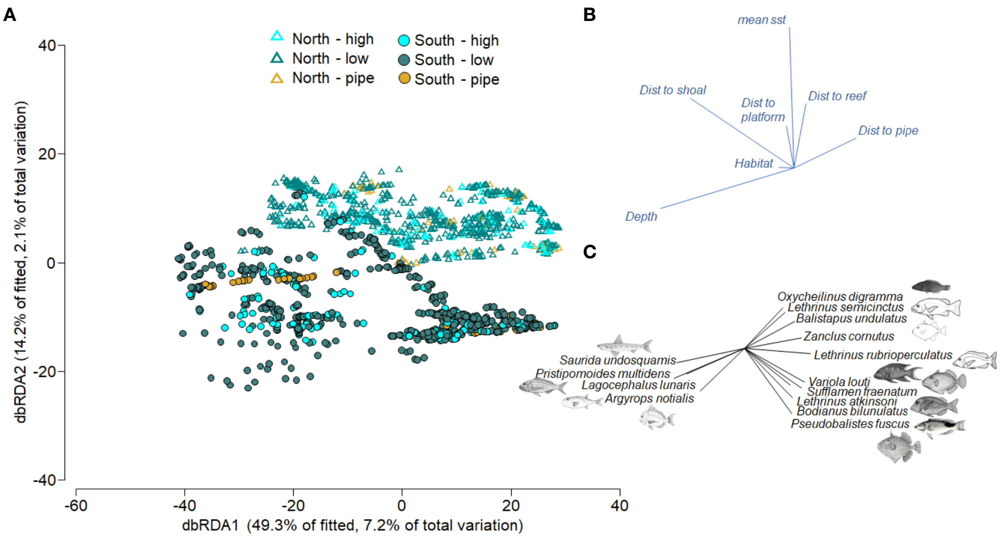

FIGURE 3
(A) dbRDA ordination plot displaying relationships between predictor variables and fish relative abundance data (MaxN of all species). Colours represent seafloor complexity (low & high refer to seafloor complexity; pipe = pipeline) while symbols represent regions along the coast of NW Australia (south = Pilbara and Dampier, north = Broome and Darwin). **(B)** Vectors indicate the direction of the relationship, and their length indicates the strength of their effect on fish abundance. **(C)** Fish species with Pearson correlations of |R| ≥ 0.30 to either axis are overlaid with vectors in the bottom right indicating the strength and direction of this association, i.e. how these fish species correlate with seafloor complexity categories and regions and predictor variables.

The near-shoal branch of the MRT was further split by depth (≥38 m) with a terminal node identifying a shoal mesophotic assemblage (Figure 4). This assemblage occurred in the northern part of the study region (Figures 5A, B, D) and was also prominent offshore from Dampier (Figures 5A, D). It was characterised by the second highest proportion of BRUV deployments (36%) yet lowest proportion of indicator taxa (7.1%) which were primarily commercially targeted generalist carnivores from Carangidae (jacks) and Lethrinidae (emperors) families (Table 2).

The shallow, near-shoal branch was further split by distance to pipeline with one terminal node at the shallow shoal assemblage (distance to pipeline ≥34.5 km) and another at the shallow shoal near pipeline assemblage (distance to pipeline <34.5 km; Figure 4). The shallow shoal assemblage was only characteristic of shoals offshore from Darwin (Figures 5A, B) and was characterised by the third lowest proportion of BRUV deployments (14.2%) and second highest proportion of DLI taxa (33.9%; Table 2). It was primarily dominated by invertebrate carnivore taxa from Labridae (wrasses) family with relatively low DLI values (≤47) for all indicator taxa in this assemblage. It had several near threatened and vulnerable taxa from the IUCN Red List particularly from Dasyatidae family (stingrays) and *Plectropomus* species (coral trout; Table 2). The shallow shoal near pipeline assemblage only occurred offshore from Dampier (Figures 5A, D). This assemblage was characterised by the lowest proportion of BRUV deployments (4.7%) yet the highest proportion of DLI taxa (35.3%; Table 2). The indicator taxa were roughly equally split between invertebrate carnivores e.g., Labridae and Chaetodontidae families, and generalist carnivores e.g., Lethrinidae family, followed by roughly equal numbers of herbivores and algae/invertebrate consumers (Table 2). In addition, it had several taxa from the IUCN Red List including two commercially targeted *Epinephelus* (grouper) species and two members of Carcharhinidae family (Table 2).

Individual-based and sample-based rarefaction curves and associated confidence bands made for the three types of seafloor complexity indicated that taxonomic richness on the pipelines was substantially lower than in both types of natural habitat (Figure 6). The three curves overlapped at lower cumulative abundance of individuals (< 150 individuals) then diverged with the curve for pipelines reaching asymptote approximately around 300 taxa whereas the other two curves and their 95% confidence bands remained closely overlapping and did not reach asymptote (Figure 6A).

Similarly, the sample-size based curves grew quickly at initial parts and overlapped at small sample sizes (< 50 BRUV sites) but quickly diverged afterwards with the pipeline-associated curve reaching asymptote at approximately 250 taxa. Fish taxonomic richness on low and high seafloor complexity diverge with increased sampling effort with both curves approaching asymptote at maximum number of samples. Overall, the curves for low and high seafloor complexity and their confidence bands mostly overlapped with increased sampling

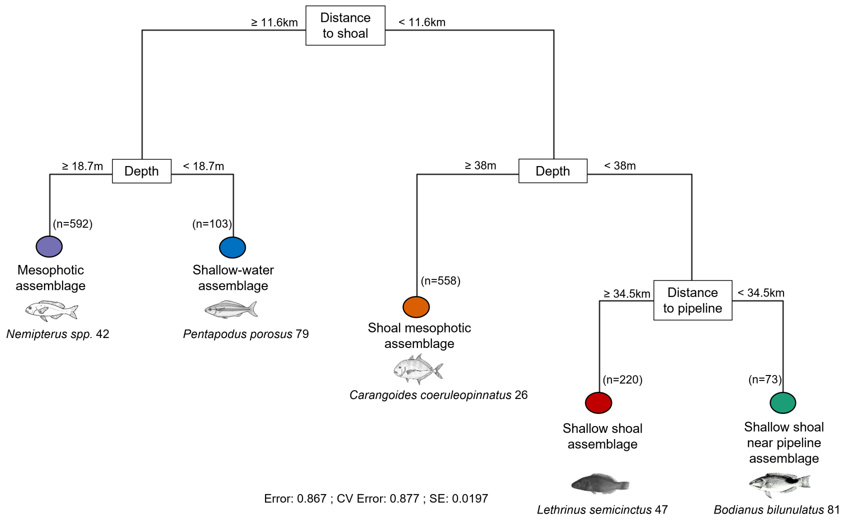

FIGURE 4
Pruned (1 SE) multivariate regression tree (MRT) defining assemblage composition of demersal fishes (n=1546 BRUV deployments) on the NW Shelf constrained by environmental predictors. The terminal nodes identified five distinct assemblages (see Table 2) with breaks labelled with the environmental predictor that best split the data into the most homogenous groups possible and the value of each predictor that best distinguished them. The number of BRUV deployments within each terminal node is also indicated (n). Top indicator taxa with highest values of Dufrene-Legendre index (DLI) are shown for each terminal node.

effort indicating that the taxonomic richness were roughly similar (Figure 6B).

Discussion

Our regional study spanned almost 2000 km of coastline to demonstrate overarching influences from oceanic shoal environments (presented as distance to shoals in our study) and depth on the composition of demersal fish assemblages across the NW region, with O&G infrastructure playing a relatively minor role in explaining the observed regional patterns in fish assemblage composition. The diversity of fishes on pipelines (in terms of taxonomic richness) was substantially lower in comparison to the diversity observed on natural habitats (both low and high seafloor complexity). The abundance of most fish feeding guilds was equal across natural and artificial habitats, except for piscivore and herbivore taxa that were more abundant on pipelines.

Submerged oceanic banks and shoals of the NW region are known hotspots of fish diversity where fish abundance and richness can exceed those recorded on similar features of the Great Barrier Reef (Nichol et al., 2013; Heyward et al., 2017; Moore et al., 2017; Heyward & Radford, 2019). Proximity to these features was the primary split in the MRT analysis, followed by depth, with strong alignment in patterns observed by the MRT with DISTLM analyses. Depth is often among the most common predictors of fish distributions (Moore et al., 2009; Monk et al., 2010; Galaiduk et al., 2017b), assemblage composition (Cappo et al., 2007; Moore et al., 2010; Harvey et al., 2013) and fish species richness (Young & Carr, 2015; McLean et al., 2021; Currey-Randall et al., 2021). Proximity to infrastructure, such as platform jackets and/or pipelines, featured in both statistical analyses but were ranked low as predictors each explaining <2% of variation in the fish abundance data in both instances. This suggests that while infrastructure can have a strong influence on fish assemblage composition at a local scale (i.e. Bond et al., 2018a; Bond et al., 2018b; McLean et al., 2021; Schramm et al., 2021), the influence of natural features (e.g., oceanic shoals) and broader scale environmental gradients (e.g., depth) are stronger factors at a regional scale.

This study represents the first quantitative bioregional scale analysis that includes O&G infrastructure among a set of environmental predictors commonly found to be important in explaining fish diversity and distributions (Pittman et al., 2007; Pittman et al., 2009; Chatfield et al., 2010; Costa et al., 2014; Galaiduk et al., 2017a; Moore et al., 2017). The relatively low explanatory performance of the MRT and DISTLM models is expected, given the high alpha diversity (taxonomic richness; 450 taxa) of the BRUV abundance data and vast span of the study area. It is likely that key variables (such as oceanographic covariates e.g., chlorophyll concentration or wave exposure) that could improve the explanatory performance and ecological realism of these analyses (Elith and Leathwick, 2009) are missing. Inclusion of additional data such as substrate type, could also provide further insights, but would require re-examination of imagery from >1500 BRUV deployments and

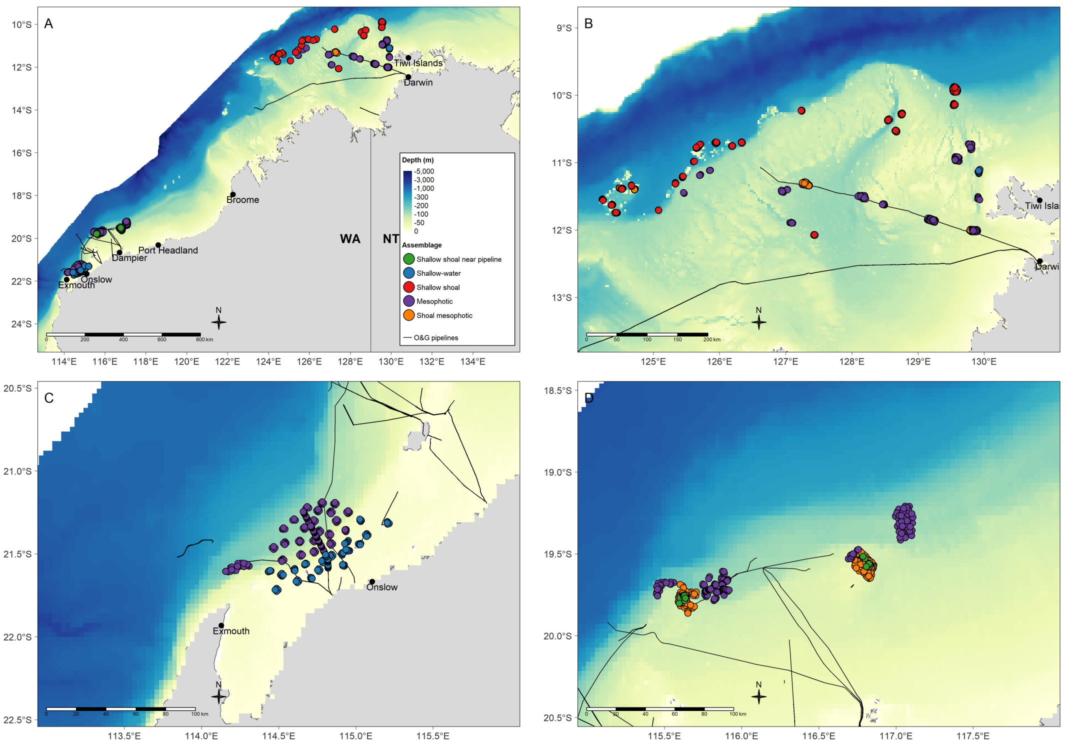

FIGURE 5
Spatial distribution of five fish assemblages obtained from the MRT analysis of BRUVs data from three pipelines and historical AIMS surveys in NW Australia. **(A)** A regional setting of the NW Australia with the five assemblages mapped. **(B)** The northern part of the study region west of Tiwi Islands and offshore from Darwin. **(C)** The southern part of the study region, southern Pilbara offshore from Onslow and north of Exmouth. **(D)** The southern part of the study region, mid-coast Pilbara and offshore from Dampier.

was beyond the scope of this study. Further, processes affecting fish population size and dynamics (e.g., competition, predation) and behaviour (e.g., attraction to O&G infrastructure to access encrusting invertebrates as a food source) are likely to have a significant influence on fish abundance and distribution, yet such population processes and behaviours require dedicated research programs to indicate their relative strength for different taxa, data which is not yet available for this region. Regardless, the results here align with previous bioregional studies on fish communities that demonstrated strong regional trends and varying scales of influence of environmental predictors (Travers et al., 2010; Galaiduk et al., 2017a; Wellington et al., 2021).

Both mesophotic fish assemblages were characterised by fishes associating with sand and hard substrata, with almost 75% of all BRUV deployments attributed to these two assemblages. This highlighting the presence of mixed habitat communities within these depths (Currey-Randall et al., 2019; Currey-Randall et al., 2021). Indeed, an assemblage characterised by Synodontidae (lizardfish), Tetraodontidae (toadfish) and Nemipteridae (threadfin bream) is typical of those ecosystems dominated by sand including those observed in impacted areas (historically trawled; Sainsbury et al., 1997; Travers et al., 2012). An indicator species for monitoring and assessment for the commercial fishery in the region and also for the mesophotic assemblage identified here was *Pristipomoides multidens* (goldband snapper), a vagile species (able to disperse widely) known to associate with hard bottom areas in depths of 60 to at least 180 m (Ovenden et al., 2002; Ovenden et al., 2004). Both mesophotic assemblages were characterised by a higher number of vagile taxa such as Carangidae (trevallies) and Carcharhinidae (whaler shark) species which were indicated by the relatively low DLI values of indicator taxa in those assemblages (Table 2). The association of trevallies and whaler species with mesophotic depths supports previous research findings in Australia for these typically wide-ranging species (e.g. Stevens and Wiley, 1986; Harry et al., 2019). Cosmopolitan distributions, conservative life-histories, and susceptibility to overfishing are primarily reasons that most of the indicator shark species surveyed in this study are found on the threatened species list (McAuley et al., 2007; Dulvy et al., 2014; Geraghty et al., 2015). Major declines in apex predator population can alter entire food webs (Estes et al., 2011). However, some practical tools such as fishing area closure, reduced fishing

TABLE 2 Summary of indicator taxa in the five fish assemblages of the multivariate regression tree (MRT; Figure 4).

Assemblage name	# ofDLI species in assemblage	Proportion of DLI species in assemblage (%)	Number of BRUV deployments allocated to an assemblage	Proportion of BRUV deployments in assemblage (%)	DLI (%) generalist carnivore (GC), invertebrate carnivore (IC), piscivore (P), zooplanktivore (Z), algae/invertebrate consumer (AI), herbivore (H)
Mesophotic assemblage ● 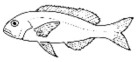	29	8.2	592	38.3	GC: Nemipterus spp (42)*, Pristipomoides multidens (26)*, Carangoides chrysophrys (18)*, Lagocephalus lunaris (14), Caranx papuensis (11)*, Saurida undosquamis (10), Lutjanus vitta (9)*, Carcharhinus sorrah (8)^{NT}, Carcharhinus sp (8)^{VU}, Lutjanus russellii (8)*, Seriola dumerili (7)*, Carcharhinus plumbeus (6)^{EN}, Caranx bucculentus (4)*, Carcharhinus obscurus (4)^{EN}, Carcharhinus limbatus (3)^{VU}, Epinephelus chlorostigma (3)*, Sphyrna lewini (3)^{CR}, Carangoides equula (2)*, Carcharhinus macloti (2)^{NT}, Pentapodus paradiseus (2) IC: Netuma thalassina (11), Terapon spp (8), Upeneus moluccensis (4), Pomadasys kaakan (2) P: Argyrops notialis (20)*, Lutjanus malabaricus (16), Sphyraena sp (2)* Z: Decapterus spp (12), Selar spp (3)
Shallow-water assemblage ● 	55	15.5	103	6.7	IC: Pentapodus porosus (79), Choerodon cauteroma (39)*, Parapercis nebulosa (27), Scolopsis monogramma (23), Paramonacanthus choirocephalus (19), Chaetodontoplus duboulayi (18), Upeneus tragula (18), Parupeneus heptacanthus (17)*, Choerodon cephalotes (16)*, Choerodon cyanodus (15)*, Parupeneus barberinoides (15), Chelmon marginalis (14), Pentapodus emeryii (13), Pentapodus vitta (13), Parupeneus indicus (12)*, Parupeneus spilurus (12)*, Choerodon schoenleinii (9)^{NT}*, Choerodon vitta (9), Halichoeres nebulosus (8), Chaetodon aureofasciatus (7), Chaetodontoplus personifer (7), Leptojulis cyanopleura (6), Canthigaster valentini (5), Parupeneus chrysopleuron (5), Abudefduf bengalensis (4), Anampses lennardi (4), Stethojulis interrupta (4), Apogonidae spp (3), Iniistius pavo (3), Bothidae spp (2)* GC: Scomberomorus spp (39)*, Lethrinus genivittatus (32)*, Lethrinus punctulatus (19)*, Gnathanodon speciosus (15)*, Lethrinus laticaudis (11)*, Epinephelus fasciatus (10)*, Atule mate (9), Lethrinus variegatus (9)*, Lethrinus nebulosus (8)*, Lethrinus miniatus (7)*, Lagocephalus sceleratus (6), Pristotis obtusirostris (5), Carangoides hedlandensis (4)*, Carcharhinus melanopterus (4)^{VU}, Stegostoma tigrinum (4)^{EN}, Lutjanus carponotatus (3)* AI: Naso annulatus (9), Chaetodon assarius (9), Monacanthus chinensis (4), Pomacentrus nagasakiensis (3) Z: Selaroides leptolepis (53), Pterocaesio chrysozona (2) H: Siganus fuscescens (21), Siganus doliatus (4) P: Plagiotremus tapeinosoma (5)
Shoal mesophotic assemblage ● 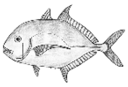	25	7.1	558	36	GC: Carangoides coeruleopinnatus (26)*, Gymnocranius grandoculis (21)*, Lethrinus ravus (14)*, Carangoides gymnostethus (14)*, Lutjanus sebae (14)*, Symphorus nematophorus (13)*, Carangoides fulvoguttatus (9)*, Pristipomoides typus (7)*, Carangoides orthogrammus (6)*, Epinephelus multinotatus (6)*, Epinephelus areolatus (5)*, Loxodon macrorhinus (5), Oxycheilinus orientalis (5), Seriola rivoliana (4)*, Aphareus rutilans (3)*, Pristipomoides filamentosus (3), Hemitriakis falcata (2), Wattsia mossambica (2)* IC: Abalistes stellatus (18)*, Pentapodus nagasakiensis (8), Abalistes filamentosus (3) Z: Ptereleotris sp (2), Cyprinocirrhites polyactis (2) P: Carcharhinus albimarginatus (9)^{NT} AI: Amblypomacentrus breviceps (4)

(Continued)

TABLE 2 Continued

Assemblage name	# ofDLI species in assemblage	Proportion of DLI species in assemblage (%)	Number of BRUV deployments allocated to an assemblage	Proportion of BRUV deployments in assemblage (%)	DLI (%) *generalist carnivore (GC), invertebrate carnivore (IC), piscivore (P), zooplanktivore (Z), algae/invertebrate consumer (AI), herbivore (H)*
Shallow shoal assemblage 🔴 	120	33.9	220	14.2	*IC: Oxycheilinus digramma (29), Scolopsis bilineata (24), Halichoeres prosopeion (23), Balistapus undulatus (20), Neoglyphidodon melas (20), Amblyglyphidodon leucogaster (18), Chaetodon lunulatus (17), Monotaxis grandoculis (15), Chaetodon baronessa (14), Halichoeres hortulanus (14), Halichoeres zeylonicus (13), Macolor niger (13), Thalassoma lunare (13), Coris gaimard (12), Naso vlamingii (12)*, Pomacanthus imperator (11), Acanthurus thompsoni (10), Bodianus diana (10), Balistoides conspicillum (8), Chaetodon trifascialis (8)^{NT}, Hologymnosus doliatus (8), Hemigymnus fasciatus (7), Scolopsis xenochrous (7), Balistoides viridescens (6), Bodianus mesothorax (6), Coris batuensis (6), Forcipiger longirostris (6), Halichoeres chrysus (6), Anampses meleagrides (5), Cirrhilabrus cyanopleura (5)^{DD}, Heniochus varius (5), Odonus niger (5), Oxycheilinus celebicus (5), Epibulus insidiator (4), Parupeneus barberinus (4), Bodianus anthioides (3), Cephalopholis spiloparaea (3)*, Chaetodon adiergastos (3), Chaetodontoplus mesoleucus (3), Cheilinus fasciatus (3), Labropsis manabei (3), Lutjanus kasmira (3), Novaculichthys taeniourus (3), Pseudobalistes flavimarginatus (3), Arothron nigropunctatus (2), Hologymnosus rhodonotus (2), Malacanthus latovittatus (2), Paracanthurus hepatus (2), Pictichromis paccagnellae (2), Siganus puellus (2)* *GC: Lethrinus semicinctus (47)*, Macolor macularis (28), Lethrinus erythracanthus (22), Aethaloperca rogaa (20), Plectropomus spp (16)$^{VU/NT}$*, Cephalopholis urodeta (11), Carangoides plagiotaenia (10)*, Labroides bicolor (9), Lethrinus amboinensis (9), Neotrygon australiae (8)^{NT}, Elagatis bipinnulata (7)*, Plectropomus laevis (7)^{VU}, Taeniura lymma (6)^{NT}, Cephalopholis leopardus (4)*, Epinephelus maculatus (3)*, Plectorhinchus vittatus (3), Aphareus furca (2)*, Aulostomus chinensis (2), Grammatorcynus bilineatus (2)*, Lethrinus erythropterus (2)** *AI: Acanthochromis polyacanthus (20), Pygoplites diacanthus (17), Chaetodon kleinii (15), Pomacentrus limosus (11), Pomacentrus amboinensis (9), Pseudodax moluccanus (9), Pomacentrus reidi (6), Chaetodon meyeri (5), Pomacentrus spp (4), Aluterus scriptus (3), Pomacentrus brachialis (3), Pomacentrus nigromarginatus (3), Arothron hispidus (2), Chaetodon selene (2), Naso brachycentron (2), Pomacentrus moluccensis (2)* *H: Acanthurus pyroferus (23), Centropyge bicolor (21), Cetoscarus ocellatus (15), Siganus argenteus (11), Chlorurus sordidus (10), Zebrasoma scopas (10), Centropyge vrolikii (7), Acanthurus nigricans (6), Scarus tricolor (6), Acanthurus nigrofuscus (5), Siganus punctatissimus (5), Scarus dimidiatus (3), Acanthurus spp (2), Scarus flavipectoralis (2), Scarus fuscocaudalis (2)* *Z: Chromis xanthura (13), Pterocaesio marri (12), Dascyllus reticulatus (10), Hemitaurichthys polylepis (10), Cirrhilabrus randalli (9), Genicanthus lamarck (9), Caesio teres (7), Chromis ternatensis (5), Amblyglyphidodon aureus (4), Pterocaesio tile (4), Dascyllus trimaculatus (3), Amphiprion clarkii (2), Canthidermis maculata (2), Pterocaesio sp (2)* *P: Triaenodon obesus (17)^{NT}, Variola albimarginata (14)*, Cephalopholis miniata (8)*, Gymnosarda unicolor (4)*, Gracila albomarginata (7)^{DD}*

(Continued)

TABLE 2 Continued

Assemblage name	# ofDLI species in assemblage	Proportion of DLI species in assemblage (%)	Number of BRUV deployments allocated to an assemblage	Proportion of BRUV deployments in assemblage (%)	DLI (%) generalist carnivore (GC), invertebrate carnivore (IC), piscivore (P), zooplanktivore (Z), algae/invertebrate consumer (AI), herbivore (H)
Shallow shoal near pipeline assemblage ● 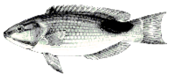	125	35.3	73	4.7	*IC: Bodianus bilunulatus (81)*, Parupeneus cyclostomus (54), Thalassoma lutescens (52), Heniochus singularius (50), Parupeneus multifasciatus (40), Sufflamen chrysopterum (38), Apolemichthys trimaculatus (36), Parapercis clathrata (35), Chaetodon ornatissimus (33), Sufflamen fraenatum (32), Halichoeres biocellatus (31), Chaetodon speculum (23), Chaetodon lineolatus (22), Coris caudimacula (20), Labroides dimidiatus (20), Chaetodon auriga (19), Chaetodon lunula (17), Heniochus diphreutes (16), Chromis weberi (14), Heniochus acuminatus (13), Pseudojuloides severnsi (12), Chaetodon unimaculatus (9), Pseudocheilinus evanidus (9), Parupeneus pleurostigma (8)*, Forcipiger flavissimus (7), Bodianus axillaris (6), Coris aygula (6), Choerodon jordani (5), Chromis fumea (5), Gomphosus varius (5), Gymnocranius microdon (5)*, Pomacanthus sexstriatus (5), Chaetodon ulietensis (4), Chaetodon plebeius (3), Cirrhilabrus exquisitus (3)^{DD}, Ostracion cubicus (3), Sufflamen bursa (3)* *GC: Lethrinus atkinsoni (68)*, Caranx melampygus (42)*, Melichthys vidua (41), Lethrinus rubrioperculatus (31)*, Epinephelus malabaricus (30)^{NT}*, Lutjanus bohar (30)*, Oxycheilinus unifasciatus (30), Epinephelus bilobatus (21)^{DD}*, Alepes vari (19), Epinephelus tukula (18), Lethrinus olivaceus (18)*, Galeocerdo cuvier (17)^{NT}, Gymnocranius euanus (17)*, Lutjanus rivulatus (17), Aprion virescens (14)*, Lethrinus microdon (12)*, Carcharhinus amblyrhynchos (11)$^{NT/EN}$, Fistularia commersonii (11), Cirrhitichthys oxycephalus (9), Echeneis naucrates (9), Lutjanus lemniscatus (9)*, Lutjanus gibbus (8), Arothron sp (7), Lutjanus quinquelineatus (6)*, Nebrius ferrugineus (6)^{VU}, Epinephelus fuscoguttatus (5)$^{VU/NT}$*, Cephalopholis formosa (3)*, Elops hawaiensis (3)^{DD}*, Epinephelus coioides (3)*, Lutjanus fulviflamma (3), Epinephelus rivulatus (2)*, Sargocentron caudimaculatum (2)* *H: Acanthurus grammoptilus (44), Naso lituratus (42), Chlorurus capistratoides (41), Scarus rubroviolaceus (37), Centropyge tibicen (31), Ctenochaetus striatus (25), Naso fageni (25), Naso hexacanthus (22), Scarus oviceps (22), Hipposcarus longiceps (17), Scarus forsteni (16), Scarus sp3 (13), Acanthurus dussumieri (12), Scarus schlegeli (11), Naso unicornis (10), Chlorurus microrhinos (8), Acanthurus nigros (7), Ctenochaetus binotatus (5), Scarus frenatus (5), Acanthurus leucocheilus (4), Scarus ghobban (4), Scarus sp (4), Acanthurus blochii (3), Naso caesius (3), Chlorurus bleekeri (2), Naso reticulatus (2)^{DD}* *AI: Acanthurus olivaceus (67), Pseudobalistes fuscus (36), Naso brevirostris (35), Zanclus cornutus (31), Melichthys niger (30), Chaetodon punctatofasciatus (24), Plectroglyphidodon johnstonianus (18), Pomacentrus vaiuli (13), Siganus punctatus (13), Acanthurus mata (10), Pomacanthus semicirculatus (8), Cantherhines dumerilii (4), Acanthurus nigricauda (3), Pomacentrus adelus (3)* *Z: Pomacentrus coelestis (54), Caesio cuning (24), Cirrhilabrus sp (23), Chromis margaritifer (21), Thalassoma amblycephalum (20), Cirrhilabrus temminckii (17)^{DD}, Pseudanthias cooperi (15), Cirrhilabrus punctatus (14), Pseudanthias sp (4), Pterocaesio digramma (3)* *P: Variola louti (55), Scomberoides lysan (12)*, Paracirrhites forsteri (9), Sphyraena qenie (4)*, Scomberoides tol (3), Plagiotremus rhinorhynchos (2)*

Values of the Dufrene-Legendre index (DLI) for each discriminant taxa are shown in brackets with asterisk (*) indicates commercial taxa. The higher DLI value (100 being the highest) the more 'indicative' the taxa is of a specific assemblage. Coloured circles match terminal nodes indicated in Figure 4 and mapped in Figure 5. Threatened taxa under IUCN Red List are indicated with superscript: data deficient (DD), near threatened (NT), vulnerable (VU), endangered (EN), critically endangered (CR). Text colours represent feeding guilds: generalist carnivore, invertebrate carnivore, piscivore, zooplanktivore, algae/invertebrate consumer, herbivore.

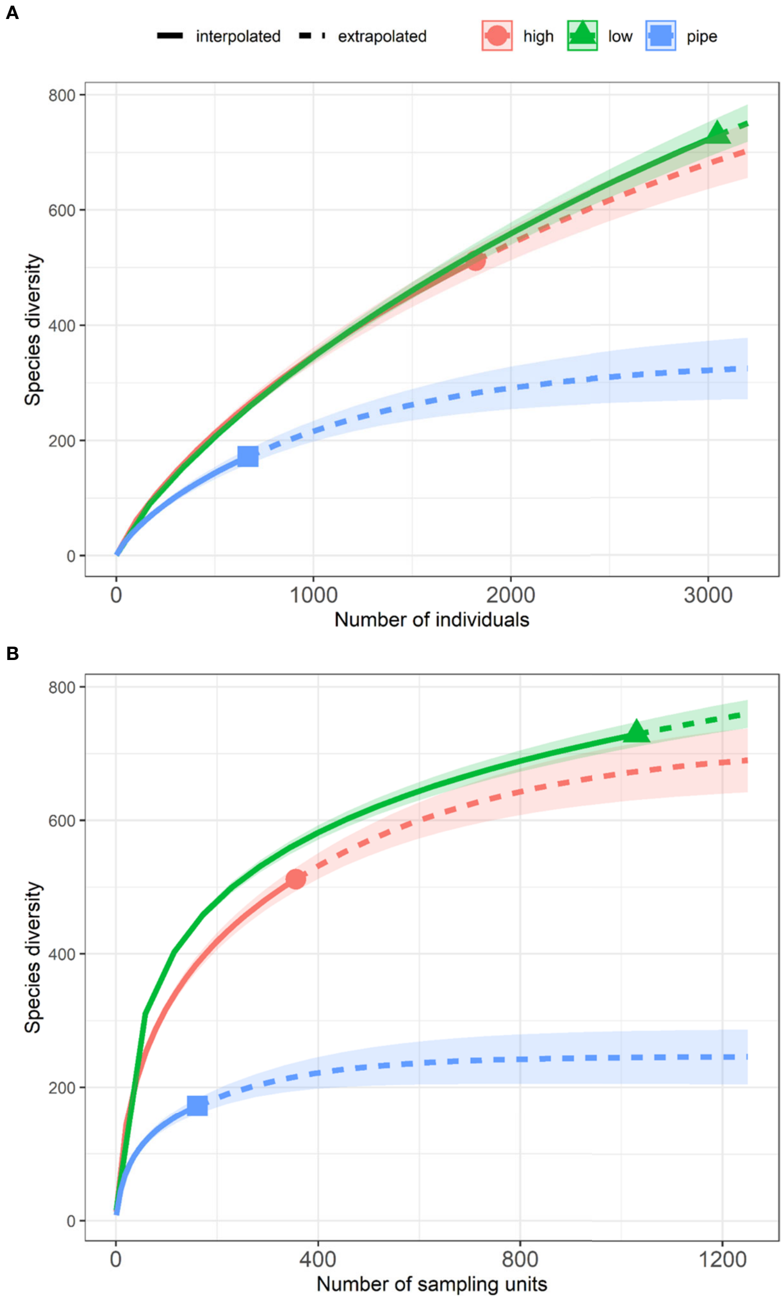

FIGURE 6
(A) Individual-based and **(B)** Sample-size-based rarefaction (solid lines) and extrapolation (dotted lines) sampling curves with 95% confidence intervals (shaded areas) for the species diversity (number of taxa) data across three seafloor complexities: pipelines, low complexity natural habitat and high complexity natural habitat. Solid line indicates the rarefied curve, dashed line indicates the extrapolated curve, symbol indicates the observed taxonomic richness, the shaded area indicates the 95% confidence interval.

effort, and various enforcement tools may improve shark management and conservation efforts and contribute to population recovery (Braccini et al., 2020; Gaughan & Santoro, 2021).

Shoal mesophotic assemblage included relatively few indicator taxa (and low DLI values), with many quite mobile and wide-ranging taxa (e.g., *Carangoides coeruleopinnatus, Carangoides fulvoguttatus, Carangoides gymnostethus, Carangoides orthogrammus, Carcharhinus albimarginatus, Loxodon macrorhinus, Hemitriakis falcata*, etc). Such species can be attracted to shoals as these habitats support high biodiversity and an abundance of prey (Pinheiro et al., 2016;

Moore et al., 2017) and deeper areas around shoals may provide refugia from physical disturbances (e.g., cyclones) or fishing pressures (Lindfield et al., 2016; Abdul Wahab et al., 2018). An abundance of mobile, predatory reef-associated finfish and sharks supports previous research by Letessier et al. (2019) that showed remote regions in the Timor Sea that were far from human influence, and possessed submerged shoals, were hotspots for shark abundance.

In contrast, the three shallow water assemblages were characterised by low proportion of BRUV deployments but collectively consist of almost 85% of indicator taxa which is a common pattern of shallow tropical environments which are often associated with higher abundance and diversity of fish (Fitzpatrick et al., 2012; McLean et al., 2016; Abdul Wahab et al., 2018). The shallow fish assemblages were characterised by many *Choerodon* (tuskfish), *Parupeneus* (goatfish) and *Lethrinus* (emperor) taxa that are known to associate with reefs and sandy patches between reefs where they can forage for invertebrates amongst the sediment (McCormick, 1995; Travers et al., 2010). The representation of various feeding guilds within these shallow ecosystems aligns strongly with previous characterisation of fish assemblages in this region, with many of the indicator taxa identified here among the most ubiquitous identified by McLean et al. (2016). High relative abundance of zooplanktivores in two shallow shoal assemblages can support high biomass of generalist carnivore and piscivore taxa in their vicinity (Bejarano et al., 2014; Pinheiro et al., 2016). While the greatest proportion of indicator taxa were observed on shallow BRUV deployments especially near to shoals, very few fishery-target taxa were observed in comparison to those in deeper areas across the region (the two mesophotic assemblages). As many of these shallow and shoal-associated taxa had high DLI values, this also could indicate site attachment (Dufrene & Legendre, 1997). A high degree of site-attachment by low-mobility species might be expected for fish observed on shallow offshore shoal features remote from similar habitat features (e.g., a break in habitat continuity) or where surrounding ecosystems are oligotrophic (Papastamatiou et al., 2009; Martinez et al., 2017).

The shallow shoal near pipeline fish assemblage comprised substantial numbers of indicator taxa with high DLI values, including numerous *Epinephelus* (grouper), *Chaetodon* (butterflyfish) and herbivorous fish taxa (e.g., *Scarus* spp.*)*. These locations offshore of Dampier are typically of a mix of hard coral habitat and patchy soft sediment communities (Abdul Wahab et al., 2018; McLean et al., 2021) and are situated near Glomar Shoal and Rankin Bank, and adjacent to several pipelines. In contrast, the shallow shoal assemblage had indicator taxa with comparatively low DLI values which may reflect an overall ubiquity of these taxa across the region (Dufrene & Legendre, 1997). The shallow shoal near pipeline assemblage included many similar families and feeding guilds to other shallow water assemblages but did have fewer Epinephelidae (grouper) species and a greater number of Pomacentridae (damsels) and Acanthuridae (surgeonfish). Scaridae (parrotfish) and various Acanthuridae and Pomacanthidae (angelfish) species, in particular, were distinctive of both shoal assemblages, aligning strongly with published works on shoals in these areas (Bellwood et al., 2012; Moore et al., 2017; Abdul Wahab et al., 2018). Herbivorous fish species play an important role in maintaining low macroalgal cover on reefs, thus enhancing juvenile coral densities (Evans et al., 2020), with parrotfishes also playing a role in removing live and dead corals and transporting sediment (Graham et al., 2006; Adam et al., 2011).

The mean relative abundance of all feeding guilds was similar across seafloor complexities except for piscivore and herbivore taxa which had higher relative abundance on pipelines than on low and high complexity seafloor. The high relative abundance of piscivores near pipelines supported previous findings by Schramm et al. (2021) where piscivore species were more abundant on shallow pipelines where they were feeding on prey from lower trophic levels. However, our results for herbivore relative abundance are different from those of Schramm et al. (2021). This difference likely reflects the local scale of research by Schramm et al. (2021) where herbivores were abundant in surrounding macroalgae habitats.

The taxonomic richness on pipelines was notably low in comparison to the taxonomic richness in the natural ecosystems. This aligns well with a previous local study identifying lower diversity of fish (number of species) on the Griffin pipeline in comparison to adjacent off-pipeline habitats (Bond et al., 2018a). Furthermore, the rising slope of all rarefaction curves indicated that there are additional fish taxa to be discovered with extra sampling. For pipelines, however, the extrapolated part of the curve reached asymptote at around 400 BRUV deployments which indicates the appropriate sample size required to exhaustively sample fish diversity on this type of infrastructure for this region. It appears that current sampling effort reported for pipeline surveys in the NW (including our study) is insufficient to adequately sample the full range of associated fish diversity. However, such sampling designs for pipelines are limited by space, with a requirement for at least 400 m between neighbouring BRUV deployments to avoid resampling of fish species capable of visiting more than one BRUV within a one-hour sampling period. Higher taxonomic richness was attributed to low seafloor complexity which likely results from the coarse resolution of the regional bathymetry raster used to derive seafloor complexity categories. While our method for deriving seafloor complexity categories is well suited for high resolution rasters and landscape-scale studies (Galaiduk et al., 2019; McLean et al., 2021) the resolution of the regional raster (cell size of 250m * 250m) likely misses many small seafloor features such as small reef outcrops and bommies and patches of sponge gardens which are known to harbour high diversity of fishes (Butler et al., 2002; Marliave et al., 2009; Kerry & Bellwood, 2012;

Abdul Wahab et al., 2018). The small seafloor features could be detected using appropriate remote sensing techniques, such as multibeam echosounder surveys. However, given the spatial extent of this regional study, obtaining these data across the study area would require significant time and resources. Further, the BRUV monitoring technique itself can draw some fish species in from surrounding areas to the bait which limits the effectiveness of the technique for targeting small habitat patches specifically, i.e., a pipeline deployment could include fish drawn from immediate surrounds. We are confident, however, that the presented patterns of difference in diversity between pipelines and natural environments are valid because the pipeline was observed directly from the BRUV video deployments. In addition, McLean et al. (2021) used real-time USBL positioning to assess drift of systems during deployment with 86% of deployments within 10 m of the pipeline. This also highlights the urgent need for expanding the fine scale bathymetric surveys for the NW region so it can facilitate future studies and sustainable management of this highly diverse region.

Conclusion and implications for the decommissioning of oil and gas infrastructure

Decommissioning decisions are typically made for singular or small groups of interconnected assets and do not consider the potential impact of cumulative decommissioning activities over large areas or through time. Our study shows that there is value in considering regional scale processes and environmental gradients to better understand potential broad ecological implications of such activities. At a regional scale, pipelines do not hold heightened fish taxonomic richness which is not surprising given the vast extent and diversity of natural habitats that exist across the NW region (Moore et al., 2017; Abdul Wahab et al., 2018; Currey-Randall et al., 2021). Such patterns may be different for other types of infrastructure, such as platform jackets which are known to be structurally more complex and consequentially have a high fish diversity (McLean et al., 2019; van Elden et al., 2019). This does not, however, suggest that removal of pipelines in this NW region will not impact fish diversity, as these anthropogenic features can influence fish communities in a manner of ways not investigated by this study, e.g., influencing fish behaviour (Bond et al., 2018b), facilitating depth range extensions of associated taxa (Sammarco et al., 2014), concentrating fishing activities (Bond et al., 2021), and potential adverse impacts of contaminants trough bioaccumulation in food webs or toxicity to local organisms (MacIntosh et al., 2021; Koppel et al., 2022). Further, there is a clear paucity of research into the influence O&G infrastructure on seascape ecological connectivity (McLean et al., 2022), yet this is a critical consideration for decommissioning (NOPSEMA, 2022). Without understanding the level and nature of connectedness across marine ecosystems that include infrastructure, it is difficult to predict the impact that decommissioning of infrastructure (complete or partial removal) might have on marine ecosystems. We suggest that a logical expansion of this research include examination of fish population and demographic processes (most notably larvae distribution, metapopulation connectivity processes and movement patterns of some of the indicator species identified in this study) to obtain a more holistic understanding of fish community processes in the region and how important infrastructure is for these processes. Such a study would also be particularly relevant for highly mobile species such as megafauna (e.g. sharks, rays, turtles, whales), many of which occur and transit across this region and are threatened by anthropogenic activities (e.g., turtles, sawsharks; Morgan et al., 2011; Wilson et al., 2018).

Data availability statement

The original contributions presented in the study are included in the article/Supplementary Material. Further inquiries can be directed to the corresponding author.

Ethics statement

Ethical review and approval was not required for the animal study because this study used historical datasets e.g. no new data was collected. All historical datasets were recorded with video using non-destructive methods. When required, Animal Ethics Committee approvals and Australian Marine Park activity permits were obtained for the individual studies and were stated in the individual reports and publications.

Author contributions

RG, BR, and DM conceived the ideas and perform the analyses. TB and MT analysed BRUVS footage and contributed BRUVS data. RG and DM prepared the manuscript. All authors contributed to the article and approved the submitted version.

Funding

This study received funding from the National Decommissioning Research Initiative (NDRI) who manages all contributing industry partners, namely Shell Australia Pty Ltd, Esso Australia Pty Ltd, Chevron Australia Pty Ltd, BHP Petroleum Pty Ltd, Woodside Energy Ltd, Santos Ltd, Vermillion Oil and Gas Australia Ltd, Cooper Energy Ltd. The funder was involved in the review of this article.

Acknowledgments

We thank Andrew Taylor for his tireless efforts as the founding Director and most recently, Sam Jarvis as the new Director of the National Decommissioning Research Initiative (NDRI). We acknowledge PTTEP Australasia Ltd., a joint voyage under the auspices of the Arafura and Timor Seas Ecosystem Action (ATSEA) program, and the Australian Government's National Environmental Research Program (NERP), Woodside Energy and BHP petroleum for supporting previous projects that contributed historical data. We thank Juliet Corley and Katrina Bornt for the hand drawn fish images. We thank all those who were involved in the collection of historical AIMS data utilised here (see References). We thank Dr Michele Thums and Dr Marji Puotinen for their detailed reviews and comments on previous drafts of the manuscript. AIMS acknowledges the Traditional Owners of the Country adjacent to where historical BRUVS surveys were undertaken. We recognise these People's ongoing spiritual and physical connection to Country and pay our respects to their Aboriginal Elders past, present and emerging.

Conflict of interest

LS is employed by Woodside Energy and TC is employed by BHP Petroleum.

The remaining authors declare that the research was conducted in the absence of any commercial or financial relationships that could be construed as a potential conflict of interest.

NDRI science advisory board, in particular Prof Peter Macreadie and Prof Iain Suthers contributed ideas and provided guidance in the conceptual framework of the study.

The authors declare that this study received funding from the National Decommissioning Research Initiative (NDRI). The funder had the following involvement with the study: review.

Publisher's note

Supplementary material

The Supplementary Material for this article can be found online at: https://www.frontiersin.org/articles/10.3389/fmars.2022.979987/full#supplementary-material

References

Abdul Wahab, M. A., Radford, B., Cappo, M., Colquhoun, J., Stowar, M., Depczynski, M., et al. (2018). Biodiversity and spatial patterns of benthic habitat and associated demersal fish communities at two tropical submerged reef ecosystems. *Coral Reefs* 37, 327–343. doi: 10.1007/s00338-017-1655-9

Adam, T. C., Schmitt, R. J., Holbrook, S. J., Brooks, A. J., Edmunds, P. J., Carpenter, R. C., et al. (2011). Herbivory, connectivity, and ecosystem resilience: Response of a coral reef to a Large-scale perturbation. *PLoS One* 6, e23717. doi: 10.1371/journal.pone.0023717

AIMS (2014). "Biodiversity survey of glomar shoal and rankin bank," in *Report prepared by the Australian institute of marine science for woodside energy Ltd*, vol. 1. (Townsville: Australian Institute of Marine Science), 153.

AIMS (2016). *Addressing strategic knowledge gaps in the oceanic shoals bioregion, Western Australia* [Perth: Australian Institute of Marine Science (AIMS)].

Almany, G. R. (2004). Differential effects of habitat complexity, predators and competitors on abundance of juvenile and adult coral reef fishes. *Oecologia* 141, 105–113. doi: 10.1007/s00442-004-1617-0

Anderson, M. J., Gorley, R. N., and Clarke, K. R. (2008). *PERMANOVA+ for PRIMER: guide to software and statistical methods* (PRIMER-E: Plymouth, UK: PRIMER-E, Plymouth).

Bejarano, I., Appeldoorn, R. S., and Nemeth, M. (2014). Fishes associated with mesophotic coral ecosystems in la parguera, Puerto Rico. *Coral Reefs* 33, 313–328. doi: 10.1007/s00338-014-1125-6

Bellwood, D. R., Hoey, A. S., and Hughes, T. P. (2012). Human activity selectively impacts the ecosystem roles of parrotfishes on coral reefs. *Proc. R. Soc. B: Biol. Sci.* 279, 1621–1629. doi: 10.1098/rspb.2011.1906

Bond, T., McLean, D. L., Wakefield, C. B., Partridge, J. C., Prince, J., White, D., et al. (2021). Quantifying fishing activity targeting subsea pipelines by commercial trap fishers. *Rev. Fish Biol. Fish.* 31, 1009–1023. doi: 10.1007/s11160-021-09686-4

Bond, T., Partridge, J. C., Taylor, M. D., Cooper, T. F., and McLean, D. L. (2018a). The influence of depth and a subsea pipeline on fish assemblages and commercially fished species. *PLoS One* 13, e0207703. doi: 10.1371/journal.pone.0207703

Bond, T., Partridge, J. C., Taylor, M. D., Langlois, T. J., Malseed, B. E., Smith, L. D., et al. (2018b). Fish associated with a subsea pipeline and adjacent seafloor of the north West shelf of Western Australia. *Mar. Environ. Res.* 141, 53–65. doi: 10.1016/j.marenvres.2018.08.003

Braccini, M., Molony, B., and Blay, N. (2020). Patterns in abundance and size of sharks in northwestern Australia: cause for optimism. *ICES J. Mar. Sci.* 77, 72–82. doi: 10.1093/icesjms/fsz187

Bradley, M., Nagelkerken, I., Baker, R., Travers, M., and Sheaves, M. (2021). Local environmental context structures animal-habitat associations across biogeographic regions. *Ecosystems.* 25 (2), 237–251 doi: rg/10.1007/s10021-021-00651-7

Brown, O. B., Minnett, P. J., Evans, R., Kearns, E., Kilpatrick, K., Kumar, A., et al. (1999). MODIS infrared sea surface temperature algorithm algorithm theoretical basis document version 2.0. *Univ. Miami* 31, 098–033. Available at: https://mmodis.gsfc.nasa.gov/data/atbd/atbd_mod25.pdf.

Butler, A., Althaus, F., Furlani, D., and Ridgway, K. (2002). *Assessment of the conservation values of the bass strait sponge beds area*, Vol. 71.

Cappo, M., De'ath, G., and Speare, P. (2007). Inter-reef vertebrate communities of the great barrier reef marine park determined by baited remote underwater video stations. *Mar. Ecol. Prog. Ser.* (Hobart, Tasmania: CSIRO Marine Research) 350, 209–221. doi: 10.3354/meps07189

Chao, A., Gotelli, N. J., Hsieh, T. C., Sander, E. L., Ma, K. H., Colwell, R. K., et al. (2014). Rarefaction and extrapolation with hill numbers: a framework for sampling and estimation in species diversity studies. *Ecol. Monogr.* 84, 45–67. doi: 10.1890/13-0133.1

Chatfield, B. S., Van Niel, K. P., Kendrick, G. A., and Harvey, E. S. (2010). Combining environmental gradients to explain and predict the structure of demersal fish distributions. *J. Biogeogr.* 37, 593–605. doi: 10.1111/j.1365-2699.2009.02246.x

Claisse, J. T., Ii, D. J. P., Love, M., Zahn, L. A., Williams, C. M., and Bull, A. S. (2015). Impacts from partial removal of decommissioned oil and gas platforms on fish biomass and production on the remaining platform structure and surrounding shell mounds. *PLoS One* 10, e0135812. doi: 10.1371/journal.pone.0135812

Claisse, J. T., Pondella, D. J., Love, M., Zahn, L. A., Williams, C. M., Williams, J. P., et al. (2014). Oil platforms off California are among the most productive marine fish habitats globally. *Proc. Natl. Acad. Sci.* 111, 15462–15467. doi: 10.1073/pnas.1411477111

Clarke, K., Chapman, M., Somerfield, P., and Needham, H. (2006). Dispersion-based weighting of species counts in assemblage analyses. *Mar. Ecol. Prog. Ser.* 320, 11–27. doi: 10.3354/meps320011

Colwell, R. K., Chao, A., Gotelli, N. J., Lin, S.-Y., Mao, C. X., Chazdon, R. L., et al. (2012). Models and estimators linking individual-based and sample-based rarefaction, extrapolation and comparison of assemblages. *J. Plant Ecol.* 5, 3–21. doi: 10.1093/jpe/rtr044

Coolen, J. W. P., Bittner, O., Driessen, F. M. F., van Dongen, U., Siahaya, M. S., de Groot, W., et al. (2020). Ecological implications of removing a concrete gas platform in the north Sea. *J. Sea Res.* 166, 101968. doi: 10.1016/j.seares.2020.101968

Core Team, R. (2019). *R: A language and environment for statistical computing, r foundation for statistical computing, Vienna, Austria* (Vienna, Austria: R Foundation for Statistical Computing).

Costa, B., Taylor, J. C., Kracker, L., Battista, T., and Pittman, S. (2014). Mapping reef fish and the seascape: using acoustics and spatial modeling to guide coastal management. *PLoS One* 9, e85555. doi: 10.1371/journal.pone.0085555

Cummings, D. O., Lee, R. W., Simpson, S. J., Booth, D. J., Pile, A. J., and Holmes, S. P. (2011). Resource partitioning amongst co-occurring decapods on wellheads from australia's north–West shelf. *Anal. carbon nitrogen stable isotopes J. Exp. Mar. Biol. Ecol.* 409, 186–193. doi: 10.1016/j.jembe.2011.08.021

Cure, K., Currey-Randall, L., Galaiduk, R., Radford, B., Wakeford, M., and Heyward, A. (2021). Depth gradients in abundance and functional roles suggest limited depth refuges for herbivorous fishes. *Coral Reefs* 40 (2), 365–379. doi: 10.1007/s00338-021-02060-7

Currey-Randall, L. M., Galaiduk, R., Stowar, M., Vaughan, B. I., and Miller, K. J. (2021). Mesophotic fish communities of the ancient coastline in Western Australia. *PLoS One* 16, e0250427. doi: 10.1371/journal.pone.0250427

Currey-Randall, L., Wakeford, M., Colquhoun, J., Cappo, M., Stowar, M., Birt, M., et al. (2019). "Temporal trends in benthic communities and demersal fishes at rankin bank and glomar shoal," in *Report prepared for woodside energy Ltd* (Perth: Australian Institute of Marine Science), 62.

Da Silva, F., and Luis Pereira, F. X. (2011). *ATSEA (Arafura and timor Sea environmental actions) cruise 2 report*. (Perth: Australian Institute of Marine Science)

De'ath, G. (2002). Multivariate regression trees: a new technique for modeling species-environment relationships. *Ecology* 83, 1105–1117.

De'ath, G. (2011). "Mvpart: multivariate partitioning," in *R package version 1.4-0.* [computer program]

De'ath, G., and Fabricius, K. (2000). Classification and regression trees: a powerful yet simple technique for ecological data analysis. *Ecology* 81, 3178–3192. doi: 10.1890/0012-9658(2000)081[3178:CARTAP]2.0.CO;2

DeVantier, L. M., De'ath, G., Turak, E., Done, T. J., and Fabricius, K. E. (2006). Species richness and community structure of reef-building corals on the nearshore great barrier reef. *Coral Reefs* 25, 329–340. doi: 10.1007/s00338-006-0115-8

DMIRS (2021). *DMIRS (Department of mines, industry regulations and safety): An overview of the latest key information on the performance of the state's resources industry*.

Dufrene, M., and Legendre, P. (1997). Species assemblages and indicator species: The need for a flexible asymmetrical approach. (Perth: Government of Western Australia) *Ecol. Monogr.* 67, 345–366. doi: 10.2307/2963459

Dulvy, N. K., Fowler, S. L., Musick, J. A., Cavanagh, R. D., Kyne, P. M., Harrison, L. R., et al. (2014). Extinction risk and conservation of the world's sharks and rays. *elife* 3, e00590. doi: 10.7554/eLife.00590

Elith, J., and Leathwick, J. R. (2009). Species distribution models: ecological explanation and prediction across space and time. *Annu. Rev. Ecol. Evolution Systematics* 40, 677–697. doi: 10.1146/annurev.ecolsys.110308.120159

Estes, J. A., Terborgh, J., Brashares, J. S., Power, M. E., Berger, J., Bond, W. J., et al. (2011). Trophic downgrading of planet earth. *Science* 333, 301–306. doi: 10.1126/science.1205106

Evans, R. D., Wilson, S. K., and Field, S. N. (2014). Importance of macroalgal fields as coral reef fish nursery habitat in north-west Australia. *Mar. Biol.* 161, 599–607. doi: 10.1007/s00227-013-2362-x

Evans, R. D., Wilson, S. K., Fisher, R., Ryan, N. M., Babcock, R., Blakeway, D., et al. (2020). Early recovery dynamics of turbid coral reefs after recurring bleaching events. *J. Environ. Manage.* 268, 110666. doi: 10.1016/j.jenvman.2020.110666

Fitzpatrick, B. M., Harvey, E. S., Heyward, A. J., Twiggs, E. J., and Colquhoun, J. (2012). Habitat specialization in tropical continental shelf demersal fish assemblages. *PloS One* 7, e39634. doi: 10.1371/journal.pone.0039634

Fowler, A. M., Macreadie, P. I., Bishop, D. P., and Booth, D. J. (2015). Using otolith microchemistry and shape to assess the habitat value of oil structures for reef fish. *Mar. Environ. Res.* 106, 103–113. doi: 10.1016/j.marenvres.2015.03.007

Froese, R., and Pauly, D. (2021a). *FishBase* (Fisheries Centre: University of British Columbia). Available at: www://www.fishbase.de, accessed 10/18/2022.

Froese, R., and Pauly, D. (2021b). The ecology table. Available at: www://www.fishbase.de, accessed 10/18/2022.

Fujii, T. (2015). Temporal variation in environmental conditions and the structure of fish assemblages around an offshore oil platform in the north Sea. *Mar. Environ. Res.* 108, 69–82. doi: 10.1016/j.marenvres.2015.03.013

Fung, T., and LeDrew, E. (1987). Application of principal components analysis to change detection. *Photogrammetric Eng. Remote Sens.* 53, 1649–1658.

Galaiduk, R., Figueira, W. F., Kingsford, M., and Curley, B. G. (2013). Factors driving the biogeographic distribution of two temperate Australian damselfishes and ramifications for range shifts. *Mar. Ecol. Prog. Ser.* 484, 189–202. doi: 10.3354/meps10300

Galaiduk, R., Halford, A. R., Radford, B. T., Moore, C. H., and Harvey, E. S. (2017a). Regional-scale environmental drivers of highly endemic temperate fish communities located within a climate change hotspot. *Diversity Distributions* 23 (11), 1256–1267. doi: 10.1111/ddi.12614

Galaiduk, R., Radford, B., Harries, S., Case, M., Williams, D., Low Choy, D., et al. (2019). *Technical report: Darwin – bynoe harbours predictive mapping of benthic communities* (Perth: Australian Institute of Marine Science).

Galaiduk, R., Radford, B. T., Saunders, B. J., Newman, S. J., and Harvey, E. S. (2017b). Characterizing ontogenetic habitat shifts in marine fishes: advancing nascent methods for marine spatial management. *Ecol. Appl.* 27, 1776–1788. doi: 10.1002/eap.1565

Gaughan, D., and Santoro, K. (2021). *Status reports of the fisheries and aquatic resources of Western Australia 2019/20: The state of the fisheries* (Perth, Australia: Department of Primary Industries and Regional Development).

Geraghty, P., Macbeth, W., and Williamson, J. (2015). "Aspects of the reproductive biology of dusky, spinner and sandbar sharks (Family carcharhinidae) from the Tasman Sea," in *Marine and freshwater research* 67 (4), 513–525.

Gilmour, J. P., Cook, K. L., Ryan, N. M., Puotinen, M. L., Green, R. H., Shedrawi, G., et al. (2019). The state of Western australia's coral reefs. *Coral Reefs* 38, 651–667. doi: 10.1007/s00338-019-01795-8

Graham, N. A. J., Wilson, S. K., Jennings, S., Polunin, N. V. C., Bijoux, J. P., and Robinson, J. (2006). Dynamic fragility of oceanic coral reef ecosystems. *Proc. Natl. Acad. Sci.* 103, 8425–8429. doi: 10.1073/pnas.0600693103

Gratwicke, B., and Speight, M. R. (2005). The relationship between fish species richness, abundance and habitat complexity in a range of shallow tropical marine habitats. *J. Fish Biol.* 66, 650–667. doi: 10.1111/j.0022-1112.2005.00629.x

Gust, N., Choat, J. H., and McCormick, M. I. (2001). Spatial variability in reef fish distribution, abundance, size and biomass: a multi-scale analysis. *Mar. Ecol. Prog. Ser.* 214, 237–251. doi: 10.3354/meps214237

Harry, A. V., Butcher, P. A., Macbeth, W. G., Morgan, J. A. T., Taylor, S. M., Geraghty, P. T., et al. (2019). Life history of the common blacktip shark, carcharhinus limbatus, from central eastern Australia and comparative demography of a cryptic shark complex. *Mar. Freshw. Res.* 70, 834–848. doi: 10.1071/MF18141

Harvey, E. S., Cappo, M., Butler, J. J., Hall, N., and Kendrick, G. A. (2007). Bait attraction affects the performance of remote underwater video stations in assessment of demersal fish community structure. *Mar. Ecol. Prog. Ser.* 350, 245–254. doi: 10.3354/meps07192

Harvey, E. S., Cappo, M., Kendrick, G. A., and McLean, D. L. (2013). Coastal fish assemblages reflect geological and oceanographic gradients within an Australian zootone. *PloS One* 8, 1–17. doi: 10.1371/journal.pone.0080955

Heyward, A., Cappo, M., Case, M., Colquhoun, J., Fisher, R., Radford, B., et al. (2015). *AIMS ARP7 shoals – annual report on the outcome of the 2015 shoals survey* (Perth: Prepared for Shell and INPEX by the Australian Institute of Marine Science).

Heyward, A., Jones, R., Meeuwig, J., Burns, K., Radford, B., Colquhoun, J., et al. (2012). "Monitoring study S5. montara: 2011 offshore banks assessment survey," in *Final report prepared by the Australian institute of marine science for PTTEP Australasia (Ashmore Cartier) pty. Ltd* (Perth: Australian Institute of Marine Science).

Heyward, A., and Radford, B. (2019). Northwest Australia. *In: Mesophotic Coral Ecosystems Springer* p, 337–349. doi: 10.1007/978-3-319-92735-0_19

Heyward, A., Radford, B., Cappo, M., Wakeford, M., Fisher, J., Colquhoun, J., et al. (2017). "Barossa environmental baseline study, regional shoals and shelf assessment 2015 final report," in *A report for ConocoPhillips Australia exploration pty Ltd by the Australian institute of marine science* (Perth: Western Australia).

Hixon, M. A., and Jones, G. P. (2005). Competition, predation, and density-dependent mortality in demersal marine fishes. *Ecol. (Washington DC)* 86, 2847–2859. doi: 10.1890/04-1455

Holmes, K. W., Van Niel, K. P., Radford, B., Kendrick, G. A., and Grove, S. L. (2008). Modelling distribution of marine benthos from hydroacoustics and underwater video. *Continental Shelf Res.* 28, 1800–1810. doi: 10.1016/j.csr.2008.04.016

Hsieh, T. C., Ma, K. H., and Chao, A. (2016). INEXT: an r package for rarefaction and extrapolation of species diversity (Hill numbers). *Methods Ecol. Evol.* 7, 1451–1456. doi: 10.1111/2041-210X.12613

Hyndes, G. A., Kendrick, A. J., MacArthur, L. D., and Stewart, E. (2003). Differences in the species-and size-composition of fish assemblages in three distinct seagrass habitats with differing plant and meadow structure. *Mar. Biol.* 142, 1195–1206. doi: 10.1007/s00227-003-1010-2

Hyndes, G. A., Potter ', I. C., and Lenanton, R. C. J. (1996). Habitat partitioning by whiting species (Sillaginidae) in coastal waters. *Environ. Biol. Fishes* 45, 21–40. doi: 10.1007/BF00000625

IUCN (2021). *The IUCN red list of threatened species. version 2021-3*. Available at: www://www.iucnredlist.org., accessed 04/01/2022.

Kerry, J. T., and Bellwood, D. R. (2012). The effect of coral morphology on shelter selection by coral reef fishes. *Coral Reefs* 31, 415–424. doi: 10.1007/s00338-011-0859-7

Koppel, D. J., Kho, F., Hastings, A., Crouch, D., MacIntosh, A., Cresswell, T., et al. (2022). Current understanding and research needs for ecological risk assessments of naturally occurring radioactive materials (NORM) in subsea oil and gas pipelines. *J. Environ. radioact.* 241, 106774. doi: 10.1016/j.jenvrad.2021.106774

Kordi, M. N., Collins, L. B., O'Leary, M., and Stevens, A. (2016). *ReefKIM: An integrated geodatabase for sustainable management of the Kimberley reefs*. (North West Australia: Ocean & Coastal Management) 119, 234–243

Langlois, T., Goetze, J., Bond, T., Monk, J., Abesamis, R. A., Asher, J., et al. (2020). A field and video annotation guide for baited remote underwater stereo-video surveys of demersal fish assemblages. *Methods Ecol. Evol.* 11, 1401–1409. doi: 10.1111/2041-210X.13470

Langlois, T. J., Radford, B. T., Van Niel, K. P., Meeuwig, J. J., Pearce, A. F., Rousseaux, C. S. G., et al. (2012). Consistent abundance distributions of marine fishes in an old, climatically buffered, infertile seascape. *Global Ecol. Biogeogr.* 21, 886–897. doi: 10.1111/j.1466-8238.2011.00734.x

Letessier, T. B., Mouillot, D., Bouchet, P. J., Vigliola, L., Fernandes, M. C., Thompson, C., et al. (2019). Remote reefs and seamounts are the last refuges for marine predators across the indo-pacific. *PLoS Biol.* 17, e3000366. doi: 10.1371/journal.pbio.3000366

Lindfield, S. J., Harvey, E. S., Halford, A. R., and McIlwain, J. L. (2016). Mesophotic depths as refuge areas for fishery-targeted species on coral reefs. *Coral Reefs* 35, 125–137. doi: 10.1007/s00338-015-1386-8

MacIntosh, A., Dafforn, K., Penrose, B., Chariton, A., and Cresswell, T. (2021). Ecotoxicological effects of decommissioning offshore petroleum infrastructure: A systematic review. *Crit. Rev. Environ. Sci. Technol.*, 52 (18), 3283–3321. doi: 10.1080/10643389.2021.1917949

Marliave, J. B., Conway, K. W., Gibbs, D. M., Lamb, A., and Gibbs, C. (2009). Biodiversity and rockfish recruitment in sponge gardens and bioherms of southern British Columbia, Canada. *Mar. Biol.* 156, 2247–2254. doi: 10.1007/s00227-009-1252-8

Martinez, A. S., Queiroz, E. V., Bryson, M., Byrne, M., and Coleman, R. A. (2017). Incorporating *in situ* habitat patchiness in site selection models reveals that site fidelity is not always a consequence of animal choice. *J. Anim. Ecol.* 86, 847–856. doi: 10.1111/1365-2656.12668

McArdle, B., and Anderson, M. (2001). Fitting multivariate models to community data: a comment on distance-based redundancy analysis. *Ecology* 82, 290–297. doi: 10.1890/0012-9658(2001)082[0290:FMMTCD]2.0.CO;2

McAuley, R. B., Simpfendorfer, C. A., and Hall, N. G. (2007). A method for evaluating the impacts of fishing mortality and stochastic influences on the demography of two long-lived shark stocks. *ICES J. Mar. Sci.* 64, 1710–1722. doi: 10.1093/icesjms/fsm146

McCormick, M. (1995). Fish feeding on mobile benthic invertebrates: influence of spatial variability in habitat associations. *Mar. Biol.* 121, 627–637. doi: 10.1007/BF00349298

McLean, D., Cure, K., Wahab, M. A., Galaiduk, R., Birt, M., Vaughan, B., et al. (2021). A comparison of marine communities along a subsea pipeline with those in surrounding seabed areas. *Continental Shelf Res.*, 219, 104394. doi: 10.1016/j.csr.2021.104394

McLean, D. L., Ferreira, L. C., Benthuysen, J. A., Miller, K. J., Schläppy, M.-L., Ajemian, M. J., et al. (2022). Influence of offshore oil and gas structures on seascape ecological connectivity. *Global Change Biol.* 28 (11), 3515–3536 doi: 10.1111/gcb.16134

McLean, D. L., Langlois, T. J., Newman, S. J., Holmes, T. H., Birt, M. J., Bornt, K. R., et al. (2016). Distribution, abundance, diversity and habitat associations of fishes across a bioregion experiencing rapid coastal development. *Estuarine Coast. Shelf Sci.* 178, 36–47. doi: 10.1016/j.ecss.2016.05.026

McLean, D. L., Partridge, J. C., Bond, T., Birt, M. J., Bornt, K. R., and Langlois, T. J. (2017). Using industry ROV videos to assess fish associations with subsea pipelines. *Continental Shelf Res.* 141, 76–97. doi: 10.1016/j.csr.2017.05.006

McLean, D. L., Taylor, M. D., Giraldo Ospina, A., and Partridge, J. C. (2019). An assessment of fish and marine growth associated with an oil and gas platform jacket using an augmented remotely operated vehicle. *Continental Shelf Res.* 179, 66–84. doi: 10.1016/j.csr.2019.04.006

McLean, D. L., Taylor, M. D., Partridge, J. C., Gibbons, B., Langlois, T. J., Malseed, B. E., et al. (2018). Fish and habitats on wellhead infrastructure on the north west shelf of Western Australia. *Continental Shelf Res.* 164, 10–27. doi: 10.1016/j.csr.2018.05.007

McLean, D. L., Vaughan, B. I., Malseed, B. E., and Taylor, M. D. (2020). Fish-habitat associations on a subsea pipeline within an Australian marine park. *Mar. Environ. Res.* 153, 104813. doi: 10.1016/j.marenvres.2019.104813

Meyer-Gutbrod, E., Love, M., Claisse, J., Page, H., Schroeder, D., and Miller, R. (2019). Decommissioning impacts on biotic assemblages associated with shell mounds beneath southern California offshore oil and gas platforms. *Bull. Mar. Sci.* 95, 683–702. doi: 10.5343/bms.2018.0077

Meyer-Gutbrod, E. L., Love, M. S., Schroeder, D. M., Claisse, J. T., Kui, L., and Miller, R. J. (2020). Forecasting the legacy of offshore oil and gas platforms on fish community structure and productivity. *Ecol. Appl.* 30, e02185. doi: 10.1002/eap.2185

Monk, J., Ierodiaconou, D., l., V. V., Bellgrove, A., Harvey, E., Rattray, A., et al. (2010). Habitat suitability for marine fishes using presence-only modelling and multibeam sonar. *Mar. Ecol. Prog. Ser.* 420, 157–174. doi: 10.3354/meps08858

Moore, C., Cappo, M., Radford, B., and Heyward, A. (2017). Submerged oceanic shoals of north Western Australia are a major reservoir of marine biodiversity. *Coral Reefs* 36, 719–734. doi: 10.1007/s00338-017-1564-y

Moore, C. H., Harvey, E. S., and Van Niel, K. P. (2009). Spatial prediction of demersal fish distributions: enhancing our understanding of species-environment relationships. *ICES J. Mar. Sci.* 66, 2068–2075. doi: 10.1093/icesjms/fsp205

Moore, C. H., Harvey, E. S., and Van Niel, K. (2010). The application of predicted habitat models to investigate the spatial ecology of demersal fish assemblages. *Mar. Biol.* 157, 2717–2729. doi: 10.1007/s00227-010-1531-4

Moore, G., Morrison, S., Hutchins, J. B., Allen, G. R., and Sampey, A. (2014). Kimberley Marine biota. *Historical data: fishes. Records Western Aust. Museum Supplement* 84, 161–206. doi: 10.18195/issn.0313-122x.84.2014.161-206

Morgan, D. L., Whitty, J. M., and Phillips, N. M. (2011). North-western Australia as a hotspot for endangered elasmobranchs with particular reference to sawfishes and the northern river shark. *J. R. Soc. Western Aust.* 14, 345–358.

Newman, S., Wakefield, C., Skepper, C., Boddington, D., and Steele, A. (2020). "North coast demersal resource status report 2020," in *Status reports of the fisheries and aquatic resources of Western Australia 2019/20: The state of the fisheries*. Eds. D. J. Gaughan and K. Santoro (Western Australia: Department of Primary Industries and Regional Development).

Nichol, S., Howard, F. J. F., Kool, J., Siwabessy, J., Przeslawki, R., Stowar, M., et al. (2013). *Oceanic shoals commonwealth marine reserve (Timor Sea) biodiversity survey: GA0339/SOL5650 post-survey report* (Canberra: Geoscience Australia).

NOPSEMA (2022). *NOPSEMA (National offshore petroleum safety and environmental management authority) research strategy*. (Perth: NOPSEMA)

Oksanen, J., Blanchet, F. G., Kindt, R., Legendre, P., Minchin, P., O'hara, R., et al. (2013). "Community ecology package," in *R package version* 2 (0), 321–326.

Ouellette, M.-H., Legendre, P., and Borcard, D. (2012). Cascade multivariate regression tree: a novel approach for modelling nested explanatory sets. *Methods Ecol. Evol.* 3, 234–244. doi: 10.1111/j.2041-210X.2011.00171.x

Ovenden, J. R., Lloyd, J., Newman, S. J., Keenan, C. P., and Slater, L. S. (2002). Spatial genetic subdivision between northern Australian and southeast Asian populations of pristipomoides multidens: a tropical marine reef fish species. *Fish. Res.* 59, 57–69. doi: 10.1016/S0165-7836(01)00415-5

Ovenden, J. R., Salini, J., O'connor, S., and Street, R. (2004). Pronounced genetic population structure in a potentially vagile fish species (Pristipomoides multidens, teleostei; perciformes; lutjanidae) from the East indies triangle. *Mol. Ecol.* 13, 1991–1999. doi: 10.1111/j.1365-294X.2004.02210.x

Papastamatiou, Y. P., Lowe, C. G., Caselle, J. E., and Friedlander, A. M. (2009). Scale-dependent effects of habitat on movements and path structure of reef sharks at a predator-dominated atoll. *Ecology* 90, 996–1008. doi: 10.1890/08-0491.1

Pinheiro, H. T., Goodbody-Gringley, G., Jessup, M. E., Shepherd, B., Chequer, A. D., and Rocha, L. A. (2016). Upper and lower mesophotic coral reef fish communities evaluated by underwater visual censuses in two Caribbean locations. *Coral Reefs* 35, 139–151. doi: 10.1007/s00338-015-1381-0

Pittman, S. J., Christensen, J. D., Caldow, C., Menza, C., and Monaco, M. E. (2007). Predictive mapping of fish species richness across shallow-water seascapes in the Caribbean. *Ecol. Model.* 204, 9–21. doi: 10.1016/j.ecolmodel.2006.12.017

Pittman, S. J., Costa, B. M., and Battista, T. A. (2009). Using lidar bathymetry and boosted regression trees to predict the diversity and abundance of fish and corals. *J. Coast. Res.* 10053, 27–38. doi: 10.2112/SI53-004.1

Pradella, N., Fowler, A. M., Booth, D. J., and Macreadie, P. I. (2014). Fish assemblages associated with oil industry structures on the continental shelf of north-western Australia. *J. Fish Biol.* 84, 247–255. doi: 10.1111/jfb.12274

Pratchett, M. S., Bay, L. K., Gehrke, P. C., Koehn, J. D., Osborne, K., Pressey, R. L., et al. (2011). Contribution of climate change to degradation and loss of critical fish habitats in Australian marine and freshwater environments. *Mar. Freshw. Res.* 62, 1062–1081. doi: 10.1071/MF10303

Priede, I. G., Bagley, P. M., Smith, A., Creasey, S., and Merrett, N. (1994). Scavenging deep demersal fishes of the porcupine seabight, north-east Atlantic: observations by baited camera, trap and trawl. *J. Mar. Biol. Assoc. U. K.* 74, 481–498. doi: 10.1017/S0025315400047615

Przeslawski, R., Alvarez de Glasby, B., Smit, N., Evans-Illidge, L., and Dethmers, K. (2013). *Benthic biota of northern Australia: SS2012t07 post-survey report.* (Canberra: Geoscience Australia)

Randin, C. F., Ashcroft, M. B., Bolliger, J., Cavender-Bares, J., Coops, N. C., Dullinger, S., et al. (2020). Monitoring biodiversity in the anthropocene using remote sensing in species distribution models. *Remote Sens. Environ.* 239, 111626. doi: 10.1016/j.rse.2019.111626

Richards, J., and Jia, X. (2006). Interpretation of hyperspectral image data. Remote Sensing Digital Image Analysis: An Introduction. 359–388.

Roberts, D. W., and Roberts, M. D. W. (2016). *Package 'labdsv.' ordination and multivariate* 775. Available at: https://cran.r-project.org/web/packages/labdsv/index.html, accessed 10/18/2022

Sainsbury, K., Campbell, R., Lindholm, R., and Whitelaw, A. (1997). *Experimental management of an Australian multi-species fishery: examining the possibility of trawl-induced habitat modification*. (Maryland, USA: American Fisheries Society).

Sammarco, P., Porter, S., Sinclair, J., and Genazzio, M. (2014). Population expansion of a new invasive coral species, tubastraea micranthus, in the northern gulf of Mexico. *Mar. Ecol. Prog. Ser.* 495, 161–173. doi: 10.3354/meps10576

Saunders, B. J., Galaiduk, R., Inostroza, K., Myers, E. M. V., Goetze, J. S., Westera, M., et al. (2021). Quantifying patterns in fish assemblages and habitat use along a deep submarine canyon-valley feature using a remotely operated vehicle. *Front. Mar. Sci.* 8, 1267. doi: 10.3389/fmars.2021.608665

Schramm, K. D., Marnane, M. J., Elsdon, T. S., Jones, C. M., Saunders, B. J., Newman, S. J., et al. (2021). Fish associations with shallow water subsea pipelines compared to surrounding reef and soft sediment habitats. *Sci. Rep.* 11, 6238. doi: 10.1038/s41598-021-85396-y

Stevens, J. D., and Wiley, P. D. (1986). Biology of two commercially important carcharhinid sharks from northern Australia. *Mar. Freshw. Res.* 37, 671–688. doi: 10.1071/MF9860671

Thomson, P. G., Pillans, R., Jaine, F. R. A., Harcourt, R. G., Taylor, M. D., Pattiaratchi, C. B., et al. (2021). Acoustic telemetry around Western australia's oil and gas infrastructure helps detect the presence of an elusive and endangered migratory giant. *Front. Mar. Sci.* 8, 631449. doi: 10.3389/fmars.2021.631449

Travers, M. J., Potter, I. C., Clarke, K. R., and Newman, S. J. (2012). Relationships between latitude and environmental conditions and the species richness, abundance and composition of tropical fish assemblages over soft substrata. *Mar. Ecol. Prog. Ser.* 446, 221–241. doi: 10.3354/meps09501

Travers, M. J., Potter, I. C., Clarke, K. R., Newman, S. J., and Hutchins, J. B. (2010). The inshore fish faunas over soft substrates and reefs on the tropical west coast of Australia differ and change with latitude and bioregion. *J. Biogeogr.* 37, 148–169. doi: 10.1111/j.1365-2699.2009.02183.x

Tuya, F., Wernberg, T., and Thomsen, M. S. (2011). The relative influence of local to regional drivers of variation in reef fishes. *J. Fish Biol.* 79, 217–234. doi: 10.1111/j.1095-8649.2011.03015.x

Underwood, A. J., Chapman, M. G., and Connell, S. D. (2000). Observations in ecology: you can't make progress on processes without understanding the patterns. *J. Exp. Mar. Biol. Ecol.* 250, 97–115. doi: 10.1016/S0022-0981(00)00181-7

UNEP-WCMC, WorldFish Centre, WRI and TNC (2021). "Global distribution of warm-water coral reefs, compiled from multiple sources including the millennium coral reef mapping project," in *Version 4.1. includes contributions from IMaRS-USF and IRD 2005)*. Ed. Spalding,, et al (Cambridge (UK: UN Environment World Conservation Monitoring Centre). doi: 10.34892/t2wk-5t34

van Elden, S., Meeuwig, J. J., Hobbs, R. J., and Hemmi, J. M. (2019). Offshore oil and gas platforms as novel ecosystems: A global perspective. *Front. Mar. Sci.* 6, 548. doi: 10.3389/fmars.2019.00548

Watson, D. L., Harvey, E. S., Anderson, M. J., and Kendrick, G. A. (2005). A comparison of temperate reef fish assemblages recorded by three underwater stereo-video techniques. *Mar. Biol.* 148, 415–425. doi: 10.1007/s00227-005-0090-6

Wellington, C. M., Harvey, E. S., Wakefield, C. B., Abdo, D., and Newman, S. J. (2021). Latitude, depth and environmental variables influence deepwater fish assemblages off Western Australia. *J. Exp. Mar. Biol. Ecol.* 539, 151539. doi: 10.1016/j.jembe.2021.151539

Whiteway, T. (2009). *Australian Bathymetry and topography grid* (Canberra: Geoscience Australia).

Willis, T. J., and Anderson, M. J. (2003). Structure of cryptic reef fish assemblages: relationships with habitat characteristics and predator density. *Mar. Ecol. Prog. Ser.* 257, 209–221. doi: 10.3354/meps257209

Wilson, S. K., Babcock, R. C., Fisher, R., Holmes, T. H., Moore, J. A. Y., and Thomson, D. P. (2012). Relative and combined effects of habitat and fishing on reef fish communities across a limited fishing gradient at ningaloo. *Mar. Environ. Res.* 81, 1–11. doi: 10.1016/j.marenvres.2012.08.002

Wilson, S. K., Fulton, C. J., Depczynski, M., Holmes, T. H., Noble, M. M., Radford, B., et al. (2014). Seasonal changes in habitat structure underpin shifts in macroalgae-associated tropical fish communities. *Mar. Biol.* 161, 2597–2607. doi: 10.1007/s00227-014-2531-6

Wilson, P., Thums, M., Pattiaratchi, C., Meekan, M., Pendoley, K., Fisher, R., et al. (2018). Artificial light disrupts the nearshore dispersal of neonate flatback turtles natator depressus. *Mar. Ecol. Prog. Ser.* 600, 179–192. doi: 10.3354/meps12649

Young, M., and Carr, M. H. (2015). Application of species distribution models to explain and predict the distribution, abundance and assemblage structure of nearshore temperate reef fishes. *Diversity Distributions* 21, 1428–1440. doi: 10.1111/ddi.12378

Zanini, F., Pellet, J., and Schmidt, B. R. (2009). The transferability of distribution models across regions: an amphibian case study. *Diversity Distributions* 15, 469–480. doi: 10.1111/j.1472-4642.2008.00556.x

frontiers | Frontiers in Marine Science

TYPE Original Research
PUBLISHED 31 October 2022
DOI 10.3389/fmars.2022.1001925

OPEN ACCESS

EDITED BY
Victoria Louise Georgia Todd,
Ocean Science Consulting Ltd.,
United Kingdom

REVIEWED BY
Jongseong Ryu,
Anyang University, South Korea
Alvar Carranza,
Universidad de la República, Uruguay

*CORRESPONDENCE
Waka Sato-Okoshi
waka.sato-okoshi.d3@tohoku.ac.jp

SPECIALTY SECTION
This article was submitted to
Marine Ecosystem Ecology,
a section of the journal
Frontiers in Marine Science

RECEIVED 24 July 2022
ACCEPTED 27 September 2022
PUBLISHED 31 October 2022

CITATION
Hashimoto A and Sato-Okoshi W
(2022) Population dynamics of
Capitella aff. *teleta* (Polychaeta,
Capitellidae) in Gamo Lagoon,
northeastern Japan, during a series of
restoration works following the 2011
Great East Japan Earthquake
and tsunami.
Front. Mar. Sci. 9:1001925.
doi: 10.3389/fmars.2022.1001925

Population dynamics of *Capitella* aff. *teleta* (Polychaeta, Capitellidae) in Gamo Lagoon, northeastern Japan, during a series of restoration works following the 2011 Great East Japan Earthquake and tsunami

Akane Hashimoto and Waka Sato-Okoshi*

Laboratory of Biological Oceanography, Graduate School of Agricultural Science, Tohoku University, Sendai, Japan

The population dynamics of the capitellid polychaete *Capitella* aff. *teleta* were studied in Gamo Lagoon, located in northeast Japan, for the subsequent 2 years from 2016, when a series of restoration works was conducted following the 2011 Great East Japan Earthquake and tsunami. *Capitella* aff. *teleta* was found to be widely distributed from the estuary side, where the levee was located, to the innermost part but was more abundant in the innermost part, which is rich in organic matter. In the lagoon, the daily maximum water level dropped from 2017 to 2018 during the reconstruction of a flow-conducting levee, which blocked water flow and isolated the inner part of the lagoon. Although the density decreased drastically for approximately 11 months under diurnal hypoxia and strongly reducing conditions, small-sized new recruits were observed and the population recovered quickly after the daily maximum water level increased. In Gamo Lagoon, *C.* aff. *teleta* inhabiting the innermost part and estuary side of the lagoon contributed to maintaining the population by dispersing planktonic larvae between them. Thus, the maximum water level had a significant effect on the maintenance of the *C.* aff. *teleta* population in the lagoon, and sufficiently high water levels enable the dispersion of planktonic larvae to help recover the population quickly, suggesting that it is important to keep the water area connected.

KEYWORDS

***Capitella* aff. *teleta*, population dynamics, lagoon, water level, planktonic larvae, restoration work**

Introduction

The annelid species belonging to the genus *Capitella* (family Capitellidae) are opportunistic species in marine eutrophic sediments and are widely distributed globally (Rouse and Pleijel, 2001). *Capitella* aff. *teleta* found only in Gamo Lagoon (Tomioka et al., 2016) predominantly appeared in Gamo Lagoon immediately after the tsunami that followed the 2011 Great East Japan Earthquake and tsunami (Kondoh, 2017; Kondoh et al., 2020).

Of the 17 *Capitella* species known (Warren, 1991; Blake et al., 2009; Magalhães and Bailey-Brock, 2012; Silva et al., 2016), *Capitella capitata* (Fabricius, 1780) is best known as an opportunistic (Kanaya and Kikuchi, 2011) species that is predominant in eutrophic sediments and widely distributed worldwide (Blake, 2009). However, studies on the anatomy, growth, and physiology of *C. capitata* (Grassle and Grassle, 1976; Eckelbarger and Grassle, 1983; Chareonpanich et al., 1993; Gamenick et al., 1996; Gamenick et al., 1998; Linke-Gamenick et al., 2000; Méndez, 2002; Méndez, 2006) have revealed that *C. capitata* comprises at least 10 different species (Blake et al., 2009). One of these species, *Capitella* sp. I, which was thought to be distributed in North America and Japan, was determined and described as *C. teleta* (Blake et al., 2009).

In Japan, five species or subspecies of the genus *Capitella* have been described: *C. capitata*, *C. capitata japonica* (Kitamori, 1960), *Capitella jonesi* (Hartman, 1959), *Capitella minima* (Langerhans, 1880), and *C. teleta* (Kitamori, 1960; Imajima and Hartman, 1964; Imajima, 2015; Kanaya et al., 2015). Before *C. teleta* was described in 2009, most *Capitella* species in Japan were considered *C. capitata* (Kitamori, 1960; Imajima and Hartman, 1964; Honma et al., 1974; Ueno and Yamamoto 1982; Tsutsumi and Kikuchi, 1984; Tsutsumi, 1987; Tsutsumi et al., 1991). However, Tsutsumi and Montani (1993) reported that the species from Tomoe Bay, Amakusa, and Kyushu are identical to *Capitella* sp. I (Grassle and Grassle, 1976) from Massachusetts, USA, in terms of the karyotype, mating ability, and life history. Subsequent ecological studies after 2009 have revealed that this species is identical to *Capitella* sp. I (Tsutsumi, 2005; Tsutsumi et al., 2005; Kinoshita et al., 2008) or *C. teleta* (Nishi et al., 2010; Kanaya, 2014; Kanaya et al., 2015).

Gamo Lagoon is a eutrophic lagoon located at the mouth of the Nanakita River in Miyagi Prefecture, northeastern Japan. Gamo Lagoon was catastrophically damaged by a megathrust earthquake—the 2011 Great East Japan Earthquake—and huge tsunamis that occurred in March 2011 (Ide et al., 2011; Ozawa et al., 2011), which have caused drastic topographic changes (Kondoh et al., 2020). Just after the disturbance, a sand dune completely disappeared but was rapidly reformed, the river mouth was completely closed, a seasonal typhoon-induced flood hit the lagoon, and an intense deluge occurred in 2015. The second tsunami followed by the Fukushima Earthquake hit this estuary again in 2016; therefore, the balance of sand sedimentation dynamics remained unstable (Kondoh et al., 2020). Restoration and reconstruction work are underway, although many years have passed since the 2011 earthquake and tsunami.

Many coastal benthic species have a planktonic larval stage in their early life history. During this period, the larvae are passively transported and may settle and grow far from their original habitats. Thus, having a pelagic period leads to habitat expansion. The extinction of local populations caused by small-scale disturbances can be recovered by transferring from neighboring local populations. In other words, the dispersal of planktonic larvae leads to not only the expansion of the habitat of the species but also its sustainable survival in the wider region. Usually, geographically distant local communities interact in this complex way through the dispersal of organisms. Such regional aggregations of local communities are called metacommunities (Wilson, 1992). The local populations of each benthic species with planktonic larvae maintain and establish their populations through larval dispersal from other water sites.

The life history and population dynamics of *C. teleta* were studied on the coast of Kyushu in Japan (Tsutsumi and Kikuchi, 1984; Tsutsumi, 1987; Tsutsumi, 1990; Tsutsumi, 2005). Genetic analysis revealed that the species in Gamo Lagoon is a sister species of *C. teleta* and was reported as *C.* aff. *teleta* by Tomioka et al. (2016). This species has only been found in Gamo Lagoon, predominantly after the 2011 earthquake. The levee that was constructed at the border between Gamo Lagoon and the Nanakita River was destroyed by tsunamis but is being reconstructed since 2017. These events have caused major topographic changes within Gamo Lagoon and allowed us to analyze the change in the population dynamics of *C.* aff. *teleta*.

In recent years, changes in the environment have become evident in the form of torrential rains and frequent typhoons. Natural disturbances, such as earthquakes and tsunamis, followed by restoration work are common. Coastal areas have been directly affected by these natural and anthropogenic disturbances, resulting in significant changes in the topography and the communities that inhabit them. In this study, to clarify the population maintenance mechanism of *C.* aff. *teleta*, which first appeared immediately after the disturbance and is one of the key species in understanding the environmental changes and community dynamics in Gamo Lagoon, we examined the environmental changes in the lagoon and the interdependence between individuals at multiple stations in different environments in the lagoon, as well as the factors affecting population dynamics at different stations.

Materials and methods

Study area

Gamo Lagoon, located at the mouth of the Nanakita River in Miyagi Prefecture, northeastern Japan, is a eutrophic shallow tidal flat with a water surface area of 13 ha: 860 m long and 250 m wide, with a mean water depth of 0.8 m (Kondoh, 2017: data before March 2011). The lagoon was separated from the estuary by a stone levee with three water gates, a flow-conducting levee, and, from Sendai Bay, by a 150 m wide dune before March 2011 (Kanaya et al., 2014). The bottom sediment of the riverside and the inner part of the lagoon are sandy and muddy, respectively, and high reduction conditions were observed in the innermost part of the lagoon. Gamo Lagoon was designated as the Gamo Special Protection Area in the nationally designated Sendai Coastal Wildlife Protection Area in 1973. Many conservation efforts have been made to protect the biological communities and brackish water environment.

The 2011 Great East Japan Earthquake, with a magnitude of 9.0, occurred in March 2011 followed by 7.2-m-high tsunamis (data from the Japan Meteorological Agency) at the nearby Sendai Port and 3–4.5 m tsunamis (data from the Sendai Science Museum) in the Gamo area. In addition to the initial disturbance, heavy rainfall occurred in the Kanto and Tohoku regions in September 2015 (Tanaka et al., 2016), and another tsunami was generated following the Fukushima Earthquake in November 2016. Thus, topographic changes have occurred continuously at Gamo Lagoon: the topography around the mouth of the Nanakita River was significantly altered by the heavy rain, and sand deposition was observed in the middle part of Gamo Lagoon by the second tsunami. In the area around the estuary, including Gamo Lagoon, a series of restoration works began in 2016. The reconstructions of the levee at the entrance to Gamo Lagoon and the embankment on the landward side have been ongoing since November and February 2017, respectively. An artificial deep channel was excavated in the middle part of the lagoon by Miyagi Prefecture in August 2018.

Environmental data

The survey was conducted at Gamo Lagoon during low tide once a month from September 2016 to October 2018. The survey was included just after the tsunami on 28 November 2016. Three measuring points (Stns A, C, and D; Figure 1) were set up in Gamo Lagoon from the estuary side to the innermost part of the lagoon to cover the entire tidal flat area. At Stn C, the water level became so low that the sediments dried out during low tide after April 2018; therefore, Stn C′ was set up nearby where the water level was higher.

Environmental measurements were taken each month at each station for water temperature, mud temperature, salinity, the dissolved oxygen (DO) concentration, and the redox potential from the bottom layer. Water temperature and DO concentration were measured using a DO meter (HACH, HQ40d). Salinity was measured using a salinity meter (DKK-TOA, CM-21P). The oxidation–reduction potential and mud temperature were measured using an ORP meter (DKK-TOA, RM-30P). A data logger (YSI, 6000MS) was also installed near Stn C to measure water temperature, salinity, DO, and depth once every 30 min.

Changes in the density and size frequency distributions

Samples were collected from September 2016 to October 2018, once for each month and at each station using the Ekman–Birge

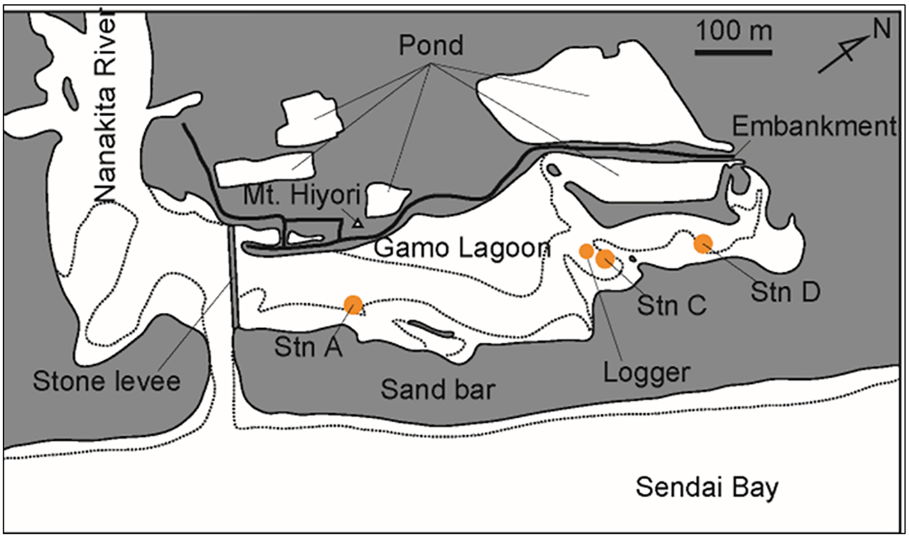

FIGURE 1
Gamo Lagoon. The bold line shows the location of Gamo Lagoon. Dashed lines show shorelines at low tide.

grab sampler [240 mm (W) × 210 mm (D) × 350 mm (H)]. An extra sample was added just after the tsunami on 28 November 2016. Mud samples were sieved through a 500 μm mesh, and all organisms remaining on the sieve were fixed and preserved with 10% neutralized formalin.

The individuals of *C.* aff. *teleta* were sorted from bottom mud samples and counted under a stereomicroscope (OLYMPUS SZX12). Thoracic maximal body segment width was used as an index of body size (Tsutsumi and Kikuchi, 1984) and measured under a stereomicroscope (OLYMPUS MZX12). Individuals with reproductive bristles on chaetigers 8 and 9 were identified as males and those with eggs in the ventral side of the abdominal chaetigers as females. Individuals lacking the characteristics of males and females were identified as immature individuals.

Results

Environmental observations at the time of the survey

Changes in water and mud temperatures at the time of the survey are shown in Figures 2A, B. The differences between water and mud temperatures were small, with a minimum water temperature of 2.4°C at Stn C in March 2018 and a maximum water temperature of 31.1°C at Stn C′ in August 2018, showing a seasonal variation with the lowest water temperature in December–March and the highest water temperature in July–August. The differences between the stations were small.

Changes in salinity, which varied between 13.9 and 31.2, at the time of the survey are shown in Figure 2C. Changes in the DO concentration during the survey are shown in Figure 2D. The lowest value during the study was 2.66 mg/L at Stn C in December 2017, and the highest value was 19.08 mg/L at Stn C in March 2018, with a weak tendency to drop in summer under 5 mg/L. In addition, the fluctuations were drastic from June 2017 both between and within stations.

Changes in the water level at the time of the survey are shown in Figure 2E. The water levels at Stns C and C′ were lower than those at Stns A and D throughout the study.

Changes in the redox potential at the time of the survey are shown in Figure 2F. The redox potential increased from September 2016 to January 2017, with a maximum value of 555 mV at Stn C in January 2017, and then remained high until March before decreasing again. The redox potential had negative

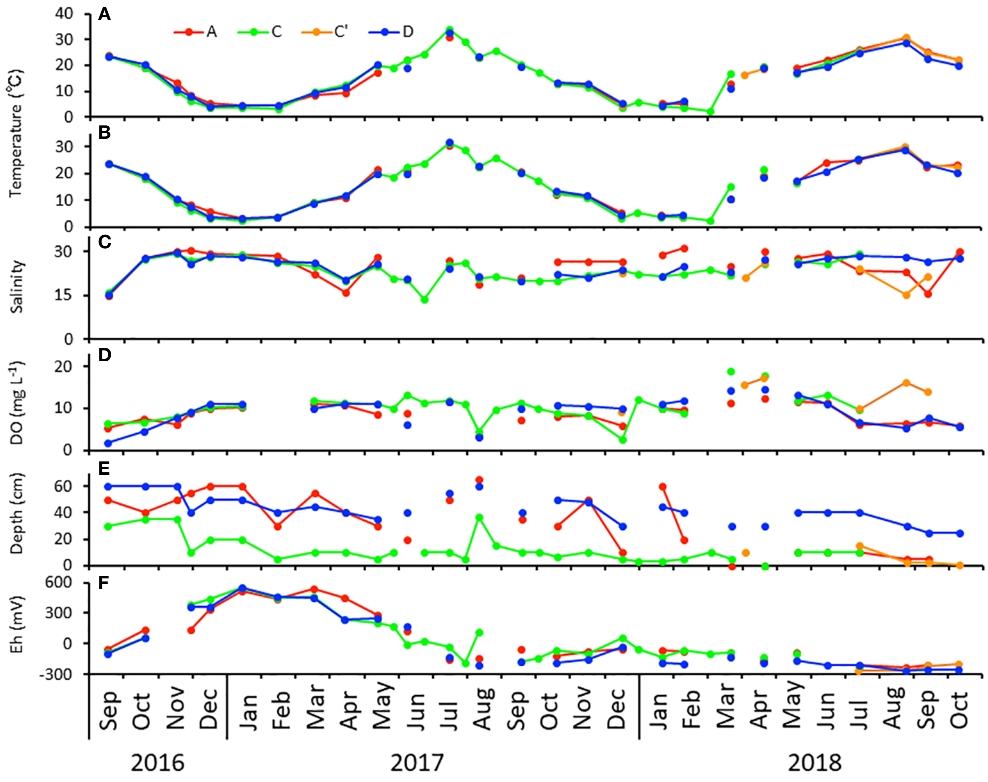

FIGURE 2
Seasonal changes in **(A)** water temperature, **(B)** sediment temperature, **(C)** salinity, **(D)** dissolved oxygen (DO) concentration, **(E)** water depth, and **(F)** the redox potential at Stns A, C (and C′), and D in Gamo Lagoon from September 2016 to October 2018. For missing data, no line connects before and after the missing data.

values in many months after June 2017, and these low levels continued. The differences between stations were relatively small, but Stn D tended to show the lowest values throughout.

Environmental observations by data logger

Figure 3 shows the results of observations made by a data logger installed near Stn C. Water temperatures varied seasonally from a minimum of −1.7°C to a maximum of 37.9° C. Compared to 2016–2017, 2017–2018 had longer periods below 0°C from December to March and higher maximum water temperatures from June to September. Salinity varied more between August and October, from approximately 10 to 30. DO concentrations during high water temperature in summer were hypoxic (see Diaz and Rosenberg, 1995), with the DO levels of 0–2.8 mg/L at night and supersaturation during the day, showing diurnal hypoxia. In addition, frequent diurnal hypoxia occurred from November 2017 to March 2018 during low-water-temperature periods. Depths showed a decrease in minimum water levels from February to March 2017, from December 2017 to June 2018, and since August 2018. Moreover, maximum water levels decreased from February to March 2017 and from December 2017 to June 2018. Daily water levels fluctuated highly from August 2018 after the channel was excavated in the middle of the lagoon.

Population dynamics of *C.* aff. *teleta* in Gamo Lagoon

Density

The population densities of *C.* aff. *teleta* at the three stations are shown in Figure 4. Although each station showed a large fluctuation in abundance, the two stations at the middle and innermost parts of the lagoon (Stns C, C', and D) showed rather similar changes in density, whereas Stn A at the estuary side showed a different change.

Capitella aff. *teleta* showed unstable density at Stn A, which varied from approximately 0–4,000 ind/m^2 from September 2016 to August 2017. During this period, a significant decline in the density was seen from December 2016 to January 2017 and March–May 2017. In addition, density did not increase from August 2017 to April 2018, continuing at almost zero level. However, after that period, density suddenly increased from May and reached 10,000 ind/m^2 in June but again began to decrease from July and dropped to almost zero in October.

At Stn C, density was higher than that at Stn A (Figure 4). It apparently plummeted just after the 2016 Fukushima Earthquake and tsunami in November. Thereafter, density fluctuated largely as it continued to increase in December 2016 and January 2017, decreased in February 2017, increased again in March, and decreased in April to one-half of the previous month's level. Thus, density was not stable after the tsunami from November 2016 to May 2017, with significant changes

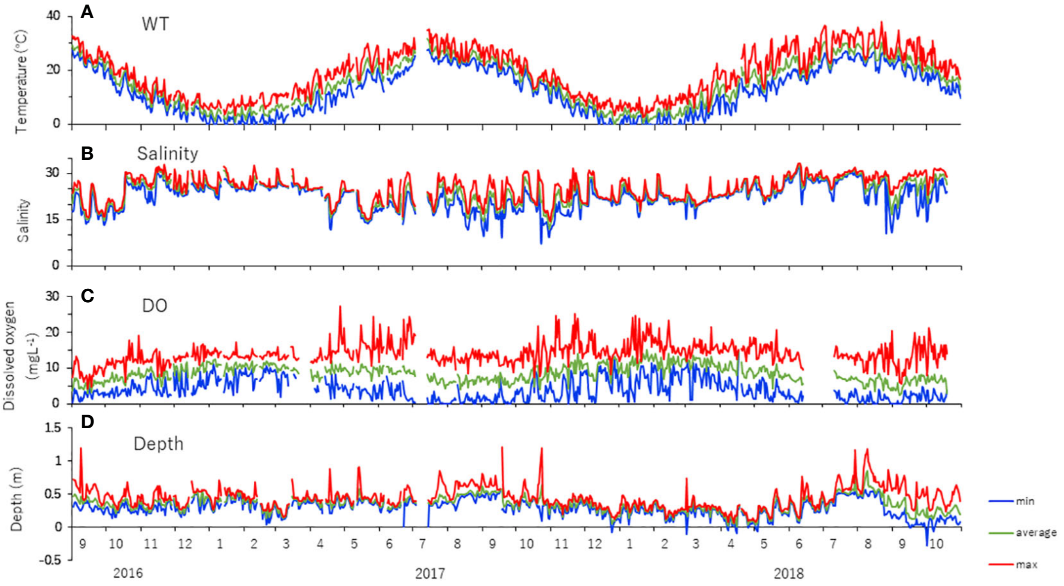

FIGURE 3
Seasonal changes in the daily minimum, average, and maximum **(A)** water temperature, **(B)** salinity, **(C)** DO, and **(D)** water depth recorded by the data logger at Stn C in Gamo Lagoon from September 2016 to October 2018.

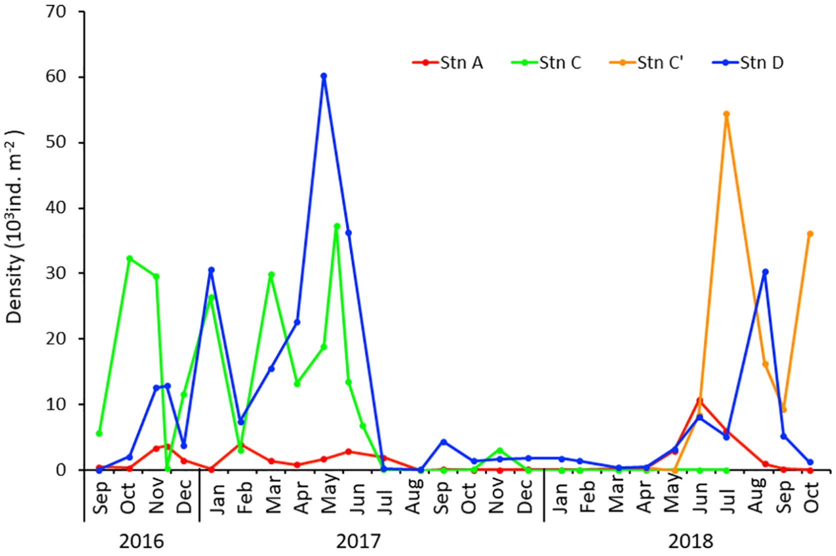

FIGURE 4
Seasonal changes in the density of *Capitella* aff. *teleta* at Stns A, C (and C′), and D in Gamo Lagoon from September 2016 to October 2018.

occurring every few months. Moreover, *C.* aff. *teleta* disappeared for approximately a year after July 2017. At nearby Stn C', an alternative station to dry up Stn C, density increased after June 2018 and reached up to >50,000 ind/m^2, decreased drastically in August and September, and increased again in October 2018.

The density at Stn D had the highest value among the three stations. Large fluctuations were observed from almost 0 (September 2016 and July 2017) to 60,000 ind/m^2 (May 2017) during September 2016–July 2017 (Figure 4). Density showed a rapid decrease in December 2016 and February 2017. The highest density of 60,000 ind/m^2 was recorded in May 2017. Density did not increase from July 2017 to April 2018. After May 2018, density showed an increasing trend and reached a maximum at approximately 30,000 ind/m^2 in August 2018.

Size frequency distribution

The size frequency distributions of the maximum width of the thoracic segment at Stn A are shown in Figure 5. At Stn A, smaller individuals with body width < 0.5 mm appeared each month, except December 2016, August and November 2017, and February and March 2018. Body width increased gradually from September to December in both 2016 and 2017 and decreased gradually from April to August in both 2017 and 2018. Larger individuals with body width >1 mm appeared from November 2016 to April 2017, except January 2017. Mature individuals appeared from November 2016 to April 2017, except January, and April–June 2018. Large mature individuals with body width approximately >1 mm appeared in November and December 2016, February–April 2017, and April and May 2018. Smaller mature individuals with body width <0.5 mm appeared in November 2016 and April and June 2018. Both the minimum and maximum body widths of mature individuals increased from November 2016 to February 2017 and decreased again from February. The presence of females and males revealed that no females appeared since April 2017.

A similar trend in change in body width was observed in Stn C, showing a gradual increase from September to December 2016 and a gradual decrease from April to June 2017 (Figure 6). In January 2017, many individuals with body width >1 mm were observed in Stn C, although very few were observed at Stn A. Small individuals (<0.5 mm) appeared, except from July to October and December 2017 and January, February, and May 2018. In November and December 2016; January, March–May, and November 2017; and April 2018, larger mature individuals (≥1 mm body width) appeared. In November 2016 and from June 2018, smaller mature individuals (<0.5 mm body width) were observed. The occurrence of males and females at both Stns C and C' showed that males tended to occur more frequently than females.

At Stn D, individuals with body width <0.5 mm appeared every month, except September 2016 and April 2018 (Figure 7). Large individuals (≥1 mm) emerged from October 2016 to April 2017 and from December 2017 to February and May 2018. Larger mature individuals (≥1 mm) emerged from October 2016 to April 2017 and January 2018. Smaller mature individuals (<0.5 mm) emerged in November 2016; January, April, and September 2017; and August and September 2018. The occurrence of males tended to be more abundant than females in Stn D.

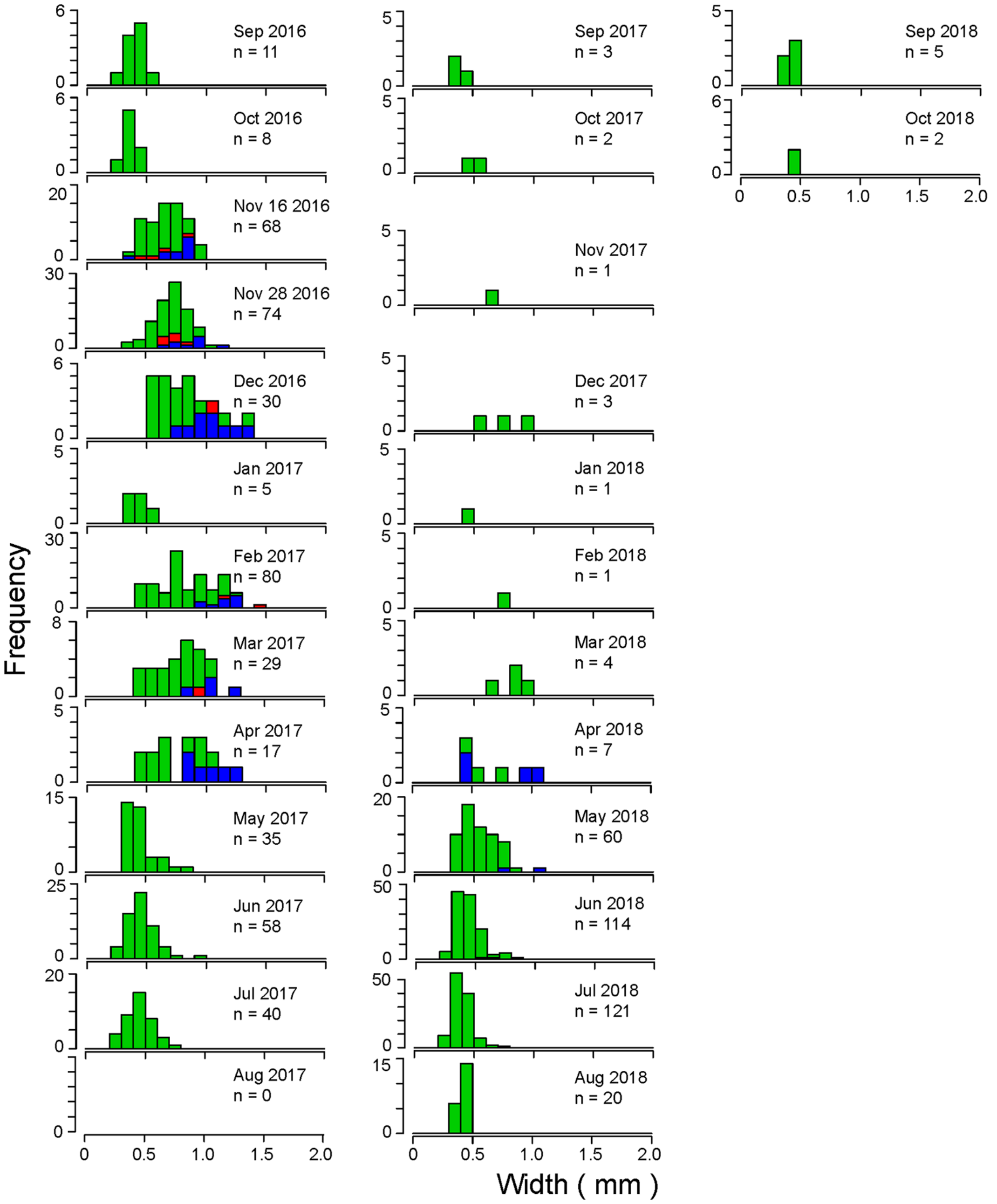

FIGURE 5
Size frequency distributions of the maximum width of the thoracic segment of *C.* aff. *teleta* at Stn A in Gamo Lagoon from September 2016 to October 2018. Red: females, blue: males, green: immature individuals.

Discussion

Environmental changes in Gamo Lagoon

The environment of Gamo Lagoon can be divided into low- and high-water-temperature periods, with a water temperature of 15°C. Diurnal hypoxia was observed mainly during the high-water-temperature period, but diurnal hypoxia was also observed from November 2017 to March 2018. Therefore, factors other than high water temperature can be related to a decrease in the levels of the DO concentration in Gamo Lagoon. Salinity fluctuated greatly from August to October, suggesting an increase in water runoff from the Nanakita River.

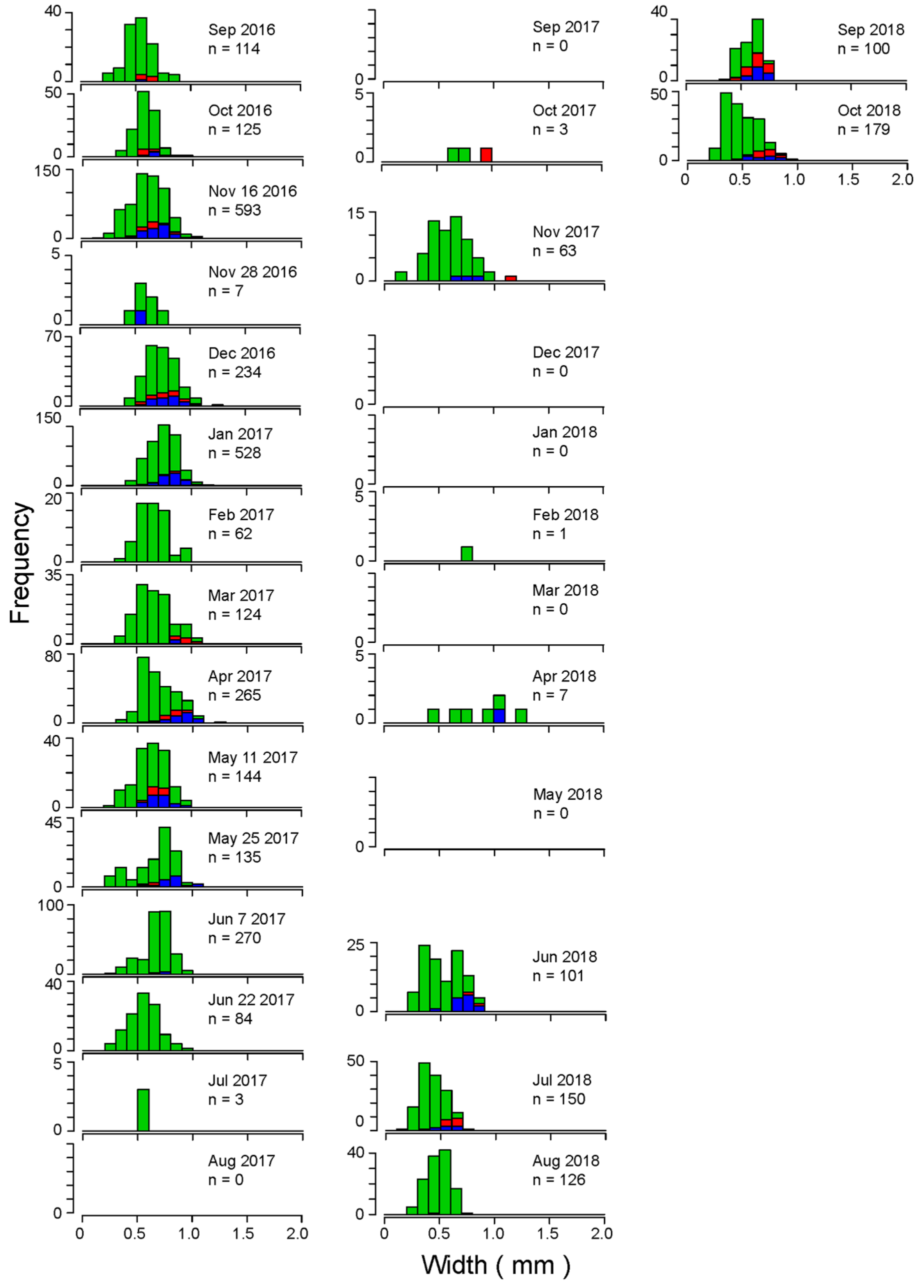

FIGURE 6
Size frequency distributions of the maximum width of the thoracic segment of *C.* aff. *teleta* at Stn C from September 2016 to March 2018 and at Stn C′ from April 2018 to October 2018 in Gamo Lagoon. Red: females, blue: males, green: immature individuals.

Seasonal fluctuations were observed in redox potential values, which tended to be higher during the low-water-temperature period and lower during the high-water-temperature period. During the low-water-temperature period from 2017 to 2018, the redox potential did not increase as much as it did from 2016 to 2017. From July 2017 onward, the redox potential continued to show negative values. This suggests that although water temperature or DO levels seemed to recover, the redox potential did not change and had low values since July 2017. Various factors, such as water temperature, DO, hydrogen sulfide, and pH, are thought to affect redox potential values—with hydrogen sulfide having a particularly strong effect—an increase in hydrogen sulfide results in a decrease in the redox potential (Muto and Kim, 1986).

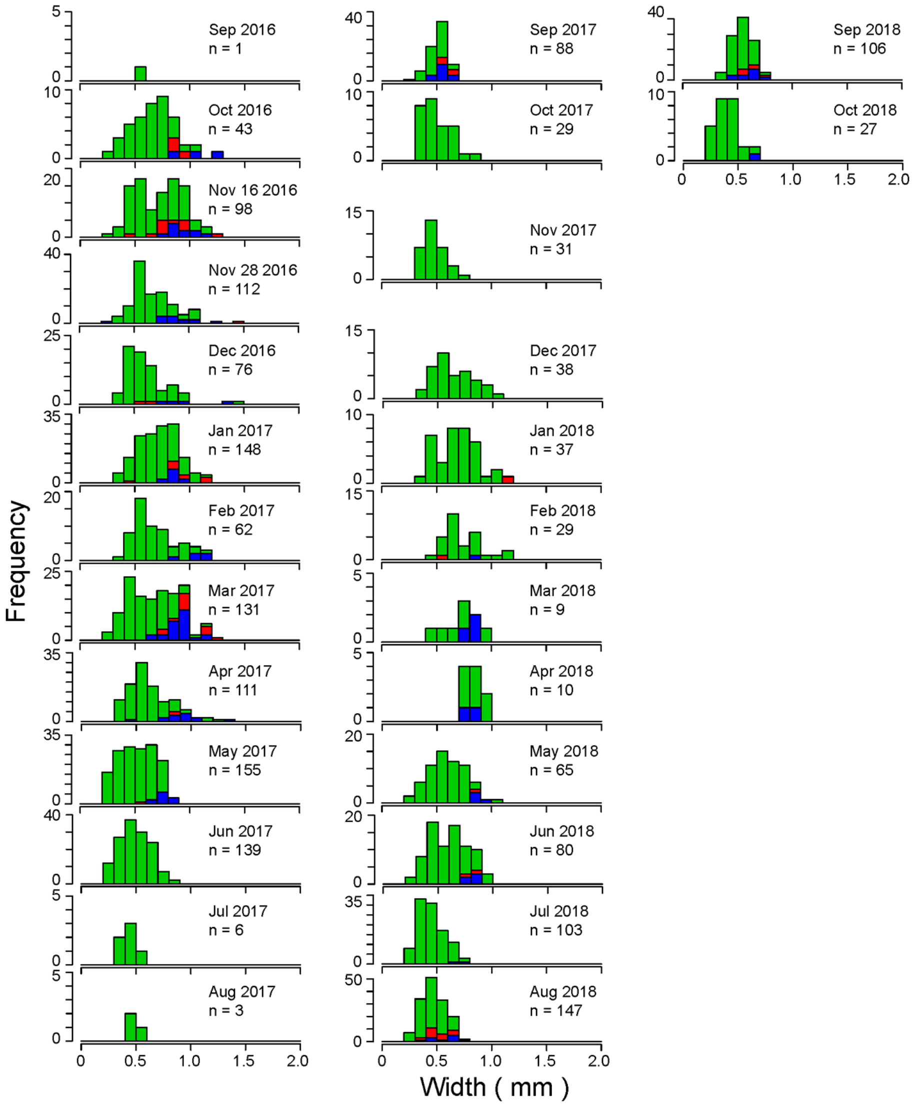

FIGURE 7

Size frequency distributions of the maximum width of the thoracic segment of *C.* aff. *teleta* at Stn D in Gamo Lagoon from September 2016 to October 2018. Red: females, blue: males, green: immature individuals.

Topographic changes in Gamo Lagoon

Water levels, both the daily minimum water depth and daily maximum water depth, declined from February to March 2017 and from December 2017 to May 2018. Moreover, sand sedimentation became noticeable in the beginning of summer 2017. Following these periods, the innermost part of the lagoon was found to be isolated in March 2017 and December 2017–April 2018 during low tide. During this period, a series of restoration works occurred at the estuarine side of the lagoon, which includes the reconstruction of the levee that was damaged by the 2011 tsunami (Figure 8) (Public Works Department, Miyagi Prefecture, 2021) and may have affected the water level of Gamo Lagoon. As the inner part of the lagoon began to dry and water flow continued to stagnate, artificial channel excavation was conducted in August 2018 to allow water to pass through the estuarine side and the innermost part of the lagoon (Figure 9) (Public Works Department, Miyagi Prefecture, 2021).

Although many periods, when the minimum water level decreased, showed a simultaneous decrease in the maximum water level, the maximum water level did not decrease after August 2018, resulting in more fluctuating water levels (Figure 3D). A possible reason for this is that a channel was excavated artificially in August (Figure 9) (Public Works Department, Miyagi Prefecture, 2021). The construction of the channel is thought to have increased the amount of flowing water, and the large fluctuations in water levels suggest that the amount of water conversion increased significantly since August 2018.

Population dynamics of *C.* aff. *teleta*

Density

Differences in the size density were observed between the three stations during September 2016–October 2018. Stn A, on the estuary side, had the lowest density throughout the period, whereas Stns C (and C′) and D, located in the inner part, had one order of magnitude higher density than Stn A. Densities at the three stations were unstable and fluctuated under 4,000 ind/m^2 at Stn A, 40,000 ind/m^2 at Stn C, and 60,000 ind/m^2 at Stn D from September 2016 to July 2017. Although each station had density peaks at different times and the pattern of increase and decrease was different and not identical during the fluctuation period, *C.* aff. *teleta* almost disappeared in all three stations beginning from July or August 2017 to April or May 2018. Although the number of individuals was very low, such that the density indicated almost zero, it was never absent for that period. Environmental observations revealed that the period coincided with the period under diurnal hypoxia and low-redox-potential conditions during high water temperatures and followed a decrease in the water level below approximately 0.5 m (Figure 3D). However, after that period, individuals suddenly started to increase from May or June, and the peak densities at Stns A, C′, and D were observed to shift by 1 month each to June (reached up to 10,000 ind/m^2), July (55,000 ind/m^2), and August (30,000 ind/m^2), respectively, resulting in the recovery of abundance. The increase in daily maximum water level coincided with the timing of abundance increase.

In the three stations in Gamo Lagoon, population density decreased drastically after the tsunami that occurred following the Fukushima Earthquake in late November 2016. However, by January 2017, density rapidly recovered to almost above pre-tsunami levels in Stns C and D. Notably, the tsunami that occurred after the 2016 Fukushima Earthquake seemed to be have a partial impact; only the density at Stn C declined

FIGURE 8
Photographs **(A)** before and **(B)** after the reconstruction of the levee in Gamo Lagoon. **(A)** Photographed in April 2017 and **(B)** March 2021 (from Public Works Department, Miyagi Prefecture, March 2021).

FIGURE 9
Photograph after channel excavation was conducted in August 2018 (from Public Works Department, Miyagi Prefecture, March 2021).

immediately and temporarily, whereas no immediate decrease was observed at Stns A and D. However, in February 2017, density again declined dramatically to below that of the immediate post-tsunami period in Stns C and D. This period coincides with a period of decreased water depth. The population density then increased through May and June but then decreased toward July. Density did not increase even after the high-water-temperature period ended, probably because diurnal hypoxia frequently occurred and the redox potential remained severely low under low water levels because of the start of the levee reconstruction work. However, densities increased from June to August 2018, even under hypoxia and high redox conditions, but the daily maximum water level increased. It appeared that the daily maximum water level had a large impact on the population density of *C.* aff. *teleta* in the entire lagoon (Figure 10). This suggests that after the water level recovered and circulated normally, *C.* aff. *teleta* would interact with other stations through water flow.

Size frequency distribution

The size histogram data from three stations (A, C and C′, and D) were combined to analyze changes in the size frequency distribution of *C.* aff. *teleta* in Gamo Lagoon as a single water area (Figure 11). Smaller individuals with body width <0.5 mm appeared each month. Even during the periods of very low density from July 2017 to April 2018, the recruitment of a small number of juveniles and smaller individuals, with body width <0.5 mm, was observed at least in one station and in most months in all stations (Figures 5–7). Body width increased gradually from September to March or April 2016–2018 and gradually decreased from May to August in both 2017 and 2018 (Figure 11). From October 2016 to April 2017 and November 2017 to May 2018, individuals with >1 mm body width were observed. No individual with >1 mm body width was observed in July–September in all stations during the 3 years. More males than females appeared in many months in Gamo Lagoon. Although females with eggs in their coeloms were few during the entire period and at all stations, females were always present in at least one station in all months, except July, August, and December 2017 and March and April 2018. From November 2016 to February 2017, the minimum body width of mature individuals increased. Mature individuals with >1 mm body width appeared from November 2016 to April 2017; November 2017; and January, April, and May 2018. Smaller mature individuals with body width ≤0.5 mm also appeared in November 2016, September 2017, April 2018, and after June 2018, mainly during the high-water-temperature period. These results did not contradict a preliminary study of the life history and lifespan of *C.* aff. *teleta* in Gamo Lagoon by Kondoh (2017) based on laboratory breeding experiments. The previous study reported that at <15°C water temperature, *C.* aff. *teleta* spawn 55 d after settling, with multiple spawning cycles and a lifespan of approximately 3 months. Body size increased in this case. Mature females spawned eggs in 10 d, and spawning to

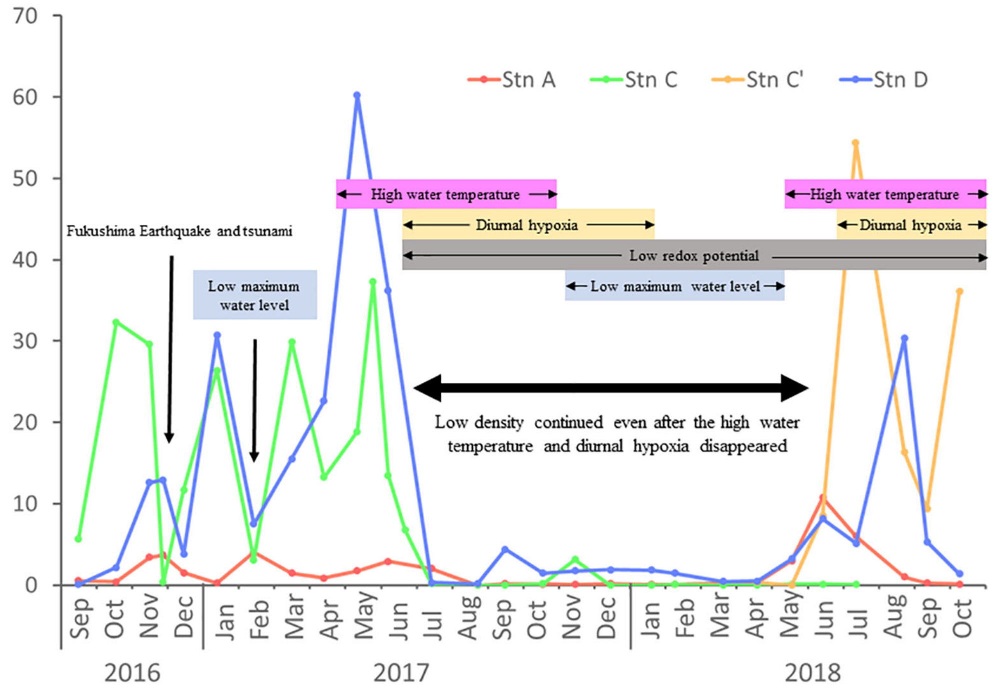

FIGURE 10
Summarizing *C.* aff. *teleta* density and environmental factors associated with water stagnation and circulation due to levee construction and channel excavation.

planktonic larval hatching took 2 weeks. During the high-water-temperature period, the size of the mature females was smaller and the lifespan seemed to be approximately 2 months after one spawning (Kondoh, 2017). Thus, during high water temperatures, they matured and spawned faster, and, during low water temperatures, their body size increased and they spawned many times.

A detailed body-width composition analysis was performed for each station. At Stn A, new recruitment was observed and abundance was maintained thereafter, although no females had appeared since April 2017. During this period, females were observed at Stns C (and C′) and D. In addition, despite the presence of females in the previous month, no new recruitment was seen in December 2016. This may indicate that the new recruitment at Stn A was largely dependent on planktonic larva recruitment from other stations. By contrast, at Stns C and D, new recruitment was observed in March 2017 although females were absent in the previous month. In February, females were observed only in Stn A, suggesting that planktonic larvae from Stn A were transferred to Stns C and D. At Stn D, although females were absent in July 2018, new recruitment was observed in August and density increased rapidly. No females were observed in Stns A, C, and D in July; however, females were observed in Stn C′. The new recruitment to Stn D may have been transferred by planktonic larvae from Stn C′. These results suggest that each station was supported by the transfer of planktonic larvae from other stations inside Gamo Lagoon.

At Stn D, from October 2016 to April 2017 and December 2017 to May 2018, individuals with body size >1 mm in width appeared for a long period of time. We believe that the presence of larger-sized individuals in Stn D during the low-temperature period contributed to the continuous increase in population.

Population density decreased dramatically in February 2017 despite the presence of mature individuals in January 2017 and new recruitment in February 2017. Similarly, although mature individuals were seen in September 2017 and many new recruitments were seen in October 2017, population density did not increase in October. The decrease in density was not likely due to the lack of new recruitment but rather other factors, such as environmental factors.

How to maintain a population in Gamo Lagoon

By comparing the change in the density and size frequency distribution of *C.* aff. *teleta* at multiple sampling stations inside the lagoon, we could examine how *C.* aff. *teleta* maintains its population in Gamo Lagoon, where the environment has been fluctuating and unstable due to restoration work.

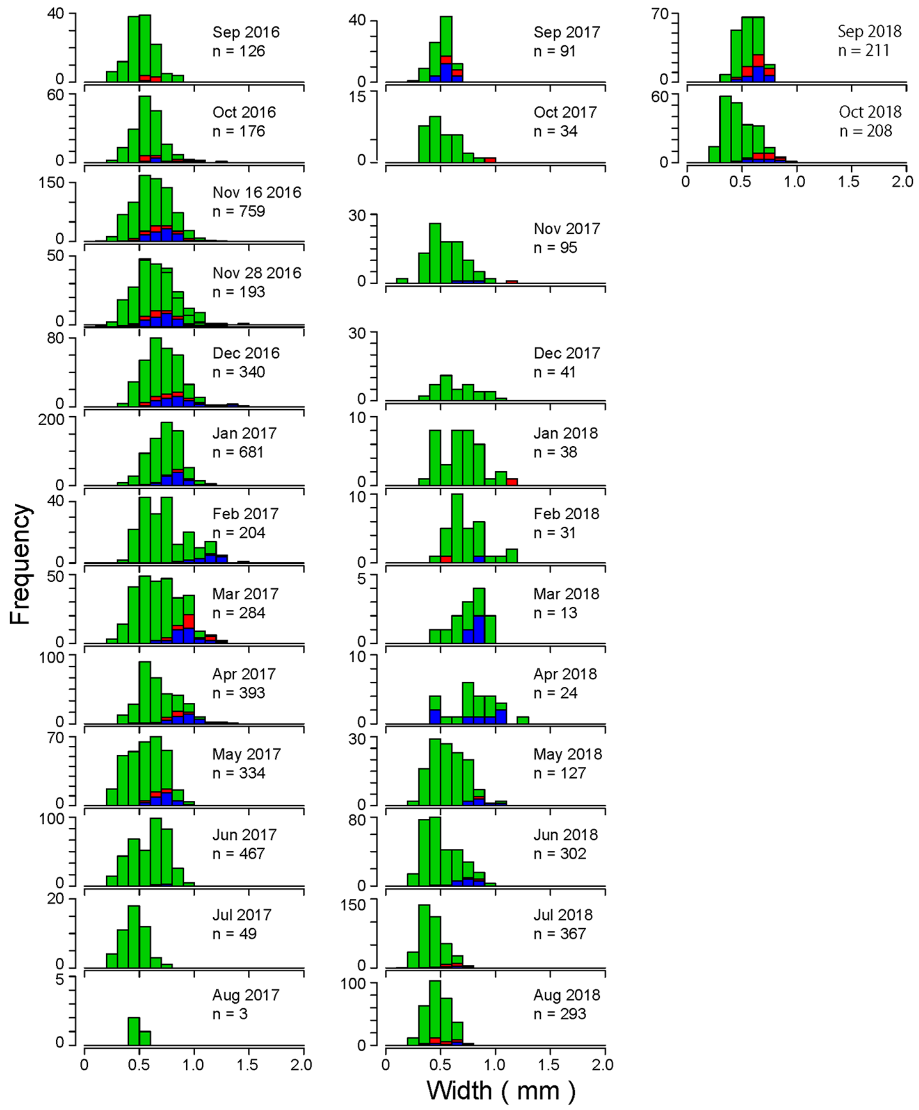

FIGURE 11
Size frequency distributions of the maximum width of the thoracic segment of total *C.* aff. *teleta* at the three stations in Gamo Lagoon from September 2016 to October 2018. Red: females, blue: males, green: immature individuals.

The Fukushima Earthquake and tsunami in November 2016 added to the initial disturbances following the 2011 Great East Japan Earthquake and tsunami in the lagoon. The reconstruction of the destroyed levee began in 2017. This resulted in destabilizing the sand sedimentation dynamics and changes in the water level. Although these changes were not as large as the disturbance caused by the 2011 Great East Japan Earthquake and tsunami (Kanaya et al., 2012; Kondoh et al., 2020), they likely had a significant impact on the population dynamics of *C.* aff. *teleta*.

We have discussed the significance of each station in Gamo Lagoon and how *C.* aff. *teleta* maintains its population at these stations by showing the environmental changes at each station and comparing and summarizing the characteristics of *C.* aff. *teleta* dynamics at each station. Stn A is located closer to the river, whereas Stns C and D are in the middle and inner parts of the lagoon, respectively. In Gamo Lagoon, only one levee exists at the riverside, which tends to stagnate topographically; the amount of organic matter increases as one moves into the inner part (Kanaya and Kikuchi, 2004). Population growth increases in organically rich muddy sediment (Kanaya et al., 2016), and, as shown in this study, densities at the inner parts of Stns C and D were higher than those at Stn A. Thus, Stns C and D—located in the inner part of the lagoon, with higher organic matter—are more suitable for increasing the density of *C.* aff. *teleta* than Stn A.

As eutrophication progresses, the bottom sediment becomes hypoxic and anaerobic metabolism becomes dominant (Hargrave, 2008), leading to the accumulation of toxic substances, such as free hydrogen sulfide (Gray et al., 2002). Microbial sulfate reduction, to release dissolved sulfides, is predominant in the anaerobic sediment layers of marine environments (Hargrave, 2008). Sulfides usually do not accumulate in the form of free hydrogen sulfide because they react quickly with metals, such as iron, and precipitate as insoluble sulfides; however, under excessive organic loading, sulfide formation exceeds the buffering capacity of iron in the sediment (Heijs et al., 1999), leading to the accumulation of free hydrogen sulfide (Marvin-DiPasquale and Capone, 1998). High hydrogen sulfide concentrations (up to 6.6 mmol/L of sediment) have been detected in Gamo Lagoon, especially in the inner part of the lagoon, with high water temperatures. These values are similar to or considerably higher than those of other eutrophic estuarine sediments (Gamenick et al., 1996; Marvin-DiPasquale and Capone, 1998; Sakai et al., 2012; Kanaya et al., 2015).

In Gamo Lagoon, the population growth of many opportunistic polychaetes, including *C.* aff. *teleta*, was shown to be inhibited by the excessive accumulation of sulfides under hypoxic conditions (Kanaya, 2014). During winter and spring, when sediment sulfide concentrations decrease, the number of opportunistic polychaetes increases rapidly (Kanaya et al., 2005; Kanaya and Kikuchi, 2011). Our findings revealed that in addition to hypoxia and high reduction conditions during the high-water-temperature period, hypoxia occurred frequently from November 2017 to March 2018 (Figure 3C). During this period, very small numbers of *C.* aff. *teleta* were observed from July 2017 to April 2018. Simultaneously, large numbers were observed after June 2018, when hypoxic conditions were also frequent. The daily maximum water level was higher after May 2018, and water level fluctuations increased in August. This may have led to a large increase in water conversion. Although sulfides in the sediments have been reported to a decrease in concentration as they are washed away after water conversion increases (Nielsen et al., 2003; Volkenborn, 2007), the reduction potential values remained low from June 2017 in this study.

We hypothesized that the formation of a large population only after June 2018, despite the same frequency of hypoxic and negative redox potential conditions, was due to differences in the water level. Therefore, the maximum water level must be maintained at a high level for enough water change so that the *C.* aff. *teleta* population can be maintained in the inner part. Moreover, our findings revealed that *C.* aff. *teleta* can maintain its population under low DO and redox conditions if water conversion is enough.

When the highest water level decreased in February 2017, a decrease in density was observed in Stns C and D, which are close to the water level observation point, whereas the opposite trend was observed in Stn A, which is close to the riverside. This suggests that the decrease in the water level has a direct impact on the population in the inner part of the lagoon. However, when the highest water level dropped again from November 2017 to May 2018, the density decreased at Stn A as well. Considering that Stn A maintains its population through larval transfers from other stations, the failure to increase densities at Stns C and D due to the drop in the water level for a long period may have affected population density at Stn A. In addition, since June 2018, *C.* aff. *teleta* could increase in abundance throughout Gamo Lagoon, although the minimum water level was lower and the maximum water level was higher. These findings suggest that the maximum and not minimum water level affects population construction.

The trend of the *C.* aff. *teleta* population at each station had the following characteristics: at Stn A, the habitat was maintained by relying heavily on larval transfers from other stations; at Stn C, the habitat was susceptible to the lowering of the water level in the lagoon, and the more time the bottom sediment had to dry out, the more difficult it became for *C.* aff. *teleta* to inhabit the low water levels. However, despite a period of almost no habitat for approximately 11 months in the lagoon, high densities were again constructed at Stn C′ due to the transfer of planktonic larvae from other stations. Stn D showed the highest density between the three stations even after the summer of 2017, when the density was low throughout. By contrast, new recruitment also occurred due to transfers from other stations. Thus, each station showed different characteristics in the density and dynamics of *C.* aff. *teleta* in Gamo Lagoon.

New recruitments were seen in many months in all stations, and there were periods when new recruitments were seen despite the absence of females nearby, indicating that they were largely supported by the supply of planktonic larvae from other stations. Although the density varied between stations, at least one station had females during the period, suggesting that each station supplied planktonic larvae to the other and that they were interdependent and maintained as a single population throughout the Gamo Lagoon area. Therefore, it is important for populations to interact to maintain the *C.* aff. *teleta* population in Gamo Lagoon.

Due to the original topography of Gamo Lagoon, water tends to stagnate in the inner side of the lagoon and becomes a hypoxic and reducing environment under high water temperatures. In this study, we examined how *C.* aff. *teleta*, a capitellid polychaete that maintains its population in such an environment, was impacted during the 2 years when restoration work was underway. During the construction of a new levee, the balance of sedimentation dynamics was disrupted, the central part dried up, and water exchange with the riverside was lost, making the inner part isolated. This disrupted the supply of larvae over the lagoon, and the density decreased drastically and continued to be low. Later, an increase in the daily maximum water level initiated water to flow between the inner part and the riverside, and the density recovered. Thus, *C.* aff. *teleta* requires both environments—the inner part and the riverside of the lagoon—to maintain its population and that it is necessary to allow the water bodies to interact with each other.

The ecological adaptation of *C.* aff. *teleta* in Gamo Lagoon can be summarized as follows: *C.* aff. *teleta* prefers to live in the middle and innermost parts, namely, stations C and D, respectively, which are organic-rich environments. However, the innermost parts have a high risk of hypoxia and a low redox potential. When the population declines due to deterioration, it recovers by recruiting floating larvae from the riverside station A, which is not a favorable habitat; therefore, only a small number is maintained. In this lagoon, the presence of stations in different environments, both at the innermost part and the riverside, may be considered necessary to maintain the population in the lagoon as a whole, because both sides supply each other with planktonic larvae. Thus, water flow, which connects different environmental stations, is the most important factor for the maintenance of *C.* aff. *teleta* populations.

Many macrobenthos, including opportunistic polychaete species such as *C.* aff. *teleta*, have been affected by human activities that have altered their habitats, such as water flow and drought, but have continued to maintain their populations. It is important to understand the ecological characteristics of these animals, minimize the impact of habitat change, and maintain a sustainable marine ecosystem and biodiversity.

Data availability statement

The raw data supporting the conclusions of this article will be made available by the authors, if necessary.

Author contributions

WS-O conceived and designed the research. AH generated and analysed the data. WS-O wrote the first draft of the manuscript. All authors contributed to the article and approved the submitted version.

Funding

This study was supported by a grant from the Tohoku Ecosystem-Associated Marine Sciences (TEAMS) research program of the Ministry of Education, Culture, Sports, Science and Technology (MEXT). This study was partially supported by a research grant from JSPS KAKENHI Grant Number: JP15K07540, JP18K05777) to Waka Sato-Okoshi.

Acknowledgments

We are grateful to the members of the Laboratory of Biological Oceanography, Graduate School of Agricultural Science, Tohoku University, for their cooperation and assistance during field observations. Thanks especially to Dr. Tomohiko Kondoh for his continuous research advice and to Akane Nishioka for her cooperation in creating figures. We thank Miyagi Prefecture for their cooperation in providing us with an overview of the Gamo restoration works and photographs during the work period.

Conflict of interest

The authors declare that the research was conducted in the absence of any commercial or financial relationships that could be construed as a potential conflict of interest.

Publisher's note

References

Blake, J. A. (2009). Redescription of *Capitella capitata* (Fabricius) from West Greenland and designation of a neotype (Polychaeta, capitellidae). *Zoosymposia* 2, 55–80. doi: 10.11646/zoosymposia.2.1.7

Blake, J. A., Grassle, J. P., and Eckelbarge, K. J. (2009). *Capitella teleta*, a new species designation for the opportunistic and experimental *Capitella* sp. I, with a review of the literature for confirmed records. *Zoosymposia* 2, 25–53. doi: 10.11646/zoosymposia.2.1.6

Chareonpanich, C., Montani, S., Tsutsumi, H., and Matsuoka, S. (1993). Modification of chemical characteristics of organically enriched sediment by *Capitella* sp. I. *Mar. Poll. Bull.* 26, 375–379. doi: 10.1016/0025-326X(93)90184-L

Diaz, R. J., and Rosenberg, R. (1995). Marine benthic hypoxia: A review of its ecological effects and the behavioural responses of benthic macrofauna. oceanogr. *Mar. Biol.* 3, 245–303.

Eckelbarger, K. J., and Grassle, J. P. (1983). Ultrastructral differences in the eggs and ovarian follicle cells of *Capitella* (Polychaeta) sibling species. *Biol. Bull.* 165, 379–393. doi: 10.2307/1541203

Fabricius, O. (1780). Fauna Groenlandica, systematice sistens animalia groenlandiae occidentalis hactenus indagata, quoad nomen specificium, triviale, vernaculumque, synonyma auctorum plurimum, descriptionem, locum, victum, generationem, mores, usum capturamque singuli, pro ut detegendi occasio fuit, maximaque parte secundum proprias observationes.

Gamenick, I., Jahn, A., Vopel, K., and Giere, O. (1996). Hypoxia and sulphide as structuring factors in a macrozoobenthic community on the Baltic Sea shore: Colonization studies and tolerance experiments. *Mar. Poll. Bull.* 114, 73–85.

Gamenick, I., Vismann, B., Grieshaber, M. K., and Giere, O. (1998). Ecophysiological differentiation of *Capitella capitata* (Polychaeta). Sibling species from different sulfidic habitats. *Mar. Ecol. Prog. Ser.* 175, 155–166. doi: 10.3354/meps175155

Grassle, J. P., and Grassle, J. F. (1976). Sibling species in the marine pollution indicator *Capitella* (Polychaeta). *Science* 192, 567–569. doi: 10.1126/science.1257794

Gray, J. S., Wu, R. S., and Or, Y. Y. (2002). Effects of hypoxia and organic enrichment on the coastal marine environment. *Mar. Poll. Bull.* 238, 249–279. doi: 10.3354/meps238249

Hargrave, B. T. (2008). Towards a classification of organic enrichment in marine sediments based on biogeochemical indicators. *Mar. Poll. Bull.* 5, 810–824. doi: 10.1016/j.marpolbul.2008.02.006

Hartman, O. (1959). Capitellidae and Nereidae (marine annelids) from the Gulf side of Florida with a review of freshwater Nereidae. *Bull. Mar Sci. Gulf Caribbean.* 9, 153–168.

Heijs, S. K., Jonhers, H. M., Gemerden, H. V., and Schaub, B. E. M. (1999). The buffering capacity towards free sulphide in sediments of a coastal lagoon (Bassin d' arcachon, France) -the relative importance of chemical and biological processes. *Estuar. Coast. Shelf. Sci.* 49, 21–35. doi: 10.1006/ecss.1999.0482

Honma, Y., Kitami, T., and Ito, S. (1974). Fauna of lake kamo-ko, sado island in the Japan Sea (a preliminary report). *Proc. Jap. Soc Syst. Zool.* 10, 63–73.

Ide, S., Baltay, A., and Beroza, G. C. (2011). Shallow dynamic overshoot and energetic deep rupture in the 2011 mw 9.0 tohoku-oki earthquake. *Science* 332, 1426–1429. doi: 10.1126/science.1207020

Imajima, M. (2015). *Annelida, Polychaeta IV* Vol. 332 (Tokyo: Seibutsu Kenkyusha).

Imajima, M., and Hartman, O. (1964). "The polychaetous annelids of Japan," in *Allan Hancock Found publications occasional paper* California, USA: University of Southern California, vol. 26, 1–452.

Kanaya, G. (2014). Recolonization of macrozoobenthos on defaunated sediments in a hypertrophic brackish lagoon: Effects of sulfide removal and sediment grain size. *Mar. Environ. Res.* 95, 81–88. doi: 10.1016/j.marenvres.2013.12.014

Kanaya, G., and Kikuchi, E. (2004). Relationships between sediment chemical buffering capacity and H2S accumulation: Comparative study in two temperate estuarine brackish lagoons. *Hydrobiologia* 528, 187–199. doi: 10.1007/s10750-004-2342-8

Kanaya, G., and Kikuchi, E. (2011). Infuences of anthropogenic eutrophication on estuarine benthic ecosystems. *Chikyu Kankyo* 16, 33–44.

Kanaya, G., Maki, H., Suzuki, T., Sato-Okoshi, W., and Kikuchi, E. (2014). Tsunami-induced changes in a shallow brackish lagoon ecosystem (Gamo lagoon) in Sendai bay, Japan. *Glob. Environ. Res.* 18, 35–46.

Kanaya, G., Nobata, E., Toya, T., and Kikuchi, E. (2005). Effects of different feeding habits of three bivalve species on sediment characteristics and benthic diatom abundance. *Mar. Ecol. Prog. Ser.* 229, 67–78. doi: 10.3354/meps299067

Kanaya, G., Suzuki, T., and Kikuchi, E. (2015). Impacts of the 2011 tsunami on sediment characteristics and macrozoobenthic assemblages in a shallow eutrophic lagoon, Sendai bay, Japan. *PloS One* 10 (8), e0135125. doi: 10.1371/journal.pone.0135125

Kanaya, G., Suzuki, T., Maki, H., Nakamura, Y., Miyajima, Y., and Kikuchi, E. (2012). Effects of the 2011 tsunami on the topography, vegetation, and macrobenthic fauna in gamo lagoon, Japan. *Jap. J. Benthol.* 67, 20–32.

Kanaya, G., Uehara, T., and Kikuchi, E. (2016). Effects of sedimentary sulfide on community structure, population dynamics, and colonization depth of macrozoobenthos in organic-rich estuarine sediments. *Mar. Poll. Bull.* 109, 393–401. doi: 10.1016/j.marpolbul.2016.05.043

Kinoshita, K., Tamaki, S., Yoshioka, M., Srithonguthai, S., Kunihiro, T., Hama, D., et al. (2008). Bioremediation of organically enriched sediment deposited below fish farms with artificially masscultured colonies of deposit-feeding polychaete *Capitella* sp. I. *Fish. Sci.* 74, 77–87. doi: 10.1111/j.1444-2906.2007.01498.x

Kitamori, R. (1960). The relation between the distribution of genus *Capitella*, polychaetous annelids, and pollution. *Bull. Naikai. Reg. Fish. Res. Lab.* 87, 1–10.

Kondoh, T. (2017). *Benthic community dynamics and life history strategies of dominant species in gamo lagoon (Miyagi prefecture, Japan) after the great East Japan earthquake and tsunami disturbance* (Sendai: Tohoku University).

Kondoh, T., Nakayama, G., and Sato-Okoshi, W. (2020). "Preliminary report of impacts of the 2011 earthquake and tsunami and subsequent events on macrobenthic community in a shallow brackish lagoon in Sendai bay, Japan," in *Evolution of marine coastal ecosystems under the pressure of global changes*, Ed. Ceccaldi, H.-J., Henocque, Y., Komatsu, T., Prouzet, P., Sautour, B., Yoshida, J., et al (Switzerland AG: Springer Nature), 163–172.

Langerhans, P. (1880). Die Wurmfauna von Madeira. III. *Z. für wissenschaftliche Zoologie.* 34, 87–143.

Linke-Gamenick, I., Forbes, V. E., and Méndez, N. (2000). Effect of chronic fluoranthene exposure on sibling species of *Capitella* with different development modes. *Mar. Ecol. Prog. Ser.* 203, 191–203. doi: 10.3354/meps203191

Magalhães, F., and Bailey-Brock, J. H. (2012). Capitellidae grube 1862 (Annelida: Polychaeta) from the Hawaiian islands with description of two new species. *Zootaxa* 3581, 1–52. doi: 10.11646/zootaxa.3581.1.1

Marvin-DiPasquale, M. C., and Capone, D. G. (1998). Benthic sulfate reduction along the Chesapeake bay central channel. i. spatial trends and controls. *Mar. Ecol. Prog. Ser.* 168, 213–228. doi: 10.3354/meps168213

Méndez, N. (2002). Experimental evidence of polymorphysm of sexual development in *Capitella* sp. b (Polychaeta: Capitellidae) from Barcelona, Spain. *Sci. Mar.* 66, 103–110. doi: 10.3989/scimar.2002.66n2103

Méndez, N. (2006). Life cycle of *Capitella* sp. y (Polychaeta: Capitellidae) from estero del yugo, mazatlán, Mexico. *J. Mar. Biol. Ass. UK* 86, 263–369. doi: 10.1017/S0025315406013117

Muto, N., and Kim, K. S. (1986). Experimental studies of factors influencing the value of ORP——Water temperature, DO, H_2S and pH——. *Jap. J. Water pollut. Res.* 9, 661–667. doi: 10.2965/jswe1978.9.661

Nielsen, O. I., Kristensen, E., and Holmer, M. (2003). Impact of *Arenicola marina* (Polychaeta) on sediment sulfur dynamics. *Aquat. Microb. Ecol.* 33, 95–105. doi: 10.3354/ame033095

Nishi, E., Ueda, L., Sakamoto, A., Sugihara, N., Shimosako, K., and Sanada, S. (2010). Benthos fauna of artificially created tidal flats in Yokohama port, Tokyo bay. *Nat. Hist. Rep. Kanagawa.* 31, 29–33.

Ozawa, S., Nishimura, T., Suito, H., Kobayashi, T., Tobita, M., and Imakiire, T. (2011). Coseismic and postseismic slip of the 2011 magnitude-9 tohoku-oki earthquake. *Nature* 475, 373–376. doi: 10.1038/nature10227

Public Works Department, Miyagi Prefecture (2021). *Environmental consideration records of the reconstruction works on the rivers and coasts in Miyagi after the Great East Japan Earthquake/tsunami* (Miyagi Prefecture: Public Works Department), 344.

Rouse, G. W., and Pleijel, F. (2001). *Polycheates* (New York: Oxford University Press).

Sakai, S., Nakaya, M., Sampei, Y., Dettman, D. L., and Takayasu, K. (2012). Hydrogen sulfide and organic carbon at the sediment-water interface in coastal brackish lake nakaumi, SW Japan. *Environ. Earth Sci.* 7, 1999–2006.

Silva, C. F., Shimabukuro, M., Alfaro-Lucas, J. M., Fujiwara, Y., Sumida, P. Y. G., and Amaral, A. C. Z. (2016). A new *Capitella* polychaete worm (Annelida: Capitellidae) living inside whale bones in the abyssal south Atlantic. *Deep-Sea. Res. I.* 108, 23–31. doi: 10.1016/j.dsr.2015.12.004

Tanaka, H., Mitobe, Y., and Hoang, V. C. (2016). Estuarine morphological changes due to the 2015 kanto-tohoku heavy rainfall and their subsequent recovery. *Tohoku. J. Natl. Disaster. Sci.* 52, 67–72.

Tomioka, S., Kondoh, T., Sato-Okoshi, W., Ito, K., and Kajihara, H. (2016). Cosmopolitan or cryptic species? A case study of *Capitella teleta* (Annelida: Capitellidae). *Zool. Sci.* 33, 545–555. doi: 10.2108/zs160059

Tsutsumi, H. (1987). Population dynamics of *Capitella capitata* (Polychaeta; capitellidae) in an organically polluted cove. *Mar. Ecol. Prog. Ser.* 36, 139–149. doi: 10.3354/meps036139

Tsutsumi, H. (1990). Population persistence of *Capitella* sp. (Polychaeta; capitellidae) on a mud flat subject to environmental disturbance by organic enrichment. *Mar. Ecol. Prog. Ser.* 63, 147–156. doi: 10.3354/meps063147

Tsutsumi, H. (2005). Production of planktonic and non-planktonic larvae in a single brood of *Capitella* sp. I and its implications for population persistence in disturbed environment due to organic enrichment of the sediments. *Benthos. Res.* 60, 17–24. doi: 10.5179/benthos1996.60.1_17

Tsutsumi, H., and Kikuchi, T. (1984). Study of the life history of *Capitella capitata* (Polychaeta: Capitellidae) in amakusa, south Japan including a comparison with other geographical regions. *Mar. Biol.* 80, 315–321. doi: 10.1007/BF00392827

Tsutsumi, H., Kikuchi, T., Tanaka, M., Higashi, T., Imasaka, K., and Miyazaki, M. (1991). Benthic fauna succession in a cove organically polluted by fish farming. *Mar. Pollut. Bull.* 23, 233–238.

Tsutsumi, H., Kinoshita, K., Srithongouthai, S., Sato, A., Nagata, S., Inoue, A., et al. (2005). Treatment of the organically enriched sediment below the fish farm with the biological activities of artificially mass-cultured colonies of a small deposit feeding polychaete, *Capitella* sp. I. *Benthos. Res.* 60, 25–38. doi: 10.5179/benthos1996.60.1_25

Tsutsumi, H., and Montani, S. (1993). Utilization of biological activities of capitellid polychaete for treatment of "hedoro" (organically enriched sediment) deposited on the marine bottom below fish net pen culture. *Nippon. Suisan. Gakkaishi.* 59, 1343–1347. doi: 10.2331/suisan.59.1343

Ueno, S., and Yamamoto, G. (1982). Physiological tolerance in the polychaetous annelids *Capitella capitata* and *Paraprionospio pinnata*. *Benthos Res.* 23, 60–68.

Volkenborn, N. (2007). Effects of bioturbation and bio irrigation by lugworms (*Arenicola marina*) on physical and chemical sediment properties and implications for intertidal habitat succession. *Estuar. Coast. Shelf. Sci.* 74, 331–343. doi: 10.1016/j.ecss.2007.05.001

Warren, L. M. (1991). Problems in capitellid taxonomy. the genera *Capitella*, *Capitomastus*, and *Capitellides* (Polychaeta). *Ophelia* Suppl 5, 272–282.

Wilson, D. S. (1992). Complex interactions in metacommunities, with implications for biodiversity and higher levels of selection. *Ecology* 73, 1984–2000. doi: 10.2307/1941449

Frontiers in Marine Science

TYPE Original Research
PUBLISHED 21 November 2022
DOI 10.3389/fmars.2022.979212

EDITED BY
Victoria Louise Georgia Todd,
Ocean Science Consulting Ltd.,
United Kingdom

REVIEWED BY
Holden Earl Harris,
University of Florida, United States
Greg Sass,
Wisconsin Department of Natural
Resources, United States
Tom Laidig,
National Marine Fisheries Service
(NOAA), United States
Sean Van Elden,
University of Western Australia,
Australia

*CORRESPONDENCE
Tiffany L. Sih
t.sih@deakin.edu.au

SPECIALTY SECTION
This article was submitted to
Marine Ecosystem Ecology,
a section of the journal
Frontiers in Marine Science

RECEIVED 27 June 2022
ACCEPTED 21 October 2022
PUBLISHED 21 November 2022

CITATION
Sih TL, Cure K, Yilmaz IN, McLean D
and Macreadie PI (2022) Marine life
and fisheries around offshore oil and
gas structures in southeastern
Australia and possible consequences
for decommissioning.
Front. Mar. Sci. 9:979212.
doi: 10.3389/fmars.2022.979212

Marine life and fisheries around offshore oil and gas structures in southeastern Australia and possible consequences for decommissioning

Tiffany L. Sih[1]*, Katherine Cure[2,3], I. Noyan Yilmaz[1], Dianne McLean[2,3] and Peter I. Macreadie[1]

[1]Centre for Integrative Ecology, School of Life and Environmental Sciences, Deakin University, Burwood, VIC, Australia, [2]Australian Institute of Marine Science, Indian Ocean Marine Research Centre, Crawley, WA, Australia, [3]Oceans Institute, The University of Western Australia, Crawley, WA, Australia

The Gippsland Basin is the location of Australia's oldest offshore oil and gas (O&G) structures, with hydrocarbon production beginning in the 1960s. The Bass Strait flows over this area with fisheries providing seafood for the major population centers of Melbourne, Sydney and beyond. Since Australia's maritime legislation restricts activities to outside of 500 meters from O&G structures as a security exclusion zone, these O&G structures may serve as *de facto* marine protected areas that may have spillover effects to local fisheries. Therefore, it is critical to understand the habitat value of O&G infrastructure to marine life in the Bass Strait and whether decommissioning of these structures affect local marine ecosystems and fisheries. We analyzed industry-collected remotely operated vehicle (ROV) imagery from 2008-2018 and compared this data with reported catch data from fishing vessels operating in this region collected by the Australian Fisheries Management Authority (AFMA) from 2008-2018. We assessed species richness and relative abundance on two platforms and two pipelines and compared the species composition with retained catch reported by commercial fishers operating in Commonwealth fisheries. We found diverse communities of fishes and invertebrates around O&G structures, with a different subset of species inhabiting pipelines than platforms. We found little overlap between the species that were targeted by commercial fishers and those found around O&G structures (10% overlap), however, species composition data from fisheries often groups species making the data coarse and under-representative of true species diversity. Fishery-independent data from ROV imagery or other methods greatly augments our understanding of deepwater marine communities, including those around O&G structures. Combining data sources provides a holistic look at these novel ecosystems and provides better insight into future decommissioning scenarios.

KEYWORDS

oil & gas infrastructure, fisheries, anthropogenic structures, marine communities, temperate marine ecosystems, remotely operated vehicle (ROV)

1 Introduction

Worldwide, as offshore oil and gas (O&G) structures reach the end of their intended use, decommissioning discussions consider what to do with these physical structures and what the resulting impact may be on the surrounding marine environment. O&G structures are analogous to ‘artificial reefs’, which may create habitat and feeding opportunities for marine communities where those are often limited or in decline (Macreadie et al., 2011; Fowler and Booth, 2012; Bull and Love, 2019). Artificial reefs may provide habitat for fishes, invertebrates and sessile biota, and serve a purpose for biodiversity or fisheries enhancement *via* habitat rehabilitation or habitat augmentation (Becker et al., 2017; Paxton et al., 2020), though O&G structures were not expressly built for these purposes. Decommissioning decisions on these structures in Australian State and Commonwealth waters is governed by the National Offshore Petroleum Safety and Environmental Management Authority (NOPSEMA) *via* an Offshore Petroleum and Greenhouse Gas Storage Act 2006 (OPGGS Act, 6.4 Restoration of the Environment). A titleholder may only leave O&G infrastructure in place if it can be demonstrated that this delivers equal or better environmental and safety outcomes compared to complete removal and that all impacts and risks are reduced to ‘as low as reasonably practicable’ (ALARP; Australian Government, 2018) and has an exemption through an accepted environment plan. Such a decision requires an understanding of the potential habitat value of a structure and its associations with fauna, as well as knowledge of the risks posed to marine ecosystems by different decommissioning options. With many countries entering an era of large-scale decommissioning, this agenda is driving focused marine research activities around the globe (Shaw et al., 2018; Sommer et al., 2018; Birchenough and Degraer, 2020; Fowler et al., 2020).

Better understanding of marine communities on O&G structures, as well as their surrounding ecosystems, are key for informing the decommissioning agenda. Further linking this information with data on local industries such as fisheries, that may benefit from spillover effects of existing infrastructure, adds key value to the decision-making process. Gippsland Basin O&G structures are placed among Australia’s ‘Great Southern Reef’ (Great Southern Reef (GSR), 2021), a series of interconnected temperate rocky reefs that are understudied yet likely highly valuable for fishery production and biodiversity. Australia’s unique marine ecosystems exhibit high rates of endemism in its flora and fauna (Australian Biological Resources Study (ABRS), 2020) and this region is also biologically and geographically distinct. More than 100 species of teleosts (bony fishes) and elasmobranchs (sharks and rays) are commercially caught in south-east Australian fisheries (Williams and Bax, 2001; Emery et al., 2021), which have been active since the early 1900s and where fishing effort has continuously intensified (Novaglio et al., 2018). Currently, the South-east Australian fishery is the largest fishery for benthic or near-bottom ‘groundfishes’ and the most important Australian fishery in terms of the domestic seafood market (Williams and Bax, 2001). The potential contributions of O&G structures to these fisheries have not yet been evaluated.

Presently, no published research exists that documents the ecological role or habitat value of O&G infrastructure for comprehensive marine communities in the Bass Strait region of Australia. Two previous research studies have investigated the role of these offshore structures specifically to ichthyoplankton (Neira, 2005) and fur seal populations (Arnould et al., 2015) but there is a direct need to understand whether decommissioning might influence the larger ecosystem. Broader research efforts have been limited due to two primary reasons: 1) historical scientific data only existed in industry-held reports and 2) 500-m exclusion zones around platforms have limited access to scientists and other sectors (e.g., fishing, shipping). During routine inspection and maintenance activities, Remotely Operated Vehicles (ROVs) collect imagery of O&G structures and their associated underwater communities (e.g., fish, invertebrates, mammals). The imagery and metadata that is collected can be a tremendous (and under-utilized) resource for scientists (Macreadie et al., 2018). When O&G infrastructure nears its end-of-use, such information is critical for understanding the consequences of different O&G decommissioning scenarios on associated marine life, and potentially more broadly to ocean health.

Offshore O&G platforms are often the only dominant underwater hard structure in the area where they are positioned, providing unique habitats for marine species. Most of these structures are large and provide vertically connected habitats that span the water column from the surface to the seabed. A 70-m structure is analogous to a > 20-story building on land and may result in micro- or macro-level changes to surrounding biological or oceanographic processes (Hastings et al., 1976; Love et al., 2000; Hernandez et al., 2003). Detailed analysis of platform ecology can provide greater insight into whether these structures provide ecological value to fish and invertebrate species. For example, O&G structures exhibit non-uniform distributions of marine communities throughout a platform’s structure (Ajemian et al., 2015; McLean et al., 2019) often with depth-driven differences in fish (e.g., North Sea, Todd et al., 2018; North-west Australia, McLean et al., 2019) and invertebrate assemblages (e.g., North Sea, van der Stap et al., 2016; North-west Australia, Thomson et al., 2018). Assessing temporal change in O&G communities colonizing structures is also important to improve understanding of ecological succession of anthropogenic structures, compared to more natural habitats. Such knowledge may inform decisions regarding the maintenance, removal or retention of structures and provide insight into potential future installations (Bull and Love, 2019). In one case study, industry ROV surveys indicated that marine communities in subsea infrastructures undergo rapid succession, with a 'first wave' of colonization by fish and invertebrates often occurring within a week (Todd et al., 2020b). What these structures represent in terms of 'attracting' marine life or 'producing' benefits for local fisheries and marine ecosystems has to date been treated largely on a case-by-case basis, with few widespread geographic (i.e., with neighboring habitats, among structures within a region) or temporal comparisons (e.g., Love et al., 2019). Describing the marine communities is only the first step, but essential, to understanding the ecological and successional role of infrastructure communities.

Pipelines are important conduits in O&G infrastructure and may have different habitat value as pipelines are laid on the seabed (or in trenches) and can become partially or fully buried in the sediment over time. Industry typically use ROVs or Autonomous Underwater Vehicles (AUVs), to conduct visual inspections of pipelines or perform specific tasks such as monitoring free-spans/anodes. Pipelines can vary in diameter from ~12 cm to > 1 m and in length from meters to > 1000 km, they can provide attachment points and available habitat where little hard substrate exists (e.g., sandy environments) and may be important structures to fish and local fisheries (McLean et al., 2020b; Bond et al., 2021). Pipelines may provide food sources and refuges for fish and invertebrates and are often characterized by high abundances of larval fishes (McLean et al., 2017; McLean et al., 2021b). Commercially important fish species can occur in higher abundance and biomass along pipelines than in nearby natural environments (Bond et al., 2018b, Bond et al., 2018b; McLean et al., 2021b). Differences in pipeline position (i.e., how much is buried and how much is exposed) and in the complexity and extent of colonizing benthic communities (marine growth) along the pipeline may account for differences in species presence or abundance. In North-west Australia for example, the high proportion of sponges along a pipeline was correlated with high abundances of Moses snapper (*Lutjanus russellii*, McLean et al., 2020b).

This research project used fishery data and historical ROV footage to address the question: What marine communities associate with O&G infrastructure in the Bass Strait, and how might decommissioning influence these communities? Our specific aims were to investigate: 1) broad patterns in fish, invertebrate and benthic communities for the region using industry-collected fishery data between 2008-2018 and 2) similarities and differences in fish and invertebrate communities among two platforms and two pipelines. This research is novel in combining two sets of industry-collected data for a region in southeastern Australia that has a long history of anthropogenic use. This information may be important for assessing the ecological value of O&G structures in temperate environments considering Australia's unique marine taxa.

2 Materials and methods

2.1 Study area

In the Bass Strait region of southeastern Australia, the Gippsland Basin is an important region for Australian industries including energy (Department of Jobs, Precincts and Regions (DJPR), 2021) and fisheries. It includes an extensive network of O&G infrastructure, operated by Esso website, on behalf of joint ventures, with the first O&G infrastructure installed in the late 1960s (Esso Australia, 2022). The O&G infrastructure operated by Esso in the Gippsland Basin includes 19 platforms and about 800 km of pipelines, with data from two platforms and two pipelines used in this study (Figure 1). There is other O&G infrastructure in the Gippsland Basin that is managed by other operators.

2.2 Fishery data

To provide a marine ecological context, we also requested commercial fishing data for the region from the same period (2008-2018). The Australian Fisheries Management Authority (AFMA) collects information on species retained and discarded from all Commonwealth commercial fishing vessels as part of the agreement to participate in those fisheries. This information, compiled across multiple years, was used to describe fleet-wide fishing behaviors, including the composition of target species going to local markets and the spatial distribution of fishing effort in areas neighboring the O&G infrastructure. Australia's Commonwealth fisheries integrate data collection and adaptive management practices (Commonwealth Scientific and Industrial Research Organisation (CSIRO), 2014; Fisheries Research and Development Corporation (FRDC), 2020), however, there are few sources of fishery-independent data.

The Australian Fisheries Management Authority provided reported data from 1 January 2008-31 December 2018 covering the area between latitudes 147.210255 to 148.703841°S and longitudes 37.782502 to 38.650937°E. This created an area around the offshore structures to help understand the spatial distribution and intensity of localised fishing effort. Commonwealth fisheries operate outside of state waters (3 nm from the coastline). Data included the date, location, participating fishery and retained and discarded catch expressed in estimated kilograms (kg) by species or species group. Taxa are reported as a species or lowest grouping, which can vary from phyla (e.g., sponges, Phylum Porifera), family (e.g., flatheads, Platycephalidae), and order (e.g., squids, Order Teuthoidea). Reports are submitted after each trip and this information contributes to fisheries management (Australian Fisheries Management Authority (AFMA), 2022).

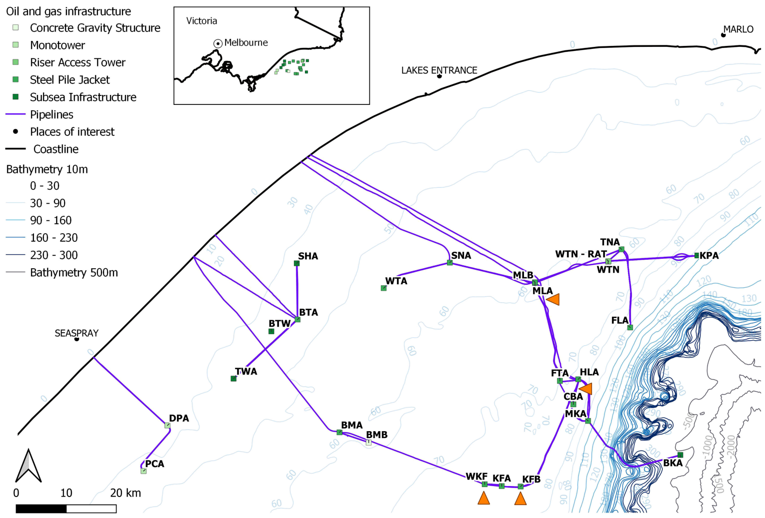

FIGURE 1
Map of Esso Australia Resources Pty Ltd (EARPL)-operated oil and gas structures in the Gippsland Basin of the Bass Strait region, south-east Australia. An inset map shows the location of the structures along the coastline east of Melbourne in the state of Victoria. Each platform is identified with the structure type. The platforms and pipelines included in this study are indicated by the orange triangles. Map created in QGIS.

2.2.1 Fishery data analysis

Fishing data was checked for quality and individual species were allocated to family for some comparisons. We then analyzed the reported catch information to understand the intensity and distribution of fishing effort around the O&G structures.

Cumulative retained and discarded catch was summed annually to understand the intensity of fishing effort over the ten-year period. The retained catch over ten years was summed for the 12 most abundantly caught families. Cumulative catch of the most important 30 fishery species or species groups was also summarized.

Spatial distribution of fishing effort was mapped by the six participating fisheries with heat maps presenting the areas of greatest to lowest retained catch. To represent the fishing activities fairly precisely, each pixel represented an area 500 m x 500 m with a radius for the quartic kernel density estimate of 1000 m. Maps were created in QGIS (QGIS.org, 2022).

2.3 ROV data

We screened imagery of many offshore assets to determine the quality and coverage of existing videos obtained between 2008 – 2018 to describe marine communities in the Bass Strait region. The assessment first established the utility of historical industry-collected ROV video and was used to inform the planning of future marine ecological surveys to address knowledge gaps, re-visit areas of interest, and/or refine ROV surveys for collection of more quantitative scientific information (e.g., McLean et al., 2019). Through this screening process we identified specific assets with good imagery coverage and quality for further assessment. We focused on two platforms (steel pile jackets) located in similar depths and distances from shore (West Kingfish-WKF and Kingfish B-KFB), and two pipelines (CBA300 and MLA100). These structures were selected from other platforms and pipelines for having better quality ROV imagery and more comprehensive coverage of each structure. Since industry ROVs were not collecting data with ecological sampling design in mind, there were some limitations to more robust sampling with the available imagery. For instance, video quality differed between years, not all structures and pipelines were sampled every year, and ROV swim distances from structures and pipelines varied considerably, altering species composition visible from the imagery (more details in imagery selection below).

2.3.1 Platform jackets

Two steel pile jackets, West Kingfish (WKF) and Kingfish B (KFB), are platforms similar in position (water depth and location). KFB became operational in November 1971 and WKF in December 1982. As such, they were 46 and 36 years of age at the time of ROV survey (2015 imagery for KFB and 2017 imagery for WKF). Both platforms are lit at night with a 500-m exclusion zone to all ships as a minimum safety precaution (Kashubsky and Morrison 2013). KFB is located in 78 m and WKF in 76 m of water depth. The structures are connected with Kingfish A in between, with WKF slightly further inshore (72 km) and KFB further offshore (78 km from shore, Figure 1). Both platforms supply crude oil but have some differences in construction. Both structures are eight-legged steel pile jackets. WKF is wider and the sub-structure weighs approximately 6955 tonnes with 32 well-conductors and KFB's sub-structure weighs about 4309 tonnes with 21 well-conductors. KFB is asymmetrical in configuration with a strut than spans the height of the structure from a few meters below the surface to the mudline.

2.3.2 Pipelines

The two subsea pipelines included "CBA300", which extends from the Cobia platform to the Halibut platform for a total length of 5.5 km, and "MLA100", which runs between the Marlin and Mackerel platforms and is 32 km long. CBA300 currently holds inhibited seawater with an outside diameter of 324 mm and 12.7 mm thickness. MLA100 has an outside diameter of 114.3 mm and 12.7 mm thickness and currently transports gas. The two pipelines run perpendicular to each other, with CBA300 following a single depth contour (73 to 78 m), while MLA100 extends across a depth gradient from 60 to 93 m. At the time of the ROV surveys of these structures, both had been installed for a similar amount of time (32 years for CBA300 and 33 years for MLA100).

2.4 ROV imagery analysis

2.4.1 Platform ROV imagery selection

Hard drives containing a combined 4.9 TB of ROV videos and associated metadata were provided by Esso Australia, documenting pipeline and platform ROV activities over a ten-year period (2008-2018). These activities included visual inspections, maintenance activities and free-span inspections. Videos were assessed using methods described in McLean et al. (2020a), which scored the suitability of imagery for facilitating ecological assessments of marine communities. Videos were discarded from further analysis if the field of view was restricted by equipment or the ROV activity was focused on a specific, small area. As ROVs operate 24-hours a day, imagery is collected at night and during the day. Typically, scientific studies only utilize day-time imagery as very different communities can be present at night, and ROV lighting can influence marine life present (Bond et al., 2018a). Day-time ROV imagery (between 730 – 1500 hours) of KFB and WKF was analyzed to quantify marine life across their full depth. This opportunistic imagery was collected for industry purposes rather than a planned scientific survey, so video replicates spanned different years and seasons (8 – 25 Oct 2015, austral spring, for KFB *vs.* 25 Apr – 5 Jun 2017, autumn to winter, for WKF). Both platforms were operational at the time the ROV imagery was collected

To test for the influence of depth on marine communities, we divided each jacket into five water column depth bands (0 – 15, 15 – 30, 30 – 45, 45 – 60, > 60 m; Supplementary Figure 1) covering the underwater span of these structures. A selection of five to seven replicate videos was then used to survey marine life associated with each of these depth bands at both platforms (Supplementary Table 1). Videos ranged in length from 1 to 21 minutes with those selected for analysis having good visibility, a field of view adequate for counting fish and benthos, and slow movement of the ROV.

A total of 4.28 hours of ROV imagery were suitable for the study (2.1 hours for KFB and 2.18 for WKF) and used to estimate: 1) relative abundance of associated marine fauna (fish, mobile invertebrates and mammals), and 2) percent cover of benthic/encrusting groups growing on the underwater structures. To supplement species diversity estimates, and obtain the best possible images for habitat analyses, we further viewed 26.8 hours of ROV imagery at high speed (*x* 2) to identify extra species that were not present in selected replicates, and took still images where appropriate for benthos identification.

2.4.2 Pipeline ROV imagery selection

Industry-collected ROV imagery for the CBA300 and MLA100 pipelines was analyzed for a quantitative assessment of marine life (fish, invertebrates and benthic communities). Imagery was collected during 2014, when both pipelines were operational, and a continuous visual inspection was conducted on sections of each pipeline. Imagery consisted of a single central view of the pipeline. A subset of this imagery recorded between 730 – 1500 hours was selected, to minimize the influence of time of day on assessments of marine life. Based on this selected time range, an approximate 1.8 km total length of imagery was available for analysis (from 0.7 to 1 KP and 4.3 to 5.2 KP for CBA300, and from 0.04 to 2 KP for MLA100). KP stands for kilometer point and provides a location (distance) along each pipeline. These pipeline sections were located in depths of 65 to 73.5 m for CBA300 (KP4.3 to 5.2) and in depths of 63.5 to 71.4 m for MLA100 (0.04 to 2 KP). The imagery was collected in March 2014 for CBA300 and April 2014 for MLA100.

Selected imagery was examined for all fish and invertebrates encountered along 50 m transects, separated from a subsequent transect by a 10 m gap. Transect and pipeline distances were defined using georeferenced KP information presented in real time. A total of 31 x 50 m transects were analyzed for each pipeline, with every fish and invertebrate encountered recorded. Observations were made along the pipeline and immediately adjacent to the pipeline to a distance of ~2 m on either side.

2.4.3 Quantifying platform and pipeline marine fauna

Analysis of ROV imagery to quantify marine fauna was conducted in EventMeasure^{TM} Stereo (SeaGIS, 2021a) aided with reference literature for the region (Edgar, 1997; Jones and Morgan, 2002; Gomon et al., 2008; Gowlett-Holmes, 2008; Wilson et al., 2010; Bray and Gomon, 2021). Each ROV video was treated as an independent sample, with the aim of getting comparable estimates of species richness and relative abundance.

All fish, mobile invertebrates (e.g., crustaceans, squids, octopus) and mammals observed were recorded to the lowest taxonomic level possible. In several cases, species could not be identified reliably to species level due to either low video quality, low visibility, or ROV swimming patterns (high speed, too close or too far from the structure). These species were recorded to genus or family level where possible (e.g., *Lepidotrigla* spp., gurnards, *Trachurus* spp., jack mackerels).

Relative abundance of all recorded fish, mobile invertebrates and mammals was estimated using *MaxN*, a relative and conservative measure of abundance that counts only the maximum number of individuals observed at a single video frame during each video sample (Ellis and DeMartini, 1995; Willis and Babcock, 2000). By using *MaxN*, possible recounting of individuals of the same species at each replicate was avoided.

2.4.4 Quantifying platform benthic biota

To test for differences in benthic biota throughout the platform, ten opportunistic quadrats were obtained at each depth band (0 – 15, 15 – 30, 30 – 45, 45 – 60, > 60 m) by taking images with the best visibility of the biota from ROV imagery. As the diameter of the horizontal, diagonal, and vertical piles of the jacket varied, benthic quadrats were 0.25 – 1 m^2 estimated based on detailed platform schematics showing the diameter of each component.

Quadrats were analyzed using TransectMeasure™ software (SeaGIS, 2021b), to assess benthic cover according to modified CATAMI categories (Collaborative and Annotation Tools for Analysis of Marine Imagery; Althaus et al., 2015). For each quadrat, 25 points were randomly allocated on the image, and benthos directly underneath the point was identified to biota categories (e.g., macroalgae, sponges, ascidians, zoanthids) and morphological characteristics (e.g., encrusting, complex or taller erect forms). For each quadrat, a measure of habitat complexity was also recorded by estimating epibenthic height according to four categories: 0: negligible; 1: low (0 – 20 cm); 2: medium (20 – 40 cm); and 3: high (> 40 cm). We used the diameter of columns and other structural elements from available platform schematics as a relative scale for these estimates. Ten quadrats of 25 random points in five depth categories resulted in 1250 data points for each platform. Similar methods have been used in other O&G studies (e.g., Thomson et al., 2018).

2.4.5 Pipeline habitat assessment

For each 50 m transect, measurements of “pipeline position” (0 to 4; completely buried to having a gap > 0.5 m) and “epibenthic height” (0 to 3; negligible to high > 40 cm; Figure 2) were taken along five points (0, 10, 20, 30 and 40 m).

Benthic composition along each pipeline was assessed using TransectMeasure by analyzing a virtual quadrat of about 4 m^2 (~150 cm x ~270 cm, depending on ROV altitude) placed on a freeze-framed image taken every 60 m along each pipeline (one per 50 m transect). Within each quadrat, 20 random points were allocated and the benthos under each point was identified to the lowest taxonomic resolution possible. This classification resulted in fourteen broad categories based on a modified CATAMI guide (Collaborative and Annotation Tools for Analysis of Marine Imagery; Althaus et al., 2015), which included biotic and abiotic components: ascidian, biofilm, calcareous, dead shell, encrusting, hydrozoa, macroalgae, rubble, sand, shells, soft coral, sponge, turf and other. The position of each random point in the allocated quadrat was recorded as either “on” or “off” the pipeline. Descriptions of benthic biota on the pipeline used just the points “on” the pipeline, whereas all habitat points (on and off pipeline) were used for assessment of relationships between

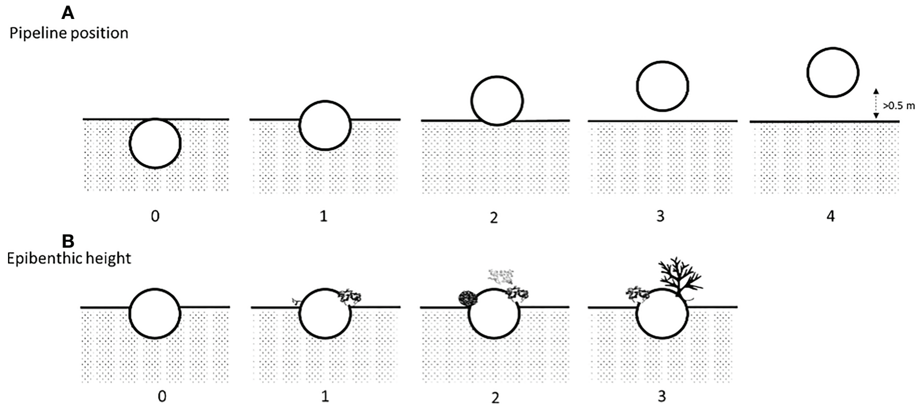

FIGURE 2
(A) Method of assessing pipeline position with 0: buried; 1: more than half buried; 2: resting on the seafloor; 3: span< 0.5 m; and 4: span > 0.5 m and **(B)** epibenthic height with 0: negligible; 1: low (0 – 20 cm); 2: medium (20 – 40 cm); and 3: high (> 40 cm). A version of this figure has previously been published in McLean et al., 2020b.

benthic biota and fish species richness and relative abundance. Habitat components were grouped (for plotting) according to the most frequent biotic categories including sponges, encrusting (e.g., ascidians and biofilm), other (e.g., macroalgae, hydroids) and the abiotic categories of dead shell, sand and rubble.

2.5 ROV data analysis

All data were exported from EventMeasure and TransectMeasure, checked, formatted, and summarized *via* plots using the R Language for Statistical Computing (R Core Team, 2020, v. 4.0.2), *via* the *tidyr*, *dplyr* (Wickham et al., 2019) and *ggplot2* (Wickham, 2016) packages. Permutational Analyses of Variance (PERMANOVA) using the PRIMER-E statistical software (Clarke and Gorley, 2005) was used to investigate multivariate species richness and relative abundance data.

2.5.1 Platform data analyses

For multivariate abundance data, PERMANOVA analyses were performed on a Bray-Curtis similarity matrix, generated from either fourth-root (fish) or square-root (invertebrates) transformed abundance data. In the case of univariate response metrics, analyses were performed on Euclidean dissimilarity matrices constructed from untransformed total abundance and species richness data for fish and invertebrates (Anderson, 2001; Anderson and Millar, 2004). PERMANOVAs were run using a two-factor design with platform (two levels; KFB and WKF), and depth band (five levels; 0 – 15 m, 15 – 30 m, 30 – 45 m, 45 – 60 m, > 60 m) as fixed effects, 9,999 permutations, Type III sums of squares, and with the option to permutate residuals under a reduced model.

To further test for differences in fish community composition between platforms and depth bands, multivariate ordination plots *via* Principal Coordinates Analysis (PCO; Anderson et al., 2008) were constructed. PCO analysis was based on a Bray-Curtis similarity matrix, generated from fourth-root transformed data on individual fish species abundance. Arrows representing species with significant correlation ($|R| \geq 0.4$) with the PCO axes, were then overlaid on the PCO (Anderson et al., 2008).

2.5.2 Pipeline data analysis

To test for differences in fish communities between pipelines and their relationship with benthic diversity/cover and pipeline characteristics, we used generalized additive models (GAMs; Hastie and Tibshirani, 1986). GAMs were chosen to account for the non-linear relationships between dependent and predictor variables in our models (Austin, 2007). We used a Tweedie GAM with a log-link function to model total fish abundance (*MaxN*) and taxonomic richness as a function of one fixed (pipeline identity; categorical with two levels), and nine continuous variables (pipeline position, epibenthic height, depth, % cover dead shell, % cover encrusting organisms, % cover other benthic organisms, % cover rubble, % cover sand and % cover sponge) (Equation 1). Eight habitat predictors were excluded because of their limited coverage (> 85% zeros; e.g., ascidians, hydrozoans). Exploratory analyses suggested kilometer point information was an important predictor of differences in fish communities along pipelines with proximity to a platform, but this variable had uneven distribution for modelling and was excluded (for example, at CBA300 imagery spanned 0.07 to 1 KP, and then 4.3 to 5.2 KP).

$$N\ (\text{Abundance/Richness})\ ij \sim \text{Tweedie}\ (\mu ij)$$

$$E\ (\text{NAbundance}\ ij/\text{Richness}\ ij) = \mu ij$$

$$\begin{aligned} log\ (\mu ij) = \ & \beta o + \text{pipeline identity}ij + f1(\text{pipeline position}ij) \\ & + f2(\text{epibenthic height}ij) + f3(\text{depth}ij) \\ & + f4(\ \%\ \text{cover dead shell}ij) \\ & + f5(\ \%\ \text{cover encrusting}ij) + f6(\ \%\ \text{cover other}ij) \\ & + f7(\ \%\ \text{cover rubble}ij) + f8(\ \%\ \text{cover sand}ij) \\ & +\ f9(\ \%\ \text{cover sponge}ij) + \epsilon \end{aligned}$$

$$\epsilon \sim N(0,\sigma^2)$$

where N(Abundance/Richness)*ij* is the *j*th observation in transect *i*, and *i*= 1, …, 31, and *f*1 to *f*8 are spline based smooth functions estimated by the model ($k = 3$)

(Equation 1)

The Tweedie distribution was selected because it allows for responses to have a mass at zero, but otherwise continuous and positive values. This distribution also provided the best fit to our data as assessed by comparing diagnostic plots of residuals with alternative distributions (least overdispersion). We chose not to evaluate interaction terms to simplify model interpretation. All observations were independent, so there were no random intercepts.

Models were fitted using package *FSSgam* (Fisher et al., 2018; Goetze et al., 2018; McLean et al., 2020b). This package allows for the construction of a complete set of competing models, which are compared to determine the most plausible fitting model. Model construction was restricted to a maximum of three predictors to avoid overfitting and excluded correlated variables ($R > 0.28$). Selection of the most plausible model was based on a multivariate analogue of the Akaike Information Criterion corrected for small sample sizes (AIC_c, Anderson et al., 2008), which was used to compare models and select the most parsimonious (fewer number of predictors and within 2 AIC_c units of the model with the lowest AICc value). Models were further cross-validated using five-fold cross validation 50 times (Brunsdon et al., 1996; Lehmann et al., 2002), and normalized root mean square errors (normalized RMSE) calculated to assess the average magnitude of predictive errors in all sub-models (Potts and Elith, 2006). Finally, to assist model interpretation and identify the most important predictors of fish relative abundance and diversity, variable importance metrics were calculated for all GAMs, based on a weighted AICc (*w*AICc, Burnham and Anderson, 2002).

2.5.3 Comparing platform and pipeline communities

To compare the overlap of marine communities from ROV imagery, a Venn diagram was created for each of the two pipelines and platforms (package ggvenn, Yan, 2021). Lastly, to compare the community composition caught in fisheries with the species identified among pipelines and platform imagery, a Euler diagram was used to illustrate the proportion of overlap between communities found in the two main fisheries, pipelines and platforms. Overlapping ellipses indicated the percent shared by those structures or fishery with the area of non-overlapping sections representing the unique number of species per assemblage (package eulerr, Wilkinson, 2012; Larsson, 2021).

3 Results

3.1 Fisheries operating around oil and gas infrastructure in Bass Strait

Six Commonwealth fisheries operated within the area from 2008-2018 (from greatest fishing effort to least): the Commonwealth Trawl Sector (CTS, 86% of the reported data), Gillnet, Hook and Trap Fishery (GHAT, 13%), Southern Squid Jig Fishery (SSJF,< 1%), Bass Strait Central Zone Scallop Fishery (BSCZSF,< 1%), High Seas Fishery (HSF,< 1%), and Small Pelagic Fishery (SPF,< 1%). Fishing gears used in this area included (in descending order, according to the percentage of reported data): Danish seine (a type of trawl fishing, 73%), bottom otter trawl (13%), set gillnet (demersal gillnet, 13%), set auto-longline (demersal longline,< 1%), set longline (demersal longline,< 1%), and squid jigs (mechanized,< 1%). Cumulative annual reported retained catch varied between 1,042,278 kg (in 2018) - 1,513,793 kg (in 2009, Figure 3). Reported discarded catch weight was a small fraction compared to retained catch (17,034 - 375,135 kg).

Species composition from reported catch was quite diverse, with 248 species or species groups reported from 110 families of fishes and invertebrates. It is important to note that this is an underestimate of true species diversity as many species are reported to family or order. Ninety-nine of these species/groups were rarely caught, being reported fewer than ten times in ten years. The most frequently retained species (in terms of cumulative catch weight) were from the following families (Figure 4): Platycephalidae (flatheads), Sillaginidae (whitings), Triakidae (houndsharks), Ophidiidae (cusk-eels), Ommastrephidae (squids), Pristiophoridae (sawsharks), Centrolophidae (medusafish), Latridae (trumpeters), Pectinidae (scallop), and Octopodidae (octopus). Other commercially important families include Monacanthidae (leatherjackets), Callorhinchidae (elephantfish), Zeidae (true dories), and Mullidae (goatfishes) with all other families contributing less than 100,000 kg over the ten-year period.

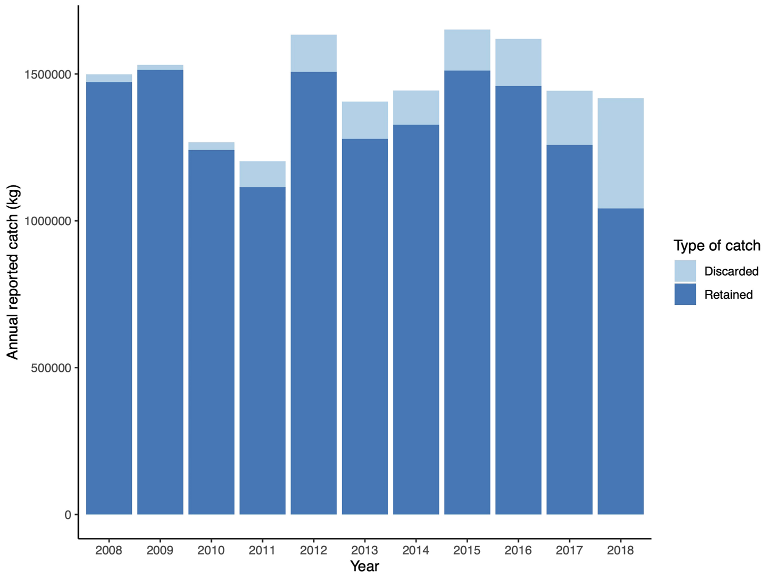

FIGURE 3
Retained and discarded catch data near oil and gas structures in the Bass Strait from 2008-2018.

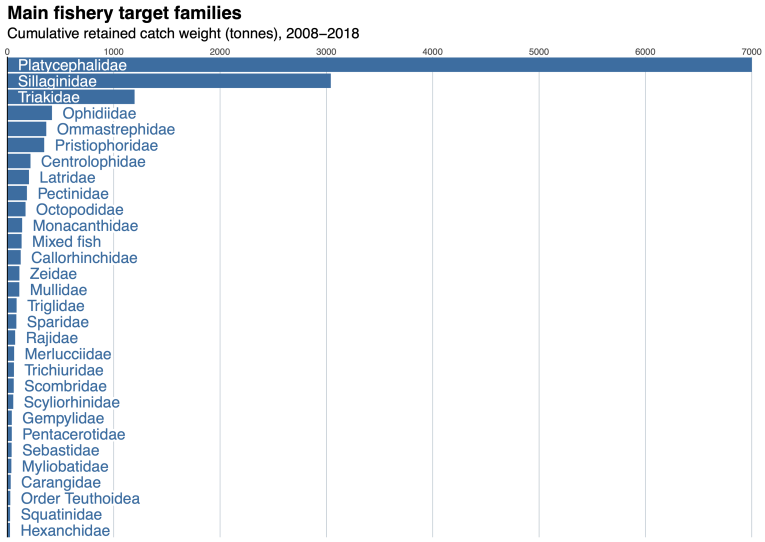

FIGURE 4
Cumulative fishery catch near oil and gas structures in the Bass Strait from 2008-2018 by family.

The category "Mixed Fish" is a frequent allocation for any species not caught in high abundance per deployment of fishing gear. This could represent any number of species caught in smaller quantities and comprised a substantial portion of the fishery catch over time.

The two main fisheries operating around O&G structures were the CTS and GHAT fisheries, which are both managed as part of the Southern and Eastern Scalefish and Shark Fishery (SESSF). These fishers operated fairly ubiquitously around all O&G infrastructure and target tiger flathead, *Platycephalus richardsoni*, eastern school whiting, *Sillago flindersi*, and gummy shark, *Mustelus antarcticus* (Figure 5, Supplementary Figures 2, 3). The SESSF catch a diverse range of species with Danish seine, bottom otter trawl and gillnet equipment. From 2008-2018 CTS caught 183 species, with only 70 species > 1000 kg cumulatively caught. The GHAT catch included 118 species with 29 species > 1000 kg over the ten-year period.

The other four fisheries had limited fishing operations in this region. The BSCZSF only targets the commercial scallop, *Pecten fumatus* (183,885 kg) and retained a small quantity of the doughboy scallop, *Mimachlamys asperrima* (85 kg), which has little commercial value. The fishing effort was not spread evenly during this period with trips only in 2009, 2010, 2012, 2013 (Figure 6). The HSF only operated in a small area outside of the 300 m bathymetric contour. During three trips in 2014 and 2016, retained catch reports included only nine species, with the majority pink ling, *Genypterus blacodes* (6970 kg), and incidental quantities of reef ocean perch, *Helicolenus percoides* (62 kg), ribaldo, *Mora moro* (24 kg), greeneye spurdog, *Squalus chloroculus*, and southern dogfish, *Centrophorus zeehaani* (15 *kg* each). The SPF rarely fished in this area during the period analyzed and retained skipjack tuna, *Katsuwonus pelamis* (15200 kg) and common jack mackerel, *Trachurus declivis* (9000 kg) in only one trip in 2008. The SSJF fishing effort was concentrated around the platforms between the 40-60 m bathymetric contours, with most of the fishing effort concentrated in 2012. SSJF targets Gould's squid, *Nototodarus gouldi* (116,696 kg), which is also referred to as arrow squid.

3.2 A description of marine communities observed around infrastructure

From the full collection of ROV imagery from Esso Australia O&G structures, we provide a brief description of the broader marine community. Species important to State and Commonwealth fisheries that were documented in the ROV imagery included the bluespotted goatfish (in local seafood markets referred to as red mullet, *Upeneichthys vlamingii*), longsnout boarfish (also known as duckfish, *Pentaceropsis recurvirostris*), trevally (*Pseudocaranx* spp.), jackass morwong (*Nemadactylus macropterus*), elephantfish (*Callorhinchus milii*), pink ling (*Genypterus blacodes*) and the bluethroat wrasse (*Notolabrus tetricus*, Figure 7). Abundant species included jack mackerels (*Trachurus* spp.), sweeps (e.g., sea sweep, *Scorpis aequipinnis*), scorpionfishes (e.g., common gurnard perch, *Neosebastes scorpaenoides*), stinkfish (e.g., common stinkfish, *Foetorepus calauropomus*), and perches (e.g., butterfly perch, *Caesioperca lepidoptera*). Larger species (often highly mobile) included the smooth stingray (*Bathytoshia brevicaudata*),

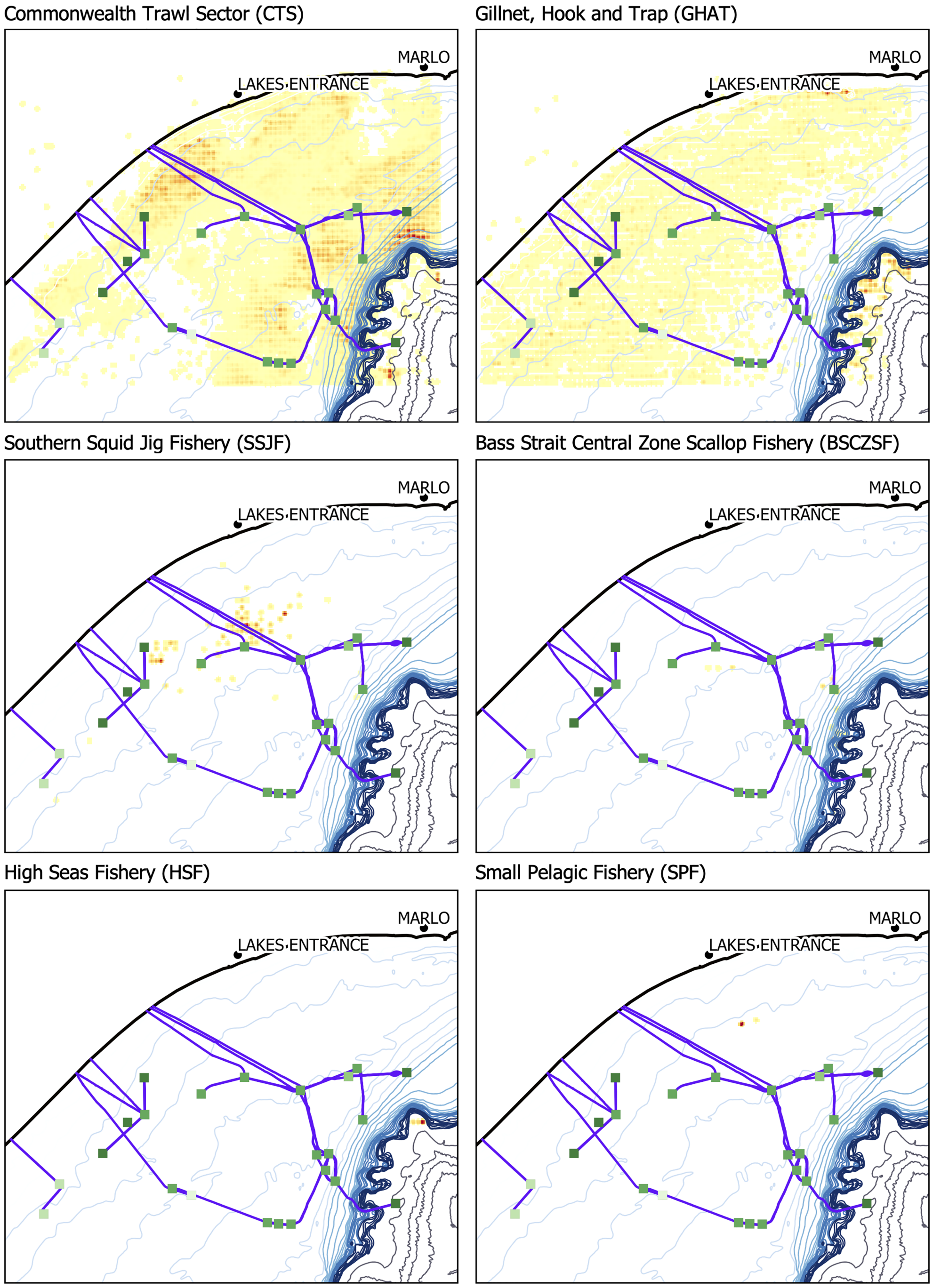
Commonwealth Trawl Sector (CTS)
Gillnet, Hook and Trap (GHAT)
Southern Squid Jig Fishery (SSJF)
Bass Strait Central Zone Scallop Fishery (BSCZSF)
High Seas Fishery (HSF)
Small Pelagic Fishery (SPF)

FIGURE 5
Spatial distribution of fishing effort for six Commonwealth fisheries among the offshore oil and gas structures in the Gippsland Basin. Maps were made in QGIS. Individual versions of these maps with accompanying legends are included in the Supplementary Materials.

banded stingaree (*Urolophus cruciatus*), Port Jackson sharks (*Heterodontus portusjacksoni*), and draughtboard sharks (*Cephaloscyllium laticeps*).

Greater richness of invertebrate taxa was generally observed near pipelines than on platforms, likely due to the proximity of the benthos and the maneuverability of the ROV. Rock lobsters (also referred to as crayfish, family Palinuridae, including southern rock lobsters *Jasus edwardsii*) were observed near the base of at least six of the platforms and other subsea infrastructure. Smaller crustaceans including shore crabs

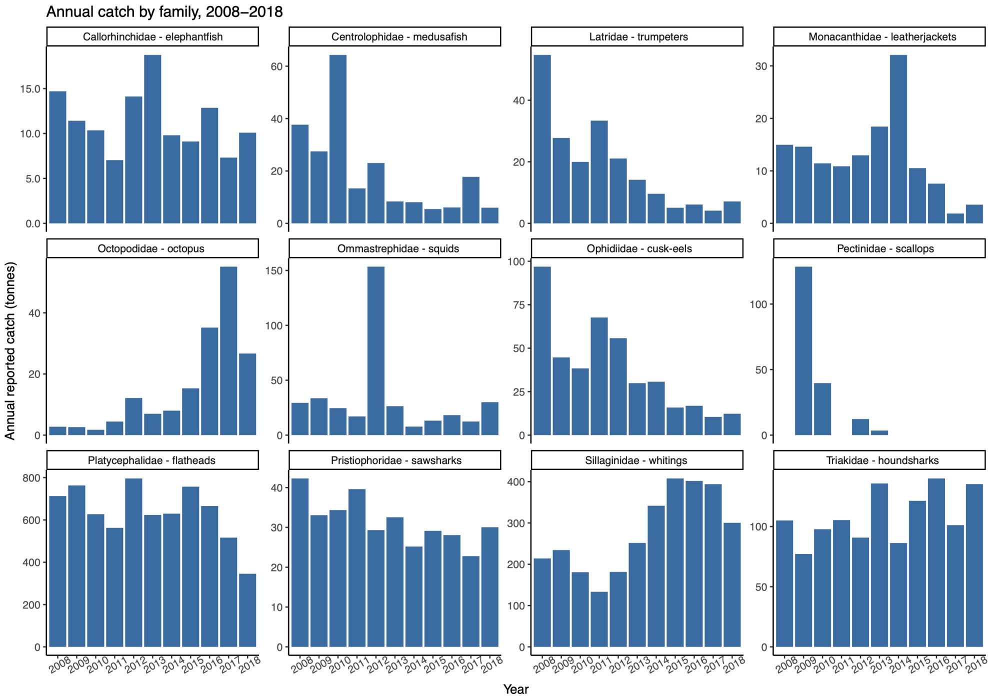

FIGURE 6
Annual catch of 12 families by fisheries operating near oil and gas structures 2008-2018.

(Grapsidae) were observed in water depths < 15 m. Jellyfish were also observed in the water column and were sometimes entrained downcurrent of the platform structures. On the benthos, hermit crabs (superfamily Paguroidea) were the most abundant, typically crawling along or beside the pipelines. Sea urchins (class Echinoidea), including the purple sea urchin, *Centrostephanus rodgersii*, were infrequently observed, but where they appeared, they were often clustered along the pipelines. Larger sea stars (*Asterodiscides truncatus*), decorator crabs (family Majidae) and mantis shrimp (order Stomatopoda) were visible in the imagery. Occasionally squid such as the southern calamari squid (*Sepioteuthis australis*), octopus such as the Maori octopus (*Octopus maorum*), and the giant cuttlefish (*Sepia apama*) were present along the pipelines. Also present in ROV videos were gastropods such as spindle shells and whelks. Near the pipelines mobile invertebrates were documented in the soft sediments, including sea cucumbers (family Holothuridae), sea pens (order Pennatulacea), and featherstars (class Crinoidea). In deep water (> 300 m), carrier crabs (family Homolidae) and large anemones (order Actinaria) were attached to the pipeline and were observed on the pipeline down to ~ 400 m depths. Squat lobsters (family Galatheidae), which have squat bodies, slender arms and claws were also only found in deep water.

The predominant forms of benthic biota documented in the ROV imagery included many forms of sponges (Phylum Porifera), bivalves (e.g., commercial scallops, oysters, doughboy scallops), hydrozoans, tunicates (e.g., sea squirts, salps), free-living and colonial ascidians, tube worms, anemones and sea whips. Platforms were covered in benthic biota, mostly encrusting morphs of colonial ascidians, jewel anemones, anemone-like zoanthids (not true anemones), and sponges. Observations suggested that the encrusting height increased with depth with erect and branching morphs of sponges found on the seabed and deepest sections of the platforms. The shallowest areas of the platforms were characterized by invertebrate complexes of barnacles, macroalgae, and smaller mounding morphs of sponges.

3.3 Steel pile jacket communities

3.3.1 General patterns across marine fauna: Univariate metrics

Sixty-seven species of marine fauna were recorded from the two steel piled jackets in the Bass Strait. Of these, 55 were fish, 11 were mobile invertebrates and one was a mammal. Seven of these species are regularly caught in commercial fisheries (redfish *Centroberyx affinis*, silver trevally *Pseudocaranx georgianus*, jackass morwong *Nemadactylus macropterus*, banded morwong *Cheilodactylus spectabilis*, blue throat wrasse *Notolabrus tetricus*, rosy wrasse *Pseudolabrus rubicundus*, and

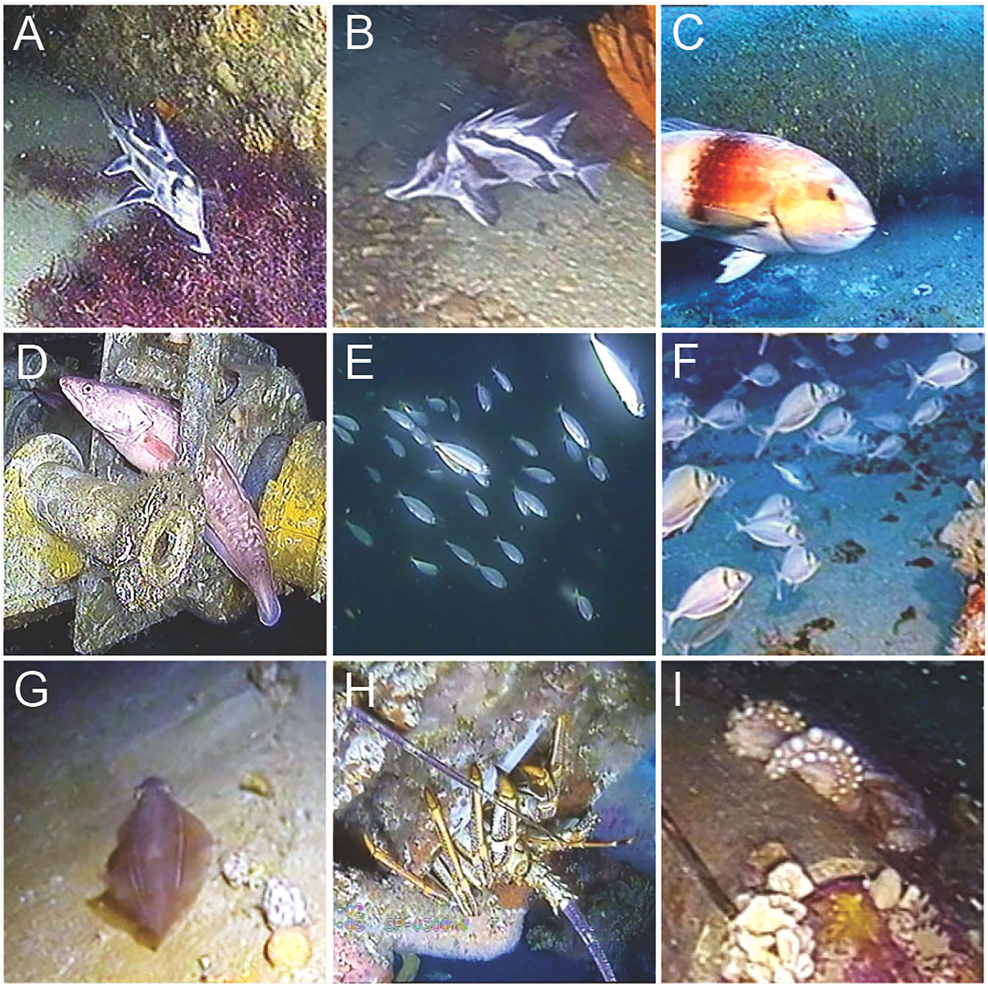

FIGURE 7
Examples of fishery species observed during industry-collected ROV surveys: **(A)** elephantfish, *Callorhinchus milii*, **(B)** longsnout boarfish, *Pentaceropsis recurvirostris* **(C)** bluethroat wrasse, *Notolabrus tetricus*, **(D)** pink ling, *Genypterus blacodes*, **(E)** jack mackerels, *Trachurus* spp., **(F)** jackass morwong, *Nemadactylus macropterus*, **(G)** squid, **(H)** southern rock lobster, *Jasus edwardsii*, and **(I)** an octopus.

southern rock lobster *Jasus edwardsii*, Supplementary Table 2). The only species of mammal found was the Australian fur seal, *Arctocephalus pusillus doriferus*, observed swimming through the water column at both platforms. Although most species richness was accounted for by fish, numerous species of crabs and jellyfishes were likely not accounted for during imagery analyses due to low video image quality (e.g., most crabs could only be identified to the level of Infraorder Brachyura).

At KFB, 43 species were recorded (34 species of fish, eight invertebrates and one mammal), and 46 at WKF (39 species of fish, six invertebrates, one mammal). Of the 67 species recorded across both platforms, only 22 species were observed at both platforms, while 21 were unique to KFB and 24 unique to WKF. Additional species included the world's largest bony fish, the sunfish (*Mola* spp.). Fish species that were common on both platforms were also abundant at each platform (e.g., *C. lepidoptera*, *N. macropterus*, Table 1). Other fish species were unique to WKF (e.g., *Trachurus* spp., *Pseudocaranx* spp.).

Marked differences in species relative abundance were observed across depths at the two platforms (Supplementary Table 3, Figure 8). Patterns also differed between fish, invertebrates and mammal species. Highest overall taxonomic richness (both total and average) was found in the deepest depth band at both platforms (> 60 m, n=33 species for KFB and n=27 species for WKF). Lowest taxonomic richness was recorded at water depths of 0 – 15 m for KFB (n=9 species), and 45 – 60 m for WKF (n=10), although average taxonomic richness (# species/video sample) was lower at 15 – 30 m at the latter. Fish accounted for most of the taxonomic richness patterns, with invertebrate taxonomic richness being more uniform across depth. Fish taxonomic richness was similar between the KFB and WKF platforms but varied significantly

TABLE 1 Summary of the ten most common (% of occurrence: #ROV videos/total ROV videos sampled), and the ten most abundant (Total MaxN) fish species present at the Kingfish B (KFB) and West Kingfish (WKF) steel jacket oil and gas platforms.

Platform	10 Most Common	% Occurrence (#ROV/Total)	10 Most Abundant	Total Max N
KFB	Butterfly perch, *Caesioperca lepidoptera*	58	Butterfly perch, *Caesioperca lepidoptera*	1680
	Splendid perch, *Callanthias australis*	32	Jack mackerel, *Trachurus* spp.	809
	Unknown spp.	29	Jackass morwong, *Nemadactylus macropterus*	365
	Silver sweep, *Scorpis lineolata*	19	Silver sweep, *Scorpis lineolata*	130
	Blennies, *Blenniidae* spp.	13	Splendid perch, *Callanthias australis*	126
	Jack mackerel, *Trachurus* spp.	13	Unknown spp.	64
	Jackass morwong, *Nemadactylus macropterus*	10	Perch, *Caesioperca* spp.	60
	Banded sweep, *Scorpis aequipinnis*	10	Common gurnard perch, *Neosebastes scorpaenoides*	46
	Marblefish, *Aplodactylus arctidens*	6	Banded sweep, *Scorpis aequipinnis*	13
	Reef ocean perch, *Helicolenus percoides*	6	Reef ocean perch, *Helicolenus percoides*	7
WKF	Butterfly perch, *Caesioperca lepidoptera*	56	Jack mackerel, *Trachurus* spp.	1513
	Jack mackerel, *Trachurus* spp.	44	Butterfly perch, *Caesioperca lepidoptera*	517
	Onespot puller, *Chromis hypsilepis*	32	Silver sweep, *Scorpis lineolata*	122
	Banded sweep, *Scorpis aequipinnis*	28	Banded sweep, *Scorpis aequipinnis*	73
	Southern red scorpionfish, *Scorpaena papillosa*	20	Southern red scorpionfish, *Scorpaena papillosa*	34
	Silver sweep, *Scorpis lineolata*	20	Splendid perch, *Callanthias australis*	30
	Splendid perch, *Callanthias australis*	16	Onespot puller, *Chromis hypsilepis*	30
	Draughtboard shark, *Cephaloscyllium laticeps*	16	Jackass morwong, *Nemadactylus macropterus*	12
	Trevally, *Pseudocaranx* spp.	16	Draughtboard shark, *Cephaloscyllium laticeps*	7
	Banded morwong, *Chirodactylus spectabilis*	12	Trevally, *Pseudocaranx* spp.	6

according to depth band (P(perm)=0.006, Supplementary Table 3, Supplementary Figure 8), with water depths > 60 m having higher species richness than all other depth bands (Platform *x* Depth band, all P(perm)<0.009).

Species relative abundance also differed across depth for both platforms (Figure 9, Supplementary Table 3). Total fish abundance (univariate) was similar between platforms but varied significantly according to depth band (P(perm)=0.006),

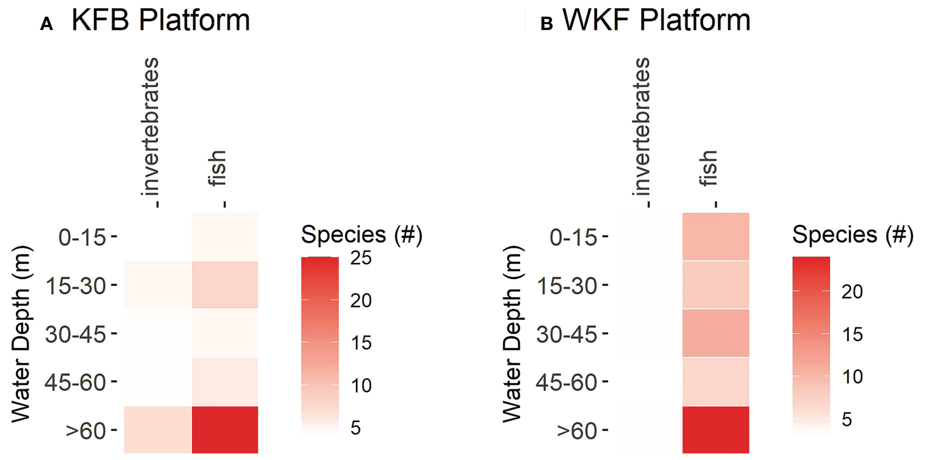

FIGURE 8
Heatmap showing species richness (total # of species) at platforms Kingfish B (KFB, **A**) and West Kingfish (WKF, **B**) surveyed for fish and invertebrates at the five depth bands for which ROV imagery were surveyed (0 – 15, 15 –30, 30 – 45, 45 – 60, – 60 m). Only one species of mammal, the Australian fur seal, *Arctocephalus pusillus doriferus*, was found.

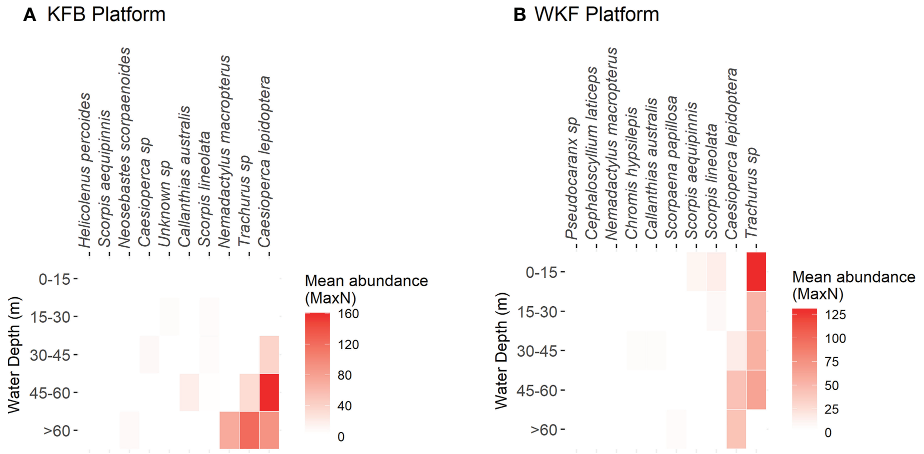

FIGURE 9
Heatmap showing average abundance (mean MaxN) of the ten most abundant species at each of the five depth bands (0 – 15, 15 – 30, 30 – 45, 45 – 60, > 60 m) for each platform Kingfish B (KFB, **A**) and West Kingfish (WKF, **B**).

with this pattern differing between platforms (Platform *x* Depth band interaction, Supplementary Figure 9). At KFB, three distinct water depth groups for total fish abundance were evident: 0 – 15, 30 – 45 and > 45 m (based on significant differences for *post-hoc* tests on the Platform *x* Depth band interaction, all P(perm)<0.04). This platform had a higher abundance of fish at its base (> 45 m) compared to shallower depths. Fish in the deeper areas included large schools of jackass morwong (*N. macropterus*), butterfly perch (*C. lepidoptera*) and splendid perch (*C. australis*). Common gurnard perch (*Neosebastes scorpaenoides*) and reef ocean perch (*Helicolenus percoides*), two types of bottom-dwelling perches were also common on the seabed around and underneath the KFB platform. In contrast, total fish abundance at the WKF platform was more evenly distributed across depths (Supplementary Figure 9). Lack of depth differentiation at this platform was largely due to abundant schools of jack mackerels (*Trachurus* spp.), a pelagic group of fishes, that was mostly ubiquitous across 0 – 60 m water depths (Figure 9). Species relative abundance patterns for the ten most abundant fish species, showed clear association of butterfly perch (*C. lepidoptera*), jack mackerels (*Trachurus* spp.), and jackass morwongs (*N. macropterus)* with deep sections of the KFB platform (> 45 m), with other species more evenly distributed across depth (Supplementary Table 2). Similar to KFB, *C. lepidoptera* were associated with deep sections of this platform, and other fish species were more evenly distributed across depth.

Invertebrate relative abundance (univariate) was significantly lower in deeper waters at both platforms (> 60 m) (all P(perm)<0.03), with other depth bands showing no statistically significant differences in abundance (Supplementary Figure 9). At KFB, the high relative abundance of invertebrates observed at 15 – 30 m water depth was accounted for by large schools of krill (*Nyctiphanes australis*), with crabs and jellyfishes more evenly distributed throughout depth. At WKF, the highest average invertebrate abundance was recorded at intermediate depths (30 – 45 m). Both platforms had significantly different invertebrate community composition (multivariate abundance, P(perm) =0.0001), which also varied according to depth band (P (perm)=0.02).

Australian fur seals, the only mammals associated with both platforms (n= 9; total mammals recorded at both platforms), were most abundant towards the water surface at KFB (0 – 15 m) (no statistics conducted due to very high proportion of zeros). Some of these individuals may be the same individuals but recorded on different videos, so true total abundance may be less than nine. Australian fur seals were found in lower relative abundance at WKF and only at the 0 – 15 and 45 – 60 m water depth bands; this is presumably due to low sampling frequency and chance observation of these mammals, with their distribution likely being ubiquitous across depths.

3.3.2 Fish assemblage composition: Multivariate patterns of abundance

Multivariate patterns in abundance showed a clear separation between shallow sections of the platforms, driven by the presence of *Trachurus* spp. and one-spot puller (*Chromis hypsilepis*) at the WKF platform (Figure 10). Both of these species were present at KFB, but in deeper waters > 45 m. At deep sections of both platforms (> 45 m), species composition appeared to be more similar, with *C. lepidoptera* common and abundant. The PCO axes presented explained a total of 50.2% variation in fish assemblage data.

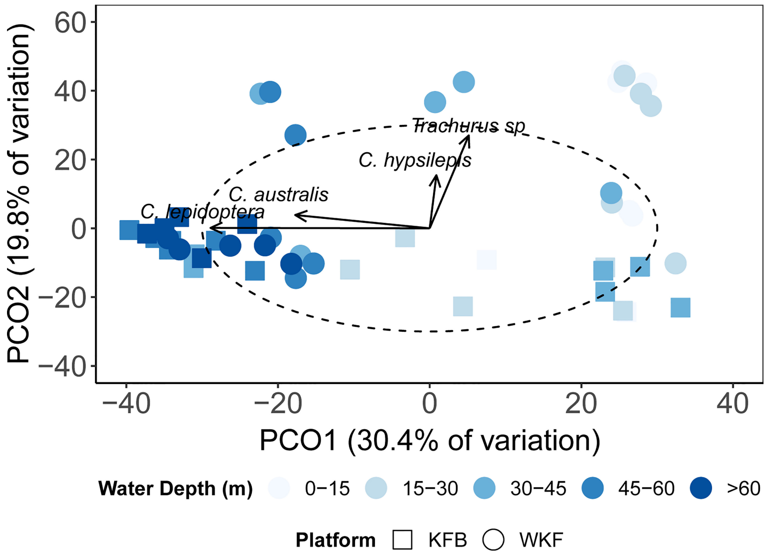

FIGURE 10
Principal Coordinates Analysis (PCO) showing multivariate fish data (fourth-root transformed) at the two platforms surveyed (KFB- squares, WKF- circles), according to the five depth bands selected. Arrows represent fish species showing significant correlation (|R| ≥ 0.4) with the PCO axes.

These multivariate patterns were validated by PERMANOVA results showing platform and depth band were significant factors separating multivariate fish species composition (P(perm) =0.0001), with a significant interaction between them (P(perm) =0.0001; Supplementary Table 3). At both platforms there were three distinct depth groups: 0 – 45 m, 45 – 60 m and > 60 m water depth (based on significant differences for *post-hoc* tests on the Platform *x* Depth band interaction; all P(perm)<0.03). However, at WKF this distinction was less clear with the fish assemblage similar among 0 – 60 m water depths.

3.3.3 Steel pile jacket benthic biota

Both KFB and WKF platforms were 100% covered by benthic biota. Colonial ascidians and sponges were the most common benthic biota categories observed (Supplementary Figure 10). Shallow sections of the platforms (0 – 15 m) had more macroalgae and 'invertebrate complexes' such as bivalves or barnacles. Most of the benthic biota were encrusting and unstalked types, forming short continuous coverage over the entire platform. Taller erect forms of sponges were present below 45 m, with similar levels at KFB and WKF. 'Small mixed' morphs and 'articulated calcareous' types of macroalgae were more common in the 0 – 15 m water depth. Small mixed morphs were also present in greater proportions below 45 m water depth creating habitat for fishes lying on or among the benthos on the structure. Epibenthic height variation was overall very low, with 20 – 30% of higher growth (2: medium 20 – 40 cm) in the shallowest and deepest categories. There was more uniformly low growth between 15 – 60 m. However, benthic quadrats were opportunistically sampled and the quality of still images from standard definition ROV videos that were not collected for this purpose limited the ability to quantify the benthic biota. This information is therefore considered qualitatively representative of the benthic communities present.

3.4 Pipelines

3.4.1 General faunal patterns among pipelines

At the CBA300 pipeline, 1200 fishes were recorded across 29 species and 20 families (Supplementary Table 4). Total fish abundance ranged from 0 to 358 individuals per 50 m transect (mean ± SD: 38.71 ± 71.57), and fish species richness ranged from 0 to 16 species per 50 m transect (mean ± SD: 4.03 ± 3.28). Only a few species of commercial importance were recorded: the jackass morwong (*Nemadactylus macropterus*), bluespotted goatfish (*Upeneichthys vlamingii*) and octopus species. Ninety-three invertebrates from five categories were recorded (sea star *Asterodiscides truncatus*, hermit crabs, crabs, decapods, octopus), with most of these being hermit crabs (86%).

At the MLA100 pipeline, 4199 fishes were recorded across 47 species and 28 families; with ~30% of species also present at the CBA300 pipeline. Abundance per each 50 m transect varied from 4 to 620 (mean ± SD: 135.45 ± 148.37), and species richness from 3 to 17 (mean ± SD: 7.16 ± 3.20). As with the CBA300 pipeline, the same commercial species were present, with *N. macropterus* in lower abundance (89 individuals recorded at

CBA300 and only 44 fish at MLA100). A total of 49 invertebrates were also recorded from nine categories, with most of them being hermit crabs (67%).

The fish assemblage along the CBA300 pipeline was dominated by small benthic species such as stinkfish (*Foetorepus calauropomus*) and grubfish (*Parapercis allporti*) (Table 2). Schools of jacks/trevallies were also common along this pipeline and responsible for a large percentage of the total fish abundance recorded (~26%). Abundance of *N. macropterus*, was ~7.5% of the total fish abundance at the CBA300 pipeline. At the MLA100 pipeline, butterfly perch were the most abundant. Schools of jacks/trevallies were also present, although in less abundance than at CBA300, and the abundance of *N. macropterus* was ~1% of total fish abundance recorded at this pipeline. Benthic and relatively sedentary fish species such as reef ocean perch (*Helicolenus percoides*) and the southern red scorpionfish (*Scorpaena papillosa*) were common and abundant at both pipelines surveyed.

Total fish abundance and species richness were higher along the MLA100 pipeline while invertebrate abundance was higher on the CBA300 pipeline and invertebrate species richness was similar between pipelines (Supplementary Figure 11, Supplementary Table 5).

3.4.2 Pipeline fish assemblages

A combination of epibenthic height and pipeline position were important variables for explaining fish total abundance and richness (Figure 11, Table 3). Total fish abundance was higher when more complex epibenthic communities were present and when the pipeline was more exposed, for both pipelines (Supplementary Figure 12A). Pipeline identity (CBA300 *vs.* MLA100) explained very little of the variation in total fish abundance and this variable was not selected in the top model. Pipeline identity and percent cover of sponges (%) were the main drivers of fish *species richness*. The MLA100 pipeline showed higher species richness on average than CBA300 (Supplementary Figure 12B). Species richness increased with availability of sponge habitat present at both pipelines.

Comparison of variable importance plots for sum abundance and species richness models confirmed GAM patterns. Pipeline identity was important for species richness but not abundance. Pipeline position was important for abundance but not species richness. Epibenthic height was important for both univariate metrics of the fish assemblage.

3.4.3 Comparison of fishery species with platform and pipeline communities

Pipelines communities comprised a different subset of fish and invertebrate species than platforms, with only ~25% of species (29 species out of 111 total species found among the four structures) observed at both types of structures (Figure 12). Overall, the platform communities of KFB and WKF were more similar to each other (20% shared species), than the pipeline communities (15% shared species).

TABLE 2 Summary of the ten most common (% of occurrence: #transects/total # of transects sampled), and the ten most abundant (Total #) fish species present at the CBA300 and MLA100 pipelines.

Pipeline	10 Most Common	% Transects	10 Most Abundant	Total Abundance
CBA300	Barred grubfish, *Parapercis allporti*	74.2	Stinkfish, *Foetorepus calauropomus*	237
	Unknown spp.	45.2	Jack mackerel, *Trachurus* spp.	178
	Perch, *Caesioperca* spp.	29.0	Barred grubfish, *Parapercis allporti*	166
	Stinkfish, *Foetorepus calauropomus*	25.8	Southern red scorpionfish, *Scorpaena papillosa*	123
	Butterfly perch, *Caesioperca lepidoptera*	22.6	Butterfly perch, *Caesioperca lepidoptera*	118
	Southern Maori wrasse, *Ophthalmolepis lineolatus*	19.4	Jack, *Carangidae* spp.	100
	Southern red scorpionfish, *Scorpaena papillosa*	19.4	Jackass morwong, *Nemadactylus macropterus*	89
	Jackass morwong, *Nemadactylus macropterus*	16.1	Splendid perch, *Callanthias australis*	45
	Jack mackerel, *Trachurus* spp.	16.1	Trevally, *Pseudocaranx* spp.	32
	Jack, *Carangidae* spp.	12.9	Reef ocean perch, *Helicolenus percoides*	25
MLA100	Barber perch, *Caesioperca razor*	87.1	Butterfly perch, *Caesioperca lepidoptera*	2899
	Butterfly perch, *Caesioperca lepidoptera*	77.4	Jack mackerel, *Trachurus* spp.	272
	Barred grubfish, *Parapercis allporti*	77.4	Southern red scorpionfish, *Scorpaena papillosa*	221
	Reef ocean perch, *Helicolenus percoides*	64.5	Barber perch, *Caesioperca rasor*	140
	Velvet leatherjacket, *Meuschenia scaber*	45.2	Barred grubfish, *Parapercis allporti*	138
	Halfbanded seaperch, *Hypoplectrodes maccullochi*	35.5	Stinkfish, *Foetorepus calauropomus*	128
	Stinkfish, *Foetorepus calauropomus*	32.3	Reef ocean perch, *Helicolenus percoides*	127
	Common gurnard perch, *Neosebastes scorpaenoides*	32.3	Velvet leatherjacket, *Meuschenia scaber*	61
	Jackass morwong, *Nemadactylus macropterus*	29.0	Jackass morwong, *Nemadactylus macropterus*	44
	Grey morwong, *Nemadactylus douglasii*	25.8	Rosy wrasse, *Pseudolabrus rubicundus*	37

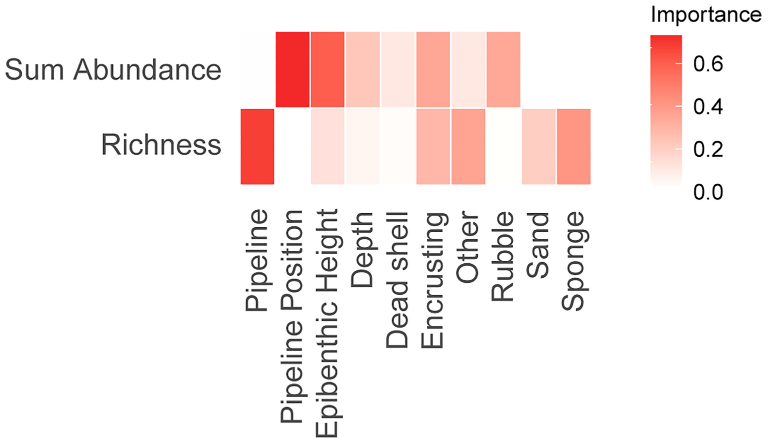

FIGURE 11
Variable importance plots for generalized additive models (GAM). Variables in dark red are the most important contributors. Variables in white were not selected in any of the fitted GAMs due to their low importance. Pipeline position refers to the extent of burial/spanning (see Figure 2). Other refers to instances where the habitat could not be determined.

When compared to the fishery data, the representation of fishery species among the O&G structures was low in terms of the number of species represented (< 10% of the total species accounted for in this study). The CTS and GHAT, the two main fisheries operating among the O&G structures, retained a diverse composition of fish and invertebrate species, with about a quarter of the total species retained in both fisheries despite differences in fishing gear and target species. The marine communities at the four O&G structures studied were diverse but hosted a different composition of species. Of the species documented in the ROV imagery, few species of commercial interest were observed (Supplementary Tables 2 and 4). ROV imagery included species not targeted for seafood markets, including fur seals, invertebrates such as sea stars, crabs and jellyfish, as well as fish species too small to be selected for in fishing gears, or considered not commercially valuable for a number of reasons.

4 Discussion

This is the first quantitative evaluation of marine communities of O&G structures comparing ROV imagery analysis with reported fishery data in Bass Strait. These descriptions also form important baseline data for future decommissioning discussions as these structures are > 40 years old with KFB one of the first platforms (installed in 1971) in Bass Strait and WKF in 1981, which make these the oldest Australian O&G structures and marine communities studied to-date (McLean et al., 2021a) and potentially the oldest *de facto* offshore ‘no-take’ areas in Bass Strait since fishing is excluded by default.

ROV imagery of the platforms showed diverse and well-established marine communities with significant depth variations. Greatest species richness and total abundance was

TABLE 3 Top Generalized Additive Models (GAM) for explaining relationships between fish abundance (total # fish/50 m) and fish species richness (# species/50 m), with explanatory variables relating to pipeline characteristics and benthic community composition (epibenthic height, pipeline position, depth, % cover of: dead shells, encrusting, other, rubble, sand, sponge).

	Best model	R^2	df	AICc	ΔAICc	Normalized RMSE (%)
Sum Abundance (total # fish per 50 m transect)	epibenthic height + pipeline position + encrusting	0.48	5.09	651.85	0	1.66
	epibenthic height + pipeline position + rubble	0.37	4.89	652.02	0.18	2.33
	epibenthic height + pipeline position	***0.35***	***3.00***	***652.05***	***0.21***	***2.21***
	pipeline position + depth + rubble	0.38	4.68	653.20	1.36	1.61
	pipeline position + encrusting + rubble	0.48	5.67	653.59	1.74	0.99
Species Richness (# fish species per 50 m transect)	***pipeline + sponge***	***0.25***	***3.00***	***311.93***	***0***	***0.55***
	encrusting + pipeline	0.29	3.68	312.37	0.44	0.52
	other + pipeline + sponge	0.29	4.64	312.41	0.48	0.54

benthic habitat categories that were uninformative for modelling purposes (> 85% proportion of zeros) were not used in modelling (ascidian, biofilm, calcareous, hydrozoa, macroalgae, shells, soft coral, turf). Selected models are shown in bold italics.

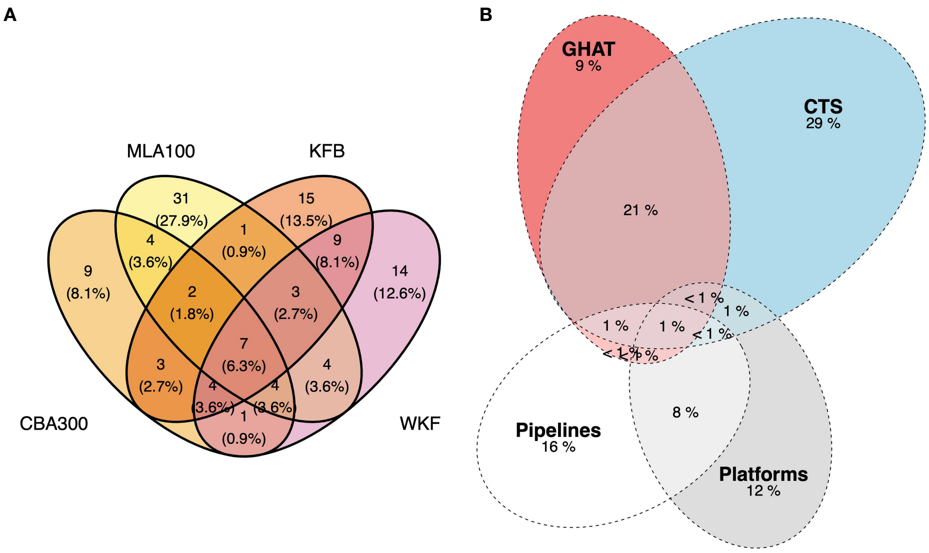

FIGURE 12
(A) Venn diagram showing the number and percent of shared species among the pipelines CBA300 and MLA100 and platforms KFB and WKF, **(B)** Euler diagram showing the percent overlap between retained catch species from commercial fisheries with oil and gas pipeline and platform communities. Species data included imagery analysis from Remotely Operated Vehicle surveys of two pipelines and two steel pile jackets and cumulative catch data from 2008-2018.

in > 60 m water depth and included many reef-associated fish species. Jackass morwong (*Nemadactylus macropterus*) and butterfly perches (*Caesioperca lepidoptera*) were abundant schooling species near the base of each platform. Jack mackerels (*Trachurus* spp.) formed large, dense schools at each platforms. These species are common to the soft sediments and rocky reefs of south-east Australia at similar depths (Williams and Bax, 2001).

Fish and invertebrate communities along pipelines were slightly more diverse (74 spp.) and comprised a different composition than platform communities (67 spp.). Pipelines, although not as vertically complex as platform environments, cover a larger spatial area across the seafloor. A few important fishery species were observed along pipelines including jackass morwong (*Nemadactylus macropterus*), bluespotted goatfish (*Upeneichthys vlamingii*), trevallies (Carangidae), rosy wrasse (*Pseudolabrus rubicundus*), flathead (Platycephalidae), flatfishes (Pleuronectiformes), gurnards (Triglidae) and octopus species. Pipeline communities included some important fishery species (e.g., flatheads *Platycephalus* spp. and octopus) not documented on platforms, as well as more benthic associated fish species. Pipelines also exhibited a different invertebrate community to platforms with sea urchins, mantis shrimps, sea stars, hermit crabs, and octopus observed. Some of these taxa burrow in the soft sediments surrounding the pipeline (e.g., octopuses' nest in soft sediments), and others may use pipelines as sources of food or shelter.

The fishing data provided an interesting direct comparison and also ecological and economic context to these marine communities. In terms of direct overlap with the fisheries data, O&G structures appear to provide little evidence for the species sought after commercially (i.e., target species), with few observations in the ROV imagery and relatively small subset of the total species included in this study (< 10%). Whether or not these O&G structures are important to fishery species and thus, important to fisheries, cannot be surmised yet and future research is needed to investigate these possible connections. Our study is the first to describe the diverse marine communities on a number of O&G structures in this region, and also the first to directly compare fishing effort and species composition. These structures may provide holistic benefits to the adjacent ecosystems by supporting abundant lower trophic level species and critical habitat for fish where comparable habitats would be few and far between. This is demonstrated by the pervasive fishing effort allocated throughout the area around O&G structures for the period studied. Fishery data and ROV imagery were collected by industry for different purposes and the historical imagery and the fishery reported species' catch data provided coarse taxonomic resolution. This lessens the ability to make meaningful interpretations from some of the data convergence as some species may be grouped together, and, therefore, result in underestimates of species diversity and richness. Further, the analysis of pipeline footage was a small proportion of the total pipeline network (~800 km) and ROV surveys were limited over short survey periods and could only provide 'snapshots' of species that may more broadly inhabit the region and structures. Each data sampling type has inherent biases, and it is noteworthy that some fishery species (e.g., whiting) may be more active at night and thus not observed in the subset of daytime imagery. Species like flatheads may be harder to observe if the benthic environment is not agitated as it is during fishing activities. It is possible to use imagery data for relative abundance estimates, however, we were limited to conservative measures as the ROV imagery was not gathered for the purposes of ecological assessment.

Of the 67 species recorded across both platforms, half of the species were unique to each platform (21 unique to KFB and 24 unique to WKF). This suggests there is high variance among O&G structures, despite similarities in age and location. Differences in the communities between KFB and WKF may point to differences between the platforms (e.g., jacket age or design) or sampling differences, such as the timing of the ROV surveys (Oct 2015 vs Apr – Jun 2017 respectively) and the limitations based on the quality and quantity of available imagery. Marine communities are temporally and spatially dynamic. There are likely differences in the seasonal distributions of fishes and invertebrates at O&G structures in Bass Strait. The presence of jellyfish and krill, as well as transitory species like sunfish (*Mola* spp.) may support this hypothesis. Jellyfish, krill (*Nyctiphanes australis*) and pyrosomes are key diet items linked to important South-east Australian fishery species (Blaber and Bulman, 1987; Young et al., 1996) and may indirectly be important to local fisheries. Gelatinous zooplankton temporarily store energy from seasonal phytoplankton blooms until they are eaten by jack mackerels or their predators southern bluefin tuna (*Thunnus maccoyii*, Young et al., 1996; Young et al., 1997). Krill is an important diet item for barracouta (*Thyrsites atun*) southern bluefin tuna, skipjack tuna (*Katsuwonus pelamis*), tiger flathead (*Platycephalus richardsoni*), and jack mackerel (*Trachurus* spp.) in continental shelf waters (Prince, 2001). The number of species common to both platforms (22 out of 67 total species observed) also highlight that greater sampling effort (both more replication and over a longer period of time) is needed to clarify which species are unique or if fish assemblages are mostly homogeneous with some seasonal differences. For instance, *Trachurus* spp., were highly abundant at WKF and KFB, these species are highly mobile and form dense schools but may be difficult to measure for accurate biomass estimates.

The frequent presence of large schools of mackerel/scads (*Trachurus* spp.) and other schooling fishes suggests that O&G platforms may attract these species. These fishes are important to the Small Pelagic Fishery of the Bass Strait and are important in marine food webs. South-east Australian fisheries may be sustained by offshore and pelagic resources with up to 90% of the primary productivity taken up by foraging fish species, which support the more commercially valuable piscivorous fishes (Prince, 2001). In other marine ecosystems these 'pelagic subsidies' support higher rates of productivity than would otherwise be expected (e.g., coral reefs, Morais and Bellwood, 2019 and deep ecosystems, Stasko et al., 2016). O&G structures are three-dimensional structures that extend throughout the water column; they may function as either a stopover or habitat refuge for transient species. Many offshore platforms are well-lit, which is the main attractant for squid jigging methods (Koopman et al., 2018) and may influence other species drawn in by light or light-attracted prey. Pelagic species are often attracted to fish aggregation devices (FADs, e.g., Rountree, 1989; Dempster and Kingsford, 2003), coastal fish farms (Sanchez-Jerez et al., 2011), and artificial reefs (Caley and St John, 1996; Champion et al., 2015). Without consistent standardized surveys it would be difficult to estimate potential fishery biomass for these (and other) species. For pelagic species egg and larval sampling are used for fishery production estimates. None of these species in the Small Pelagic Fishery are considered overfished or subject to overfishing. Compared to other fishery species, they are not of high commercial value, but total fishery value is not disclosed due to the small number of participating fishers (Australian Fisheries Management Authority (AFMA), 2021).

Analyzing marine communities around O&G pipelines revealed interesting parallels to other O&G regions around Australia, despite differences between tropical and temperate marine ecosystems. Quantitative models highlighted the importance of the type of benthic biota growing on pipelines and the space available under pipelines (free-spans), as drivers of higher fish abundance and species richness in North-west Australia (McLean et al., 2017; Bond et al., 2018b; McLean et al., 2020b). Sponges form important components of marine communities in tropical and temperate Australia (e.g., Pitcher et al., 2009; Schultz et al., 2014) and provide important habitats for many species. In this study, fish species richness increased with the extent of sponge habitat present, with this result similar to other studies where the percent cover of sponges was correlated with commercial fish species (McLean et al., 2017; McLean et al., 2020b). Parts of Bass Strait are known for extensive sponge habitats (Butler et al., 2002), and many of these benthic habitats have been modified by various fishing techniques (e.g., scallop dredges, trawl). Pipelines and platforms may provide large enough exclusion zones for pockets of habitat needed for fish and invertebrates to shelter, reproduce and forage similar to how wildlife corridors are used in terrestrial conservation practices (Lindenmayer and Nix, 1993).

O&G structures may fill similar roles to artificial reefs to augment habitat for marine communities, with the aim of benefitting local fisheries. O&G platforms demonstrate high productivity to comparable marine habitats (Claisse et al., 2014; Smith et al., 2016; Meyer-Gutbrod et al., 2020). Established (~20 year old) deeper O&G structures (82-135 m) could sustain both juvenile and adults of the serranid *Pseudanthias rubrizonatus* (Fowler and Booth, 2012) in NW Australia, which provide evidence that these structures do not just attract mobile species but may be self-sustaining. While research on offshore Australian temperate O&G structures is limited, there is a longer history of placing artificial reefs in near-coastal (e.g., Becker et al., 2017; Smith et al., 2017), or estuarine Australian temperate environments (e.g., Lowry et al., 2014) to benefit recreational fishers. These artificial reefs are not at similar depths or scales of construction, and therefore, can only cautiously inform how larger O&G structures in deeper (> 50 m depths), offshore environments may perform in this capacity. Artificial reefs have demonstrated that size, placement and design are important to consider (Champion et al., 2015; Blount et al., 2021) and this would be necessary if decommissioned O&G platforms are to be converted to artificial reefs. Becker et al., 2017 monitored a purpose-built artificial reef for fisheries enhancement in 38 m of water near Sydney Harbour. Over the four years of monitoring, they recorded high species richness (53 species) on the high-relief structure on par with the taxonomic richness of the steel pile jackets KFB and WKF. Similar to a caveat of this study, Becker et al. (2017) found it difficult to compare to 'control reefs' that differed fundamentally in design and isolation. A converted O&G structure off of Exmouth in NW Australia was repurposed in 2018 and artificial reef modules were added to increase the available habitat to 27,000 m^3, and within two years over 90 fish species were observed (Florisson et al., 2020). If decommissioned O&G structures are to be used to enhance local fisheries, then the autecology of target fishes should be considered (Champion et al., 2015; Smith et al., 2015). The optimal design and placement of underwater structures will differ for commercial and recreational fisheries, which use different fishing gears. Decommissioned O&G structures could provide both positive and negative impacts on fisheries and deep marine habitats and these should be carefully considered (reviewed in Macreadie et al., 2011).

South-east Australia is the largest fishery for benthic or near-bottom 'groundfishes' and is important for the domestic Australian seafood market (Williams and Bax, 2001). Many types of commercial fishing off the Victorian coast target soft-bottomed habitats, to prevent benthic gear (e.g., Danish seine, trawl, gillnets, scallop dredges) from being destroyed or lost (Prince, 2001; Williams and Bax, 2001). Ensnarement on the seabed is one of the most common causes of lost fishing gear (Richardson et al., 2019). Fishers avoid unknown habitats (where they have not fished before) and rely on benthic sounders to investigate the seabed and look for acoustic fish signals (Prince, 2001). Future decommissioning decisions that involve leaving pipelines in place may result in impacts to fishers, dependent on their subsequent ability to fish around these pipelines. For example, commercial trap fishers in North-west Australia target subsea pipelines (Bond et al., 2021) while commercial trawlers in the North Sea experience gear loss associated with pipelines (Rouse et al., 2020). Pipelines host a different subset of fishery species and fishers may avoid risky situations depending on fishing gear type (e.g., pipeline spans that may hook gear). If pipelines are left in place, they will have different consequences for future Bass Strait navigation and fishing activities.

The O&G structures are likely important fishing exclusion zones for certain length classes of important fishery species, but without accurate length information (e.g., confirmation from extractive surveys or calibrated stereo imagery) and information on the movements of these species (e.g., tag-recapture, acoustic tracking), we can only hypothesize as to the potential ecological role of these structures. Based on what has been documented in other areas of south-east Australia (New South Wales, Tasmania), these O&G platforms off the Victorian coast may benefit local fisheries but these direct links have not been established. How far offshore these species move, either with adult or larval dispersal, is not known. Neira (2005) used opportunistic plankton surveys on O&G structures and provided some evidence that these structures may be important for early life history stages of some fish species. The plankton catch included larval forms of adult fish observed by ROV around the KFB and WKF platforms (e.g., *Trachurus* spp., *Pseudocaranx* spp. and *C. affinis*) but these plankton surveys also sampled many fish species not documented in the ROV imagery. Plankton surveys will collect a different subset of species, which may connect O&G structures to other components of the Bass Strait ecosystem. For instance, some of the plankton caught included species not found among the platforms from shallow water (e.g., dragonet, *Bovichtus angustifrons* and king gar, *Scomberesox saurus*), inshore species (e.g., eastern Australian salmon, *Arripis trutta*), pelagic species (e.g., mahi mahi, *Coryphaena hippurus*) and deep mesopelagic species (e.g., Myctophidae, Neira, 2005). Other complementary sampling methods will be necessary to establish larval connectivity and evidence of juveniles recruiting to local fisheries. Research on the role of platforms for larval fish in California (Love et al., 2019) and the Gulf of Mexico (Hernandez et al., 2003), indicate platforms can perform functions similar to nursery grounds for commercially important fish species. Genetic techniques such as parentage analysis may also be useful for establishing if platform communities have direct linkages to fishes caught elsewhere (Harrison et al., 2012).

Australian fur seals (*Arctocephalus pusillus*) were observed in footage from both platforms. These marine mammals are known to associate with O&G structures (Todd et al., 2020a) but the types of interactions have not been quantified for Bass Strait platforms. Fur seals have been documented foraging along O&G pipelines in this region (Arnould et al., 2015). From the ROV imagery this is also a common behavior that may be correlated with ROV activities (i.e., using lights or waiting for the ROV to stir up prey). Prey items including jack mackerels (*Trachurus* spp.), rock cods (*Pseudophycis* spp.), wrasses (Labridae), marblefish (*Aplodactylus arctidens*), common gurnard perch (*Neosebastes scorpaenoides*), reef ocean perch (*H. percoides*) and leatherjackets (Monocanthidae) were identified from otoliths retrieved from fur seal diet and scat samples

(Kirkwood et al., 2008). The northern Bass Strait has been a key location of fur seal breeding since the 1980s and Australian populations are still in recovery (Kirkwood et al., 2010). Primary pupping occurs on neighboring Bass Strait islands and fur seals may use platforms for teaching and hunting opportunities. Fur seals that use platforms may also gain some temporary protection from fishing as fur seals are sometimes accidental bycatch during fishing activities in south-east Australia (Australian Fisheries Management Authority (AFMA), 2019).

Although there were limitations on both data types used in this study, both are important to document the ecology of the region, which has been anthropogenically modified through fishing and O&G activities, resulting in a 'novel ecosystem' (Hobbs et al., 2006; Morse et al., 2014; van Elden et al., 2019). Visual imagery is useful to understand the behavior and location of marine life within O&G structures (Macreadie et al., 2018), which complements the fishery-dependent data of how communities vary in space and time. Future studies would benefit from more precise and robust data collection. The implementation of electronic logbooks has improved the timeliness of data capture, for example, but there is still room for improvement in species identification. When O&G structures began being built off the Victorian coastline in the late 1960s, these anthropogenic structures also influenced the marine communities but the direct and indirect effects of these physical structures on the biological community have largely been unknown. Many of these offshore structures are deep (> 30 m), restricting the ability of direct observations until the advent of underwater visual survey methods (e.g., towed cameras, ROVs, BRUVS). The marine communities around O&G structures may resemble some natural communities but are 'novel ecosystems' from the intentional or unintentional results of human activities (Hobbs et al., 2006). Novel ecosystems may have different species compositions and relative abundances than natural states (van Elden et al., 2019). The information on marine communities in the region is largely fishery-dependent data (e.g., Coleman and Mobley, 1984), with some O&G-specific information from limited past surveys on larval fish abundances near O&G structures (Neira, 2005). There have been no other published studies of the marine communities associated with these structures, which include some of the oldest O&G assets in Australia's Exclusive Economic Zone, providing a historical element to the ecosystem modifications through time. Therefore, the information on fish and invertebrate species near and around O&G structures from this study provide useful 'snapshots' for this area of Australia. This information also contributes to understanding how Australian O&G structures compare to the infrastructure in other places of the world (e.g., North Sea, Gulf of Mexico, California) and provides a better understanding of how fish and invertebrate communities are adapting in the Anthropocene.

In summary, platforms house diverse and well-established communities of fish, invertebrates and benthic biota, with the greatest abundance of marine life at the base of these structures. Further, pipelines provide complex habitat where abundant invertebrates and fish are found but the composition of species is different among platforms and pipelines, with different subsets of fishery species observed near the platforms and pipelines surveyed. This means that pipeline and platform may have different decommissioning scenarios with some structures left in place for their habitat value. Although there was some overlap in fishery species observed between O&G structures it would be difficult to quantify direct and measured consequences of decommissioning with the caveats of the available data. We have described the marine communities around O&G structures using the existing industry-collected data, which is a critical first step to both understanding the ecological and successional role of O&G structures and how decommissioning these structures may affect the broader ecosystem. We have also identified a number of ways to improve future data collection for this region. It is important to remember that decommissioning activities will have direct effects on other local industries, such as fishing, with the greatest influence on local fishing fleets that regularly fish near the O&G structures.

Data availability statement

The original contributions presented in the study are included in the article/Supplementary Material. Further inquiries can be directed to the corresponding author.

Ethics statement

Ethical review and approval was not required for the animal study because no animals were collected as part of this research. This study included existing data sets of commercial fishing catch and underwater video methods.

Author contributions

TS, PM and DM conceived the study. TS and KC analyzed video data. TS analyzed fishery data. IY assisted with figures and formatting. TS and KC wrote the first draft of the manuscript and all authors contributed during multiple rounds of feedback. All authors contributed to the article and approved the submitted version.

Funding

EARPL provided the funding for publication fees of this manuscript and for the research allocation for TS, IY and KC.

Acknowledgments

We appreciate Esso Australia Resources Pty Ltd. for providing us access to their ROV imagery. Azivy Che Aziz and Sheela Veluayitham supported this research and provided contextual information on EARPL operations. Part of this manuscript appeared as an internal report for EARPL in 2021. We would like to thank Kehani Manson for fulfilling our AFMA data request. Thanks to our colleagues Martin Gomon, Dianne Bray and Joanne Taylor at Museums Victoria, Jeff Leis and Rudy Kuiter for their expertise and invaluable resources.

Conflict of interest

The reviewer SVE declared a shared affiliation with the authors KC and DM to the handling editor at the time of review.

The remaining authors declare that the research was conducted in the absence of any commercial or financial relationships that could be construed as a potential conflict of interest.

Publisher's note

Supplementary material

The Supplementary Material for this article can be found online at: https://www.frontiersin.org/articles/10.3389/fmars.2022.979212/full#supplementary-material

References

Ajemian, M. J., Wetz, J. J., Shipley-Lozano, B., and Stunz, G. W. (2015). Rapid assessment of fish communities on submerged oil and gas platform reefs using remotely operated vehicles. *Fisheries Res.* 167, 143–155. doi: 10.1016/j.fishres.2015.02.011

Althaus, F., Hill, N., Ferrari, R., Edwards, L., Przeslawski, R., Schönberg, C. H. L., et al. (2015). A standardised vocabulary for identifying benthic biota and substrata from underwater imagery: the CATAMI classification scheme. *PLOS ONE* doi: 10.1371/journal.pone.0141039

Anderson, M. J. (2001). A new method for non-parametric multivariate analysis of variance. *Aust. Ecol.* 26, 32–46. doi: 10.1111/j.1442-9993.2001.01070.pp.x

Anderson, M., Gorley, R. N., and Clarke, R. K. (2008). *Permanova+ for primer: Guide to software and statistical methods* (Plymouth, UK: Primer-E).

Anderson, M. J., and Millar, R. B. (2004). Spatial variation and effects of habitat on temperate reef fish assemblages in northeastern New Zealand. *J. Exp. Mar. Biol. Ecol.* 305, 191–221. doi: 10.1016/j.jembe.2003.12.011

Arnould, J. P. Y., Monk, J., Ierodiaconou, D., Hindell, M. A., Semmens, J., Hoskins, A. J., et al. (2015). Use of anthropogenic sea floor structures by Australian fur seals: potential positive ecological impacts of marine industrial development? *PloS One* 10 (7), e0130581. doi: 10.1371/journal.pone.0130581

Austin, M. (2007). Species distribution models and ecological theory: A critical assessment and some possible new approaches. *Ecol. Model.* 200, 1–19. doi: 10.1016/j.ecolmodel.2006.07.005

Australian Biological Resources Study (ABRS) (2020) *Australian Faunal directory*. Available at: https://biodiversity.org.au/afd/home.

Australian Fisheries Management Authority (AFMA) (2019) *Commonwealth trawl sector (Otterboard trawl and Danish seine) bycatch and discarding workplan 2018-2019*. Available at: https://www.afma.gov.au/sites/default/files/cts_bycatch_and_discarding_workplan_2018-19_0.pdf?acsf_files_redirect.

Australian Fisheries Management Authority (AFMA) (2021) *Small pelagic fishery* (Canberra, ACT). Available at: https://www.afma.gov.au/fisheries/small-pelagic-fishery.

Australian Fisheries Management Authority (AFMA) (2022) *Reported retained annual catch from commonwealth fisheries logbooks - dataset*. Available at: https://data.gov.au/data/dataset/reported-retained-annual-catch-from-commonwealth-fisheries-logbooks (Accessed April 11, 2022).

Australian Government (2018). *Offshore petroleum decommissioning guideline* (Canberra, ACT: Australian Government Department of Industry, Science, Energy and Resources). Available at: www.nopta.gov.au.

Becker, A., Taylor, M. D., and Lowry, M. B. (2017). Monitoring of reef associated and pelagic fish communities on australia's first purpose built offshore artificial reef. *ICES J. Mar. Sci.* 74, 277–285. doi: 10.1093/icesjms/fsw133

Birchenough, S. N. R., and Degraer, S. (2020). Science in support of ecologically sound decommissioning strategies for offshore man-made structures: taking stock of current knowledge and considering future challenges. *ICES J. Mar. Sci.* 77 (3), 1075–1078. doi: 10.1093/icesjms/fsaa039

Blaber, S. J. M., and Bulman, C. M. (1987). Diets of fishes of the upper continental slope of eastern Tasmania: content, calorific values, dietary overlap and trophic relationships. *Mar. Biol.* 95 (3), 345–356. doi: 10.1007/BF00409564

Blount, C., Komyakova, V., Barnes, L., Smith, M. L., Zhang, D., Reeds, K., et al. (2021). Using ecological evidence to refine approaches to deploying offshore artificial reefs for recreational fisheries. *Bull. Mar. Sci.* 97, 665–698. doi: 10.5343/bms.2020.0059

Bond, T., Langlois, T. J., Partridge, J. C., Birt, M. J., Malseed, B. E., Smith, L., et al. (2018a). Diel shifts and habitat associations of fish assemblages on a subsea pipeline. *Fisheries Res.* 206, 220–234. doi: 10.1016/j.fishres.2018.05.011

Bond, T., McLean, D. L., Wakefield, C. B., Partridge, J. C., Prince, J., White, D., et al. (2021). Quantifying fishing activity targeting subsea pipelines by commercial trap fishers. *Rev. Fish Biol. Fish.* 31, 1009–1023. doi: 10.1007/S11160-021-09686-4/FIGURES/8

Bond, T., Partridge, J. C., Taylor, M. D., Langlois, T. J., Malseed, B. E., Smith, L. D., et al. (2018b). Fish associated with a subsea pipeline and adjacent seafloor of the north West shelf of Western Australia. *Mar. Environ. Res.* 141, 53–65. doi: 10.1016/j.marenvres.2018.08.003

Bray, D. J., and Gomon, M. F. (2021) *Fishes of australia. museums Victoria and OzFishNet*. Available at: http://fishesofaustralia.net.au.

Brunsdon, C., Fotheringham, A. S., and Charlton, M. E. (1996). Geographically weighted regression: A method for exploring spatial nonstationarity. *Geogr. Anal.* 28, 281–298. doi: 10.1111/j.1538-4632.1996.tb00936.x

Bull, A. S., and Love, M. S. (2019). Worldwide oil and gas platform decommissioning: A review of practices and reefing options. *Ocean Coast. Manage.* 168 (October 2018), 274–306. doi: 10.1016/j.ocecoaman.2018.10.024

Burnham, K., and Anderson, D. (2002). *Model selection and multimodel inference: A practical information-theoretic approach* (Berlin, New York: Springer-Verlag).

Butler, A., Althaus, F., Furlani, D., and Ridgway, K. (2002). *Assessment of the conservation values of the bass strait sponge*. Available online: https://parksaustralia.gov.au/marine/pub/scientific-publications/archive/conservation-assessment-bass.pdf.

Caley, M. J., and St John, J. (1996). Refuge availability structures assemblages of tropical reef fishes. *J. Anim. Ecol.* 65, 414–428. doi: 10.2307/5777

Champion, C., IM, S., and JA, S. (2015). Zooplanktivory is a key process for fish production on a coastal artificial reef. *Mar. Ecol. Prog. Ser.* 541, 1–14. doi: 10.3354/meps11529

Claisse, J. T., Pondella, D. J., Love, M., Zahn, L. A., Williams, C. M., Williams, J. P., et al. (2014). Oil platforms off California are among the most productive marine fish habitats globally. *Proc. Natl. Acad. Sci.* 111, 15462–15467. doi: 10.1073/pnas.1411477111

Clarke, K. R., and Gorley, R. N. (2005). PRIMER: Getting started with v6. PRIMER-e Ltd: Plymouth, UK.

Coleman, N., and Mobley, M. (1984). Diets of commercially exploited fish from bass strait and adjacent Victorian waters, south-eastern Australia. *Mar. Freshw. Res.* 35 (5), 549–560. doi: 10.1071/MF9840549

Commonwealth Scientific and Industrial Research Organisation (CSIRO) (2014) *Securing the future of australia's commercial fisheries - CSIRO*. Available at: https://www.csiro.au/en/research/animals/Fisheries/Harvest-Strategy-Policy (Accessed May 3, 2022).

Dempster, T., and Kingsford, M. J. (2003). Homing of pelagic fish to fish aggregation devices (FADs): the role of sensory cues. *Mar. Ecol. Prog. Ser.* 258, 213–222. doi: 10.3354/meps258213

Department of Jobs, Precincts and Regions (DJPR) (2021) *Oil and gas in Victoria - earth resources*. Available at: https://earthresources.vic.gov.au/geology-exploration/oil-gas/oil-and-gas-in-victoria (Accessed March 24, 2022).

Edgar, G. J. (1997). "Australian Marine life the plants and animals of temperate waters," in *Reed books* (Victoria, Australia: New Holland).

Ellis, D., and DeMartini, E. (1995). Evaluation of a video camera technique for indexing abundances of juvenile pink snapper, *Pristipomoides filamentosus*, and other Hawaiian insular shelf fishes. *Fish Bull.* 93, 67–77. Available at: https://spo.nmfs.noaa.gov/content/evaluation-video-camera-technique-indexing-abundances-juvenile-pink-snapper-pristipomoides

Emery, T., Marton, N., Woodhams, J., and Curtotti, R. (2021). "Commonwealth trawl and scalefish hook sectors," in *Department of agriculture, water and the environment commonwealth trawl and scalefish hook sectors* (Canberra, ACT: Department of Agriculture). Available at: https://www.agriculture.gov.au/abares/research-topics/fisheries/fishery-status/trawl-scalefish-hook-sectors.

Esso Australia (2022) *Esso history*. Available at: https://www.exxonmobil.com.au/company/who-we-are/esso-history (Accessed October 11, 2022).

Fisheries Research and Development Corporation (FRDC) (2020) *Status of Australian fish stocks reports*. Available at: https://www.fish.gov.au (Accessed May 3, 2022).

Fisher, R., Wilson, S. K., Sin, T. M., Lee, A. C., and Langlois, T. J. (2018). A simple function for full-subsets multiple regression in ecology with r. *Ecol. Evol.* 8, 6104–6113. doi: 10.1002/ece3.4134

Florisson, J. H., Rowland, A. J., Harvey, E. S., Allen, M. B., Watts, S. L., Saunders, B. J., et al. (2020). King reef: An Australian first in repurposing oil and gas infrastructure to benefit regional communities. *APPEA J.* 60, 435–439. doi: 10.1071/AJ19134

Fowler, A. M., and Booth, D. J. (2012). Evidence of sustained populations of a small reef fish on artificial structures. does depth affect production on artificial reefs? *J. Fish Biol.* 80, 613–629. doi: 10.1111/j.1095-8649.2011.03201.x

Fowler, A. M., Jørgensen, A. M., Coolen, J. W. P., Jones, D. O. B., Svendsen, J. C., Brabant, R., et al. (2020). The ecology of infrastructure decommissioning in the north Sea: what we need to know and how to achieve it. *ICES J. Mar. Sci.* 77 (3), 1109–1126. doi: 10.1093/icesjms/fsz143

Goetze, J. S., Langlois, T. J., McCarter, J., Simpfendorfer, C. A., Hughes, A., Leve, J. T., et al. (2018). Drivers of reef shark abundance and biomass in the Solomon islands. *PlosONE* 13, e0200960. doi: 10.1371/journal.pone.0200960

Gomon, M., Bray, D., and Kuiter, R. H. (2008). *Fishes of australia's southern coast* (Australia: New Holland Publishers).

Gowlett-Holmes, K. (2008). *A field guide to the marine invertebrates of south Australia* (Tasmania, Australia: Notomares).

Great Southern Reef (GSR) (2021). *Great southern reef* (Australia: The Great Southern Reef project). Available at: https://greatsouthernreef.com.

Harrison, H. B., Williamson, D. H., Evans, R. D., Almany, G. R., Thorrold, S. R., Russ, G. R., et al. (2012). Larval export from marine reserves and the recruitment benefit for fish and fisheries. *Curr. Biol.* 22, 1023–1028. doi: 10.1016/j.cub.2012.04.008

Hastie, T., and Tibshirani, R. (1986). Generalized additive models. *Stat. Sci.* 1, 297–310. doi: 10.1214/ss/1177013604

Hastings, R. W., Ogren, L. H., and Mabry, M. T. (1976). Observations on the fish fauna associated with offshore platforms in the northeastern gulf of Mexico. *Fish. Bull.; (United States)* 74 (2), 387–402. Available at: https://spo.nmfs.noaa.gov/content/observations-fish-fauna-associated-offshore-platforms-northeastern-gulf-mexico

Hernandez, F. J., Shaw, R. F., Cope, J. S., Ditty, J. G., Farooqi, T., and Benfield, M. C. (2003). The across-shelf larval, postlarval, and juvenile fish assemblages collected at offshore oil and gas platforms west of the Mississippi river delta. *Am. Fisheries Soc. Symposium* 36, 39–72.

Hobbs, R. J., Arico, S., Aronson, J., Baron, J. S., Bridgewater, P., Cramer, V. A., et al. (2006). Novel ecosystems: Theoretical and management aspects of the new ecological world order. *Global Ecol. Biogeography* 15 (1), 1–7. doi: 10.1111/j.1466-822X.2006.00212.x

Jones, D. S., and Morgan, G. J. (2002). *A field guide to crustaceans of Australian waters: 2nd edition* (Australia: New Holland Publishers).

Kashubsky, M., and Morrison, A. (2013). Security of offshore oil and gas facilities: exclusion zones and ships' routeing. *Aust. J. Maritime Ocean Affairs* 5 (1), 1–10. doi: 10.1080/18366503.2013.10815725

Kirkwood, R., Hume, F., and Hindell, M. (2008). Sea Temperature variations mediate annual changes in the diet of Australian fur seals in bass strait. *Mar. Ecol. Prog. Ser.* 369, 297–309. doi: 10.3354/meps07633

Kirkwood, R., Pemberton, D., Gales, R., Hoskins, A. J., Mitchell, T., Shaughnessy, P. D., et al. (2010). Continued population recovery by Australian fur seals. *Mar. Freshw. Res.* 61, 695–701. doi: 10.1071/MF09213

Koopman, M., Knuckey, I., and Cahill, M. (2018) *Improving the location and targeting of economically viable aggregations of squid available to the squid jigging method and the fleet's ability to catch squid* (Queenscliff, VIC). Available at: https://www.afma.gov.au/sites/default/files/afma_project_2016_0809_-_improving_targeting_of_squid.pdf (Accessed May 3, 2022).

Larsson, J. (2021) *Eulerr: Area-proportional Euler and Venn diagrams with ellipses_. r package version 6.1.1*. Available at: https://CRAN.R-project.org/package=eulerr.

Lehmann, A., Overton, J. M., and Leathwick, J. R. (2002). GRASP: generalized regression analysis and spatial prediction. *Ecol. Modell* 157, 189–207. doi: 10.1016/S0304-3800(02)00195-3

Lindenmayer, D. B., and Nix, H. A. (1993). Ecological principles for the design of wildlife corridors. *Conserv. Biol.* 7, 627–630. doi: 10.1046/j.1523-1739.1993.07030627.x

Love, M. S., Caselle, J. E., and Snook, L. (2000). Fish assemblages around seven oil platforms in the Santa Barbara channel area. *Fishery Bull.* 98 (1), 96–117. Available at: https://spo.nmfs.noaa.gov/content/fish-assemblages-around-seven-oil-platforms-santa-barbara-channel-area

Love, M. S., Claisse, J. T., and Roeper, A. (2019). An analysis of the fish assemblages around 23 oil and gas platforms off California with comparisons with natural habitats. *Bull. Mar. Sci.* 95 (4), 477–514. doi: 10.5343/bms.2018.0061

Lowry, M. B., Glasby, T. M., Boys, C. A., Folpp, H., Suthers, I., and Gregson, M. (2014). Response of fish communities to the deployment of estuarine artificial reefs for fisheries enhancement. *Fisheries Manage. Ecol.* 21, 42–56. doi: 10.1111/fme.12048

Macreadie, P. I., Fowler, A. M., and Booth, D. J. (2011). Rigs-to-reefs: will the deep sea benefit from artificial habitat? *Front. Ecol. Environ.* 9, 455–461. doi: 10.1890/100112

Macreadie, P. I., McLean, D. L., Thomson, P. G., Partridge, J. C., Jones, D. O. B., Gates, A. R., et al. (2018). Eyes in the sea: unlocking the mysteries of the ocean using industrial, remotely operated vehicles (ROVs). *Sci. Total Environ.* 634, 1077–1091. doi: 10.1016/j.scitotenv.2018.04.049

McLean, D., Bond, T., Harvey, E. S., Ierodiaconou, D., Cure, K., Taylor, M., et al. (2021a). Importance of australia's offshore oil and gas infrastructure for fish. *APPEA J.* 61, 429–437. doi: 10.1071/AJ20106

McLean, D. L., Cure, K., Abdul Wahab, M. A., Galaiduk, R., Birt, M., Vaughan, B., et al. (2021b). A comparison of marine communities along a subsea pipeline with those in surrounding seabed areas. *Continental Shelf Res.* 219, 104394. doi: 10.1016/j.csr.2021.104394

McLean, D. L., Parsons, M. J. G., Gates, A. R., Benfield, M. C., Bond, T., Booth, D. J., et al. (2020a). Enhancing the scientific value of industry remotely operated vehicles (ROVs) in our oceans. *Front. Mar. Sci.* 7 (April). doi: 10.3389/fmars.2020.00220

McLean, D. L., Partridge, J. C., Bond, T., Birt, M. J., Bornt, K. R., and Langlois, T. J. (2017). Using industry ROV videos to assess fish associations with subsea pipelines. *Continental Shelf Res.* 141 (December 2016), 76–97. doi: 10.1016/j.csr.2017.05.006

McLean, D. L., Taylor, M. D., Ospina, A. G., and Partridge, J. C. (2019). An assessment of fish and marine growth associated with an oil and gas platform jacket using an augmented remotely operated vehicle. *Continental Shelf Res.* 179, 66–84. doi: 10.1016/j.csr.2019.04.006

McLean, D. L., Vaughan, B. I., Malseed, B. E., and Taylor, M. D. (2020b). Fish-habitat associations on a subsea pipeline within an Australian marine park. *Mar. Environ. Res.* 153, 104813. doi: 10.1016/j.marenvres.2019.104813

Meyer-Gutbrod, E. L., Love, M. S., Schroeder, D. M., Claisse, J. T., Kui, L., and Miller, R. J. (2020). Forecasting the legacy of offshore oil and gas platforms on fish community structure and productivity. *Ecol. Appl.* 30 (8), 1–16. doi: 10.1002/eap.2185

Morais, R. A., and Bellwood, D. R. (2019). Pelagic subsidies underpin fish productivity on a degraded coral reef. *Curr. Biol.* 29 (9), 1521–1527.e6. doi: 10.1016/j.cub.2019.03.044

Morse, N. B., Pellissier, P. A., Cianciola, E. N., Brereton, R. L., Sullivan, M. M., Shonka, N. K., et al. (2014). Novel ecosystems in the anthropocene: A revision of the novel ecosystem concept for pragmatic applications. *Ecol. Soc.* 19 (2), 12. doi: 10.5751/ES-06192-190212

Neira, F. J. (2005). Summer and winter plankton fish assemblages around offshore oil and gas platforms in south-eastern Australia. *Estuarine Coast. Shelf Sci.* 63 (4), 589–604. doi: 10.1016/j.ecss.2005.01.003

Novaglio, C., Smith, A. D. M., Frusher, S., Ferretti, F., Klaer, N., and Fulton, E. A. (2018). Fishery development and exploitation in south East Australia. *Front. Mar. Sci.* 5, 145. doi: 10.3389/fmars.2018.00145

Paxton, A. B., Shertzer, K. W., Bacheler, N. M., Kellison, G. T., Riley, K. L., and Taylor, J. C. (2020). Meta-analysis reveals artificial reefs can be effective tools for fish community enhancement but are not one-Size-Fits-All. *Front. Mar. Sci.* doi: 10.3389/fmars.2020.00282

Pitcher, C. R., Doherty, P. J., and Anderson, T. J. (2009). "Seabed environments, habitats and biological assemblages," in *The great barrier reef: biology, environment and management* (Dordrecht: Springer), 551–558.

Potts, J. M., and Elith, J. (2006). Comparing species abundance models. *Ecol. Modell* 199, 153–163. doi: 10.1016/j.ecolmodel.2006.05.025

Prince, J. D. (2001). Ecosystem of the south East fishery (Australia), and fisher lore. *Mar. Freshw. Res.* 52 (4), 431–449. doi: 10.1071/MF00042

QGIS.org (2022). *QGIS geographic information system* (QGIS Association). Available at: https://www.qgis.org/en/site/.

R Core Team (2020). "R: A language and environment for statistical computing," in *R foundation for statistical computing* (Vienna, Austria: the R Project). Available at: https://www.R-project.org/.

Richardson, K., Hardesty, B. D., and Wilcox, C. (2019). Estimates of fishing gear loss rates at a global scale: A literature review and meta-analysis. *Fish Fisheries* 20 (6), 1218–1231. doi: 10.1111/faf.12407

Rountree, R. A. (1989). Association of fishes with fish aggregation devices: effects of structure size on fish abundance. *Bull. Mar. Sci.* 44 (2), 960–972. Available at: https://www.ingentaconnect.com/content/umrsmas/bullmar/1989/00000044/00000002/art00040#

Rouse, S., Hayes, P., and Wilding, T. A. (2020). Commercial fisheries losses arising from interactions with offshore pipelines and other oil and gas infrastructure and activities. *ICES J. Mar. Sci.* 77 (3), 1148–1156. doi: 10.1093/icesjms/fsy116

Sanchez-Jerez, P., Fernandez-Jover, D., Uglem, I., Arechavala-Lopez, P., Dempster, T., Bayle-Sempere, J. T., et al. (2011). "Coastal fish farms as fish aggregation devices (FADs)," in *Artificial reefs in fishery management* (FL, USA: CRC Press. Taylor & Francis Group), 187–208.

Schultz, A. L., Malcolm, H. A., Bucher, D. J., Linklater, M., and Smith, S. D. A. (2014). Depth and medium-scale spatial processes influence fish assemblage structure of unconsolidated habitats in a subtropical marine park. *PloS One* 9 (5). doi: 10.1371/journal.pone.0096798

SeaGIS (2021a) *EventMeasure software*. Available at: https://www.seagis.com.au/event.html.

SeaGIS (2021b) *TransectMeasure software*. Available at: https://www.seagis.com.au/transect.html.

Shaw, J. L., Seares, P., and Newman, S. J. (2018). *Decommissioning offshore infrastructure: A review of stakeholder views and science priorities* (Perth: Western Australian Marine Science Institute). Available at: www.wamsi.org.au/decommissioning-offshore-infrastructure-reviewstakeholder-views-and-science-priorities.

Smith, J. A., Cornwell, W. K., Lowry, M. B., and Suthers, I. M. (2017). Modelling the distribution of fish around an artificial reef. *Mar. Freshw. Res.* 68, 1955. doi: 10.1071/MF16019

Smith, J. A., Lowry, M. B., Champion, C., and Suthers, I. M. (2016). A designed artificial reef is among the most productive marine fish habitats: new metrics to address 'production versus attraction.'. *Mar. Biol.* 163, 188. doi: 10.1007/s00227-016-2967-y

Smith, J. A., Lowry, M. B., and Suthers, I. M. (2015). Fish attraction to artificial reefs not always harmful: A simulation study. *Ecol. Evol.* 5, 4590–4602. doi: 10.1002/ece3.1730

Sommer, B., Fowler, A. M., Macreadie, P. I., Palandro, D. A., Aziz, A. C., and Booth, D. J. (2018). Decommissioning of offshore oil and gas structures - environmental opportunities and challenges. *Sci. Total Environment.* 658, 973–981. doi: 10.1016/j.scitotenv.2018.12.193

Stasko, A. D., Swanson, H., Majewski, A., Atchison, S., Reist, J., and Power, M. (2016). Influences of depth and pelagic subsidies on the size-based trophic structure of Beaufort Sea fish communities. *Mar. Ecol. Prog. Ser.* 549, 153–166. doi: 10.3354/meps11709

Thomson, P. G., Fowler, A. M., Davis, A. R., Pattiaratchi, C. B., and Booth, D. J. (2018). Some old movies become classics – a case study determining the scientific value of ROV inspection footage on a platform on australia's north West shelf. *Front. Mar. Sci.* 5 (DEC). doi: 10.3389/fmars.2018.00471

Todd, V. L. G., Lavallin, E. W., and Macreadie, P. I. (2018). Quantitative analysis of fish and invertebrate assemblage dynamics in association with a north Sea oil and gas installation complex. *Mar. Environ. Res.* 142, 69–79. doi: 10.1016/j.marenvres.2018.09.018

Todd, V. L. G., Lazar, L., Williamson, L. D., Peters, I. T., Hoover, A. L., Cox, S. E., et al. (2020a). Underwater visual records of marine megafauna around offshore anthropogenic structures. *Front. Mar. Sci.* 7, 230. doi: 10.3389/fmars.2020.00230

Todd, V. L. G., Williamson, L. D., Cox, S. E., Todd, I. B., and Macreadie, P. I. (2020b). Characterizing the first wave of fish and invertebrate colonization on a new offshore petroleum platform. *ICES J. Mar. Sci.* 77 (3), 1127–1136. doi: 10.1093/icesjms/fsz077

van der Stap, T., Coolen, J. W. P., and Lindeboom, H. J. (2016). Marine fouling assemblages on offshore gas platforms in the southern north Sea: Effects of depth and distance from shore on biodiversity. *PloS One* 11 (1), e0146324. doi: 10.1371/journal.pone.0146324

van Elden, S., Meeuwig, J. J., Hobbs, R. J., and Hemmi, J. M. (2019). Offshore oil and gas platforms as novel ecosystems: A global perspective. *Front. Mar. Sci.* 6 (548). doi: 10.3389/fmars.2019.00548

Wickham, H. (2016). *ggplot2: Elegant graphics for data analysis* (Verlag New York: Springer).

Wickham, H., Averick, M., Bryan, J., Chang, W., McGowan, L. D., Francois, R., et al. (2019). Welcome to the tidyverse. *J. Open Source Software* 4 (43), 1686. doi: 10.21105/joss.016861

Wilkinson, L. (2012). Exact and approximate area-proportional circular Venn and Euler diagrams. *IEEE Trans. Visualization Comput. Graphics (Internet).* 18 (2), 321–31. doi: 10.1109/TVCG.2011.56

Williams, A., and Bax, N. J. (2001). Delineating fish-habitat associations for spatially based management: An example from the south-eastern Australian continental shelf. *Mar. Freshw. Res.* 52 (4), 513–536. doi: 10.1071/MF00017

Willis, T., and Babcock, R. (2000). A baited underwater video system for the determination of relative density of carnivorous reef fish. *Mar. Freshw. Res.* 51, 755–763. doi: 10.1071/MF00010

Wilson, R., Norman, M., and Syme, A. (2010). *An introduction to marine life* (Melbourne, Australia: Museums Victoria), 166 p.

Yan, L. L. (2021) *Ggvenn: Draw Venn diagram by 'ggplot2'. r package version 0.1.9*. Available at: https://CRAN.R-project.org/package=ggvenn.

Young, J. W., Bradford, R. W., Lamb, T. D., and Lyne, V. D. (1996). Biomass of zooplankton and micronekton in the southern bluefin tuna fishing grounds off eastern Tasmania, Australia. *Mar. Ecol. Prog. Ser.* 138, 1–14. doi: 10.3354/meps138001

Young, J. W., Lamb, T. D., Le, D., Bradford, R. W., and Whitelaw, A. W. (1997). Feeding ecology and interannual variations in diet of southern bluefin tuna, *Thunnus maccoyii*, in relation to coastal and oceanic waters off eastern Tasmania, Australia. *Environ. Biol. Fishes* 50 (3), 275–291. doi: 10.1023/A:1007326120380

frontiers | Frontiers in Marine Science

TYPE Original Research
PUBLISHED 10 January 2023
DOI 10.3389/fmars.2022.1022168

Influence of oyster and seaweed cultivation facilities on coastal environment and eukaryote assemblages in Matsushima Bay, northeastern Honshu, Japan

Yutaka Okumura[1]*, Yoshio Masuda[2],
Minenosuke Matsutani[3] and Akihiro Shiomoto[4]

[1]Fisheries Resource Institute/Fisheries Technology Institute, Japan Fisheries Research and Education Agency, Shiogama, Japan, [2]Miyagi Prefecture Fisheries Technology Institute, Ishinomaki, Japan, [3]NODAI Genome Research Center, Tokyo University of Agriculture, Tokyo, Japan, [4]Faculty of Bioindustry, Tokyo University of Agriculture, Abashiri, Japan

OPEN ACCESS

EDITED BY
Daniel Joseph Pondella,
Occidental College, United States

REVIEWED BY
Hideki Fukuda,
The University of Tokyo, Japan
Gouranga Biswas,
Central Institute of Fisheries Education (ICAR), India

*CORRESPONDENCE
Yutaka Okumura
✉ okumura@affrc.go.jp

SPECIALTY SECTION
This article was submitted to Marine Ecosystem Ecology, a section of the journal Frontiers in Marine Science

RECEIVED 18 August 2022
ACCEPTED 19 December 2022
PUBLISHED 10 January 2023

CITATION
Okumura Y, Masuda Y, Matsutani M and Shiomoto A (2023) Influence of oyster and seaweed cultivation facilities on coastal environment and eukaryote assemblages in Matsushima Bay, northeastern Honshu, Japan. *Front. Mar. Sci.* 9:1022168. doi: 10.3389/fmars.2022.1022168

The northeastern coast of Japan suffered a massive tsunami in 2011, a natural disaster which ‘reset’ the coastal ecosystem when it destroyed much of the original sealife and scoured the seabed. This has presented an opportunity to learn more about the load on coastal ecosystems exerted by human exploitation such as aquaculture rafts and areas of anchored and float-suspended ropes. We surveyed the coastal environment in Matsushima Bay for approximately four years following the year after the occurrence of the 2011 tsunami. Phytoplankton abundance increased with increasing water temperature. Nutrient concentrations were high at the exit of a small branch of the Ofuna-iri Canal (entering the southwestern inner part of the bay at Shiogama) but no significant differences in nutrient concentrations were observed at other stations, so it is considered that the aquaculture installations in Matsushima Bay currently have no significant effect on observed nutrient concentrations. The composition of eukaryotes in the surface seawater varied with the year and the season, but there were no clear differences between sampling stations. The lack of any differences in nutrient concentrations or eukaryote assemblages between areas with or without aquaculture installations is considered to be a result of efficient seawater exchange, despite the presence of many small islets separating Matsushima Bay from the open ocean. In addition, the aquaculture installations at present number less than half of the maximum number before the tsunami, so the bay is by no means overexploited by aquaculture. It is concluded that the current aquaculture installations have no major negative impact on the environment in Matsushima Bay.

KEYWORDS

natural disaster, aquaculture, microorganisms, next generation sequencing, coast

1 Introduction

Matsushima Bay is a small sheltered region of Sendai Bay, just northwest of Sendai in northeastern Honshu, Japan (Figure 1). The area ranges from 35 km^2 to about 50 km^2 with a maximum depth of 4 to 5 m (Watanabe 1977, Ota et al., 2019). It is the site of many rafts for oyster (*Crassostrea gigas*) cultivation (Ito and Oshino, 2018), and rope-based installations for cultivation of seaweeds such as wakame (*Undaria pinnatifida*) and konbu (*Saccharina japonica*) (Nagaki et al., 2015). These installations comprise natural- or non-feeding aquaculture. Oysters feed themselves by filtering seawater to remove phytoplankton (Akashige et al., 2005), and seaweeds compete with phytoplankton to use nutrients in seawater as they grow (Nagaki et al., 2015; Yoshida et al., 2011). The periphyton attached to the surfaces of oyster shells, ropes, and aquaculture installations also filters seawater and removes phytoplankton (Ciavatta et al., 2020). In addition, larvae derived from shellfish and the periphyton are periodically present in the seawater (Kakehi et al., 2016; Ciavatta et al., 2020).

Aquaculture installations may affect the abundance and the composition of the eukaryote assemblages in seawater, and sheltered bays can be affected easily by anthropogenic sources such as the inflow of water from sewage treatment plants (Okumura et al., 2021a), as well as inflows from rivers during heavy rainfall (Kakehi et al., 2020). Major nutrients include dissolved inorganic nitrogen (DIN) and dissolve inorganic phosphate (DIP) in river water (Officer and Ryther, 1980), and DIN contained in the effluent from wastewater plants (Okumura et al., 2021a). Silica is supplied to the coast by rivers (Officer and Ryther, 1980; Taniuchi et al., 2017).

Both anthropogenic and natural nutrient input can affect phytoplankton growth, since phytoplankton organisms absorb nitrogen (N) and phosphorus (P) for growth, and in addition diatoms require silicate (Si) for frustule formation (Treguer et al., 1995). If nutrient loading is excessive, eutrophication results (Breitburg et al., 2018), and if the balance between N, P and Si is disrupted, phytoplankton composition changes (Officer and Ryther, 1980). Also, eutrophication causes anoxia (Breitburg et al., 2018), and an imbalance of nutrient concentrations leads to an increase in the presence of phytoplankton communities unsuitable for aquaculture (Officer and Ryther, 1980). To ensure that natural- and non-feeding aquaculture are sustainable, it is necessary to avoid overexploitation by overcrowding, which leads to poor growth due to a reduction in available feed and nutrients, extended time for successful cultivation, and culture products of poor quality. Therefore, if the number of aquaculture facilities is properly managed, the effects of eutrophication or problems with the reduced availability of natural feed organisms can be minimized. In this study, we investigated whether the oyster and seaweed culture facilities have an impact on the marine environment and eukaryote assemblages in Matsushima Bay, and the significance of the impact of culture facilities compared with other anthropogenic influences and the natural environment.

Matsushima Bay is located within a region severely affected by the 2011 Great East Japan Earthquake and tsunami. Since it is a sheltered bay protected from the open sea by numerous small islets, the tsunami height in Matsushima Bay was lower than outside the bay (Nagashima et al., 2016; Ota et al., 2019). Even so, the tsunami destroyed almost all of the aquaculture installations in the bay and the environment related to natural- and non-feeding aquaculture was ‘reset’. Outside Matsushima Bay, the broader effects of the tsunami on phytoplankton have been investigated in Sendai Bay: there were apparently no tsunami effects on phytoplankton phenology (Taniuchi et al., 2017) or diatom assemblages (Watanabe et al., 2017) but toxic dinoflagellate species increased after the disaster (Kamiyama et al., 2014; Masuda et al., 2014; Ishikawa et al., 2015), because of easy cyst germination after redeposition of cysts to the seafloor surface following seafloor disturbance by the tsunami. It has been reported that the environment of the seafloor in Matsushima Bay has improved after the tsunami (Oota et al., 2017; Ota et al., 2019), and that deterioration of the functioning of a sewage treatment plant had an unexpectedly small impact (Okumura et al., 2021a). However, there have been few reports concerning phytoplankton other than diatoms and dinoflagellates, microbial assemblages other than phytoplankton, and or the minor phyla.

In Matsushima Bay, a mass mortality of oysters occurred in 2013, which apparently was caused by the oysters being covered with periphyton to which suspended matter was attached, reducing oxygen availability and resulting in death of the oysters (Ito and Oshino, 2018). It is important to understand whether the amount of periphyton increased dramatically due to post-tsunami effects, or was at the same level as before the tsunami, but unfortunately there were no data available on this prior to 2011. In recent years, the development of next-generation sequencing (NGS) has enabled study of a wide range of organisms, from bacteria and other microorganisms to fish (De Vargas et al., 2015; Miya et al., 2015; Nimnoi and Pongsilp, 2020). If appropriate samples have been preserved over the study period required, it is possible to use NGS retrospectively to investigate fluctuations in periphyton organisms.

The present study makes use of samples preserved from environmental and eukaryotes surveys that were conducted in Matsushima Bay over a two-year period a few years before the tsunami. These samples enable comparison with samples taken after the tsunami, from which it is possible to investigate the effects of the presence versus absence of aquaculture installations on the environment and on the eukaryote composition.

2 Materials and methods

2.1 Measurements

The samples used in this study were obtained from Matsushima Bay from 2004 to 2005 (12 stations, B1 to B12), and from 2012 to 2016 (18 stations, non-prefixed numbers; Figure 1). Surface seawater samples were collected with a bucket and analyzed for nutrient concentrations as reported previously (Okumura et al., 2021a). Seawater was also filtered to obtain DNA samples for sequencing and pigment analysis (although no pigment analysis was possible for the 2004 to 2005 samples). Since 2012, salinity, water temperature, dissolved oxygen (DO), and pH have been measured routinely using a Conductivity, Temperature, and Depth (CTD) profiler (RINKO-Profiler, JFE-Advantech, Hyogo, Japan). Water clarity was measured routinely using Secchi Disk depth. The data on salinity and water temperature for the 16 post-tsunami stations have been published already (Okumura et al., 2021a).

2.2 Pigment analyses

The variations in phytoplankton abundance per taxon were approximated by determining seawater pigment composition. Samples (150 ml) of seawater were filtered through Whatman GF/F glass microfiber filters (GE Healthcare UK Ltd., Buckinghamshire, England). Phytoplankton pigments were extracted from the filter with 1 ml methanol at -18°C for at least one day. The methanol-soluble fraction was centrifuged at 17,000 × g for 10 min, and the supernatant was subjected to pigment analysis by high performance liquid chromatography (HPLC; Shimadzu, Kyoto, Japan) using the method of Zapata et al. (Zapata et al., 2000), with the additional insertion of an HPLC guard column before the analytical column. The HPLC system included the following components: auto injector (SIL-10ADvp), degasser (DGU-14A), low pressure gradient unit (FCV-10ALvp), pump (LC-20AD), column oven (CTO-20AC), diode array detector (SPD-M10Avp), fluorescence detector (RF-10AXL), and a communication bus module (CBM-20A). It was controlled by Class-vp software (Shimadzu, Kyoto, Japan).

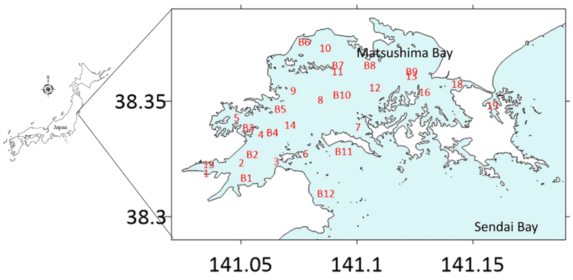

FIGURE 1
Sampling stations in Matsushima Bay (enlarged map, with the position of Matsushima Bay indicated on a smaller-scale map of Japan at left). Large numerals in black are longitude and latitude coordinates. Alphanumerics in red indicate the position of individual sampling stations. Matsushima Bay is roughly divided into areas of seaweed cultivation (Stn. 2 to Stn. 4), areas free of cultivation (Stn. 1, Stn. 15 to Stn. 2 and Stn. 6), and oyster cultivation (other stations). Stn. 1 (at Shiogama, at the southwestern edge of Matsushima Bay) is at the entrance to the bay from a small branch of Ofuna-iri Canal (the southern portion of the Teizan Canal system, which runs parallel to the coast of Sendai Bay a few hundred metres inland). Stations 13 and B9 are the closest to the entrance to Tona Canal (the northeastern continuation of the canal system which connects with the Naruse River before continuing as the Kitakami Canal to Ishinomaki). Investigations for 2004 to 2005 were conducted at stations B1 to B12.

2.3 DNA sequencing of 18S rDNA by Miseq DNA sequencer and data analysis

To understand the composition of eukaryotic organisms in the seawater in Matsushima Bay and compare them before and after the earthquake, DNA sequencing was conducted on 18SrRNA genes isolated from seawater. Samples (500 ml) of seawater were filtered through a 0.45μm PVDF Durapore membrane filter (Merck, Darmstadt, Germany) and DNA was extracted using 1mL SNET-Cl buffer (20mM Tris•HCl(pH 8.0), 5 mM EDTA, 0.3% SDS; Shimadzu Corporation, (2019)) containing 200 µg/mL proteinase K (final concentration), vortexed and then incubated at 55°C for 2 h and then at 90°C for 10 min. After the filter was removed from the lysis buffer, the liquid phase containing nucleic acids was separated by centrifugation at 17,000 × g for 10 min. The supernatant from each sample was used as a PCR template. The PCR enzyme was KOD FX of DNA polymerase (Toyobo, Osaka, Japan) (TOYOBO, 2019). The primer pair was TAReuk454FWD1 and TAReukREV3 (Stoeck et al., 2010), with an adapter attached outside of the primer for analysis by Miseq (Illumina, California, U.S.A.). All procedures, such as the PCR reaction, treatment of amplicons, DNA sequencing, and data analysis, were performed as reported previously (Okumura et al., 2021b).

2.4 Changes in aquaculture production and the number of aquaculture facilities

To estimate the number of aquaculture facilities in Matsushima Bay, we examined the amounts of oyster, wakame seaweed, and kelp cultivated in each survey year and the number of aquaculture facilities after the earthquake. Cultivation volumes for each organism were aggregated from statistical data (https://www.maff.go.jp/j/tokei/kouhyou/kaimen_gyosei/index.html). The production volume of wakame in Shiogama (near Matsushima Bay) after the earthquake was not available from data provided by the Ministry of Agriculture, Forestry and Fisheries, Japan (MAFF), so we used data provided by the fishery cooperatives.

The number of aquaculture installations for oyster, wakame and konbu was counted based on information provided by the fishing cooperatives of Matsushima Bay.

Annual statistical data in Japan are often published for the financial year period from April to March of the following year, rather than as a complete calendar year from January to December. The data reported here therefore range from April of year 'n' to March of year 'n+1'. The members of some fishing cooperatives used aquaculture rope lengths of 3.9 m up to 2012, but increased the length to 4.5 m after 2013. The rope length was longer, and as a result, the number of aquaculture installations decreased after 2013. In order to make valid comparisons of the amount of aquaculture conducted across the years 2011 to 2017, the number of installations before 2012 was converted to the equivalent of the number of installations for 2012 by multiplying by 3.9/4.5. Data from 2004 to 2005 is not available because records had already been discarded by the fishery cooperatives.

2.5 Statistical analyses

To understand the influence of sampling sites on environmental factors, multiple comparisons were performed using EZR ver. 1.54 (a GUI-based addition to the 'R' package; (Kanda, 2013) to test for differences of environment among sampling stations. All data for dissolved inorganic nitrogen (NH_4-N, NO_3+NO_2-N), dissolved inorganic phosphate (DIP), DO, and chlorophyll a (Chl *a*) concentration were aggregated by station. Multiple comparisons by the nonparametric Kruskal-Wallis test of Steel-Dwass were then performed to make comparisons among three or more groups.

To understand the influence of environmental factors on phytoplankton abundance, the major pigment concentrations and environmental parameters (nutrients NH_4-N, NO_3+NO_2-N, DIP, DO and pH) were subjected to Redundancy Analysis (RDA) using Canoco 5 (ter Braak and Šmilauer, 2018). The pigment concentrations used were Chl *a*, Chl *b*, Fucoxanthin (Fuco) and Peridinin (Perid). The concentrations of the four pigments in each sample were entered into Canoco 5 as "samples" items, and the environmental data (NH_4-N, NO_3+NO_2-N, DIP, DO and pH) in each sample were entered as "environment" items.

To assess the yearly, monthly and station variation in diversity of eukaryotes in the seawater samples, non-metric multi-dimensional scaling (MDS) was performed using Primer 6 (Quest Research Ltd., Massey University, Auckland, New Zealand) according to the provider's manual. MDS proceeded in the following order: data transformation to fourth roots; Bray-Curtis matrix similarity; cluster of group average; and finally MDS. To compare the composition of eukaryotes by year, the ratio of all data obtained by NGS were analyzed by MDS. As the eukaryote composition from 2004 to 2005 was largely different from those after 2012, only data after 2012 were used in the MDS comparison by month and station.

3 Results

3.1 Changes in aquaculture volumes and number of aquaculture facilities

After the earthquake, production figures for oyster and konbu were less than half of pre-earthquake levels, while wakame production increased (Table 1). Oyster production exceeded 1,000 t in 2005, but was halved to approximately 350 t in 2016. Konbu production exceeded 400 t before the earthquake, but was only approximately 100 t at most after the earthquake, although accurate data for 2012 and 2013 are not available due to the post-disaster confusion. Wakame production increased after the earthquake compared to pre-disaster values. In particular, production in 2012 exceeded 600 t, and was more than seven times the pre-disaster level of approximately 80 t. Wakame production declined to around 100 t after 2013.

The numbers of aquaculture facilities from April 2012 to March 2016 are displayed in Table 2. The mean number of each type of installation was 744 oyster rafts, 1724 wakame ropes, and 100 konbu ropes. There were more konbu installations in 2012: approximately 150 (more than 40 more than in any other year).

TABLE 1 Harvest in Matsushima Bay.

	2004	2005	2012	2013	2014	2015	2016
Oyster (soft body)	769	1048	75	169	341	330	347
Konbu	472	418	*	*	31*	101*	99*
Wakame	70	80	627	196	168	134	174

unit tonne, *:data were obtained from fishery cooperative association.

TABLE 2 The number of aquaculture installations in Matsushima Bay.

	2012Ap. ~2013Mar.	2013Ap. ~2014Mar.	2014Ap. ~2015Mar.	2015Ap. ~2016Mar.
Oyster	628	766	796	786
Konbu	147	102	92	60
Wakame	1899	1571	1762	1666

3.2 Seasonal changes of water temperature, salinity, phytoplankton pigment content, nutrients, and water clarity

To understand the effect of the environment on phytoplankton communities in Matsushima Bay, mean monthly values (± S.D.) of environmental parameters in surface seawater were compared (Figure 2). The monthly mean water temperature in Matsushima Bay ranged from 3.2°C to 29.9°C, with annual fluctuations of more than 20°C (Figure 2A). The temperature exceeded 20°C from June to October in 2012-2014 and from June to September in 2015. The monthly mean of salinity ranged from 20.2 PSU to 32.5 PSU: salinity declined during the summer to below 30 PSU from June to August 2012, July to October 2013, April to September 2014, May 2015, and July to September 2015. Water temperatures 0.5 m above the seabed tended to be higher than those at the surface during winter, and lower during summer (Supplemental Figure 1A). Salinity 0.5 m above the seabed tended to be higher than at the surface (Supplemental Figure 1A).

The monthly mean of dissolved inorganic nitrogen (DIN) and dissolved inorganic phosphorus (DIP) ranged from 0.56 to 22.68 µM, and 0.06 to 1.55 µM, respectively (Figure 2B). DIN and DIP tended to be high in the autumn.

Concerning pigment concentrations, the monthly mean for Chl *a* tended to be lower from autumn to winter, when water temperatures were lower, and ranged from 0.83 to 6.9 µg/L (Figure 2C). For the periods in October 2012, from November 2013 to February 2014, from November 2014 to February 2015, and from November 2015 to February 2016, mean monthly Chl a was below 2 µg/L. The trend of variation in Chl *a* was similar to that of other pigments. In particular, there was higher correlation between Fuco and Chl *a* (correlation r^2 = 0.81), than the other pigments measured (for Peridinin, Alloxanthin, and Chl *b*; r^2 = 0.44, 0.57, and 0.67, respectively; Supplemental Figure 2). The monthly mean of water clarity (as measured by Secchi disc) ranged from 1.4 to 4 m, and tended to be clearer during autumn and winter, when Chl *a* levels were low (Figure 2D).

Although pigment concentrations changed with environmental parameters, and were particularly influenced by

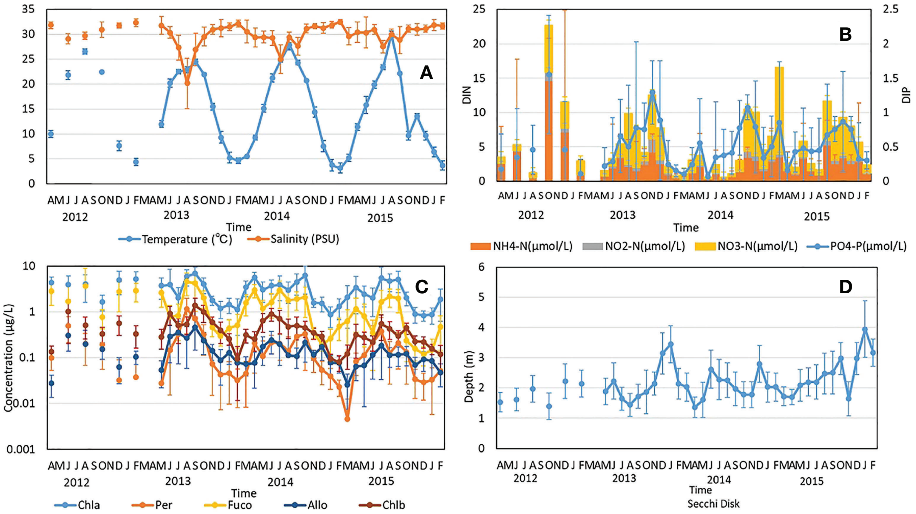

FIGURE 2
Monthly fluctuations in environmental parameters and pigment concentrations from April, 2012 to Feb., 2016. **(A)** Sea surface temperature and salinity. **(B)** Inorganic nitrogen-containing compounds and phosphate. **(C)** Pigment concentrations (see text for key to abbreviations). **(D)** Secchi Disk depth.

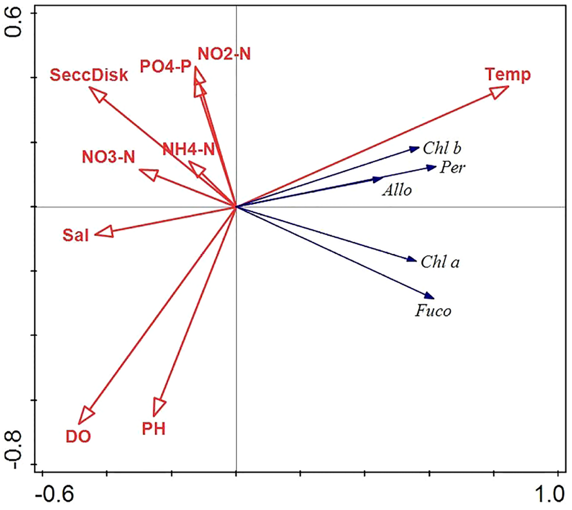

FIGURE 3
Biplot. Redundancy Analysis loading plot of the influence of environmental factors on phytoplankton abundance. Sal, salinity); DO, dissolved oxygen. Nutrients are represented by measurements of PO_4-P, NH_4-N, NO_2-N and NO_3-N. Secchi Disk, Secchi disk depth measure of water clarity.

water temperature in Matsushima Bay, RDA (Figure 3) reveals that changes of pigment concentrations (measures of total photosynthetic tissue present) were positively related to temperature and negatively related to salinity, nutrient concentrations, Secchi disk reading (indicator of seawater turbidity), DO and pH. The magnitude of the water-temperature vector was the largest among the environmental parameters.

3.3 The composition of eukaryotes as indicated by 18S rRNA genes

The occurrence of eukaryotes classified according to the Silva database showed the following order of abundance (expressed as mean frequency of occurrence for all periods measured): SAR supergroup (0.63) > Archaeplastida (0.14) > Opisthokonta (0.13) > Cryptophyceae (0.08), and these four taxa accounted for 98% of the total (Figure 4). The SAR monthly means of all stations fluctuated between 0.3 and 0.89, tending to decrease in winter, such as in December 2013, December 2014, and December 2015, except for June 2013. In these periods, Chl *a* and Fuco concentrations also decreased (Figure 2B). In 2005 (before the earthquake), the mean SAR was 0.64 and the pigment compositions resembled those after the earthquake (Figure 4). However, in 2004, SAR (0.44) and Opisthokonta (0.40) were present in similar amounts, while the occurrence of eukaryotes differed compared to other years.

The monthly mean frequency of Archaeplastida fluctuated between 0.03 and 0.41, tending to increase during periods when SAR organisms were relatively scarce. The monthly means for Opisthokonta varied between 0.02 and 0.51, with particularly high occurrence (mean 0.40) in 2004. The occurrence of Cryptophyceae varied from almost zero to 0.36, and increased when SAR organisms were relatively scarce, as also with Archaeplastida.

The taxa detected were mostly phytoplankton, ciliates and zooplankton. Among the SAR taxa, Alveolata and Straminopila accounted for a large proportion (with fewer Rhizaria), with means for the entire period of 48% and 42%, respectively (Figure 5A). Within the Alveolata, Dinoflagellata formed the largest proportion, followed by Ciliophora (= ciliates)

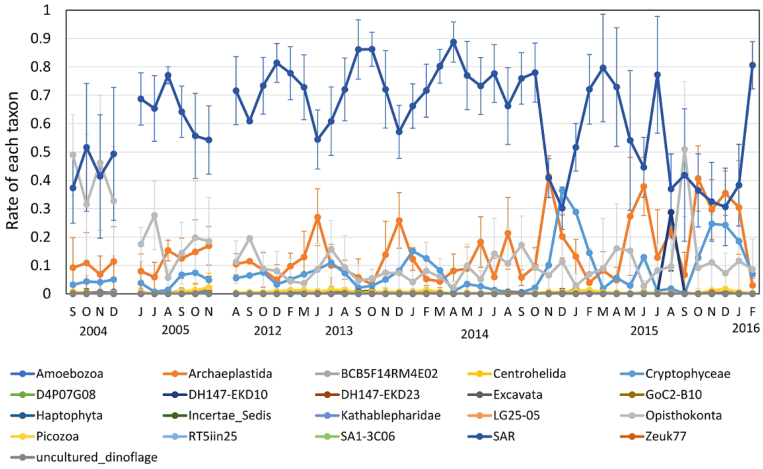

FIGURE 4
18S rRNA gene composition in surface seawater analyzed by NGS. Classification follows the Silva Database.

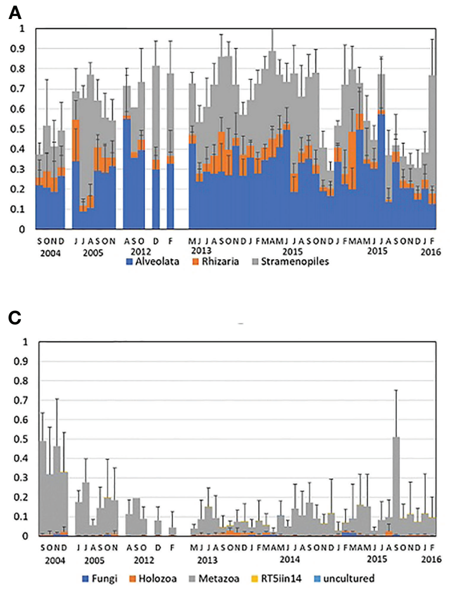

FIGURE 5
Periodic mean relative composition of the three components of **(A)** the SAR supergroup for Sept. 2004 to Nov. 2005, and for Aug. 2012 to Feb. 2016; **(B)** the Chloroplastida and Rhodophyceae; and **(C)** the Fungi, Holozoa, and Metazoa. The original data is the same as in Figure 5. All classification follows the Silva Database.

(Supplemental Figure 3). Within the Straminopila, the commonest were the Bacillariophyceae (= diatoms). Among the Archaeplastida (Rhodophyceae and Chlorophyceae), Chlorophyceae were dominant at more than 90% (Figure 5B, Supplemental Figure 4). Except for the ciliates, almost all the four major taxa were phytoplankton. Among the Opisthokonta, the bryozoan *Alcyonidium* (Metazoa) was associated with aquaculture rafts and was dominant in 2004; and members of the crustacean group Maxillopoda were the dominant metazoans throughout the period (Figure 5C, Supplemental Figure 5).

3.4 Horizontal distribution of environmental parameters

Chl *a* and nutrient concentrations at some stations showed significant differences from those at others, while DO was fairly consistent across all stations (Figure 6). The medians of Chl *a* ranged from 1.1 to 3.9 μg/L, and the concentration showed a three-fold difference among stations (Figure 6A). Chl *a* at Stn. 19, at the eastern end of the bay (Figure 1), was significantly lower than at the other stations. Chl *a* in Stns. 2 and 15 (at the western and eastern inner parts of the bay, respectively) appear to be at higher concentrations than the other stations, but the differences were not significant. The median of monthly values of DO ranged from 7.9 to 9.6 mg/L (Figure 6B). DO at Stn. 1, at the mouth of a small branch off the Ofuna-iri Canal, appears to be lower than at the other stations, but there were no significant differences among the stations. The medians of PO_4-P (Figure 6C), NH_4-N (Figure 6D), and NO_2+NO_3 (Figure 6E) ranged from 0.19 to 2.16 μM, 0.21 to 10.28 μM, and 0.07 to 14.63 μM, respectively. The median concentrations of PO_4-P, NH_4-N, and NO_2+NO_3 differed across stations by about 10, 50, and 200 times, respectively. Both DIP and DIN were significantly higher at Stn. 1 near the mouth of the canal branch (Figures 6C–E). Except for Stn.1, there were no significant differences among the other stations.

3.5 Non-metric multi-dimensional scaling (MSD) analysis

The degree of biodiversity detected in the seawater of Matsushima Bay tended to vary with the year (Figure 7). Eukaryote assemblages in 2004 differed greatly from other years (Figure 7A). Biodiversity also tended to show monthly variation (Figure 7B). The data after 2012 tended to aggregate as monthly clusters, and the data for July, August, and September each year clustered differently than for the other months (Figure 7B). Composition beyond 2012 showed no clear differences among the stations (Figure 7C). Rather than differences by location, composition tended to vary by month and year (Figures 7A–C).

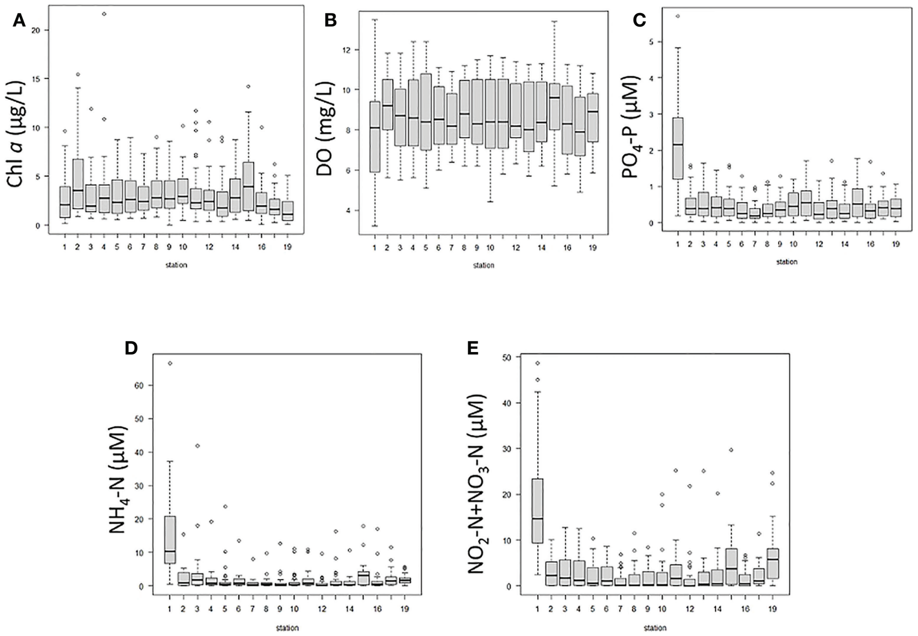

FIGURE 6
Box plots comparing sampling stations 1-19 (see Figure 1) for each environmental parameter from Oct. 2012 to Feb. 2016, analyzed by EZR. Dark horizontal lines are medians, within boxes indicating lower and upper quartiles. Dotted lines indicate 95 percentile minima and maxima. Circles indicate outliers.

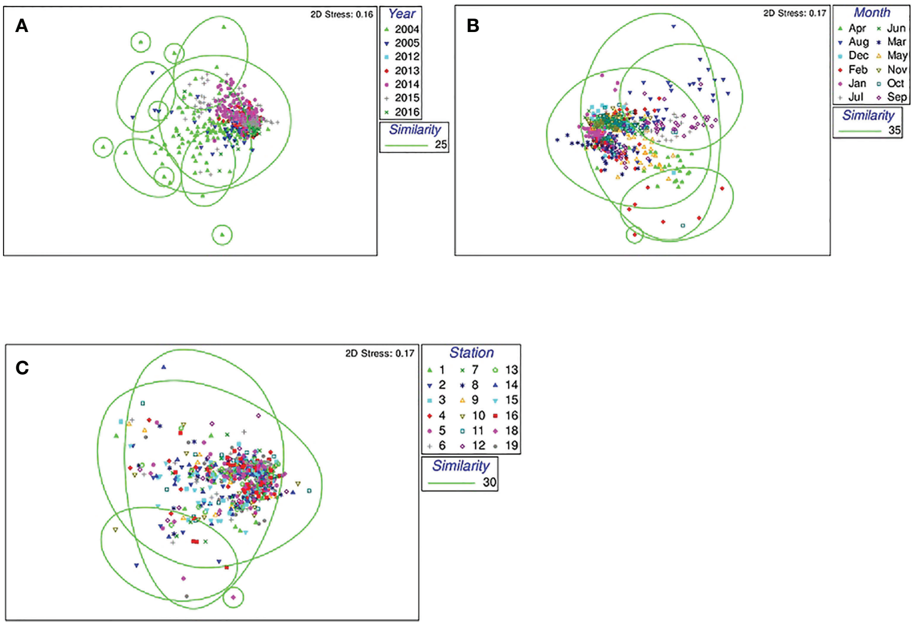

FIGURE 7
Diversity of eukaryote communities **(A)** comparing different years; **(B)** comparing different months of the year after 2012; and **(C)** sampling stations 1-19 after 2012 by MDS.

4 Discussion

The growth characteristics of phytoplankton in Matsushima Bay differed from the general mechanism of the spring bloom. Normally, vertical mixing in winter raises nutrients from lower layers to the surface layer, where increased solar radiation and water temperature cause a spring bloom; then in summer the nutrient supply is interrupted by establishment of the thermocline, and the bloom ends when phytoplankton have consumed all the dissolved nutrients available. In the rest of Sendai Bay outside Matsushima Bay (see Figure 1), Chl *a* concentration peaks from winter to spring, while nutrients increase from fall to winter and decrease from spring to summer (Watanabe et al., 2017). From July (after the end of the spring bloom) to January, Chl *a* concentrations was lower, sometimes less than 1 μg/L (Taniuchi et al., 2017). However Chl *a* concentrations in Matsushima Bay were often remained above 2 μg/L, and was high almost continuously from spring to fall or even extending into winter (Figure 2C).

RDA analysis showed a negative relationship for salinity, nutrients, turbidity, DO, and pH; and a strong positive relationship between water temperature and pigment concentrations (Figure 3). Therefore, phytoplankton growth in Matsushima Bay was not limited by nutrient concentrations, and changed in line with increasing or decreasing water temperature. Regarding the relationship between nutrients and major pigment concentrations, nutrient levels were low during periods of high Chl *a* and Fuco concentrations during the spring and autumn in 2014 (Figures 2B, C). The reason for this is considered to be consumption and decrease of nutrients by phytoplankton growth.

Salinity was continuously below 30 during the same period (Figure 2A). The salinity in Sendai Bay, excluding Matsushima Bay, has been reported to decrease in summer in the range of 26.9 to 34.2 (Watanabe et al., 2017), while the salinity in Matsushima Bay was found to be generally lower, in the range of 20.2 to 32.5 (Figure 2A). The lower salinity in Matsushima Bay is attributed to the constant inflow of river water, which is also higher in nutrient concentrations than the seawater nearby (Okumura et al., 2021a). Although lower in quantity than river water, there was also treated-water inflow from wastewater plant *via* the canal mouth near Stn. 1 (Okumura et al., 2021a). Indeed, the highest concentrations of nutrients in Matsushima Bay were higher than those in the surrounding seawater of Sendai Bay. Even excluding Stn. 1 at the canal mouth (where nutrient concentrations are extremely high due to anthropogenic influences), the highest concentrations of NO_2-N+NO_3-N and DIP was 29.62 μM and 1.77 μM, respectively, in Matsushima Bay (Figures 6C–E). In Oginohama, further up the coast in the northern part of Sendai Bay, NO_2-N+NO_3-N and DIP were 18.1 μM and 0.96 μM, respectively (Kamiyama et al., 2005), and 3.07 μM and 0.36 μM in Sendai Bay (Taniuchi et al., 2017). Also, diatoms can store nutrients in vacuoles (Raven, 1987; Falkowski et al., 1998; Falkowski and Oliver, 2007) and may be able to withstand starvation for a short period of time. Since nutrients were maintained at levels that did not cause starvation (because they were constantly being supplied from rivers and anthropogenic sources), it seems that phytoplankton growth was maintained during low nutrient concentrations. As a result, Chl *a* and Fuco were high even during conditions of low nutrient concentrations.

The NGS results showed that most of the microorganisms detected in the seawater were phytoplankton, with a high proportion of diatoms and dinoflagellates (Figures 4, 5A). High proportions of diatoms and dinoflagellates were also detected in other offshore areas by the sequences of the 18SrRNA genes (De Vargas et al., 2015), and the main phytoplankton composition in Matsushima Bay was similar. Diatoms were the dominantly abundant phytoplankton, since Chl *a* and Fuco (the latter being a major pigment of diatoms) showed similar fluctuations, and a correlation was also observed (Figure 2, Supplemental Figure 2). A lower correlation than Fuco was observed between Chl *a* and Peridinin, which is a major pigment of dinoflagellates. It is therefore considered that most of the Chl *a* obtained was associated with diatoms, although the NGS data showed that diatoms and dinoflagellates in the SAR group were in roughly equal proportions (Supplemental Figure 3). Diatoms are thought to account for about 20% of all phytoplankton on Earth (Malviya et al., 2016), and are generally considered to be dominant in temperate coastal areas (Armbrust, 2009) due to a supply of silicate from rivers (Officer and Ryther, 1980; Treguer et al., 1995; Falkowski et al., 1998; Taniuchi et al., 2017). Diatoms have also been reported to be dominant in Sendai Bay, outside Matsushima Bay (Taniuchi et al., 2017; Watanabe et al., 2017). Resting cells of various diatoms have been recorded from the sediments of Matsushima Bay in the past (Ichinomiya and Taniguchi, 2003), and if they germinate from the sediment, they may be the dominant species. The reason why diatoms appear to be dominant in abundance, while diatoms and dinoflagellates are recorded in almost equal numbers from DNA sequencing, is due to the difference in the copy number of 18SrRNA genes, which is thought to depend on cell volume, so dinoflagellates have more copies of 18SrRNA genes per cell than diatoms (Godhe et al., 2008). In Sendai Bay, dinoflagellates have been reported to be present at an abundance approximately 1/10 that of diatoms (Taniuchi et al., 2017), and in Matsushima Bay, too, dinoflagellate abundance was not dominant.

It is considered that there is no problem with the fact that the preservation period of the DNA samples from 2004-2005 was more than 10 years, because DNA has been sequenced successfully from sediment core samples following tens of thousands of years earlier (Lejzerowicz et al., 2013). Similarly, we have also confirmed that DNA sequencing is possible from samples several hundred years old (Okumura et al., 2021b), so decomposition of DNA samples over several decades preserved in a freezer is expected to be minimal.

If the aquaculture of oyster and seaweeds using rafts and rope installations were too intensive, it may affect the environment, the abundance and composition of phytoplankton and other microorganisms in Matsushima Bay. The total filtration rate by oysters cultured on rafts in Matsushima Bay is calculated to be enormous: the total number of oysters is calculated to be more than 40,000 per culture raft because oyster rafts in Matsushima Bay are installed as a 2 m x 27 m bamboo grid, from which hang 270 ropes with 10 to 20 scallop shells fixed within the twists of each rope (Miyagi Prefectural government, 1994). If oysters were cultured from 15 to 20 per scallop shell, the total number of suspended oysters per raft is 40,500 to 108,000. If one oyster filters 400 L of water per day (Fisheries Agency), the total filtration capacity per raft would be at least 16,200 tonnes per raft. Although the actual filtration rate varies greatly depending on oyster size and water temperature (Akashige et al., 2005), in the presence of more than 100 rafts the overall filtration volume is expected to be enormous. Filtration by oysters will therefore have a large effect on cleaning the marine environment, as well as the amount and composition of the microorganism population.

In addition, seaweed cultivation competes with phytoplankton for nutrients, which in seaweed are assimilated at a rate of about 5.7 mgN/gDW/h, depending on the type of seaweed (Yoshida et al., 2011). However, it is considered that the current number of aquaculture installations in Matsushima Bay probably does not affect the phytoplankton community in surface waters because nutrients, Chl *a* concentrations, and eukaryote assemblages did not clearly differ between cultured and non-cultured areas (Figures 6A, 7C; refer to Figure 1). The nutrient concentrations at Stn.1 (the canal mouth) appear different, presumably due to a higher anthropogenic effect, but otherwise there were no clear differences in nutrient concentrations among cultivated and non-cultivated areas (Figures 6C–E). Chl *a* concentration, too, showed no clear differences, except for a lower concentration at the Ofuna-iri Canal mouth (Figure 6A).

Eukaryote assemblages in seawater tended to show similar composition during the same year (Figure 7A), and during the same month each year (Figure 7B), while there were no clear differences among stations (Figure 7C). One reason may be that the biomass of diatoms was strongly dependent on water temperature, a natural environmental change unrelated to the presence or absence of aquaculture facilities (Figures 2A, C). The month-by-month population composition may be related to phenology. The dominant phytoplankton in Matsushima Bay were the diatoms, growth of which is temperature-dependent, so they are more abundant in the summer, declining in winter.

The timing of maturation of shellfish, such as oysters, is known to depend on the accumulated empirical water temperature, and oysters in Matsushima Bay spawn in the summer (Miyagi Prefectural government, 1994; Kakehi et al., 2016). The periphyton, including organisms such as hydrozoans, also demonstrate life cycle turnover (Ciavatta et al., 2020). One of the reasons why composition tended to vary by month (Figure 7B) is the fact that the entire biological community tended to change depending on the season.

In particular, the distribution of eukaryotes in 2004 was different from other years (Figure 7A), and we infer that this was due to the high proportion of Opisthokonta, which is not phytoplankton (Figure 5C). We consider the difference in the distribution of eukaryotes in 2004 to be an annual variation rather than a difference before and after the earthquake because the taxon composition in 2005 was similar to that after the earthquake. Even if there are similar annual seasonal changes, related to phenology, environmental factors fluctuated only slightly (Figure 2). Consequently, it is inferred that the distribution of eukaryotic communities also changed slightly from year to year (Figure 7C).

The shallow depth of Matsushima Bay (5 m maximum; Okumura et al., 2021a), and the associated frequency of seawater exchange (including a tidal range occasionally exceeding 1 m (Japan Meteorological Agency), probably exerts a stronger effect on changes to the phytoplankton assemblages in Matsushima Bay than the amount of cultured oysters and seaweed present. When the tidal range is large, it is estimated that this results in a daily replacement of approximately 1/5 of the seawater in Matsushima Bay. Indeed, seawater exchanges have been shown to be accelerated by the presence of a persistent rain front (Kakehi et al., 2016), flooding from rain over the nearby land (Kakehi et al., 2017), or by marine environmental changes of other kinds (Okumura et al., 2021a). Therefore, although there are more than 600 oyster rafts and 1,300 seaweed rope installations in Matsushima Bay, it is considered that the extent of seawater replacement exceeds the impact of aquaculture facilities on the bay's environment and phytoplankton assemblages.

Periphyton is also considered to affect aquaculture in Matsushima Bay, contributing as one factor in the occurrence of mass mortality of oysters, such as that which occurred in 2013 (Ito and Oshino, 2018). However, it is considered that the scouring of aquaculture facilities by the 2011 tsunami probably had little effect on oyster mass mortality phenomena. The occurrence of periphyton Metazoa such as *Alcyonidium* was found to show irregular fluctuations, and although it was much higher in 2004 than in 2013 (Figure 5C), it is considered that periphyton outbreaks were not affected by environmental changes following the tsunami.

It is considered also that the current number of aquaculture installations in Matsushima Bay has little impact on the environment and eukaryote assemblages. The number of fishermen in Miyagi Prefecture, including Matsushima Bay, has been decreasing year by year, as a direct result of the effects of the tsunami (Okumura et al., 2019). As a result, the number of oysters being cultured is less than half what it was in 1960 (Miyagi Prefectural government, 1994). Similarly, current seaweed cultivation is about half of that recorded for 1989 (Nagaki et al., 2015). Oyster and seaweed cultivation in Matsushima Bay are therefore not over-intensive and are within an appropriate range, with little effect on the marine environment and eukaryote assemblages.

5 Conclusion

According to results from NGS analysis of samples, phytoplankton comprised a high proportion of the eukaryote assemblages in Matsushima Bay. Diatoms were the dominant phytoplankton. The growth of diatoms in Matsushima Bay was seen to be dependent on water temperature, and was independent of anthropogenic influences, so aquaculture installations in Matsushima Bay apparently have little effect on the natural microorganisms. Because of the high rate of filtration of phytoplankton in oyster culture, and the competition for nutrients in seaweed cultivation, differences were expected in the phytoplankton and eukaryote assemblages present in comparison with non-cultured areas. However, no such differences were observed, perhaps because of the shallow water depth in Matsushima Bay, the high turnover of seawater replacement, and culture installations probably well below exploitation capacity. However, feces from shellfish, dead shellfish and the periphyton in culture areas generally sink to the seafloor, so it is possible that the bottom environment differs from the environment of the seawater column. Since analysis in this study was conducted using only surface seawater, further investigation of the near-bottom layer and bottom sediment will be necessary to provide a more detailed and comprehensive understanding of the effects of culture facilities in Matsushima Bay.

Data availability statement

The data presented in the study are deposited in the DDBJ repository, BioProject accession number; PRJDB13931, and DRA accession number; DRA014705.

Author contributions

YO designed and wrote manuscript in the study. YM investigated in the Matsushima Bay, and analyses nutrients in the seawater. MM helped with data processing and AS advised on analysis. All authors contributed to the article and approved the submitted version.

Funding

This work was supported by a Grant-in-Aid for Scientific Research B (18H03414) of the Japan Society for the Promotion of Science; the Tohoku Marine Science Project (a grant to assist with recovery from earthquake damage) provided by the Reconstruction Agency of Japan; and a Cooperative Research Grant of the Genome Research for BioResources, NODAI Genome Research Center, Tokyo University of Agriculture.

Conflict of interest

The authors declare that the research was conducted in the absence of any commercial or financial relationships that could be construed as a potential conflict of interest.

Publisher's note

Supplementary material

The Supplementary Material for this article can be found online at: https://www.frontiersin.org/articles/10.3389/fmars.2022.1022168/full#supplementary-material

SUPPLEMENTARY FIGURE 1
(A). Vertical distribution of water temperature (°C) at the surface and 0.5 m above the seafloor. **(B)**. Vertical distribution of salinity (PSU) at the surface and 0.5 m above the seafloor.

SUPPLEMENTARY FIGURE 2
The relationship between Chl *a* and other pigment concentrations.

SUPPLEMENTARY FIGURE 3
Percentage of the major taxonomic groups detected which belong to the SAR supergroup.

SUPPLEMENTARY FIGURE 4
Percentage of major taxonomic groups detected which belong to the Archaeplastida.

SUPPLEMENTARY FIGURE 5
Percentage of major taxonomic groups detected which belong to the Opisthokonta.

References

Akashige, S., Hirata, Y., Takayama, K., and Soramoto, K. (2005). Seasonal changes in oxygen consumption rates and filtration rates of the cultured pacific oyster *Crasssotrea gigas*. *Nippon Suisan Gakkaishi (Japanese Ed.* 71, 762–767. doi: 10.2331/suisan.71.762

Armbrust, E. V. (2009). The life of diatoms in the world's oceans. *Nature* 459, 185–192. doi: 10.1038/nature08057

Breitburg, D., Levin, L. A., Oschlies, A., Grégoire, M., Chavez, F. P., Conley, D. J., et al. (2018). Declining oxygen in the global ocean and coastal waters. *Science* 359, eaam7240. doi: 10.1126/science.aam7240

Ciavatta, M. L., Lefranc, F., Vieira, L. M., Kiss, R., Carbone, M., van Otterlo, W. A. L., et al. (2020). The phylum bryozoa: From biology to biomedical potential. *Mar. Drugs* 18, 1–32. doi: 10.3390/md18040200

De Vargas, C., Audic, S., Henry, N., Decelle, J., Mahé, F., Logares, R., et al. (2015). Eukaryotic plankton diversity in the sunlit ocean. *Science* 348, 1261605. doi: 10.1126/science.1261605

Falkowski, P. G., Barber, R. T., and Smetacek, V. (1998). Biogeochemical controls and feedbacks on ocean primary production. *Science* 200, 200–207. doi: 10.1126/science.281.5374.200

Falkowski, P. G., and Oliver, M. J. (2007). Mix and match- how climate selects phytoplankton- falkowski and Oliver. *Nature* 5, 813–819. doi: 10.1038/nrmicro1751

Fisheries Agency *Environmental conservation through fishing activities*. Available at: https://www.jfa.maff.go.jp/j/kikaku/tamenteki/kaisetu/gyogyou_katudou/.

Godhe, A., Asplund, M. E., Härnström, K., Saravanan, V., Tyagi, A., and Karunasagar, I. (2008). Quantification of diatom and dinoflagellate biomasses in coastal marine seawater samples by real-time PCR. *Appl. Environ. Microbiol.* 74, 7174–7182. doi: 10.1128/AEM.01298-08

Ichinomiya, M., and Taniguchi, A. (2003). Seasonal variation in abundance and species composition of a planktonic diatom assemblage including viable cells on the bottom in matsushima bay, northeastern japan. *J. Ocean Univ. Qingdao* 2, 160–166. doi: 10.1007/s11802-003-0045-9

Ishikawa, T., Kusaka, K., Oshino, A., Nishitani, G., and Kaniyama, T. (2015). Distribution patterns of *Alexandrium* vegetative cells and resting cysts, and paralytic shellfish poisoning in kesennuma bay, after the great East Japan earthquake. *Nippon Suisan Gakkaishi* 81, 256–266. doi: 10.2331/suisan.81.256

Ito, H., and Oshino, A. (2018). The sessile organisms of cultured oyster and removal methods in matsushima bay. *Miyagi Pref. Rep. Fish. Sci.* 18, 47–50. Available at: https://www.pref.miyagi.jp/documents/1138/18-7.pdf.

Japan Meteorological Agency *A tide table in shiogama*. Available at: https://www.data.jma.go.jp/gmd/kaiyou/db/tide/suisan/suisan.php?stn=SG.

Kakehi, S., Kamiyama, T., Abe, H., Hanawa, S., Oota, H., Matsuura, R., et al. (2016). Mechanisms leading to the decline in pacific oyster *Crassostrea gigas* seedlings in matsushima bay, Japan. *Fish. Sci.* 82, 499–508. doi: 10.1007/s12562-016-0982-z

Kakehi, S., Shirai, H., Magome, S., Takagi, T., Okabe, K., Takayanagi, K., et al. (2020). Predicting the larval transport of pacific oyster *Crassostrea gigas* during the seedling collection season. *Fish. Oceanogr.* 29, 484–504. doi: 10.1111/fog.12491

Kakehi, S., Takagi, T., Okabe, K., and Takayanagi, K. (2017). Circulation in a bay influenced by flooding of a river discharging outside the bay. *Estuar. Coast. Shelf Sci.* 187, 204–215. doi: 10.1016/j.ecss.2017.01.013

Kamiyama, T., Yamauchi, H., Iwai, T., Hanawa, S., Matsuyama, Y., Arima, S., et al. (2005). Comparison of environmental conditions in two representative oyster farming areas: Hiroshima bay, western Japan and oginohama bay (a branch of ishinomaki bay), northern Japan. *Fish. Sci.* 71, 1295–1130. doi: 10.1111/j.1444-2906.2005.01096.x

Kamiyama, T., Yamauchi, H., Nagai, S., and Yamaguchi, M. (2014). Differences in abundance and distribution of *Alexandrium* cysts in Sendai bay, northern Japan, before and after the tsunami caused by the great East Japan earthquake. *J. Oceanogr.* 70, 185–195. doi: 10.1007/s10872-014-0221-0

Kanda, Y. (2013). Investigation of the freely available easy-to-use software "EZR" for medical statistics. *Bone Marrow Transplant.* 48, 452–458. doi: 10.1038/bmt.2012.244

Lejzerowicz, F., Esling, P., Majewski, W., Szczucinski, W., Decelle, J., Arbizu, P. M., et al. (2013). Ancient DNA complements microfossil record in deep-sea subsurface sediments. *Biol. Lett.* 9, 20130283. doi: 10.1098/rsbl.2013.0283. doi: 10.5061/dryad.b5m0j.

Malviya, S., Scalco, E., Audic, S., Vincent, F., Veluchamy, A., Poulain, J., et al. (2016). Insights into global diatom distribution and diversity in the world's ocean. *Proc. Natl. Acad. Sci.* 113, E1516–E1525. doi: 10.1073/pnas.1509523113

Masuda, Y., Okumura, Y., and Ohta, H. (2014). Monitoring of causative plankton of shellfish poisoning two decades (from 1993 to 2013) in the middle and southern coastal area of miyagi prefecture. *Miyagi Pref. Rep. Fish. Sci.* 14, 41–56. Available at: https://www.pref.miyagi.jp/documents/1138/14-6.pdf.

Miyagi Prefectural government (1994) *Traditional fishing gear fishing methods in miyagi prefecture VII aquaculture (Oyster)*. Available at: https://www.pref.miyagi.jp/documents/25039/309091.pdf.

Miya, M., Sato, Y., Fukunaga, T., Sado, T., Poulsen, J. Y., Sato, K., et al. (2015). MiFish, a set of universal PCR primers for metabarcoding environmental DNA from fishes: Detection of more than 230 subtropical marine species. *R. Soc Open Sci.* 2, 150088. doi: 10.1098/rsos.150088

Nagaki, M., Suto, A., Nobuhisa, A., and Hanawa, S. (2015). Growth of undaria pinnatifida and laminaria japonica cultivated in matsushima bay and water temperature and nutrient concentration in the cultivating area. *Miyagi Pref. Rep. Fish. Sci.* 8, 54–61. Available at: https://www.pref.miyagi.jp/documents/1138/15-7.pdf.

Nagashima, H., Ishida, A., Yoneyama, N., and Pringle, W. J. (2016). Numerical study on the tsunami reduction factor in matsushima bay during the great east Japan earthquake. *J. Japan Soc Civ. Eng. Ser. B3 (Ocean Eng.* 72, I_151–I_156. doi: 10.2208/jscejoe.72.I_151

Nimnoi, P., and Pongsilp, N. (2020). Marine bacterial communities in the upper gulf of Thailand assessed by illumina next-generation sequencing platform. *BMC Microbiol.* 20, 1–11. doi: 10.1186/s12866-020-1701-6

Officer, C. B., and Ryther, J. H. (1980). The possible importance of silicon in marine eutrophication. *Mar. Ecol. Prog. Ser.* 3, 83–91. doi: 10.3354/meps003083

Okumura, Y., Masuda, Y., Suzuki, N., Kakehi, S., and Hara, M. (2021a). Temporal changes in the nutrient status of matsushima bay after a wastewater plant was destroyed by a tsunami on 11 march 2011. *Fish. Sci.* 87, 845–859. doi: 10.1007/s12562-021-01553-2

Okumura, Y., Matsuoka, H., Arakawa, H., Tokanai, F., Suzuki, A., Irizuki, T., et al. (2021b). The influence and impact of tsunamis on the microorganism assembly of nagatsura-ura lagoon, miyagi, northeastern Japan. *Fish. Sci.* 87, 121–130. doi: 10.1007/s12562-020-01472-8

Okumura, Y., Nawata, A., Ito, H., Oshino, A., and Hara, M. (2019). "Suitable oyster culture density in oginohama bay, miyagi, Japan," in *Oceanography challenges to future earth* (Cham: Springer International Publishing), 351–363. doi: 10.1007/978-3-030-00138-4_28

Oota, H., Suzuki, N., and Gambe, S. (2017). Sedimentary environment before and after the great East Japan earthquake in matsushima bay. *Miyagi Pref. Rep. Fish. Sci.* 17, 35–41. Available at: https://www.pref.miyagi.jp/documents/1138/17-5.pdf.

Ota, Y., Suzuki, A., Yamaoka, K., Nagao, M., Tanaka, Y., Irizuki, T., et al. (2019). Sediments of matsushima bay, northeastern Japan: Insights gained from 5 years of sedimentological analysis following the 2011 tohoku earthquake-tsunami. *Geochemistry Geophys. Geosystems* 20, 3913–3927. doi: 10.1029/2019GC008381

Raven, J. A. (1987). The role of vacuoles. *New Phytol.* 106, 357–422. doi: 10.1111/j.1469-8137.1987.tb00149.x

Shimadzu Corporation. (2019). *Ampdirect® Plus Procedure*. Availabe at: https://www.an.shimadzu.co.jp/bio/reagents/amp/amp_emn.pdf.

Stoeck, T., Bass, D., Nebel, M., Christen, R., Jones, M. D. M., Breiner, H. W., et al. (2010). Multiple marker parallel tag environmental DNA sequencing reveals a highly complex eukaryotic community in marine anoxic water. *Mol. Ecol.* 19, 21–31. doi: 10.1111/j.1365-294X.2009.04480.x

Taniuchi, Y., Watanabe, T., Kakehi, S., Sakami, T., and Kuwata, A. (2017). Seasonal dynamics of the phytoplankton community in Sendai bay, northern Japan. *J. Oceanogr.* 73, 1–9. doi: 10.1007/s10872-015-0334-0

ter Braak, C. J. F., and Šmilauer, P. (2018). Canoco reference manual and user's guide: software for ordination (version 5.10). *Biometris Wageningen Univ. Res.* 356.

TOYOBO (2019) *Instruction manual KOD FX 1110*. Available at: https://www.toyobo-global.com/.

Treguer, P., Nelson, D. M., Van Bennekom, A. J., DeMaster, D. J., Leynaert, A., and Queguiner, B. (1995). The silica balance in the world ocean: A reestimate. *Science* 268, 375–379. doi: 10.1126/science.268.5209.375

Watanabe, T., Taniuchi, Y., Kakehi, S., Sakami, T., and Kuwata, A. (2017). Seasonal succession in the diatom community of Sendai bay, northern Japan, following the 2011 off the pacific coast of tohoku earthquake. *J. Oceanogr.* 73, 133–144. doi: 10.1007/s10872-016-0387-8

Watanabe, T. (1977). Problems of water exchange in productivity development studies of shallow waterfisheries ground. *Bull.Coast.Oceanogr.* 14, 65–77. doi: 10.32142/engankaiyo.14.1_65

Yoshida, G., Niimura, Y., Tarutani, K., and Hamaguchi, M. (2011). Research review on the relationship between macroalgal-production and nutrients, and relative assessment of the nutrient conditions on macroalgae in the seto inland Sea. *Bull. Fish. Res. Agen.* 34, 1–34. Available at: https://www.fra.affrc.go.jp/bulletin/bull/bull34/1-31.pdf.

Zapata, M., Rodríguez, F., and Garrido, J. L. (2000). Separation of chlorophylls and carotenoids from marine phytoplankton: A new HPLC method using a reversed phase C8 column and pyridine-containing mobile phases. *Mar. Ecol. Prog. Ser.* 195, 29–45. doi: 10.3354/meps195029

frontiers | Frontiers in Marine Science

TYPE Original Research
PUBLISHED 25 January 2023
DOI 10.3389/fmars.2022.1020334

A framework for a net environmental benefit analysis based comparative assessment of decommissioning options for anthropogenic subsea structures: A North Sea case study

Joseph P. Nicolette[1]*, Nicholas A. Nelson[1], Michael K. Rockel[1], Mark L. Rockel[1], Alex N. Testoff[1], Larry L. Johnson[2], Laura D. Williamson[3,4] and Victoria L. G. Todd[3,4]

[1]Montrose Environmental Solutions, Inc., Sandy Springs, Georgia, GA, United States, [2]Global Decommissioning Advisor, Former Oil and Gas Operator, Florida, FL, United States, [3]Ocean Science Consulting Limited., Scotland, United Kingdom, [4]Environmental Research Institute, University of the Highlands & Islands, Thurso, United Kingdom

Check for updates

OPEN ACCESS

EDITED BY
Stelios Katsanevakis,
University of the Aegean, Greece

REVIEWED BY
Ibon Galparsoro,
Technological Center Expert in Marine and Food Innovation (AZTI), Spain
Rafael Sarda,
(CSIC), Spain

*CORRESPONDENCE
Joseph P. Nicolette
✉ Jnicolette@Montrose-env.com

SPECIALTY SECTION
This article was submitted to Marine Ecosystem Ecology, a section of the journal Frontiers in Marine Science

RECEIVED 16 August 2022
ACCEPTED 07 December 2022
PUBLISHED 25 January 2023

CITATION
Nicolette JP, Nelson NA, Rockel MK, Rockel ML, Testoff AN, Johnson LL, Williamson LD and Todd VLG (2023) A framework for a net environmental benefit analysis based comparative assessment of decommissioning options for anthropogenic subsea structures: A North Sea case study. *Front. Mar. Sci.* 9:1020334.
doi: 10.3389/fmars.2022.1020334

Taxpayers and operators worldwide have significant current liabilities associated with decommissioning of offshore Oil & Gas (O&G) assets. Consequently, decommissioning is at the forefront of industrial, governmental, and non-governmental agendas. Decommissioning is a highly complex activity with health, safety, environmental, social, economic, and technical implications. Increasing scientific evidence supports that manmade subsea structures create hard, artificial reef habitats that provide ecological and social benefits to society. Given the significant uncertainty regarding how subsea structures should be retired at the end of their operational lifetimes, it is necessary for governments, taxpayers, and operators to understand the risks and benefits associated with potential decommissioning options. Currently, the North Sea decommissioning process is based on the policies and direction of the Oslo and Paris Convention's (OSPAR) Decision 98/3 and follow comparative assessment (CA) multiple-criteria decision analysis (MCDA) guidelines to determine the best overall strategy for decommissioning subsea structures; however, CA MCDA processes can be biased, ambiguous, difficult to use, interpret, and replicate, and limited in their consideration of multigenerational benefits. Consequently, to assist decision-makers in understanding and evaluating options and associated benefits for decommissioning subsea structures, this study adapted the net environmental benefit analysis (NEBA) framework to supplement and strengthen the CA process for evaluating decommissioning options for offshore O&G facilities. The net environmental benefit analysis based comparative assessment (NEBA-CA) framework is presented that addresses the growing need for a practical, quantitative, scientifically robust, defendable, and transparent MCDA approach to determine optimized decommissioning strategies for subsea assets. Increased transparency in CAs will provide an additional layer of credibility with regulators and society. The approach is data driven and a desktop analysis mainly relying on existing data. Using a North Sea case study, this work demonstrates the ability of NEBA-CA to resolve inherent complexity in comparing decommissioning options, thereby supporting operators in working with regulators to decommission assets in a way that maximizes ecosystem service benefits to society while managing site-related risks and costs. The NEBA-CA framework supplements and strengthens the standard CA process by 1) incorporating quantified metrics including multigenerational ecosystem service benefits and risks, 2) excluding front ranking (scoring) or weighting of metrics, and 3) providing consistent graphical displays to support visual differentiation of options and metrics.

KEYWORDS

net environmental benefit analysis, comparative assessment, decommissioning, offshore platform, North Sea, multiple criteria decision analysis, NEBA, NEBA-CA

1 Introduction

As of the end of 2020, there were at least 6,000 fixed or floating Oil & Gas (O&G) platforms in operation globally (Gourvenec, 2018). Between 2017 and 2030, a global estimated annual average of 100 offshore O&G assets will require decommissioning. The annual average is expected to rise to 150 assets between 2031 and 2040 (IEA, 2019b). The majority of these assets will necessitate complete removal under current global regulations with an associated cost in the hundreds of billions (USD) to 2040 (Gourvenec et al., 2022). With nearly 800 platforms operating in the North Sea as of 2016 (Todd et al., 2016), cumulative expenditure estimates for decommissioning in the United Kingdom (UK) range from £40 billion to more than £66 billion over the next 40 years (O&G UK, 2021). Consequently, decommissioning is at the forefront of industrial, governmental, and non-governmental agendas, acknowledging that removal is a highly complex activity with health, safety, environmental, social, economic, and technical implications.

Recent peer-reviewed independent scientific and regulatory processes for decommissioning decision-making for subsea structures worldwide have not only revealed significant uncertainty associated with how subsea structures should be decommissioned, but also overlooked the potential benefits subsea infrastructure may provide to society, marine stakeholders, and the environment (Fowler et al., 2018; IOGP, 2022). This paper presents a practical, quantitative, scientifically robust, defendable, and transparent multiple-criteria decision analysis (MCDA) framework to support optimized decommissioning strategies for subsea assets.

1.1 Decommissioning planning and comparative assessment

Operator "end-of-life" decommissioning plans identify specific options for subsea structures within a field. Subsea structures comprise a myriad of components, such as *inter alia*, platform jackets, production flowlines and bundles, risers and riser turrets, towheads, wellheads and associated protection units, production manifolds, umbilicals, pipeline end manifolds, concrete mattresses, mooring anchors, and chains.

In the context of offshore decommissioning, a comparative assessment process was first referenced within the Oslo and Paris Convention's (OSPAR) policies and directions (OSPAR, 1998) with respect to assets designated as candidates for derogation based on a variety of specific considerations. The term comparative assessment (CA) is used to describe the general process used to evaluate decommissioning options and identify proposed options. Guidelines for implementing CAs have been published by O&G UK (2015) and the Department of Energy and Climate Change (DECC) [Offshore Petroleum Regulator for Environment & Decommissioning (OPRED), 2018], both of which satisfy OSPAR's regulatory requirements for CA, including cases of derogation. No detailed procedures for the CA process are prescribed in OSPAR Decision 98/3, O&G UK guidance, or DECC guidance (OSPAR, 1998; O&G UK, 2015; OPRED, 2018). To determine proposed decommissioning options for subsea structures, CAs typically consider the following five factors:

health and safety, environmental, social, technical feasibility, and economic impacts associated with the implementation of various decommissioning options (O&G UK 2015; DMIRS, 2017; OPRED, 2018; IOGP, 2022).

1.2 Comparative assessment and evaluation

In general, decommissioning processes and CA protocols include both qualitative and quantitative analyses with front grouping, ranking (or scoring), and/or weighting schemes for parameter evaluation. For example, O&G UK proposed three evaluation methods where qualitative and/or quantitative data for each option are grouped into simple classes by color and/or numerical scores (O&G UK 2015). Depending on which of the three evaluation methods is used, the evaluation may include weighting of the scored data (O&G UK 2015). In the subsequent OPRED guidelines, the effects of decommissioning options on the five main factors were ranked on a scale of low to medium to high and assigned a correlating color of green, amber and red, respectively (OPRED, 2018).

However, the current CA techniques have several disadvantages:

1. *Guidance is vague*: Although the CA process is referenced within decommissioning guidelines from multiple geographical locales (O&G UK 2015; Petroleum Safety Authority, 2020; APPEA, 2016; NOPSEMA, 2018; OPRED, 2018; ANP, 2020; Government of New Zealand, 2021; UNEP/MED, 2022; Petroleum Institute of Thailand, 2008), guidance available is arcane, obscure, and non-standardized, leading to ambiguity associated with varying methods, analysis techniques, presentations, interpretations, conclusions, and data transparency, even between similar projects spanning across geographical and regulatory boundaries (O&G UK 2015; DMIRS, 2017; OPRED, 2018);
2. *Insufficient rigor*: Empirical data are often analyzed and presented in a qualitative, unrepeatable, and non-scientifically robust manner, challenging independent scientific peer-review, thereby diminishing their value to stakeholders;
3. *Reduced transparency*: Given the multiple layering of metrics and risk evaluations that define an option within CA approaches, results can increase the overall subjectivity of metric comparisons between options, which can lead to reduced transparency and ambiguity in how results were derived;
4. *Qualitative data lumping where differences obscured*: Multiple options may be identified as having the same color and/or ranking, which indicates that there are no disparities between these options, even though the metric values may be different;
5. *Potential to introduce stakeholder bias*: CA approaches have potential to, *inter alia*, bias stakeholders participating in the weighting and ranking exercise and can also obscure quantitative differences when data are grouped into rankings (i.e., become increasingly subjective with each layer of weights and ranks);
6. *Ecological and social benefits understated*: CA approaches often tend to focus on option risks over benefits; that is, within the standard CA evaluation process, the incorporation of multigenerational benefits, also known as intergenerational benefits (Nicolette et al., 2013a), appears limited; and,
7. *Ineffective presentation of results*: CA results have been presented in a variety of non-standardized and inconsistent graphical displays that can be confusing to regulators.

Fortunately, operators are obliged to release CAs into the public domain (such as British Petroleum, 2011; CNR International, 2012; Shell International Petroleum, 2017; Spirit Energy, 2018; INEOS, 2021; Ithaca Energy Group, 2021; and Xodus Group, 2021). This enables stakeholders to familiarize themselves with the CA process. Nonetheless, disadvantages of the CA process have the potential to generate significant uncertainty and incorrect inferences by stakeholders. This could lead to the identification of inaccurate quantitative metric data differences or scoring between options, rendering the time-consuming and costly CA exercises of little value to society.

As part of the decommissioning planning process, a CA approach that limits subjectivity, increases transparency, incorporates multigenerational benefits and risks, focuses on quantitative analysis, and provides a consistent and systematic approach to option evaluation, with readily comparable data displays, is needed. This study presents a framework for supplementing and strengthening the standard CA process including incorporation of a risk management approach to support decision-making. Additionally, a North Sea case study is used to demonstrate the application and results of the net environmental benefit analysis based comparative assessment (NEBA-CA) framework applied to an offshore jacket, including resulting graphics and risk management approach.

1.3 NEBA background

Net environmental benefit analysis (NEBA) is a risk-benefit approach for comparing the net environmental benefits and risks between competing management actions. Management actions include a wide variety of actions that affect the environment, such as restoration, remediation, conservation, and development. The first formalized NEBA framework (Efroymson et al., 2003; Efroymson et al., 2004) is recognized, *inter alia*, by the United States Environmental Protection Agency (USEPA), the USEPA Science Advisory Board (USEPA SAB, 2009), and the National Oceanic and Atmospheric Administration (NOAA, 2011) for its value in providing a defendable basis for environmental decision-making. Net environmental benefits are gains in the value of environmental services or other ecological properties attained by an action(s) minus the value of the adverse environmental effects caused by the action(s) (Efroymson et al., 2004). Thus, NEBA considers the overall impact, positive or negative, of proposed or implemented actions(s) and manages site risks.

Efroymson et al. (2004) noted that NEBA is an extension or elaboration of ecological risk assessment (USEPA, 1997). They identified that the key difference between the two processes was the consideration of environmental benefits in NEBA, which were not incorporated in traditional risk assessments. Gradually, NEBA evolved to include, *inter alia*, ecological services and the social and economic benefits derived from the presence of ecological services (Nicolette et al., 2013a), jointly known as ecosystem services (Millennium Ecosystem Assessment, 2005).

Efroymson et al. (2004) summarized the major advantages of NEBA in supporting management decisions.

"The NEBA framework should be useful when the balance of risks and benefits from an action at a site is ambiguous. That ambiguity arises when the site retains significant ecological value; when the actions are themselves environmentally damaging; when the ecological risks from the *in-situ* condition are relatively small, uncertain, or limited to a component of the ecosystem."

In the context of offshore decommissioning, the NEBA framework directly addresses the ambiguity that can arise when making decisions regarding the selection of appropriate decommissioning options. Ambiguity associated with decommissioning option decision-making arises because recent evidence suggests that subsea structure has a beneficial consequence: the creation of hard-structure habitat areas that support benthos, fish, and marine mammals that in turn, provide a variety of ecological and social benefits to society (Fowler and Booth, 2012; Claisse et al., 2014; Todd et al., 2021; McLean et al., 2022; Todd et al., 2022a). These habitats contribute to human well-being by providing passive use values such as existence, bequest, and aesthetic values, as well as active use values such as recreational fishing, commercial fishing, diving, photography, and scientific research. The provision of specific ecosystem services is site dependent. It stands to reason that these benefits will be provided by the infrastructure for as long as it is in place (i.e., centuries), establishing multigenerational value (Kenter et al., 2013).

To assist decision makers in understanding and evaluating options and associated benefits for decommissioning subsea structures, we adapted the NEBA framework (Efroymson et al., 2004) to supplement and strengthen the CA process for evaluating decommissioning options for offshore O&G assets. The framework is based on international experience with NEBA-based comparative assessment studies integrating ecosystem service values, site data, and readily available scientific information at sites in Australia, California, Caribbean, Gulf of Mexico, Gulf of Thailand, and the North Sea. The developed framework is holistic in that it considers environmental, social, health and safety, technical feasibility, and economic factors, including the multigenerational benefits and risks associated with option implementation.

2 The NEBA-based comparative assessment framework

The NEBA-based CA (NEBA-CA) framework presented herein is a MCDA approach with which the potential range of offshore decommissioning options for a given field can be compared (IOGP, 2022). The NEBA-CA is focused on option selection through an analysis of the trade-offs between benefits and risks and involves comparison of several management options that may include: (1) leaving the structure in place, (2) physically removing the structure, (3) partially removing the structure, (4) improving ecological value through onsite and offsite restoration options (e.g., rigs-to-reefs, creation of designated reefing areas, and *in-situ* management); or (5) a combination of these options.

The NEBA-CA framework supplements and strengthens the standard CA process by 1) incorporating quantified metrics including multigenerational ecosystem service benefits and risks, 2) excluding front ranking (scoring) or weighting of metrics, and 3) providing consistent graphical displays to support visual differentiation of options and metrics.

Incorporating quantified multigenerational ecosystem service benefits and risks - Incorporating formally quantified benefit and risk metrics, including the time frame over which these benefits and risks would be impacted (i.e., multigenerational or the duration of the decommissioning campaign, depending upon the metric being evaluated), provides decision-makers with an opportunity to make informed choices about the net benefits of decommissioning options that affect the environment. Informed decisions are systematic, transparent, understandable to stakeholders, non-arbitrary, scientifically-based and defendable, quantitative in nature (where possible), based on internationally recognized concepts and approaches, and considerate of stakeholder concerns.

Additionally, multigenerational value is important because future generations are unable to participate in decisions that will affect them and thus, they cannot defend their interests in the current decision-making process, even though present decisions can have irreversible impacts on their welfare. Correction for multigenerational valuation issues to capture potential irreversible wealth/benefit transfers between generations can be accomplished using a discount rate that gives more weight to future generations' preferences (Lowe, 2008). The discount rate reflects the time preference that society has to receive benefits sooner rather than later (Lowe, 2008).

Excluding front ranking or weighting of metrics - NEBA-CA quantified values for options analyzed are graphically displayed in relation to one another, providing a level of objectivity and transparency to stakeholders for the initial evaluation of the data. Weighting of select quantified metrics, where it is determined necessary, can be integrated into NEBA-CA once the original data graphics are produced. Weighting various metrics at this latter stage, once the quantified data are final and evaluated by key stakeholders, ensures increased transparency. It is important that all stakeholders are represented should latter weighting or ranking be conducted.

Objective graphical displays - NEBA-CA provides objective graphics that allow for benefits, losses, and risks for all metrics to be displayed in a manner that can be readily ascertained by the viewer, thereby increasing their confidence in the outcome.

The NEBA-CA framework for offshore decommissioning consists of the following components (Figure 1):

- Analysis Planning
- Options Analysis and Graphics
- Risk Management Decision-Making

It should be noted that long-term monitoring, in some form, may be required by the local regulatory authority should any assets remain in place. While potential monitoring is not addressed in this framework, monitoring typically does not alter the optimum benefit versus detriment outcome. Each of the above-mentioned components are described in the following sections.

2.1 Analysis planning

Analysis planning in NEBA-CA is comparable to the planning and problem formulation aspects of risk assessment (USEPA, 1997) and NEBA (Efroymson et al., 2004). Analysis planning outlines the scope of the work to be conducted to compare alternative decommissioning actions. Analysis planning provides for the upfront development of the assessment to identify those environmental services, properties, or potential risks of concern, as well as the methods and metrics by which those services, properties, or risks will be measured. Analysis planning for NEBA-CA for offshore decommissioning includes the following considerations (Figure 1):

- Identification of Management and Assessment Goal(s);
- Regulatory Guidance and Consistency with the Precautionary Principle;
- Incorporation of the Spatial and Temporal Scope of the Assessment;
- Subsea Structure Component Identification;
- Decommissioning Option Identification, Feasibility, and Assumptions;
- Decommissioning Option Campaign Characteristics;
- Characterization of Site-Specific Ecosystem Services and the Reference State;
- Characterization and Quantification of Ecosystem Services Potentially Affected by Option Implementation;
- Characterization and Quantification of *In-Situ* Risks Associated with Leaving Hard Structure in Place;
- Health and Safety Option Implementation Risks; and
- Comparative Metrics and Data Requirements

2.1.1 Management and assessment goal(s)

The overarching management goal of a NEBA-CA is to provide a scientifically defendable, transparent, non-arbitrary, and systematic approach for evaluating decommissioning options in support of decision-making that maximizes short-term and multigenerational ecosystem service benefits to society while managing site and implementation risks. NEBA-CA supports the understanding of the net ecosystem service benefits and risks (ecological, human use, and economic) between competing decommissioning alternatives to support an overall risk-benefit analysis so that operators, regulators, and other stakeholders can make informed decisions regarding a preferred decommissioning program.

2.1.2 Regulatory guidance and consistency with the precautionary principle

As part of the planning process and in pursuit of management goal(s) identified, NEBA-CA considers decommissioning options in terms of health and safety, environmental, societal, technical, and economic considerations, as generally required by current CA guidance (OSPAR, 1998; O&G UK 2015; OPRED, 2018). Additionally, NEBA-CA's inclusion of multigenerational ecosystem services addresses the essence of sustainable development by quantitatively assessing the impact of actions taken today on future generations and their ability to meet their needs (Brundtland, 1987).

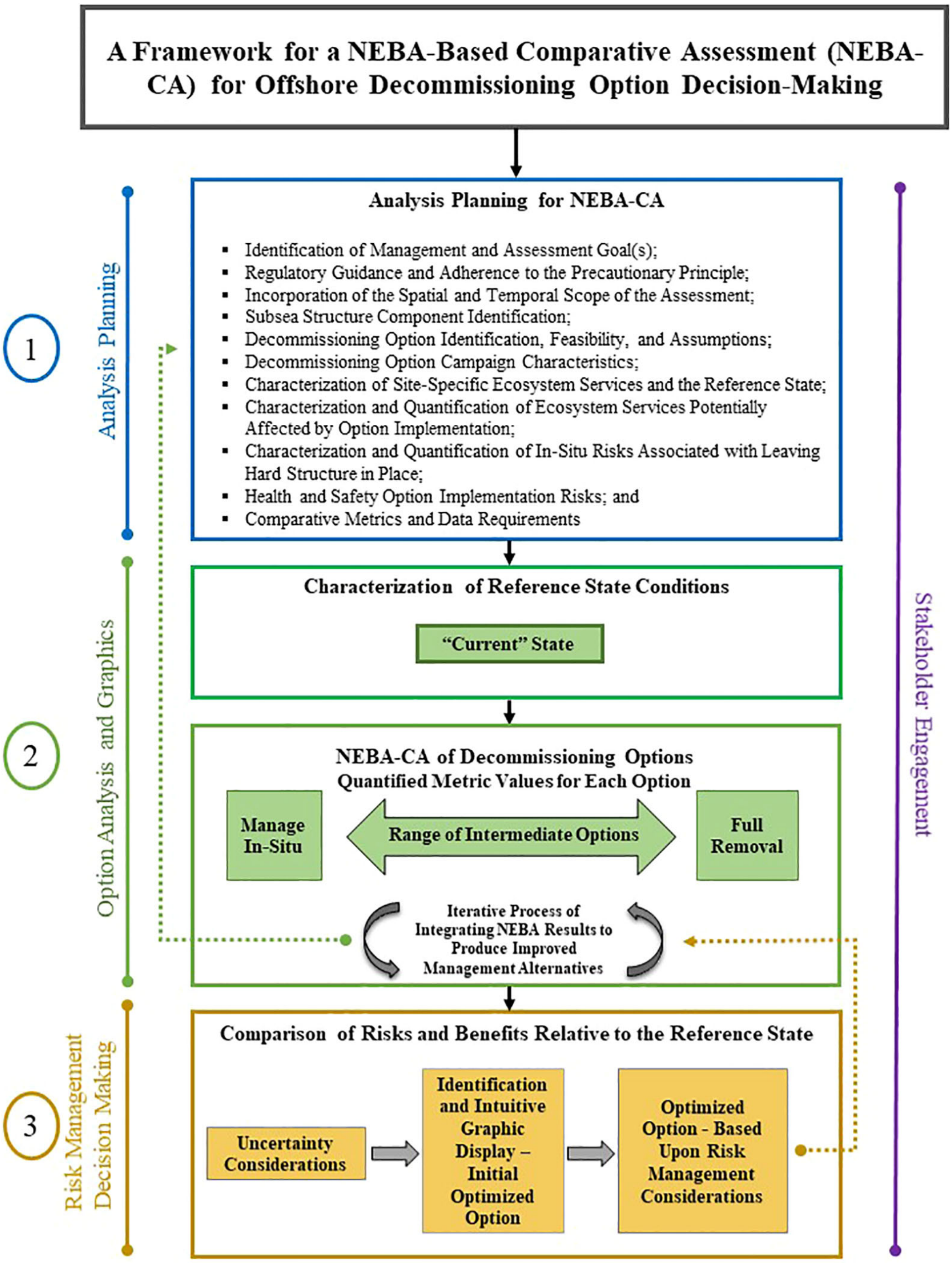

FIGURE 1
The NEBA-CA Framework for Offshore Decommissioning Option Selection.

2.1.2.1 Consistency with the precautionary principle

The precautionary principle of risk management implies that if an action or policy has a suspected risk of causing harm to the public or environment, in the absence of scientific consensus (that the action or policy is not harmful), the burden of proof that it is not harmful falls on those taking that action. The precautionary principle encourages policies that protect human health and the environment in the face of uncertain risks and is meant to ensure that the societal good is represented. Adherence to the precautionary principle is a key component of decommissioning under the OSPAR (Raffensperger and Tickner, 1999). Additionally, the 1992 treaty that created the

European Union (EU) made the precautionary principle the foundation of EU environmental policy (Article 130R) (European Commission, 1992).

Because ongoing research has identified a variety of ecosystem service benefits provided by subsea infrastructure, options to decommission and remove subsea structures should be evaluated, on a case by case basis, because these actions have the potential to create a plausible risk to these ecosystem service benefits. These risks include potential significant (and possibly irreversible) adverse effects on fish stock protection and abundance, which further relate to potential adverse effects to commercial fishing, marine mammals and prey abundance, and protection of species of special concern (e.g., endangered species), all of which can adversely affect future generations. The NEBA-CA satisfies the precautionary principle in that it supports a transparent, quantitative, and scientifically defendable approach for environmental decision-making and ensures that the societal good is represented in decisions made under scientific uncertainty where ambiguity exists.

The applicability and consistency of the NEBA-CA framework with select International, European, and UK decommissioning guidance and legislation are presented in Supplementary Table 1. A NEBA-CA should be conducted irrespective of constraints associated with aged regulations (e.g., OSPAR 98/3), especially where these regulations did not have the benefit of our current knowledge regarding the potential multigenerational ecological, social, and economic benefits of subsea structures.

2.1.3 Incorporation of the spatial and temporal scope of the assessment

2.1.3.1 Spatial

It is important to determine the spatial and temporal scales over which the analysis will be conducted before one can begin to understand the environmental benefits or impacts. The spatial scale of a NEBA-CA is dependent on the assets to be evaluated and their locations within the field. A NEBA-CA can be conducted for a specific component (e.g., a jacket) or developed to address all assets and types of subsea structures within a field. Spatially, the analysis focuses on the assets themselves and the areas over which they influence the local ecology. The analysis also considers areas outside the influence of the structures for comparison purposes. As an example, Claisse et al. (2014) estimated that secondary fish production near O&G platforms off the California coast was 18 to 150 times greater than that of nearby soft-bottom habitats.

2.1.3.2 Temporal

Removal of subsea structure can immediately remove habitat and its associated ecosystem, which would have been predicted to provide ecological and socioeconomic value for multiple generations (i.e., centuries) into the future. Thus, the analysis of options must consider the predicted multigenerational timeframe over which ecological and socioeconomic benefits and risks would be influenced by the implementation of the options. Understanding component degradation rates supports an understanding of predicted multigenerational timeframes associated with structure left in-situ.

2.1.3.3 Degradation rates

Degradation rates can be used to estimate the period over which benefits (i.e., presence of hard structure and associated ecological value) and risks (navigation, trawling, potential contaminant releases, etc.) would be projected to occur. For example, carbon steel is commonly used in the construction of fixed production jackets in the North Sea. Although jackets are built to last, the structure will eventually oxidise and corrode in the seawater (O&G UK, 2013). Corrosion rates and cathodic protection information can be used to approximate the longevity of a structure in place (O&G UK, 2013).The corrosion rate depends on a variety of factors such as: protective structures, depth, temperature, salinity, pH, flow, pressure, and fouling (O&G UK, 2013). O&G UK (2013) presented a general rate of corrosion for carbon steel in the North Sea on the exterior (5-10mm/century) and interior (1-2mm/century), not accounting for cathodic protection.

As there is some uncertainty as to predicting future conditions over multiple generations, conservative and internally consistent assumptions can be made within NEBA-CA for the purposes of differentiating between options (Section 4).

2.1.4 subsea structure component identification

As presented earlier, subsea structures are comprised of many types of components of varying sizes and materials. In developing the subsea structure list, physical parameters by component should be developed to consider the composition (steel, plastics, coatings, etc.), structural dimensions (hard structural surface area (m^2) and volume/complexity), water depth, and structure weight (t). These data will support the estimation of available habitat structure, environmental health and safety risks, and greenhouse gas emissions required for component lifts and/or transport associated with each option.

Plastics, coatings, and potential contaminants (e.g., mercury, naturally occurring radioactive material (NORM), and residual hydrocarbons) present on/in each component should also be identified along with the volume, type/composition, thickness, and/or extent on/in the structure. These data support the ecological and human health risk evaluation associated with component degradation and potential contaminant releases into the environment.

2.1.4.1 Halo effect area

Along with the understanding of the physical characteristics of the subsea structures, the analysis should also consider the physical condition of the sea bottom under and near the structure. O&G offshore facilities are known to enhance surrounding benthic communities by altering flow patterns and subsequent deposition of organic matter (Wolfson et al., 1979; Todd et al., 2018; Todd et al., 2021). The increased input of organic matter to the benthic community, creates a "halo" effect (also known of as a "shadow" or "umbrella" area) surrounding the structures, resulting in an affected area that can be 15 times larger than the structure by itself (Reeds et al., 2018). "Halo" areas in shallower water environments can be found at large distances from the subsea structures and while these distances are not known for deep water environments, an area of altered habitat that is two–to-four times the area of the structure is not unlikely. Thus, removal of subsea structures and their "reef" inhabitants will not only directly impact the reef communities but will also influence the altered benthic communities adjacent to the artificial reef that has been created by the subsea structure. Thus, aside from the subsea structures to be considered, the effect of decommissioning options on the "halo" effect area should also be incorporated into the NEBA-CA.

2.1.5 Decommissioning option identification, feasibility, and assumptions

2.1.5.1 Option identification

Decommissioning options to be evaluated for each structure group should be identified. Both *in-situ* and implementation risks and benefits for each option will be compared. Various decommissioning options can be developed for each structure within a given field. Similar structures (i.e., structural groups) are likely to have similar options. The identified options should range from a no-action option to a full-removal option and include potential intermediate options.

Full removal involves complete removal of the component. For jackets, full removal likely requires cutting footings below the mudline. It should be noted that to cut the footings below the mudline, it may be necessary to remove surrounding sediments/drill cuttings piles to a depth of several meters, so that the cutting tool can maneuver to make the cut; therefore, it is necessary to understand the ramifications of full removal in terms of sediment disturbance in relation to the cuttings pile(s) and the potential to release contaminants, if any, that may be present in the cuttings pile sediments into the environment. Additionally, cuttings piles may extend vertically upward and cover cross braces within a jacket. Removal of the lower portions of a jacket may also have the potential to disturb cuttings piles and release potential contaminants into the environment, if any are present in the cuttings pile. In some cases, the shell hash layer that covers cuttings piles has been shown to entomb potential contaminants (Gala et al., 2008).

Additionally, various intermediate options may be developed within the bounds of the no-action and full removal options. These include the partial removal of the structure where the removed portion is transported to the shore for recycling, reefed in-place, or transported to a designated reefing location. For example, partial removal options for a jacket could include toppling the jacket (with or without conductors and/or the topside) or cutting sections of the jacket at various depths, and either placing cut portions near the base of the jacket or removing cut portions to a recycling facility.

2.1.5.2 Exclusion zones

Option selection and evaluation should consider the potential to remove or maintain the existing exclusion zone (Nelson et al., 2022). No-action options can include both a "Leave-In-Place" option (LIP), referring to leaving the structure in-place, in whole or in part, without an exclusion zone, or a "Protect-in-Place" option (PIP) that refers to leaving the structure in-place, in whole or in part, while retaining the exclusion zone. Exclusion zones protect the habitat, along with the associated ecosystem benefits, that have developed around the subsea structure, or portions thereof, by limiting the intrusion of trawling gear into the developed ecosystem. The adverse physical impacts of trawl fishing on the sea bottom, as well as the impacts of incidental bycatch, have been well documented (Daan et al., 2005; Mannocci et al., 2012; Eigaard et al., 2017). Bycatch, in the fishing industry, is a fish or other marine species that is caught unintentionally while catching certain target species and target sizes of fish, crabs etc.

Exclusion zones also assist in managing navigation and trawling risks by limiting the vessel traffic within the exclusion zone. The exclusion of commercial fishing within the 500 m exclusion zone around each installation in the North Sea is regarded as "further enhancing the properties of these reefs as refuges for marine life" (Todd et al., 2009). Owing to these fishing restrictions, offshore oil platforms have served as de facto marine protected areas (MPAs) for years (Fujii and Jamieson, 2016), allowing for high colonization rates of fish and benthic invertebrates on large steel structures throughout the water column (Bell & Smith, 1999; Roberts, 2002; Soldal et al., 2002). These benefits may increase the carrying capacity of fish in the North Sea, similar to that observed in the Gulf of Mexico (Scarborough-Bull et al., 2008). Thus, the removal of offshore structures and associated exclusion zones should be considered and incorporated into any fisheries management plan because the removal of these structures has the potential to cause ecological and economic impacts (Scarborough-Bull et al., 2008).

2.1.5.3 Technical feasibility and option assumptions

When selecting potential decommissioning options, it is important to understand the technical feasibility of the proposed options and document why certain options, including their assumptions, are selected or rejected for evaluation. While considering and evaluating decommissioning options, adaptive management of the options can be used to adjust existing options or introduce new decommissioning options into the analysis for consideration on an iterative basis.

2.1.6 Decommissioning option campaign characteristics

For each identified decommissioning option, it is necessary to define the characteristics of the decommissioning campaign necessary to implement each option. This information includes the type of vessels to be used, fuel types burned, personnel tasks and associated manhours expected for each task (onshore and offshore), weight of the structure to be transported, distances to be travelled, and outgoing and receiving port locations. This information will be used to support the development of multiple metric values, including health and safety risks (onshore and offshore), greenhouse gas emissions, and the estimated costs of option implementation. Implementation campaign characteristics should consider the synergies between tasks for all subsea structures in the field. Campaign characteristics, and associated costs for option implementation, are typically developed by the operator.

2.1.7 Characterization of site-specific ecosystem services and the reference state

To understand the potential positive or negative effects associated with the implementation of various decommissioning options, it is imperative to identify the key ecosystem services associated with the structure in its "current condition". Analysis planning should clearly identify the condition that will serve as the "reference" state from which changes in metric values will be measured. Since decommissioning actions (e.g., removal, partial removal) proposed as part of the decommissioning program may affect the current "in-situ" condition of ecosystem services, the "reference state" should represent the "current condition," and metrics adjusted appropriately in relation to this condition. Thus, an understanding of the reference state requires an understanding of the marine ecosystem that has developed in relation to the presence of subsea structure(s) under current conditions and its level of maturity. These ecosystem services include both ecological and socioeconomic services. Ecological services include, *inter alia*, benthic invertebrate and fish production and nursery areas; provisioning of food resources for benthos, fish, and marine mammals; and refuge areas for fish. Socio-economic services include, *inter alia*, multigenerational production and harvest of commercial and recreational fish stocks, long-term fish stock protection, and provision of existence and bequest value of species of special significance. Socioeconomic services exist because the habitat exists. Thus, actions that affect habitats have the potential to affect the flow of socioeconomic values.

2.1.8 Characterization and quantification of ecosystem services potentially affected by option implementation

Once site-specific ecosystem services have been identified, the next step is to determine which of these services may benefit or be adversely impacted through the implementation of each decommissioning option. In the context of a NEBA-CA, ecosystem service impacts associated with option implementation refer to the impacts that are predicted to arise from the implementation of the options being analyzed and include the following:

- Ecological impacts associated with physical changes of habitat (e.g., removal, partial removal);
- Ecological risks associated with chemical/polymer short and long-term exposure (e.g., NORM, mercury, PAHs, plastics);
- Risks to socioeconomic active and passive use values associated with the above-mentioned ecological risks; and
- Greenhouse gas emissions associated with option implementation.

The physical removal of hard-structure habitat can create ecological impacts such as the reduction of benthic biomass and associated fish production and densities, resulting in subsequent risks to marine biota that may use these sites as feeding stations (Scarborough-Bull et al., 2008; Arnould et al., 2015; Todd et al., 2018; Todd et al., 2022a; Todd et al., 2022b). Changes in hard structure surface area, a key habitat metric, are estimated within NEBA-CA. Hard structure surface area can serve as a surrogate metric to understand potential changes in ecological metrics such as fish biomass, benthic biomass, etc.

In case any component or decommissioning option results in the release of a contaminant into the environment, an ecological risk assessment, in some form, should be considered to understand the extent of potential risk to ecological populations (USEPA, 2004; Barnthouse, 2008). For example, the effect of degradation of plastics associated with components to be left *in situ* should be considered (Testoff et al., 2022) and similarly, screening level ecological risk assessment of multiple chemical constituents can also be considered (USEPA, 1997; USEPA, 2004).

Both physical and chemical risks to marine ecology may occur following the implementation of decommissioning options and have the potential to result in related adverse risks to socioeconomic values to society (Scarborough-Bull et al., 2008). Socioeconomic risks include loss of commercial and recreational fishing value associated with less fish, decreased stock protection, and loss of species of special significance where society holds existence and bequest value for these species. For example, *Desmophyllum pertusum*, a slow-growing cold-water coral of conservation importance, was found on multiple jackets in the North Sea (Gass and Roberts, 2006). Removal of these jackets may thus, affect the long-term protection of this species through the reduction of physical habitat, a metric quantified within the NEBA-CA.

Natural reef habitats are declining worldwide (Pandolfi et al., 2003). In areas where many offshore platforms exist (e.g., North

Sea, Gulf of Mexico, Australia, and California), mass removal may have the potential to adversely affect ecological and socioeconomic values on a larger scale through loss of physical habitat and connectivity benefits (McLean et al., 2022). Evidence shows that the artificial habitat supplied by platforms in the Gulf of Mexico has increased the regional carrying capacity for economically important reef fish species (Scarborough-Bull et al., 2008).

An improved understanding of potential impacts and risks allows us to evaluate the consequences of the removal of hard structures and to meet the social responsibility associated with the precautionary principle.

2.1.9 Quantifying ecosystem service values

To evaluate how implementation of an action affects ecological and socioeconomic conditions, quantification of changes, negative or positive, in ecosystem services is necessary. It is also important to recognize that ecosystem services are not static measurements but represent a flow of benefits over time (i.e., multigenerational services). Quantified estimates of ecosystem services sufficient for environmental decision-making can be obtained through the use of the natural resource service valuation approaches developed and refined under the United States natural resource damage assessment (NRDA) process (Unsworth and Bishop, 1994; NOAA, 1999; Nicolette et al., 2013b). Within NRDA, these approaches are used to balance compensatory restoration with adverse impacts to maintain the flow of ecological and socioeconomic services provided to society (Nicolette et al., 2013b). These approaches include service-to-service approaches such as habitat equivalency analysis (HEA) and resource equivalency analysis (REA) (NOAA, 1999; Chapman and LeJeune, 2007). In a NEBA-CA decommissioning context, these approaches can be used to evaluate changes in ecological and socioeconomic service values, over time, associated with option implementation. It is within this context that the use of these economic-based methods is considered and takes advantage of the experience gained within the NRDA process over the past 30 years.

2.1.9.1 Ecological service quantification

Many ecological habitat services are not traded in the marketplace and therefore do not have a direct monetary value. A method for evaluating ecological habitat service flows is provided in King and Adler, 1991. This concept led to the development of the HEA approach (NOAA, 1999). HEA is an environmental economics-based approach used for determining appropriately scaled compensatory restoration. HEA uses environmental metric (s) to measure changes to ecological habitat services and focuses on quantifying the area (e.g., hectares, acres) and level of impact over time in units typically represented as service-hectare-years (SHYs), service-acre-years (SAYs), and service-tonne-years (STYs) (Nicolette et al., 2013a); however, other metrics can be used and developed appropriate to the site and the key services being evaluated. Within this method, changes in one or more metrics (e.g., fish biomass, species diversity) may be selected as a surrogate or proxy to represent the loss or gain of ecological services associated with changes to a habitat (Chapman et al., 1998; Chapman and LeJeune, 2007; Nicolette et al., 2013a). The calculation of ecological services involves a discount rate that allows for the gains and losses of ecological services to be evaluated from a net present value (NPV) standpoint; however, using a non-monetary environmental metric (e.g., NPV fish biomass SHYs or NPV benthic invertebrate STYs). The discount rate is the rate at which the public is indifferent to consuming goods now or sometime in the future (Moore et al., 2013).

An overview of the information, technical approach, and input parameters required to conduct habitat equivalency analysis is detailed in published articles and government sponsored reports (Chapman et al., 1998; NOAA, 1999; Dunford et al., 2003; Chapman and LeJeune, 2007; Bateman et al., 2011; Nicolette et al., 2013a). The use of HEA has been upheld in the US Federal Court (United States, 1997; United States, 2001). Additionally, the European Environmental Liabilities Directive (ELD) gives preference to resource equivalency approaches over monetary valuation when determining compensatory restoration (Nicolette et al., 2013b).

2.1.9.2 Human use service quantification

Ecosystems generate several different types of benefits for humans including those that are enjoyed directly through consumption (boating, fishing, diving, etc.), indirectly through their support and production of directly enjoyed goods and services (clean water, food production, etc.) and through non-consumptive means such as bequest and existence values (Nicolette et al., 2013a). Human use service values are typically quantified in monetary metrics, however, for use data, metrics might include user-days or visitor-days as non-monetary metrics. Multiple economics methods are available to quantify changes in human use services. These include hedonic pricing, stated preference methods, and the travel cost models (Freeman, 2003). Each method measures a different type of public value.

Conducting primary economic studies may not be feasible given the cost and time required to collect and analyze the data; therefore, many analysts estimate publicly valued ecosystem services using benefit transfer methods. Benefit transfer refers to methodologies that use knowledge gained from past studies regarding the value of similar services at comparable locations and employs this knowledge at a new location (Rosenberger and Loomis, 2001; Nicolette et al., 2013a). Transferred values are adjusted for population, income, and other factors to obtain an estimate of the value at the project site.

Service to service human use valuation approaches are also preferred approaches for compensatory restoration within the ELD.

2.1.10 Characterization and quantification of *In-Situ* risks associated with leaving hard structure in place

In addition to evaluating the effects on ecological and socioeconomic services, it is important to consider the *in-situ* management risks associated with structures that are managed in place. A variety of *in-situ* risks may be associated with the various options and should be identified with the intent of quantifying these risks and how they would be predicted to change through implementation of the various options. For example, if an option identifies that a certain subsea component, or portion thereof, is to be left in place, it is important to consider the potential and magnitude of the *in-situ* risks associated with that action over the period in which that component is predicted to last in the environment. The types of *in-situ* risks that are likely to be encountered with subsea structures that are left in place can vary based on the type of structure (e.g., fixed structure, buoyant structure) and include chemical risks (e.g., component specific, drill cuttings piles), navigational hazard risks, and trawl fishing hazard risks (i.e., snagging), among others. These risks vary according to the site-specific location, depth, and type of structure being evaluated. Assumptions regarding risks should be consistent among options for a given component. Although the predicted risk will only be as precise as the available data allows, internal consistency in the assumptions across options, where appropriate, for the same subsea component provides a mechanism to support option differentiation, i.e., a key outcome of the NEBA-CA process.

It should also be noted that option development can be used to manage *in-situ* management risks. For example, navigation and trawl snagging risks can be managed by maintaining the existing exclusion zone around a structure as well as by reducing ecological impacts by limiting impacts to benthic habitat within the exclusion zone (Nelson et al., 2022).

2.1.11 Health and safety, implementation risks

Decommissioning options entail various equipment, tasks and associated manhours that are predicted to occur. As these activities increase in difficulty and/or the man hours needed for option execution increase, human health and safety risks may increase as well. These risks include both physical injury and potential loss of life (PLL) during both onshore and offshore activities.

2.1.12 Comparative metrics and data requirements

Given the options identified, the next step is to determine what metrics would be evaluated for understanding the benefits and risks associated with implementation of each option. Metric selection should focus on how each decommissioning option may affect specific parameters related to environmental, health and safety, short and long-term risks, economic, and technical feasibility. Assessment metrics should be evaluated for each option and include a combination of ecosystem service (benefit) and risk metrics.

Net environmental benefits and risks are assessed using the "reference" state of the environmental condition, against which the potential change in environmental values and risks associated with each of the decommissioning options will be compared. NEBA-CA incorporates a variety of quantitative and semi-quantitative assumptions. These assumptions should be identified, along with their basis, during analysis and within reporting. Given the uncertainty in some assumptions, the assessment should attempt to be conservative in any estimates to not overestimate benefits or underestimate adverse impacts and risks.

Since it would be difficult to measure every ecosystem service associated with a site, metrics that serve as a surrogate for potentially affected ecosystem services should be identified (Section 2.1.8). Additionally, human health and safety risk metrics associated with navigation, trawling, and option implementation are important as they relate to long and short-term conditions that should be considered along with ecosystem service values. Example ecosystem service and risk metrics that the authors have used for various offshore decommissioning applications of NEBA-CA are presented in Table 1.

Risk analysis and modeling may be required to further understand how chemicals or actions influence ecosystem services. For example, combining water column dispersion modeling and associated chemical toxicity reference values may help understand the relationship between chemicals released into the environment and potential risks to ecological or human receptors. When conducting a NEBA-CA analysis, sufficient information should be collected and evaluated for each metric so that a relative differentiation of the trade-offs between options can be compared. Within NEBA-CA, quantified metric estimates are approximate values and are not intended to be exact, but sufficient enough for identifying impacts and differences between options to a reasonable degree of certainty.

2.2 Data requirements

Since offshore O&G sites are generally different in composition, design, water depth, and location, NEBA-CA is a site-by-site analysis. Analysis planning should identify data requirements and data gaps for the proposed analysis. NEBA-CA is primarily a desktop analysis and relies on existing data, although supplemental data can be collected to address significant data gaps where deemed necessary. Data are needed to establish the ecological and chemical condition around and away from the structure. Field layout and engineering diagrams are needed to establish structural surface areas and physical characteristics of the site, and data associated with option

TABLE 1 Example Metrics Used for Offshore Decommissioning Applications of NEBA-CA.

Ecosystem Service Beneficial Metrics	Detrimental Risk Metrics
Total Hard Steel Surface Area in Water (ha)	Navigation Risks
Surface Area - Shell Hash Habitat (ha)	Bouyancy Risks
Surface Area - Halo Area (ha)	Trawling Snagging Risks
Habitat Volume in Water (m^3)	Trawling PLL (Potential Loss of Life) Risks
Hard Plastics Surface Area (ha)	Residual Chemical Risks (PAHs, NORM, Hg, etc.)
Benthic Coverage (ha)	Plastics Ecological Degradation Risk
NPV Benthic Biomass (t)	Onshore and Offshore Implementation PLL Risks
NPV Fisheries Biomass (t)	Onshore and Offshore Implementation Injury Risks
NPV Net Ecosystem Service Value (SHYs)	Onshore and Offshore Man-Hours
NPV Commercial Fisheries Value (£)	Greenhouse Gas Emissions (CO_2, CH_4, N_2O, SO_2)
NPV Fish Processing Sector (£)	Energy Usage (GJ)
NPV Recreational Fisheries Value (£)	Fuel Usage (liters)
NPV Other Active Use Values (£)	Implementation Costs (£)
NPV Passive Use Values (£)	

[1] Net Ecosystem Service Value combines available hard structure surface area (hard structure, shell hash habitat, and halo areas) and overall ecological impact projected with trawling to represent the overall ecological condition of the specific component area.

[2] Option implementation costs are evaluated; however, cost is considered as a secondary evaluation metric within a NEBA-CA, since the focus is on maximizing benefits to the public while managing site risks. The cost metric is relevant in decision-making in cases where the benefit and risk metrics themselves do not sufficiently distinguish an optimized option, in which case, cost can be used to further support a decision.

[3] Passive use values can include other metrics such as existence, bequest, and aesthetic values.

campaigns are needed to evaluate onshore and offshore implementation risks, option costs, and greenhouse gas emissions. Options should describe the changes in surface area and other physical actions that will alter the existing habitat. Our experience has shown that operators have developed most of the data needed as part of their development, monitoring, and regulatory submissions which includes:

- Historical marine environmental and subsea surveys;
- Environmental appraisals;
- Jacket and subsea structure removal studies/estimates;
- Previously conducted CA's, if any;
- Prior environmental monitoring reports – sediment and water quality, biota surveys, and human use activities;
- Remotely operated vehicle (ROV) survey reports and video;
- Detailed field layout diagrams and tables listing dimensions and material composition of each component; and
- Regulatory submissions relating to facilities included in the scope.

Review of ROV footage is critical in establishing the ecological condition near the structure. In some cases, examination of the existing ROV footage may be necessary to identify the biological makeup of the ecosystem associated with the subsea structure. In other cases, collection of ROV footage may be necessary. For example, collection of high-resolution videos so that fish can be identified at a species level and differentiated based on their commercial or recreational value, as well as for the identification of species of special significance, may be warranted for the site if not available.

Additionally, marine mammal acoustical or observational surveys within a field can provide further evidence as to the use of the field as feeding grounds by seals, whales, etc.

For cutting piles and "halo" areas, the biological and chemical characteristics, as well as physical dimensions of these habitat areas, help to further establish the ecological condition associated with the field. The collection of these data, if not available, would support an understanding of the effects that these actions (i.e., disturbance) might have on the ecosystem services associated with the field. Once the analysis of individual components is completed, a field-level decommissioning plan can be proposed that represents the decision for the overall campaign across the field.

2.3 Option analysis and graphics

A key aim of the NEBA-CA process is to provide a mechanism to differentiate how assessment metrics are predicted to change, given the implementation of each decommissioning option. A NEBA-CA provides a graphical summary of the data so that differentiation between options becomes readily apparent while providing a clear basis for that differentiation, thus providing an improved understanding of individual metric trade-offs between options based on quantified data. This is necessary because stakeholders tend to focus on metrics of specific interest to themselves at the expense of other metrics. For example, commercial fishermen may focus more on commercial fishery values, an environmental group may focus on overall ecosystem habitat values, or O&G operators may focus on economic benefits of leaving structure in-situ. The separation of various metrics within a graphical presentation is critical for allowing stakeholders to understand the following:

- Their own metric interests;
- Metric interests of others; and
- Trade-offs that need to be made to arrive at a final decision.

A stakeholder may not initially support a final decision; however, a data presentation that clearly depicts scientifically-based, transparent, and defendable metrics and the individual trade-offs between options, will be helpful for stakeholder discussions regarding understanding the basis of option selection.

Graphics presented as part of a NEBA-CA are developed to provide an understanding of the relative beneficial (positive) and detrimental (negative) impacts associated with the metrics evaluated for each option so that trade-offs between options can be evaluated. Note that, for clarity within a structure, if there is no difference in an assessment metric across all decommissioning options, that metric is not included in the associated graphics. The justification behind this approach is to focus on metrics that help differentiate between options to select a preferred decommissioning option.

For example, if exposure risks to chemical constituents associated with structural components are considered negligible across all options, and therefore do not help differentiate between options, the chemical exposure risks associated with structural components are not presented in the graphic displays, although they are documented as part of the NEBA-CA. Additionally, duplicative metrics can be removed from the comparative graphics to avoid overinfluencing the visual effect, impact, or clarity of the evaluation metrics.

2.3.1 Benefit–detriment graphical understanding

Given the variety of units in which various metrics are displayed, it is necessary to develop a process whereby all differentiating metrics can be displayed on the same graph. Consequently, graphics are developed such that each specific metric can be plotted in proportion to its specific metric values across options. Metrics with beneficial ecological and human use service attributes are scaled to a value between 0 and 1, as shown in example Figure 2. Note that shell hash habitat is recognized as a beneficial attribute; however, in the case of full removal, shell hash habitat value can be adversely impacted compared to baseline soft-bottom habitat, and as such, can result in a negative impact for the full removal option.

Each beneficial metric is scaled across all options by setting the best value for that metric to 1. All subsequent values for that specific metric are scaled to a proportion of 1, so that their graphical bar heights are relative to one another. For example, a bar that goes to a value of 0.5, provides 50% of the beneficial value when compared to the option where that metric has the greatest beneficial value of 1. This allows all values for each specific beneficial metric to be plotted on the same relative scale, for that specific metric, across the options for comparison. Note that the actual data values are provided above each bar to provide stakeholders a basis to understand the metric tradeoffs.

Similarly, each detrimental metric is scaled across all options by setting the most detrimental value for a metric value equal to −1. All subsequent values for that specific metric are scaled to a proportion of −1 so that their graphical bar heights are relative to one another. Thus, the bar that is predicted to provide the greatest adverse impact (i.e., highest risk) for each specific detrimental metric receives a value of −1, and the metric values for that specific metric for the other options are plotted proportional to the bar at a value between 0 and −1. Graphics presented in this manner help to identify NEBA-CA optimized options, considering that all risk drivers are managed to as low as reasonably practical (ALARP). ALARP is a best common practice of judgement of the balance of risk and societal benefit (NOPSEMA, 2022).

2.4 North Sea case example

A NEBA-CA was conducted for an end-of-life jacket located in the North Sea in approximately 150 meters water depth (Confidential Client Report, 2020). The purpose of presenting this case study is to demonstrate the application and results of the NEBA-CA framework applied to an actual site, including resulting graphics. The case study included analysis of the following four scenarios for the jacket with various exclusion zone (presence or absence) and partial removal options:

- Protect-In-Place - Recycle
- Leave-In-Place - Recycle
- Protect-In-Place - Reef
- Leave-In-Place - Reef

Although detailed metric evaluations were conducted for the case study, underlying detailed analysis of the individual metrics

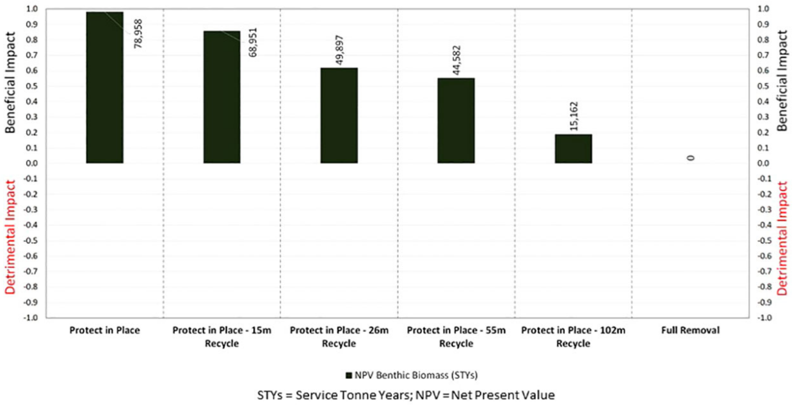

FIGURE 2
Example graphic of one metric, [net present value (NPV) of benthic biomass (Service Tonne Year)], scaled to between 0 and 1 for each of the options evaluated. All bars are in proportion to one another.

on which the graphics for the case study were based are not included. This is because the NEBA-CA framework presents metrics to consider, while not being prescriptive. Metrics and their evaluation methods will be site by site considerations and may depend upon available data, and as well, provide flexibility in the application of the approach.

The options analysis and quantitative metric evaluation results of the case study are presented using benefit-detriment graphics, whereby a visual assessment of the data can be conducted. The options evaluated ranged from *in-situ* management to full removal, with multiple partial removal options. For partial removal options, the removed portion of the jacket is either reefed alongside the remaining portion of the jacket or transported to a recycling facility. These conditions are also examined by considering alternate exclusion zone options (i.e., to fully remove the exclusion zone or maintain the zone). The case study evaluation options framework is shown in Figure 3.

2.4.1 Case study option identification and nomenclature

The options identified for the North Sea jacket were designated as follows on corresponding graphics:

- Leave-In-Place (LIP) refers to leaving the structure, in whole or in part, in place without an exclusion zone (NOEZ);
- Protect-in-Place (PIP) refers to leaving the structure, in whole or in part, in place with a 500 m exclusion zone (EZ) that serves to protect the habitat and associated ecosystem benefits that have developed around the jacket, or portions thereof, and manage navigation and trawling risks;

Both the Leave-In-Place and Protect-in-Place options assumed that the jacket remained in-place after topside removal. For scenarios in which the jacket is managed in place with a portion extending above the water level, it was assumed that there would likely be a requirement for functional navigational aids, including the need for periodic access and associated maintenance.

- Partial Removal: For both of the above options, the option name included the following if a partial removal action:

O Final depth of cut in meters; and
O Cut section disposition (Reef or Recycle)

■ Reefing refers to placing the cut portion in the sea next to the jacket.

■ Recycling refers to transporting the cut section to shore to be recycled.

O Four cut depths were evaluated for the partial removal options as follows:

2.4.1.1 Partial removals and cut depth intervals

For options that involved some form of partial removal, it was assumed that the removed structure would be either transported to shore for recycling or the removed structure would be reefed in place near the base of the jacket. Partial removal options were considered for multiple depth intervals in either case (recycle or reef).

To determine depth intervals appropriate for evaluating partial removal options, it was necessary to understand the characteristics of various vessels, from heavy lift vessels (HLVs) to fishing vessels, which may occur in the North Sea. The analysis considered the transit and lifting drafts (where appropriate) of these vessels with the likelihood of being used in the North Sea.

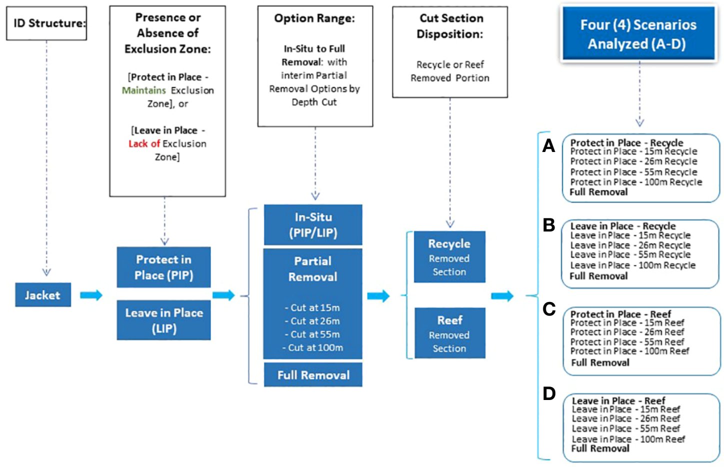

FIGURE 3
The NEBA-CA North Sea Jacket Option Analysis.

The basis for partial removal cut depths that were evaluated follows:

2.4.1.1.1 Partial removal - 0 (sea level) to 15 m

The transit draft of any of the HLVs evaluated (likely the largest vessels in the area) ranged from 10 m to 12 m. The drafts of various types of fishing vessels ranged from 1.25 m to 8.5 m. It should be noted that an HLV, especially in a lifting draft, will have a detailed route plan, and as such, we focused on the transit draft rather than lifting the draft in determining this first depth cut. A 15 m depth cut was estimated to provide sufficient clearance for vessels in use in the North Sea, as these would be in transit when operating at or near the jacket location.

2.4.1.1.2 Partial removal - 0 to 26 m

The Seawise Giant was the largest ship built to date and had a draft of 24.6 m. The decision to include partial removal at 26 m reflects the largest potential draft of a vessel and coincides with the 85-foot clearance guideline in the Gulf of Mexico.

2.4.1.1.3 Partial removal - 0 to 55 m

Partial removal at 55 m was selected as an option because it met the International Maritime Organization (IMO) guidelines.

2.4.1.1.4 Partial removal - 0 to approximately 100 m

This option is the "derogation option" under OSPAR Decision 98/3, which requires the jacket to be removed down to the top of the footings. The top of the footings of the jacket was approximately 100 m deep.

- Full removal (assumes cut 3 m below the mudline, NOEZ, and removed structure prepared for recycling.

2.4.2 Ecosystem services and metric identification

For this case study, the NEBA-CA drew upon the UK National Ecosystem Assessment (UK NEA) framework (UK Government, 2011) as the basis for the identification and selection of key ecosystem service assessment metrics. Ecosystem service values are recognized by UK and International authorities as legitimate uses of the sea (UK Government, 2011). Several key findings of the UK NEA related to the importance of ecosystem services to UK society are listed below. Each key finding was assigned a level of scientific certainty, based on a 4-box model and complemented, where possible, with a likelihood scale (*well established, virtually certain, very likely, likely*) (UK Government, 2011).

- The diversity of organisms in marine habitats provide a range of ecosystem services and benefits of significant value to UK society. (*well established)*
- Many of the benefits are accrued directly by coastal dwellers and visitors, but also indirectly by much of the UK's society. (*well established, virtually certain*)
- The quantity of wild fish caught in UK waters is insufficient to meet the UK demand for this food. (*well established, virtually certain)*
- The sustainability of food provision from marine habitats is threatened by overexploitation of fisheries; fishing is also damaging other marine ecosystem services. (*well established, virtually certain)*

- The UK's seas are important to people's quality of life but are less well protected than terrestrial environments. (*virtually certain*)
- The UK population has a strong affinity for the sea and has always derived inspiration from it. More people are using the sea for leisure and recreation, education, research and health benefits. (*virtually certain*)
- Many organisms create living habitats such as reefs and seagrass meadows. These can provide essential feeding, breeding and nursery space that can be particularly important for commercial fish species. (*well established, likely*)
- Building coastal defences and offshore structures, such as wind turbines, oil platforms and reefs, provides artificial habitats which can have positive impacts, particularly for species usually associated with rocky environments. (*very likely*)
- The use of monetary and non-monetary valuation of ecosystem services will aid the process of considering the impacts and benefits of development on marine habitats. (*virtually certain*)

As can be ascertained from the key findings of the UK NEA, ecosystem services and associated valuation play a key role in UK society and as such, require consideration as to actions that affect these services. Although multiple metrics were calculated as part of the study, only those metrics plotted on the graphics (as described earlier) are highlighted in Table 2. These metrics encompassed ecosystem services, risks, and costs.

2.4.3 Case study results

The results of the case study, without any weighting of the data and for demonstration purposes, are graphically presented for the Protect-In-Place - Recycle scenario (Figure 4). Note that the graphics produced within NEBA-CA depict the quantified value associated with each bar to help the reviewer understand the differences between metric values by option. The graphics for all four scenarios are provided in Figures 5A–D for visual comparison. The results summary for the four scenarios is provided in Table 3. The quantified metric values were removed from Figures 5A–D to aid the reader in visually observing the trends among the four scenarios.

2.4.4 Observations

Overall, the following trends become apparent:

- The presence of an exclusion zone provides greater ecological and socioeconomic value and less risk than the same option with no exclusion zone; and

TABLE 2 North Sea Case Study Metrics (metrics bolded were plotted in graphics).

Ecosystem Service Beneficial Metrics	Detrimental Risk Metrics
Total Hard Steel Surface Area in Water (ha)	**Navigation Risks**
Surface Area - Shell Hash Habitat (ha)	Bouyancy Risks
Surface Area - Halo Area (ha)	**Trawling Snagging Risks**
Habitat Volume in Water (m^3)	**Trawling PLL (Potential Loss of Life) Risks**
Hard Plastics Surface Area (ha)	Residual Chemical Risks (PAHs, NORM, Hg, etc.)
Benthic Coverage (ha)	Plastics Ecological Degradation Risk
NPV Benthic Biomass (t)	**Onshore and Offshore Implementation PLL Risks**
NPV Fisheries Biomass (t)	Onshore and Offshore Implementation Injury Risks
NPV Net Ecosystem Service Value (SHYs)	Onshore and Offshore Man-Hours
NPV Commercial Fisheries Value (£)	**Greenhouse Gas Emissions (CO_2, CH_4, N_2O, SO_2)**
NPV Fish Processing Sector (£)	Energy Usage (GJ)
NPV Recreational Fisheries Value (£)	Fuel Usage (liters)
NPV Other Active Use Values (£)	**Implementation Costs (£)**
NPV Passive Use Values (£)	

[1] Net Ecosystem Service Value combines available hard structure surface area (hard structure, shell hash habitat, and halo areas) and overall ecological impact projected with trawling to represent the overall ecological condition of the specific component area.

[2] Option implementation costs are evaluated; however, cost is considered as a secondary evaluation metric within a NEBA-CA, since the focus is on maximizing benefits to the public while managing site risks. The cost metric is relevant in decision-making in cases where the benefit and risk metrics themselves do not sufficiently distinguish an optimized option, in which case, cost can be used to further support a decision.

[3] Passive use values can include other metrics such as existence, bequest, and aesthetic values.

- Reefing (i.e., habitat retention) provides greater ecological and related socioeconomic value and lower risks than the recycling option.
- Full removal option is predicted to create the most negative impact compared to all the options and should be considered as the least preferable option.

It is important to understand that any calculated values for the various options are to be used in the comparative assessment to differentiate between the options and are therefore most relevant when compared against each other. Although some data may not be precise, internal consistency of assumptions, between options, provides the level of evaluation necessary for option comparison.

If stakeholders determine that weighting of metrics is appropriate, they can adjust the graphics by changing the individual weights of select metrics; however, in the example graphics provided, visual comparison of the data did not require weighting of metrics while allowing the reviewer the ability to evaluate all data simultaneously so that the trade-offs between options could be understood and discussed with confidence.

2.5 Optimized decommissioning option for the jacket

The overall NEBA-CA optimized decommissioning option across all option groups was determined as follows:

First, the graphical approach used to identify the preferred individual group options was used to visually evaluate how the data from each of the four option groups compared to one another (Figures 5A–D). The visual display provides the relative difference between the predicted metrics for each option group.

As seen in Figures 5A–D, the option group considering Leave-in-Place with Recycling would create the least amount of ecosystem service benefit and the greatest amount of risk. The option group considering Protect-in-Place with Reefing would create the greatest amount of ecosystem service benefit and the least amount of risk. Based on the visual display of the data, the optimized decommissioning option was initially identified as the Protect-in-Place - 15 m Reef option (Figure 5C).

2.6 Risk management decision-making

Given the visual analysis, risk management tolerance considerations can also be incorporated into the evaluation of the data to adjust, if necessary, the initially identified optimized option to account for the understanding of the magnitude of risk and how that risk might influence health, safety, or the environment. For example, an option may have an identified risk; however, that risk might be small in scale or be considered negligible in absolute terms, even if the bar tracks to -1 as the highest assessed risk option for the asset. As such, this step can be used to help confirm or refine the initially identified

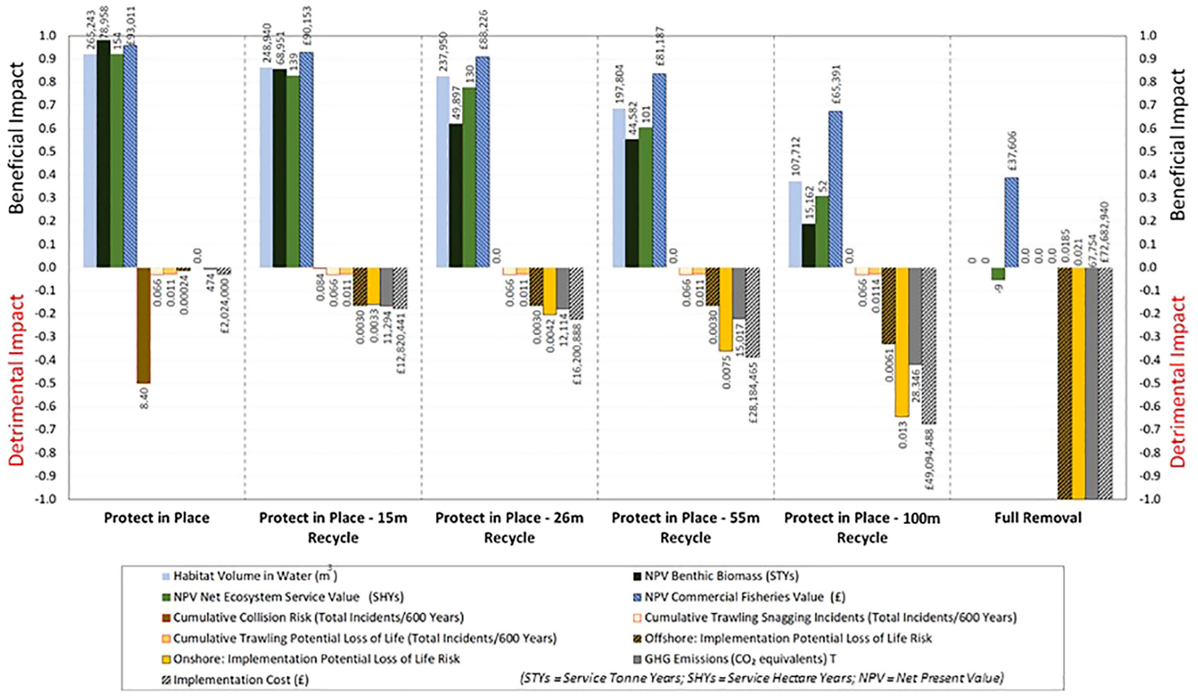

FIGURE 4
Beneficial and Detrimental Trade-offs Associated with the Jacket and the Protect-In-Place Recycle Options.

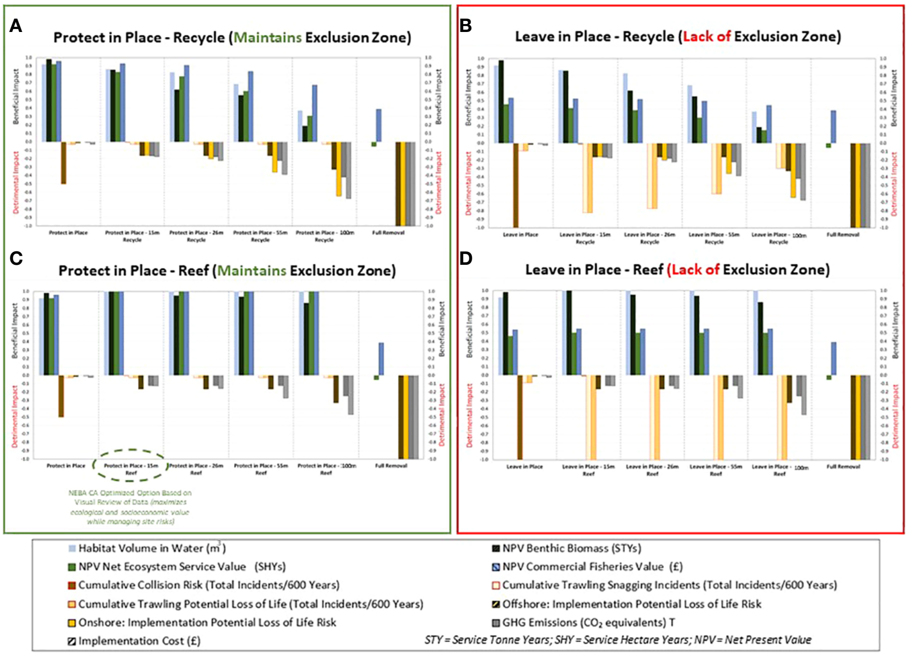

FIGURE 5
(A–D) The NEBA-CA Optimized Decommissioning Option Based on Visual Observation with Data Comparison for the Jacket. Note that metric values were removed from this graphic to enhance the visual comparison.

TABLE 3 North Sea Case Study Results Summary.

(A) **Protect-In-Place - Recycle**	**(Maintains Exclusion Zone)**	The predicted changes (i.e., trade-offs) in the beneficial and detrimental metrics associated with partial removal protect in place recycle option, with an exclusion zone, are presented in Figure 4. As portions of the jacket are removed and transported to the shore, benthic biomass and net ecosystem service values are predicted to decline steadily as cuts proceed at deeper depths and removed portions are taken to shore for recycling. These declines are due to the permanent removal of hard structural habitat and volume with related subsequent adverse impacts on the shell hash habitat (i.e., in the form of reduced shell hash deposition). The maintained exclusion zone prevents further discounting of benefits because commercial fishing pressure will be significantly reduced, thus negating adverse effects on benthic invertebrates, commercial and non-commercial fish species, and small marine mammals from direct catch and by-catch, as well as physical impacts to the sea bottom, including the shell hash and halo areas that lie outside the structure.
		As seen in Figure 4, beneficial impacts decrease as detrimental impacts increase as the level of effort to implement each option increases and hard structure is removed, with the full removal option being the most detrimental. As seen in Figure 4, 8.40 navigation incidents are expected to occur over the 600-year period for the in-situ management option (i.e. one incident every 71 years.). This assumes that there are no advances in technology, etc. that reduce potential risks over this period. As such, this assumption is conservative in that it overestimates risk relative to the period over which ecological and commercial fishing benefits were calculated (300 years).
		Full removal was predicted to provide little beneficial value and results in the lowest commercial fishing value (an approximate 60% decline compared to the current Protect in Place condition). Moreover, full removal was predicted to create short-term environmental damage associated with the disturbance to the shell hash habitat and cuttings pile.

(Continued)

TABLE 3 Continued

		Based on the information in Figure 4 and 5A, the full removal option is predicted to create the most negative impact and least benefit compared to all the options, and thus should be considered as the least preferable option.
(B) **Leave-In-Place - Recycle**	**(Lack of Exclusion Zone)**	As seen in Figure 5B, as portions of the jacket are removed and transported to the shore, benthic biomass and net ecosystem service values are predicted to decline steadily as cuts proceed to deeper depths. These declines are due to 1) the permanent removal of hard structural habitat and volume with related subsequent adverse impacts on the shell hash habitat, and 2) removal of the exclusion zone allowing the area to be open to trawling, increasing the likelihood of adverse effects on fish and mammal species, as well as impacts to the sea bottom in the shell hash and halo areas that lie outside the structure.
		For the recycling options, options that remove the least amount of the jacket are predicted to provide more ecosystem service benefits and less detrimental impacts when compared to the other recycling options (i.e., the less amount removed, the better).
		Based on the information in Figure 5B, the full removal option is predicted to create the most negative impact compared to all the options and should be considered as the least preferable option.
(C) **Protect-In-Place - Reef**	**(Maintains Exclusion Zone)**	As seen in Figure 5C, as portions of the jacket are removed and laid down (reefed) next to the remaining jacket portion, impacts on benthic biomass are predicted to be minor because the portions reefed in the water column will regenerate benthic biomass over time; with additional hard surface area and habitat volume reefed underwater. Additionally, with an exclusion zone, the net ecosystem service value is projected to remain relatively constant, as the area will not be open to trawling, thus avoiding adverse effects on fish, benthos, marine mammals, and the sea bottom. However, the existing shell-hash habitat under the jacket will no longer benefit from the additional shell hash and organic deposits when the upper structure portions (15 m and 26 m) are removed. The Net Ecosystem Service Value incorporates both the quality and quantity of hard surface area habitat provided by the shell hash layer, halo area, and the jacket structure itself. It should be noted that hard surface area and habitat volume is the highest with the 15 m cut when compared to the current Protect in Place condition. This is due to reefing which adds surface area associated with the portion of the jacket extending above the water column but below the topside with limited impact to the quantity of marine snow that accumulates at the base of the jacket forming the shell hash layer. Further depth cuts slightly diminish the value of the shell hash layer over time. The area where the newly reefed sections are placed will benefit from the organic deposits around the reefed structure over time. Shell hash from mollusks under and around newly reefed sections will, however, be quite limited as these species thrive in the upper portions of the water column, not at depth.
		Ecological and commercial fishing value was calculated over a 300-year period and is predicted to increase slightly across all partial-removal options. As more structure is reefed near the seafloor, it creates additional habitat volume and surface area above and beyond the current condition. This is because the reefed sections include the portion of the jacket that was above sea level and subsequently reefed, along with the portions that were below sea level thus increasing the overall volume and surface area of structure on the sea floor. Additionally, the increased structure at the reefed depths is likely to provide increased habitat and stock protection for many adult commercial and non-commercial fish species.
		There is negligible risk associated with a 15 m cut given the review of vessel transit drafts and conditions that could create a risk at this depth cut in the North Sea (i.e., a combination of a 12 m draft, swells greater than 6 m in height, and vessel contact within the exclusion zone). The 15 m cut option is predicted to reduce the navigation risk by two orders of magnitude, i.e., to 0.084 incidents every 600 years or one incident every 7,142 years. The detrimental impacts increase as the options increase in the effort level to implement each option, with the full removal option being the most detrimental.
		Trawl snagging and PLL risks were not predicted to be significant when the structure is laid down in the water column and the exclusion zone is maintained (compared to the scenario where there is no exclusion zone).

(Continued)

TABLE 3 Continued

		Based on the information in Figure 5C, the full removal option is predicted to create the most negative impact compared to all the options and should be considered as the least preferable option.
(D) **Leave-In-Place - Reef**	**(Lack of Exclusion Zone)**	As seen in Figure 5D, as portions of the jacket are removed and laid down (reefed alongside the jacket), impacts on benthic biomass are predicted to be minor because the portions reefed in the water column will regenerate benthic biomass over time, and additional hard surface area and habitat volume are laid under the water. It is important to note that, with no exclusion zone, the net ecosystem service value is predicted to decrease substantially because fishing pressure will increase in the area. Opening the area to trawling will increase the likelihood of adverse effects on benthic invertebrates, commercial and non-commercial fish species, marine mammals from direct catch and by-catch, as well as physical impacts on the sea bottom, and some of the shell hash and halo areas that lie outside the structure footprint. Bycatch is a fishing industry term that references a fish or other marine species that is caught unintentionally while catching certain target species and target sizes of fish, crabs etc. Commercial fishing and stock protection benefits are also predicted to decline with no exclusion zone.
		The detrimental impacts are predicted to increase as the options increase in the effort level to implement, with the full removal option being the most detrimental. Full removal was predicted to provide very little beneficial value and result in the lowest commercial fishing value (a 60% decline compared to the current Protect in Place condition). Based on available information (Løkkeborg et al., 2002), fish catch near platforms can be 3x to 4x the size of the surrounding (background) soft bottom habitat areas. Once the structure is fully removed, catch will eventually decrease to the background level. As such, for the North Sea case study, although this indicates a potential loss of 66% to 75% of the catch, we assumed a 60% loss to be conservative (i.e., not overestimate the impact). Moreover, it was predicted to create short-term environmental damage associated with the disturbance to the shell hash habitat and cuttings pile.
		As seen in Figure 5D, the removal of the exclusion zone is predicted to increase (double) navigation risks compared to the presence of an exclusion zone because of increased boat traffic, including trawlers, will be prevalent in the area. Based on the assumptions herein, approximately 16.8 navigation incidents are expected to occur over the 600-year period, i.e., one incident every 36 years with the Leave in Place option. The 15 m cut option reduces the navigation risk by two orders of magnitude, i.e., to 0.168 incidents every 600 years or one incident every 3,571 years.
		Additionally, for the Leave in Place reefing options, trawling risks (PLL and snagging) are predicted to increase from the Leave in Place option to the partial removal options by one order of magnitude because it is assumed that a NAVAID and visual confirmation will help reduce trawl snagging risks.
		Based on the information in Figure 5D, the full removal option is predicted to create the most negative impact compared to all the options and thus should be considered as the least preferable option.

optimized decommissioning option based on an understanding of the identified risks and achieving ALARP thresholds. The risk management process and preferences (i.e., ALARP thresholds) will likely vary on a case-by-case basis, but in most cases would include both operator and other stakeholder engagement.

For this North Sea case study, a risk management process and preferences were used to examine the initial optimized option to further consider a final optimized decommissioning option. This process included the following four steps, as seen in Figure 6:

1. Step 1: Navigation and trawl snagging and potential loss of life (PLL) risks were identified as key long-term risks associated with the potential decommissioning options.

Thus, the first step was the identification and removal of options deemed to have unacceptable risks based on the identified criteria. In this case, collision and trawling risks were presented in relation to a preferred risk-management threshold return period (the period of years it would take to have one occurrence) of 1,000 years. Options in which a navigation or trawling incident was predicted to occur in less than 1,000 years[1] were removed from consideration, given the predicted risk. Unacceptable risks based on the 1,000-

---

[1] A 1,000-year period was used as this represents a potential long-term period over which the structure would remain in place.

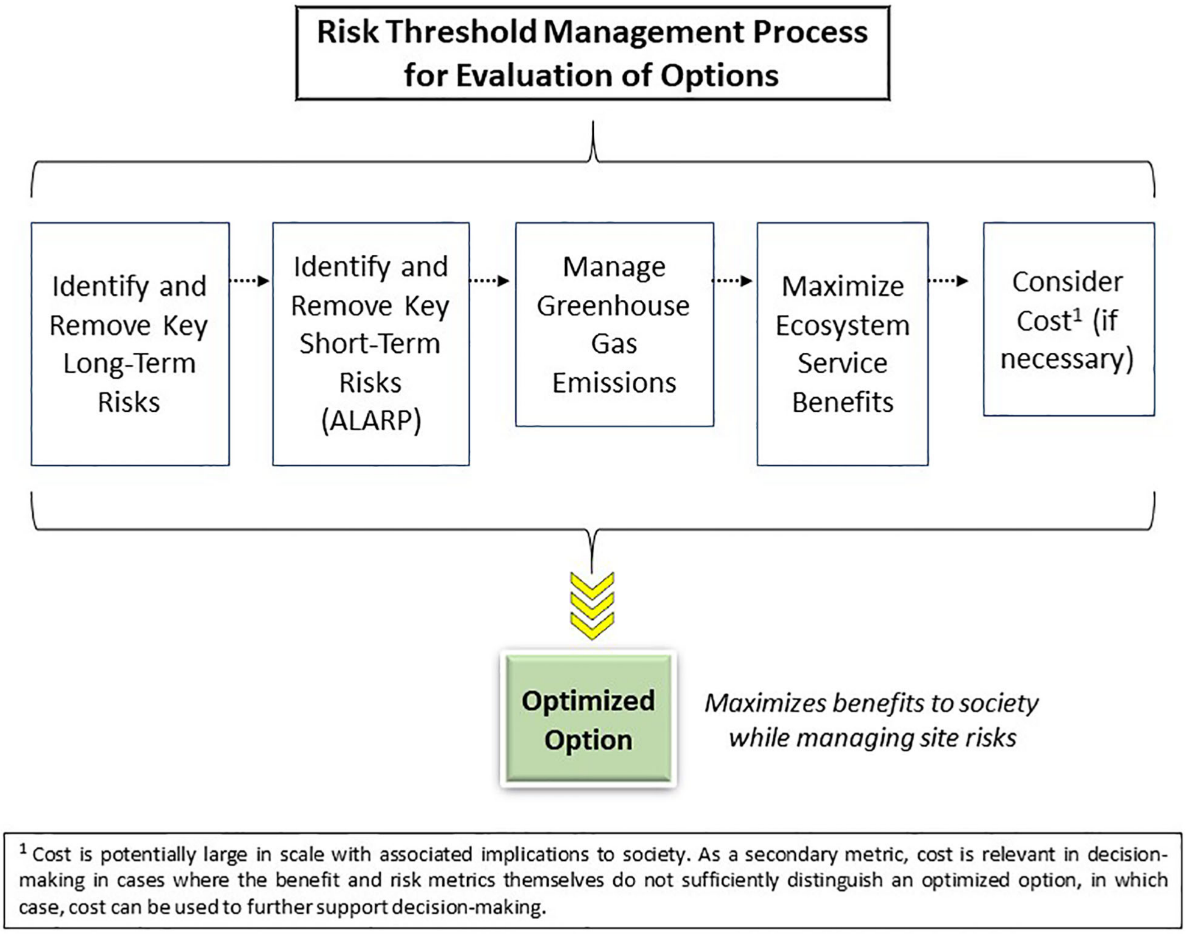

[1] Cost is potentially large in scale with associated implications to society. As a secondary metric, cost is relevant in decision-making in cases where the benefit and risk metrics themselves do not sufficiently distinguish an optimized option, in which case, cost can be used to further support decision-making.

FIGURE 6
A Schematic Representation of the Process for Risk Threshold Management and Option Selection.

year threshold are shown in red in Figure 7. Accordingly, the Protect-in-Place Reef option was not considered acceptable because a navigation incident was predicted to occur within 71 years. The return period for the Protect-in-Place - 15 m Reef option was 7,142 years, which was considered an acceptable risk. The options with acceptable and unacceptable risk return periods for navigation and trawling risks are presented in Figure 7, with unacceptable risk options removed from consideration and presented as "grey" text in Figure 7.

2. Step 2: The next evaluation criterion for those options with acceptable navigation and trawling risks was the consideration of both onshore and offshore implementation PLL risks. In this case, options with a PLL risk of greater than 1% were not considered acceptable. The unacceptable onshore and offshore implementation PLL risks and associated options are presented in Figure 7.
3. Step 3: After managing navigation, trawling, and implementation risks, GHG emissions were considered next to differentiate between the remaining options. Options with acceptable navigation, trawling, and implementation risks were evaluated based on the level of GHG emissions. Steps 1, 2, and 3 lead to options that best manage the risks (Figure 7).
4. Step 4: Since the goal of NEBA-CA is to maximize ecosystem service benefits while managing site risks, the next step was to evaluate the remaining options to identify the option(s) that maximizes the ecosystem service value, which was determined to be the Protect-In-Place Reef with Partial Removal at 15 m option (Figure 7).

For the North Sea case study, based upon the preferences evaluated, the optimized option was confirmed to be the Protect-

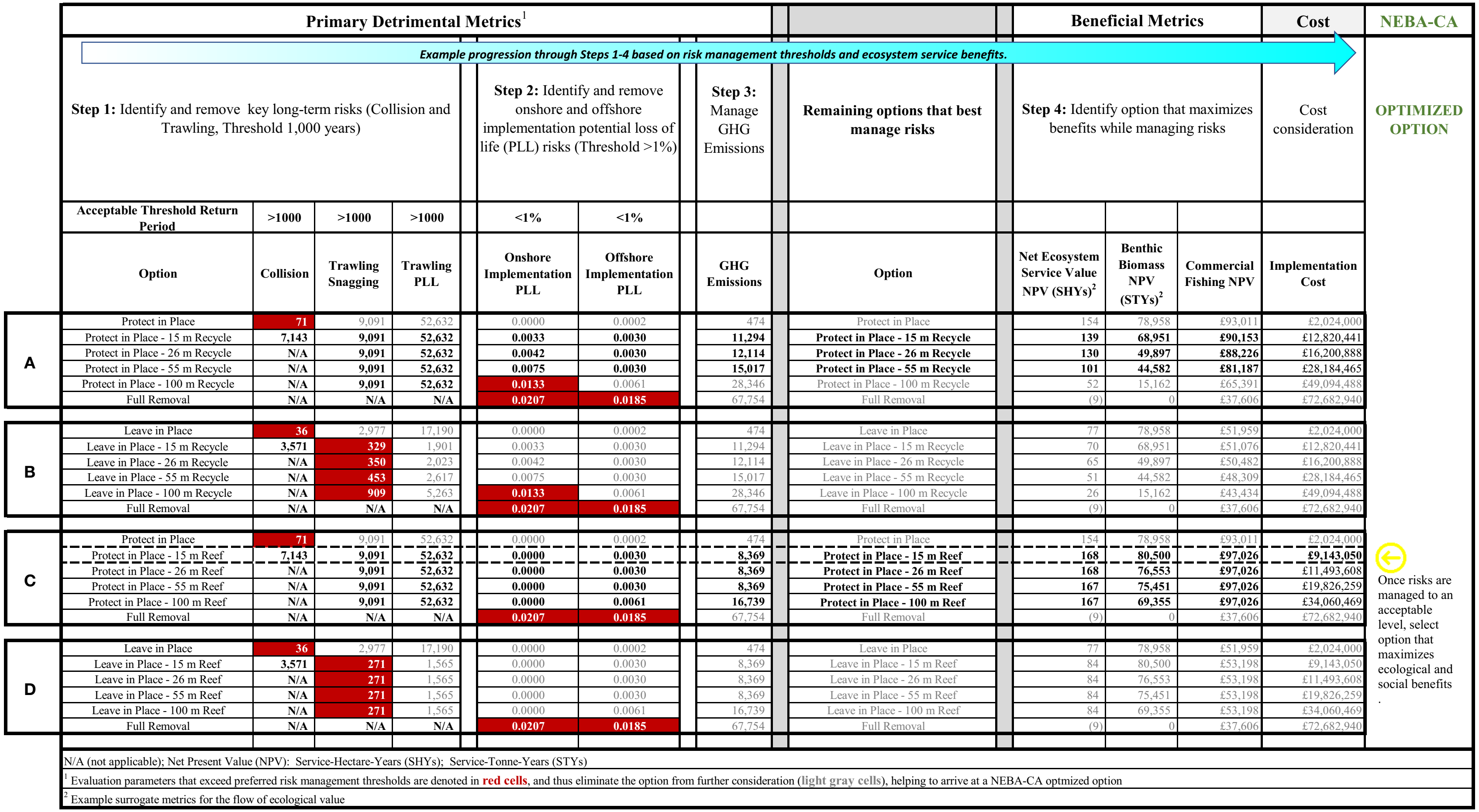

Example progression through Steps 1-4 based on risk management thresholds and ecosystem service benefits.

	Primary Detrimental Metrics[1]								Beneficial Metrics			Cost	NEBA-CA
	Step 1: Identify and remove key long-term risks (Collision and Trawling, Threshold 1,000 years)				**Step 2:** Identify and remove onshore and offshore implementation potential loss of life (PLL) risks (Threshold >1%)		**Step 3:** Manage GHG Emissions	**Remaining options that best manage risks**	**Step 4:** Identify option that maximizes benefits while managing risks			Cost consideration	**OPTIMIZED OPTION**
	Acceptable Threshold Return Period	**>1000**	**>1000**	**>1000**	**<1%**	**<1%**							
	Option	**Collision**	**Trawling Snagging**	**Trawling PLL**	**Onshore Implementation PLL**	**Offshore Implementation PLL**	**GHG Emissions**	**Option**	**Net Ecosystem Service Value NPV (SHYs)[2]**	**Benthic Biomass NPV (STYs)[2]**	**Commercial Fishing NPV**	**Implementation Cost**	
A	Protect in Place	71	9,091	52,632	0.0000	0.0002	474	Protect in Place	154	78,958	£93,011	£2,024,000	
	Protect in Place - 15 m Recycle	7,143	9,091	52,632	0.0033	0.0030	11,294	Protect in Place - 15 m Recycle	139	68,951	£90,153	£12,820,441	
	Protect in Place - 26 m Recycle	N/A	9,091	52,632	0.0042	0.0030	12,114	Protect in Place - 26 m Recycle	130	49,897	£88,226	£16,200,888	
	Protect in Place - 55 m Recycle	N/A	9,091	52,632	0.0075	0.0030	15,017	Protect in Place - 55 m Recycle	101	44,582	£81,187	£28,184,465	
	Protect in Place - 100 m Recycle	N/A	9,091	52,632	0.0133	0.0061	28,346	Protect in Place - 100 m Recycle	52	15,162	£65,391	£49,094,488	
	Full Removal	N/A	N/A	N/A	0.0207	0.0185	67,754	Full Removal	(9)	0	£37,606	£72,682,940	
B	Leave in Place	36	2,977	17,190	0.0000	0.0002	474	Leave in Place	77	78,958	£51,959	£2,024,000	
	Leave in Place - 15 m Recycle	3,571	329	1,901	0.0033	0.0030	11,294	Leave in Place - 15 m Recycle	70	68,951	£51,076	£12,820,441	
	Leave in Place - 26 m Recycle	N/A	350	2,023	0.0042	0.0030	12,114	Leave in Place - 26 m Recycle	65	49,897	£50,482	£16,200,888	
	Leave in Place - 55 m Recycle	N/A	453	2,617	0.0075	0.0030	15,017	Leave in Place - 55 m Recycle	51	44,582	£48,309	£28,184,465	
	Leave in Place - 100 m Recycle	N/A	909	5,263	0.0133	0.0061	28,346	Leave in Place - 100 m Recycle	26	15,162	£43,434	£49,094,488	
	Full Removal	N/A	N/A	N/A	0.0207	0.0185	67,754	Full Removal	(9)	0	£37,606	£72,682,940	
C	Protect in Place	71	9,091	52,632	0.0000	0.0002	474	Protect in Place	154	78,958	£93,011	£2,024,000	
	Protect in Place - 15 m Reef	7,143	9,091	52,632	0.0000	0.0030	8,369	**Protect in Place - 15 m Reef**	**168**	**80,500**	**£97,026**	**£9,143,050**	← Once risks are managed to an acceptable level, select option that maximizes ecological and social benefits .
	Protect in Place - 26 m Reef	N/A	9,091	52,632	0.0000	0.0030	8,369	Protect in Place - 26 m Reef	168	76,553	£97,026	£11,493,608	
	Protect in Place - 55 m Reef	N/A	9,091	52,632	0.0000	0.0030	8,369	Protect in Place - 55 m Reef	167	75,451	£97,026	£19,826,259	
	Protect in Place - 100 m Reef	N/A	9,091	52,632	0.0000	0.0061	16,739	Protect in Place - 100 m Reef	167	69,355	£97,026	£34,060,469	
	Full Removal	N/A	N/A	N/A	0.0207	0.0185	67,754	Full Removal	(9)	0	£37,606	£72,682,940	
D	Leave in Place	36	2,977	17,190	0.0000	0.0002	474	Leave in Place	77	78,958	£51,959	£2,024,000	
	Leave in Place - 15 m Reef	3,571	271	1,565	0.0000	0.0030	8,369	Leave in Place - 15 m Reef	84	80,500	£53,198	£9,143,050	
	Leave in Place - 26 m Reef	N/A	271	1,565	0.0000	0.0030	8,369	Leave in Place - 26 m Reef	84	76,553	£53,198	£11,493,608	
	Leave in Place - 55 m Reef	N/A	271	1,565	0.0000	0.0030	8,369	Leave in Place - 55 m Reef	84	75,451	£53,198	£19,826,259	
	Leave in Place - 100 m Reef	N/A	271	1,565	0.0000	0.0061	16,739	Leave in Place - 100 m Reef	84	69,355	£53,198	£34,060,469	
	Full Removal	N/A	N/A	N/A	0.0207	0.0185	67,754	Full Removal	(9)	0	£37,606	£72,682,940	

N/A (not applicable); Net Present Value (NPV): Service-Hectare-Years (SHYs); Service-Tonne-Years (STYs)

[1] Evaluation parameters that exceed preferred risk management thresholds are denoted in **red cells**, and thus eliminate the option from further consideration (**light gray cells**), helping to arrive at a NEBA-CA optmized option

[2] Example surrogate metrics for the flow of ecological value

FIGURE 7
NEBA-CA Risk Management Process.

In-Place Reef with Partial Removal at 15 m. It should be noted that in some cases, comparison to preferences and thresholds might further adjust the final optimized option. It should be noted that consideration of cost was not necessary to identify the initial optimized decommissioning option.

3 Discussion

With aged regulations, both precedent and bias appear to have influenced the advancement of decommissioning planning, in which support for a complete removal option is not typically substantiated by robust science, and complete removal is simply assumed to be the best option. For example, in the 1990s, there was a public and political outcry over the proposed plans to dispose of the Brent Spar oil storage and tanker loading buoy by sinking it in deeper water. This influenced development of the North Sea decommissioning policy and a 'return to a clean seabed' was promoted as the default decommissioning decision. Consequently, OSPAR Decision 98/3 was adopted in 1998, which prohibits dumping or leaving, whole or in part, any offshore installation after the end of its working life. Recent assessments have since allowed for some exceptions to this rule (termed 'derogations'); however, this has largely been based on the technical complexity of removing certain types of, often larger, gravity-based structures and not on the health, safety, environmental, economic, and social implications of the removal options. Based on evolving science, and in full compliance with the precautionary principle, full removal has the potential to be harmful to society and the environment.

In the North Sea case study, the NEBA-CA analysis indicated that the removal of the jacket structure, in full or in part, will adversely impact the established ecological community. Additionally, adverse effects may disrupt ecosystem connectivity and associated networks across multiple fields and structures in the North Sea (Henry et al., 2018; McLean et al., 2022).

In general, the level of ecosystem services affected by decommissioning is based on the location and attributes of the structure(s), as well as on the characteristics of the option(s) to be implemented. A key characteristic associated with each potential option is its effect on the hard surface area of structure that remains in the sea, and its relation to "halo" area productivity. The high level of heterotrophic growth per area of the seafloor is due to the large amount of habitat provided by the structural surface area of subsea structure (Claisse et al., 2014); therefore, site-by-site and option-by-option NEBA-CA analyses within the decommissioning planning process are warranted to facilitate decision-making.

The North Sea case study results indicate that, for the jacket examined, the full removal option for the jacket is the least preferable option. Given the potential for adverse impacts associated with full and partial removal options for the jacket, leaving as much steel structure in the sea as possible is projected to maximize ecosystem service benefits to society while managing site risks. The analysis further refines the jacket partial removal options and indicates that the less steel removed (i.e., a lesser depth cut combined with a reefing action) as part of a partial removal, the greater the projected ecosystem service benefits provided to society. That is, in an area where hard structure is lacking to support reef colonization and thus limit ecological production (i.e., in the North Sea), the availability of hard structure provided by subsea infrastructure is a valuable multigenerational habitat for benthic invertebrate colonization that further attracts fish (including commercially fished species) and other marine biota (e.g., marine mammals; Todd et al., 2022b), helping to maintain ecosystem benefits for multiple generations of the UK public; therefore, the financial expenditure and opportunity cost to society should be considered in the decision-making process. If it is possible to maximize ecological and human use service benefits and manage site risks with less removal, the value of these cost savings should be considered by both government regulators and society.

Scientific evidence pertaining to the ecological and social multigenerational values associated with subsea structures is increasing. Decisions made today can have positive or negative risks to future generations with the potential for long-term impacts; therefore, decisions regarding the decommissioning of offshore structures should consider the ecological and social values associated with the subsea structure and the basic tenets of the precautionary principle. There is no reason that these same concepts cannot be applied to decommissioning and development of other offshore subsea structures, such as wind energy development.

4 Limitations and uncertainties

The NEBA-CA framework is a data driven approach that entails the evaluation of multiple option and site-specific metrics that represent ecological and human use services, ecological and human health risks, and costs. The approach is primarily a desktop analysis that relies on readily available data and as such, data availability may be a limitation of the approach in some cases; however, based on the authors experience related to decommissioning projects in the North Sea, Australia, Gulf of Mexico, California, and the Caribbean, most data required to conduct the analysis and associated modelling have been previously generated by the site operator as part of their development, monitoring, and regulatory requirements. In many cases, ROV data may be available; however, detailed analysis of this footage may be necessary to understand the ecological and physical conditions present. In cases where data were lacking, the operator commissioned the collection of data necessary to fill any significant data gaps. For example, the collection of additional ROV video at and around the site is necessary to establish the physical and ecological condition of the site, as well as outside of the influence of the structure. Data gaps should be identified up-front during the planning phase of the NEBA-CA.

The NEBA-CA framework is intended to provide a differentiating weight of evidence regarding identifying and optimizing decommissioning options for maximizing ecosystem service benefits to society while managing both site risks and costs. Indication of changes in ecosystem service value, both ecological and socioeconomic, is developed from the identification of surrogate or proxy metrics to represent the flow of ecological and socioeconomic value. For example, site-specific changes in hard structure surface area, fish biomass, fish diversity, benthic biomass, and benthic diversity, or some combination thereof, may be used as a proxy to evaluate how various options may affect overall ecological habitat value. Likewise, site-specific changes in recreational fishing, commercial fishing, diving photography, and the fish processing sector, or some combination thereof, may be used to evaluate how various options might affect socioeconomic direct use value. Quantified metric estimates are approximate values and are not intended to be exact, but sufficient enough for identifying impacts and differences between options to a reasonable degree of certainty.

The approach used in NEBA-CA is to approximate the metric values for each of the options based on consistent assumptions where applicable. Assumptions should be kept internally consistent, where applicable, to account for their influence across all options. Internally consistent refers to the use of an assumption that remains constant among options so that all options are treated in a consistent manner. For example, for calculation purposes, a 300-year time frame was used to capture changes over multiple generations. Future predictions of changes in value are just that, predictions. However, by keeping the same predicted rate of change consistent throughout options, relative differences of the effects of implementing various options can be ascertained.

Conservative assumptions used within the North Sea case study are listed in Supplementary Table 2.

5 Conclusions

The NEBA-CA framework provides a transparent, objective, science-based decommissioning option selection approach that can assist decision makers in maximizing ecological, economic, and social benefits to the public while managing site risks and costs. Although the approach is data driven, it is primarily a desktop analysis that relies on readily available data and as such, data availability may be a limitation of the approach in some cases; however, based on the authors experience, most data required to conduct the analysis and associated modelling have been previously generated by the site operator as part of their development, monitoring, and regulatory requirements. Application of NEBA-CA to offshore decommissioning is consistent with the advantages of NEBA in that NEBA-CA directly addresses the ambiguity within available CA techniques that can arise when making decisions regarding the selection of appropriate decommissioning options. Offshore subsea structures have been shown to retain significant ecological value, physical removal of structure can adversely affect these values, and the ecological risks of the *in-situ* condition, if any, appear to be relatively small and limited in scale. The NEBA-CA framework supplements and strengthens the standard CA process by 1) incorporating quantified metrics including multigenerational ecosystem service benefits and risks, 2) excluding front ranking (scoring) or weighting of metrics, and 3) providing consistent graphical displays to support visual differentiation of options and metrics. Evaluation of risk management preferences and thresholds can further refine the NEBA-CA results to support an optimized option. Increased transparency in CAs will provide an additional layer of credibility with regulators and society.

Data availability statement

The datasets presented in this article are not readily available because the datasets for the case study are client confidential and provided for demonstration purposes. Requests to access the datasets should be directed to jnicolette@montrose-env.com.

Ethics statement

Ethical review and approval was not required for the animal study because non intrusive ROV data were used to observed benthic and fisheries populations. ROV data were collected as part of regulatory required monitoring.

Author contributions

JN: Conceptualization, Methodology, Formal analysis, Writing - Original Draft NN: Formal analysis, Writing - Original Draft MKR: Review and Editing - case study support MLR: Review and Editing - case study support AT: Review and Editing - case study support LW Writing - Review and Editing VT: Writing - Review and Editing. LJ Review and editing. All authors contributed to the article and approved the submitted version.

Funding

Montrose Environmental Solutions, Inc. had no funding role in the development of the framework presented in this paper or the decision to submit this paper for publication. The paper was

developed independently by the authors. All authors declare no other competing interests.

Acknowledgments

The authors would like to thank a confidential operator for their approval to publish the case study results. We would also like to thank Montrose Environmental Solutions, Inc. for their contribution in paying the open-access publication fee. Lastly, copy editing by Editage author services was appreciated.

Conflict of interest

Authors JN, NN, MKR, MLR, and AT are employed by Montrose Environmental Solutions, Inc.

Authors LW and VT are employed by Ocean Science Consulting, Ltd. (OSC).

This paper presents an adaptation of the NEBA framework, a framework that the lead author co-authored and has over 30 years of experience, that supplements and strengthens the comparative assessment (CA) process for evaluating decommissioning options for offshore oil and gas facilities. The framework incorporates, in part, ecosystem service valuation approaches that several of the authors pioneered as part of US NRDA regulation development. The framework presented herein includes the culmination of over 10 years of offshore decommissioning option CA experience and was developed independent of any direction from either MEG or OSC. Additionally, a confidential operator, through a non-disclosure agreement, gave permission to the authors to publish site data based on this framework. All authors declare no other competing interests.

Publisher's note

Supplementary material

The Supplementary Material for this article can be found online at: https://www.frontiersin.org/articles/10.3389/fmars.2022.1020334/full#supplementary-material

References

ANP (2020) *Body of mines and energy* (National Agency for Petroleum, Natural Gas and Biofuels). Available at: https://www.in.gov.br/web/dou/-/resolucao-n-817-de-24-de-abril-de-2020-254001378 (Accessed July 5, 2022). Resolution No. 817Section 1.

APPEA (2016) *Offshore oil and gas decommissioning decision-making guidelines*. Available at: https://www.stfs.com.au/wp-content/uploads/2016/12/APPEA-Decommissioning-Guidelines.pdf (Accessed July 5, 2022).

Arnould, J. P. Y., Monk, J., Ierodiaconou, D., Hindell, M. A., Semmens, J., Hoskins, A. J., et al. (2015). Use of anthropogenic sea floor structures by Australian fur seals: Potential positive ecological impacts of marine industrial development? *PLoS One* 10, e0130581–e0130581. doi: 10.1371/journal.pone.0130581. iss. 7.

Barnthouse, L. (2008). The strengths of the ecological risk assessment process: linking science to decision making. *Integrated Environ. Assess. Manage.* 4 (3), 299–305. doi: 10.1897/IEAM_2007-065.1

Bateman, I. J., Mace, G. M., Fezzi, C., Atkinson, G., and Turner, K. (2011). Economic analysis for ecosystem service assessment. *Environ. Resour. Econ.* 48, 177–218. doi: 10.1007/s10640-010-9418-x

Bell, N., and Smith, J. (1999). Coral growing on north Sea oil rigs. *Nature* 402 (6762), 601. doi: 10.1038/45127

British Petroleum (2011). *Miller decommissioning programme. document number: MLR-A-D0-PM-PRO-00217* 198 pp. Accessible at: https://www.bp.com/content/dam/bp/country-sites/en_gb/united-kingdom/home/pdf/Miller_Decomm_Programme.pdf. (Accessed 5 July 2022).

Brundtland, G. (1987). *Report of the world commission on environment and development: Our common future* (United Nations General Assembly Document A/42/427) pp. 374. Accessible at: https://digitallibrary.un.org/record/139811?ln=en. (Accesed on 11 November, 2021)..

Chapman, D., Iadanza, N., and Penn, T. (1998). *Calculating resource compensation: an application of the service-to-service approach to the blackbird mine hazardous waste site* Vol. 97-1 (National Oceanic and Atmospheric Administration Damage Assessment and Restoration Program Technical Paper), 18. Accessible at: https://repository.library.noaa.gov/view/noaa/33285. (Accessed 5 July 2021).

Chapman, D., and LeJeune, K. (2007). "REMEDE: Resource equivalency methods for assessing environmental damage in the EU," in *6th framework programme of the European commission, deliverable no. 6A: Review report on resource equivalence methods and applications*, 36.

Claisse, J. T., Pondella, D. J., Love, M., Zahn, L. A., Williams, C. M., Williams, J. P., et al. (2014). Oil platforms off California are among the most productive marine fish habitats globally. *Proc. Natl. Acad. Sci.* 111 (43), 15462–15467. doi: 10.1073/pnas.1411477111

CNR International (2012) *Murchison Decommissioning comparative assessment report. document number: MURDECOM-CNR-PM-REP-00225*. Available at: http://www.cnri-northsea-decom.com/Comparative-Assessment.pdf (Accessed July 5, 2022).

Confidential Client Report (2020). *Net environmental benefit analysis based comparative assessment for the X jacket and associated subsea structures* (North Sea Operator), 302.

Daan, N., Gislason, H., Pope, J. G., and Rice, J. C. (2005). Changes in the north Sea fish community: Evidence of indirect effects of fishing? *ICES J. Mar. Sci.* 62 (2), 177–188. doi: 10.1016/j.icesjms

DMIRS (2017) *Petroleum decommissioning guideline* (Government of Western Australia). Available at: https://dmp.wa.gov.au/Documents/Petroleum/PET-DecommissioningGuideline.pdf (Accessed July 5, 2022).

Dunford, R., Ginn, T., and Desvousges, W. (2003). The use of habitat equivalency analysis in natural resource damage assessments. *Ecol. Econ.* 48, 49–70. doi: 10.1016/j.ecolecon.2003.07.011

Efroymson, R. A., Nicolette, J. P., and Suter, II, GW. (2003). *A framework for net environmental benefit analysis for remediation or restoration of petroleum-*

contaminated sites Vol. 2003 (Oak Ridge, Tennessee: Oak Ridge National Laboratory) 34, 17.

Efroymson, R. A., Nicolette, J. P., and Suter, II, GW (2004). *A framework for net environmental benefit analysis for remediation or restoration of contaminated sites* Vol. 34 (Environmental Management), 315–331. Available at: https://link.springer.com/article/10.1007/s00267-004-0089-7.

Eigaard, O., Bastardie, F., Hintzen, N. T., Buhl-Mortensen, L., Buhl-Mortensen, P., Catarino, R., et al. (2017). The footprint of bottom trawling in European waters: Distribution, intensity, and seabed integrity. *ICES J. Mar. Sci.* 74 (3), 847-865. doi: 10.1093/icesjms/fsw194

European Commission (1992). Council directive 92/43/EEC of 21 may 1992 on the conservation of natural habitats and of wild fauna and flora. *Off. J. Eur. Communities* 206, 7–50.

Fowler, A. M., and Booth, D. J. (2012). Evidence of sustained populations of a small reef fish on artificial structures. does depth affect production on artificial reefs? *J. Fish Biol.* 80 (3), 613–629. doi: 10.1111/j.1095-8649.2011.03201.x

Fowler, A. M., Jørgensen, A.-M., Svendsen, J. C., Macreadie, P. I., Jones, D. O., Boon, A. R., et al. (2018). Environmental benefits of leaving offshore infrastructure in the ocean. *Front. Ecol. Environ.* 16, 571–578. doi: 10.1002/fee.1827

Freeman, A. M. (2003). *The measurement of environmental and resource values: Theory and methods. 2nd ed* (Washington, DC, USA: Resources for the Future).

Fujii, T., and Jamieson, A. J. (2016). Fine-scale monitoring of fish movements and multiple environmental parameters around a decommissioned offshore oil platform: A pilot study in the north Sea. *Ocean Eng.* 126, 481–487. doi: 10.1016/j.oceaneng.2016.09.003

Gala, W. R., Hill, R. W., and Hostetter, L. A. (2008). "Use of habitat equivalency analysis (HEA) to determine the environmentally superior project alternative". *Soc. Petroleum Engineers* (SPE) Paper No. 111760, SPE International Conference on Health, Safety, and Environment in Oil and Gas Exploration and Production, Nice, France. 9 pp.

Gass, S. E., and Roberts, J. M. (2006). The occurrence of the cold-water coral lophelia pertusa (Scleractinia) on oil and gas platforms in the north Sea: Colony growth, recruitment and environmental controls on distribution. *Mar. pollut. Bull.* 52, 549–559. doi: 10.1016/j.marpolbul.2005.10.002

Gourvenec, S. (2018). Shaping the offshore decommissioning agenda and next-generation design of offshore infrastructure. *Proc. Institution Civil Engineers-Smart Infrastructure Construction* 171, 54–66. doi: 10.1680/jsmic.18.00002

Gourvenec, S., Sturt, F., Reid, E., and Trigos, F. (2022). Global assessment of historical, current and forecast ocean energy infrastructure: Implications for marine space planning, sustainable design and end-of-engineered-life management. *Renewable Sustain. Energy Rev.* 154, 111794. doi: 10.1016/j.rser.2021.111794

Government of New Zealand (2021) *Exclusive economic zone and continental shelf (Environmental effects - decommissioning plans) regulations 2021*. Available at: https://www.legislation.govt.nz/regulation/public/2021/0272/latest/whole.html#LMS548501 (Accessed July 5, 2022). Sections 29E-30.

Henry, L. A., Ayorga-Adame, C. G., Fox, A. D., Polton, J. A., Ferris, J. S., McLellan, F., et al (2018). Ocean sprawl facilitates dispersal and connectivity of protected species. *Scientific Reports* 8, 11346 doi: 10.1038/s41598-018-29575-4

IEA (2019b). *Annual average decommissioning need for offshore oil and gas assets by region 2000-2040* (Paris: International Energy Association, IEA). Available at: https://www.iea.org/data-and-statistics/charts/annual-average-decommissioning-need-for-offshore-oil-and-gas-assets-by-region-2000-2040.

INEOS UK SNS Ltd (2021) *Topaz decommissioning project comparative assessment. document number: RD-TOP-ZPL005-7*. Available at: https://assets.publishing.service.gov.uk/government/uploads/system/uploads/attachment_data/file/962320/RD-TOP-ZPL005_7_Topaz_Comparative_Assessment_JAN2021_FINAL.pdf (Accessed July 5, 2022).

IOGP (2022). *Habitat retention strategies for decommissioned offshore jacket structures* (International Association of Oil and Gas Producers, IOGP Report 650), 54. Accessible at: https://www.iogp.org/bookstore/product/habitat-retention-strategies-for-decommissioned-offshore-jacket-structures/. (Accessed 5 July 2022).

Ithaca Energy Group Ltd (2021) *Causeway-fionn decommissioning pipelines and umbilical comparative assessment*. Available at: https://www.ithacaenergy.com/sites/ithaca/files/decommissioning/cfi-lla-it-de-re-0001-02-1-comparative-assessment.pdf (Accessed July 5, 2022). Document number: CFI-LLA-IT-DE-RE-0001.

Kenter, J. O., Bryce, R., Davies, A., Jobstvogt, N., Watson, V., Ranger, S., et al. (2013). *The value of potential marine protected areas in the UK to divers and sea anglers* (Cambridge, UK: UNEP-WCMC).

King, D. M., and Adler, K. J. (1991). *Scientifically defensible compensation ratios for wetland mitigation* (Washington, DC, USA: United States Environmental Protection Agency, Office of Policy, Planning and Evaluation).

Løkkeborg, S., Humborstad, O. B., Jørgensen, T., and Soldal, A. V. (2002). Spatiotemporal variations in gillnet catch rates in the vicinity of north Sea oil platforms. *ICES J. Mar. Sci.* 59, S294–S299. doi: 10.1006/jmsc.2002.1218

Lowe, J. (2008). *Intergenerational wealth transfers and social discounting: Supplementary green book guidance* (Her Majesty's Treasury. The Crown) 9. ISBN: 978-1-84532-419-3. Accessible at: https://assets.publishing.service.gov.uk/government/uploads/system/uploads/attachment_data/file/193938/Green_Book_supplementary_guidance_intergenerational_wealth_transfers_and_social_discounting.pdf (Accessed on 5 June 2019).

Mannocci, L., Dabin, W., Augeraud-Véron, E., Dupuy, Jean-François, and Ridoux, V. (2012). Assessing the impact of bycatch on dolphin populations: The case of the common dolphin in the Eastern north Atlantic. *PloS One* 7, e32615. doi: 10.1371/journal.pone.0032615

McLean, D. L., Ferreira, L. C., Benthuysen, J. A., Miller, K. J., Schläppy, M.-L., Ajemian, M. J., et al. (2022). Influence of offshore oil and gas structures on seascape ecological connectivity. *Global Change Biol.* 28(11), 3515–3536.

Millennium Ecosystem Assessment (Program) (2005). *Ecosystems and human well-being* (Washington, D.C: Island Press).

Moore, M. A., Boardman, A. E., and Vining, A. R. (2013). More appropriate discounting: the rate of social time preference and the value of the social discount rate. *J. Benefit-Cost Anal.* 4 (1), 1–16. doi: 10.1515/jbca-2012-0008

Nelson, N. A., Nicolette, J. P., Testoff, A. N., and Duguid, A. D. (2022). Safety zones and decommissioning in Situ/Artificial reefing in the Australian regulatory context: A net environmental benefit analysis-based comparative assessment (NEBA-CA) intergenerational value proposition. *APPEA J.* 62 (S1), S327–S333. doi: 10.1071/AJ21112

Nicolette, J., Burr, S., and Rockel, M. (2013a). A practical approach for demonstrating environmental sustainability and stewardship through a net ecosystem service analysis. *Sustainability* 2013(5), 2152–2177. doi: 10.3390/su5052152

Nicolette, J., Goldsmith, B., Wenning, R., Barber, T., and Colombo, F. (2013b). "Experience with restoration of environmental damage'. chapter 9 of the book entitled," in *The E.U. liability directive: A commentary*. Eds. L. Berkamp and B. Goldsmith (Oxford Press), 181–219. Published March 14, 2013. Available at: https://www.mdpi.com/2071-1050/5/5/2152.

NOAA (National Oceanic and Atmospheric Administration) (1999). *Habitat equivalency analysis: an overview* (Silver Springs, Maryland: Damage Assessment and Restoration Program, Damage Assessment Center).

NOAA (National Oceanic and Atmospheric Administration) (2011). "Summary report for fate and effects of remnant oil remaining in the environment," in *Annex m - net environmental benefit analysis* (National Oceanic and Atmospheric Administration). Shigenaka, G. pp 48. Accessible at: https://www.restorethegulf.gov/sites/default/files/documents/pdf/Annex%20M%20NEBA.pdf (Accessed on 26 June 2019).

NOPSEMA (2022). *ALARP guidance note, n-04300-GN0166, revision 6* Australia National Offshore Petroleum Safety and Environmental Management Authority. Available at: https://www.nopsema.gov.au/sites/default/files/documents/N-04300-GN0166%20-%20ALARP%20%28A138249%29.pdf

NOPSEMA (2018) *The regulator* (National Offshore Petroleum Safety and Environmental Management Authority). Available at: https://www.nopsema.gov.au/sites/default/files/documents/2021-04/A619419.pdf (Accessed July 5, 2022).

O&G UK (2013). *Long term degradation of offshore structures and pipelines: Decommissioned and left in-situ*, Report No. 002-121-RPT-001. pp 47. Accessible at: https://oeuk.org.uk/product/guidelines-for-long-term-degradation-of-offshore-structures-and-pipelines-issue-1/. (Accessed 10 January 2021)

O&G UK (2015). *Guidelines for comparative assessment in decommissioning programmes*. Issue 1, pp 49. ISBN: 1903004551. Accessible at: http://oeuk.org.uk/product/guidelines-for-comparative-assessment-in-decommissioning-programmes-issue-1/ (Accessed 10 March 2019).

O&G UK (2021) *Decommissioning insight 2021*. Available at: https://oeuk.org.uk/product/decommissioning-insight-report/.

OPRED (2018). "Decommissioning of offshore oil and gas installations and pipelines," in *ANNEX a - a guide to comparative assessments* (Offshore Decommissioning Unit, Offshore Petroleum Regulator for Environment and Decommissioning, Department of Business, Energy and Industrial Strategy) pp 138. Accessible at: https://assets.publishing.service.gov.uk/government/uploads/system/uploads/attachment_data/file/760560/Decom_Guidance_Notes_November_2018.pdf (Accessed on 9 January 2020).

OSPAR (1998). *Decision 98/3 on the disposal of disused offshore installations, OSPAR convention for the protection of the marine environment of the north-East Atlantic* (Sintra: Ministerial Meeting of the OSPAR Commission), 12. 22-23 July 1998, Annex 33 (Ref. § B-5.6).

Pandolfi, J. M., Bradbury, R. H., Sala, E., Hughes, T. P., Bjorndal, K. A., Cooke, R. G., et al. (2003). Global trajectories of the long-term decline of coral reef ecosystems. *Sci. (American Assoc. Advancement Science)* 301 (5635), 955–958. doi: 10.1126/science.1085706

Petroleum Institute of Thailand (2008) *Draft Thailand decommissioning guidelines for upstream installations* (Accessed 5 July 2022). Petroleum Institute of Thailand. 2008. Draft Thailand Decommissioning Guidelines for Upstream. International Decommissioning. The guidelines cover the onshore and offshore decommissioning of installations for - [PDF Document] (vdocuments.net).

Petroleum Safety Authority (Norway) (2020) *Regulation guidelines for petroleum activities, chapter 6 sections 43-45a*. Available at: https://www.npd.no/en/regulations/regulations/petroleum-activities/#Section-43 (Accessed July 5, 2022).

Raffensperger, C. and J. Tickner (Eds.) (1999). *Protecting public health and the environment: Implementing the precautionary principle* (Washington, DC: Island Press).

Reeds, K. A., Smith, J. A., Suthers, I. M., and Johnston, E. L. (2018). An ecological halo surrounding a Large offshore artificial reef: Sediments, infauna, and fish foraging. *Mar. Environ. Res.* 141, 30–38. doi: 10.1016/j.marenvres.2018.07.011

Roberts, J. M. (2002). The occurrence of the coral lophelia pertusa and other conspicuous epifauna around an oil platform in the north Sea. *Underwater Technol.* 25 (2), 83–92. doi: 10.3723/175605402783219163

Rosenberger, R. S., and Loomis, J. B. (2001). *Benefits transfer of outdoor recreation use values; rocky mountain research station* Vol. 2001 (Fort Collins, CO, USA: U.S.D.A. Forest Service).

Scarborough-Bull, A., Love, M. S., and Schroeder, D. M. (2008). Artificial reefs as fishery conservation tools: Contrasting the roles of offshore structures between the gulf of Mexico and the southern California bight. *Am. Fisheries Soc. Symposium* 49, 899-915.

Shell International Petroleum Co. Ltd (2017) *Gaupe decommissioning programme comparative assessment report. document number: GAUPD-PT-S-AA-7480-00001 rev A02*. Available at: https://assets.publishing.service.gov.uk/government/uploads/system/uploads/attachment_data/file/891475/Gaupe_Comparative_Assessment.pdf (Accessed July 5, 2022).

Soldal, A. V., Svellingen, I., Jørgensen, T., and Løkkeborg, S. (2002). Rigs-to-reefs in the north Sea: hydroacoustic quantification of fish in the vicinity of a "semi-cold" platform. *ICES J. Mar. Sci.* 59, S281–S287. doi: 10.1006/jmsc.2002.1279

Spirit Energy (2018) *Ensign comparative assessment for pipelines. document number: SPT-DCM-SNS0104-REP-0003*. Available at: https://www.spirit-energy.com/media/1297/spt-dcm-sns0104-rep-0003-a3-signed.pdf (Accessed July 5, 2022).

Testoff, A. N., Nelson, N. A., and Nicolette, J. P. (2022). A quantitative method for evaluating ecological risks associated with long-term degradation of deep-Sea plastic-containing infrastructure. *APPEA J.* 62 (1), 141–158. doi: 10.1071/AJ21113

Todd, V. L. G., Lavallin, E. W., and Macreadie, P. I. (2018). Quantitative analysis of fish and invertebrate assemblage dynamics in association with a north Sea oil and gas installation complex. *Mar. Environ. Res.* 142, 69–79. doi: 10.1016/j.marenvres.2018.09.018

Todd, V., McLean, D. L., Ferreira, L. C., Benthuysen, J. A., Miller, K. J., Schläppy, M., et al. (2022a). Influence of offshore oil and gas structures on seascape ecological connectivity. *Global Change Biol.* 28, 3515–3536. doi: 10.1111/gcb.16134

Todd, V. L. G., Pearse, W. D., Tregenza, N. C., Lepper, P. A., and Todd, I. B. (2009). Diel echolocation activity of harbour porpoises (Phocoena phocoena) around north Sea offshore gas installations. *ICES J. Mar. Sci.* 66, 734–745. doi: 10.1093/icesjms/fsp035

Todd, V. L. G., Susini, I., Williamson, L. D., Todd, I. B., McLean, D. L., and Macreadie, P. I. (2021). Characterising the second wave of fish and invertebrate colonisation and production potential of an offshore petroleum platform. *ICES J. Mar. Sci.* 78, 1131–1145. doi: 10.1093/icesjms/fsaa245

Todd, V. L. G., Warley, J. C., and Todd, I. B. (2016). Meals on wheels? a decade of megafaunal visual and real-time passive acoustic monitoring detections from on-tow and stationary offshore oil and gas rigs and platforms in the north and Irish seas. *PLoS One* 11, 25. doi: 10.1371/journal.pone.0153320

Todd, V. L. G., Williamson, L. D., Couto, A. S., Todd, I. B., and Clapham, P. J. (2022b). Effect of a new offshore gas platform on harbor porpoises in the dogger bank. *Mar. Mammal Sci.* 38 (4), 1609–1622. doi: 10.1111/mms.12949

UK Government (2011). "National ecosystems assessment. technical report. chapter 12," in *Marine* (Cambridge: UNEP-WCMC).

UNEP/MED (2022) *Decision IG.24/9. Mediterranean offshore guidelines and standards: (a) common standards and guidance on the disposal of oil and oily mixtures and the use and disposal of drilling fluids and cuttings; (b) common standards and guidelines for special restrictions or conditions for specially protected areas (SPA) within the framework of the Mediterranean offshore action plan*. Available at: https://wedocs.unep.org/bitstream/handle/20.500.11822/31707/19ig24_22_2409_eng.pdf (Accessed July 5, 2022).

United States (1997). *United states v. Melvin Fisher*, United States District Court for the Southern District of Florida, Key West Division Case Numbers 92–10027-CIV-DAVIS, and 95–10051-CIV-DAVIS. Decided 30 July 1997, Filed 30 July 1997. 977 F. Supp. 1193; 1997 U.S. Dist. LEXIS 16767.

United States (2001). *United states of America and internal improvement trust fund v. great lakes dredge and dock company* (United States District Court for the Southern District of Florida D. C). Docket No. 97–02510-CV-EBD. Available at: https://caselaw.findlaw.com/us-11th-circuit/1302158.html.

Unsworth, R. E., and Bishop, R. C. (1994). Assessing natural resource damages using environmental annuities. *Ecol. Economics* 11, 35–41. doi: 10.1016/0921-8009(94)90048-5

USEPA (1997). *Ecological risk assessment guidance for superfund: Process for designing and conducting ecological risk assessments (EPA 540-R-97-006)* (Washington, DC: USEPA, OSWER).

USEPA (2004). *An examination of EPA risk assessment principles and practices: Staff paper prepared for the U.S* (Environmental Protection Agency by members of the Risk Assessment Task Force). EPA/100/B-04/001. March. pp 193. Accessible at: https://semspub.epa.gov/work/10/500006305.pdf. (Accessed on 5 March 2019)

USEPA Science Advisory Board (SAB) (2009). *Valuing the protection of ecological systems and services (EPA-SAB-09-012)* (Washington, DC: USEPA Science Advisory Board).

Wolfson, A., Van Blaricom, G., Davis, N., and Lewbel, G. S. (1979). The marine life of an offshore oil platform. *Mar. Ecol. Prog. Ser.* 1, 81–89. doi: 10.3354/meps001081

Xodus Group (2021) *Dunlin alpha decommissioning comparative assessment report. document number: A-301649-S07-REPT-005* (Fairfield Betula Ltd). Available at: http://www.fairfield-energy.com/assets/documents/A-301649-S07-REPT-005.pdf (Accessed July 5, 2022).

Frontiers in Marine Science

TYPE Original Research
PUBLISHED 09 February 2023
DOI 10.3389/fmars.2023.1095906

EDITED BY
Victoria Louise Georgia Todd,
Ocean Science Consulting Ltd.,
United Kingdom

REVIEWED BY
Ilana Rosental Zalmon,
State University of the North Fluminense
Darcy Ribeiro, Brazil
Jordi Grinyó,
Royal Netherlands Institute for Sea
Research (NIOZ), Netherlands

*CORRESPONDENCE
Daniel Ierodiaconou
✉ daniel.ierodiaconou@deakin.edu.au

SPECIALTY SECTION
This article was submitted to
Marine Ecosystem Ecology,
a section of the journal
Frontiers in Marine Science

RECEIVED 11 November 2022
ACCEPTED 17 January 2023
PUBLISHED 09 February 2023

CITATION
Ierodiaconou D, McLean D, Birt MJ, Bond T, Wines S, Glade-Wright O, Morris J, Higgs D and Whitmarsh SK (2023) Industry remotely operated vehicle imagery for assessing marine communities associated with subsea oil and gas infrastructure on the continental shelf of South-East Australia. *Front. Mar. Sci.* 10:1095906. doi: 10.3389/fmars.2023.1095906

Industry remotely operated vehicle imagery for assessing marine communities associated with subsea oil and gas infrastructure on the continental shelf of South-East Australia

Daniel Ierodiaconou[1*], Dianne McLean[2,3], Matthew Jon Birt[2], Todd Bond[3,4], Sam Wines[1], Ollie Glade-Wright[5], Joe Morris[5], Doug Higgs[5] and Sasha K. Whitmarsh[1]

[1]School of Life and Environmental Sciences, Deakin University, Warrnambool, VIC, Australia, [2]The Australian Institute of Marine Science, Indian Ocean Marine Research Centre, Perth, WA, Australia, [3]Oceans Institute, The University of Western Australia, Perth, WA, Australia, [4]School of Biological Sciences, The University of Western Australia, Perth, WA, Australia, [5]Cooper Energy, Adelaide, SA, Australia

Introduction : Offshore oil and gas (O & G) infrastructure provides hard substrata of structural complexity in marine environments and has been shown to have ecological value, particularly in oligotrophic environments. As infrastructure approaches end of life, understanding such values is critical to inform decommissioning decisions.

Methods: This study uses a decade of industry remotely operated vehicle (ROV) imagery to describe fish, invertebrate, and benthic communities on gas field infrastructure. Sampling was conducted over 22 km of flowline, three wells and one manifold in the temperate waters of Bass Strait, south east Australia in depths of 155 to 263 m.

Results: A total of 10,343 mobile animals from 69 taxa were observed. A higher diversity of fishes were observed on flowlines (28 taxa) compared to wells (19 taxa). Fish and invertebrate communities observed along flowlines were distinct from those observed on wells/manifold, however, there was also high spatial variability among the different flowlines surveyed and between the three wells and manifold. These differences appear to be driven by habitat and depth preferences of the species observed. Many sand-affiliated species were associated with buried sections of flowlines (Tasmanian giant crab Pseudocarcinus gigas, Balmain bug Ibacus peronii, slender sand burrower Creedia haswelli, red cod Pseudophycis spp., blue grenadier Macruronus novaezelandiae) whilst reef-associated and schooling species were observed on the wells/manifold (jackass morwong Nemadactylus macropterus, redbait Emmelichthys nitidus, splendid perch Callanthias australis). Species of ecological importance were also noted including the Australian fur seal (Arctocephalus pusillus doriferus), long-lived foxfish (Bodianus frenchii), and handfish (Brachionichthyidae spp).

Discussion: This study describes the habitat value of oil and gas infrastructure in a data poor temperate region that is important for understanding how the decommissioning of these structures may affect local marine ecosystems and fisheries. Therefore, it is critical to understand the habitat value of O&G infrastructure to marine life in the Bass Strait and whether decommissioning of these structures affect local marine ecosystems and fisheries. This study shows the complexity of determining temporal change in biodiversity values associated with these O & G structures from historical industry datasets that will be key for informing future decommissioning options. We also provide some guidance on how future quantitative data can be obtained in a systematic way using industry ROV data to better inform ecological investigations and decommissioning options.

KEYWORDS

ROV, fish, flowline, wells, invertebrates, time-series

1 Introduction

Offshore oil and gas (O&G) infrastructure features in much of the world's oceans and includes large-scale platforms and extensive networks of subsea pipelines and wells (Bugnot et al., 2021; Gourvenec et al., 2022). An understanding of the potential habitat value of O&G structures and their associations with fauna, is high on the research agenda for many countries, as structures reach the end of field life and must be decommissioned (Shaw et al., 2018; Sommer et al., 2019; Melbourne-Thomas et al., 2021; Schläppy et al., 2021).

Scientists are beginning to understand the potential fishery production value of jackets (Gallaway et al., 2009; Claisse et al., 2014; Claisse et al., 2019), the drivers behind high diversity on structures (Meyer-Gutbrod et al., 2019; Page et al., 2019; Love et al., 2019a;) and how marine communities compare on structures to those in surrounding ecosystems (Boswell et al., 2010; Love et al., 2019b). In Australia, an increasing number of studies are examining marine communities associated with subsea infrastructure (e.g. McLean et al., 2017; Thomson et al., 2018; Bond et al., 2018a; McLean et al., 2020a;), how communities on pipelines compare to those in natural ecosystems (Bond et al., 2018b; Bond et al., 2018c; Schramm et al., 2020), the potential value of pipelines to commercial fisheries (Bond et al., 2021) and the drivers of marine community structure on infrastructure across regions (McLean et al., 2018; Galaiduk et al., 2022). Scientists are also working closely with industry to conduct quantitative scientific surveys of oil and gas infrastructure (McLean et al., 2019; Schramm et al., 2020). To date however, the majority of published scientific research in Australia has been on tropical marine communities associated with infrastructure in the north-west (exceptions being Neira, 2005; Arnould et al., 2015; McLean et al., 2022; Sih et al., 2022). A critical knowledge gap exists for most infrastructure present in the temperate south-east, particularly given that the region has hosted oil and gas infrastructure for the longest period in Australia (since 1968) in tandem with high species endemism (Butler et al., 2002), many protected and migratory species (Gill et al., 2011; Arnould et al., 2015), and important commercial fisheries (Hobday and Hartmann, 2006).

Bass Strait is positioned on the eastward extent of Australia's unique southern coast. Isolated for some 65 million years, the high endemic species richness and diversity is influenced by the confluence of ocean currents (Ridgway, 2007). The repeated submergence and emergence of Bass Strait has strongly shaped the present-day composition and distribution of species, along with the geomorphology and oceanography of the area (Schultz et al., 2009; Miller et al., 2013). The region is oceanographically complex with subtropical influences from the north and subpolar influences from the south. The eastern parts of the region are strongly influenced by the East Australian Current (EAC) carrying warm equatorial waters and recent range expansion of species such as the black urchin (*Centrostephanus rodgersii*) impacting biodiversity and fisheries values on kelp dominated reefs (Johnson et al., 2011). Seasonal and transient upwellings are important ecological features of the region. The Bonney upwelling, a strong seasonal upwelling in the shelf waters between Cape Jaffa and Cape Otway supports one of the most productive marine regions in Australian coastal waters (Gill et al., 2011). At the shelf break east of Bass Strait, nutrient-rich waters rise to the surface in winter as part of the processes of the Bass Strait Water Cascade, where the eastward flushing of the shallow waters of the strait over the continental shelf mix with cooler, deeper nutrient-rich waters. Bass Strait supports a range of State and Commonwealth marine protected areas implemented to conserve key ecological features, vulnerable and endemic species and diverse benthic communities (Commonwealth of Australia, 2015). Commercial fisheries target 15 different species using a variety of different fishing gears (Butler et al., 2002) including otterboard trawl, Danish seine, demersal gill nets, demersal longlines, droplines, scallop dredges and rock lobster traps (Boag and Koopman, 2021).

The waters support 81 species listed under the Environmental Protection and Biodiversity Conservation Act (EPBC) including large populations of blue and southern right whales, Australian fur seals, sharks, and southern blue-fin tuna (Butler et al., 2002). The region also supports growing charter and recreational fishing industries alongside areas of high ecological value including diverse sponge beds and macroalgae communities that are home to species-rich invertebrate and fish assemblages (Bax and Williams, 2001; Butler et al., 2002).

Despite the ecological significance of the area considering Australia's unique temperate taxa present and the age of the oil and gas infrastructure, few studies have attempted to quantify the marine assemblages in the area and how they may be influenced by the presence of such infrastructure (but see McLean et al., 2022; Sih et al., 2022). The present study used industry-collected historical remotely operated vehicle (ROV) video to examine marine communities associated with subsea flowlines and wells of an offshore subsea facility field in the Gippsland basin of the Bass Strait, south-east Australia. Using time series data (11 years), our research describes fish, and sessile and mobile invertebrate communities that associate with these structures and examines how these communities change over time and how might decommissioning influence these communities. Our specific aims were to 1) Explore patterns in fish and invertebrate community composition and abundance between 2009-2020, including benthic community cover, depth, survey time of day, and structural features of the infrastructure itself and 2) evaluate the similarities and differences in fish and invertebrate communities among 9 subsea flowlines and 3 wells and a manifold. Our results provide the first in depth assessment of assemblages associated with subsea gas infrastructure in south-east Australia and are one of the only studies using historical industry ROV data to explore change in assemblages over time.

2 Materials and methods

2.1 Study location and infrastructure

In depths of 155–263 m in the Gippsland basin region of south-east Australia, the studied offshore field possesses ~22 km of flowlines and umbilicals (herein termed 'flowline'), one manifold and seven wells. Most subsea infrastructure was installed between 2006-2008 with sections of flowline trenched in 2011 (Table 1) to enable trawl fisheries to re-access the area. This survey examined ROV video imagery obtained by Industry during their routine operational surveys which included imagery of nine flowlines, the manifold and three wells (Figure 1). Industry ROV surveys typically operate 24-hours a day and, as such, we considered time of day in our analyses (actual time). For simplicity we refer to surveys as occurring either in the night (20:00 – 6:30) or day (6:30 – 20:00), with raw Australian Eastern Daylight Time (AEDT) retained in statistical analyses.

2.2 ROV video analyses

The purpose-built software program, TransectMeasure (SeaGIS, 2020), was used to record broad classifications of benthic habitat on structures using an adaptation of the CATAMI (Collaborative and Annotation Tools for Analysis of Marine Imagery; Althaus et al., 2015) classification scheme. An additional specialized program, EventMeasure Stereo (SeaGIS, 2020), was used to annotate mobile fauna from ROV video. Both software programs were designed specifically to allow fast, and efficient analysis of biological information from video sequences and have been used previously to analyze ROV videos (McLean et al., 2017; McLean et al., 2018; Bond et al., 2018a; McLean et al., 2019;).

2.2.1 ROV video analysis of flowlines

In total, ~22 km of flowline had ROV video imagery that was suitable for analysis across the years (Table 1), with most of this collected in 2020 (17.8 km – single data collection across all flowlines). Imagery was deemed suitable for analysis if the ROV video provided a good view of the flowline, without obstruction or being focused on a small area only (see McLean et al., 2020b). Prior to 2020, standard definition imagery was collected from port, center and starboard cameras providing an oblique and often grainy view of each flowline, however, only sections of flowlines were sometimes surveyed (not the entire flowline) (Table 1). In contrast, the 2020 survey collected high-resolution downfacing video using a CathX system.

The abundance of all fish, mobile invertebrates, and other animals (e.g. seals) encountered along each flowline were recorded and identified to lowest taxonomic rank. Several fish could not be consistently or reliably identified to species level and were therefore recorded to the next lowest taxonomic level possible which was often genus or family (e.g. *Pseudophycis* spp. and *Helicolenus* spp.). Analyst's cross checked their identifications to reduce the chance of interobserver biases. Unlike previous surveys in north-west Australia (McLean et al., 2017), no fish were observed to swim along in front of the ROV, leaving the field of view (FOV) and as such the chances of recounting any individuals was deemed low for flowlines. Fish length (snout to tail fork) was estimated in size class categories <20, 20–30, 30–40, 40–50, >50 cm, using the known diameter of each flowline (Table 1) as a guide. Consistent ROV fly heights and field of views within surveys enabled estimated size categories to be determined when flowlines were not visible when trenched.

A virtual quadrat measuring ~4 m^2 (~150 cm x ~270 cm, derived from the relatively constant ROV altitude) was placed on a freeze-framed image taken every 50 m along flowlines and spanned the flowline and seafloor to either side. Within each quadrat, a 20-point grid was allocated, and biota identified to the lowest taxonomic resolution possible within the grid. Benthos and substrate were categorized using quadrats and a modified CATAMI classification schema (Althaus et al., 2015) that included black/octocorals, encrusting sponges, massive sponges, Actiniaria (anemones), bryozoans, ascidians, biofilm, rubble, burrows, shells, pebble/gravel, sand, open water, fish and scores for unidentifiable and not useable data as an indication of image quality. Biofilm refers to flowlines that appear somewhat bare but have a thin layer of biota, likely a mix of cnidaria and bryozoans. In addition to benthic biota, the density of burrows in the sediment immediately adjacent to the flowline (within the quadrat), indicating infauna presence, were assessed as low (burrows present in <5% of seafloor within quadrat), medium (5–25%) and dense (>25%) and the size of each burrow estimated as <2, 2–8 cm and >8 cm, using the known size of the flowline as a guide. Benthic community height and density were scored in the FOV of the pipeline at the same location as quadrats to examine potential relationships with fish and invertebrate abundance. For height, this included 0 = none; 1 = low (0–20 cm), 2 = medium (20–40 cm) and 3 = high (>40 cm). Density scores included 0 = none, 1 = sparse (<25% percentage cover for entire FOV), 2 = medium (between 25–75% percent cover for entire FOV), 3 = dense (>75% percent cover for

TABLE 1 Length of flowline assessed (m) for each asset and year, and the age, size, timing and length of ROV survey (minutes) of the manifold and wells studied.

Flowline #	Type	Date installed	Diameter of flowline (mm)	Flowline depth (m)	Flowline length (m)	Metres of flowline surveyed by ROV during the day (D) or night (N)					Total length surveyed	Total overlap across years in metres (# years)
						2020 (Feb)	2017 (Nov)	2014 (Nov)	2012 (Sept)	2009 (Oct)		
1	Umbilical	2006	93.5	131–261	1900	1532 (N)	–	–	–	–	1532	–
2	Flowline	2006	304	132–138	1360	1360 (D)	–	–	–	–	1367	–
3	Flowline	2006	106	131–153	2797	2797 (N)	–	–	–	–	2811	–
4	Umbilical	2006	145	141–152	1750	1392 (D)	–	–	–	1464 (D)	2856	1464 (*2)
5	Flowline	2008	220	141–152	1550	1550 (D)	541 (D)	–	675 (D)	1543 (N)	4326	541 (*4)
6	Flowline	2006	279	142–153	1450	1450 (D)	–	–	–	1100 (D)	2574	1100 (*2)
7	Umbilical	2008	159	147–153	1135	1132 (N)	–	–	–	–	1132	–
8	Umbilical ^{T}	2008	159	145–261	4385	4385 (N)	1443 (D)	898 (D)	–	–	4471	1143/898 (*3)
9	Flowline ^{T}	2008	279	226–270	5567	2211 (D)	634 (D)	–	–	–	2845	634 (*2)
Total (m)					**21,894**	**17,877**	**2618**	**898**	**675**	**4107**	**21,550**	**3312**

Well #	Type	Date installed	Size (h × w × l) (m)	Depth (m)	Length of survey in minutes and time of day (D/N)					
					2020 (Feb)	2017 (Nov)	2014 (Nov)	2012 (Oct)	2011 (Mar)	2009 (Oct)
1	Manifold	2006	5 × 11 × 13	155	141 (N)	–	100 (D)	41 (D)	–	30 (N)
2	Well	2006	4 × 5 × 5	155	100 (D)	6 (D)	6 (D)	–	11 (D)	–
3	Well	2008	4 × 5 × 5	261	101 (N)	6 (D)	43 (D)	–	–	18 (N)
4	Well	2006	4 × 5 × 5	128	106 (D)	–	30 (D)	–	–	23 (N)

^{T}Trenched in 2011. This involved excavating two separate trenches then relocating the flowline into the trenches. The trenches were left to naturally backfill (become buried naturally).
The time of day each was surveyed is also indicated with Day = D, Night = N. Total overlap is the length of flowline in metres with overlapping time series data. Brackets (*) indicate number of time steps available for analysis.
Bold value indicate the totals.

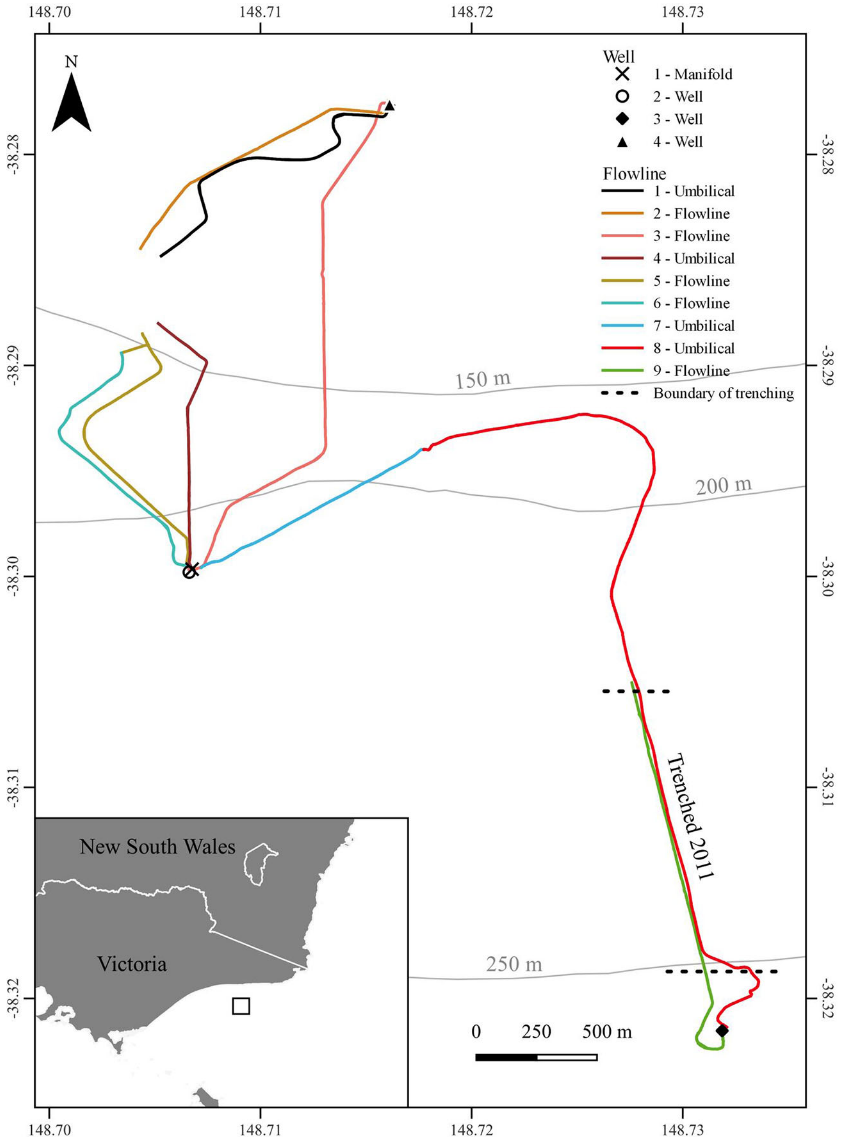

FIGURE 1
Location of studied offshore field and assets investigated in this study.

entire FOV). Video quality was also scored at these points; 1 being poor quality, 2 indicating moderate quality, and 3 indicating good quality. The same analyst undertook all benthic assessments to avoid any inter-observer variability.

To examine relationships between fish, benthic biota, and the position of flowlines relative to the seafloor, 'flowline position' was scored similarly to McLean et al. (2020b) with 0 = completely buried, 1 = flowline showing but more than halfway buried, 2 = flowline touching the seafloor but making a closed crevice, 3 = underside of flowline not touching the seafloor (spanning), and 4 = flowline >0.5 m above the seafloor. Flowline position was recorded in tandem with every fish observation.

2.2.2 ROV video analysis of wells and the manifold

For analysis of fish and mobile invertebrates on the wells/manifold, each structure was divided into six sections to determine the role of structure position in shaping communities observed. For wells, these sections included: tree cap assembly (top of the well), Christmas tree general (main middle section of the well), flow base (base of the well), seafloor around structure, seafloor beneath structure and water column around structure as described by McLean et al., 2022. The same general locations were identified on the manifold, namely the cap assembly, manifold module, base, seafloor beneath structure and water column around structure. The height of each of these structure sections was similar however the width and length of the manifold was greater resulting in more surface area for benthic habitats, fish and mobile invertebrate communities on this structure (Table 1).

To prevent repeated counts of the same individuals leaving and re-entering the field of view, the conservative measure MaxN (the maximum number of individuals of the same species present in the field of view at one time) was used to estimate relative abundance (Cappo et al., 2007). The length of ROV surveys of each structure varied dramatically across the years (Table 1) from rapid general visual inspections (6 mins) to detailed structural assessments (>100 mins). As a result, a more conservative measure of the 'maximum

MaxN' observed for the entire well (highest MaxN observed across all sections) for each species was used for temporal comparisons. Therefore abundances are likely conservative.

Benthic habitats on wells/manifold were analyzed by obtaining 10 non-overlapping FOV images per section of the structure (n = 60 total) and randomly allocating 20 points per FOV image. It was not possible to standardize the size of these FOV images due to high variability in ROV movements relative to the wells/manifold, however the point classification enabled the percent cover of each biotic component, identified to the lowest taxonomic resolution, to be quantified.

2.3 Data analyses

2.3.1 Spatial distribution of marine communities

Analyses were conducted to assess whether faunal assemblages differed among flowlines or wells/manifold using the comprehensive 2020 dataset only. For flowlines, fish and mobile invertebrate observations were grouped into 50 m transects, with this distance chosen to provide sufficient replication along each flowline while also capturing spatial variability in communities observed. For wells, too few mobile invertebrate taxa were observed for inclusion in statistical analyses, but these communities are described.

The separate multivariate fish and mobile invertebrate data sets were compared among flowlines in 2020 in PRIMER V7 (Clarke and Gorley, 2015) with the PERMANOVA+ add on (Anderson et al., 2008). Each assemblage was assessed using shade plots to determine the appropriate transformation level (Clarke et al., 2014), which for fish was dispersion weighting by flowline, while the invertebrate data needed no transformation. Dispersion weighting is becoming a commonly used transformation that enables better representation across species and down-weighs spatially clumped species (e.g. fish schools; Clarke et al., 2014). A Bray-Curtis dissimilarity matrix was constructed for each data set (Anderson et al., 2008) using a dummy variable on the factor of Flowline (nine levels, fixed) to include 50 m sections of flowline without taxa.

A canonical analysis of principal coordinates (CAP; Anderson and Robinson, 2003; Anderson and Willis, 2003) was undertaken for both fish and invertebrate datasets to visually examine patterns among flowlines. A leave-one-out allocation test (Anderson and Robinson, 2003) was used to provide a statistical estimate of misclassification error and demonstrate how distinct assemblages were in multivariate space (Anderson and Willis, 2003). Individual species that were likely responsible for any of the observed differences were identified using Pearson correlations of their abundance with the canonical axes. A Pearson correlation of $|R| \geq 0.3$ was used as an arbitrary cut-off to display potential relationships between individual species and the CAP axes. These relationships are graphically illustrated through the use of vectors that are superimposed onto the CAP plot made using the R packages ggplot2 (Wickham, 2016) and gridExtra (Auguie, 2017).

Separate analyses were undertaken for those four flowlines with over-lapping temporal data and aimed to assess change in fish and mobile invertebrate assemblages (combined data set) over time. The first analysis was conducted on Flowline 5 and involved assessing ~550 m of the same sections of flowline across four time periods (2009, 2012, 2017, and 2020). Data were visualized using shade plots before applying a dispersion weighted transformation (by flowline; Clarke et al., 2014) and calculating a Bray-Curtis similarity matrix. A repeated measures PERMANOVA with the lowest replication level, 'Transect' was conducted to assess change across years (four levels, fixed) and included video quality (Supplementary Table 1) as a covariate, with subsequent pairwise tests used to investigate significant differences. A CAP plot was used to visually assess patterns and differences across years.

The same analysis was undertaken for Umbilical 8 (2014, 2017, 2020). However, transects in 2017 and 2014 were not overlapping due to the surveys being conducted on different flowline sections, thus an additional qualifier was added to the 2020 dataset to match to either 2017 or 2014 (<1500 m section or >1500 m section). We combined data obtained from Umbilical 4 and Flowline 6, as they were surveyed at the same time (2009 and 2020) and included a second factor 'Flowline' into the PERMANOVA analysis. Flowline 9 had two time points (2017 and 2020) and was analyzed separately.

Analyses of fish communities observed on wells/manifold used the same methods described above for the 2020 data using a dispersion-weighted Bray-Curtis similarity matrix, but according to the factors Structure (4 levels, fixed) and Section (6 levels, fixed). Due to differences in the time of survey, duration of survey (Table 1) and video quality (Supplementary Table 1), well and manifold temporal data were only able to be examined heuristically with data presented in descriptive figures rather than undergoing formal statistical analysis. This included metric multidimensional scaling (mMDS) to visually represent patterns of fish communities among years and depths (Clarke et al., 2014).

2.3.2 Influence of survey-specific, environmental, and benthic variables on fish and mobile invertebrate communities

Relationships between the fish and mobile invertebrate Bray-Curtis dissimilarity (described above) and normalized benthic habitat, flowline position, depth and distance to the nearest structure variables (n = 11) were explored using distance-based linear models (DISTLM) and distance-based redundancy analysis (dbRDA; McArdle and Anderson, 2001; Anderson et al., 2008) in the PRIMER-E statistical software package. Variables were checked for correlations using draftsmen plots, with percent cover of shell/pebble strongly negatively correlated with percent cover of sand (-0.95). Thus, percent cover of shell/pebble was excluded from analyses. A stepwise selection procedure was used in which the contribution of each variable was assessed for statistical significance using marginal tests (from 9999 permutations) and percentage contribution of each set of variables (Anderson et al., 2008). A dbRDA plot was produced using the R packages ggplot2 (Wickham, 2016) and gridExtra (Auguie, 2017) for visualizing relationships between the assemblages and associated variables.

The influence of epibenthic community percent cover and complexity, and of flowline position on fish and mobile invertebrate diversity, total abundance, abundance of ubiquitous (species with <80% zero samples and those identified in CAP) and commercial fishery species were investigated using generalized additive models (GAMs; Hastie and Tibshirani, 1986). Because of strong collinearity, a full subsets approach was used to fit all combinations of predictor variables up to a maximum of three (to prevent over-fitting and ensure models remained ecologically interpretable). Time of day was treated as a circular variable using the function (bs='cc') in mgcv (Wood, 2011). Models containing combinations of variables with correlations >0.28 were excluded. The best model had the fewest variables (most parsimonious) and was the one with lowest Akaike information criterion (AIC). Best models were also within two AIC units of the lowest AIC value (Burnham and Anderson, 2003; Symonds and Moussalli, 2011).

As recommended in the literature (O'Hara and Kotze, 2010), we used untransformed abundance metrics as our response variables. Models were fitted using a Tweedie error distribution (Tweedie, 1984). A Tweedie model is an extension of a compound Poisson model derived from the stochastic process where a gamma distribution is used for the counted or measured objects (i.e. number of fishes) and has an advantage over delta-type two-step models by handling the zero data in a unified way. All GAM modelling and plots were performed using the R language for statistical computing (R Development Core Team, 2019) with the package mgcv (Wood, 2011) and ggplot2 (Wickham, 2016), and based on the approach by Fisher et al. (2018).

Linear regression models were produced to understand if the cover of colonizing invertebrates (summed cover of ascidians, bryozoans, sponges, and black/octocorals) correlated with well/manifold age and depth. Benthic habitat data from wells/manifold in this study were combined with those reported by McLean et al. (2019) to see if relationships held with those previously documented in north-west Australia. Analysis was undertaken using the R language for statistical computing (R Development Core Team, 2019) and plotted with ggplot2 (Wickham, 2016).

3 Results

3.1 Overview of species richness and abundance

A total of 10,343 individual animals were observed and comprised 69 taxa including bony and cartilaginous fishes, mammals, and invertebrates (Supplementary Tables 2, 3; Supplementary Figures 1, 2). There were 16 species observed of commercial fisheries interest, and three species of conservation value including, handfish (Brachionichthyidae spp.), stingaree (*Urolophus* spp.), and foxfish (*Bodianus frenchii*); although these are tentative identifications unable to be verified from the imagery obtained. Australian fur seals (*Arctocephalus pusillus doriferus*) were observed multiple times along flowlines in 2009, including juvenile males and adult females (Supplementary Data Table 2).

More species of fish were recorded on flowlines ($n = 28$ species) compared to wells and manifold ($n = 19$ species). An average of 295 ± 45 individual fish were recorded per km of pipeline. Considering the comprehensive 2020 dataset on its own, 16 species of fish were recorded on the flowlines that were not observed on the wells or manifold, including species closely associated with the benthos e.g. banded cucumberfish (*Paraulopus balteatus*), ghost flathead (*Hoplichthys* spp.). Eight species of fish were unique to the wells and manifold which included more mobile, schooling species such as Australian sandpaper fish (*Paratrachichthys macleayi*) and redfish (*Centroberyx affinis*). Eight species were observed on both infrastructure types, including commercial fishery species such as ocean perch (*Helicolenus* spp.), jackass morwong (*Nemadactylus macropterus*) and pink ling (*Genypterus blacodes*).

A total of 2,066 individual invertebrates comprised of 32 species were observed on flowline surveys across all survey years (Supplementary Data Table 2). Invertebrate taxa were identified from four phyla, of which Arthropoda and Cnidaria had the highest abundance. A total of 27 individual invertebrates were observed on the wells and manifold across all years and comprised seven taxa (Supplementary Data Table 3). Pancake urchin (*Araeosoma thetidis*) was the only mobile invertebrate species recorded on both types of infrastructure.

3.2 Extent of burial of flowlines

Using the 2020 data only, forty one percent of flowlines surveyed were classed as 'buried'. This was most prevalent on Umbilical 7 and 8, and Flowline 9 where 97- 100% was buried. Where flowlines were classified as exposed; 32% of observations were less than 50% exposed, 15% were greater than 50% exposed and 11% were completely exposed and spanning. There were no observations of any flowline with a span of greater than 0.5 m above the substrate.

3.3 Epibenthic cover of flowlines and wells

Using the 2020 data only, epibenthic cover of flowlines was predominantly abiotic, i.e. sand (>80% cover) for all flowlines except flowline 3 which was a mix of sand (49%) and pebble/gravel (50%). The most prevalent biotic cover was 'biofilm' accounting for 3% of the total cover. Overall, all sponge classes accounted for only 0.3% of cover. Among all flowlines, most epibenthic communities were encrusting (61–91%; negligible in height), with very few of low (9–39% values) and moderate (0–4%) complexity. Infauna burrows were observed beside all flowlines, generally in low densities; between 9% (Umbilical 7) and 39% (Umbilical 4) sparse coverage (<25% cover).

For surveys prior to 2020, poor video quality had the largest impact on benthic assessments because it affected our ability to identify epibenthic organisms. As such, large amounts (49%) of historic imagery was classed as either "unidentifiable" (biota too blurry to identify; 20.3%), "not useable" (biota/flowlines not visible; 7.9%) or "open water" (where the ROV view was at an oblique angle, causing some quadrat points to be placed in the water column; 21.5%) (Figure 2), thus, further analyses on these biota metrics was not undertaken. Sand was the dominant habitat scored on flowlines through the time series, but an overall increase in biofilm was also observed among flowlines over time.

Similar to historic epibenthic habitat classifications of flowlines, a substantial amount (58%) of habitat classifications on wells and the manifold for all years were classed as either "unidentifiable" (37%; video too blurry to identify), "not useable" (0.7%; benthos and flowlines not visible), "fish" (0.9%; where a quadrat point has landed on a fish and the underlying benthos cannot be identified),

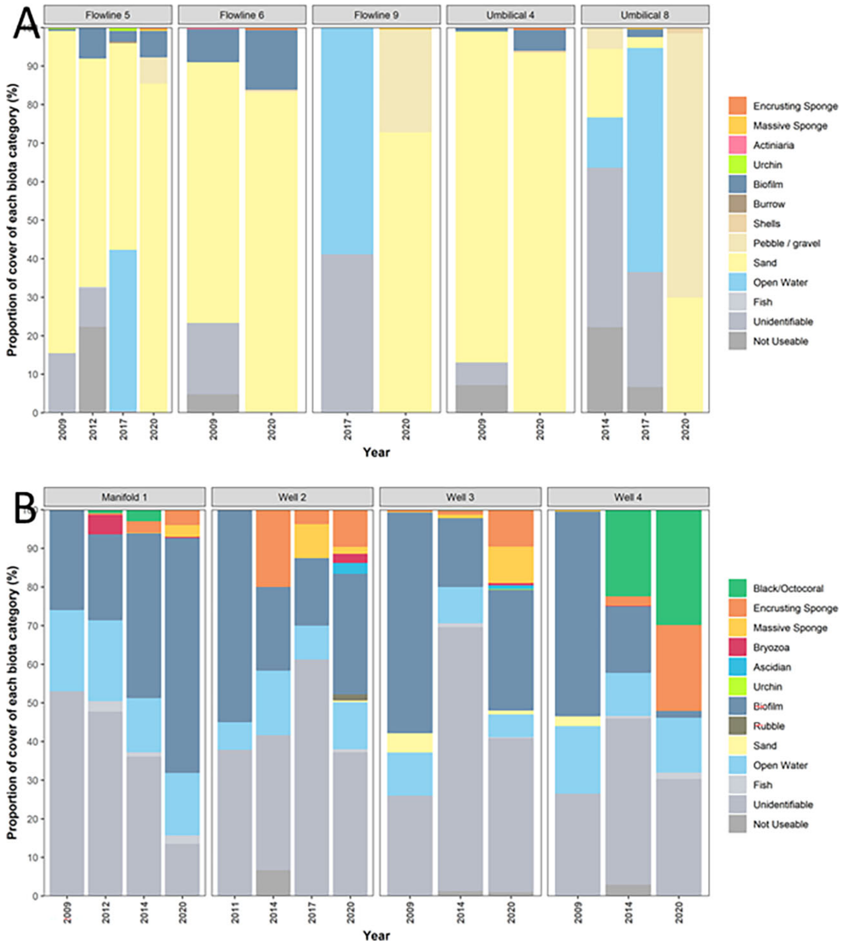

FIGURE 2
Percentage cover of each benthic biota grouping observed on **(A)** comparable sections of flowline between 2009 and 2020 and **(B)** wells and manifolds between 2009 and 2020.

or "open water" (12%; video where the quadrat point is in the water column). Biofilm was the most common class of biota able to be scored, making up 32% of all classifications (Figure 2). Other types of biotas that were observed in lower densities included sponges (8%; encrusting and massive), black/octocorals (6%) and bryozoans (0.5%). A greater cover of black/octocorals and massive sponge classes were observed in 2020 compared to previous years, although whether this is a true increase rather than a product of improved visibility is not known.

Epibenthic cover was predominantly biotic for all wells and dominated by biofilm for the manifold (61%), Well 2 (31%) and Well 3 (31%). Well 4 had a comparatively high proportion of black/octocorals (22%) and encrusting sponge communities (22%; Figure 2). Black/octocorals, bryozoans and ascidians were not observed on flowlines (Figure 2).

A linear regression of total percent cover of colonizing epibenthic communities on wells and the manifold sampled for this study and reported by McLean et al. (2019) showed weak positive correlation with well and manifold age, suggesting an increase in invertebrate epibiota with increasing time *in-situ* (Figure 3). The addition of samples from this study reduced the R^2 reported by McLean et al. (2019) from 0.43 to 0.29 (Figure 3), noting that McLean et al. (2019) reported on tropical fish assemblages which may exhibit different patterns to those in temperate ecosystems such as those surveyed here. A stronger negative correlation existed between the depth of the well or manifold and the total cover of epibenthos (Figure 3). Similarly, adding samples from this study to the model, reduced the R^2 reported by McLean et al. (2019) from 0.74 to 0.57.

3.4 Fish communities observed along flowlines in 2020

Across the 17.8 km of flowlines assessed in 2020, 5,697 individual fish were identified from 24 taxa equating to a relative abundance of 295 ± 45 individual fish per kilometer (Supplementary Table 4). The most abundant species were also the most ubiquitous (>80% of the observations) and included: *Parapercis* sp2 (species complex, not including *P. allporti*); ocean perch (*Helicolenus* spp.); slender sandburrower (*Creedia haswelli*); barred grubfish (*Parapercis allporti*); banded cucumberfish (*Paraulopus balteatus*); and trevally (Carangidae spp.). Six commercial fishery species were observed along flowlines in 2020 including the aforementioned Carangidae spp. and *Helicolenus* spp., along with blue grenadier (*Macruronus novaezelandiae*), jackass morwong (*Nemadactylus macropterus*), pink ling (*Genypterus blacodes*), tiger flathead (*Platycephalus richardsoni*).

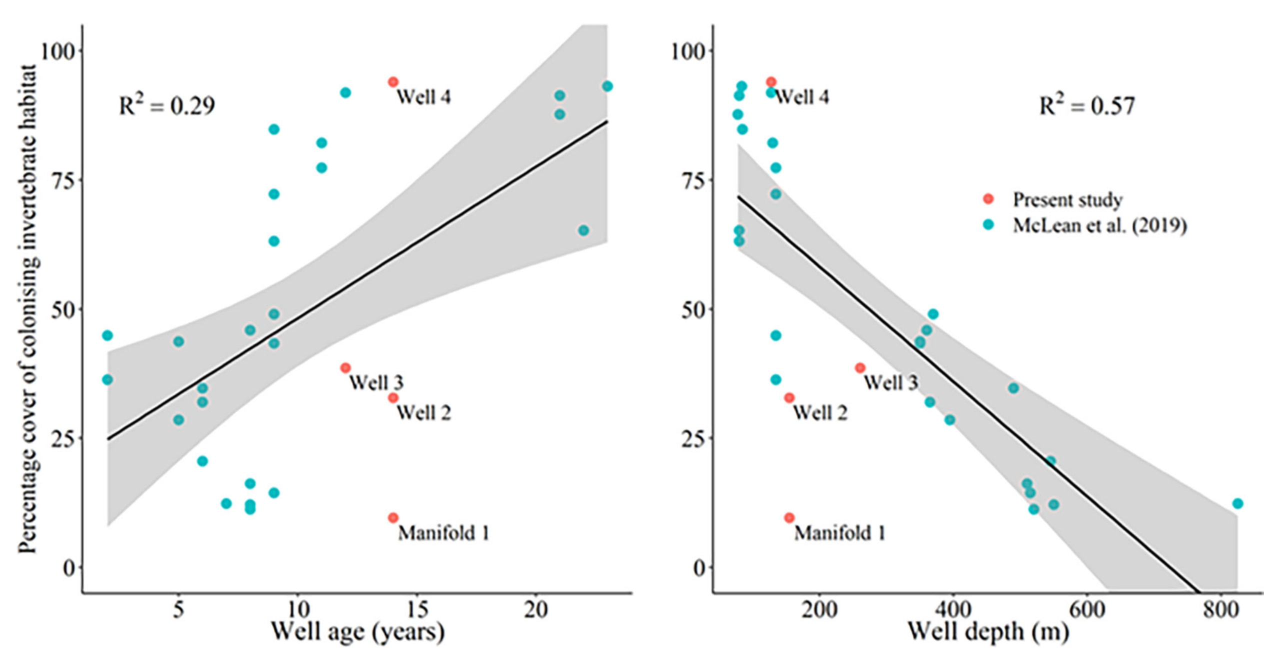

FIGURE 3
Linear regression of the percent cover of colonising invertebrates against wellhead age and wellhead depth. Shaded regions represent the 95% confidence interval. Samples are presented with those recorded by McLean et al. (2019) which reflect fish communities around wells on the north-west shelf of Australia.

The relative abundance of commercial fishery species across the flowlines varied, ranging from 0.4–79.1 individuals/km, with Flowline 5 having the highest, mainly comprised of *Helicolenus* spp. Species of ecological interest included the rarely seen broad duckbill (*Enigmapercis reducta*) and handfish (anglerfish) within the family Brachionichthyidae. The majority of fish species observed on flowlines were <20 cm in size (snout to tail fork) with frequency substantially declining with increasing size classes (Supplementary Figure 3). Commercial fishery species accounted for 83% of all length observations over 20 cm. For commercial fishery species, 98% of length estimates in the <20 cm class were of *Helicolenus* spp. (Supplementary Figure 3).

Spatial distribution of total abundance and fish species richness along flowlines (Figure 4) in addition to the abundance distribution of ubiquitous species (Figure 4) show some patterns according to positions along flowlines. Individual species show affinity to particular sections of flowline. *Parapercis allporti* and *C. haswelli* were present in higher abundance in northern sections of flowlines, compared to flounder (Bothidae spp.) and *Parapercis* sp2 which had high abundance at the southern, deeper sections of Umbilical 8 and Flowline 9 (Figure 4).

3.4.1 Influence of survey-specific, environmental, and benthic variables on fish communities observed in 2020

Fish assemblages differed across flowlines in 2020 (Pseudo-F = 25.78, P = 0.001), with all flowline pairs significantly different (t > 1.5, P <0.05; Supplementary Table 5). Fish assemblages also showed distinct clusters on each flowline, particularly for Umbilical 1, Flowline 3, Umbilical 7 and Umbilical 8 (CAP analysis p < 0.01; Figure 5). This distinction between the seven flowlines was illustrated by an overall CAP leave-one-out allocation success rate of 67%. Fish species associated with Flowline 3 included barred grubfish (*P. allporti*), slender sandburrower (*C. haswelli*), cocky gurnard (*L. modesta*), and red cod (*Pseudophycis* spp.), while the whiptail (*Coelorinchus* spp.) was correlated with Umbilical 8 (Figure 5). Blue grenadier (*M. novaezelandiae*) had high abundance at both Flowline 3 and Umbilical 7. While *Parapercis* sp2 also had high abundances at Flowline 3 and Umbilical 8. Ocean perch (*Helicolenus* spp.) had the highest abundance on Flowline 6 (Figure 4).

Flowline position, depth, percent cover of sand, percent of biofilm on flowlines, and burrow density, all had a significant relationship with the variation in the fish assemblage data cloud when considered alone (p < 0.01). Flowline position explained the greatest amount of variation in the fish relative abundance data cloud at 12%. The variables that reduced the value of AICc the most after fitting flowline position, in the stepwise additive model, were depth (10%, cumulative = 22%), percent cover of sand (3%, cumulative = 25%) and biofilm on flowlines (1%, cumulative = 27%). All of the conditional tests associated with each of these sequential additions were statistically significant (p < 0.05). The best solution contained the five stated variables, flowline position, depth, percent cover of sand, percent of biofilm on flowlines and burrow density and explained 27% of the variation in the fish relative abundance data cloud (Figure 6). The first two dbRDA axes captured 86.4% of the variability in the fitted model and 23.6% of the total variation in the data cloud (Figure 6). The grubfish (*Parapercis* sp2) and whiptail (*Coelorinchus* spp.) showed similar correlations to increasing depth, while slender sandburrower (*C. haswelli*), red cod (*Pseudophycis* spp.) and blue grenadier (*M. novaezelandiae*), were more strongly correlated with sand coverage (Figure 6).

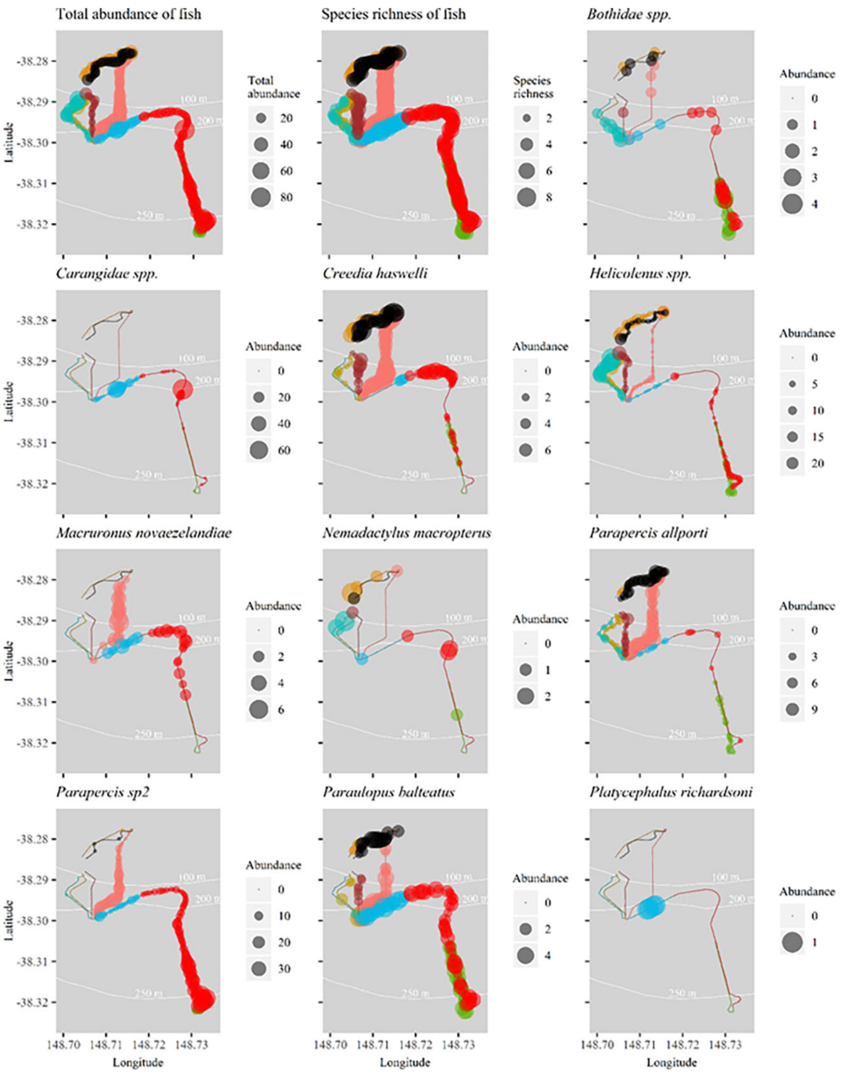

FIGURE 4
Spatial distribution of total abundance and species richness of fish, and the abundance of key species of fish per transect along flowlines surveyed in 2020. Abundance bubble sizes reflect exact abundance per transect, and therefore bubble size may be larger or smaller than those shown in the legend's categories. Flowline numbers are indicated in Figure 1.

Univariate GAMs were produced for total abundance and fish species richness, as well as the abundance of those species identified in the CAP (Figure 5), species with >80% non-zero samples, and commercial fishery species. No GAM was produced for commercially targeted *N. macropterus*, *M. novaezelandiae*, and *Platycephalus richardsoni* due to low abundances (*n* = 20, *n* = 104, and *n* = 4, respectively).

Percent cover of biofilm was present in the top model for total abundance, species richness, *C. haswelli*, *Parapercis allporti*, *Parapercis* sp2, *Paraulopus balteatus*, *Pseudophycis* spp., and *Helicolenus* spp. (Table 2). Total abundance and the abundance of *Helicolenus* spp. increased with higher percent cover of biofilm compared to species richness, and abundance of *C. haswelli, Parapercis allporti, Parapercis* sp2, *Pseudophycis* spp., and *P. balteatus*, which generally decreased with increasing percent cover of biofilm (Supplementary Figure 4). Time of day was also included with biofilm in the top models for total abundance and abundance of *C. haswelli*, *P. allporti*, *Parapercis* sp2, and *P. balteatus* (Table 2). Total abundance and the abundance of *Parapercis* sp2, and *P. balteatus* were highest during the night and into sunrise, compared to the abundance of *C. haswelli* and *P. allporti* which peaked in abundance at sunset and into night (Figure 7). *P. balteatus* also showed a pulse in abundance at midday, but abundance peaked at night (Figure 7).

Depth was the only variable in the top models for *Coelorinchus* spp. and *L. modesta* and included in the top models for *Pseudophycis* spp. and Carangidae spp. (Table 2). Abundance of *L. modesta* and *Pseudophycis* spp. decreased with increasing depth, compared to *Coelorinchus* spp. which increased with depth (Figure 7). Carangidae spp. peaked in abundance at 140 m and at 260 m water depth (Supplementary Figure 4). Distance to nearest structure was included in models for species richness and *Helicolenus* spp. (Table 2). Species richness peaked at approximately 750 m from structures and was lowest for transects close to structures and those >1500 m away (Supplementary Figure 4). *Helicolenus* spp. decreased in abundance with increasing distance from structures (Supplementary Figure 4). The percent cover of pebble/gravel was included in the top model for Carangidae spp. only (Table 2) and

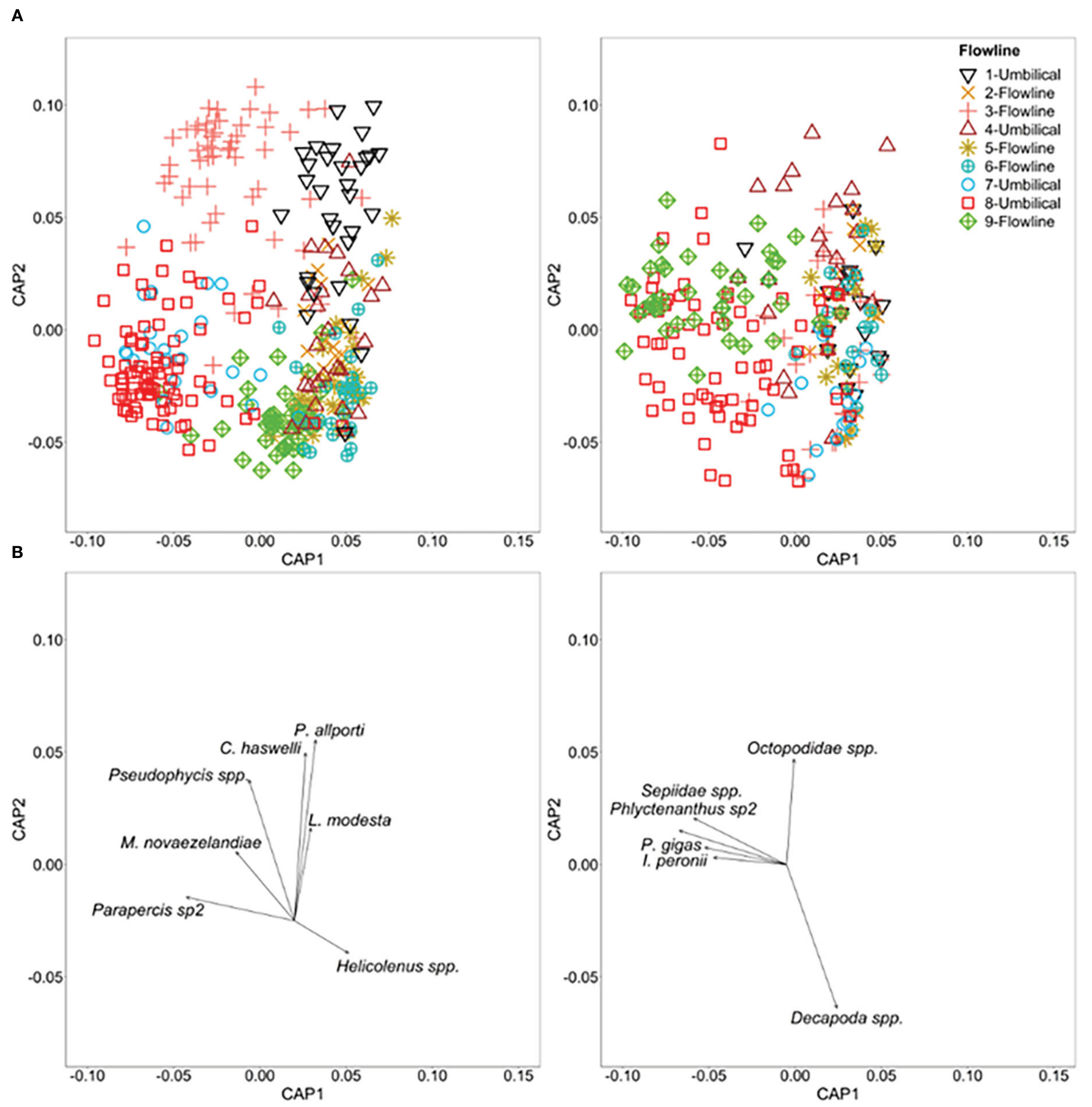

FIGURE 5
(A) A Canonical analysis of principal coordinates (CAP) ordination based on Bray-Curtis dissimilarities for 1) (Top left) multivariate fish abundance on flowlines and 2) (Top right) mobile invertebrate abundance on flowlines, showing the first two (out of *m* = 10) axes. Each point represents the assemblage structure (all species) within each 50 m transect of each flowline in relation to the other locations (similarity), with points that are closer together more similar than those further apart. **(B)** Pearson correlations (|R| ≥ 0.3) for species are displayed as vectors with the length and direction of these vectors representing the strength and direction (relative to the data cloud **(A)**) of this species association.

showed highest predicted abundance at approximately 40% pebble/gravel and lowest predicted abundance when pebble/gravel was not present (Supplementary Figure 4).

3.5 Mobile invertebrate communities observed along flowlines in 2020

For the 2020 survey, a total of 1,466 mobile invertebrates from 31 taxa were identified, equating to 71 ± 12 individuals/km of flowline (Supplementary Table 2). Mobile invertebrate taxa were identified from four phyla with Arthropoda and Cnidaria dominating the assemblage, in particular, hermit crabs (n = 443) and anemone sp2 (n = 328). Invertebrates of commercial importance included the Tasmanian giant crab (*Pseudocarcinus gigas*, n = 47), cuttlefish (Sepiidae spp., n = 93), octopus (Octopodidae spp., n = 44), arrow squid (*Nototodarus gouldi*, n = 1), and Balmain bug (*Ibacus peronii*, n = 35).

Total abundance and species richness of mobile invertebrates varied spatially, with higher abundance and diversity below 200 m depth (Figure 8). Individual species show affinity to particular sections of flowline. For example, *I. peronii*, *P. gigas*, anemone sp2, *Phlyctenanthus* sp2 and Sepiidae spp. were observed in comparatively high abundance at the southern section of Umbilical 8 and Flowline 9 (Figure 8).

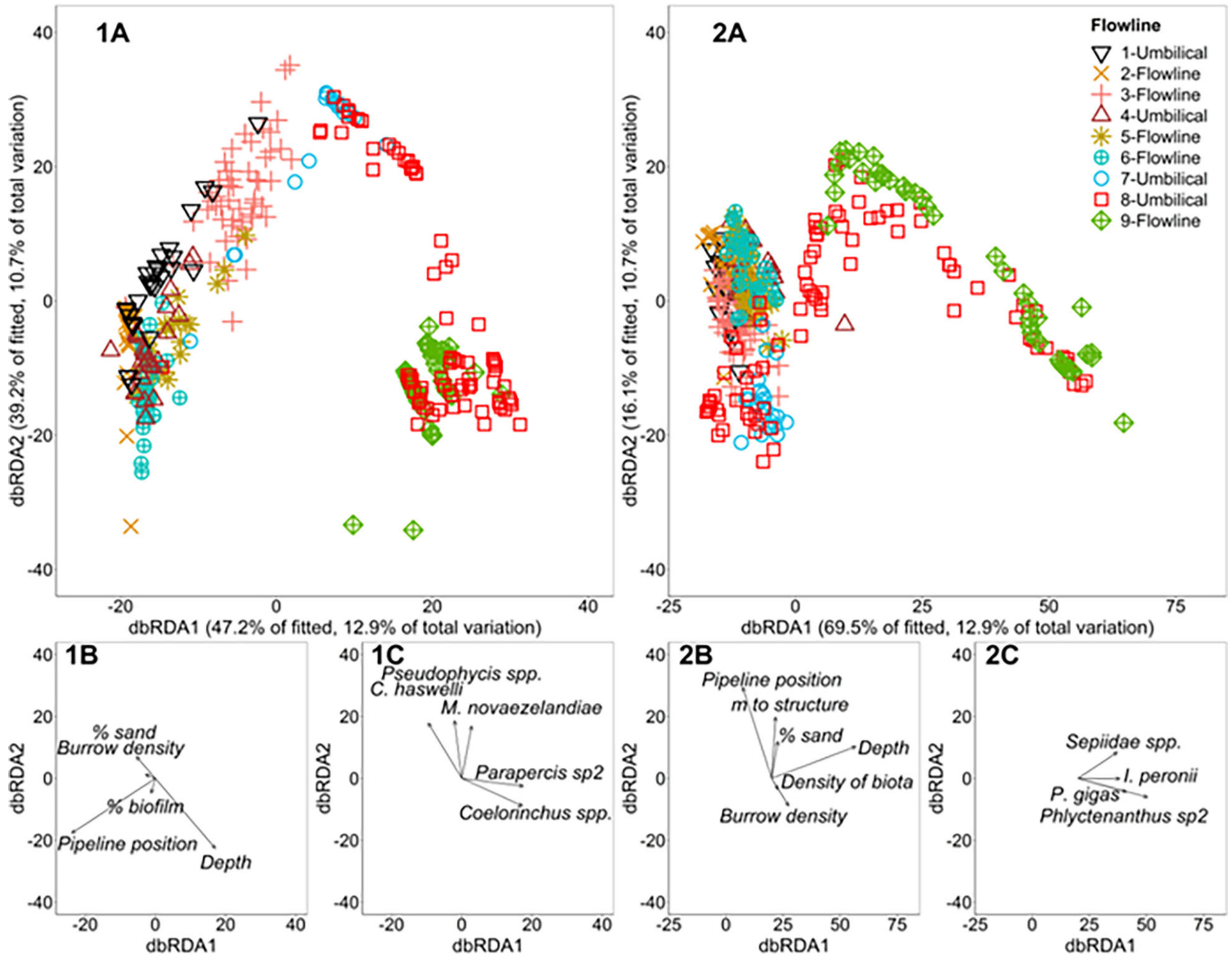

FIGURE 6

(A) Distance-based redundancy analysis (dbRDA) displaying the relationship between the most important explanatory variables (depth, flowline position, % biofilm on flowline, % sand and burrow density) for 1) (Top left) multivariate fish abundance on flowlines and 2) (Top right) mobile invertebrate abundance on flowlines. **(B)** Vectors indicate the direction of the relationship with the explanatory variables and their length indicates the strength of their effect on fish abundance. **(C)** Species with a Pearson correlation of |R| ≥ 0.4 to either axis is displayed as vectors indicating the strength and direction (relative to the data cloud **(A)** and variables **(B)**) of their association.

3.5.1 Influence of survey-specific, environmental, and benthic variables on mobile invertebrate communities observed in 2020

Mobile invertebrate assemblages differed across flowlines (Pseudo-*F* = 11.92; *P* = 0.001), however, six pairs of flowlines showed no significant difference, with three pairs involving Flowline 6 (Supplementary Table 5). A CAP analysis, constrained by 'flowline', shows some separation between flowlines, particularly for Umbilical 8 and Flowline 9 ($p < 0.01$; Figure 5). There was generally a poor level of distinction between the seven flowlines as illustrated by an overall CAP leave-one-out allocation success rate of only 35%. Mobile invertebrate species associated with the deeper, more southern flowlines Umbilical 8, and Flowline 9, included cuttlefish (Sepiidae spp.), anemone sp2 (*Phlyctenanthus* sp2), Tasmanian giant crab (*P. gigas)*, and Balmain bug (*I. peronii)*.

Depth, distance to nearest structure, flowline position, burrow density, percent cover of sand and the density of biota all had a significant relationship with the variation in the invertebrate assemblage data cloud when considered alone (all $p < 0.01$). Depth explained the greatest amount of variation in the mobile invertebrate relative abundance data cloud at 17%. The variables that increased the value of AICc the most after fitting depth, in the stepwise additive model, were distance to nearest structure (5%, cumulative = 22%), flowline position (4%, cumulative = 27%) and burrow density (1%, cumulative = 28%). All of the conditional tests associated with each of these sequential additions were statistically significant ($p < 0.05$). The best solution contained the aforementioned six variables and explained 28% of the variation in the mobile invertebrate relative abundance data cloud (Figures 5, 6).

Univariate GAMs were produced for the total abundance and species richness of mobile invertebrates, as well as the abundance of those species identified in the CAP (Figure 5), species with >80% non-zero samples, and commercial fishery species. As evident from spatial distribution plots (Figure 8), depth was an important predictor variable and present in the top model for total abundance, species richness, anemones (*Phlyctenanthus* spp), Balmain bug (*I. peronii*) and octopus (Octopodidae spp.) (Table 2). Models including depth showed increasing species richness and abundances of mobile invertebrates

TABLE 2 Generalised additive models (GAMs) for predicting total abundance and species richness of fish and mobile invertebrates, and the abundance of key species and commercial species along flowlines within 2 AIC of the top model. The best model is indicated in bold.

Dependent variable	eDF	AIC	wAIC	R^2	Top model
Fishes					
Total	5.85	2519.19	1.00	0.19	**Biofilm + Time of day**
Species richness	5.71	1352.31	0.99	0.12	**Biofilm + Distance to nearest structure**
Creedia haswelli	4.84	1139.44	0.66	0.44	**Biofilm + Time of day**
	3.84	1140.77	0.34	0.43	Time of day
Coelorinchus spp.	3.49	380.24	1.00	0.45	**Depth**
Lepidotrigla modesta	3.88	338.98	0.89	0.23	**Depth**
Parapercis allporti	4.93	1068.19	0.87	0.46	**Biofilm + Time of day**
Parapercis sp2	4.84	1348.79	0.91	0.56	**Biofilm + Time of day**
Paraulopus balteatus	4.83	913.14	0.59	0.15	**Biofilm + Time of day**
	3.84	913.88	0.41	0.14	Time of day
Pseudophycis spp.	8.60	382.18	0.79	0.33	**Sand + Biofilm + Depth**
Commercial fish					
Carangidae spp.	7.39	539.87	0.49	0.69	**Pebble/Gravel + Depth**
	8.29	540.08	0.44	0.71	Undefined biota + Pebble/Gravel + Depth
Helicolenus spp.	6.93	1543.90	0.54	0.32	**Biofilm + Distance to nearest structure**
	8.82	1544.27	0.45	0.33	Biofilm + Pebble/Gravel + Depth
Macruronus novaezelandiae	5.87	497.56	0.35	0.24	**Biofilm + Distance to nearest structure**
	6.63	497.64	0.34	0.29	Biofilm + Depth
Invertebrates					
Total	5.62	1410.07	0.32	0.40	**Sand + Depth**
	5.63	1411.13	0.19	0.40	Pebble/Gravel + Depth
	4.68	1411.41	0.16	0.39	Depth
	7.50	1412.04	0.12	0.40	**Biofilm** + Pebble/Gravel + Depth
Species richness	3.04	860.89	0.41	0.31	**Biofilm + Depth**
	2.40	862.85	0.15	0.30	Depth
Araeosoma thetidi	1.00	424.17	0.78	0.00	NULL
Decapoda spp.	4.87	2435.02	1.00	0.20	**Biofilm + Time of day**
Pycnogonidae spp.	3.18	357.52	0.80	0.80	**Time of day**
Phlyctenanthus spp.	4.58	322.20	0.57	0.22	**Pebble/Gravel + Depth**
Phlyctenanthus sp2	3.92	505.13	0.46	0.85	**Time of day**
	4.35	506.40	0.25	0.85	Pebble/Gravel + Depth
	5.63	507.04	0.18	0.85	Biofilm + Time of day
Commercial invertebrates					
Ibacus peronii	2.84	330.67	0.94	0.57	**Depth**
Octopodidae spp.	4.83	315.93	0.52	0.15	**Depth**
	3.00	317.46	0.24	0.13	Biofilm + Pebble/Gravel
Pseudocarcinus gigas	4.16	330.96	1.00	0.35	**Sand + Flowline position**
Sepiidae spp.	1.00	315.01	0.67	0.00	NULL
	2.00	316.73	0.28	0.01	Pebble/Gravel

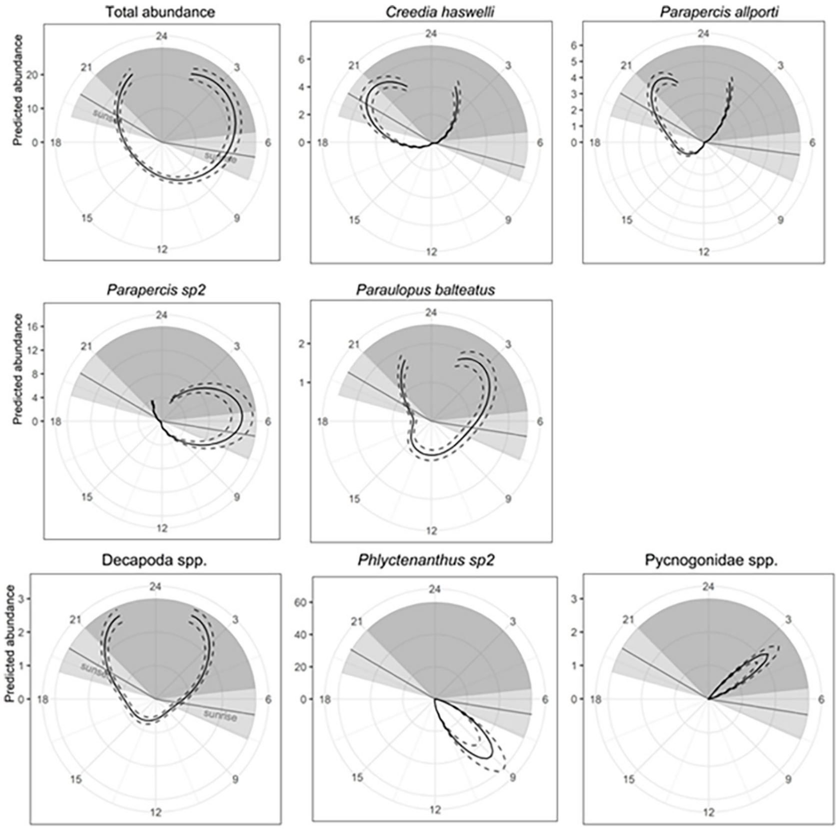

FIGURE 7
Predicted fish and mobile invertebrate abundance per transect as a function of time of day for all fish (total abundance), common and commercial fishery species plotted over a 24 hour 'clockface'. Solid lines indicate fitted GAM curves and dashed lines represent ±2×SE of predicts. Light grey shading is the crepuscular period defined as one hour either side of sunset and sunrise. The dark grey shading is night, beginning one hour after sunset and finishing one hour before sunrise. Gaps in the curve indicate the time of the day where no sampling occurred. GAM was circular for available data only, therefore predicted abundance is equal at both ends of the curved displayed.

with increasing depth. Octopus (Octopodidae spp.) also showed a peak in abundance in shallower depths. Time of day was included in the top model for hermit crabs (Decapoda spp.), sea spiders (Pycnogonidae spp.), and anemones (*Phlyctenanthus* sp2) (Table 2). Hermit crabs (Decapoda spp.) displayed higher abundances at night, anemones (*Phlyctenanthus* sp2) peaked after sunrise, and sea spiders (Pycnogonidae spp.) peaked during the night (Figure 7). Species richness and Decapoda spp. included percent cover of biofilm in their top models (Table 2) and both increased with increasing percent cover (Supplementary Figure 5). Percent cover of sand and flowline position were the only two variables in the top model for *P. gigas* (Table 2) with a higher abundance when the flowline is buried by sand.

3.6 A comparison of marine communities observed on flowlines from 2009 - 2020

Prior to 2020, the majority of ROV imagery of flowlines (75% of transects) was of poor video quality, while 25% was of moderate quality. In contrast, 100% of 2020 ROV imagery was of good quality, although the downward nature did make identification of some fish species difficult (Supplementary Table 1). Only one commercial fish species was observed in historical video imagery (2014) but not also observed in 2020; the gemfish (*Rexea solandri*, n = 3). All others that were observed in historical imagery were observed in 2020 (Supplementary Table 2).

For fish and mobile invertebrates, the same sections of five flowlines were assessed over time enabling evaluation of change to these communities (Table 1; Flowline 5, Flowline 6, Umbilical 4, Umbilical 8, Flowline 9). For these repeated measures assessments, the 'video quality' covariable had a significant impact on assemblages on all flowlines (Table 3). Even considering large differences in video quality, fish, and mobile invertebrate assemblages along two flowlines (Flowline 5 and Umbilical 8) changed across years (Table 3). Assemblages observed in 2020 had higher abundance and species richness than those in previous years for Umbilical 8, while Flowline 5 only had higher abundance for fish in 2020 (Figure 9), but not for species richness or for mobile invertebrate abundance or richness, with these remaining relatively constant over time (Figure 9).

Separation of assemblages by Year is evident for both Flowline 5 and Umbilical 8 (Figure 10), with a moderate level of distinction between years for Flowline 5 (67% allocation success rate) and a good level for Umbilical 8 (89% allocation success rate). Species correlated with the CAP axes for Flowline 5 were distinct for each year with Australian fur seal (*A. pusillus doriferus*), pancake urchin (*A. thetidis*), and *P. balteatus* correlated with 2009, Decapoda spp. and *P. allporti* correlated with 2012, Octopodidae spp. with 2017, and *Helicolenus* spp. with 2020. While for Umbilical 8, Sepiidae spp. were correlated

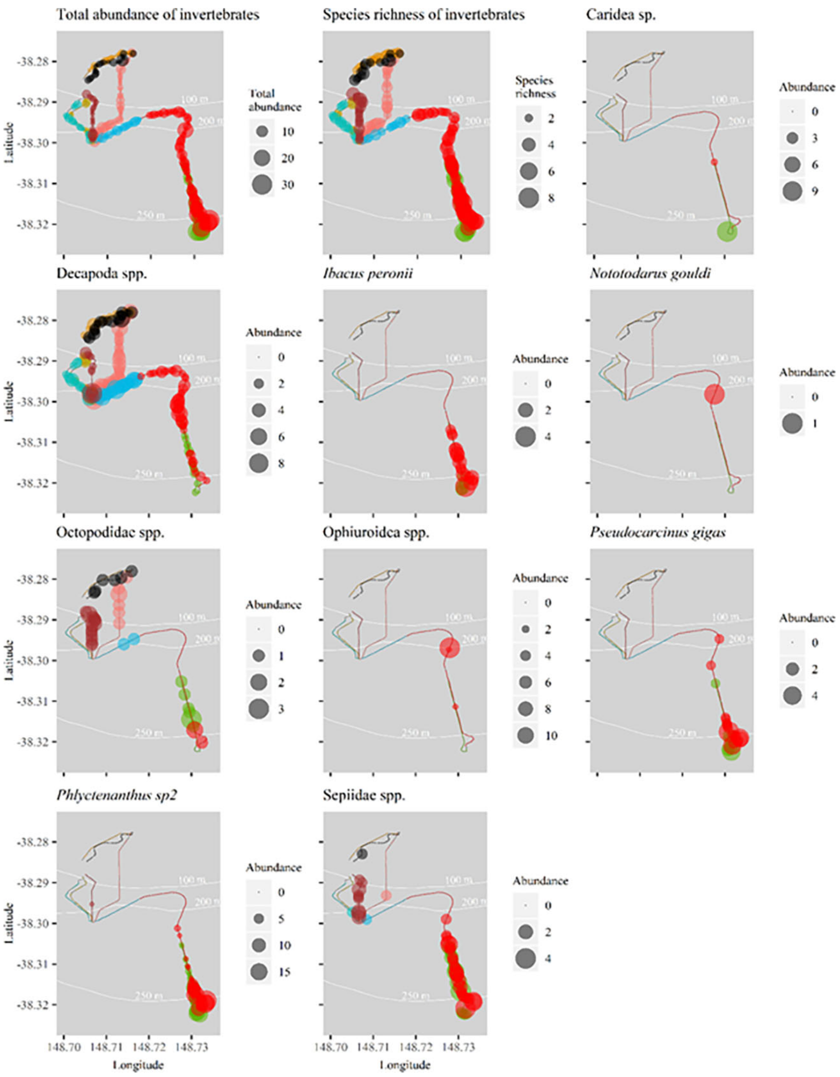

FIGURE 8
Spatial distribution of total abundance (top left), species richness (top right) and the abundance of common mobile invertebrate species per transect along flowlines surveyed in 2020. Abundance bubble sizes reflect exact abundance per 50m transect, and therefore bubble size may be larger or smaller than those shown in the legend's categories. Refer to Figure 1 for flowline names.

with 2014, and *A. thetidis* with 2017. Multiple species were correlated with 2020 including Decapoda spp., squat lobsters (*Galathea australiensis*), *Coelorinchus* spp., *Phlyctenanthus* spp., and *Parapercis* sp2 for the section >1500 m along the flowline that matched with the area surveyed in 2014 and *Pseudophycis* spp., *M. novaezelandiae*, Pycnogonidae spp., and *C. haswelli*, in the section <1500 m along the flowline that matched with 2017.

3.7 Marine communities around the manifold and wells

3.7.1 Fish and mobile invertebrate communities on the manifold and wells in 2020

For 2020, over 787 individuals were identified from 16 fish species (Supplementary Table 3) were observed. An estimated additional 2,517 additional individual fish were noted but not able to be identified to species level, primarily due to the angle of the imagery (not reported on further). Eight of these species were unique to wells and not encountered on flowlines. Wells 2- 4 had high abundances of Australian sandpaper fish (*P. macleayi)* while the manifold had a greater abundance of redbait (*Emmelichthys nitidus*) and jackass morwong (*N. macropterus*). A range of perch species were also abundant on wells e.g. splendid perch (*Callanthias australis*) and butterfly perch (*Caesioperca* spp.). Six species of commercial importance were observed including redfish (*Centroberyx affinis*), redbait (*E. nitidus*), pink ling (*Genypterus blacodes*), ocean perch (*Helicolenus* spp.), striped trumpeter (*Latris lineata*) and *N. macropterus.*

MaxN is a conservative and relative abundance metric which cannot be converted into an absolute density as done for flowline. However, the total relative abundance of fish can be expressed relative to the surface area of the structure if each structure is considered as basic cuboid. The surface area of Well 2 – 4 is 105 m^2 and the surface area of the manifold is 365.19 m^2. The total relative abundance of identified fish species per m^2 ranged from 0.79 fish m^{-2} at Well 2 to 1.90 fish m^{-2} at Well 4.

TABLE 3 Repeated measures PERMANOVA results and pairwise test results for historic flowline comparison on the fish and mobile invertebrate assemblage combined, using a video quality metric as a covariate. Significant values are shown in bold. Unique permutations varied from 992–999.

Factor	df	MS	Pseudo-*F*	*P*	Pairs	*t*	*P*
Flowline 5							
Video quality	1	7621.8	5.93	**0.001**	2009 *vs* 2012	1.83	**0.01**
Year	3	3283.1	2.55	**0.001**	2009 *vs* 2017	1.98	**0.003**
Transect	10	1872.9	1.46	**0.048**	2009 *vs* 2020	1.78	**0.006**
Residual	29	1285.3			2012 *vs* 2017	1.37	0.12
					2012 *vs* 2020	1.06	0.357
					2017 *vs* 2020	0.89	0.517
Flowline 9							
Video quality	1	10747	5.35	**0.005**			
Year	0	No test					
Transect	8	1440.8	0.72	0.882			
Residual	8	2007.4					
Flowline 6 and Umbilical 4							
Video quality	1	21516	16.99	**0.001**	**Flowline 6**		
Flowline	1	18156	11.05	**0.001**	2009 *vs* 2020	0.80	0.638
Year	1	2081.8	1.46	0.197	**Umbilical 4**		
Transect (Flowline)	46	1630.7	1.30	**0.013**	2009 *vs* 2020	1.20	0.214
Flowline x Year	1	8680.9	6.92	**0.001**			
Residual	45	1255.1					
Umbilical 8							
Video quality	1	41677	35.48	**0.001**	2014 >1500 *vs* 2017 <1500	No test	
Year	3	10917	9.29	**0.001**	2014 >1500 *vs* 2020 <1500	No test	
Transect	48	1622.4	1.38	**0.002**	2014 >1500 *vs* 2020 >1500	1.58	**0.013**
Residual	47	1174.6			2017 <1500 *vs* 2020 <1500	1.98	**0.004**
					2017 <1500 *vs* 2020 >1500	No test	
					2020 <1500 *vs* 2020 >1500	No test	

Across all wells and the manifold, the tree cap assembly had the highest abundance of fish taxa followed by the Christmas tree and the flow base. The tree cap and Christmas tree also had the highest diversity at 11 and 12 species, respectively, compared to 10 for the flow base and four for other areas. The majority of fish species for which length estimates were made on wells were in the 20-30 cm size range, with 30% of these commercial fishery species. *Helicolenus* spp. were mostly 30-40 cm in size and *N. macropterus* 40-50 cm (Supplementary Figure 3).

For 2020 observations, fish communities differed across wells and across sections of each wells ($p = 0.001$; Supplementary Table 5). All wells possessed distinct fish communities ($p = <0.04$) with the exception of Well 2 and Well 4 ($p = 0.06$; Supplementary Table 5). *Callanthias australis* was associated with Well 4 while all other species were correlated with the manifold (Figure 11). There was a good level of distinction between the wells, as illustrated by an overall CAP allocation success rate of 80%, with each group equally distinct (80% success rate per group).

3.7.2 A comparison of marine communities around the manifold and wells across years

A total of 2,196 individual fish from 19 species were observed on the wells across the six surveys spanning 11 years using the conservative measure of ‘maximum MaxN’ for each well (Supplementary Table 3). Fish assemblages were dominated by the Australian sandpaper fish (*P. macleayi*) which was at least six times more abundant than any other species. Species of ecological interest included the Australian fur seal (*A. pusillus doriferus*) with one observation in 2009 and the western foxfish *B. frenchii*.

Comparisons across years for the well and manifold surveys need to be interpreted with caution given the differing time of day sampled, duration of surveys, depth, and size of the structures. Metric multi-dimensional scaling plots show a distinct separation of fish assemblages observed during the first 2009 survey from surveys in later years (Figures 11B, C). Surveys beyond 2009 were characterized by Australian sandpaper fish (*P. macleayi*) and

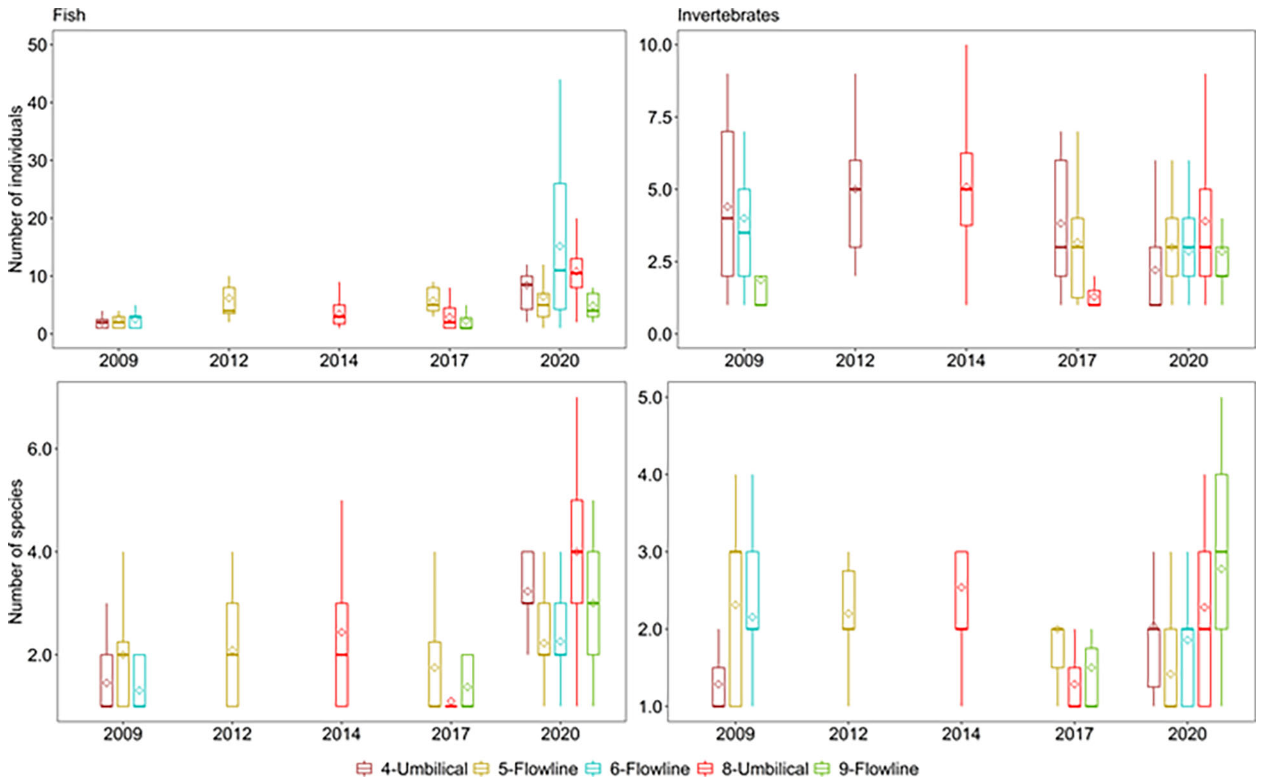

FIGURE 9
Comparisons of the mean (◊) and median (|) number of fish species (left) and mobile invertebrates (right) and individuals per 50 m transect on the flowlines across years surveyed. The upper and lower hinges represent the first and third quartiles (the 25 and 75 percentiles). The whiskers extend from the hinge to the largest and smallest value, but no further than 1.5 × the interquartile range.

Helicolenus spp. Two clusters were evident among the years beyond 2009 with one grouping being comprised of Well 2 and Well 3 and the other cluster primarily the manifold and Well 4 (Figure 11B). *Callanthias australis* (Figure 11A) and *N. macropterus* (Figure 11C) were strongly associated with the manifold and Well 4.

Total abundance and species richness generally increased across the years at each well, however, the duration of the survey also increases through time with the exception of some short six-minute surveys conducted in 2014 and 2017 (Figure 12). The highest number of species (14) were observed on Well 2 in 2020 whilst the highest number of individuals (650) were observed on the manifold in 2012 which was largely comprised of *P. macleayi* (Figure 12). Three species *P. macleayi, Helicolenus* spp. and *Pseudophycis* spp. were consistently present at all wells and across all years with the exception of the first 2009 survey.

4 Discussion

An improved understanding of marine communities associated with oil and gas infrastructure in the Bass Strait region is particularly important given the ecological and socio-economic importance of the region. Industry-collected ROV video provides a unique opportunity to examine marine communities associated with subsea flowlines and wells. While historical ROV video has, in recent years, been used to survey marine communities around infrastructure in Australia's tropical north-west (e.g. Thomson et al., 2018; Bond et al., 2018a; McLean et al., 2020a;), only a small handful of published papers exist for the temperate Bass Strait region, one focused on using animal-borne imagery to evaluate infrastructure space use (Arnould et al., 2015), another examining plankton communities around platforms (Neira, 2005) and two recent studies that use historical industry ROV imagery to describe fish and benthic communities on a small number of wells, pipelines and platforms (McLean et al., 2022; Sih et al., 2022). The data for wells presented in McLean et al. (2022) was obtained from the present study and included data for Well 2 and 4 only. Here, we demonstrate the potential utility of industry collected ROV data for documenting biodiversity values of offshore infrastructure.

Using imagery collected by industry gives us a unique opportunity to observe areas that are often difficult and expensive to assess. However, given industry surveys are not specifically designed for scientific data collection, there are naturally issues with standardizing methodology and design to make experimentally robust comparisons. Historical comparisons here are interpreted with caution, given the different video quality, time of day, and duration of surveys. While a generally low diversity of fishes might be expected on poor quality video obtained from historical ROV surveys, the 2020 high-definition imagery was likely also be hindered by the downward-facing camera not capturing species in front of the ROV. As downward facing high-definition imagery is essential for epibenthic communities and invertebrates, a combination of downward and forward-looking HD cameras, ideally with a boom-camera set up for flowlines, would improve sampling for all aspects of marine communities. At these

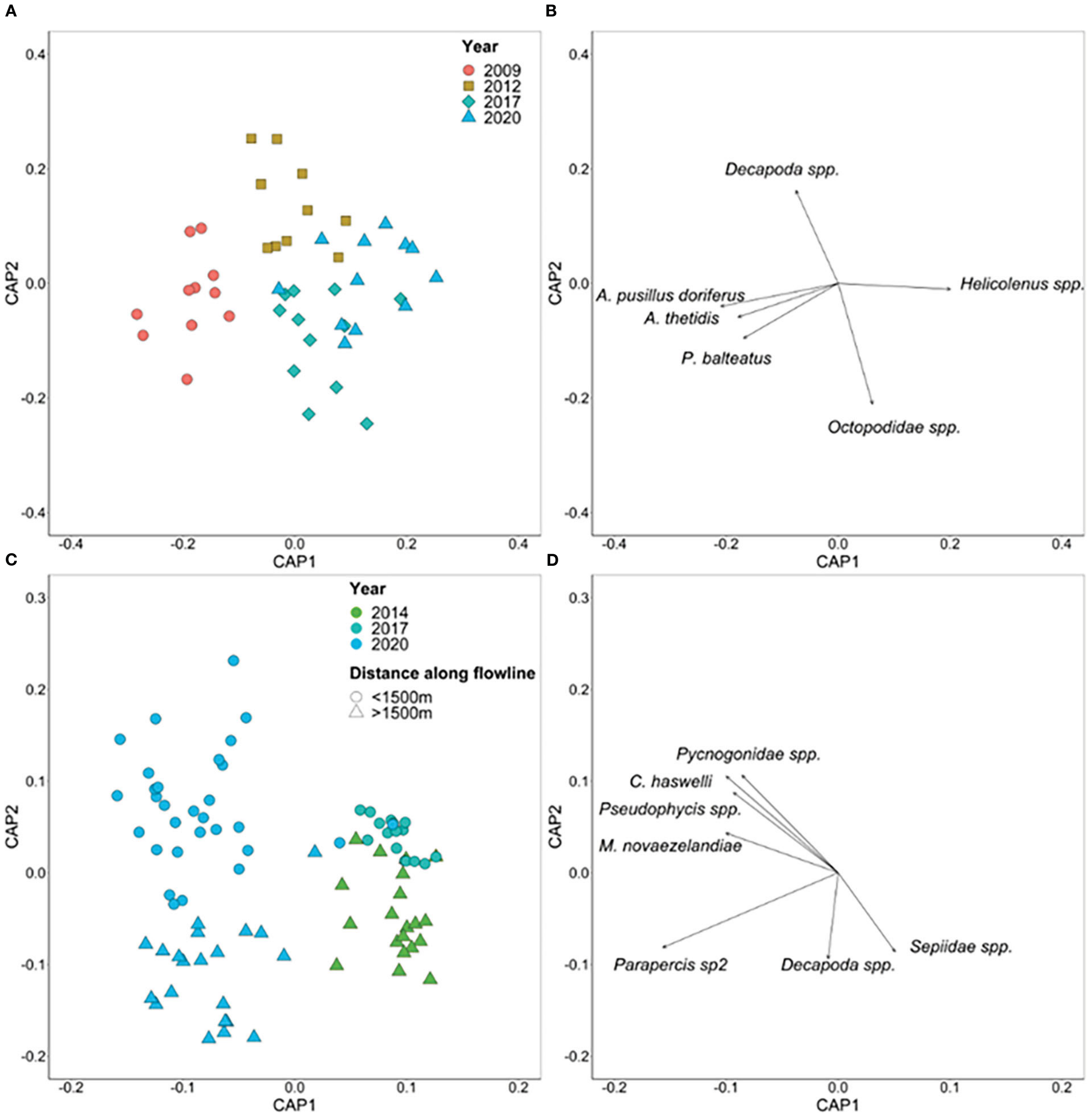

FIGURE 10
Canonical analysis of principal coordinates (CAP) ordination based on Bray-Curtis dissimilarities for multivariate fish and invertebrate abundance on the **(A)** Flowline 5 and **(C)** Umbilical 8 flowlines. Each point represents the assemblage structure (all species) within each 50 m transect of each flowline in relation to the other locations (similarity), with points that are closer together more similar than those further apart. Pearson correlations (|R| ≥ 0.4) are displayed as vectors for **(B)** Flowline 5 and **(D)** Umbilical 8 flowlines with the length and direction of vectors representing the strength and direction, respectively, of the relationship.

depths (beyond natural light), ROVs may have less of an influence on fish behavior if they were to use red lights, rather than white, as at these depths red lights may not be visible to fishes (Widder et al., 2005; Raymond and Widder, 2007; Birt et al., 2019).

While the science value of historical ROV video has been thought to be enormous, particularly for depths not easily accessible to scientists (Macreadie et al., 2018), it does have limitations when assessing biodiversity values, particularly of sessile biota, and for rigorously addressing hypotheses associated with the value of infrastructure communities. Traditionally, industry ROV operations have either not possessed the ability or had the requirement for HD imagery and, as a result, analysis of historical ROV imagery for science is hampered by difficulties in species identification and counting due to low image resolution (McLean et al., 2020b). Here, assessments of change in marine communities through time were confounded by video quality and survey duration that made it impossible to determine if assemblages changed or our ability to detect them did. Given the poor quality of imagery and the vast differences in ROV movement and survey duration, it is most likely that the observed increase in abundance and richness with time is a product of sampling, rather than time itself. However repeated surveys of same sections of flowlines enabled the detection of

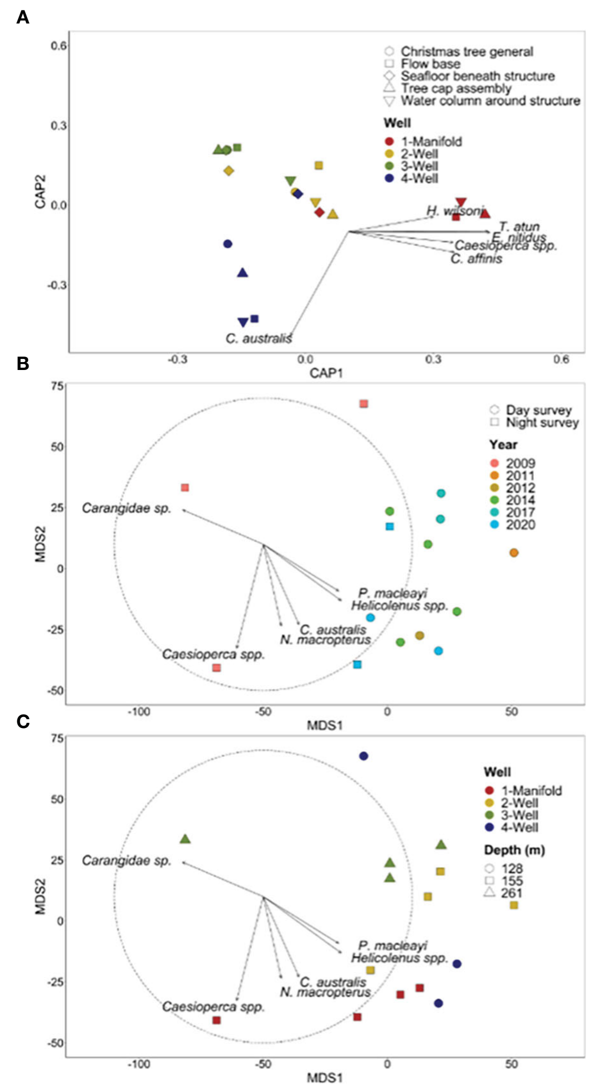

FIGURE 11
(A) Canonical analysis of principal coordinates (CAP) ordination based on Bray-Curtis dissimilarity for fish species abundance for well assets. Each point represents the assemblage structure (of all species) for each well/manifold in relation to the other locations (similarity), with points that are closer together more similar than those further apart. Species with a Pearson's correlation of |R| > 0.4 are represented as vectors in an overlay. The length and direction of vectors indicate the strength and direction, respectively, of the relationship. Metric multi-dimensional scaling (mMDS) ordination of all well surveys with plot **(B)** illustrating patterns among year and time of survey and plot **(C)** illustrating patterns among depth and well; species with the strongest positive (>0.55) and negative (<–0.55) Pearson's correlation values are displayed as vectors.

change in fish and invertebrate assemblages taking in to consideration the influence of the variability in video quality in the analyses.

The present study observed 10,343 individual animals around subsea oil and gas infrastructure across 11 years, spanning 69 taxa that included bony and cartilaginous fishes, mammals, and invertebrates, and provides the first comprehensive understanding of biodiversity associated with flowlines and wells in temperate waters of Australia. Further, the historical archive of imagery and analyses undertaken as part of this work provided a unique opportunity to determine if this imagery can be used to assess temporal change in communities associated with infrastructure across multiple assets. To our knowledge, all previous research in Australia has been limited to single time periods (e.g., Bond et al., 2018a; Bond et al., 2018b; McLean et al., 2019) or several time periods for single structures (McLean et al., 2017).

We recorded higher diversity of fishes on flowlines (28 species) than wells (19 species). Despite the different measures of abundance (count vs MaxN) and units of measure (individuals per linear meter vs individuals per square meter), we saw lower a density of fish at ~0.3 individuals per linear meter of flowline than wells at 0.8-2 per m^2 which we would expect to be a more conservative measure being derived from the maximum MaxN abundance. Differences in the apparent density of fish between wells and flowlines might be driven by the overall structural complexity of infrastructure and associated sclerobionts, or the traits of fishes unique to infrastructure-type. i.e. schooling versus solitary organisms. Love et al., 2019b found midwater assemblages on offshore platforms to harbor higher densities of juvenile fishes compared to natural sites closer to the seabed. They hypothesize that recruits are more likely to encounter these tall structures than natural habitats that have relatively little relief above the seafloor, and perhaps secondarily to comparatively reduced predation in midwaters compared to natural sites. It is possible that high densities observed on wells and the manifold compared to flowlines in this study may have similar structural complexity influences on the assemblages observed, however further research is required.

4.1 Marine communities along flowlines

Flowlines possessed an array of demersal fishes and mobile invertebrates known to exist in the region. However, fish assemblages recorded here represent only a small proportion (~10%) of the diversity of fishes known to occur across a diversity of habitats in the Bass Strait region (200 species; Butler et al., 2002). Species relatively common across the region but absent on ROV imagery of flowlines include dories, dogfish, frostfish, burrfish, warehou, leatherjackets, demersal shark species such as gummy, school and draughtboard sharks, sawsharks and elephantfish (Knuckey, 2006). This is perhaps not surprising as research has shown that ROV lights, sound, and speed can impact fish behavior in different ways, with variability across species (Popper, 2003; Trenkel et al, 2004; Stoner et al., 2008; Ryer et al., 2009; Schramm et al., 2020). Using industry ROV imagery of a pipeline on the north-west shelf, Bond et al. (2018c) theorized that the absence of regionally common *Lethrinus punctulatus* (blue-lined emperor) and *Lethrinus erythropterus* (crimson snapper) on surveys was likely a result of these species fleeing with the approach of the ROV. Schramm et al. (2020) found that in soft sediment habitats in north-west Australia, baited video techniques were more effective at sampling a diversity of species than ROV suggesting bait and behavior-related responses. Such a response to the ROV here may account for the absence of other species which are known to occur in similar depths across this region (Williams and Bax, 2001) or lower abundances of some species on flowlines (e.g. jackass morwong *N. macropterus*). Alternately it may be that the flowlines may not provide a suitable habitat for these species, or there are some other environmental factors specific to this location that do not suit their presence. We note that several of these

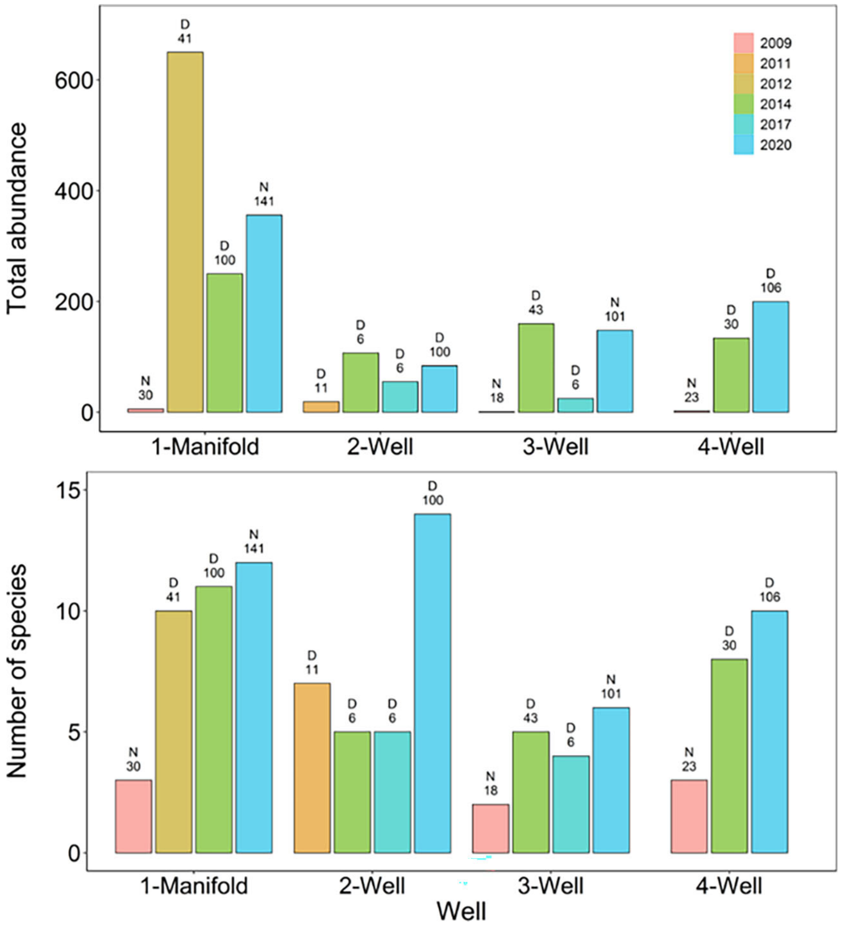

FIGURE 12
Total abundance (maximum MaxN's) and number of species of fish sampled for each well survey. Above the bars, the letter 'D' indicates a daytime survey whilst 'N' indicates a night survey. The number above the bars refers to the duration of the survey in minutes.

absent species (elephantfish, draughtboard sharks, leatherjackets) were observed in low numbers around platform infrastructure in the Gippsland region to the east and in shallower waters <100 m depth (Sih et al., 2022).

Fish assemblages were surprisingly distinct on each flowline with diversity varying between 8–18 taxa per flowline (out of 24 total species in 2020), and assemblages varied even for flowlines occupying similar areas. The reasons for these spatially explicit communities could be due to a variety of factors. In this study, depth, the position of the pipeline relative to the seafloor and the percent cover of biofilm, sand and burrows were all associated with variation in the structure of marine communities. Depth is a common environmental driver in structuring marine communities (Baldwin et al., 2018; Stefanoudis et al., 2019) and can be tied to other environmental changes such as differences in temperature, dissolved oxygen content, and nutrient and plankton availability. Here, the Balmain bug (*Ibacus peronii*) and the whiptail (*Coelorinchus* spp.) both increased in abundance with increasing depth, concurring with previous research on the ecology and distribution of these species (Haddy et al., 2005; McLean et al., 2015). In general, the number of mobile invertebrate species and total abundance also increased with depth, however this relationship was not strong. *I. peronii* also tended to be more abundant where burrow numbers were higher although it is unknown whether the burrows observed were created by this species or not. Balmain bugs are known for spending a good proportion of their time in burrows (Faulkes, 2006). The cocky gurnard (*L. modesta*) increased in abundance as depth became shallower. This species is widely distributed between southern and eastern Australian waters, particularly in depths <50 m (Hyndes et al., 1999; Park et al., 2017). *Parapercis allporti* was also commonly observed in the space underneath the flowlines (46% of observations) and 86% of observations were recorded when the flowline was not completely buried. Recent research in tropical north-west Australia has documented higher abundances of many species where pipelines span the seafloor (gap between bottom of pipeline and the seabed) linked to species behavior and higher cover of epibenthic communities (McLean et al., 2017; McLean et al., 2020a). Here, however, there were very few spans and biotic cover was minimal.

Low epibenthic cover observed across the flowlines (such as sponges) and high proportion of biofilm and sand meant that these two latter habitats featured as variables of importance for structuring communities observed on flowlines. Slender sandburrower (*C. haswelli*), red cod (*Pseudophycis* spp.), and blue grenadier (*M. novaezelandiae*) were each associated with areas of higher percent cover of sand. Each of these species are sand-affiliated, *C. haswelli* burrows into sandy and loose gravel bottoms and *Pseudophycis* spp. (likely *Pseudophycis bachus*) feeds on fishes, cephalopods, crabs in muddy and sandy areas (Horn et al., 2012). *M. novaezelandiae* also occur in sandy, muddy regions, but undertake vertical migrations at night, up to within 50 m of the surface, to feed on other fishes, decapods, krill, and squid (Bulman and Blaber, 1986). Interestingly, *M. novaezelandiae* were observed in greatest abundance at night on flowlines when it might be expected that they would not be present due to feeding activity up in the water column. Absence of fish species at night along pipelines on the north-west shelf has been documented by Bond et al. (2018a) and predicted this to be linked to species departure to feed in surrounding areas. Here, it seemed that nocturnally active species were observed in higher abundance on night surveys, including hermit crabs (*Decapoda* spp.), sea spiders (*Pycnogonidae* sp.), several *Parapercis* (grubfish) species, the slender sand burrower (*C. haswelli*), banded cucumberfish (*P. balteatus*) and red cod (*Pseudophycis* spp.). This has clear implications for the future timing of ROV surveys of marine communities around infrastructure. Based on these results, and those of Bond et al. (2018a), we predict that many fish and mobile invertebrate species will exhibit diurnal patterns of habitat (infrastructure) usage. Knowledge of these patterns will facilitate improved understanding of residency rates around structures (required to inform estimates of production on structures) in addition to nutrient transfer among infrastructure and surrounding ecosystems, i.e., how connected are artificial and natural ecosystems and how is this influenced by diurnal movements? Additional diurnal investigations are needed to better understand the role that infrastructure plays in the day-to-day behaviors of fish and invertebrate species and how this might differ between tropical and temperate ecosystems.

A number of commercial fishery species were observed along flowlines with the most numerically abundant in 2020 including octopus (Octopodidae spp; $n = 46$), Tasmanian giant crab (*P. gigas;* 47), cuttlefish (*Sepiidae* spp.; 93), Balmain bug (*I. peronii;* 35), ocean perch (*Helicolenus* spp.; 1207), trevally (Carangidae spp.; 335) and blue grenadier (*M. novaezelandiae;* 104). The most abundant commercial fish, *Helicolenus* spp. could be either *H. barathi* (bigeye ocean perch) or *H. percoides* (reef ocean perch) however the two could not be reliably distinguished from imagery. *Helicolenus* spp. comprised the majority of commercial taxa size estimates on flowlines (98% in the <20 cm range, n = 1127) with few individuals (n = 78) 20-30 cm in length. Females of both *H. barathri* and *H. percoides* are believed to reach sexual maturity at 15-20 cm (5 years) while males mature at 19-25 cm (5-7 years) (Paul and Francis, 2002 cited from Morrison et al., 2014). It is therefore quite likely that a high proportion of individuals observed here are not sexually mature and therefore not available to the fishery which take individuals predominantly in the 20-40 cm size range in this region (AFMA, 2020). *Helicolenus* spp. were also among the most common and abundant commercially fished species observed on pipelines to the east of this study in the Gippsland region (McLean et al., 2022; Sih et al., 2022).

The phenomena of pipelines acting as 'corridors' has recently been noted for various species around the globe. Previous research has shown that benthic foraging marine mammals and seabirds benefit from seafloor infra-structure as they act as artificial reefs which provide habitat for prey species. Australian fur seals (*A. pusillus doriferus*) have previously been observed to exhibit foraging behavior along pipelines in the Bass Strait (Arnould et al., 2015), with similar behavior observed in other species in the North Sea (Todd et al., 2016) around windfarm turbine piles and pipelines (Russell et al., 2014) and platforms (Todd et al., 2020). *A. pusillus doriferus* forage on a large variety of prey observed on the infrastructure (see list of 40-60 species in Kirkwood et al., 2008), but here were observed chasing schools of redbait (*E. nitidus*). Observations of seals only occurred in 2009 with the time of year of image capture (October) coinciding with heightened foraging activity before breeding season. *A. pusillus doriferus* are protected under the Environment Protection and Biodiversity Conservation Act 1999 (EPBC Act) and represent a significant predator biomass in south-eastern Australia (Kirkwood et al., 2010). In Arnould et al. (2015) pipelines and cable (electricity and telephone) routes were the most visited and most influential structures associated with foraging locations despite such features having limited vertical scope and habitat complexity (and, thus, diversity in prey habitat) in comparison to wells and shipwrecks. They hypothesized, pipelines/cable routes may represent greater overall area and provide habitat connectivity for prey species potentially making them more profitable sites to exploit.

Two additional species of conservation value were observed on the seafloor above buried flowlines (Brachionichthyidae spp., handfish, and *Urolophus* spp., stingaree). The poorly studied handfish are considered the most threatened of all marine bony fishes, especially at greater depths (Stuart-Smith et al., 2020). Seven of 14 species were recently listed as Critically Endangered or Endangered by the International Union for Conservation of Nature (IUCN) and this family has the only marine bony fish to be recognized as Extinct – the Smooth handfish (*Sympterichthys unipennis*) (Stuart-Smith et al., 2020). Imagery obtained of handfish was not sufficient to accurately identify to species level the 10 individuals observed; therefore, their conservation listing is not known. The unidentified stingaree is likely one of three species of *Urolophus* recorded from the region in a previous study, of which two are listed as Vulnerable (IUCN), wide stingaree (*Urolophus expansus)* and greenback stingaree *Urolophus viridis* (Knuckey, 2006) and one listed as least concern (banded stingaree *Urolophus cruciatus*).

4.2 Marine communities at wells and the manifold

In general, wells had a less diverse community of fishes than flowlines but possessed a high density of individuals per occupancy space. Topographic complexity that the structures provide is known to be a major surrogate for diversity and biomass in previous studies (Wedding et al., 2008; Wines et al., 2020). Areas of high complexity are also commonly related to higher fish abundance and species richness than less complex areas (Galaiduk et al., 2017). The Christmas tree and tree cap assembly were structurally complex and possessed the highest abundances of fish but were also sections where the ROV spent proportionally more time. The most abundant fish observed on wells was the Australian sandpaper fish (*P. macleayi*), a slimehead endemic to south-eastern Australia. Little is known about this species, with no published scientific works describing its ecology. We noted 144 individuals on a single well (conservative MaxN estimate) which is a higher density than any fish species observed on well infrastructure on the north-west shelf (McLean et al., 2018). While the species does not feature in commercial catches for the region, it is in the same family as highly targeted roughies (Trachichthyidae) (Knuckey, 2006).

Of the 16 fish species observed across the structures in 2020, six are retained by commercial fisheries operating in this region (Boag and Koopman, 2021); redfish (*C. affinis, n* = 3), redbait (*E. nitidus;* 164), pink ling (*G. blacodes;* 1), ocean perch (*Helicolenus* spp.; 14), striped trumpeter (*L. lineata;* 1) and jackass morwong (*N. macropterus;* 140). While *E. nitidis* was observed in high numbers, this was due to the presence of one school only on Manifold 1. The jackass morwong, *N. macropterus*, is a commercially important groundfish that is common in coastal and continental shelf waters of southern Australia and New Zealand commonly caught in depths from 80–170 meters with major nursery grounds for this species identified in Bass Strait (Bruce et al., 2001). Structural complexity of habitat has been found to be an important in shaping fish assemblages (Wedding et al., 2008) with the vertical relief and complexity of the wells and manifold likely to provide food and shelter from predators in an area of seafloor where we would expect low relief in the majority of surrounding natural habitat.

Similar epibenthic communities were observed on each well when first surveyed in 2009, but there was subsequently some variation through the years. Time series data showed more complex habitat forms in subsequent years (e.g. black/octocorals on Well 4 in 2014 and 2020). This suggests that this benthic community has recruited to and developed on this structure over time, aligning with previous research by McLean et al. (2018) that documents a strong positive relationship between the cover of epibenthic communities and well age. Here, this relationship was comparatively weak, which could be due to variations in sampling effort, depth of structures and/or reflect a different pattern of establishment for temperate ecosystems and locality such as oceanographic parameters influencing recruitment. Further research is required to assess how epibenthic communities on infrastructure in the Bass Strait establish and change through time.

4.3 Future research opportunities

Industry would benefit from incorporating HD scientific surveys (e.g. stereo-ROV) into offshore ROV campaigns (see McLean et al., 2019) where quantitative data can be obtained in a systematic way to better inform decommissioning.

Advances in our understanding of the impacts of oil and gas infrastructure in marine ecosystems will require dedicated science programs. For ecology, this includes research to examine:

- diversity of benthic and encrusting communities and how these influence development and succession in fish communities,
- primary and secondary productivity supported by structures,
- the role these structures play in the life history (ontogeny) of species, including residency rates, movement patterns,
- how communities on infrastructure are connected to surrounding ecosystems (connectivity, diel behavior patterns, food webs),
- contribution of structures to surrounding fisheries.

There is also an opportunity to increase the potential benefits of industry ROV data collection for biodiversity assessments. However, it is acknowledged that they would need to be taken into consideration regarding their primary use for inspection, maintenance, and repair campaigns. This would include:

- obtaining both day and night data to ensure diurnal effects can be assessed on fish and invertebrate assemblages observed for structures of interest (e.g. individual flowline sections, wells across years),
- ensure that tracking data from USBL systems are available and accessible to undertake spatially explicit analyses, in tandem with infrastructure schematics,
- maintain consistency of ROV survey methods (survey heights, speed, duration, and coverage through time) and across assets so similar effort of data capture can be compared across years,
- consider the addition of HD stereo video allowing for accurate size estimates, and better identification of species,
- discuss survey design options with science team to optimize benefits for biodiversity assessments.

Data availability statement

The raw data supporting the conclusions of this article will be made available by the authors, without undue reservation.

Ethics statement

Ethical review and approval was not required for the animal study because we used observation data from historical imagery from industry ROVs.

Author contributions

DI, DM, JM, and OG-W conceived the project. DH coordinated data capture. SW, SKW, TB, MB, DM, and DI contributed data analyses. All authors contributed to the article and approved the submitted version.

Funding

Funding provided by Cooper Energy. The funder had the following involvement in the study: study design, data collection, analysis and preparation of the manuscript.

Acknowledgments

We thank Cooper Energy for their project support, in particular Phil Deshon. We thank Dr Rick Stuart-Smith from IMAS and John Pogonoski from CSIRO for assistance with fish identifications. Thanks to Jamie Colquhoun (AIMS) for assistance with verifications of identifications used in benthic scoring.

Conflict of interest

Authors OG-W, JM and DH were employed by company Cooper Energy.

The remaining authors declare that the research was conducted in the absence of any commercial or financial relationships that could be construed as a potential conflict of interest.

Publisher's note

Supplementary material

The Supplementary Material for this article can be found online at: https://www.frontiersin.org/articles/10.3389/fmars.2023.1095906/full#supplementary-material

References

AFMA (2020). Available at: https://www.afma.gov.au/fisheries-management/species/ocean-perch.

Althaus, F., Hill, N., Ferrari, R., Edwards, L., Przeslawski, R., Schönberg, C. H. L., et al. (2015). A standardised vocabulary for identifying benthic biota and substrata from underwater imagery: The CATAMI classification scheme. *PloS One* 10, e0141039–e0141039. doi: 10.1371/journal.pone.0141039

Anderson, M., Gorley, R., and Clarke, K. (2008). *PERMANOVA+ for PRIMER: Guide to software and statistical methods* (Plymouth, UK: PRIMER-E Ltd).

Anderson, M. J., and Robinson, J. (2003). Generalized discriminant analysis based on distances. *Aust. New Z. J. Stat* 45, 301–318. doi: 10.1111/1467-842X.00285

Anderson, M. J., and Willis, T. J. (2003). Canonical analysis of principal coordinates: A useful method of constrained ordination for ecology. *Ecology* 84, 511–525. doi: 10.1890/0012-9658(2003)084[0511:CAOPCA]2.0.CO;2

Arnould, J. P. Y., Monk, J., Ierodiaconou, D., Hindell, M. A., Semmens, J., Hoskins, A. J., et al. (2015). Use of anthropogenic Sea floor structures by Australian fur seals: Potential positive ecological impacts of marine industrial development? *PLoSONE* 10 (7), e0130581. doi: 10.1371/journal.pone.0130581

Auguie, B. (2017). *gridExtra: Miscellaneous functions for "Grid" graphics* (R package version 2.3). Available at: https://CRAN.R-project.org/package=gridExtra.

Baldwin, C. C., Tornabene, L., and Robertson, D. R. (2018). Below the mesophotic. *Sci. Rep.* 8, 4920. doi: 10.1038/s41598-018-23067-1

Bax, N. J., and Williams, A. (2001). Seabed habitat on the south-eastern Australian continental shelf: Context, vulnerability and monitoring. *Mar. Freshw. Res.* 52, 491–512. doi: 10.1071/MF00003

Birt, M. J., Stowar, M., Currey-Randall, L. M., McLean, D. L., and Miller, K. J. (2019). Comparing the effects of different coloured artificial illumination on diurnal fish assemblages in the lower mesophotic zone. *Mar. Biol.* 166, 154. doi: 10.1007/s00227-019-3595-0

Boag, S., and Koopman, M. (2021). *Commercial fishing catch and value in the area of the basker-Manta-Gummy oil and gas field* (Atlantis and Fishwell Consulting).

Bond, T., Langlois, T. J., Partridge, J. C., Birt, M. J., Malseed, B. E., Smith, L., et al. (2018a). Diel shifts and habitat associations of fish assemblages on a subsea pipeline. *Fisheries Res.* 206, 220–234. doi: 10.1016/j.fishres.2018.05.011

Bond, T., McLean, D. L., Wakefield, C., Partridge, J., Prince, J., White, D., et al. (2021). Quantifying fishing activity targeted subsea pipelines by commercial trap fishers. *Rev. Fish Biol. Fisheries* 31, 1009–1023. doi: 10.1007/s11160-021-09686-4

Bond, T., Partridge, J., Taylor, M. D., Cooper, T., and McLean, D. L. (2018b). The influence of depth and a subsea pipeline on fish assemblages and commercially fished species in north-west Australia. *PloS One* 13 (11), e0207703. doi: 10.1371/journal.pone.0207703

Bond, T., Partridge, J. C., Taylor, M. D., Langlois, T. J., Malseed, B. E., Smith, L. D., et al. (2018c). Fish associated with a subsea pipeline and adjacent seafloor of the north West shelf of Western Australia. *Mar. Environ. Res.* 141, 53–65. doi: 10.1016/j.marenvres.2018.08.003

Boswell, K. M., Wells, D. R. J., Cowan, J. H.Jr, and Wilson, C. A. (2010). Biomass, density and size distributions of fishes associated with a large-scale artificial reef complex in the gulf of Mexico. *Bull. Mar. Sci.* 86 (4), 879–889. doi: 10.5343/bms.2010.1026

Bruce, B. D., Evans, K., Sutton, C. A., Young, J. W., and Furlani, D. M. (2001). Influence of mesoscale oceanographic processes on larval distribution and stock structure in jackass morwong (Nemadactylus macropterus: Cheilodactylidae). – *ICES J. Mar. Sci.* 58, 1072–1081. doi: 10.1006/jmsc.2001.1099

Bugnot, A. B., Mayer-Pinto, M., Airoldi, L., Heery, E. C., Johnston, E. L., Critchley, L. P., et al. (2021). Current and projected global extent of marine built structures. *Nat. Sustainability* 4, 33–41. doi: 10.1038/s41893-020-00595-1

Bulman, C. M., and Blaber, S. J. M. (1986). Feeding ecology of *Macruronus novaezelandiae* (Hector) (Teleostei: Merlucciidae) in south-eastern Australia. *Aust. J. Mar. Freshw. Res.* 37, 621–639. doi: 10.1071/MF9860621

Burnham, K. P., and Anderson, D. R. (2003). *Model selection and multimodel inference: A practical information-theoretic approach* (New York, NY: Springer New York). doi: 10.1007/b97636

Butler, A., Althaus, F., Furlani, D., and Ridgway, K. (2002). Assessment of the conservation values of the bass strait sponge beds area. CSIRO marine research. *Rep. to Environ. Aust.* 1–64

Cappo, M., Harvey, E., and Shortis, M. (2007). "Counting and measuring fish with baited video techniques – an overview," in *Proceedings of the 2006 Australian society of fish biology conference and workshop cutting edge technologies in fish and fisheries science*. Eds. J. M. Lyle, D. M. Furlani and C. D. Buxton (Hobart, Hobart: ASFB).

Claisse, J. T., Love, M. S., Meyer-Gutbrod, E. L., Williams, C. M., and Pondella DJ, I. I. (2019). Fishes with high reproductive output potential on California offshore oil and gas platforms. *Bull. Mar. Sci.* 95 (4), 514–534. doi: 10.5343/bms.2019.0016

Claisse, J. T., Pondella DJ, I. I., Love, M., Zahn, L. A., Williams, C. M., Williams, J. P., et al. (2014). Oil platforms off California are among the most productive marine fish habitats globally. *PNAS* 11 (43), 15462–15467. doi: 10.1073/pnas.1411477111

Clarke, K., and Gorley, R. (2015). *PRIMER v7: User Manual/Tutorial* (Plymouth, UK: PRIMER-E Ltd).

Clarke, K. R., Tweedley, J. R., and Valesini, F. J. (2014). Simple shade plots aid better long-term choices of data pre-treatment in multivariate assemblage studies. *J. Mar. Biol. Assoc. UK* 94, 1–16. doi: 10.1017/S0025315413001227

Commonwealth of Australia (2015). "South-east marine region profile: A description of the ecosystems, conservation values and uses of the south-east marine region," in *Commonwealth of Australia 2015*. Available at: https://www.environment.gov.au/system/files/resources/7a110303-f9c7-44e4-b337-00cb2e4b9fbf/files/south-east-marine-region-profile.pdf.

Faulkes, Z. (2006). Digging mechanisms and substrate preferences of shovel nosed lobsters, ibacus peronii (Decapoda: Scyllaridae). *J. Crustacean Biol.* 26 (1), 69–72. doi: 10.1651/C-2628.1

Fisher, R., Wilson, S. K., Sin, T. M., Lee, A. C., and Langlois, T. J. (2018). A simple function for full-subsets multiple regression in ecology with R. *Ecology and Evolution.* 8 (12), 6104–13. doi: 10.1002/ece3.4134

Galaiduk, R., Halford, A. R., Radford, B. T., Moore, C. H., and Harvey, E. S. (2017). Regional-scale environmental drivers of highly endemic temperate fish communities located within a climate change hotspot. *Diversity Distributions* 23, 1256–1267. doi: 10.1111/ddi.12614

Galaiduk, R., Radford, B., Case, M., Bond, T., Taylor, M., Cooper, T., et al. (2022). Regional patterns in demersal fish assemblages among subsea pipelines and natural habitats across north-west Australia. *Front. Mar. Science.* 9. doi: 10.3389/fmars.2022.979987

Gallaway, B. J., Szedlmayer, S. T., and Gazey, W. J. (2009). A life history review for red snapper in the gulf of Mexico with an evaluation of the importance of offshore petroleum platforms and other artificial reefs. *Rev. Fisheries Sci.* 17 (1), 48–67. doi: 10.1080/10641260802160717

Gill, P. C., Morrice, M. G., Page, B., Pirzl, R., Levings, A. H., and Coyne, M. (2011). Blue whale habitat selection and within-season distribution in a regional upwelling system off southern Australia. *Mar. Ecol. Prog. Ser.* 421, 243–263. doi: 10.3354/meps08914

Gourvenec, S., Sturt, F., Reid, E., and Trigos, F. (2022). Global assessment of historical, current and forecast ocean energy infrastructure: Implications for marine space planning, sustainable design and end-of-engineered-life management. *Renewable Sustain. Energy Rev.* 154, 111794. doi: 10.1016/j.rser.2021.111794

Haddy, J. A., Courtney, A. J., and Roy, D. P. (2005). Aspects of the reproductive biology and growth of balmain bugs (*Ibacus* spp.) (Scyllaridae). *J. Crustacean Biol.* 25 (2), 263–273. doi: 10.1651/C-2521

Hastie, T., and Tibshirani, R. (1986). Generalized additive models. *Stat. Sci.* 1, 297–310. doi: 10.1214/ss/1177013604

Hobday, A. J., and Hartmann, K. (2006). Near real-time spatial management based on habitat predictions for a longline bycatch species. *Fisheries Manage. Ecol.* 13 (6), 365–380. doi: 10.1111/j.1365-2400.2006.00515.x

Horn, P. L., Forman, J. S., and Dunn, M. R. (2012). Dietary partitioning by two sympatric fish species, red cod (*Pseudophycis bachus*) and sea perch (*Helicolenus* percoides) on chatham rise, new Zealand. *Mar. Biol. Res.* 8, 624–634. doi: 10.1080/17451000.2011.653543

Hyndes, G. A., Platell, M. E., Potter, I. C., and Lenanton, R. C. J. (1999). Does the composition of the demersal fish assemblages in temperate coastal waters change with depth and undergo consistent seasonal changes? *Mar. Biol.* 134, 335–352. doi: 10.1007/s002270050551

Johnson, C. R., Banks, S. C., Barrett, N. S., Cazassus, F., Dunstan, P. K., Edgar, G. J., et al. (2011). Climate change cascades: Shifts in oceanography, species' ranges and subtidal marine community dynamics in eastern Tasmania. *J. Exp. Mar. Biol. Ecol.* 400, 17–32. doi: 10.1016/j.jembe.2011.02.032

Kirkwood, R., Hume, F., and Hindell, M. (2008). Sea Temperature variations mediate annual changes in the diet of Australian fur seals in bass strait. *Mar. Ecol. Prog. Ser.* 369, 297–309. doi: 10.3354/meps07633

Kirkwood, R., Pemberton, D., Gales, R., Hoskins, A. J., Mitchell, T., Shaughnessy, P. D., et al. (2010). Continued population recovery by Australian fur seals. *Mar. Freshw. Res.* 61, 695–701. doi: 10.1071/MF09213

Knuckey, I. A. (2006). *Southern and Eastern scalefish and shark fishery – bycatch utilisation scoping study* (Victoria: Department of Primary Industries Agribusiness Group).

Love, M. S., Claisse, J. T., and Roeper, A. (2019b). An analysis of the fish assemblages around 23 oil and gas platforms off California with comparisons to natural habitats. *Bull. Mar. Sci.* 95 (4), 477–514. doi: 10.5343/bms.2018.0061

Love, M. S., Nishimoto, M. M., Snook, L., and Kui, L. (2019a). An analysis of the sessile, structure-forming invertebrates living on California oil and gas platforms. *Bull. Mar. Science.* 95 (4), 583–596. doi: 10.5343/bms.2017.1042

Macreadie, P. I., McLean, D. L., Thomson, P. G., Partridge, J. C., Jones, D. O. B., Gates, A. R., et al. (2018). Eyes in the sea: Unlocking the mysteries of the ocean using industrial, remotely operated vehicles (ROVs). *Sci. Total Environ.* 634, 1077–1091. doi: 10.1016/j.scitotenv.2018.04.049

McArdle, B. H., and Anderson, M. J. (2001). Fitting multivariate models to community data: A comment on distance-based redundancy analysis. *Ecology* 82, 290–297. doi: 10.1016/j.csr.2021.104394

McLean, D. L., Green, M., Harvey, E. S., Williams, A., Daley, R., and Graham, K. J. (2015). Comparison of baited longlines and baited underwater cameras for assessing the composition of continental slope deepwater fish assemblages off southeast Australia. *Deep-Sea Res. Part I: Oceanographic Res. Papers* 98, 10–20. doi: 10.1016/j.dsr.2014.11.013

McLean, D. L., Parsons, M. J. G., Gates, A. R., Benfield, M. C., Bond, T., Booth, D. J., et al. (2020b). Enhancing the scientific value of industry remotely operated vehicles (ROVs) in our oceans. *Front. Mar. Sci.* 7, 220. doi: 10.3389/fmars.2020.00220

McLean, D. L., Partridge, J. C., Bond, T., Birt, M. J., Bornt, K. R., and Langlois, T. J. (2017). Using industry ROV videos to assess fish associations with subsea pipelines. *Continental Shelf Res.* 141, 76–97. doi: 10.1016/j.csr.2017.05.006

McLean, D., Speed, C. W., Birt, M. J., Colquhoun, J., Case, M., Stowar, M., et al. (2022). Habitat value of subsea wells and pipelines for fishery target species in Australia. *Front. Mar. Science.* 9. doi: 10.3389/fmars.2022.960496

McLean, D. L., Taylor, M. D., Giraldo, A., and Partridge, J. C. (2019). An assessment of fish and marine growth associated with an oil and gas platform jacket using an augmented remotely operated vehicle. *Continental Shelf Res.* 179, 66–84. doi: 10.1016/j.csr.2019.04.006

McLean, D. L., Taylor, M. D., Partridge, J. C., Gibbons, B., Langlois, T. J., Malseed, B. E., et al. (2018). Fish and habitats on wellhead infrastructure on the north west shelf of Western Australia. *Continental Shelf Res.* 164, 10–27. doi: 10.1016/j.csr.2018.05.007

McLean, D. L., Vaughan, B. I., Malseed, B. E., and Taylor, M. D. (2020a). Fish-habitat associations on a subsea pipeline within and Australian marine park. *Mar. Environ. Res.* 153, 104813. doi: 10.1016/j.marenvres.2019.104813

Melbourne-Thomas, J., Hayes, K. R., Hobday, A. J., Little, R., Strzelecki, J., Thomson, D. P., et al. (2021). Decommissioning research needs for offshore oil and gas infrastructure in Australia. *Front. Mar. Sci.* 8. doi: 10.3389/fmars.2021.711151

Meyer-Gutbrod, E. L., Kui, L., Nishimoto, M. M., Love, M. S., Schroeder, D. M., and Miller, R. J. (2019). Fish densities associated with structural elements of oil and gas platforms in southern California. *Bull. Mar. Sci.* 95 (4), 639–656. doi: 10.5343/bms.2018.0078

Miller, A. D., Versace, V. L., Matthews, T. G., Montgomery, S., and Bowie, K. C. (2013). Ocean currents influence the genetic structure of an intertidal mollusc in southeastern Australia – implications for predicting the movement of passive dispersers across a marine biogeographic barrier. *Ecol. Evol.* 3, 1248–1261. doi: 10.1002/ece3.535

Morrison, M. A., Jones, E. G., Parsons, D. P., and Grant, C. M. (2014). Habitats and areas of particular significance for coastal finfish fisheries management in new Zealand: A review of concepts and life history knowledge and suggestions for future research. *New Z. Government*. 1–205

Neira, F. J. (2005). Summer and winter plankton fish assemblages around offshore oil and gas platforms in south-eastern Australia. *Estuar. Coast. Shelf Sci.* 63, 589–604. doi: 10.1016/j.ecss.2005.01.003

O'Hara, R. B., and Kotze, D. J. (2010). Do not log-transform count data. *Methods Ecol. Evol.* 1, 118–122. doi: 10.1111/j.2041-210X.2010.00021.x

Page, H. M., Zaleski, S. F., Miller, R. J., Dugan, J. E., Schroeder, D. M., and Doheny, B. (2019). Regional patterns in shallow water invertebrate assemblages on offshore oil and gas platforms along the pacific continental shelf. *Bull. Mar. Sci.* 95 (4), 617–638. doi: 10.5343/bms.2017.1155

Park, J. M., Coburn, E., Platell, M. E., Gaston, T. F., Taylor, M. D., and Williamson, J. E. (2017). Diets and resource partitioning among three sympatric gurnards in northeastern Tasmanian waters, Australia. *Mar. Coast. Fisheries* 9, 305–319. doi: 10.1080/19425120.2017.1320342

Paul, L. J., and Francis, M. P. (2002). "Estimates of age, growth, and mortality parameters of sea perch (Helicolenus percoides) off the east coast of the south island, new Zealand," in *Ministry of fisheries, final research report for the ministry of fisheries* (Wellington: Ministry for Primary Industries), 52.

Popper, A. N. (2003). Effects of anthropogenic sounds on fishes. *Fisheries* 28, 24–31. doi: 10.1577/1548-8446(2003)28[24:EOASOF]2.0.CO;2

Raymond, E. H., and Widder, E. A. (2007). Behavioral responses of two deep-sea fish species to red, far-red, and white light. *Mar. Ecol. Prog. Ser.* 350, 291–298. doi: 10.3354/meps07196

R Development Core Team (2019). *R: A language and environment for statistical computing, r foundation for statistical computing, Vienna, Austria* (Vienna, Austria: R Foundation for Statistical Computing).

Ridgway, K. R. (2007). Seasonal circulation around Tasmania: An interface between eastern and western boundary currents. *J. Geophysical Res.* 112, C10016. doi: 10.1029/2006JC003898

Russell, D. J. F., Brasseur, S. M. J. M., Thompson, D., Hastie, G. D., Janik, V. M., Aarts, G., et al. (2014). Marine mammals trace anthropogenic structures at sea. *Curr. Biol.* 24 (14), R638. doi: 10.1016/j.cub.2014.06.033

Ryer, C. H., Stoner, A. W., Iseri, P. J., and Spencer, M. L. (2009). Effects of simulated underwater vehicle lighting on fish behavior. *Mar. Ecol. Prog. Ser.* 391, 97–106. doi: 10.3354/meps08168

Schläppy, M.-L., Robinson, L. M., Camilieri-Asch, V., and Miller, K. (2021). Trash or treasure? considerations for future ecological research to inform oil and gas decommissioning. *Front. Mar. Sci.* 8. doi: 10.3389/fmars.2021.642539

Schramm, K. D., Harvey, E. S., Goetze, J. S., Travers, M. J., Warnock, B., and Saunders, B. J. (2020). A comparison of stereo-BRUV, diver operated and remote stereo-video transects for assessing reef fish assemblages. *J. Exp. Mar. Biol. Ecol.* 524, 151273. doi: 10.1016/j.jembe.2019.151273

Schultz, M., Ierodiaconou, D., Smith, S., Horwitz, P., Richardson, A., Crandall, K., et al. (2009). Sea-Level changes and palaeo-ranges: Reconstruction of ancient shorelines and river drainages and the phylogeography of the Australian land crayfish *Engaeus sericatus* Clark (Decapoda: Parastacidae). *Mol. Ecol.* 17, 5291–5314. doi: 10.1111/j.1365-294X.2008.03996.x

SeaGIS (2020). *EventMeasure (Stereo)* (Bacchus Marsh: SeaGIS Pty Ltd). Available at: http://www.seaGIS.com.au.

Shaw, J. L., Seares, P., and Newman, S. J. (2018). *Decommissioning offshore infrastructure: A review of stakeholder views and science priorities* (Perth, Western Australia: WAMSI), 74.

Sih, T. L., Cure, K., Yilmaz, I. N., McLean, D., and Macreadie, P. I. (2022). Marine life and fisheries around offshore oil and gas in southeastern Australia and possible consequences for decommissioning. *Front. Mar. Sci.* 9. doi: 10.3389/fmars.2022.979212

Sommer, B., Fowler, A. M., Macreadie, P. I., Palandro, D. A., Aziz, A. C., and Booth, D. J. (2019). Decommissioning of offshore oil and gas structures – environmental opportunities and challenges. *Sci. Total Environ.* 658, 973–981. doi: 10.1016/j.scitotenv.2018.12.193

Stefanoudis, P. V., Gress, E., Pitt, J. M., Smith, S. R., Kincaid, T., Rivers, M., et al. (2019). Depth-dependent structuring of reef fish assemblages from the shallows to the rariphotic zone. *Front. Mar. Sci.* 6. doi: 10.3389/fmars.2019.00307

Stoner, A. W., Ryer, C. H., Parker, S. J., Auster, P. J., and Wakefield, W. W. (2008). Evaluating the role of fish behavior in surveys conducted with underwater vehicles. *Can. J. Fisheries Aquat. Sci.* 65, 1230–1243. doi: 10.1139/F08-032

Stuart-Smith, J., Edgar, G. J., Last, P., Linardich, C., Lynch, T., Barrett, N., et al. (2020). Conservation challenges for the most threatened family of marine bony fishes (handfishes: Brachionichthyidae). *Biol. Conserv.* 252, 108831. doi: 10.1016/j.biocon.2020.108831

Symonds, M. R. E., and Moussalli, A. (2011). A brief guide to model selection, multimodel inference and model averaging in behavioural ecology using akaike's information criterion. *Behav. Ecol. Sociobiology* 65, 13–21. doi: 10.1007/s00265-010-1037-6

Thomson, P. G., Fowler, A. M., Davis, A. R., Pattiaratchi, C. B., and Booth, D. J. (2018). Some old movies become classics – a case study determining the scientific value of ROV inspection footage on a platform on australia's north West shelf. *Front. Mar. Sci.* 5. doi: 10.3389/fmars.2018.00471

Todd, V. L. G., Lazar, L., Williamson, L. D., Peters, I. T., Hoover, A. L., Cox, S. E., et al. (2020). Underwater visual records of marine megafauna around offshore anthropogenic structures. *Front. Mar. Sci.* 7, 230. doi: 10.3389/fmars.2020.00230

Todd, V. L. G., Warley, J. C., and Todd, I. B. (2016). Meals on wheels? a decade of megafaunal visual and acoustic observations from offshore oil & gas rigs and platforms in the north and Irish seas. *PloS One* 11, e0153320. doi: 10.1371/journal.pone.0153320

Trenkel, V. M., Lorance, P., and Mahe´vas, S. (2004). Do visual transects provide true population density estimates for deepwater fish? *ICES J. Mar. Sci.* 61, 1050. doi: 10.1016/j.icesjms.2004.06.002

Tweedie, M. (1984). "An index which distinguishes between some important exponential families," in *Statistics: Applications and new directions: Proc. Indian statistical institute golden jubilee international conference*, 579–604.

Wedding, L. M., Friedlander, A. M., McGranaghan, M., Yost, R. S., and Monaco, M. E. (2008). Using bathymetric lidar to define nearshore benthic habitat complexity: Implications for management of reef fish assemblages in Hawaii. *Remote Sens. Environ.* 112, 4159–4165. doi: 10.1016/j.rse.2008.01.025

Wickham, H. (2016). *ggplot2: Elegant graphics for data analysis*. doi: 10.1007/978-0-387-98141-3

Widder, E. A., Robison, B. H., Reisenbichler, K. R., and Haddock, S. H. D. (2005). Using red light for *in situ* observations of deep-sea fishes. *Deep-Sea Res. Part I: Oceanographic Res. Papers* 52, 2077–2085. doi: 10.1016/j.dsr.2005.06.007

Williams, A., and Bax, N. J. (2001). Delineating fish-habitat associations for spatially based management: An example from the south-eastern Australian continental shelf. *Mar. Freshw. Res.* 52, 513–536. doi: 10.1071/MF00017

Wines, S. L., Young, M. A., Zavalas, R., Logan, J. M., Tinkler, P., and Ierodiaconou, D. (2020). Accounting for spatial scale and temporal variation in fish-habitat analyses using baited remote underwater video stations (BRUVS). *Mar. Ecol. Prog. Ser.* 640, 171–187. doi: 10.3354/meps13292

Wood, S. N. (2011). Fast stable restricted maximum likelihood and marginal likelihood estimation of semiparametric generalized linear models. *J. R. Stat. Society. Ser. B: Stat. Method.* 73, 3–36. doi: 10.1111/j.1467-9868.2010.00749.x

Frontiers in
Marine Science

Explores ocean-based solutions for emerging global challenges

The third most-cited marine and freshwater biology journal, advancing our understanding of marine systems and addressing global challenges including overfishing, pollution, and climate change.

Discover the latest Research Topics

See more →

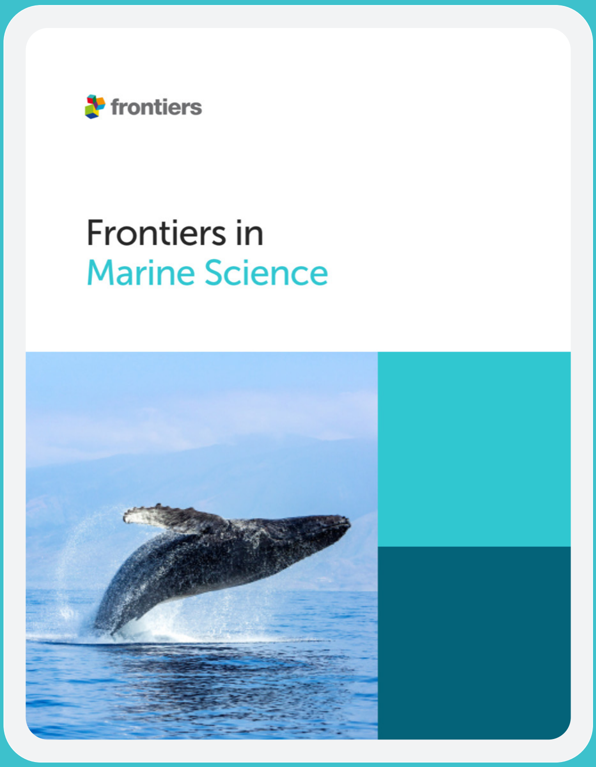

Frontiers

Avenue du Tribunal-Fédéral 34
1005 Lausanne, Switzerland
frontiersin.org

Contact us

+41 (0)21 510 17 00
frontiersin.org/about/contact